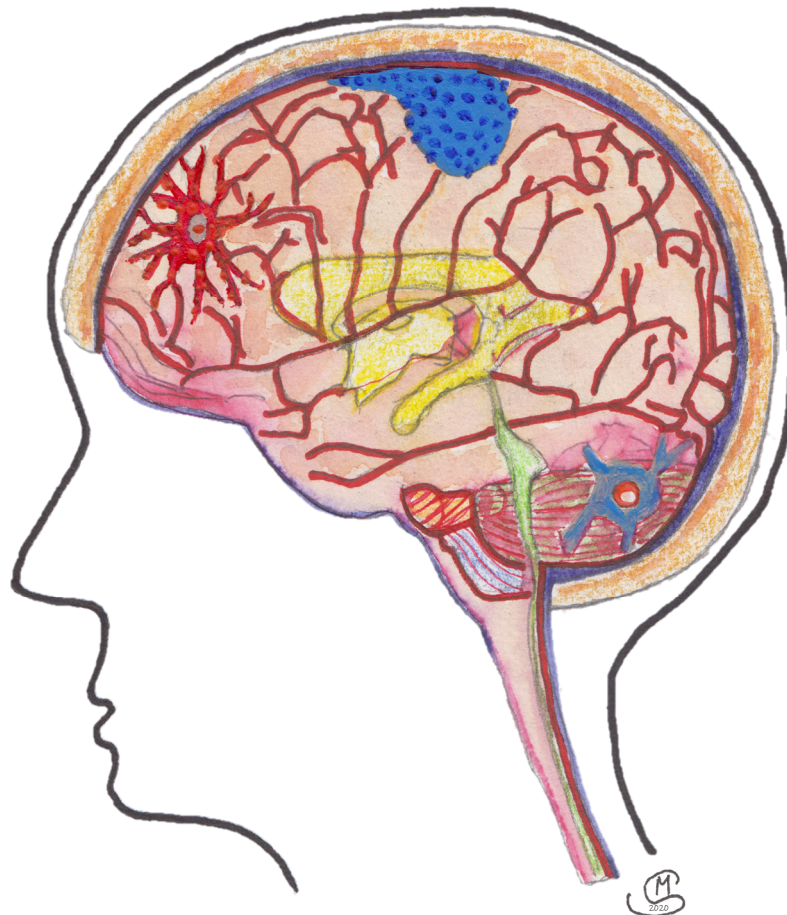


The immunopeptidomic landscape of intracranial neoplasias – Target identification for immunotherapy of glioblastoma, medulloblastoma, and meningioma

Lena Katharina Freudenmann

**University of Tübingen, Interfaculty Institute for Cell Biology,
Department of Immunology**

DKFZ Partner Site Tübingen, German Cancer Consortium (DKTK)



**The immunopeptidomic landscape of intracranial neoplasias –
Target identification for immunotherapy of glioblastoma,
medulloblastoma, and meningioma**

**Das Immunpeptidom intrakranieller Neoplasien –
Identifizierung von Zielen für die Immuntherapie von
Glioblastomen, Medulloblastomen und Meningeomen**

Dissertation

der Mathematisch-Naturwissenschaftlichen Fakultät
der Eberhard Karls Universität Tübingen
zur Erlangung des Grades eines
Doktors der Naturwissenschaften
(Dr. rer. nat.)

vorgelegt von
M.Sc. Lena Katharina Freudenmann
aus Hechingen

Tübingen
2020

Gedruckt mit Genehmigung der Mathematisch-Naturwissenschaftlichen Fakultät der
Eberhard Karls Universität Tübingen.

Tag der mündlichen Qualifikation:

30.07.2020

Dekan:

Prof. Dr. Wolfgang Rosenstiel

1. Berichterstatter:

Prof. Dr. Stefan Stevanović

2. Berichterstatter:

Prof. Dr. Hans-Georg Rammensee

3. Berichterstatter:

Prof. Dr. Oliver Bozinov

für meine Eltern

Content

PREFACE	1
PUBLICATIONS	2
SUMMARY	3
ZUSAMMENFASSUNG	4
CHAPTER 1: INTRODUCTION	
1 INTRACRANIAL NEOPLASIAS	7
1.1 INCIDENCE AND CLASSIFICATION	7
1.2 GLIOBLASTOMA	8
1.3 MEDULLOBLASTOMA	13
1.4 MENINGIOMA	16
2 CANCER IMMUNOTHERAPY	18
2.1 KEY ACTORS FOR EFFECTIVE ANTI-CANCER IMMUNE RESPONSES	18
2.2 HUMAN LEUKOCYTE ANTIGENS PRESENT PEPTIDES TO T LYMPHOCYTES	19
2.3 CANCER IMMUNOTHERAPY FOR INTRACRANIAL NEOPLASMS.....	23
3 IMMUNOPEPTIDOMICS	39
3.1 THE IMMUNOPEPTIDOME	39
3.2 MATERIALS AND METHODS FOR IMMUNOPEPTIDOME ANALYSES.....	41
4 AIM OF THE STUDY	55
5 REFERENCES	56
CHAPTER 2: MULTI-OMICS ANALYSIS IDENTIFIES NOVEL ANTIGENS FOR GLIOBLASTOMA IMMUNOTHERAPY AND DELINEATES DYNAMICS DURING PROGRESSION FROM PRIMARY TO RECURRENT DISEASE	
1 ABSTRACT	77
2 INTRODUCTION	77
3 METHODS	78
4 RESULTS	85
4.1 PEPTIDE YIELDS OF HLA-IPS AND HLA CLASS I ALLOTYPIC COVERAGE	85
4.2 DEFINITION OF GLIOBLASTOMA-ASSOCIATED ANTIGENS	87
4.3 THE HLA PEPTIDOME OF PRIMARY <i>VERSUS</i> RECURRENT GLIOBLASTOMA	98
4.4 NATURAL HLA PRESENTATION OF NEO-ANTIGENS	105
5 DISCUSSION	110
6 REFERENCES	114
CHAPTER 3: HLA PEPTIDOME ANALYSIS OF MEDULLOBLASTOMA UNCOVERS POTENTIAL TARGETS FOR CANCER IMMUNOTHERAPY	
1 ABSTRACT	120
2 INTRODUCTION	120
3 METHODS	121
4 RESULTS	123
4.1 HLA CLASS I ALLOTYPIC COVERAGE AND PEPTIDE YIELDS OF HLA-IPS.....	123
4.2 IDENTIFICATION OF MEDULLOBLASTOMA-ASSOCIATED ANTIGENS	126
5 DISCUSSION	136
6 REFERENCES	140

CHAPTER 4: THE IMMUNOPEPTIDOME OF MENINGIOMA REVEALS CANDIDATE TARGETS FOR IMMUNOTHERAPIES AND DELINEATES MODULATED PRESENTATION OF HLA LIGANDS IN COMPARISON WITH AUTOLOGOUS DURA

1 ABSTRACT	144
2 INTRODUCTION	144
3 METHODS	145
4 RESULTS	147
4.1 PEPTIDE YIELDS OF HLA-IPs AND HLA CLASS I ALLOTYPIC COVERAGE	147
4.2 DEFINITION OF MENINGIOMA-ASSOCIATED ANTIGENS	150
4.3 RELATIVE HLA LIGAND ABUNDANCES ON MENINGIOMA <i>VERSUS</i> DURA	161
5 DISCUSSION	165
6 REFERENCES	168

CHAPTER 5: A META-ANALYSIS COMPARING THE IMMUNOPEPTIDOMIC LANDSCAPE OF INTRACRANIAL NEOPLASIA

1 ABSTRACT	172
2 INTRODUCTION	172
3 METHODS	173
4 RESULTS	173
4.1 HLA CLASS I ALLOTYPES ASSOCIATED WITH INTRACRANIAL NEOPLASIA	173
4.2 THE IMMUNOPEPTIDOME OF INTRACRANIAL NEOPLASIA IN COMPARISON	175
5 DISCUSSION	176
6 REFERENCES	178

CHAPTER 6: IMPLEMENTATION OF A MIX OF TEN SYNTHETIC HEAVY ISOTOPE-LABELED PEPTIDES AS RETENTION TIME STANDARD

1 ABSTRACT	181
2 INTRODUCTION	181
3 METHODS	182
4 RESULTS	185
4.1 COMPATIBILITY OF PROCAL PEPTIDES WITH IMMUNOPEPTIDOMICS	185
4.2 TITRATION OF IN-HOUSE HEAVY ISOTOPE-LABELED RT PEPTIDES	186
4.3 PERFORMANCE MONITORING OF LC-MS/MS SYSTEMS BY RT PEPTIDES	191
4.4 COMPARISON OF LC-MS/MS SYSTEMS FOR A PROCUREMENT MEASURE.....	194
5 DISCUSSION	196
6 REFERENCES	198

CHAPTER 7: GENERAL DISCUSSION AND PERSPECTIVE

1 GENERAL DISCUSSION AND PERSPECTIVE	200
2 REFERENCES	203
DANKSAGUNG	208

APPENDIX

ABBREVIATIONS	210
SUPPLEMENTARY FIGURES AND TABLES	216

Preface

During the course of my PhD thesis, I had the possibility and the pleasure to work on various projects dealing with the exploration of the human leukocyte antigen (HLA) peptidome of primary human samples originating predominantly from different solid tumor entities. However, this thesis can only provide a deeper insight into a few of these studies. I decided to present my results on the immunopeptidomic landscape of intracranial neoplasias, namely glioblastoma, medulloblastoma, and meningioma as well as to include a meta-analysis comparing these three brain tumors originating from different cell types.

A detailed introduction into the biology of antigen presentation on HLA molecules as well as the tumor entities covered by this thesis is provided in **CHAPTER 1**. Further, the ingenious and ground-breaking principle of cancer immunotherapy is introduced supplemented with information on previous and current immunotherapeutic approaches targeting glioblastoma, medulloblastoma, or meningioma. **CHAPTER 2** focuses on the insights gained by multi-omics analyses including whole exome and RNA sequencing in combination with immunopeptidomics of samples of a large cohort of glioblastoma patients. The availability of autologous primary and recurrent tumors of several patients allows investigating antigen presentation, mutation, and RNA expression dynamics during the course of disease progression. Results from studying the HLA peptidome of medulloblastomas and meningiomas including label-free quantitation of relative HLA ligand abundances on meningeal tumors as compared with autologous dura are presented in **CHAPTER 3** and **CHAPTER 4**. A comparison of these three intracranial neoplasias of different cellular origin is provided in **CHAPTER 5** in the form of a meta-analysis. The implementation of a mix of ten heavy isotope-labeled synthetic peptides as retention time standard is described as technical excursus in **CHAPTER 6**. This peptide mix is a tool to not only monitor mass spectrometric performance, but also to compare different systems and to perform e.g. data-independent acquisition with subsequent normalization of retention times between measurements. A general discussion and summary of the most important findings as well as an outlook beyond this thesis are provided in **CHAPTER 7**.

I am convinced that investigating the entirety of naturally presented HLA ligands is a cornerstone to state-of-the-art patient-tailored immunotherapies. It was a pleasure to get into the fascinating techniques of immunopeptidomics and mass spectrometry and I highly appreciate the previous work of colleagues in this field establishing methods, workflows, and bioinformatic tools on the basis of which I conducted my studies.

Publications

Research articles

Neidert MC, Kowalewski DJ, Silginer M, Kapolou K, Backert L, Freudenmann LK, Peper JK, Marcu A, Wang SS, Walz JS, Wolpert F, Rammensee HG, Henschler R, Lamszus K, Westphal M, Roth P, Regli L, Stevanović S, Weller M, Eisele G. The natural HLA ligandome of glioblastoma stem-like cells: antigen discovery for T cell-based immunotherapy. *Acta Neuropathol.* 2018;135(6):923-938.

Löffler MW, Mohr C, Bichmann L, Freudenmann LK, Walzer M, Schroeder CM, Trautwein N, Hilke FJ, Zinser RS, Mühlenbruch L, Kowalewski DJ, Schuster H, Sturm M, Matthes J, Riess O, Czernel S, Nahnsen S, Königsrainer I, Thiel K, Nadalin S, Beckert S, Bösmüller H, Fend F, Velic A, Maček B, Haen SP, Buonaguro L, Kohlbacher O, Stevanović S, Königsrainer A, Rammensee HG. Multi-omics discovery of exome-derived neoantigens in hepatocellular carcinoma. *Genome Med.* 2019;11(1):28.

Freudenmann LK, Mayer C, Rodemann HP, Dittmann K. Reduced exosomal L-Plastin is responsible for radiation-induced bystander effect. *Exp Cell Res.* 2019;383(1):111498.

Marcu A, Bichmann L, Kuchenbecker L, Backert L, Kowalewski DJ, Freudenmann LK, Löffler MW, Lübke M, Walz JS, Velz J, Moch H, Regli L, Silginer M, Weller M, Schlosser A, Kohlbacher O, Stevanović S, Rammensee H-G, Neidert MC. The HLA Ligand Atlas. A resource of natural HLA ligands presented on benign tissues. *bioRxiv.* 2019:778944.

Review articles

Freudenmann LK, Marcu A, Stevanović S. Mapping the tumour human leukocyte antigen (HLA) ligandome by mass spectrometry. *Immunology.* 2018;154(3):331-345.

Summary

Intracranial neoplasias account for more than 80,000 new cases in the US every year representing the eighth most common tumors in adults older than 40 years and even the most frequent pediatric tumor entity. They comprise malignancies of the brain parenchyma such as glioblastoma or medulloblastoma as well as meningeal neoplasms. Throughout the last decades, the outcome of intracranial neoplasias has remained poor calling for intensive research to establish novel therapies. Especially recurrent and non-resectable tumors are characterized by a profound lack of evidence-based therapeutic options, while irradiation of the developing brain in children causes severe long-term sequelae. With the development and successful administration of checkpoint antibodies, a new era of multimodal anti-tumor therapies has dawned. Patients suffering from intracranial neoplasias have, however, not clinically benefited from the recent advancements. The response to checkpoint blockade, in particular, positively correlates with mutational burden, which is low in brain tumors. This also reasons why neo-antigens have not yet been confirmed to be presented on HLA molecules of brain tumor cells. In a recent clinical trial, the administration of a multi-peptide vaccine targeting non-mutated HLA ligands has elicited remarkable immune responses in primary glioblastoma. Although we succeeded in proving the first two neo-antigenic HLA ligands in glioblastoma, we are convinced that non-mutated antigens will coin peptide-specific immunotherapeutic efforts for intracranial neoplasias with low mutational burden.

To define candidate targets for cancer immunotherapy, a large-scale study of the HLA class I and II peptidomes of glioblastoma (n=62), medulloblastoma (n=28), and meningioma (n=33) was performed. We defined a novel set of antigens and peptides characterized by natural, frequent, and tumor-exclusive HLA presentation on native human tumor tissue, whereby established tumor-associated and cancer-testis antigens did not fulfill these criteria. Tumor exclusivity was assessed by comparison with a reference immunopeptidome dataset acquired from approximately 400 benign human tissues covering 30 different organs. For glioblastoma, an additional comparison of primary and recurrent tumors was performed delineating not only dynamics of antigen presentation during disease progression, but also enabling further restriction of candidate targets to those robustly presented at both disease conditions. The implementation of a mix of ten synthetic heavy isotope-labeled peptides as retention time standard will guide future immunopeptidomic studies fostering innovative mass spectrometric data acquisition strategies and quantitative approaches with enhanced identification and reproducibility rates.

In conclusion, we investigated the immunopeptidomic landscape of glioblastoma, medulloblastoma, and meningioma in an unprecedented depth unveiling a large novel set of entity-specific tumor-associated antigens and peptides. Being naturally, frequently, and tumor-exclusively presented on HLA class I or II molecules, these represent prime candidates to deliver the power of T cells *via* antigen-specific immunotherapies to intracranial neoplasias. This may contribute to meet the urgent demand for alternatives to radiotherapy in the treatment of pediatric brain tumors as well as for therapeutic regimens to manage non-resectable neoplasms and disease recurrence.

Zusammenfassung

Jedes Jahr werden in den Vereinigten Staaten mehr als 80.000 neue Fälle intrakranieller Neoplasien, welche die achthäufigste Tumorart bei Erwachsenen über 40 Jahren und sogar die häufigste Tumorerkrankung im Kindesalter sind, diagnostiziert. Dazu zählen Neubildungen des Hirnparenchyms wie Glioblastome oder Medulloblastome und Tumore der Hirnhäute. Während der letzten Jahrzehnte blieb die Prognose intrakranieller Neoplasien schlecht, was intensive Forschung zur Etablierung neuer Therapien unabdingbar macht. Besonders für rezidivierende und nicht resezierbare Tumore gibt es keine evidenzbasierte Behandlung, wohingegen die Bestrahlung des kindlichen sich entwickelnden Gehirns schwere Langzeitschäden verursacht. Die Entwicklung und erfolgreiche Anwendung von Immuncheckpoint-Antikörpern hat eine neue Ära multi-modaler Tumorthérapien eingeläutet. Patienten mit intrakraniellen Neoplasien haben von den jüngsten Fortschritten klinisch gesehen jedoch nicht profitiert. Besonders das Ansprechen auf Immuncheckpoint-Inhibitoren korreliert positiv mit der Mutationslast, welche in Hirntumoren niedrig ist. Das erklärt unter anderem auch, weshalb es bislang nicht möglich war, die HLA-Präsentation von Neo-Antigenen auf Hirntumorzellen nachzuweisen. In einer kürzlich durchgeführten klinischen Studie rief die Anwendung eines Multi-Peptidimpfstoffs, der sich gegen nicht-mutierte HLA-Liganden richtet, beachtliche Immunantworten in Patienten mit primärem Glioblastom hervor. Obwohl wir den Nachweis für die ersten beiden mutierten HLA-Liganden im Glioblastom erbringen konnten, sind wir davon überzeugt, dass nicht-mutierte Antigene peptid-spezifische immuntherapeutische Ansätze für intrakraniellen Neoplasien mit geringer Mutationslast prägen werden.

Um mögliche Zielantigene für Immuntherapien zu bestimmen, wurde eine groß angelegte Untersuchung des HLA Klasse I- und II-Peptidoms in Glioblastomen (N=62), Medulloblastomen (N=28) und Meningeomen (N=33) durchgeführt. Wir haben eine neuartige Zusammenstellung von Antigenen und Peptiden definiert, welche sich durch natürliche, häufige und tumor-exklusive HLA-Präsentation auf nativem humanem Tumorgewebe auszeichnen – etablierte tumor-assoziierte und Cancer-Testis ("Tumor-Hoden") Antigene erfüllten diese Kriterien dagegen nicht. Die Bestimmung von Tumor-Exklusivität erfolgte durch den Abgleich mit einem Referenzdatensatz, welcher Immunpeptidome von circa 400 benignen humanen Geweben aus 30 verschiedenen Organen beinhaltet. Bei Glioblastomen wurden zudem primäre und rezidivierende Tumore verglichen, was nicht nur Dynamiken der Antigenpräsentation im Laufe des Fortschreitens der Erkrankung aufdeckte, sondern bot auch die Möglichkeit, eine Beschränkung auf jene möglichen Zielantigene vorzunehmen, welche in beiden Krankheitsstadien robust präsentiert sind. Die Implementierung einer Mischung aus zehn isotopen-markierten synthetischen Peptiden als Retentionszeitstandard wird zukünftige Studien des Immunpeptidoms leiten, was innovative massenspektrometrische Datenaufzeichnungsstrategien und quantitative Ansätze mit verbesserten Identifikations- und Reproduzierbarkeitsraten unterstützen wird.

Zusammenfassung

Zusammenfassend haben wir das Immunpeptidom des Glioblastoms, des Medulloblastoms sowie des Meningeoms in einer beispiellosen Tiefe untersucht, was die Zusammenstellung einer umfangreichen und neuartigen Liste tumor-assoziiertes Antigenen und Peptide ermöglichte. Da diese natürlich, häufig und tumor-exklusiv auf HLA Klasse I- oder II-Molekülen präsentiert sind, stellen diese erstklassige Kandidaten dar, um intrakranielle Neoplasien durch antigen-spezifische Immuntherapien vermittelt durch T-Zellen anzugreifen. Das könnte dazu beitragen, der dringenden Forderung nach Alternativen zur Strahlentherapie bei der Behandlung kindlicher Hirntumoren sowie nach Leitlinien für die Behandlung nicht resezierbarer und rezidivierender Neoplasien nachzukommen.

CHAPTER 1



Introduction

1 Intracranial neoplasias

1.1 Incidence and classification

In the United States (US), neoplasms of the central nervous system (CNS) are the most common pediatric tumors (0-14 years), the third most frequent cancer among people from 15-39 years, and the eighth most common tumors in adults older than 40 years. From 2012-2016, 405,740 new cases of primary brain and CNS tumors were reported. Among these, malignant neoplasias (30.2%) were less than half as common as benign ones (69.8%). 5-year relative survival rates accounted for 35.8% for malignant and 91.5% for benign CNS tumors, respectively. Meningioma was the most frequent non-malignant brain and CNS tumor (53.3% of non-malignant / 37.6% of all neoplasms), whereas glioblastoma represented the most common malignant CNS tumor (48.3% of malignant / 14.6% of all neoplasms) (Table 1).¹

Table 1. Incidence and survival rates of three selected intracranial neoplasms in the US (2012-2016). Information were obtained from Ostrom *et al.*¹ * Median age at diagnosis reported for embryonal tumors, from which medulloblastomas constitute 64%. Missing data are marked as not available (n.a.).

	Glioblastoma	Medulloblastoma	Total	Meningioma	
				Malignant	Non-malignant
Proportion of all brain and CNS tumors	14.6%	0.6%	37.6%	0.4%	37.2%
5-year incidence	59,164	2,234	152,756	1,774	150,982
0-14	503	1,475	293	23	270
15-39	2,713	596	9,260	118	9,142
40+	55,948	163	143,203	1,633	141,570
Average annual incidence	11,833	446	30,551	355	30,196
0-14	101	295	59	5	54
15-39	543	119	1,852	24	1,828
40+	11,190	33	28,641	327	28,314
Median age at diagnosis	65	8*	66	65	66
Incidence rate male : female ratio	1.58	1.66 (age 0-14)	n.a.	0.89	0.43
5-year relative survival	6.8%	73.7%	n.a.	68.2%	88.0%
0-14	21.8%	72.3%	n.a.	75.3%	95.7%
15-39	26.2%	78.5%	n.a.	84.1%	97.0%
40+	5.5%	66.2%	n.a.	66.6%	87.3%

Besides distinguishing benign and malignant tumors, primary CNS neoplasias are grouped into glial and non-glial tumors according to their cell type of origin (Figure 1).² Gliomas arise from glial cells (astrocytes, oligodendrocytes, ependymal cells, and microglia), non-neuronal cells in the CNS that are supportive to neurons. Astrocytes fulfill homeostatic functions by regulating water and ion levels, modulating neurotransmission in tripartite synapses, and contributing to the formation of the blood-brain barrier. The insulating myelin sheath of axons is formed by oligodendrocytes and allows rapid conduction of electrical impulses. Microglia represent brain-resident phagocytic immune cells, whereas ependymal cells line the ventricular system, the central canal of the spinal cord as well as the choroid plexus, and produce cerebrospinal fluid (CSF).^{3,4} Glial intracranial neoplasias, namely astrocytoma, oligodendroglioma, and ependymoma can either grow in a diffuse or non-diffuse manner, whereby diffuse growth goes along with deep infiltration of surrounding benign brain tissue. Non-gliomas originate from hematopoietic / lymphoid cells (CNS lymphoma), the meninges (meningioma), or embryonal neuroepithelial / cerebellar granule neural precursor cells (medulloblastoma).^{1,2,5,6}

In 2016, grading of intracranial neoplasms as recommended by the World Health Organization (WHO) was for the first time not only based on histological and clinical, but also on molecular patterns which are of major importance for sub-classification of tumor types. Glioblastomas that have progressed from anaplastic astrocytoma or low-grade glioma, designated as secondary glioblastomas, have mutations of the isocitrate dehydrogenase (IDH) 1/2 genes (IDH^{mut}), whereas primary glioblastomas have non-mutated / wild-type (WT) IDH1/2 genes in most cases (IDH^{WT}).² Medulloblastomas (MB) are subdivided into four groups by means of expression and mutational profiles. In the first group, the Wingless and Int-1 (Wnt) pathway has a key role (WNT-activated; 11%), whereas the second group is characterized by strong activation of the Sonic Hedgehog (SHH) pathway (SHH-activated; 30%). Within this group, tumors with mutated and WT tumor suppressor p53 (TP53) are further distinguished from each other (SHH-activated/TP53^{mut}; SHH-activated/TP53^{WT}). Group 3 (25-28%) and Group 4 (35%) medulloblastomas are both non-WNT/non-SHH with dominant signaling through the photoreceptor/gamma-aminobutyric acid (GABA)-ergic or the neuronal/glutamatergic pathway instead (Figure 1).^{2,7,8}

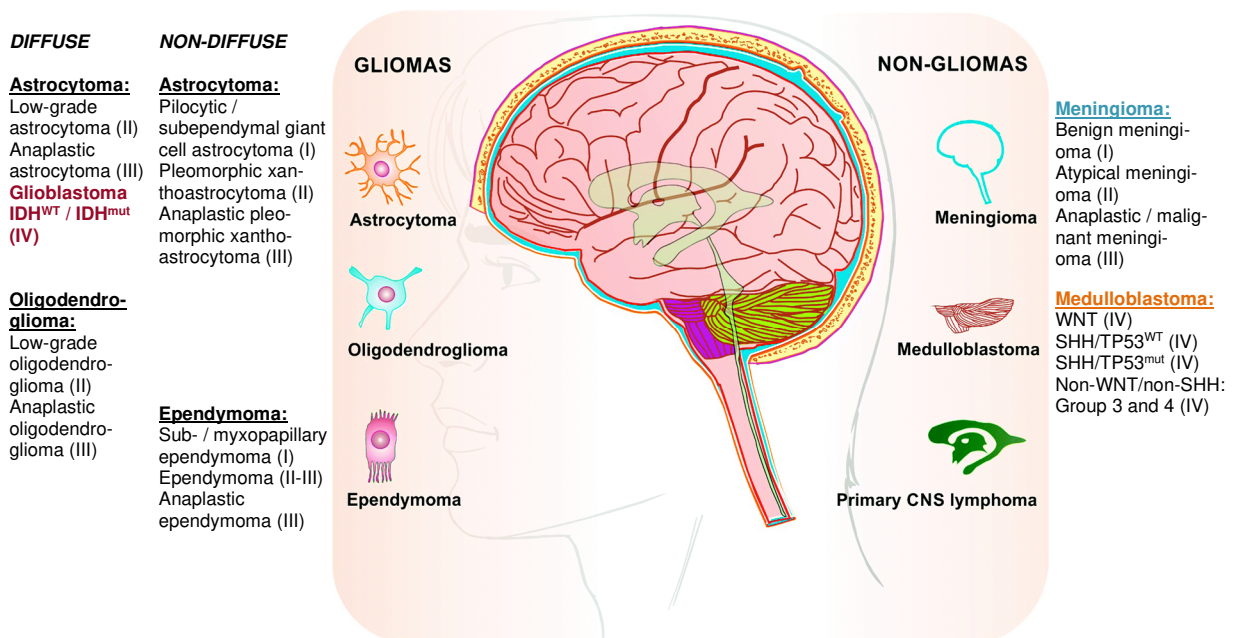


Figure 1. Overview of glial- and non-glial brain tumors. WHO grades are indicated in Roman numerals for selected CNS neoplasms. Tumor entities that are part of the subsequent experimental section are color-marked. Image adapted from Malhotra *et al.*⁹ and supplemented with information from Louis *et al.*²

1.2 Glioblastoma

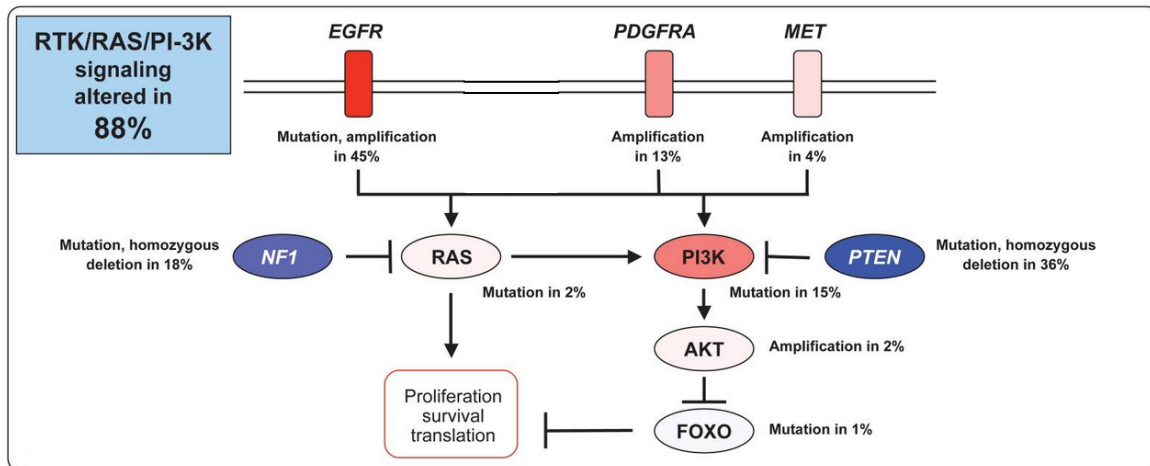
Etiology, common mutations, and epigenetic features

Glioblastoma is the most frequent and most malignant primary intracranial neoplasia. It mainly affects adults at a median age of 65 years and is characterized by the poorest 5-year relative survival rate of 6.8% among all brain tumors (Table 1). It constitutes 57.3% of all gliomas and only little is known about its etiology.¹ Hereditary cancer syndromes including Lynch or Li-Fraumeni syndrome, neurofibromatosis type 1 and 2, Turcot's syndrome (brain tumor-polyposis syndrome), Gorlin syndrome (nevroid basal cell carcinoma syndrome), and Cowden's

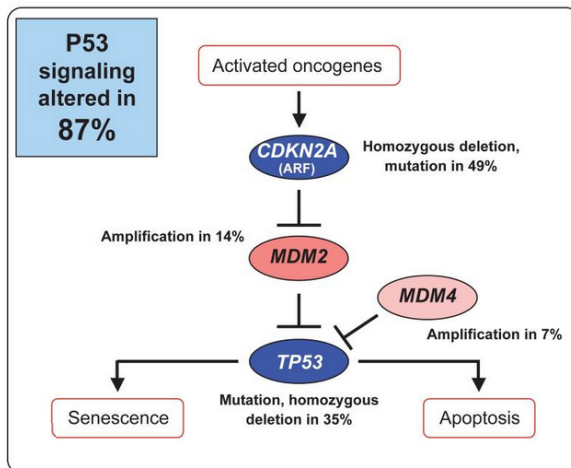
disease contribute to only 5% of glioblastoma cases.¹⁰⁻¹⁶ While (therapeutic) ionizing radiation represents a well-known risk factor, the neurocarcinogenic effect of polycyclic aromatic hydrocarbons, *N*-nitroso compounds, or other chemicals is still under investigation.^{10-12,17-19} Likewise, the association of glioblastoma with simian virus 40 (SV40) and different human herpes viruses (HHV) such as human cytomegalovirus (HCMV) in glioblastoma is controversially discussed.^{10,20-23} Heterozygous IDH1/2 mutations (IDH1: predominantly R132H (90%),^{2,24-26} less frequently R132C and R132G;²⁴ IDH2: mostly R172K²⁶⁻²⁹) occur in only 5% of primary or *de novo* glioblastomas, whereas these non-synonymous mutations are characteristic of secondary glioblastoma (approximately 80%).^{10,24,30} Determination of the IDH-status is part of routine clinical diagnostics, since IDH-mutant tumors are associated with better prognosis (median overall survival after surgery and radiochemotherapy 31 *versus* 15 months).^{2,13} Non-mutated IDH catalyzes the reaction of isocitrate into α -ketoglutarate (α -KG), which is subsequently converted into D-2-hydroxyglutarate (D2HG) by mutant IDH exhibiting neo-enzymatic activity. D2HG acts as an oncometabolite by competitive inhibition of α -KG-dependent enzymes affecting collagen synthesis, cell signaling, and epigenetic regulation.^{10,26} Secondary glioblastomas occurring in younger patients are relatively rare (5-10% of all glioblastomas) and subsequent information therefore focuses on classical *de novo* glioblastoma.^{2,10,31-33}

The core pathways driving glioblastoma comprise enhanced phosphatidylinositol-3-OH kinase (PI3K) signaling, impaired activation of the Rb and p53 pathways, and uncontrolled growth factor signaling (Figure 2).^{10,33-35} Amplification of the epidermal growth factor receptor (EGFR), the cyclin-dependent kinase 4 (CDK4), and the p53 inhibitor mouse double minute 2 homolog (MDM2) are common genetic events in glioblastoma.^{10,12,32-34,36} The truncated epidermal growth factor receptor variant III (EGFRvIII) is a gain-of-function mutation resulting in constant activation of the EGFR pathway and is present in around 30% of newly diagnosed glioblastomas.^{10,12,33,34,37} Homozygous deletion of neurofibromin-1 (NF1), phosphatase and tensin homolog (PTEN), the cyclin-dependent kinase inhibitor 2A (CDKN2A / p16^{Ink4a}), or the cyclin-dependent kinase 4 inhibitor 2B (CDKN2B / p15^{Ink4b}) cause a loss of Ras, PI3K, or CDK4 inhibition, respectively. Besides p16^{Ink4a}, CDKN2A encodes the p53 activator alternative open reading frame (ARF / p14^{ARF}), which is lacking in case of CDKN2A deletion.^{10,12,32-34,36} Impaired p53 and Rb signaling can also be due to p53 and Rb mutations. PI3K mutations and deletions of PTEN as well as CDKN2A and Rb mutations seem to be mutually exclusive.^{10,24,31,34,38} PIK3CA mutations can either render the p110 α catalytic subunit of the PI3K complex constitutively active or reduce its affinity to the inhibitor p85 α .^{10,34,39-41} Figure 2 visualizes the frequencies of these mutations as well as the role of mutated proteins in the pathways driving glioblastoma. Common chromosomal aberrations comprise gain of chromosome 7, 19, and 20, loss of chromosome 10, 13, and Y as well as rearrangements affecting chromosome 12q.^{24,42-46}

A



B



C

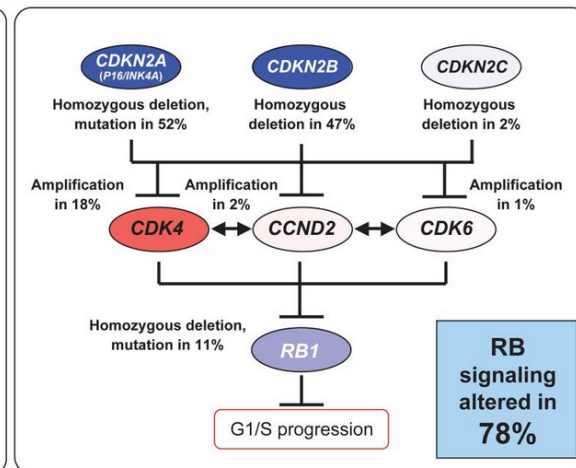


Figure 2. Pathways driving glioblastoma. Color-coded frequencies of gain-of-function (red) and loss-of-function mutations (blue) in glioblastoma patients. **(A) Increased Ras and PI3K signaling.** Loss of NF1 or PTEN, EGFR amplification, and PI3K mutations occur in many patients. **(B) Impaired senescence and apoptosis induction via p53.** In glioblastoma, TP53 or CDKN2A loss-of-function mutations and amplification of MDM2 are frequent genomic events. **(C) Reduced Rb signaling.** CDK4 gene amplification as well as CDKN2A, CDKN2B, or Rb loss can lead to uncontrolled progression of the cell cycle. Image adapted from McLendon *et al.*³⁴ and corrected with information from McLendon *et al.*⁴⁷.

Mutant IDH-derived D2HG competitively inhibits tet methylcytosine dioxygenase 2 (TET2). As a consequence, demethylation of DNA is impaired creating the so-called glioma CpG island methylator phenotype (G-CIMP).^{10,26,48,49} G-CIMP is associated with better prognosis of glioblastoma patients.^{10,50,51} Promoter methylation is a common epigenetic mechanism to silence gene transcription. DNA methylation of the O⁶-methylguanine-DNA methyltransferase (MGMT) promoter region is observed in 35% of glioblastoma patients. Alkylating chemotherapeutics such as temozolomide (TMZ) cause O⁶-alkylated guanine nucleobases. Repair of this DNA damage is mediated by MGMT, whereby decreased MGMT levels owing to promoter methylation can improve the efficacy of alkylating chemotherapies.^{10,13,27,52-57} The MGMT-status of glioblastoma patients is routinely determined in clinical practice.¹³ Recently, primary IDH^{WT} glioblastomas have been found to exhibit distinct DNA methylation patterns laying the foundation for annotation to the following epigenetic subclasses: mesenchymal,

midline, MYCN, RTK I, RTK II, RTK III, H3.3 G34 mutant, and infantile hemispheric glioma. The latter are observed in infants with supratentorial localization and at a median age of 0 years, whereby molecular characteristics have so far not been specified. Patients at a median age of 11 years with supratentorial or posterior fossa tumors are often affected by glioblastomas of the MYCN subtype with characteristic MYCN oncogene amplifications. Midline-type glioblastomas predominantly affect younger patients (median age of 13 years), are localized in the cerebellum, thalamus, or spine and have various copy number alterations on gene level (e.g. CDKN2A/B loss, platelet-derived growth factor receptor alpha (PDGFR α) amplification).⁴⁶ H3.3 G34 mutant glioblastomas harbor mutations of the histone H3.3-encoding gene in codon 34 and occur at a median age of 19.5 years with supratentorial hemispheric localization. Gain of chromosome 7 or 1q as well as loss of chromosome 13, 10q, and 4q represent common chromosomal aberrations in this subgroup. Mesenchymal glioblastomas reside within the cerebral hemispheres, occur at a median age of 59 years and are characterized by loss of chromosome 10 and 9p21 as well as gain of chromosome 7. Glioblastomas of the RTK I type with prominent loss of chromosome 10 and 9p21 and gain of chromosome 7 affect the cerebral hemispheres of people at a median age of 64 years. RTK II glioblastomas affect patients at a median age of 61 years, reside within the cerebral hemispheres, and present with gain of chromosome 7, 19, or 20 and loss of chromosome 10 or 9p21. Glioblastomas of the subclass RTK III comprise childhood tumors occurring at a median age of 9 years. Localization within the cerebral hemispheres, EGFR amplification, and loss of chromosome 10 represent typical features of this subgroup.⁴⁶

Symptoms and standard treatment of glioblastoma

Primary glioblastoma typically occurs in the white matter of the cerebrum (supratentorial), whereby the spectrum of symptoms can vary depending on the exact localization.² Glioblastoma patients present with headaches and, in severe cases, nausea or vomiting. Confusion, focal neurological deficit, changes of personality, loss of memory, and seizures are associated with glioblastoma as well.^{10,12,14} Despite having high migratory potential, dissemination of glioblastoma cells remains usually CNS-restricted without distant metastases.^{10,13}

The so-called Stupp protocol includes surgery and adjuvant radiochemotherapy as standard-of-care for newly diagnosed WHO grade IV glioma.¹³ The extent of surgical resection correlates with patient outcomes, but it is impossible to achieve complete surgical resection while fully preserving surrounding benign brain tissue^{10,13,58} Fractionated radiotherapy applied post-surgery delivers a total of 60 Gy split into 30-33 individual doses.^{10,13,59} The excellent bioavailability in the CNS distinguishes TMZ from other chemotherapeutics rendering it the first choice for glioblastoma patients. Concomitant administration during radiotherapy amounts to 75 mg/m² daily, whereas adjuvant chemotherapy lasting additional six months comprises five monthly doses of 150-200 mg/m² each. In elderly patients (> 70), maintenance TMZ is tailored to the individual performance status and health situation.^{10,12,13,60,61} Median survival of patients with newly diagnosed glioblastoma treated as recommended by the Stupp protocol accounts to 14.6 months, whereas radiotherapy alone achieves 12.1 months.⁶¹

Seizure management is based on valproate and second-generation antiepileptic drugs such as levetiracetam, lamotrigine, or pregabalin. Carbamazepine, phenobarbital, and phenytoin are avoided as anticonvulsants in glioblastoma, since they accelerate the metabolism of other medication.^{10,13,62,63} Dexamethasone (8-16 mg daily) and other corticosteroids symptomatically treat neurological deficits and elevated intracranial pressure caused by glioblastoma-associated brain edema.^{10,13}

Propensity for disease recurrence

Glioblastoma cells deeply infiltrate into surrounding benign brain tissue rendering complete surgical resection impossible.^{12,49} In addition, glioma stem cells acquire resistance to radiotherapy and TMZ by upregulation of MGMT and activation of other DNA repair pathways.^{10,12,64} Moreover, a pronounced high degree of intratumoral heterogeneity is a typical feature of glioblastomas. Under evolutionary pressure exerted by the applied therapies, tumor subclones constantly acquire new mutations leading to an intensified therapeutic situation.^{10,49,65} As a consequence, glioblastoma inevitably recurs in most patients accompanied by a decline of median overall survival to 6.2 months.^{13,49,66} Of note, a fraction of patients (37% in a study of The Cancer Genome Atlas Research Network) develops a so-called hypermutation phenotype, which is induced by alkylating chemotherapy.^{10,34,67} MutS homolog 2 (MSH2) / mutS homolog 6 (MSH6) heterodimers recognize mismatch base pairs formed by thymine and O⁶-alkylated guanine. MSH6-dependent apoptosis is induced when the number of these mismatches exceeds a certain threshold.^{10,67-69} In case loss-of-function mutations affect mismatch repair (MMR) genes such as MSH6 and TMZ is continued, glioblastoma cells acquire therapy resistance. Alkylating agents then facilitate the accumulation of mutations, clonal evolution, and glioblastoma progression instead of inducing apoptosis. Loss of either mutL homolog 1 (MLH1), MSH2, MSH6, or the endonuclease postmeiotic segregation increased 2 (PMS2) is designated as MMR deficiency and occurs predominantly in patients where the primary tumor had MGMT promoter methylation. Hypermutated recurrent grade IV glioma harbor > 30 mutations instead of less than five in primary tumors.^{10,34,67}

So far, no standard-of-care has been established to manage disease recurrence in glioblastoma. Up to one third of patients are eligible for surgical resection. However, clinical benefit of re-surgery and re-irradiation is usually very limited. Upon progression on first-line chemotherapy, TMZ dosage can be increased or nitrosoureas such as carmustine can serve as second-line medication. In case inclusion criteria are met, patients may receive experimental therapies evaluated in clinical trials.^{10,12,13,49,66,70,71} Constant application of electric fields alternating at a frequency of 200 kHz is capable of interrupting mitosis and inducing apoptosis. Applied subsequently to radiochemotherapy and concomitantly to maintenance TMZ, tumor treating fields (TTF) prolonged overall survival of patients with newly diagnosed glioblastoma by 4.9 months as compared with maintenance chemotherapy alone.⁷² In recurrent glioblastoma, TMZ-free TTF therapy *versus* chemotherapy resulted in a median survival of 6.6 or 6.0 months, respectively.⁷³ The device NovoTTF/Optune[®] was approved by the U.S. Food and Drug Administration (FDA) for the treatment of recurrent glioblastoma in 2011.⁷⁴ The monoclonal antibody bevacizumab is directed against vascular endothelial growth factor (VEGF) to target angiogenesis. It received FDA approval for recurrent glioblastoma in

2009, although an effect on overall survival has so far not been observed.^{70,75-77} Molecular therapies are further trying to exploit the regulators of PI3K, mitogen-activated protein kinase (MAPK), and DNA repair pathways as well as EGFR / EGFRvIII, VEGF receptor (VEGFR), platelet-derived growth factor receptor (PDGFR), and transforming growth factor β (TGF- β) as targets.^{10,12,78} Targeted monotherapies, however, elicit a response in only 0-15% of patients and these rare responses are only transient.^{12,79} The reason for this lies in the glioblastoma-driving signaling network harboring a high degree of functional redundancy. Targeting one molecule of this network results in upregulation or activation of another to circumvent effects on proliferation or survival of the tumor cell.^{10,12,80} Hence, ongoing and future studies aim at overcoming the mechanisms of therapy resistance in (recurrent) glioblastoma by combining various targeted therapies.^{10,12,79}

1.3 Medulloblastoma

Etiology and subgroup-associated mutational and pathway signatures

Behind pilocytic astrocytoma and malignant glioma, embryonal tumors constitute the third most common brain and CNS tumors (13.1%) in children younger than 14 years. Embryonal tumors comprise medulloblastomas (MB; 64.1%), atypical teratoid rhabdoid tumors (ATRT; 15.9%), and primitive neuroectodermal tumors (PNET; 10.4%), whereby medulloblastomas represent the most common pediatric intracranial malignancies. The peak incidence of medulloblastomas accounting for 66.0% (1,475 cases in the US from 2012-2016) is observed in children aged between 0 and 14 years, whereas only 7.3% of total cases occur in patients older than 40 years (Table 1). The total incidence in children younger than 14 years in the US from 2012-2016 distributed to 36% at age group 0-4 (535 cases), to 41% at age group 5-9 (603 cases), and to 23% at age group 9-14 (337 cases).¹

The underlying causes of medulloblastoma are in general unclear, with most cases being designated as sporadic.^{81,82} High birth weight, maternal diet – especially the uptake of *N*-nitroso compounds – during pregnancy, exposure to pesticides during childhood or the prenatal period as well as HCMV infection have been suggested as risk factors.^{8,83} As for glioblastoma, hereditary cancer syndromes are associated with a small proportion (5-6%) of medulloblastoma diagnoses, whereas this fraction is highest in the SHH-activated subgroup (14-20%). Germline mutations of deleted in polyposis 2.5 / adenomatous polyposis coli protein (DP2.5 / APC; Turcot's syndrome) or of suppressor of fused homolog (SUFU) and protein patched homolog 1 (PTCH1) (both Gorlin syndrome) are linked to WNT-activated or SHH-activated medulloblastomas, respectively. The latter distinguish into TP53^{WT} and TP53^{mut} tumors, whereby germline TP53^{mut} (Li-Fraumeni syndrome) medulloblastomas are always pediatric cases. Deficiency of homologous recombination expressed by germline breast cancer type 2 susceptibility protein (BRCA2; Fanconi anemia) or partner and localizer of BRCA2 (PALB2) mutations occurs across SHH-activated, Group 3, and Group 4 subtypes.^{81,82,84}

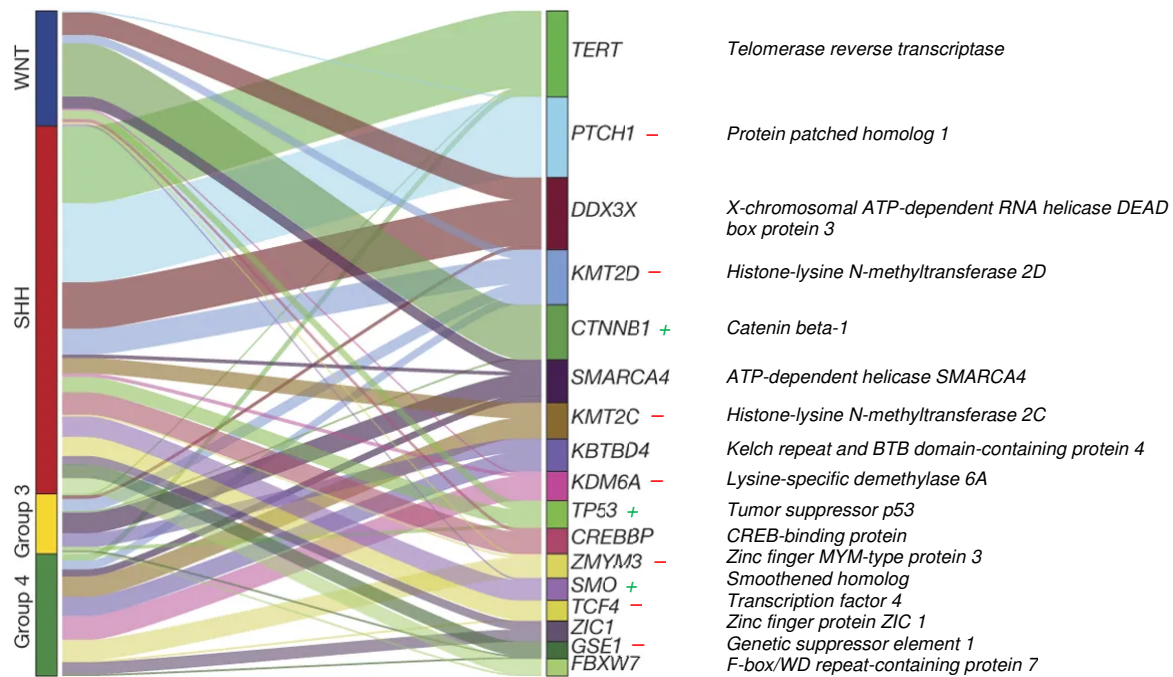


Figure 3. Recurrently mutated genes in medulloblastoma subgroups. Genes exceeding a mutation frequency of 5% in the respective study cohort (n=491 medulloblastomas; median age of 8 years [1 month – 50 years]) are depicted in a subgroup-specific manner. Driver genes affected by gain-of function mutations are marked with a +, whereas - indicates loss-of function driver mutations. Figure taken from Northcott *et al.*⁸⁵ and supplemented with information from Northcott *et al.*⁸⁵ and UniProt⁸⁶.

Recurrent mutations in medulloblastoma are shown on a subgroup-specific level in Figure 3. These participate in the regulation of neuronal development, cell-cell contacts, chromatin modification, cell signaling, and the cell cycle. WNT-activated medulloblastomas show a clear enrichment of mutations affecting histone lysine methylation, the β -catenin nuclear pathway, and the differentiation of CNS neurons. Catenin beta-1 (CTNNB1) mutations and monosomy 6 are present in >80% of WNT-activated tumors, whereas molecules of the SWI/SNF nucleosome-remodeling complex (AT-rich interactive domain-containing protein 1A/2 (ARID1A, ARID2), ATP-dependent helicase SMARCA4) together reach a mutation frequency of around 30%. SHH-activated medulloblastomas recurrently harbor mutations altering CNS neuron differentiation and the SHH-Gli pathway. Mutations of the histone acetyltransferases KAT6B, p300, and CREB-binding protein (CREBBP) as well as of peregrin (BRPF1) and KAT8 regulatory NSL complex subunit 1 (KANSL1), which regulate histone acetyltransferase complexes, are observed in 19% of SHH-activated medulloblastomas. In turn, recurrent mutations in Group 3 and Group 4 medulloblastomas show a mixed pattern of pathway annotations. Group 3 tumors are rather enriched for mutations involved in the Notch and TGF- β pathway, whereas recurrent Group 4 mutations are rather assigned to mechanisms of chromatin modification. Amplifications of the myc proto-oncogene are specific for subgroup 3 (17%), whereas the cases of amplified N-myc proto-oncogene distribute equally to Group 3 and Group 4 medulloblastomas (5-6% each).⁸⁵ Further, medulloblastomas have recently been described to exhibit subgroup-characteristic DNA methylation patterns.⁴⁶

Pathology and standard treatment

Medulloblastomas are infratentorial tumors arising in the posterior fossa, whereby a cerebellar localization is most common.⁵ WNT-activated tumors typically grow in the cerebellar peduncles or the cerebellopontine angle connecting cerebellum and pons (brain stem). They can infiltrate into the brain stem and the fourth ventricle. SHH-activated medulloblastomas preferentially reside within the cerebellar hemisphere, whereby a small proportion is localized in the midline vermis. Group 3 and Group 4 occupy the midline of the fourth ventricle (median sulcus).^{7,8,87,88} Medulloblastoma is *per se* graded as malignant WHO grade IV tumor.² CNS-internal metastatic spread is frequently observed in cases of Group 3 and Group 4, whereas SHH- or WNT-activated medulloblastomas rarely disseminate. Overall, two out of five patients present with metastases affecting the thoracic and lumbar spine or the sacrum. Ventricular or subependymal dissemination, not uncommonly already at diagnosis, occurs as well.^{5,8} Depending on the assignment to a tumor subgroup, children suffering from medulloblastoma have a 5-year overall survival between <50% (very high-risk: SHH-activated/TP53^{mut} and metastatic Group 3) and >90% (low-risk: WNT-activated and non-metastatic Group 4). High-risk medulloblastomas (metastatic SHH or Group 4 tumors and N-myc-amplified SHH) are characterized by a 5-year overall survival rate of 50-75%, whereas patients with average-risk tumors (non-metastatic / TP53^{WT} / non-N-myc-amplified SHH, non-metastatic / non-myc-amplified Group 3, and non-metastatic Group 4 without loss of chromosome 11) have a 5-year overall survival rate of 75-90%.⁸⁷

Symptoms of medulloblastoma comprise headache, visual and motor coordination disorders, clumsiness, cranial nerve palsies, reduced food intake, general indisposition, nausea, and vomiting.^{89,90} Standard-of-care following near or gross total resection depends on subgroup annotation and age. Children older than three to five years suffering from average-risk tumors undergo radiochemotherapy comprising craniospinal irradiation (CSI) with a total dose of 54-55.8 Gy (1.8 Gy per day) from one month post-surgery. 23.4 Gy are delivered to the whole brain and spinal cord, whereby the residual dose is directed to the posterior fossa or tumor bed. For WNT-activated tumors, a reduced dosing regimen is conceivable. Adjuvant chemotherapy lasts around seven weeks and can be followed by maintenance chemotherapy administered every four to six weeks. Chemotherapeutics of choice include vincristine (weekly 1.5 mg/m²), cisplatin (75 mg/m² for six cycles), cyclophosphamide (1,000 mg/m²/dose for three cycles of two doses each), and lomustine (75 mg/m² for six cycles). When diagnosed with high- or very high-risk medulloblastoma, protocols comprising radiotherapy (standard, higher, or altered dose) with adjuvant standard or high-dose chemotherapy are applied. Infants younger than three to five years suffering from low- or average-risk tumors receive post-surgery standard chemotherapy only, eventually supplemented with intratumoral chemotherapy. High- or very high-risk disease is treated with standard chemotherapy, optional high-dose chemotherapy, and, if needed, focal or CSI radiotherapy. Treatment of adult medulloblastomas is similar to high-risk tumors in children, whereby the dose delivered to the whole brain and spine is increased to 36 Gy.^{8,90}

Risk of recurrence and long-term sequelae

Although response rates to extensive multimodal therapies are high and immediate, metastatic and high-risk medulloblastomas tend to acquire therapy resistance *via* apoptosis evasion.^{5,8} WNT-activated tumors rarely recur, whereas recurrence in SHH-activated medulloblastomas occurs, but remains local. In turn, recurrent Group 3 and Group 4 tumors are mostly even metastatic.⁸ Three-quarter of pediatric recurrences are observed within two years. As for primary medulloblastoma, the age of the patient decides on the application of radiotherapy. However, a treatment protocol to manage recurrent medulloblastoma has so far not been established.⁸

Those children belonging to the 70-75% designated as cured, will experience long-term treatment-associated sequelae comprising neurological, developmental, psychosocial, and neuroendocrine deficits or even secondary malignancies such as glioblastoma and meningioma. These are primarily attributed to irradiation of the developing brain. The development of novel, especially targeted or immunotherapies, is aimed at replacing radiotherapy.^{5,8,90-92} SMO (SHH pathway) inhibitors such as vismodegib, recombinant soluble tumor necrosis factor-related apoptosis inducing ligand (TRAIL), TRAIL receptor (TRAILR)-agonistic antibodies, N-myc inhibition, targeting of anti-apoptotic Bcl-2 proteins, and pro-apoptotic Bcl-2 homology protein mimetics belong to the most promising approaches. To circumvent mechanisms of early therapy resistance, the preferential use of combination therapies is suggested, whereas targeted monotherapies should be avoided.^{5,8,93}

1.4 Meningioma

Risk factors and genetic basis

Meningiomas constituted 37.6% of all primary intracranial neoplasms diagnosed in the US from 2012-2016. They occur at a median age of 66 years and are subdivided into benign (WHO grade I; 80.5%), atypical (WHO grade II; 17.7%), and anaplastic or malignant meningiomas (WHO grade III; 1.7%). Malignant meningiomas make up only 0.4% with an annual average of 355 cases in the US, whereas non-malignant tumors account to a yearly incidence of 30,196 (Table 1).^{1,2} Irradiation, e.g. for childhood medulloblastoma, represents an established risk factor for the development of meningeal neoplasia, whereas the role of head trauma, neurosurgery, and sex hormones, especially progesterone, has so far not been clarified.^{90,94-97} Hereditary predisposition applies to a minority of meningiomas and occurs in the context of neurofibromatosis type 2 characterized by germline mutations of the tumor suppressor gene neurofibromin-2 (NF2).^{95,98,99} Moreover, meningiomas have been associated with Turcot's, BRCA-associated protein-1 (BAP1) tumor predisposition, Cowden, Werner, Li-Fraumeni, Gorlin, multiple endocrine neoplasia type 1, von Hippel-Lindau, and Gardener's syndrome.^{16,84,95,99-106} Familial meningiomatosis is caused by germline mutations affecting two components of the SWI/SNF nucleosome-remodeling complex: SWI/SNF-related matrix-associated actin-dependent regulator of chromatin subfamily E member 1 and subfamily B member 1 (SMARCE1; SMARCB1).^{99,107,108}

NF2 is not only affected by germline, but also by somatic loss-of function mutations present in 40-60% of meningiomas.^{95,99,109,110} Related thereto, loss of chromosome 22q harboring both

the NF2 region and SMARCB1 was identified to be causative of sporadic meningiomas.^{95,99,108,111} Moreover, BAP1, TERT, SMARCB1, SMO, SUFU, TNF receptor-associated factor 7 (TRAF7), RNA polymerase II subunit A (POLR2A), Krueppel-like factor 4 (KLF4) as well as the protein kinases AKT1, AKT3, and PI3K have been identified to be recurrently mutated in meningiomas, especially such harboring WT NF2. These mutated gene products mainly participate in the mammalian target of rapamycin (mTOR), SHH, and p53 pathway.^{110,112-117} High-grade meningiomas harbor a significantly increased mutational load as compared with low-grade meningiomas, apparent on the level of both non-synonymous mutations (on average 23 *versus* ~10 per tumor) and chromosomal copy number alterations (on average 19% *versus* 3% of the tumor genome disrupted). Despite that, no recurrent mutations (defined by a frequency of $\geq 5\%$ in the respective study cohort) apart from NF2 have so far been identified for high-grade meningiomas. Thus, mutated NF2 is designated a driver of meningioma across all WHO grades.¹¹⁰

Symptoms, structures affected by meningioma, and standard-of-care

Meningiomas arise from both cerebral and spinal meninges and show a characteristic tail of thickened dura on radiological images.^{1,2,118,119} Meningeal neoplasias invade both intra- and extracranial structures comprising the skull, dura mater, and dural sinuses or soft tissue, scalp, and the orbits, respectively.^{95,96,119,120} From WHO grade II, an invasion of the brain is observed.² Meningiomas manifest with symptoms of increasing intracranial pressure which include – depending on localization and size – headaches, nausea and vomiting, seizures, and visual impairment.⁹⁵⁻⁹⁷ A small proportion of meningiomas (estimated at 0.1%) forms extracranial and even extraneural metastases affecting predominantly the lungs as well as the pleura, bones, the liver, the mediastinum, and lymph nodes.¹²⁰⁻¹²²

Benign meningiomas are usually treated with surgical resection to the maximum possible extent alone. However, the specific localization of some tumors, particularly at the skull base, which is affected by 38% of grade I tumors and is rich in neurovascular structures, impedes surgery. This causes considerable morbidity and a 5-year recurrence rate of 22%.^{123,124} Atypical meningiomas receive optional adjuvant radiotherapy, whereas irradiation is a fixed pillar in the therapeutic regimen of anaplastic meningiomas. Radiotherapy typically comprises a total dose of 50 to 60 Gy applied in fractions of 1.5 to 2 Gy to the tumor bed and a margin of 0.5 to 1.5 cm.^{124,125} Stereotactic radiosurgery represents a sophisticated technique to direct irradiation emitted from a gamma knife to tumor tissue during the course of surgical resection, especially of skull base or posterior fossa meningiomas.^{124,126,127} So far, there is no FDA-approved chemotherapeutic agent – neither for primary nor for recurrent or refractory meningeal neoplasms.^{120,124} 5-year overall survival is stratified by WHO grade and comes up to 92% for grade I tumors, 78% for atypical meningiomas, and 44% for patients diagnosed with grade III.^{123,128}

Recurrent meningiomas and emerging targeted treatment strategies

Local recurrence of grade I meningiomas is rare (5-10%), whereas 5-year recurrence rates mount up to 40% for atypical meningiomas and to 50-80% when diagnosed with a malignant meningeal tumor. Recurrence of grade III meningiomas goes along with a decline in median survival to less than 24 months. So far, no effective therapies have been established to

manage recurrent meningioma.^{95,121,124,129,130} Of note, primary tumors treated with adjuvant radiotherapy show an increased amount of non-synonymous mutations and copy number alterations at recurrence.¹¹⁰

Recurrent meningiomas can be treated – if possible – with salvage resection and adjuvant radiotherapy or radiosurgery. In addition, these patients may receive hydroxyurea, anti-hormonal therapy (e.g. anti-progesterone with mifepristone), or somatostatin analogs (e.g. octreotide), whereby all these agents can mainly mediate stabilizing effects.^{124,131-133} Moreover, mTOR inhibitors such as everolimus and vistusertib are under investigation for use in recurrent or progressive meningioma.^{124,134} Anti-angiogenic therapy is increasingly applied and can be based on bevacizumab or small molecules (e.g. sunitinib and vatalanib) targeting VEGFR or PDGFR.^{124,135,136} As for medulloblastoma, the SMO inhibitor vismodegib is evaluated for use in meningeal neoplasias.^{93,124} In case eligibility criteria are fulfilled, participation in clinical trials represents a further option for patients suffering from recurrent meningioma.¹²⁴

2 Cancer immunotherapy

2.1 Key actors for effective anti-cancer immune responses

To protect the host from pathogens, infected or transformed cells, the immune system discriminates between self and non-self. It is made up of two major pillars: the innate and the adaptive system, which both have cellular as well as humoral components. The cellular part of the innate immune system encompasses macrophages, dendritic cells (DCs), granulocytes, mast cells, and natural killer cells, whereas the complement system and antimicrobial peptides predominantly build the humoral part.^{137,138} Professional antigen-presenting cells (APCs), especially DCs, connect the two subsystems by presenting fragments of incorporated antigens to naïve T lymphocytes of the adaptive immune system. These peptide fragments are bound to cell surface molecules of the major histocompatibility complex (MHC) and are specifically recognized by a T-cell receptor (TCR).¹³⁸ When naïve antigen-specific T cells bind to peptide-MHC complexes and receive co-stimulatory signals as well as cytokines from an APC, they get activated, proliferate, and differentiate into CD4⁺ helper T cells (Th cells; Th1 and Th2 as subtype), CD8⁺ cytotoxic T lymphocytes (CTLs), or CD4⁺CD25⁺ regulatory T cells (Treg cells). CTLs are responsible for the elimination of affected host cells, whereas Tregs suppress immune effector functions.¹³⁸⁻¹⁴⁰ In secondary lymphoid tissues, Th2 cells can induce the differentiation of antigen-experienced B lymphocytes into plasma cells. The latter produce antibodies, the humoral effectors of the adaptive immune system.^{138,141} Besides antigen specificity and clonality, the formation of long-lived memory B and T lymphocytes is a hallmark of adaptive immunity.^{138,142} Immune responses are orchestrated and regulated by numerous cytokines and chemokines produced by both innate and adaptive cells.^{137-139,142}

2.2 Human leukocyte antigens present peptides to T lymphocytes

2.2.1 Expression and structure of HLA molecules

For adaptive immunity, MHC presentation of peptides derived from intracellular or incorporated proteinaceous antigens to T cells is an essential feature. In humans, the MHC is called human leukocyte antigen complex (HLA).^{10,143} The short arm of chromosome 6 (6p21.3) harbors the HLA gene cluster comprising the regions HLA class I-III. Molecules belonging to the tumor necrosis factor (TNF) family and the complement system are encoded by HLA class III, whereas HLA class I and II transcripts are translated into proteins involved in the processing and presentation of antigens.^{10,144} The α chains of both the classical (HLA-A, -B, -C) and the non-classical (HLA-E, -F, -G) HLA class I molecules are gene products of the HLA class I region. In addition, the stress-induced MHC class I polypeptide-related sequence proteins (MIC-A, -B) and the human hemochromatosis protein (HFE) are transcribed from this region as well.^{10,145} The genes for HLA class II α and β chains, the peptide transporter associated with antigen processing (TAP), the chaperone tapasin, and the low molecular weight proteins (LMP) 2 and 7, two proteasome subunits induced by interferon (IFN), are included in the HLA class II region. Further, HLA-DM and HLA-DO, two non-classical HLA class II molecules involved in antigen processing, are encoded here (Figure 4 A).^{10,146}

Chromosome 15 harbors the genetic information for β_2 microglobulin (β_2m). β_2m is neither polymorphic nor participates in building the peptide-binding cleft, but forms heterodimers with the α chains of classical HLA class I molecules (Figure 4 B). All nucleated cells express HLA-A, -B, and -C on their surface to provide CTLs with antigenic peptides. To fulfill their function as professional APCs, DCs, macrophages, B lymphocytes, Kupffer, and Langerhans cells express HLA class II.^{10,143,145,147} However, in recent years it has become evident that HLA class II expression is not absolutely restricted to APCs, but may also occur on epithelial (e.g. thyroidal or intestinal cells), endothelial, further lymphoid cells (e.g. granulocytes and mast cells), and even on solid malignancies (e.g. glioblastoma and renal cell carcinoma)^{10,145,147-149} – either constitutively or IFN- γ -induced.^{145,150} In heterodimeric HLA class II molecules, both the α and β chain participate in formation of the peptide-binding cleft (Figure 4 B) exposing antigenic peptides to TCRs.^{143,145}

Polygenicity and polymorphism characterize the HLA gene cluster. Per chromosome, one HLA-A, -B, and -C allele each is encoded, which together constitute the HLA class I haplotype (Figure 4 A). Thus, every individual can have cell-surface expression of up to six HLA class I allotypes.^{10,145} The IPD-IMGT/HLA Database (release 3.40.0, 2020-04-20) listed a total of 6,082 HLA-A alleles (3,794 proteins), 7,255 HLA-B alleles (4,648 proteins), and 5,842 HLA-C alleles (3,503 proteins), in June 2020. Among the 7,301 HLA class II alleles, were 3,357 isoforms of HLA-DR β chain alleles (2,378 proteins), 1,556 HLA-DP β allele (1,016 proteins), and 1,826 HLA-DQ β allele (1,213 proteins) variants.¹⁵¹ In some haplotypes, the expression of two functional HLA-DR β chains is observed (HLA-DRB1, -DRB3, -DRB4, and -DRB5 loci).¹⁴⁵ In contrast to HLA class II β chains, α polypeptides are hardly subject to polymorphism (2 HLA-DR α , 68 HLA-DP α , and 106 HLA-DQ α protein isoforms).¹⁵¹

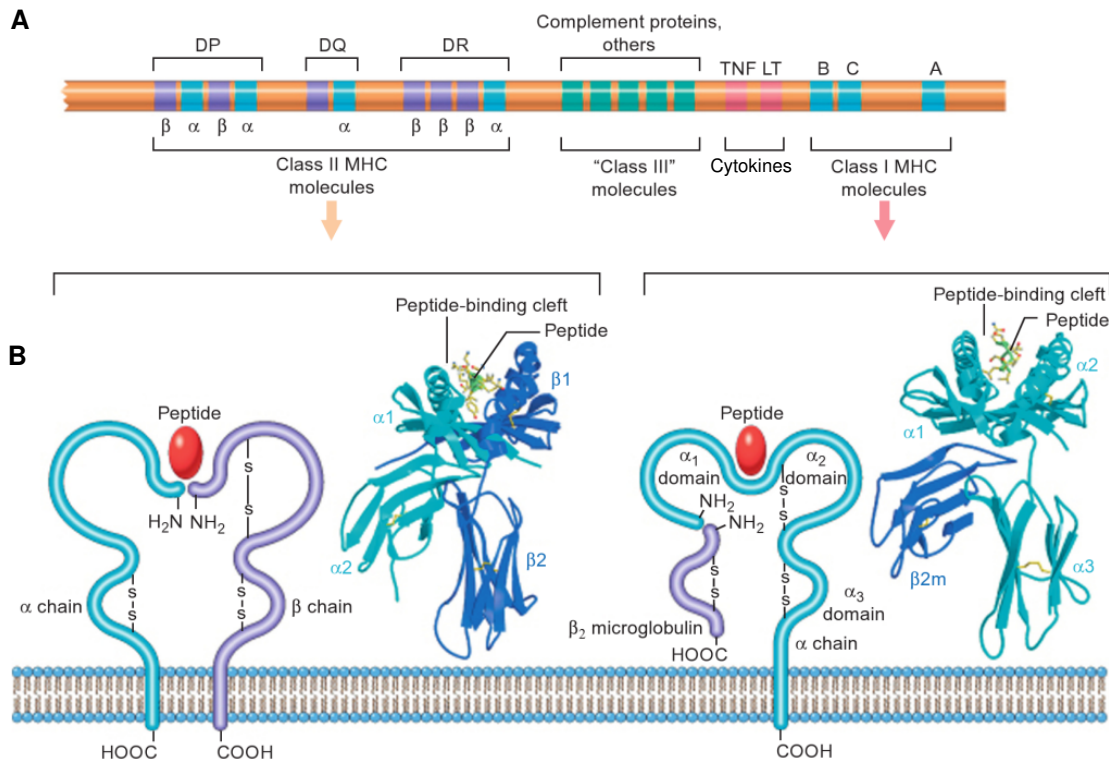


Figure 4. Structure of the HLA on genomic and protein level. (A) Organization of the HLA gene cluster on the sixth chromosome (6p21.3). The three gene regions (I-III) harbor the protein-coding information for HLA molecules themselves, other proteins of the antigen processing and presentation machinery as well as for cytokines and complement factors. **(B) Schematic illustration of HLA class I- and II-peptide complexes.** HLA class I-presented epitopes have only contact to the α polypeptide of the heterodimer (right), whereas the peptide-binding cleft of HLA class II molecules is formed by both the α and β chain (left). Figure taken from Bhagavan *et al.*¹⁵²; slightly modified.

2.2.2 Antigen processing and HLA-peptide complex formation

HLA class I ligands primarily originate from intracellular antigens deriving from both the host cell itself and from pathogens such as viruses residing inside the cell.¹⁵³ Multicatalytic complexes with proteinase activity, so-called proteasomes, show nuclear and cytoplasmic localization. The catalytic activity is harbored by a core barrel of 20 Svedberg units (S) that is capped by two 19S subunits. These caps recognize proteins marked with ubiquitin for degradation. Upon unfolding of the substrate, it is introduced into the barrel, where peptide bonds are cleaved hydrolytically.^{10,154} Cleavage products are released into the cytoplasm,¹⁵⁴ from where TAP selectively translocates them into the endoplasmic reticulum (ER).¹⁵⁵ There, peptides are further trimmed by aminopeptidases, especially the ER aminopeptidase associated with antigen processing (ERAAP), to be of appropriate length for association with HLA class I molecules. HLA class I α polypeptides are synthesized at ER-bound ribosomes, are simultaneously imported into the rough ER lumen, and are bound by calnexin, an integral membrane chaperone. Upon binding of β ₂m to the α chain, the complex associates with the chaperone calreticulin and the thiol reductase ERp57 assisting HLA molecules in proper folding.^{10,155,156} TAP, calreticulin, ERp57, and the TAP-associated tapasin form the peptide-loading complex (PLC). The PLC recognizes processed peptides and α chain- β ₂m heterodimers and allows them to form a stable complex. HLA class I-peptide complexes dissociate from the PLC and undergo vesicular transport from the ER to the Golgi apparatus.

In secretory Golgi vesicles, the complexes traffic to the plasma membrane in which they are integrated through membrane fusion (Figure 5 A).^{10,155,156} HLA class I ligands have a typical length of eight to ten amino acids (AA) and an extended conformation.^{157,158} Slightly longer peptides may be accommodated by bulging out in the center and slightly protruding from the groove.^{158,159} HLA class I molecules have five exceptionally polymorphic peptide-binding pockets (A-F), whereby the second and last pocket (B and F) authoritatively define biochemical properties of binding peptides for most allotypes. The interacting AAs of the ligand are designated as anchor residues and represent the peptide motif of the corresponding HLA class I allotype. Usually, these anchors are the C-terminal residue and the second AA counted from the N-terminus.^{10,160,161}

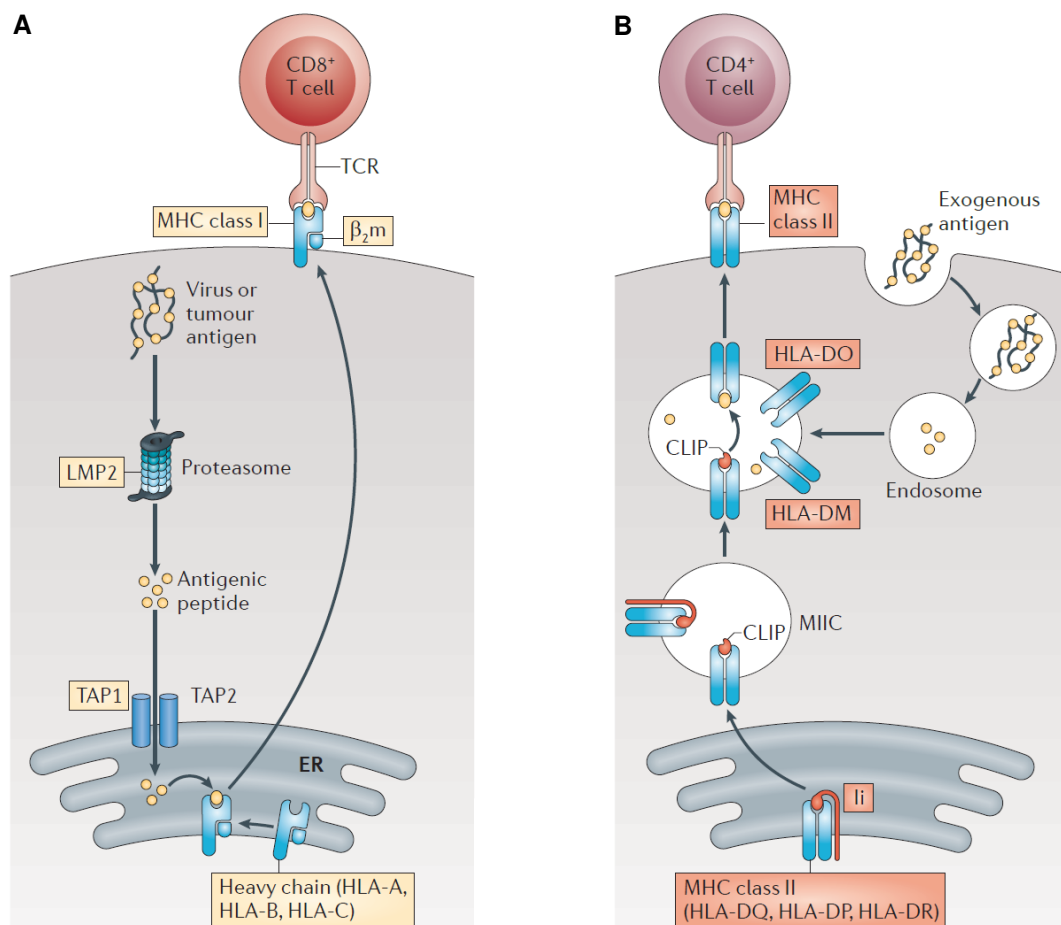


Figure 5. Loading of HLA molecules with antigenic peptides. (A) Processing of HLA class I antigens. Antigenic peptides are generated by the proteasome, bind to newly synthesized HLA class I molecules in the ER, and HLA-peptide complexes are integrated into the plasma membrane. **(B) Generation of HLA class II-peptide complexes.** Membrane proteins or extracellular antigens are broken down in vesicles and resulting peptides are loaded in MIIC on HLA class II molecules. This schematic leaves out the step of initial translocation of the HLA class II-Ii complexes to the plasma membrane and subsequent endocytosis. Figure adapted from Kobayashi *et al.*¹⁶².

Extracellular antigens as well as membrane proteins can be incorporated by phagocytosis, (clathrin-mediated) endocytosis, or by macropinocytosis and do subsequently undergo proteolytic degradation in phagolysosomes, early endosomes, macropinosomes, and the antigen-processing compartment. Through autophagy, parts of the cytosol can be engulfed by membranes and degraded in autophagosomes. This allows intracellular antigens to be

presented on HLA class II, which is of utmost importance in DCs and thymic epithelial cells to establish central and peripheral tolerance to self-antigens.^{10,163-165} HLA class II α and β chains newly synthesized at ER-resident ribosomes heterodimerize and the peptide-binding cleft is occupied by the non-polymorphic invariant chain (Ii). The complex passes the trans-Golgi network and traffics to the plasma membrane. Clathrin-mediated endocytosis of the complex and translocation to multivesicular late endosomal-lysosomal MHC class II antigen-processing compartments (MIIC) is facilitated by Ii.^{10,163,164,166} Ii is cleaved in intraluminal vesicles within the MIIC, whereby the class II-associated invariant chain peptide (CLIP), a remnant of Ii, is still bound to the peptide-binding cleft. HLA-DO regulates the enzyme HLA-DM which removes CLIP from the HLA class II heterodimer to render it peptide-receptive.^{10,163,164,166} Association of ligands and HLA class II molecules takes place in (auto-)phagolysosomes and in the MIIC. HLA class II-peptide complexes become plasma membrane-bound *via* vesicles or tubules originating from the MIIC that fuse with the cell membrane (Figure 5 B).^{10,163,164,166} HLA class II ligands have a typical length of 15 to 17 AA.¹⁶⁷ However, longer peptides of up to 25 AA can be accommodated by protrusion of the C- and N-terminus from the groove as well.¹⁶⁸ The anchor residues of HLA class II-presented peptides which mediate binding specificity reside within the approximately central core region spanning nine AA.^{10,158,169} HLA class II molecules are renowned for promiscuous binding of peptides (with distinct core regions) due to decreased length preferences and degenerate peptide motifs.¹⁶⁹⁻¹⁷¹

The phenomenon of cross-presentation describes HLA class I presentation of extracellular antigens on DCs for the activation of naïve CTLs. One of the mechanisms accomplishing this is the phagosome-to-cytosol pathway. Macropinosomes and phagosomes are believed to derive from ER membranes and do hence comprise tapasin, TAP, and the protein transporter complex Sec61. The latter allows antigens to escape from endocytic vesicles into the cytoplasm.^{10,172} Proteins are proteasomally degraded, cleavage products are imported into the ER and occupy the peptide-binding cleft of HLA class I molecules. Alternatively, peptides leaving the proteasome may undergo phagosomal import *via* TAP, where they encounter ER-derived HLA class I heterodimers. A third mechanism depends on cathepsin S, a cysteine protease that is contained in endosomes. Besides taken up antigens that are broken down by cathepsin S, endosomes do also encompass HLA class I molecules either deriving from the ER or from the plasma membrane in the course of recycling processes. Upon association of peptides and HLA class I molecules, complexes are integrated into the cell membrane.^{10,172}

2.3 Cancer immunotherapy for intracranial neoplasms

2.3.1 Immunotherapy – a contemporary concept to treat malignancies

The idea that recognition and elimination of tumor cells through cells of the innate and adaptive immune system is as simple as it is ingenious.^{173,174} The beginnings of cancer immunotherapies reach back to 1893, when William Bradley Coley observed concomitant tumor regression in cancer patients suffering from *Streptococcus*-induced erysipelas after surgery. Based on a first hypothesis, he systematically infected patients with *Streptococcus* inducing remarkable anti-tumor effects.¹⁷⁵ Immune responses directed against cancer cells have two classes of antigens as targets: tumor-specific antigens (TSAs) and tumor-associated antigens (TAAs). Processing of mutation-bearing proteins (TSAs) can produce so-called neo-epitopes. These can represent deletions or insertions, single nucleotide variants (SNVs), gene fusions, and frameshift mutations. Further, neo-antigenic HLA ligands can originate from mutations leading to splice site alterations or from defective products of usually untranslated RNA sequences.^{174,176,177} Cryptic peptides arising from cancer-specific antisense transcripts, novel unannotated open reading frames, non-coding regions (5' and 3' untranslated regions (UTR), introns, intergenic regions), non-canonical reading frames of protein-coding regions, or unconventional (proteasomal) splicing events as well as peptides harboring tumor-exclusive post-translational modifications (PTMs) can also be (non-mutated) neo-epitopes.¹⁷⁷⁻¹⁸⁶ WT genes can encode for tissue-specific differentiation antigens (TAAs) and cancer-testis (CTAs) or germline antigens (TSAs).^{174,187-190} Viral antigens, particularly when derived from oncogenic viruses, are another source of TSAs,^{10,174,191-194} whereas protein overexpression in malignant cells gives rise to TAAs.^{10,174,191,195} The major advantage of TSAs over TAAs is real tumor specificity rendering 'on-target off-tumor' toxicities virtually impossible. Additionally, TSA-specific T cells do not underlie central tolerance to self-antigens that has to be overcome for anti-tumor responses and are thus expected to be strongly immunogenic. However, this might not be applicable for CTAs with ectopic expression in the thymus resulting in the deletion of highly affine TCRs.^{196,197} Targeting early oncogenic driver mutations by immunotherapy further has the advantage of homogenous expression (and probably HLA presentation) across subclones, which is highly preferable in heterogenous tumors such as glioblastoma.^{49,65,198}

Despite this large variety of potential targets, immune responses against tumors may be inefficient or even absent. In 2011, the famous hallmarks of cancer as defined by Hanahan and Weinberg were supplemented with 'immune evasion'.¹⁹⁹ Robert Schreiber summarized the steps to immune evasion as the three phases of immunoediting which are governed by interaction and co-evolution of immune and tumor cells. In the elimination phase, the immune system successfully defeats outgrowth of tumor cells, as it eliminates transformed cells during immunosurveillance. Few surviving cells enter the second phase. Tumor formation is not yet possible, since tumor cell division and eradication are at equilibrium. Selection pressure caused by the immune system in combination with genetic instability foster the development of new variants and subclones. Once cancer cells succeed in immune evasion, this results in clinical manifestation of tumor formation.^{200,201} The reasons for insufficient or even lacking tumor antigen-specific immune responses encompass inadequate HLA presentation of the tumor antigen (on APCs), scarceness of cytokines (e.g. interleukin 2 (IL-2), IL-12) and/or co-stimulatory molecules (e.g. CD80, CD86) required for T-cell activation, a lack of immune

effector cells at the site of action, and immunosuppression originating from the tumor microenvironment (TME).^{202,203} The latter can be mediated by immunosuppressive cells (e.g. Tregs, myeloid-derived suppressor cells (MDSCs), inhibitory B lymphocytes), high levels of inhibitory cytokines (TGF- β , IL-10) and signals (e.g. cytotoxic T-lymphocyte-associated antigen 4 (CTLA4, CD152), inhibitory Ig-like transcripts (ILTs), programmed cell death protein 1 (PD-1, CD279), programmed cell death ligand 1 / 2 (PD-L1, CD274, B7-H1 / PD-L2, CD273, B7-DC), Fas cell surface death receptor (Fas), Fas ligand (FasL), TRAIL, TRAILR, impaired antibody-mediated opsonization, a metabolic milieu which is adverse for immune cells, or elevated levels of enzymes degrading factors essential for T cells or producing inhibitory metabolites (e.g. arginase-1 (ARG1), heme oxygenase-1 (HO-1), indoleamine 2,3-dioxygenase-1 (IDO1)).²⁰³⁻²⁰⁶ Cancer immunotherapy aims at breaking immune evasion by reconstituting or modulating anti-cancer immune responses.^{10,173,176,203,207} In general, this is pursued by three strategies: provision of the (appropriate) antigen (1), supply of T-cell co-stimulation or blockade of T-cell co-inhibition (2), and transfer of effector cells (3).²⁰² The so far most common approaches include vaccination with antigenic substances (1) or antigen-presenting DCs (1, 2), monoclonal antibodies intervening in T-cell activation (2), recombinant cytokines (2), adoptive T-cell transfer (3), and oncolytic viruses (multifaceted mode of action).^{10,174,203}

Cancer vaccines

For vaccination-based immunotherapies, whole tumor cell lysates, antigen- or epitope-encoding expression vectors, processable long peptides or recombinant antigens as well as short peptides in the form of exact CD8⁺ or CD4⁺ T-cell epitopes directly binding to HLA molecules, are employed. *In vitro*, the antigen presentation of DCs can be modified by pulsation with antigens or peptides, cancer cell lysate, or nucleic acids (RNA / DNA) encoding the respective TAA or TSA. Upon administration, these antigen-presenting DCs are capable of priming adaptive immunity. Vaccines can increase both the repertoire and the number of (targetable) antigens presented on HLA paving the way to induce anti-cancer immune responses.^{10,196,203,208,209} However, sipuleucel-T (Provenge), a vaccine for metastatic castration-resistant prostate carcinoma composed of autologous APCs,²¹⁰ has so far remained the only therapeutic cancer vaccine receiving FDA approval.²⁰³

Short peptide vaccines have several clear advantages as compared to other vaccination approaches. On the one hand, they have a clearly defined composition which is also beneficial to evaluate immunogenicity prior to administration as well as to monitor CD8⁺ and CD4⁺ T-cell responses.²¹¹ On the other hand, peptide synthesis is well feasible in good manufacturing practice (GMP) grade without being disproportionately expensive allowing for *de novo* synthesis for single patients. Despite the high degree of individuality of peptide vaccines inherent to the HLA system, peptides for vaccine composition may also be chosen 'off-the-shelf' from a previously built up warehouse.^{196,212} Peptide vaccines using a mix of targetable epitopes have demonstrated to both have an exceptional safety profile and to elicit clinically significant anti-tumor responses. The latter is most likely not possible by targeting a single antigen.^{196,203} However, overall clinical response rates come up to a maximum of 5% indicating that the effectiveness of cancer vaccines does not solely depend on the selection of the right target. Great potential is seen for the combination with other immunotherapies such as

checkpoint inhibition or adoptive T-cell transfer (discussed in the next sections) and the use of an appropriate adjuvant has a decisive impact.^{185,196,213}

Adjuvants can protect the delivered peptide and mediate a depot effect, promote antigen uptake by APCs, and, most importantly, provide a more general stimulus to APCs inducing antigen-specific responses of the desired Th1/CTL type.¹⁹⁶ Montanide™ ISA 51, also designated as analogue of incomplete Freund's adjuvant, is a delivery adjuvant used for oil-in-water formulations of vaccines and has both protective and depot effects.^{196,214} In turn, the popular adjuvant granulocyte-macrophage colony-stimulating factor (GM-CSF) is capable of recruiting and activating APCs at the site of injection. However, this effect is far weaker than expected and doses above 100 µg can even lead to T-cell inhibition and proliferation of MDSCs.^{196,215} Other adjuvants bind to so-called toll-like receptors (TLR) resulting in strong stimulation of APCs accompanied by an increase in HLA expression, cytokine and chemokine secretion, as well as the number of costimulatory and adhesion molecules.¹⁹⁶ Deoxycytidyl-deoxyguanosin oligodeoxynucleotides (CpG ODNs), a TLR9 ligand, was the first TLR agonist tested in a clinical trial of a therapeutic cancer vaccine (in combination with Montanide™ ISA 51) eliciting outstanding T-cell responses.^{196,216} Hiltonol® is composed of polyinosinic-polycytidylic acid stabilized by polylysine and carboxymethylcellulose (Poly-ICLC) which activates TLR3, but has not been tested in large cohorts yet. Single-stranded RNA or Imiquimod (Aldara® 5% cream) represent TLR7/8 activators. The results whether patients benefit from topical Aldara® application at the site of injection are controversial, whereas RNA adjuvants are still under development.¹⁹⁶ Recently, Pam₃Cys-GDPKHPKSF (XS15), a novel adjuvant mimicking the bacterial lipopeptide Pam₃Cys-Ser-Ser, has been described. First applications of this TLR1/2 ligand as adjuvant for peptide vaccines appear very promising (internal data created at the Department of Immunology, University of Tübingen).^{196,217} The optimal composition of therapeutic cancer vaccines remains an open question and is under intense investigation. Combinations of adjuvants acting in different manner, chimeric TLR agonists, as well as concomitant administration of other immunotherapies such as monoclonal antibodies or recombinant cytokines are possibilities to enhance the efficacy of cancer vaccines.¹⁹⁶

Recombinant cytokines

Recombinant cytokines are supposed to supplement the immune system with missing signals to elicit anti-tumoral T-cell responses. Their use was the first proof of the effectiveness of cancer immunotherapy.²¹⁸ IL-2 is a stimulator of T-cell proliferation and acts *via* the highly affine α chain (CD25) of the IL-2 receptor complex. Natural killer (NK) and B cells have IL-2 receptors lacking CD25. In these cells, IL-2 induces proliferation as well as stimulation of NK-cell cytotoxicity and B-cell differentiation, respectively.^{10,203,219} Despite having been approved by the FDA, recombinant IL-2 (Proleukin®, former aldesleukin) is rarely used in clinical routine owing to severe toxicities and limited efficacy.²⁰³ The latter is in part reasoned by the coincident expansion of CD4⁺CD25⁺ Tregs.^{203,220} Novel approaches to reduce IL-2 toxicity by altering pharmacokinetic properties include coupling to polyethylene glycol (PEG) or to Fc domains of antibodies thus increasing half-life of the molecule. Further, the pharmacodynamic profile is optimized by inhibiting binding to highly affine IL-2 receptors expressed by Tregs. Targeting IL-2 to the site of action can be achieved by chimeric molecules equipped with TME-specific

antibodies.²¹⁸ Besides IL-2, FDA approval was only given to one further recombinant cytokine: type I interferon (IFN- α), as native molecule and as half-life-optimized PEGylated version.^{218,221} IFN- α acts both on the TME by being anti-angiogenic and on tumor cells by promoting apoptosis and inhibiting proliferation.^{218,222} DCs and T cells mature under the influence of IFN- α , which is also an immunostimulant.^{218,223} However, recombinant IFN- α is rarely used in the clinics. This might be overcome by engineering novel variants with reduced toxicity and optimized binding properties. Fusion of IFN- α and apolipoprotein A-I improves the pharmacokinetic profile, whereas so-called Actakines (activity-on-Target cytokines) deliver the cytokine to DCs *via* a Clec9A-specific antibody domain. Moreover, mutation of the cytokine itself can contribute to improved binding affinity.^{218,224,225}

CTLs and NK cells exert their cytotoxic activity, proliferate, and release cytokines upon stimulation with IL-15.^{218,226,227} In contrast to IL-2, it does not promote the concomitant expansion of Tregs.^{218,228} First in-human applications failed due to severe side effects and later studies did not show a clear clinical benefit of IL-15 treatment.^{218,229} Current approaches try to increase stability of this small molecule and to generate fusion proteins with better binding properties. RLI is a chimeric molecule consisting of IL-15 and the sushi domain bearing the binding domain of the IL-15 receptor α .^{218,230} Inclusion of apolipoprotein A-I might be a way to optimize delivery of the construct.^{218,231} IL-12, IL-21, and even IL-10, which has so far been designated as immunosuppressive cytokine but was shown to prevent apoptosis of CTLs following antigen recognition, are currently under intense investigation for application as cancer immunotherapies. In addition, there are ongoing studies evaluating the effects of targeting pro-tumor cytokines such as TNF- α , TGF- β , or the colony stimulating factor 1 (CSF-1) by antibodies, small interfering RNA (siRNA), cytokine traps, and inhibitors of cytokine receptor signaling.²¹⁸

Agonistic and antagonistic monoclonal antibodies

The category of monoclonal antibodies comprises agonistic ones acting on co-stimulatory molecules and antagonistic ones blocking co-inhibitory receptors, so-called checkpoint inhibitors. In 2018, Tasuku Honjo and James P. Allison were honored with the Nobel Prize in Physiology and Medicine for their work on immune checkpoints.²³² CTLA4 exceeds the affinity of CD28 to CD80 (B7-1) and CD86 (B7-2) expressed on APCs thus preventing CD28-CD80 or CD28-CD86 interactions that enable T-cell activation.^{233,234} CTLA-4-blocking antibodies (Ipilimumab) both facilitate T-cell effector function and deplete Tregs that constitutively express CTLA4 by antibody-dependent cellular cytotoxicity (ADCC).^{10,235-237} When PD-1⁺ T cells bind to PD-L1 or PD-L2, this induces an inhibitory signaling cascade rendering the T cell anergic. While hematopoietic and parenchymal cells express PD-L1 to prevent autoimmunity, PD-L2 is preferentially expressed by APCs and Th2 cells. Various types of cancer cells hijack the PD-1–PD-L1/PD-L2 axis as mechanism of immune evasion.^{10,203,206,238-240} Monoclonal antibodies blocking PD-1 (Pembrolizumab, Nivolumab, Cemiplimab) or PD-L1 (Atezolizumab, Durvalumab, Avelumab) have the capability to elicit anti-tumor responses and have been approved by the FDA for several cancer entities.²⁴¹⁻²⁴⁸ Antibodies blocking V-domain immunoglobulin suppressor of T-cell activation (VISTA), lymphocyte activation gene-3 (LAG-3, CD223), B- and T-cell lymphocyte attenuator (BTLA, CD272), T-cell immunoglobulin and mucin-domain containing-3 (TIM-3), B7 homolog 3 protein (B7-H3, CD276), T-cell

immunoglobulin and ITIM domain (TIGIT), or sialic acid-binding immunoglobulin-like lectin 15 (Siglec-15) are currently under development and designated as 'next-generation checkpoint inhibitors'. Furthermore, the combination of several checkpoint antibodies is considered to have high therapeutic potential.^{203,241,243,249} The response to checkpoint inhibition correlates with the mutational burden and, for antibodies targeting the PD-1–PD-L1/PD-L2 axis, with PD-1, PD-L1, and PD-L2 expression on tumor and T cells. Further predictive biomarkers include the pre-therapy tumor burden and site of metastases, the diversity and (relative) composition of the peripheral immune cell repertoire, cytokine profiles, levels of immunosuppressive cells (e.g. MDSCs, Tregs), the amount and type of tumor-infiltrating lymphocytes (TILs), the patient's performance status, or the occurrence of immune-mediated side effects. The exploitation of predictive biomarkers is of importance to weigh up the side effects of checkpoint blockade and the expected clinical benefit.²⁴¹

Engagement of co-stimulatory molecules can also contribute to the enhancement of anti-tumor T-cell responses. So far, none of these agonistic antibodies have received FDA approval for cancer immunotherapy. OX40 (CD134) belongs to the TNF receptor family and is expressed by CD8⁺ and CD4⁺ T lymphocytes upon antigen recognition. OX40-activating antibodies promote T-cell proliferation and activation of effector functions.^{203,250} Agonistic antibodies acting on 4-1BB (CD137) can enhance NK-mediated ADCC and even restore cytotoxicity of T cells.^{203,251} Engagement of the glucocorticoid-induced tumor necrosis factor receptor (GITR), which is expressed on activated DCs, NK cells, regulatory and effector T cells as well as B cells, enhances the activity of the targeted cell. In the T-cell compartment, the immunosuppressive effect of Tregs is reduced, whereby TCR signaling and proliferation of CTLs and Th cells are enhanced.^{203,252} CD40-targeted immunotherapy stimulates APCs, T cells, and anti-tumoral responses mediated by cytotoxic cells of the myeloid lineage^{203,253}

A more sophisticated approach to target co-stimulatory or -inhibitory molecules is based on aptamers. The specificity and affinity of these RNA or DNA oligonucleotides is comparable to monoclonal antibodies. Thus, they represent an additional tool to unleash anti-cancer T-cell responses.²⁵⁴ Another technique for future cancer immunotherapies are bi-specific antibody formats, so-called bi-specific antibodies for T-cell redirection and activation (BiTes). Antibodies with dual specificity are aimed at redirecting immune cells to the tumor. Blinatumomab, an anti-CD19/CD3 BiTe, brings CD3⁺ T lymphocytes into spatial proximity of CD19⁺ leukemia cells.²⁵⁵ Similar effects can be achieved with fusion proteins consisting of a soluble TCR and an antigen-binding domain, named immune-mobilizing monoclonal T-cell receptors against cancer (ImmTACs). Upon TCR binding to the tumor cell, polyclonal T lymphocytes are recruited *via* the CD3-specific part of the ImmTAC.²⁵⁶

Adoptive T-cell transfer

It is suggested that the affinity, frequency, and functionality of tumor-specific T cells correlate with the efficacy in eliminating cancer cells. Autologous T cells that recognize tumor antigens can be enriched and expanded *in vitro* to be subsequently used as passive immunotherapy. Enrichment of TAA- or TSA-specific T cells can be achieved by selecting peripheral or tumor-infiltrating T-cell clones.^{10,203,257-259} Upon lympho-depleting chemotherapy which eliminates immunosuppressive factors such as Tregs or so-called 'homeostatic cytokine sinks', expanded

T cells are re-infused.^{203,260} Lymphodepletion goes along with the risk of severe infections and T-cell reconstitution is not only deferred, but often also incomplete which may ultimately also contribute to cancer recurrence.^{261,262} Therefore, alternative treatment regimens try to circumvent lymphodepletion by concomitant administration of CTL-promoting cytokines such as IL-15.²⁶² Despite eliciting clinically relevant responses e.g. in melanoma,²⁵⁹ adoptive T-cell therapy faces several obstacles: collection and expansion of T cells, especially TILs, is laborious and tumor-specific T cells are often rare and/or of low affinity.²⁰³ Genetic modification represents an option to equip T lymphocytes with highly affine TCRs specific for a pre-defined target antigen.^{203,263} Nevertheless, this approach does still require the target antigen to be processed and presented on HLA. Chimeric antigen receptors (CARs) link TCR signaling and antigen recognition of an antibody in one molecule thus rendering T-cell binding HLA-independent. CAR-expressing T cells can not only recognize unprocessed surface antigens, but also gangliosides, carbohydrates, proteoglycans, and glycosylated proteins.^{10,203,264} Moreover, co-stimulatory molecules and T cell-activating factors can be introduced into CAR-T cells by transfection.^{203,265,266}

CAR-T cells have enormous potential for immunotherapies and two CD-19-specific constructs, tisagenlecleucel and axicabtagene ciloleucel, have already been approved by the FDA for use in hematological malignancies.²⁶⁷ However, a major drawback of CARs is an unfavorable profile of adverse events including cytokine release syndrome and neurotoxicity as well as limited ability to target solid tumors.^{203,267} So-called suicide genes (e.g. Cetuximab-targetable truncated EGFR (EGFRt), ganciclovir-sensitive hygromycin phosphotransferase-herpes simplex virus 1 thymidine kinase (HyTK), truncated CD19 (CD19t), or drug-inducible caspase-9) increase the safety of CAR-T-cell therapies.²⁶⁸⁻²⁷³ To overcome immunosuppression in the TME, CAR-T cells redirected for universal cytokine killing (TRUCKs) are a sophisticated approach. TRUCK-T cells express stimulatory cytokines such as IL-18 upon CAR engagement at the site of disease. This might be an option to locally augment CAR-T-cell activity.^{203,274,275} Homing of CARs to the TME may be facilitated by using constructs with an antigen-binding domain similar to BiTes.^{203,276}

Oncolytic viruses

Employing so-called oncolytic viruses for immunotherapy is in concept similar to the experiments of Coley.^{277,278} Virotherapy is based on the idea that lytic replication happens almost exclusively in tumor cells instead of affecting all replicating cells. It is expected that the immunosuppressive mechanisms exhibited by the tumor itself as well as the TME facilitate the infection of cancer cells.²⁷⁷ This results in immunogenic cell death characterized by the release of danger signals and tumor antigens. Additionally, oncolytic viruses have been shown to enhance the number of TAAs cross-presented on HLA class I.^{10,203,279,280} This way, they are capable of both enhancing pre-existing and inducing *de novo* anti-tumor immunity. In contrast to targeted therapies, the big advantage of oncolytic viruses is being not solely dependent on one specific receptor.²⁷⁷ So far, Talimogene laherparepvec (T-Vec, Imlygic), a herpes virus modified to express GM-CSF, has remained the only oncolytic virus with FDA approval for use in metastatic melanoma.^{203,277,281} Besides herpes viruses, virus families tried to be exploited for virotherapy encompass *Paramyxo-* (e.g. *measles morbillivirus*, *mumps rubulavirus*), *Retro-* (e.g. *Moloney Leukemia Virus*), *Adeno-*, *Pox-* (e.g. *Vaccinia virus*, *Fowlpox*), *Parvo-*,

Rhabdo- (e.g. *Vesicular Stomatitis Virus*), *Reo-*, and *Picornaviridae* (e.g. *Seneca Valley Virus*, *Coxsackie-*, *Rhino-*, *Poliovirus*) as well as the *Newcastle disease virus*.^{10,277,282} Reduced off-target tropism and increased virulence for cancer cells is achieved by genetic modification.^{277,283} Intratumorally injected, the safety profile of oncolytic viruses – measured by the rate of (serious) adverse events – is superior to that of checkpoint inhibitors. Despite local injection, oncolytic viruses such as T-Vec are capable of inducing distant responses, for instance in metastases.^{277,283,284}

2.3.2 Current status of immunotherapy for intracranial neoplasias

For decades, the brain has been denoted an immune privileged organ shielded by the blood-brain barrier of the cerebrovascular endothelium. This begs the question, whether immunotherapy is a realistic therapeutic concept for brain tumors. In 1948, Peter Brian Medawar provided the first evidence for intracranial immune effector cells. Following allogeneic skin transplantation, heterotopic skin grafts of the same donor were rejected in the brain.^{10,285,286} Likewise, transplants into the brain parenchyma were shown to be responsible for accelerated rejection of orthotopic skin grafts.^{286,287} Upon injection of T cells and DCs into the brain, these migrated to cervical lymph nodes indicating that the brain is not segregated from peripheral immunity and immunosurveillance.^{288,289} In 2014, the existence of meningeal lymphatic vessels located along dural sinuses was proven by two independent groups. This system accomplishes the drainage of immune cells as well as cerebrospinal and brain interstitial fluid from the CNS to deep cervical lymph nodes.^{290,291}

Microglia express MHC class II as well as co-stimulatory molecules and are responsible for the phagocytosis of tumor cells (e.g. gliosarcoma) damaged by CD8⁺ T cells. Consequently, they constitute an interface for interaction with peripheral immune cells.^{10,292-300} Activated T cells were also evidenced to penetrate into the CNS where final maturation and proliferation of tumor-specific CTLs takes place.^{10,301-307} In melanoma patients, i.v. administered T cells have reached brain metastases eliciting clinical responses.³⁰⁸ Three routes allow leukocytes to penetrate from the periphery into the CNS: leptomeningeal vessels (blood-to-subarachnoid space), the blood-brain barrier (blood-to-perivascular space), and the choroid plexus (blood-to-CSF) (Figure 6). Under pathological conditions, traffic rates increase dramatically.³⁰⁹⁻³¹¹ Following antigenic challenge, both the CSF and the brain parenchyma home memory T cells.^{309,311,312} As explained in 1.4, meningiomas originate from the meninges lying beyond the blood-brain barrier. Thus, these should be more easily accessible to drugs and immune cells as compared with glioblastomas or medulloblastomas.³¹³

Human glioblastomas, medulloblastomas, and meningiomas are infiltrated by both CD4⁺ and CD8⁺ T cells indicated by the detection or isolation of TILs from surgical specimens.^{129,314-317} In glioblastoma and high-grade meningioma, low amounts of CD3⁺CD8⁺FOXP3⁻ TILs (relative to CD4⁺ TILs) are described as negative prognostic factor for disease progression^{129,318} and survival of glioma-bearing mice was shown to be CTL-mediated.²⁸⁹ For medulloblastomas, no correlation between T-cell infiltration and clinical outcome has been observed.³¹⁷ Spontaneous intratumoral T-cell responses seem to be rare in glioblastoma. However, peptide vaccination is capable of promoting T-cell infiltration and eliciting TIL responses to both mutated neo-

epitopes and WT antigens, which is another indicator of the invalidity of an absolute immune privilege concept.^{314,315}

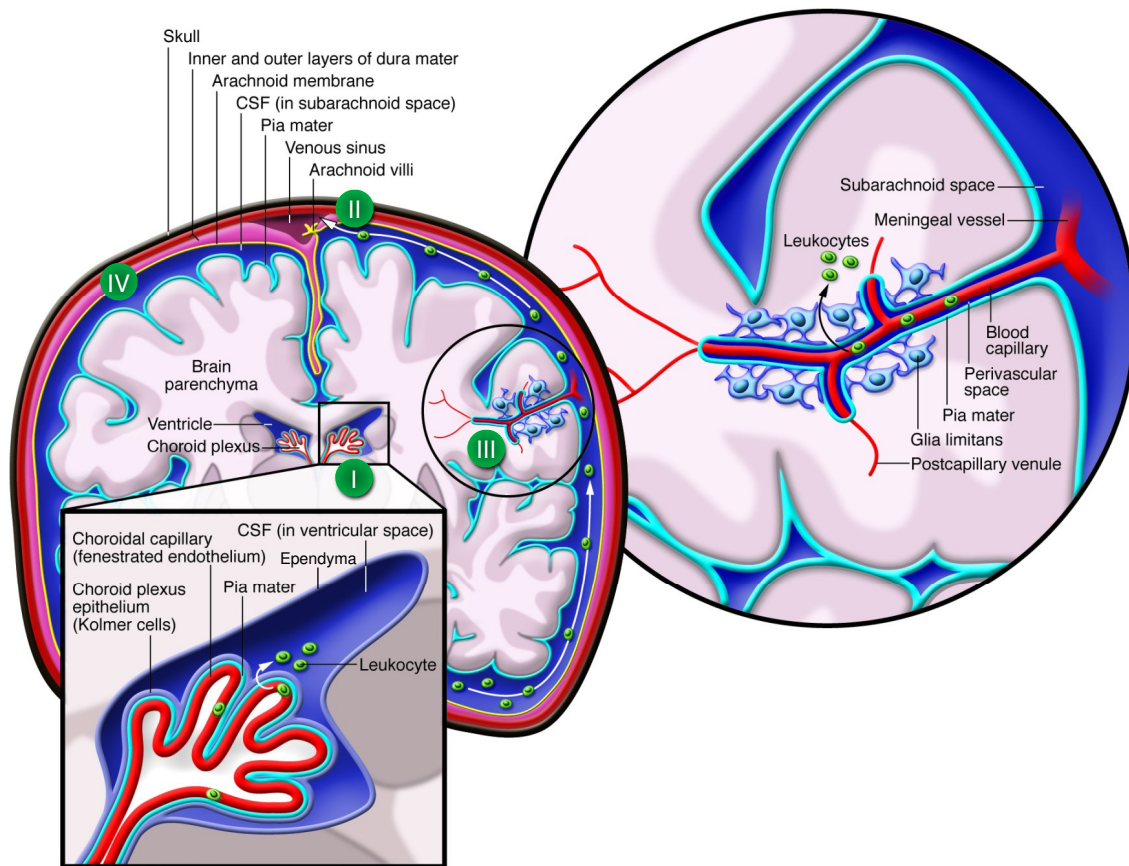


Figure 6. Leukocyte routes into and within the CNS. The brain parenchyma is separated from the skull by three meningeal layers, namely the pia mater, the arachnoid membrane, and the dura mater (from inside to outside). The subarachnoid space lies between pia mater and arachnoid membrane and is filled with CSF. The latter is produced in the choroid plexus, where leukocyte transmigration from the blood into CSF takes place (I). CSF-resident leukocytes penetrate the pia mater and the glia limitans, which is formed by astrocytes, to access the brain parenchyma. Alternatively, leukocytes can enter the parenchyma *via* the ependyma which lines the ventricular system. At the venous sinus, the uptake of leukocytes from CSF into the blood is mediated by arachnoid villi (II). The brain is supplied with blood by branches from meningeal vessels. Blood capillaries are located in the so-called perivascular space and reach deeply into the brain parenchyma. Immune cells can pass the blood-brain barrier by trafficking across vascular endothelium, the subarachnoid space, the pia mater, and the glia limitans (III). Leukocytes may also leave the blood by diapedesis to enter the CNS *via* the leptomeninges encompassing the arachnoid membrane and the pia mater (IV). Image taken from Wilson *et al.*³¹¹; slightly modified.

In order to reach the designated site of action, acellular immunotherapeutic agents have to permeate into the brain. The proportion of drugs which can do so was estimated at less than 5%.³¹⁹ Recombinant cytokines such as IFN- α can be engineered to be blood-brain barrier-permeable by coupling to Apolipoprotein A-I.²²⁴ The ability to cross the human blood-brain barrier was also evidenced for oncolytic viruses such as ParvOryx01 applied in an early clinical trial for the therapy of glioblastoma.³²⁰ So-called nanoscale immunoconjugates (NICs), chimeric molecules of antibodies and biopolymer scaffolds, can pass the blood-brain barrier, which is not applicable e.g. for unmodified anti-CTLA4 or anti-PD-L1 antibodies.^{319,321,322} Likewise, integration of a 'Brain Shuttle module' into therapeutic antibodies enables transferrin

receptor-dependent transcytosis into and optimized lysosome sorting in the CNS.³²³ Primary intracranial neoplasms – excepting hypermutated recurrent glioblastomas – are in general characterized by low mutational loads.³²⁴ Checkpoint blockade has significant clinical benefit e.g. in metastatic melanoma or non-small cell lung cancer, whereby response rates correlate with the mutational burden. Thus, checkpoint inhibitors as monotherapy are not expected to have the same therapeutic efficacy in brain tumors as observed for other cancer entities.³²⁵⁻³²⁷ Glioblastomas largely express PD-L1,³²⁸ whereas medulloblastomas are mostly PD-L1 negative³¹⁷ and PD-L1 expression is rarely observed in meningiomas.³²⁹ This further diminishes the expected clinical benefit of anti-PD-L1 therapy for the latter two cancer entities. Checkpoint antibodies represent passive immunotherapies that are not capable of priming *de novo* immune responses rendering pre-existing anti-cancer T cells a prerequisite for their effectiveness. This suggests that patients suffering from brain tumors and lacking endogenous anti-tumor immunity do not benefit from checkpoint inhibition as monotherapy. However, combinations of checkpoint blockade with other (active) immunotherapies such as cancer vaccines might be promising for intracranial neoplasias.^{10,203,330}

In conclusion, it can be stated that the anatomically reasoned dogma of the brain being devoid of immunity is no longer sustainable. Especially under pathological conditions, immune cells and cytokines enter the CNS and there is growing evidence for effective intracranial immune responses. This suggests to pursue cancer immunotherapy as means to counteract immunosuppression unleashing intracranial anti-cancer immune responses. As recently shown for peptide vaccination in glioblastoma, the timing and dosage of concomitant medication such as dexamethasone has a major impact on the effectiveness of immunotherapy and consequently requires in-depth evaluation.³¹⁵ Immunotherapy has shown to be feasible for immunologically cold brain tumors with low mutational burden, whereby the clinical benefit of standard therapy has still not been outcompeted by immunotherapeutic approaches. In the following, the current knowledge on tumor antigens in glioblastoma, medulloblastoma, and meningioma as well as a summary of recent or ongoing clinical trials will be presented. Searching the PubMed database for publications dealing with immunotherapy yielded 1,582 hits for glioblastoma and only 140 or 68 entries for medulloblastoma or meningioma, respectively.³³¹ The imbalance between these three tumor entities with a profound lack of immunotherapeutic approaches in medulloblastoma and meningioma is also reflected by the number of clinical trials registered at ClinicalTrials.gov to investigate immunotherapeutic intervention in glioblastoma (n=92), medulloblastoma (n=8), or meningioma (n=6).³³²

Tumor antigens in glioblastoma

For immunotherapeutic approaches targeting glioblastoma, a large variety of TAAs has been suggested. The target selection of WT antigens in a recent phase I clinical trial of multi-peptide vaccination conducted by the Glioma Actively Personalized VAccine Consortium (GAPVAC) was based on natural HLA presentation as well as RNA expression data. The source proteins of vaccine peptides comprised ankyrin repeat domain-containing protein 40 (ANR40), chondroitin sulfate proteoglycan 7 / brevican core protein (CSPG7), CDK4, ceramide synthase 1 (CerS1), clusterin (CLUS), cysteine and glycine-rich protein 2 (CSRP2), serine/threonine-protein kinase DCLK2 (DCLK2), dihydropyrimidinase-related protein 4

(DRP-4), eukaryotic translation initiation factor 4E (eIF4E), elongation of very long chain fatty acids protein 2 (ELOV2), glutamate receptor 4 (GluR4), ionotropic glutamate receptor kainate 3 (GluK3), ATP-sensitive inward rectifier potassium channel 10 (KCJ10), melanoma-associated antigen F1 (MAGE-F1), membrane-associated guanylate kinase inverted 2 (MAGI2), protein MTSS 2, X-linked neuroligin-4 (NLGNX), Y-linked neuroligin-4 (NLGNY), neuronal cell adhesion molecule (NRCAM), ORM1-like protein 1 (ORML1), protocadherin gamma-C5 (PCDGM), pecanex-like protein 3 (PCX3), pleckstrin homology domain-containing family A member 4 (PKHA4), receptor-type tyrosine-protein phosphatase zeta (PTPRZ), DNA repair and recombination protein RAD54B (RAD54B), seizure 6-like protein (SE6L1), transforming acidic coiled-coil-containing protein 3 (TACC3), ubiquitin carboxyl-terminal hydrolase 11 (UBP11), vacuolar protein sorting-associated protein 13B (VP13B), abnormal spindle-like microcephaly-associated protein (ASPM), protein crumbs homolog 1 (CRUM1), dedicator of cytokinesis protein 7 (DOCK7), brain-type fatty acid-binding protein (B-FABP), acyl-CoA 6-desaturase (FADS2), constitutive coactivator of PPAR-gamma-like protein 2 (F120C), neuronal membrane glycoprotein M6-b (GPM6B), HEAT repeat-containing protein 1 (HEAT1), heparan sulfate 2-O-sulfotransferase 1 (HS2ST), integrin alpha-7 (ITA7), the uncharacterized protein LOC728392, leucine zipper putative tumor suppressor 1 (LZTS1), oligodendrocyte transcription factor 2 (OLIG2), E3 ubiquitin-protein ligase Praja-2 (PJA2), 60S ribosomal protein L7a (RL7A), excitatory amino acid transporter 4 (EAA4), structural maintenance of chromosomes protein 4 (SMC4), alpha-2,8-sialyltransferase 8E (SIA8E), transmembrane protein 231 (TM231), transmembrane protein 255A (T255A), zinc finger protein 3 (ZNF3), and baculoviral IAP repeat-containing protein 5 / survivin (BIRC5).³¹⁴ The development of GAPVAC-101 included a phase I trial of the invariant peptide cocktail IMA950, which contained additional peptides derived from chondroitin sulfate proteoglycan 4 (CSPG4), insulin-like growth factor 2 mRNA binding protein 3 (IF2BP3), met proto-oncogene / hepatocyte growth factor receptor (c-Met), and tenascin C (TN-C).³³⁰

The glioblastoma-associated antigens IL-13 receptor alpha 2 (IL13R α 2), receptor tyrosine-protein kinase erbB-2 (HER2), tyrosinase-related protein 2 (TRP2), Wilms' tumor gene 1 (WT1), absent in melanoma 2 (AIM2), melanocytes lineage-specific antigen gp100 (gp100), and melanoma-associated antigen 1 (MAGE-A1 / CT1.1) have also been evaluated in in-human trials employing e.g. DCs pulsed with peptides, CAR-T cells, or peptide vaccination.³³³⁻³³⁶ Besides MAGE-A1, expression of the CTAs X antigen family member 3 (XAGE3 / CT12.3), Opa-interacting protein 5 / protein Mis18-beta (OIP5 / CT86), transcriptional repressor CTCFL (CTCFL / CT27), and actin-like protein 8 (ACTL8 / CT57) was evidenced in WHO grade IV glioma.^{10,209,337,338} By comparing the repertoire of HLA ligands naturally presented on both primary glioblastoma and glioblastoma stem-like cells but not on healthy tissues, Neidert *et al.* described Ras and Rab interactor 1 (RIN1), hepatocyte cell adhesion molecule (HEPACAM), glypican-1 (GPC1), DnaJ homolog subfamily C member 25 (DJC25), alpha-tubulin N-acetyltransferase 1 (ATAT), paired box protein Pax-6 (PAX6), raftlin-2 (RFTN2), transforming growth factor beta-2 proprotein (TGFB2), protein AF1q, EF-hand domain-containing protein 1 (EFHC1), MICOS complex subunit MIC25 (MIC25), NmrA-like family domain-containing protein 1 (NMRL1), transmembrane prolyl 4-hydroxylase (P4HTM), plasminogen activator inhibitor 1 (PAI1), and prostaglandin F2 receptor negative regulator (FPRP) as further candidate targets for cancer immunotherapy.¹⁴⁹ Overexpression renders ephrin type-A

receptor 2 (EphA2), B7-H3, telomerase, and EGFR candidates for glioblastoma immunotherapy as well.³³⁹⁻³⁴³

Neo-epitopes are mainly eligible for fully individualized immunotherapeutic approaches. However, the EGFRvIII and IDH1R132H mutations may be exploited as targetable neo-antigens in larger cohorts, as they occur in 25-30% or 5-15% of adults suffering from primary glioblastoma, respectively.^{27,37,342,344,345} Targeting the histone H3 K27M variant is currently under investigation for pediatric high-grade as well as diffuse midline (non-hemispheric) glioma characterized by a subgroup-specific mutation frequency of up to 30%.^{198,346} HCMV-directed immunotherapy, especially against the tegument protein pp65, has been subject of multiple clinical trials in glioblastoma and was even associated with clinical benefit. However, this therapeutic option is still under controversial discussion.^{10,209,341,347-350}

Targets for the immunotherapy of medulloblastoma

The number of potential targets for the immunotherapy of medulloblastoma is substantially lower as compared with glioblastoma. However, several CT antigens have been proposed based on expression data and correlation with poor patient outcome. These comprise melanoma antigen preferentially expressed in tumors (PRAME), sperm autoangiogenic protein 17 (SPA17 / CT22), MAGE-A1, New York esophageal squamous cell carcinoma-1 (NY-ESO-1 / CT6.1), G antigen 1 (GAGE-1 / CT4.1), synaptonemal complex protein 1 (SYCP1 / CT8), solute carrier organic anion transporter family member 6A1 (SO6A1 / CT48) as well as the melanoma-associated antigens 3, 4, 6, C1, and C2 (MAGE-A3 / CT1.3; MAGE-A4 / CT1.4; MAGE-A6 / CT1.6; MAGE-C1 / CT7.1; MAGE-C2 / CT10).^{268,351,352} Non-CTAs suggested for medulloblastoma immunotherapy include disialoganglioside GD2, Her2, EGFR, glypican-2 (GPC2), and B7-H3, whereby all antigens excepting the latter two have been subject of recent or ongoing clinical trials.³⁵³⁻³⁵⁷

Despite low mutational burden, somatic mutations in medulloblastoma were found to yield immunogenic predicted neo-epitopes. However, shared mutations translating into targetable neo-antigens for a larger number of patients have so far not been identified.^{324,358} As for glioblastoma, targeting HCMV-derived antigens has been suggested for medulloblastoma, but remains under controversial debate.^{83,347}

Antigens in meningioma immunotherapies

Immunotherapeutic approaches in meningioma face a profound lack of suitable target antigens. Most of the candidates including B7-H3,³⁵⁹ gp100,³⁶⁰ NY-ESO-1,^{361,362} IL13R α 2,³⁶³ survivin³⁶⁴, TRP-2,³⁶⁰ and WT1³⁶⁵ have also been proposed as targets for glioblastoma or medulloblastoma. In addition, members of the CT45 gene family (CT45A1-3, CT45A5-10) having $\geq 90\%$ sequence identity^{86,362,366} and synaptonemal complex protein 1 (SYCP1 / CT8) have been suggested as immunotherapeutic targets.^{230,232,233} Besides having in general low mutational load, little is known about the presence of neo-antigens in meningioma. In high-grade meningiomas characterized by a higher number of somatic mutations as compared with low-grade meningiomas, no common mutational signature (apart from NF2 alterations) has been identified so far. Thus, one can expect that targeting neo-epitopes in meningioma remains suitable for fully individualized approaches only.¹¹⁰

Evaluation of immunotherapy for intracranial neoplasms

Recent and ongoing clinical trials evaluating different immunotherapeutic approaches in glioblastoma, medulloblastoma, or meningioma are summarized in Table 2.

Table 2. Exemplary clinical trials evaluating immunotherapies for the treatment of intracranial neoplasms (pp. 34-39). Design and results of immunotherapeutic studies in glioblastoma (red), medulloblastoma (orange), and meningioma (blue). Listed adverse events do only refer to applied immunotherapies and not to concomitantly administered standard therapy. Abbreviations not introduced in the text above: anaplastic astrocytoma (AAST), Autologous Lymphoid Effector Cells Specific Against Tumour Cells (ALECSAT), brain stem glioma (BSG), complete response (CR), cobalt gray equivalent (CGE), delayed-type hypersensitivity (DTH), Epstein-Barr Virus (EBV), glioblastoma (GBM), intradermal (i.d.), intranodal (i.n.), intratumoral (i.t.), intravenous (i.v.), keyhole limpet hemocyanin (KLH), meningioma (MNG), months (mo), overall survival (OS), peripheral blood mononuclear cells (PBMCs), progressive disease (PD), progression-free survival (PFS), partial response (PR), PEP-CMV in Recurrent Medulloblastoma / Malignant Glioma (PRiME), radiological response (RR), subcutaneous (s.c.), stable disease (SD), time to progression (TTP), total tumor RNA (TTRNA), *ex vivo* expanded Autologous Lymphocyte Transfer (xALT), year (y), plaque-forming units (pfu).

Treatment Reference	Therapeutic schedule	Phase # Patients	Immuno-genicity	Outcome	Adverse events
Monoclonal antibodies					
Monoclonal antibodies: checkpoint inhibitors					
Atezolizumab ³⁶⁷	Post-radiochemotherapy ± bevacizumab 1,200 mg atezolizumab i.v. every 3 rd week	Ia n=16 recur- rent GBM		n=1 PR n=3 SD 4.2 mo me- dian OS 1.2 mo me- dian PFS	n=3 grade 3 toxicities (brain edema, asthenia, aspartate aminotransferase elevation)
CheckMate 143 ³⁶⁸ : nivolumab ± ipilimumab	Group 1: 3 mg/kg nivolumab every 2 nd week Group 2: 4 doses 1 mg/kg nivolumab + ipilimumab 3 mg/kg every 3 rd week, then 3 mg/kg nivolumab Group 3: 4 doses 3 mg/kg nivolumab + ipilimumab 1 mg/kg every 3 rd week, then 3 mg/kg nivolumab	I recurrent GBM Group 1: n=10 Group 2: n=10 Group 3: n=20		n=1/0/1 PR n=2/2/4 SD 1.9/1.5/2.1 mo median PFS 10.4/9.2/7.3 mo OS	n=0/9/6 grade 3-4 toxicities Nivolumab mono- therapy tolerated best, side effects determined by ipilimumab dose
Pembrolizumab ³⁶⁹	Group 1: 200 mg pembrolizumab i.v. 19-9 days before surgery (neoadjuvant), adjuvant 200 mg i.v. every 3 rd week Group 2: 200 mg i.v. every 3 rd week (adjuvant)	II, randomized recurrent GBM Group 1: n=16 Group 2: n=16		13.7 / 7.5 mo median OS 3.3 / 2.4 mo median PFS	n=10/7 grade 3-4 adverse events; n=1 grade 3 pneu- monitis and n=1 grade 4 elevation of alanine ami- notransferase (both in group 1)
Nivolumab ³⁷⁰	Nivolumab i.v., 4 doses of 240 mg every 2 nd week, 12 monthly doses of 480 mg	II, ongoing n=180 adults with re- current / refractory rare CNS tumors		Planned: OS, 6mo-PFS, RR	
Avelumab ³⁷¹	Post-surgery Avelumab i.v., 10 mg/kg every 2 nd week for 3 mo, concomitant proton therapy 20 CGE / week	Ib, ongoing n=12 recur- rent / progres- sive grade I-III MNG	Planned: changes in TILs	Planned: RR, PFS, OS	

Treatment Reference	Therapeutic schedule	Phase # Patients	Immuno-genicity	Outcome	Adverse events
Monoclonal antibodies: others					
Bevacizumab ³⁷²	60 Gy (2 Gy/day, 6 weeks) + 75 mg/m ² TMZ daily (max. 49 days), subsequent maintenance TMZ 150-200 mg/m ² 5 successive days/mo (6-12 mo) Experimental treatment from week 4 of radiotherapy Group 1: bevacizumab 10 mg/kg i.v. every 2 nd week Group 2: placebo	III newly diagnosed GBM Group 1: n=320 Group 2: n=317		15.7 / 16.1 mo median OS 10.7 / 7.3 mo median OS	Hypertension, thromboembolism, visceral perforation, thrombocytopenia, neutropenia, fatigue in both groups, but more common in group 1
Bevacizumab ³⁷³	Bevacizumab + irinotecan ± TMZ Group 1: n=5 10 mg/kg bevacizumab + 125-150 mg/m ² irinotecan i.v. every 2 nd week + 150 mg/m ² oral TMZ 5 days/mo Group 2: n=2 bevacizumab + irinotecan (as group 1) Group 3: n=2 15 mg/kg bevacizumab i.v. + 90 mg/m ² oral irinotecan for 5 successive days + 1.5 mg/m ² vincristine i.v. every 3 weeks	Retrospective n=9 children with recurrent MB		11 mo median TTP 13 mo median OS n=6 PR, n=3 CR, n=3 PD, n=1 SD	n=2 grade III neutropenia, n=2 grade III thrombocytopenia, n=1 grade III elevated liver function test, n=1 grade III diarrhea
¹³¹ I-3F8 anti-GD2 ³⁵⁵ : radioimmunotherapy	Oral potassium iodide and liothyronine (5-7 days before and until 2 weeks after therapy) Max. 4 intraventricular injections (2 mg with 10 mCi/dose) + oral prior acetaminophen and diphenhydramine + oral / i.v. 0.5-1 mg dexamethasone 2x/day for 3 days + ceftriaxone 1 h post-infusion	II n=43 high-risk / recurrent MB / PNET		24.9 mo median OS, 11 mo median PFS, 5y-OS 44.9%, 6mo-PFS 57.1%	Self-limiting fever, headache, nausea, vomiting n=2 bradycardia, headache, fatigue, n=1 CSF pleocytosis
Bevacizumab ³⁷⁴	Monthly cycles (8 in median) of 10 mg/kg bevacizumab i.v. (day 1, 15) + oral 10 mg everolimus	II n=17 refractory progressive grade I-III MNG		22 mo median PFS n=15 SD (in median for 10 mo), n=1 PD	Grade 1-2 adverse events: n=9 thrombocytopenia, n=1 proteinuria, Grade 3 adverse events: n=2 proteinuria, n=1 colitis, n=1 thrombocytopenia
Cancer vaccines					
Cancer vaccines: peptide vaccination					
GAPVAC-101 ³¹⁴ : warehouse WT peptides (APVAC1; 33 HLA-A*02:01 / 26 HLA-A*24:02 ligands of 9-10 AA; 3 HLA-DR peptides of 14-18 AA) and individualized neo-epitopes (APVAC2; 19 AA)	Following surgery and radiochemotherapy; 400 µg/peptide i.d. + 75 µg GM-CSF i.d. + 1.5 mg poly-ICLC s.c.; maintenance TMZ APVAC1: 7 warehouse peptides according to transcriptome and immunopeptidome data + 2 promiscuous HLA-DR peptides + 1 viral marker peptide; 12 applications in median (n=15 patients) APVAC2: predicted neo-epitopes, naturally presented WT peptides of 9-10 AA not part of APVAC1 as 2 nd choice; 10 applications in median (n=11 patients)	I, single-arm n=15 newly diagnosed GBM (HLA-A*02:01+ / -A*24:02*)	APVAC1: 12/13 patients sustained CD8 ⁺ central memory responses; functional T cells (killing assay) APVAC2: 8/10 neo-epitope-specific multifunctional Th1 responses; 1/6 WT antigens immunogenic	29 mo median OS, 14.2 mo median PFS	Mild-to-moderate injection site reactions; n=2 anaphylactic reaction; n=1 brain edema

Treatment Reference	Therapeutic schedule	Phase # Patients	Immuno-genicity	Outcome	Adverse events
NOA-16 ³⁴⁴ : IDH1R132H (20 AA)	Peptide in Montanide s.c. + topical Imiquimod Group 1: 4-6 weeks post radiotherapy Group 2: at day 10 of 4 th TMZ cycle Group 3: post radiochemotherapy at day 10 of 1 st maintenance TMZ cycle 8 vaccinations (completed by n=29)	I, completed n=32 IDH1R132H ⁺ newly diagnosed grade III-IV astrocytoma	24/30 patients IDH1R132H-specific T cells 26/30 IDH1R132H-specific antibodies	n=4 PD; n=28 SD Planned: PFS	Grade 1 reactions, n=1 serious adverse event
ACT IV ³⁷ : Rindopepimut (13 AA EGFRvIII peptide-KLH conjugate)	Following surgery and radiochemotherapy Group 1: 500 µg rindopepimut + 150 µg GM-CSF i.d. Group 2: 100 µg KLH i.d. 2 priming doses (day 1 + 15), then monthly injections + maintenance TMZ until progression / intolerance	III EGFRvIII-expressing newly diagnosed GBM, group 1 n=369; group 2 n=372	Robust anti-EGFRvIII response (humoral)	Group 1: 20.1 mo OS, 2-y survival 30% Group 2: 20.0 mo OS, 2-y survival 19%	Mild-to-moderate injection site reactions and single cases of rash (both groups); n=2 allergic reactions; n=1 fatal pulmonary thromboembolism
PRiME ^{347,375} : PEP-CMV (26 AA human pp65 peptide + CMV glycoprotein B conjugated to KLH)	PEP-CMV + Montanide (1:1) i.d. 3 doses every 2 nd week, followed by monthly administration for a maximum of 10 y	I, ongoing n=30 recurrent MB or grade III-IV glioma	Planned: vaccine-specific T-cell and antibody responses		
Cancer vaccines: tumor cells and lysates					
ERC1671 ³⁷⁶ : autologous and allogeneic (3 GBM patients) whole inactivated tumor cells (1×10^5 - 1×10^6 cells) and lysates (1×10^5 - 1×10^6 cells)	Group 1: from 1 mo post-surgery monthly ERC1671 + 500 µg GM-CSF i.d., 50 mg / day oral cyclophosphamide for 4 days (beginning of every cycle) + 10 mg/kg bevacizumab every 2 nd week Group 2: placebo vaccination + oral placebo, bevacizumab as group 1	II, randomized recurrent GBM Group 1: n=5 Group 2: n=4	Group 1: CD4 ⁺ T-cell numbers correlate with OS	12.1/7.6 mo median OS 7.3/5.4 mo median PFS	n=4/8 grade 3 adverse events
Autologous formalin-fixed tumor ³⁷⁷	1 mo after surgery and radiochemotherapy, 1 vaccination/week (5 i.d. injections each) + 500 ng tuberculin (1:1 soluble and microparticles), maintenance TMZ	I/IIa n=24 primary GBM	n=23 tested patients: DTH response to autologous GBM tissue induced by vaccination	8.2 mo median PFS 22.2 mo median OS n=9 with strong DTH response: 29.5 mo median PFS	n=19/1 grade 1/2 injection site reactions n=3 fever, n=2 headache, n=2 seizures, n=1 appetite loss
Autologous tumor cell vaccine, stem cell transplantation and xALT ³⁷⁸	Post-surgery induction chemotherapy i.v., tumor cell vaccine + GM-CSF every 2 nd week (up to 5 doses) s.c., high-dose chemotherapy i.v., autologous stem cell transplantation, ~3 mo later autologous lymphocytes i.v. + 5 doses IL-2 every 2 nd day	II, completed n=30 recurrent / refractory primary high-grade brain tumors	Planned: deconvolute cellular anti-tumor response		
Cancer vaccines: DCs					
DCVax ^{®-L} ³⁷⁹ : autologous DCs pulsed with autologous tumor lysate	Post-surgery + radiochemotherapy, experimental treatment (day 0/10/20, then mo 2/4/8, from mo 12 half-yearly) + maintenance TMZ 150-200 mg/m ² for 5 days / mo Group 1: DCVax ^{®-L} 2.5 × 10 ⁶ DCs i.d. Group 2: placebo PBMCs Cross-over: upon progression, DCVax ^{®-L} for patients from group 2	III, cross-over design newly diagnosed GBM Group 1: n=232 Group 2: n=99 Cross-over: n=54		23.1 mo median OS (both groups incl. cross-over patients)	Grade 3-4 reactions: n=3 cerebral edema, n=2 seizures, n=1 lymph gland infection

Treatment Reference	Therapeutic schedule	Phase # Patients	Immuno-genicity	Outcome	Adverse events
Audencel ^{380,381} : autologous DCs loaded with autologous tumor lysate	Group 1: 60 Gy radiation (2 Gy/fraction) + 75 mg/m ² TMZ, adjuvant TMZ 150-200 mg/m ² for 5 days / mo Group 2: radiochemotherapy as group 1, from week 3 of adjuvant TMZ n=3 weekly, then monthly i.n. vaccinations of 1-5×10 ⁶ DCs (for 7 mo in median), 3-mo intervals until vaccines were used up	II, randomized newly diagnosed GBM Group 1: n=42 Group 2: n=34	Enhanced Th1 anti-tumor immune responses upon vaccination	28.4%/24.5% 12 mo-PFS 18.9/18.8 mo median OS	n=7 flu-like symptoms, n=6 injection site reactions
Autologous DCs pulsed with HLA-A*01-/A*02-restricted peptides derived from Her2, TRP-2, gp100, MAGE-1, AIM-2, IL13Rα2 ³³⁴	Post-surgery + radiochemotherapy I.d. injection every 2 nd week, n=3 vaccinations	I HLA-A*01+/-A*02+ patients with confirmed expression of ≥ 3 TAAs n=17 primary GBM, n=3 recurrent GBM, n=1 BSG	33% of primary GBM respond (≥ 1.5-fold increased IFN-γ secretion by peptide-stimulated PBMCs after vaccination)	Primary GBM: 16.9 mo median PFS, 38.4 mo median OS	n=9 grade 1, n=2 grade 2 toxicities
Autologous DCs loaded with an allogeneic brain tumor stem cell line ³⁸²	DCs i.d. + topical Imiquimod Group 1: 5×10 ⁶ DCs Group 2: 10×10 ⁶ DCs Group 3: 15×10 ⁶ DCs 4 vaccinations every 2 nd week + 10 monthly vaccinations	I, completed n=8 recurrent MB / GBM / ependy-moma / AAST		Planned: TTP	
Autologous DCs loaded with autologous tumor lysate ³⁸³	Post-surgery, 0.25-11.9×10 ⁶ DCs i.d. for 2 lymph node regions each + topical Imiquimod Group 1: 2 vaccinations every 2 nd week, then monthly Group 2: 5 vaccinations every 2 nd week, then monthly Group 3: 4 weekly vaccinations, monthly i.d. injection of tumor lysate (220-3,125 μg protein) Group 4: treatment as group 3, altered DC maturation	Feasibility study in children n=33 glioma, n=5 MB / PNET, n=4 ependymoma, n=3 ATRT		MB / PNET: 5.7 mo median OS; 3.7 mo median PFS	Mild injection site reactions; n=8 fatigue, n=5 headache, n=3 fever, n=1 flu-like symptoms
Adoptive T-cell transfer					
IL13Rα2-specific CAR-T cells ^{384,385} : autologous T cells transduced with IL13Rα2-specific, 4-1BB-costimulatory CAR and CD19t	3 weekly intracavitary / intratumoral / intraventricular infusions, continued until product is used up Case report: 6 intracavitary + 10 intraventricular infusions of 2-10×10 ⁶ CAR-T cells	I n=92 recurrent / refractory IL13Rα2+ GBM Case report: n=1 recurrent multifocal GBM	Planned: cytokine, CAR-T-cell, TIL levels Case report: Increased cytokine and immune cell levels in CSF	Planned: PFS, OS, RR Case report: regression of all foci for 7.5 mo (upon intraventricular administration), possible IL13Rα2-low recurrence	Case report: grade 1-2 headache, fatigue, myalgia, olfactory auras
Her2-specific CAR-T cells ³³³ : autologous EBV-, adenovirus-, and CMV-specific CD4+ and CD8+ T cells (optimized persistence) transduced with Her2-specific CAR	1×10 ⁶ – 1×10 ⁸ CAR-T cells/m ² i.v. n=11 1 infusion, n=6 multiple infusions	I n=17 progressive / recurrent Her2+ GBM	CAR-T-cell persistence for ≥ 6 weeks and ≤ 18 mo in 7/15 patients	n=1 PR; n=7 SD; n=8 PD 11.1 mo median OS from 1 st infusion 24.5 mo median OS from diagnosis	n=2 grade 2 seizures, n=1 grade 2 headache
ALECSAT ³⁸⁶ : autologous CTLs and NK cells	3 i.v. infusions of 10×10 ⁶ -1×10 ⁹ activated and expanded cells	I, completed n=23 recurrent GBM		Planned: RR	

Treatment Reference	Therapeutic schedule	Phase # Patients	Immuno-genicity	Outcome	Adverse events
Re-MATCH³⁸⁷ : TTRNA-loaded xALT and TTRNA-loaded autologous DCs	Following myeloablative chemotherapy 1 dose TTRNA-xALT i.v. (3×10^7 /kg) 3 doses TTRNA-DCs i.d. (1×10^7 ; every 2 nd week)	I/II, ongoing I: n=9 II: n=35 Recurrent MB, PNET	Planned: T-cell and antibody response, cytokine profile, TLR activation, lymphocyte subset phenotypes	Planned: PFS, OS, RR	
Her2-specific CAR-T cells³⁵³ : autologous CD4 ⁺ and CD8 ⁺ T cells transduced with Her2-specific CAR and EGFRt	2 cycles of 1 weekly infusion for 3 weeks each, 1 week off between cycles Group 1: tumor cavity infusion Group 2: ventricular infusion	I, ongoing n=36 children / adolescents with Her2 ⁺ recurrent / refractory CNS tumors		Planned: RR	
EGFR806-specific CAR-T cells³⁵⁶ : autologous CD4 ⁺ and CD8 ⁺ T cells transduced with EGFR-specific CAR and EGFRt	Intra-patient dose escalation supratentorial tumors: tumor cavity infusion infratentorial / leptomeningeal tumors: ventricular infusion	I, ongoing n=36 children / adolescents with EGFR ⁺ recurrent / refractory CNS tumors		Planned: RR	
NY-ESO-1-specific T cells³⁶¹ : autologous T cells transduced with TCR recognizing HLA-A*02:01-presented NY-ESO-1	Conditioning non-myeloablative lymphodepleting chemotherapy, 7 days later T cells + IL-2 720,000 IU/kg i.v. every 8 h for max. 5 days	II, ongoing NY-ESO-1 ⁺ HLA-A*02:01 ⁺ recurrent / refractory MNG, melanoma, breast / non-small cell lung / hepatocellular cancer		Planned: clinical response	
GRm13Z40-2 CAR-T cells^{271,363} : allogeneic glucocorticoid-resistant ganciclovir-sensitive CTL line expressing IL-13-Zetakine (IL13Ra2-specific CAR) and HyTK	Bi-weekly i.t. infusion (day 1, 3) + IL-2 i.t. (day 1/2-5) until progression / toxicity \pm dexamethasone	I, completed Recurrent / refractory brain tumors	Planned: anti-GRm13Z40-2 responses (allograft rejection)		
Oncolytic viruses					
ParvOryx01^{320,388} : replication-competent parvovirus H-1	Group 1: 1 i.t. injection (50% of total dose), 10 days later tumor resection + virus application (remaining 50%) in resection cavity Group 2: 5 i.v. infusions (10% of total dose each), 2 nd dose as group 1 Dose escalation: 1×10^6 - 1×10^9 pfu total dose in both groups	I/IIa Recurrent / refractory GBM Group 1: n=12 Group 2: n=6	n=18 dose-dependent anti-viral antibodies, n=9 (of 12 tested patients) anti-viral CD8 ⁺ T-cell responses n=3 (of 6 tested patients) anti-tumor T-cell response	n=12 PD 27% 6-mo PFS, 3.7 mo median PFS 15.5 mo median OS	n=1 consciousness upon administration
G207³⁸⁹ : oncolytic herpes simplex 1 virus	1.15×10^9 pfu split into 1 pre- (2-5 days) and 1 post-surgery dose	Ib n=6 recurrent GBM	n=5 virus-infected tumor cells n=4 increased CD3 ⁺ TIL numbers	3 mo median PFS 23 mo median OS from primary diagnosis 6.6 mo median OS from administration	n=2 seizure, n=2 hemiparesis, n=2 fever, n=1 somnolence, n=1 motor neuropathy, n=1 neglect, n=1 decreased mental status

Treatment Reference	Therapeutic schedule	Phase # Patients	Immuno-genicity	Outcome	Adverse events
Delta-24-RGD ³⁹⁰ : replication-competent adenovirus	Intracerebral infusion of 10 ⁷ / 10 ⁸ / 10 ⁹ / 10 ¹⁰ / 3×10 ¹⁰ / 10 ¹¹ virus particles	I/II n=30 recurrent GBM n=3 per dose level + n=6-9 after dose escalation treated with 10 ¹¹ virus particles		Planned: PFS, 6mo-PFS, OS, 6mo-OS, 12mo-OS	
G207 ³⁹¹ : oncolytic herpes simplex 1 virus	1 st cohort: 1 intracranial infusion (close to tumor site) 2 nd cohort: 1 intracranial infusion + 5 Gy after 24 h	I, ongoing n=15 children with recurrent / refractory cerebellar brain tumors	Planned: HSV-1 antibody titers	Planned: PFS, OS, performance status	
PVSRIPO ³⁹² : oncolytic polio-rhinovirus recombinant	1 i.t. infusion	Ib, ongoing n=12 children / adolescents with recurrent supratentorial grade III glioma / GBM / MB / ATRT		Planned: 24mo-OS	

3 Immunopeptidomics

3.1 The immunopeptidome

The entirety of peptides presented by the HLA molecules of a cell or tissue is designated as the immunopeptidome, HLA ligandome, or HLA peptidome. Isolating these HLA ligands and employing subsequent liquid chromatography-coupled tandem mass spectrometry (LC-MS/MS) is a way to comprehensively view the antigenic signature of human neoplasms. Here, mass spectrometry (MS) represents the central component warranting unbiased peptide identification. In contrast to epitope prediction-based studies, the major strength of immunopeptidomics as approach to define candidate targets for cancer immunotherapies is focusing on those peptides that are naturally presented and thus of pathophysiological relevance.¹⁷⁷ Target discovery approaches based on genome or transcriptome sequencing with subsequent *in silico* prediction of HLA ligands yield a considerable number of false positives while missing others. This is reasoned by the poor stoichiometric relationship between RNA transcripts and HLA-presented peptides. The immunopeptidome represents an autonomous layer strongly influenced by the antigen processing machinery and can thus not be expected to mirror the proteome or even the transcriptome.^{177,393-396} Moreover, it has become evident that not the entire antigen translates into HLA ligands, but mainly so-called hotspot regions give rise to HLA-presented peptides thus shaping the immunopeptidome.^{177,397-400}

As shown e.g. for renal cell and epithelial ovarian carcinoma, glioblastoma, acute myeloid and chronic lymphocytic leukemia, or multiple myeloma, downregulation of surface HLA expression by tumors is far less common than originally expected and should thus not be designated a hallmark of cancer immune evasion anymore.^{149,177,315,401-405} For immuno-peptidomics, primary human samples clearly outcompete artificial systems, especially permanent monoclonal cell lines, as they substantially more accurately reflect the biology of human malignancies, the genetical diversity among patients, and provide a high degree of translationability into individualized treatment attempts.¹⁷⁷ Analyses of the HLA peptidome can be performed with bulk or dissociated tumor tissue,^{149,401} primary cell lines established from solid tumors,⁴⁰⁶ leukemia cells,⁴⁰³⁻⁴⁰⁵ cancer cell-derived soluble HLA molecules,⁴⁰⁷ or extracellular vesicles as starting material.^{177,408} Immuno-peptidomics can in principle cover all sources of HLA ligands and associated PTMs, whereby the majority of HLA ligands originates from WT canonical proteins. Cryptic peptides (2.3.1) were estimated to contribute with 6.5-13% to the entirety of HLA ligands.^{177,179} Proving neo-antigenic peptides to be naturally presented on cancer tissue by LC-MS/MS, has remained a major obstacle.^{177,409} The proportion of neo-antigenic HLA ligands is expected to be even smaller than that of cryptic ones, with only one mutated peptide being on average identified among 1.1×10^4 HLA class I peptides and from 1,800 non-synonymous somatic mutations.¹⁷⁷

In recent years, the concomitant development of orbitrap mass analyzers, chromatographic systems with enhanced performance, and algorithms for automated spectra interpretation have vastly improved speed, sensitivity, resolution, and mass accuracy of data acquisition and/or data analysis. Altogether, this enabled the fast ascent of immuno-peptidomics as method of choice for state-of-the-art antigen discovery studies.¹⁷⁷ Nowadays, it is possible to extract and identify several thousands of unique HLA ligands from a single primary tissue sample.^{397,401,410} Four immuno-peptidomic studies in glioblastoma have been performed, whereby not the entire datasets have been made publicly available.^{149,313,402,403} The published content of one study was even restricted to those HLA-A*02:01, -A*24:02, and -DR-presented peptides applied in a clinical trial of peptide vaccination (GAPVAC-101).³¹⁴ Two of the remaining datasets were acquired on a time of flight mass spectrometer (Q-TOF) or an LTQ Orbitrap XL, allowing the presumption that peptide identifications will increase when using another device such as the Orbitrap Fusion Lumos with higher resolution and scan rate. Moreover the number of primary samples came up to only four and nine, respectively.^{149,411} The fourth publication focuses on comparing the immuno-peptidome of ten glioblastoma tissues to that of 142 samples of soluble HLA molecules obtained from 52 glioblastoma patients as well as 30 ankylosing spondylitis patients and 6 healthy donors as control. These data were also searched for known CTAs, however, tissue samples were part of the same cohort as used for the GAPVAC-101 project.^{314,396} So far, no study investigating the immuno-peptidome of medulloblastoma has been published. HLA class I ligands have been isolated from twelve primary meningioma samples. These data were part of a training dataset (n=2) and used as benchmark dataset (n=10) for a model predicting length distribution and binding specificity across HLA class I allotypes and not reviewed for potential targets for cancer immunotherapy.⁴¹²

3.2 Materials and methods for immunopeptidome analyses

3.2.1 Materials

Substantial parts of the material lists presented on the following pages are congruent with listings in 'Freudenmann LK. Mapping the HLA Ligandome of Primary *versus* Recurrent Disease in Glioblastoma Multiforme by Mass Spectrometry'¹⁰.

Chemicals

Acetonitrile CH ₃ CN (AcN; MS grade)	J.T.Baker®, Center Valley (USA)
Baker water H ₂ O (MS grade)	J.T.Baker®, Center Valley (USA)
CHAPS 3-[(3-cholamidopropyl) dimethyl-ammonio]-1-propanesulfonate 1.2% (w/v)	PanReac AppliChem, Darmstadt (Germany)
Cyanogen bromide (CNBr)-activated sepharose 4B	GE Healthcare, Little Chalfont (UK)
Dimethyl sulfoxide (DMSO) (CH ₃) ₂ SO	Merck Millipore, Billerica (USA)
Dulbecco's phosphate-buffered saline (DPBS) without CaCl ₂ and MgCl ₂	Gibco™ / Thermo Fisher Scientific, Waltham (USA)
Formic acid (FA; MS grade)	Merck, Darmstadt (Germany)
Glycine	Merck, Darmstadt (Germany)
Hydrogen chloride HCl	Carl Roth, Karlsruhe (Germany)
Phosphate-buffered saline (PBS) without CaCl ₂ and MgCl ₂	Produced in-house by Claudia Falkenburger
Protease inhibitor cocktail tablets	cOmplete™ / Roche, Basel (Switzerland)
Sodium bicarbonate NaHCO ₃	Merck Millipore, Billerica (USA)
Sodium chloride NaCl	VWR Chemicals / VWR International, Leuven (Belgium)
Sodium hydroxide NaOH	Carl Roth, Karlsruhe (Germany)
Trifluoroacetic acid C ₂ HF ₃ O ₂ (TFA; MS grade)	Sigma-Aldrich, St. Louis (USA)

Solutions and buffers

A*	0.1% TFA in Baker H ₂ O
AB _E	32.5% AcN / 0.2% TFA in Baker H ₂ O
A _{Load}	1% AcN / 0.05% TFA in Baker H ₂ O
Coupling buffer	0.5 M NaCl / 0.1 M NaHCO ₃ in ddH ₂ O adjusted to pH 8.3 with HCl (at room temperature)
Lysis buffer (1×)	2× lysis buffer / PBS mixed 1:1
Lysis buffer (2×)	33 ml PBS / 0.4 g CHAPS / 1 protease inhibitor cocktail tablet

Antibodies

Table 3. HLA class I- or II-specific murine monoclonal antibodies employed for HLA-immunoprecipitation. All antibodies were kindly produced in-house by Claudia Falkenburger using murine B lymphocyte hybridoma cells.

Clone	Isotype	Specificity	Reference
W6/32 (ATCC® HB-95™)	IgG _{2α}	HLA-A, -B, -C	413
L243 (ATCC® HB-55™)	IgG _{2α}	HLA-DR	414
Tü39	IgG _{2α}	HLA-DP, -DQ, -DR	415

Chapter 1: Immunopeptidomics

Consumable supplies

Acclaim® C18 PepMap RSLC column 50 µm × 25 cm	Thermo Fisher Scientific, Waltham (USA)
Acclaim® C18 PepMap RSLC column 75 µm × 2 cm	Thermo Fisher Scientific, Waltham (USA)
Amicon-Ultra 0.5 ml centrifugal filter unit 10 kDa	Merck Millipore, Billerica (USA)
Amicon-Ultra 0.5 ml centrifugal filter unit 3 kDa	Merck Millipore, Billerica (USA)
DeckWorks® low binding pipet tips 1-200 µl	Corning, Corning (USA)
Eppendorf adapter for rotors with 15 ml bore holes (allows using 5 ml conical tubes)	Eppendorf, Hamburg (Germany)
Eppendorf Safe-Lock tubes 1.5 ml	Eppendorf, Hamburg (Germany)
Eppendorf Safe-Lock tubes 2 ml	Eppendorf, Hamburg (Germany)
Eppendorf screw cap tubes 5 ml	Eppendorf, Hamburg (Germany)
Falcon tubes 15 ml	Greiner Bio-One, Frickenhausen (Germany)
Falcon tubes 50 ml	Greiner Bio-One, Frickenhausen (Germany)
Maxymum Recovery® universal filter tips 1000 µl	Axygen, Union City (USA)
Maxymum Recovery® universal tips 0.5-10 µl	Axygen, Union City (USA)
Millex®-SV low protein binding PVDF Durapore® syringe filter unit 5.0 µm	Merck Millipore, Billerica (USA)
Petri dishes ø 30 mm	Greiner Bio-One, Frickenhausen (Germany)
Petri dishes ø 60 mm	Greiner Bio-One, Frickenhausen (Germany)
Polypropylene autosampler vials 250 µl	Thermo Fisher Scientific, Waltham (USA)
Polypropylene caps for 250 µl vials	Thermo Fisher Scientific, Waltham (USA)
Protein LoBind tubes 1.5 ml	Eppendorf, Hamburg (Germany)
Protein LoBind tubes 2 ml	Eppendorf, Hamburg (Germany)
SafeSeal® SurPhob filter tips 1250 µl	Biozym Scientific, Hessisch Oldendorf (Germany)
Surgical disposable scalpels	Aesculap AG, Tuttlingen (Germany) / B. Braun Melsungen AG, Melsungen (Germany)
Syringe Luer-Lok™ Tip 20 ml	Becton Dickinson, Drogheda (Ireland)
Syringe Luer-Lok™ Tip 30 ml	Becton Dickinson, Drogheda (Ireland)
Syringe Luer-Lok™ Tip 50 ml	Becton Dickinson, Drogheda (Ireland)
ZipTip _{C18} ® Pipette Tips with 0.6 µl resin bed volume	Merck Millipore, Billerica (USA)

Basic equipment

Double socket, 13 mm span	neoLab Migge, Heidelberg (Germany)
Econo-Column® low pressure glass chromatography columns, 0.5 cm × 5 cm	Bio-Rad, München (Germany)
Econo-Column® low pressure glass chromatography columns, 1 cm × 5 cm	Bio-Rad, München (Germany)
Hamilton syringe 50 µl	Sigma-Aldrich, St. Louis (USA)
Hamilton syringe 500 µl	Sigma-Aldrich, St. Louis (USA)
Lyophilization glass 600 ml, 105 mm outer diameter	Martin Christ Gefriertrocknungsanlagen, Osterode am Harz (Germany)
Micro pestle for 1.5 ml Eppendorf tubes	Carl Roth, Karlsruhe (Germany)
Polypropylene Luer adapters with 1/8" lock rings and 1/8" teflon tubing	Cole-Parmer, Vernon Hills (USA)
Potter glass	Wheaton, Milville (USA)

Chapter 1: Immunopeptidomics

Rotilabo® tripod mount, 250 mm x 142 mm, M10 threaded hole	Carl Roth, Karlsruhe (Germany)
Rotilabo® tripod rod, 600 mm, M10 thread	Carl Roth, Karlsruhe (Germany)
Two-way stopcocks with female to male Luer fitting	Bio-Rad, München (Germany)
Tygon® 3350 2 stopper 104 mm distance, 2.06 mm inner diameter, 381 mm silicone tube	Hirschmann, Neckartenzlingen (Germany)
Tygon® 3350, 2.4 mm inner diameter, 0.8 mm wall thickness, 15 m silicone tube	neoLab Migge, Heidelberg (Germany)
Universal stand clamp Remanit 4301, 240 mm length, 90 mm span	Carl Roth, Karlsruhe (Germany)

Devices

Autosampler WPS-3000PL (RS) UltiMate™ 3000 Series	Dionex, Sunnyvale (USA)
Biofuge Pico centrifuge	Heraeus, Pforzheim (Germany)
Branson sonifier 250	Emerson Industrial Automation, Danbury (USA)
Chiller ThermoFlex 900	Thermo Fisher Scientific, Waltham (USA)
DURAN® beaker glass 1000 ml	Schott, Wertheim (Germany)
E2M28 rotary vacuum pump	Edwards, Feldkirchen (Germany)
Freeze dryer VaCo 2	ZIRBUS technology, Bad Grund (Germany)
IKA® KS 250 basic shaker	Sigma-Aldrich, St. Louis (USA)
IKA® MS 3 basic vortex mixer	Sigma-Aldrich, St. Louis (USA)
KF-2-110 cold trap	H. Saur Laborbedarf, Reutlingen (Germany)
LTQ Orbitrap XL	Thermo Fisher Scientific, Waltham (USA)
Megafuge 1.0 R centrifuge	Heraeus, Pforzheim (Germany)
MIKRO 200 R centrifuge	Andreas Hettich, Tuttlingen (Germany)
Nano/Cap System NCS-2500RS UltiMate™ 3000 Series	Dionex, Sunnyvale (USA)
Nano/Pump System NCP-3200RS UltiMate™ 3000 Series	Dionex, Sunnyvale (USA)
Nanospray Flex™ ion source	Thermo Fisher Scientific, Waltham (USA)
Nanospray ion source	Thermo Fisher Scientific, Waltham (USA)
Orbitrap Fusion Lumos	Thermo Fisher Scientific, Waltham (USA)
Potter-Elvehjem tissue homogenizer	Omni International, Kennesaw (USA)
RC6 chemistry-HYBRID-vacuum-pump	vacuubrand, Wertheim (Germany)
rotarus® smart 30 peristaltic pump	Hirschmann, Neckartenzlingen (Germany)
RV8 oil-sealed rotary high vacuum pump	Edwards, Feldkirchen (Germany)
Sogevac® single-stage, oil-sealed rotary vane pump SV 65 BIFC	oerlikon leybold vacuum, Köln (Germany)
Solvent Rack SRD-3x00 UltiMate™ 3000 Series	Dionex, Sunnyvale (USA)
SpeedVac vacuum concentrator	BACHOFER, Reutlingen (Germany)
Tube rotator L28	LABINCO, Breda (Netherlands)
Ultra-low freezer DF8517GL	Skadi, Wilmington (USA)
Ultrasonic cleaner	JSP, Los Angeles (USA)
VM-300 vortex mixer	neoLab Migge, Heidelberg (Germany)

Software and databases

Allele Frequency Net Database	416
area_picker.R (2015)	In-house R script, written by Linus Backert
BioVenn	417
Catalogue of Somatic Mutations in Cancer (COSMIC)	418
Chromeleon™ 6.80 Chromatography Data System	Thermo Fisher Scientific, Waltham (USA)
DAVID Bioinformatics Resources 6.8	419,420
DCMS Link 2.14 for Xcalibur	Thermo Fisher Scientific, Waltham (USA)
DB Browser for SQLite 3.11.2	Open-source software
dbSNP	421
Discoverer Daemon 1.4	Thermo Fisher Scientific, Waltham (USA)
GraphPad Prism 6.0	GraphPad Software, La Jolla (USA)
Genotype-Tissue Expression (GTEx) database	422
HLA-C motifs	423
Hotspots.R (2018)	In-house R script, written by Leon Bichmann
Inkscape 0.92.4	Open-source software
Immune Epitope Database (IEDB): population coverage	424
In-house HLA class I SQL database (version 2019/04/25)	<p><u>Benign primary samples (n=418):</u> n=10 adrenal glands, 10 aortae, 98 peripheral blood samples, 27 bone marrows, 12 brains, 11 cerebella, 8 colons, 10 esophagi, 4 gall bladders, 11 hearts, 12 kidneys, 14 livers, 14 lungs, 17 lymph nodes, 5 mammae, 10 skeletal muscles, 31 ovaries, 9 pancreases, 18 prostates, 11 skins, 12 small intestines, 1 spinal cord, 12 spleens, 10 stomachs, 13 thyroid glands, 9 tongues, 7 tracheae, 10 urinary bladders, 2 uteri</p> <p><u>Malignant primary samples (n=874):</u> n=4 acute lymphocytic leukemias, 97 acute myeloid leukemias, 1 anaplastic astrocytoma, 10 atypical teratoid rhabdoid tumors, 3 bladder cancers, 59 breast cancers, 98 chronic lymphocytic leukemias, 21 chronic myeloid leukemias, 38 colorectal cancers, 23 ependymomas, 6 esophageal cancers, 4 fibroses, 30 gastric cancers, 1 gastrointestinal stromal tumor, 2 germ cell tumors, 50 glioblastomas, 28 hepatocellular carcinomas, 1 leiomyosarcoma, 1 melanoma, 33 meningiomas, 1 merkel-cell carcinoma, 13 multiple myelomas, 24 neuroblastomas, 18 non-small cell lung carcinomas, 1 oligodendroglioma, 28 oropharyngeal squamous cell carcinomas, 3 osteosarcomas, 139 ovarian carcinomas, 1 pancreatic cancer, 1 paraganglioma, 1 parotis carcinoma, 13 polycythemia veras, 8 primary myelofibroses, 28 prostate carcinomas, 79 renal cell carcinomas, 1 sarcoma, 5 subependymomas</p> <p>The number of leukemia samples includes few genetic duplicates due to multiple HLA ligand isolations from sorted cell populations or treated cells</p>

Chapter 1: Immunopeptidomics

In-house HLA class II SQL database
(version 2019/04/25)

Benign primary samples (n=364):

n=10 adrenal glands, 10 aortae, 85 peripheral blood samples, 23 bone marrows, 12 brains, 11 cerebella, 8 colons, 10 esophagi, 4 gall bladders, 11 hearts, 13 kidneys, 13 livers, 14 lungs, 17 lymph nodes, 5 mammae, 10 skeletal muscles, 2 ovaries, 9 pancreases, 6 prostates, 12 skins, 12 small intestines, 1 spinal cord, 12 spleens, 9 stomachs, 4 thymi, 13 thyroid glands, 9 tongues, 7 tracheae, 10 urinary bladders, 2 uteri

Malignant primary samples (n=626):

n=2 acute lymphocytic leukemias, 125 acute myeloid leukemias, 1 anaplastic astrocytoma, 3 bladder cancers, 59 breast cancers, 69 chronic lymphocytic leukemias, 20 chronic myeloid leukemias, 2 colorectal cancers, 23 ependymomas, 4 fibroses, 41 glioblastomas, 4 hepatocellular carcinomas, 1 melanoma, 33 meningiomas, 13 multiple myelomas, 16 neuroblastomas, 18 non-small cell lung carcinomas, 1 oligodendroglioma, 28 oropharyngeal squamous cell carcinomas, 3 osteosarcomas, 78 ovarian carcinomas, 1 pancreatic cancer, 1 paraganglioma, 1 parotis carcinoma, 11 polycythemia veras, 8 primary myelofibroses, 54 renal cell carcinomas, 1 sarcoma, 5 subependymomas

The number of leukemia samples includes few genetic duplicates due to multiple HLA ligand isolations from sorted cell populations or treated cells

jVenn

425

Ligandosphere

In-house software

List of 366 established TAAs and CTAs collected and translated into UniProt accessions by Lena Mühlenbruch and Michael Ghosh from the following resources: Cancer-related proteins deposited in UniProt (search term: disease:cancer AND reviewed:yes AND organism:"Homo sapiens (Human) [9606]"; 2017/09/01) Cheever *et al.* (2009) CTDdatabase (2019/08/16) Cancer Immunity Peptide Database (version: 2016)

86

426

427

191

LTQ Tune Plus 2.5.5 SP2

Thermo Fisher Scientific, Waltham (USA)

MHC Motif Viewer

428

Microsoft Office 2010 and Professional Plus 2016

Microsoft Corporation, Redmond (USA)

NetMHC 4.0 Motif Viewer

429

NetMHCpan-4.0

430-432

Notepad++ v7.8.1

Open-source software

Orbitrap Fusion Lumos Tune Application 2.1.1565.23

Thermo Fisher Scientific, Waltham (USA)

Percolator 2.04 (2012)

Department of Genome Science at the University of Washington, Seattle (USA)

PhosphoMotif Finder of the Human Protein Reference Database

433

Proteome Discoverer 1.4.1.14

Thermo Fisher Scientific, Waltham (USA)

replicate_merger.R (2016)

In-house R script, written by Linus Backert

RStudio 3.4.2

Open-source software

Chapter 1: Immunopeptidomics

saturation_analysis.R (2016)	In-house R script, written by Linus Backert
Scintilla and SciTE	Open-source software
SEQUEST search engine	434
<u>Scripts for complex SQL queries:</u>	In-house R scripts, written by Leon Bichmann
sql_protein_benign_counter_classI_groupedtissue.R (2017)	
sql_protein_benign_counter_classII_groupedtissue.R (2017)	
sql_protein_counter_malignant_classI.R (2017)	
sql_protein_counter_malignant_classII.R (2017)	
sql_sequence_counter_benign_classI_exactMatch_case-insensitive.R (2018)	
sql_sequence_counter_benign_classII_exactMatch_case-insensitive.R (2018)	
sql_sequence_counter_malignant_classI_exactMatch_case-insensitive.R (2018)	
sql_sequence_counter_malignant_classII_exactMatch_case-insensitive.R (2018)	
Skyline	435
SYFPEITHI	436
UniProt	86
Venn Diagram Plotter 1.5.5228.29250	Open-source software
volcano_plotter_from_area_all_conds_hardcoded_lim2_new_style.R (2015)	In-house R script, written by Linus Backert
Xcalibur 2.1.0.1160 with Foundation 1.0.2.65	Thermo Fisher Scientific, Waltham (USA)
Xcalibur 2.2 SP1 with Foundation 2.0 SP1	Thermo Fisher Scientific, Waltham (USA)
Xcalibur 4.0.27.10 with Foundation 3.1 SP1	Thermo Fisher Scientific, Waltham (USA)

3.2.2 Methods

Following the pioneering work of Kirsten Falk and Olaf Rötzschke in the laboratory of Hans-Georg Rammensee, the protocol underwent several optimization processes, but core components have been retained. In brief, the workflow is composed of seven steps: preparation of tissue or cell lysate, immunoaffinity chromatography to pull down HLA-peptide complexes, acidic elution of HLA molecules and their ligands, purification of HLA ligands, peptide identification by LC-MS/MS, and subsequent data analysis (Figure 7).^{437,438} The major part of the protocol presented on the following pages resembles the methods section in 'Freudenmann LK. Mapping the HLA Ligandome of Primary *versus* Recurrent Disease in Glioblastoma Multiforme by Mass Spectrometry'¹⁰.

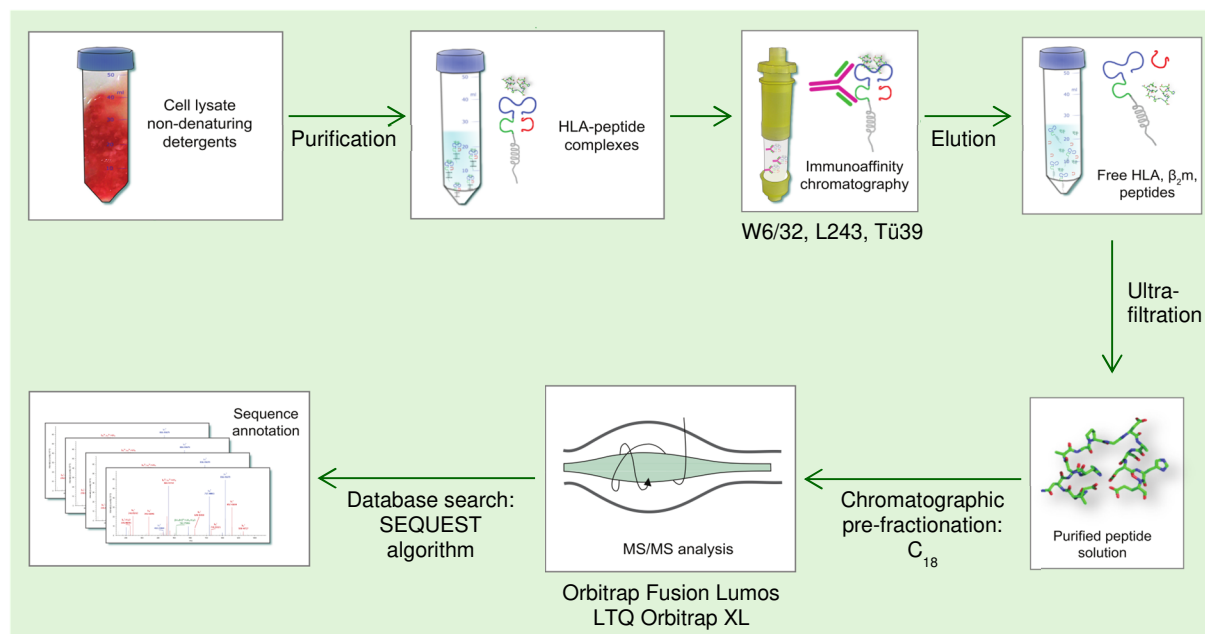


Figure 7. Isolation and analysis of HLA ligands from intracranial neoplasias. Here, icons depict schematics of HLA class I-peptide complexes. Modified from Freudenmann *et al.*¹⁷⁷

Preparation of lysate from tumor tissue

All steps for preparation of tissue lysate from fresh frozen surgical specimens were performed at 4°C in the cold room. The entire amount of tissue was never used up for immuno-peptidomics alone in order to perform parallel analyses including whole exome (glioblastoma) and RNA sequencing (glioblastoma and medulloblastoma), DNA methylation profiling (planned for glioblastoma and medulloblastoma), and HLA typing (all samples) from the identical piece of tissue. As mentioned in 1.2, the degree of intratumoral heterogeneity is especially high in glioblastoma. In order to subject cells of every subclone – as far as possible – to every analytical method, tissue was chopped first and tiny pieces were then collected to either isolate DNA and RNA (≥ 20 mg) or HLA ligands. Since RNA degradation sets in as soon as tissue thaws, samples were kept on dry ice throughout almost the whole time and immediately returned to -80°C after tissue collection for sequencing until analysis at CeGaT GmbH (Tübingen).

Tissue for the preparation of cell lysate was weighed in appropriately sized petri dishes (30 or 60 mm in diameter). Having added one volume of 2× lysis buffer, tissue was chopped finely using forceps and scalpel. Tissue was transferred into a potter glass cleaned with 70% ethanol, dH₂O, and flushed out with PBS before. Two volumes of 1× lysis buffer each were used to rinse the petri dish twice and added to the potter glass as well. With a Potter-Elvehjem tissue homogenizer, samples were mashed for approximately 2 min, whereby the potter glass was kept on ice to avoid warming of the lysate. The latter was transferred into appropriately sized tubes (5 / 15 / 50 ml) and the potter glass was rinsed twice with two volumes of 1× lysis buffer each, that were subsequently added to the lysate. In case a substantial amount of sample was still left in the potter glass, another washing step – if necessary, with a slightly increased volume of lysis buffer – was performed. Samples were then incubated on the shaker at 200 revolutions per minute (rpm) for 1 h. To further disrupt cell membranes, five cycles of pulsed sonification (duty cycle output control = 5; 60% duty cycle) each lasting 20 s were applied to

the samples. To prevent lysates from warming, tubes were kept on ice and cool-down breaks of 20 s were performed after every cycle. After another incubation on the shaker for 1 h, samples were centrifuged at 4,000 rpm and 4°C for 1 h. For lysates prepared from ≥ 1 g of tissue, centrifugation of the supernatant was repeated once. Employing 5.0 μm low protein binding filter units, samples were subsequently sterile filtrated into appropriately sized tubes (5 / 15 / 50 ml).

For tissue samples weighing less than 150 mg, tissue was manually minced with a micro pestle in 1.5 ml Eppendorf tubes instead of using the Potter-Elvehjem tissue homogenizer. Sonification was performed in an ultrasonic bath for five times 20 s with cool-down breaks on ice of 20 s each in between. Moreover, these samples were spun down only once at 13,000 rpm and 4°C for 1 h. Lysates with a volume of less than 2 ml (corresponds to ~ 222 mg tissue) were not filtered before being directly injected into either only the upper column equipped with W6/32 antibodies or into both columns. The outflow of the lower column with HLA class II-specific antibodies was straightly transferred to the upper column instead of being collected in and aspirated from a Falcon tube in between.

Isolation of HLA ligands by immunoaffinity chromatography

Immunoaffinity chromatography requires a solid phase, CNBr sepharose, to which HLA-specific antibodies are bound. Per 1 mg of antibody, 40 mg of CNBr-activated sepharose were weighed in and resuspended in 45 ml 1 mM HCl (in ddH₂O) by inverting for five times. At room temperature, the suspension was rotated for 1 h to be then spun down at 300 rpm and without break for 4 min. Having carefully decanted the supernatant, 20 ml coupling buffer and the respective antibody were added. Falcon tubes in which the antibodies had been stored were rinsed with ~ 10 ml of coupling buffer, added to the sepharose as well, and the total volume was adjusted to 45 ml with coupling buffer. After inverting for five times, tubes were rotated for 2 h and centrifuged as previously. The sepharose-antibody matrix was resuspended in 45 ml 0.2 M glycine (in ddH₂O) and rotated for 1 h to reduce unspecific binding activity. Sepharose was pelleted, washed twice with DPBS, adjusted with DPBS to a concentration of 1 mg antibody/40 mg sepharose per ml, and stored at 4°C. Newly coupled antibodies were only approved for patient samples upon passing quality control comprising isolation of HLA-peptide complexes from a standardized lysate (equivalent to 4.5×10^7 cells) prepared from the B-lymphoblastoid cell line JY.

Glass chromatography columns were cleaned thoroughly with 70% ethanol and afterwards with dH₂O by means of a 50 ml syringe. Before assembly of the chromatographic system in the cold room, possible sample residues were removed from peristaltic pumps, cassettes as well as tubes and the latter were examined for tightness. All cassettes mounted in the same peristaltic pump were manually adjusted to an equal flow rate at 10 rpm pump speed. For each sample, two columns were set up one above the other, so that the flowthrough of the upper column equipped with HLA class I-specific antibodies directly dropped into the lower column equipped with HLA class II-specific antibodies. By pipetting, sepharose-antibody matrices were resuspended and a minimum volume of 1 ml was added to each column. To precipitate HLA class II-peptide complexes, the antibodies L243 and Tü39 were mixed 1:1. For samples weighing more than 1 g, the amount of antibody was proportionally increased to an equivalent

of 1 mg per 1 g of tissue. Econo-Columns[®] with a diameter of 0.5 cm have a maximum capacity of 3 mg antibody-sepharose matrix so that columns with a diameter of 1 cm were used for samples above 3 g. The peristaltic pump was connected to the upper column equipped with W6/32 so that PBS flowed through both columns into a waste beaker glass. The liquid phase was changed to 1× lysis buffer and the system was subsequently cycled until preparation of tissue lysates had been finished.

Having linearized the system again, filtrated samples were aspirated from tubes and the system was cycled as soon as the lysate reached the lower column or before the tube ran dry, respectively. To manually load small samples, liquid was drained from either the upper or both chromatography columns and the lysate was directly pipetted onto the sepharose-antibody matrix. In order to prevent technical artefacts, samples subjected to relative quantitation of HLA ligands later on, were always run with the same peristaltic pump and under use of the identical antibody batches. Immunoaffinity chromatography was then performed overnight. To wash columns the next morning, PBS was pumped linearly through the system for 30 min followed by ddH₂O for 1 h. Having let columns run dry and washed the lids with ddH₂O in a beaker glass, 1 µl 10% TFA per 1 mg antibody and 100 µl 0.2% TFA were added with a 50 µl or a 500 µl Hamilton syringe, respectively. In case of large tissue samples, the amount of 0.2% TFA was increased until the entire antibody-sepharose matrix was covered. In a rack on the shaker, columns were incubated at 300 rpm and 4°C for 30 min. Using an air-filled 50 ml syringe, HLA molecules and peptides were eluted into 1.5 or 2 ml Protein LoBind Eppendorf tubes. This procedure was repeated for a total of four times, whereby incubation time on the shaker was reduced to 15 min and 0.2% TFA was used solely from the second to the fourth elution. Having completed the elution of HLA-peptide complexes, chromatography columns were cleaned thoroughly with dH₂O, 70% ethanol, and again with dH₂O using a 50 ml syringe.

Purification of peptides and preparation for mass spectrometry

In parallel to washing the chromatography columns and later shaking them for 30 min, Amicon filter units to separate peptides from HLA molecules were prepared. HLA class I peptides were ultrafiltrated at a pore size of 3 kDa, whereas longer HLA class II peptides were purified at a pore size of 10 kDa. As leak test, filters were filled with 500 µl Baker H₂O and spun down at 13,000 rpm and room temperature for 7 min. Remaining volume inside all filters of the same pore size was then compared and filter units with significantly divergent fill level were replaced. After discarding the flowthrough and banging the filters upside down onto paper towels to empty them, four more washing steps were performed. Centrifugation time was increased to 15 min for all of them. Washing was performed by sequentially adding 500 µl 0.1 N NaOH, Baker H₂O, and 0.2% TFA. 500 µl 0.2% TFA were again pipetted into the filter unit and run through only upon the elution of HLA-peptide complexes had been completed.

Eluates were centrifuged at 13,000 rpm and 4°C for 5 min, before not more than 500 µl supernatant were filled into the respective filter inlay which had been placed into a new collection tube. Amicon filters were spun down, until the volume had completely run through and the flowthrough was collected in appropriately sized Protein LoBind Eppendorf tubes (1.5 / 2 ml). This was repeated until the entire amount of eluate had been ultrafiltrated. Predominantly to elute hydrophobic peptides from the membrane, filters were then washed

with 450 μl AB_E which was subsequently added to the sample. An additional loose lid was perforated and placed on each Protein LoBind tube. These were frozen to the core at -80°C for at least 1 h. Peptide extracts were subsequently lyophilized to a target volume of ~ 30 μl .

Desalting of peptide solutions was achieved by reversed-phase liquid chromatography using ZipTip_{C18}[®] Pipette Tips.⁴³⁹ During the entire procedure, a volume of 10 μl was repetitively aspirated and dispensed in different solvents as well as the sample, whereby it was strictly avoided to introduce any air into the C₁₈ matrix. First, the resin was cleansed by quickly pipetting up and down in ~ 500 μl AB_E for ten times followed by equilibration in ~ 500 μl A^* for ten pipetting cycles as well. Peptides contained in the respective sample, which had been centrifuged at 13,000 rpm and 4°C for 5 min, were bound to the C₁₈ matrix by slowly aspirating and dispensing for ten times. Desalting was achieved during three very slow pipetting cycles in another tube containing ~ 500 μl A^* . Bound peptides were subsequently eluted from the resin by quickly pipetting up and down in an autosampler vial filled with 35 μl AB_E for ten times. The steps from A^* , *via* sample and A^* , to the autosampler vial (AB_E) were repeated for another four times. Upon completion of five cycles, ZipTip_{C18}[®] Pipette Tips were cleansed in ~ 500 μl AB_E as before and stored until next use. Samples planned to be compared by relative quantitation of HLA ligands (e.g. primary and recurrent tumor pairs or meningioma and autologous dura), were desalting using the identical ZipTip_{C18}[®] Pipette Tip in order to reduce technical variability. The hydrophobic solvent content of AB_E was removed by reducing the volume to 1 to 5 μl in the SpeedVac and A_{Load} was subsequently added to the desired target volume of 25 to 35 μl .

After establishment of direct injection, a method to subject peptide solutions to LC-MS/MS without prior purification *via* ZipTip_{C18}[®] Pipette Tips, this was done for every possible sample. Besides less cumbersome sample handling, the big advantage of direct injection is a reduction in possible technical artefacts and thus better reproducibility and comparability of samples. This is of particular importance when relative quantitation of peptides in two autologous samples (e.g. primary *versus* recurrence or tumor *versus* benign) is performed. Direct injection worked well for glioblastoma and medulloblastoma, but not for meningioma samples, since these tended to be sticky throughout the whole experiment and blocked – despite sterile filtration – not only the sepharose-antibody matrices during immunoaffinity chromatography, but also the trapping and separation columns of the liquid chromatography system. However, it should be noted that remnants of CHAPS might cause ion suppression during electrospray ionization and this method should therefore not be applied for big samples lysed with large amounts of this zwitterionic detergent.⁴⁴⁰ For direct injections, samples lyophilized to ~ 30 μl were spun down at 13,000 rpm and 4°C for 10 min, supernatants were transferred into autosampler vials and reduced to 1 to 5 μl by vacuum centrifugation. A_{Load} was added to the desired target volume of 25 to 35 μl .

Autosampler vials were stored at -80°C , thawed in an ultrasonic bath for 2.5 min, sublimated A_{Load} was replenished, and air bubbles were removed thoroughly prior to LC-MS/MS.

Peptide identification by LC-MS/MS and subsequent database search**LC-MS/MS**

Analysis of peptide extracts was performed by nanoflow high-performance liquid chromatography (Dionex UltiMate™ 3000 Series liquid chromatography system) and tandem mass spectrometry. For each tissue and HLA class, a minimum of three technical replicates consuming 5 µl sample and lasting 130 min each were acquired. During the first 10 min, sample was loaded onto the trapping column at 50°C and a flow rate of 4 µl/min, whereas it was gradually eluted from the separation column from min 10 to 100 at 50°C and 175 nl/min (LTQ Orbitrap XL) or 300 nl/min (Orbitrap Fusion Lumos), respectively. During this 90 min gradient, the proportion of hydrophobic solvent (NC pump solvent B) increased from 3 to 40% (equivalent to 2.4 to 32.0% AcN). Between min 101 and 106, it mounted up to 95% to remove remaining sample from the column. Pre-fractionated peptides eluting from the separation column were introduced into an online-coupled tandem mass spectrometer, either the LTQ (linear trap quadrupole) Orbitrap XL (meningioma samples) or the Orbitrap Fusion Lumos (glioblastoma, medulloblastoma, and meningioma samples). Both devices were equipped with a nanospray ion source and were operated in data-dependent acquisition (DDA) mode. In a survey scan, masses of protonated precursor ions of a defined mass-to-charge ratio (m/z) were determined (MS^1 spectra) and the 5 (LTQ Orbitrap XL) or n (Orbitrap Fusion Lumos: top n) most intense / abundant peptides were isolated for fragmentation, respectively. Peptides were fragmented by collision with nitrogen and fragment (MS^2) spectra were subsequently recorded. Detailed settings of both LC-MS/MS systems are listed in Table 4.

Table 4. LC-MS/MS settings for the identification of peptides eluted from HLA class I or II molecules. Abbreviations not introduced in the text above: collision-induced dissociation (CID), higher-energy induced dissociation (HCD). Table layout and listed parameters for the Orbitrap Fusion Lumos are largely congruent with Table 4 in ¹⁰.

Parameter	LTQ Orbitrap XL		Orbitrap Fusion Lumos	
	HLA class I peptides	HLA class II peptides	HLA class I peptides	HLA class II peptides
Internal name of the method used	top5CID_400-650mz_90min Gradient_3sDynExcl	top5CID_300-1500mz_90min Gradient_3sDynExcl	DDA_400-650mz_ qIS_CIDOT(_6Port)	DDA_400-1000mz_ qIS_HCDOT(_6Port)
LC flow rate				
Loading pump [µl/min]	4		4	
Nano pump [nl/min]	0-100 min: 175; 101-130 min: 275		300	
LC solvents				
Loading pump solvent A	0.1% FA / 1% AcN		0.05% TFA / 1% AcN	
Loading pump solvent B	0.1% FA / 80% AcN		0.15% FA / 80% AcN	
Nano pump solvent A	0.15% FA		0.15% FA	
Nano pump solvent B	0.15% FA / 80% AcN		0.15% FA / 80% AcN	
MS¹				
Permitted positive charge states	2-3	≥ 2	2-3	2-5
Permitted m/z	400-650	300-1,500	400-650	400-1,000
Detector type	Orbitrap		Orbitrap	
Resolution	60,000		120,000	
MS¹ precursor selection	Top 5; quadrupole		Top n ; quadrupole	

MS²			
Fragmentation type	CID	CID	HCD
Normalized collision energy [%]	35	35	30
Localization	Ion trap	Ion trap	Ion-routing multipole
Detector type	Ion trap detector		Orbitrap
Resolution	not specified		30,000
Data type	Centroid		Centroid
Dynamic exclusion			
Exclusion after <i>n</i> times	1	1	1
Duration [s]	3	7	10
Mass tolerance [ppm]	± 10		± 2.5

Sequence annotation to uninterpreted MS/MS spectra and data export

So far, MS/MS spectra had only been recorded, but not yet interpreted. Annotation to a peptide sequence was accomplished by database search using the SEQUEST search algorithm⁴³⁴ which Proteome Discoverer 1.4.1.14 embeds as processing node. To identify peptides derived from canonical WT antigens, the Swiss-Prot release from September 27th 2013 (20,279 reviewed protein sequences) served as reference database. Subsequently, the Percolator algorithm 2.04 estimated the false discovery rate (FDR) by decoy database search. Target FDR was set to ≤ 5%. Parameters for processing of raw files compiled by either the LTQ Orbitrap XL or the Orbitrap Fusion Lumos are given in Table 5.

To guarantee that every single measurement was technically accurate, not only the total ion chromatogram, loading and nano pump pressures were reviewed, but also a database search was performed for every technical replicate. For all analyses excepting those aimed at relative quantitation of HLA ligand abundances, the maximum number of available technical replicates was co-processed and exported peptide and protein lists served as base for downstream analyses. Due to the permission of methionine oxidation as dynamic modification, sequence duplicates with either oxidized (m) or reduced (M) methionine residues were included in the peptide lists. These two peptide variants were treated equally, whereby only the oxidized version was reported, in case the reduced one was present as well.

Table 5. Parameters for database search and data export in Proteome Discoverer. Abbreviations not introduced in the text above: signal-to-noise ratio (S/N), Fourier Transform Mass Spectrometry (refers to Orbitrap detection; FTMS). Table layout and listed parameters for the analysis of data compiled by the Orbitrap Fusion Lumos are congruent with Table 5 in ¹⁰.

Parameter	LTQ Orbitrap XL		Orbitrap Fusion Lumos	
	HLA class I peptides	HLA class II peptides	HLA class I peptides	HLA class II peptides
Raw file processing				
Internal name of workflow	SequestIT	SequestIT_ClassII	SequestOT	SequestOT_ClassII
Spectrum properties filter				
Precursor mass [Da]	800-5,000		800-5,000	
Minimum peak count	1		1	
S/N threshold (FTMS)	1.5		1.5	

Input data				
Enzyme name	No-enzyme (unspecific)		No-enzyme (unspecific)	
Maximum missed cleavage sites	0		0	
Peptide length [# of AA]	8-12	8-25	8-12	8-25
Scoring options				
Maximal delta Cn	0.05		0.05	
Tolerances				
Precursor mass tolerance [ppm]	± 5		± 5	
Fragment mass tolerance [Da]	± 0.5		± 0.02	
Spectrum matching				
Use of neutral loss ions	a, b, y ions		a, b, y ions	
Weight of a, c, x, z ions	0		0	
Weight of b or y ions	1		1	
Modifications				
Permitted dynamic modification	Oxidation / +15.995 Da (M)		Oxidation / +15.995 Da (M)	
Maximum modifications per peptide	3		3	
Permitted static modification	None		None	
Data export				
Internal name of filter set	Class I.filters	Class II.filters	Class I.filters	Class II.filters
Minimum peptide confidence	Medium (≤ 5% FDR)		Medium (≤ 5% FDR)	
Peptide length [# of AA]	8-12	8-25	8-12	8-25
Search engine rank	1		1	
Peptide grouping	Enabled		Enabled	
Protein grouping	Disabled		Disabled	

Deconvolution of HLA class I datasets

As elucidated in 2.2.2, HLA class I allotypes have relatively strict binding preferences to particular peptide motifs. Peptides obtained from HLA-immunoprecipitation (HLA-IP) with W6/32 originate from up to six different HLA-A, -B, and -C molecules. To deconvolute this multi-allelic dataset, binding prediction algorithms are employed, which calculate the probability for each peptide to bind to one of the patient's HLA class I allotypes. Ligandosphere is an in-house software which offers, among others, a stand-alone version of NetMHCpan-4.0^{431,432} and an enhanced version of SYFPEITHI.⁴³⁶ Peptides were designated as HLA class I ligands, when predicted as such by at least one of the two algorithms. The binding threshold for SYFPEITHI predictions was set to $\geq 60\%$ of the maximum score of the respective position-specific scoring matrix. Binding peptides according to NetMHCpan-4.0, which is based on artificial neural networks and trained with both binding affinity and immunopeptidomic data,⁴³² had a percentile rank score $\leq 2\%$. Proteins not represented by HLA class I ligands were subsequently removed from the protein lists. HLA annotation of class II peptides is still difficult owing to degenerate peptide motifs and promiscuous binding.¹⁷⁷

Label-free quantitation of relative HLA ligand abundances

For label-free quantitation (LFQ) of relative HLA ligand abundances in two autologous samples (primary and recurrent glioblastoma, meningioma and tumor-free dura), the total amount of substance analyzed per technical replicate, represented by the summed area under the curve (AUC) of all peptides, was adjusted for the two conditions. For this purpose, a so-called dose-

finding measurement was performed for every sample, separately for HLA class I and II. LFQ was only performed when both samples yielded at least 500 peptides and a total AUC of 1×10^9 or 400 peptides and a total AUC of 9×10^8 in the dose-finding run for the Orbitrap Fusion Lumos or the LTQ Orbitrap XL, respectively. For HLA class I-eluted peptides, the total AUC was only calculated from those assigned as HLA class I ligands. The higher concentrated sample was diluted with A_{Load} accordingly to reach the same amount of substance as the lower concentrated one. In case a dilution factor of more than eight was calculated, a new dose-finding run was acquired upon 1:8 dilution. A total number of five (adjusted) technical replicates were measured per condition and HLA class for LFQ experiments. As quality control, the HLA class I ligand or HLA class II peptide yield of each technical replicate was not permitted to deviate by $> 30\%$ of the mean peptide yield of all five adjusted measurements. In case a sample had to be heavily diluted for adjustment, two further undiluted replicates were performed in terms of qualitative analyses.

The five adjusted replicates of each condition were co-processed, protein and peptide lists were exported with standard filters, and peptide lists were merged for both conditions to compile the seedlist. For semi-quantitative HLA class I Volcano plots, this seedlist was filtered for ligands, as described previously. In addition, peptides of each replicate were exported without any filter being applied to the data, so that every peptide spectrum match (PSM) including such with a rank ≥ 2 was reported with corresponding scores. Intensities (AUC of the extracted ion chromatogram of precursor ions) of those peptides contained in the seedlist were subsequently picked from the unfiltered lists. Reproducibility of intensities across technical replicates is exemplarily shown in Supplementary Figure 4 and Supplementary Figure 11. For each peptide and each condition, mean AUC across all LFQ-MS runs as well as the ratio of mean AUC in condition A *versus* condition B was calculated. So-called 'one hit wonders' (peptides not detected in at least two technical replicates) were excluded from semi-quantitative Volcano plots. The fold-change of peptides exclusively detected in one condition was calculated by replacing zero values with the median of the five least intensities, which represents the limit of detection specific for the respective sample. Further, a normalization step computing PSM intensities in proportion to the total intensity of precursor ions in technical replicates was included. To test for significance, two-tailed *t*-tests with implemented correction for multiple testing according to the Benjamini-Hochberg (BH) procedure were conducted.

Comparative profiling against an in-house database and definition of presentation hotspots for HLA class II-presented antigens

To define glioblastoma-, medulloblastoma-, and meningioma-associated peptides and antigens, protein and peptides were queried against an in-house SQL database (3.2.1) comprising immunopeptidomic datasets from 30 benign primary human organs other than testis ($n=418$ samples for HLA class I; $n=364$ samples for HLA class II). The term tumor-exclusive was assigned to peptides and antigens that were never identified on CNS-related tissues (brain, cerebellum, spinal cord, and for meningiomas also dura which was not part of the benign database) and for which a maximum of one non-CNS-related sample was positive. Likewise, the presence of glioblastoma-, medulloblastoma-, or meningioma-associated peptides and proteins was checked in HLA peptidome datasets of up to 37 different primary human malignancies ($n=874$ samples for HLA class I; $n=626$ samples for HLA class II).

Comparative profiling is not capable of reflecting length variants and common core sequences of HLA class II-restricted peptides. Vimentin yielded a total of 29 distinct meningioma-exclusive peptides with presentation frequencies up to 67%, however, almost identical peptide sequences differing only in 1 AA in length were identified on benign tissues (Figure 36 A, Supplementary Figure 10 A). To circumvent this problem, all source proteins represented by at least one tumor-exclusive HLA class II-presented peptide were subjected to hotspot analysis. Unique peptides were aligned to human source protein sequences (as deposited in the UniProt⁸⁶ database for taxonomy ID 9606) and the proportion of all peptides covering a given position was calculated separately for identifications on malignant and benign tissues. Tumor-associated hotspots were defined to have a minimum length of eight AA and to be covered by peptides identified in at least five (medulloblastoma / meningioma) or eight (glioblastoma) patients, while not having matching sequences in benign samples.

4 Aim of the study

Primary brain and CNS tumors account for an average yearly incidence of 81,148 new cases in the US with 15,944 people dieing from malignant CNS cancers every year. They represent the eighth most common tumors in adults older than 40 years and even the most common pediatric tumor entity. Throughout the last decades, the outcome of intracranial neoplasms has remained poor calling for intensive research to establish novel therapies. Especially for recurrent glioblastomas, medulloblastomas, and meningiomas, no treatment protocols or standard-of-care guidelines have been established so far. Cancer immunotherapy has elicited remarkable responses in various cancer entities including glioblastoma. This suggests to employ immune-based therapies for intracranial neoplasias aimed at both preventing (or at least prolonging the time to) relapse, which is a common event especially in glioblastoma, and offering an option to manage disease recurrence. Peptide-specific immunotherapy targeting antigens with natural and tumor-specific presentation on HLA molecules may contribute to significantly improve prognosis and quality of life of patients suffering from glioblastoma, medulloblastoma, or meningioma. Despite extensive research on immunotherapeutic targets in gliomas, this has so far not translated into clinical benefit for patients. Of note, especially the antigenic landscape of recurrent tumors has so far not been investigated at all. Medulloblastoma and meningioma are even characterized by a profound lack of potential targets for cancer immunotherapy. HLA class II-presented antigens have not been adequately adressed for any of these three tumor entities. The aim of the present thesis is to define such tumor-associated peptides by employing an immunopeptidome-centric approach to a large number of primary human glioblastoma, medulloblastoma, and meningioma samples. This will allow adressing both HLA class I- and II-restricted peptides in future immunotherapeutic efforts. In the form of a meta-analysis, the immunopeptidomic data acquired from these three intracranial neoplasias will be compared. This will provide insight into whether the immunopeptidome views the different cellular origin of glioblastoma, medulloblastoma, and meningioma cells. Moreover, it will be analyzed whether shared or even pan-brain tumor antigens exist. These projects are intended to contribute to the development of innovative therapeutic strategies for patients suffering from intracranial neoplasms.

5 References

1. Ostrom QT, Cioffi G, Gittleman H, Patil N, Waite K, Kruchko C, Barnholtz-Sloan JS. CBTRUS Statistical Report: Primary Brain and Other Central Nervous System Tumors Diagnosed in the United States in 2012-2016. *Neuro Oncol.* 2019;21(Supplement_5):v1-v100.
2. Louis DN, Perry A, Reifenberger G, von Deimling A, Figarella-Branger D, Cavenee WK, Ohgaki H, Wiestler OD, Kleihues P, Ellison DW. The 2016 World Health Organization Classification of Tumors of the Central Nervous System: a summary. *Acta Neuropathol.* 2016;131(6):803-820.
3. Jäkel S, Dimou L. Glial Cells and Their Function in the Adult Brain: A Journey through the History of Their Ablation. *Front Cell Neurosci.* 2017;11:24.
4. Del Bigio MR. Ependymal cells: biology and pathology. *Acta Neuropathol.* 2010;119(1):55-73.
5. Johnsen JI, Kogner P, Albiñá A, Henriksson MA. Embryonal neural tumours and cell death. *Apoptosis.* 2009;14(4):424-438.
6. Schüller U, Heine VM, Mao J, Kho AT, Dillon AK, Han YG, Huillard E, Sun T, Ligon AH, Qian Y, Ma Q, Alvarez-Buylla A, McMahon AP, Rowitch DH, Ligon KL. Acquisition of granule neuron precursor identity is a critical determinant of progenitor cell competence to form Shh-induced medulloblastoma. *Cancer Cell.* 2008;14(2):123-134.
7. Taylor MD, Northcott PA, Korshunov A, Remke M, Cho YJ, Clifford SC, Eberhart CG, Parsons DW, Rutkowski S, Gajjar A, Ellison DW, Lichter P, Gilbertson RJ, Pomeroy SL, Kool M, Pfister SM. Molecular subgroups of medulloblastoma: the current consensus. *Acta Neuropathol.* 2012;123(4):465-472.
8. Massimino M, Biassoni V, Gandola L, Garre ML, Gatta G, Giangaspero F, Poggi G, Rutkowski S. Childhood medulloblastoma. *Crit Rev Oncol Hematol.* 2016;105:35-51.
9. Malhotra M, Toulouse A, Godinho BM, Mc Carthy DJ, Cryan JF, O'Driscoll CM. RNAi therapeutics for brain cancer: current advancements in RNAi delivery strategies. *Mol Biosyst.* 2015;11(10):2635-2657.
10. Freudenmann LK. Mapping the HLA Ligandome of Primary versus Recurrent Disease in Glioblastoma Multiforme by Mass Spectrometry. *Master Thesis, Master of Science in Molecular Medicine, Eberhard Karls Universität Tübingen, Faculty of Medicine.* 2017.
11. Schwartzbaum JA, Fisher JL, Aldape KD, Wrensch M. Epidemiology and molecular pathology of glioma. *Nat Clin Pract Neurol.* 2006;2(9):494-503.
12. Alifirios C, Trafalis DT. Glioblastoma multiforme: Pathogenesis and treatment. *Pharmacol Ther.* 2015;152:63-82.
13. Stupp R, Brada M, van den Bent MJ, Tonn JC, Pentheroudakis G. High-grade glioma: ESMO Clinical Practice Guidelines for diagnosis, treatment and follow-up. *Ann Oncol.* 2014;25 Suppl 3:iii93-101.
14. Wen PY, Kesari S. Malignant gliomas in adults. *N Engl J Med.* 2008;359(5):492-507.
15. Farrell CJ, Plotkin SR. Genetic causes of brain tumors: neurofibromatosis, tuberous sclerosis, von Hippel-Lindau, and other syndromes. *Neurol Clin.* 2007;25(4):925-946.
16. Rieske P, Zakrzewska M, Biernat W, Bartkowiak J, Zimmermann A, Liberski PP. Atypical molecular background of glioblastoma and meningioma developed in a patient with Li-Fraumeni syndrome. *J Neurooncol.* 2005;71(1):27-30.
17. Ohgaki H, Kleihues P. Epidemiology and etiology of gliomas. *Acta Neuropathol.* 2005;109(1):93-108.
18. Fisher JL, Schwartzbaum JA, Wrensch M, Wiemels JL. Epidemiology of brain tumors. *Neurol Clin.* 2007;25(4):867-890.
19. Wrensch M, Minn Y, Chew T, Bondy M, Berger MS. Epidemiology of primary brain tumors: current concepts and review of the literature. *Neuro Oncol.* 2002;4(4):278-299.
20. Miller G. Brain cancer. A viral link to glioblastoma? *Science.* 2009;323(5910):30-31.
21. Chi J, Gu B, Zhang C, Peng G, Zhou F, Chen Y, Zhang G, Guo Y, Guo D, Qin J, Wang J, Li L, Wang F, Liu G, Xie F, Feng D, Zhou H, Huang X, Lu S, Liu Y, Hu W, Yao K. Human herpesvirus 6 latent infection in patients with glioma. *J Infect Dis.* 2012;206(9):1394-1398.
22. Poltermann S, Schlehofer B, Steindorf K, Schnitzler P, Geletneky K, Schlehofer JR. Lack of association of herpesviruses with brain tumors. *J Neurovirol.* 2006;12(2):90-99.
23. Holdhoff M, Guner G, Rodriguez FJ, Hicks JL, Zheng Q, Forman MS, Ye X, Grossman SA, Meeker AK, Heaphy CM, Eberhart CG, De Marzo AM, Arav-Boger R. Absence of cytomegalovirus in glioblastoma and other high-grade gliomas by real-time PCR, immunohistochemistry and in situ hybridization. *Clin Cancer Res.* 2016.
24. Brennan CW, Verhaak RG, McKenna A, Campos B, Nounshmehr H, Salama SR, Zheng S, Chakravarty D, Sanborn JZ, Berman SH, Beroukhi R, Bernard B, Wu CJ, Genovese G, Shmulevich I, Barnholtz-Sloan J, Zou L, Vegesna R, Shukla SA, Ciriello G, Yung WK, Zhang W, Sougnez C, Mikkelsen T, Aldape K, Bigner DD, Van Meir EG, Prados M, Sloan A, Black KL, Eschbacher J, Finocchiaro G, Friedman W, Andrews DW, Guha A, Iacocca M, O'Neill BP, Foltz G, Myers J, Weisenberger DJ, Penny R, Kucherlapati R, Perou CM, Hayes DN, Gibbs R, Marra M, Mills GB, Lander E, Spellman P, Wilson R, Sander C, Weinstein J, Meyerson M, Gabriel S, Laird PW, Haussler D, Getz G, Chin L. The somatic genomic landscape of glioblastoma. *Cell.* 2013;155(2):462-477.
25. Preusser M, de Ribaupierre S, Wohrer A, Erridge SC, Hegi M, Weller M, Stupp R. Current concepts and management of glioblastoma. *Ann Neurol.* 2011;70(1):9-21.
26. Cairns RA, Mak TW. Oncogenic isocitrate dehydrogenase mutations: mechanisms, models, and clinical opportunities. *Cancer Discov.* 2013;3(7):730-741.

Chapter 1: References

27. Weller M, Pfister SM, Wick W, Hegi ME, Reifenberger G, Stupp R. Molecular neuro-oncology in clinical practice: a new horizon. *Lancet Oncol*. 2013;14(9):e370-379.
28. Ward PS, Patel J, Wise DR, Abdel-Wahab O, Bennett BD, Collier HA, Cross JR, Fantin VR, Hedvat CV, Perl AE, Rabinowitz JD, Carroll M, Su SM, Sharp KA, Levine RL, Thompson CB. The common feature of leukemia-associated IDH1 and IDH2 mutations is a neomorphic enzyme activity converting alpha-ketoglutarate to 2-hydroxyglutarate. *Cancer Cell*. 2010;17(3):225-234.
29. Raynaud S, Carubbia N, Colin C, Adelaide J, Mozziconacci MJ, Metellus P, Chinot O, Birnbaum D, Chaffanet M, Figarella-Branger D. Absence of R140Q mutation of isocitrate dehydrogenase 2 in gliomas and breast cancers. *Oncol Lett*. 2010;1(5):883-884.
30. Cheng HB, Yue W, Xie C, Zhang RY, Hu SS, Wang Z. IDH1 mutation is associated with improved overall survival in patients with glioblastoma: a meta-analysis. *Tumour Biol*. 2013;34(6):3555-3559.
31. Parsons DW, Jones S, Zhang X, Lin JC, Leary RJ, Angenendt P, Mankoo P, Carter H, Siu IM, Gallia GL, Olivi A, McLendon R, Rasheed BA, Keir S, Nikolskaya T, Nikolsky Y, Busam DA, Tekleab H, Diaz LA, Jr., Hartigan J, Smith DR, Strausberg RL, Marie SK, Shinjo SM, Yan H, Riggins GJ, Bigner DD, Karchin R, Papadopoulos N, Parmigiani G, Vogelstein B, Velculescu VE, Kinzler KW. An integrated genomic analysis of human glioblastoma multiforme. *Science*. 2008;321(5897):1807-1812.
32. Kleihues P, Ohgaki H. Primary and secondary glioblastomas: from concept to clinical diagnosis. *Neuro Oncol*. 1999;1(1):44-51.
33. Louis DN. Molecular pathology of malignant gliomas. *Annu Rev Pathol*. 2006;1:97-117.
34. McLendon R, Friedman A, Bigner D, Van Meir EG, Brat DJ, Mastrogiannis GM, Olson JJ, Mikkelsen T, Lehman N, Aldape K, Yung WK, Bogler O, Weinstein JN, Vandenberg S, Berger M, Prados M, Muzny D, Morgan M, Scherer S, Sabo A, Nazareth L, Lewis L, Hall O, Zhu Y, Ren Y, Alvi O, Yao J, Hawes A, Jhangiani S, Fowler G, San Lucas A, Kovar C, Cree A, Dinh H, Santibanez J, Joshi V, Gonzalez-Garay ML, Miller CA, Milosavljevic A, Donehower L, Wheeler DA, Gibbs RA, Cibulskis K, Sougnez C, Fennell T, Mahan S, Wilkinson J, Ziaugra L, Onofrio R, Bloom T, Nicol R, Ardlie K, Baldwin J, Gabriel S, Lander ES, Ding L, Fulton RS, McLellan MD, Wallis J, Larson DE, Shi X, Abbott R, Fulton L, Chen K, Koboldt DC, Wendl MC, Meyer R, Tang Y, Lin L, Osborne JR, Dunford-Shore BH, Miner TL, Delehaunty K, Markovic C, Swift G, Courtney W, Pohl C, Abbott S, Hawkins A, Leong S, Haipok C, Schmidt H, Wiechert M, Vickery T, Scott S, Dooling DJ, Chinwalla A, Weinstock GM, Mardis ER, Wilson RK, Getz G, Winckler W, Verhaak RG, Lawrence MS, O'Kelly M, Robinson J, Alexe G, Beroukhir R, Carter S, Chiang D, Gould J, Gupta S, Korn J, Mermel C, Mesirov J, Monti S, Nguyen H, Parkin M, Reich M, Stransky N, Weir BA, Garraway L, Golub T, Meyerson M, Chin L, Protopopov A, Zhang J, Perna I, Aronson S, Sathiamoorthy N, Ren G, Yao J, Wiedemeyer WR, Kim H, Kong SW, Xiao Y, Kohane IS, Seidman J, Park PJ, Kucherlapati R, Laird PW, Cope L, Herman JG, Weisenberger DJ, Pan F, Van den Berg D, Van Neste L, Yi JM, Schuebel KE, Baylin SB, Absher DM, Li JZ, Southwick A, Brady S, Aggarwal A, Chung T, Sherlock G, Brooks JD, Myers RM, Spellman PT, Purdom E, Jakkula LR, Lapuk AV, Marr H, Dorton S, Choi Y, Han J, Ray A, Wang V, Durinck S, Robinson M, Wang NJ, Vranizan K, Peng V, Van Name E, Fontenay GV, Ngai J, Conboy JG, Parvin B, Feiler HS, Speed TP, Gray JW, Brennan C, Succi ND, Olshen A, Taylor BS, Lash A, Schultz N, Reva B, Antipin Y, Stukalov A, Gross B, Cerami E, Wang WQ, Qin LX, Seshan VE, Villafania L, Cavatore M, Borsu L, Viale A, Gerald W, Sander C, Ladanyi M, Perou CM, Hayes DN, Topal MD, Hoadley KA, Qi Y, Balu S, Shi Y, Wu J, Penny R, Bittner M, Shelton T, Lenkiewicz E, Morris S, Beasley D, Sanders S, Kahn A, Sfeir R, Chen J, Nassau D, Feng L, Hickey E, Barker A, Gerhard DS, Vockley J, Compton C, Vaught J, Fielding P, Ferguson ML, Schaefer C, Zhang J, Madhavan S, Buetow KH, Collins F, Good P, Guyer M, Ozenberger B, Peterson J, Thomson E. Comprehensive genomic characterization defines human glioblastoma genes and core pathways. *Nature*. 2008;455(7216):1061-1068.
35. Mischel PS, Nelson SF, Cloughesy TF. Molecular analysis of glioblastoma: pathway profiling and its implications for patient therapy. *Cancer Biol Ther*. 2003;2(3):242-247.
36. Ichimura K, Bolin MB, Goike HM, Schmidt EE, Moshref A, Collins VP. Deregulation of the p14ARF/MDM2/p53 pathway is a prerequisite for human astrocytic gliomas with G1-S transition control gene abnormalities. *Cancer Res*. 2000;60(2):417-424.
37. Weller M, Butowski N, Tran DD, Recht LD, Lim M, Hirte H, Ashby L, Mechtler L, Goldlust SA, Iwamoto F, Drappatz J, O'Rourke DM, Wong M, Hamilton MG, Finocchiaro G, Perry J, Wick W, Green J, He Y, Turner CD, Yellin MJ, Keler T, Davis TA, Stupp R, Sampson JH. Rindopepimut with temozolomide for patients with newly diagnosed, EGFRvIII-expressing glioblastoma (ACT IV): a randomised, double-blind, international phase 3 trial. *Lancet Oncol*. 2017;18(10):1373-1385.
38. Ichimura K, Schmidt EE, Goike HM, Collins VP. Human glioblastomas with no alterations of the CDKN2A (p16INK4A, MTS1) and CDK4 genes have frequent mutations of the retinoblastoma gene. *Oncogene*. 1996;13(5):1065-1072.
39. Samuels Y, Wang Z, Bardelli A, Silliman N, Ptak J, Szabo S, Yan H, Gazdar A, Powell SM, Riggins GJ, Willson JK, Markowitz S, Kinzler KW, Vogelstein B, Velculescu VE. High frequency of mutations of the PIK3CA gene in human cancers. *Science*. 2004;304(5670):554.
40. Liu Z, Roberts TM. Human tumor mutants in the p110alpha subunit of PI3K. *Cell Cycle*. 2006;5(7):675-677.
41. Gallia GL, Rand V, Siu IM, Eberhart CG, James CD, Marie SK, Oba-Shinjo SM, Carlotti CG, Caballero OL, Simpson AJ, Brock MV, Massion PP, Carson BS, Sr., Riggins GJ. PIK3CA gene mutations in pediatric and adult glioblastoma multiforme. *Mol Cancer Res*. 2006;4(10):709-714.
42. Hassler M, Seidl S, Fazeny-Doerner B, Preusser M, Hainfellner J, Rössler K, Prayer D, Marosi C. Diversity of cytogenetic and pathohistologic profiles in glioblastoma. *Cancer Genet Cytogenet*. 2006;166(1):46-55.

Chapter 1: References

43. Rey JA, Bello MJ, de Campos JM, Kusak ME, Ramos C, Benitez J. Chromosomal patterns in human malignant astrocytomas. *Cancer Genet Cytogenet.* 1987;29(2):201-221.
44. Geisenberger C, Mock A, Warta R, Rapp C, Schwager C, Korshunov A, Nied AK, Capper D, Brors B, Jungk C, Jones D, Collins VP, Ichimura K, Bäcklund LM, Schnabel E, Mittelbron M, Lahrmann B, Zheng S, Verhaak RG, Grabe N, Pfister SM, Hartmann C, von Deimling A, Debus J, Unterberg A, Abdollahi A, Herold-Mende C. Molecular profiling of long-term survivors identifies a subgroup of glioblastoma characterized by chromosome 19/20 co-gain. *Acta Neuropathol.* 2015;130(3):419-434.
45. Kim DH, Mohapatra G, Bollen A, Waldman FM, Feuerstein BG. Chromosomal abnormalities in glioblastoma multiforme tumors and glioma cell lines detected by comparative genomic hybridization. *Int J Cancer.* 1995;60(6):812-819.
46. Capper D, Jones DTW, Sill M, Hovestadt V, Schrimpf D, Sturm D, Koelsche C, Sahm F, Chavez L, Reuss DE, Kratz A, Wefers AK, Huang K, Pajtler KW, Schweizer L, Stichel D, Olar A, Engel NW, Lindenberg K, Harter PN, Braczynski AK, Plate KH, Dohmen H, Garvalov BK, Coras R, Hölsken A, Hewer E, Bewerunge-Hudler M, Schick M, Fischer R, Beschorner R, Schittenhelm J, Staszewski O, Wani K, Varlet P, Pages M, Temming P, Lohmann D, Selt F, Witt H, Milde T, Witt O, Aronica E, Giangaspero F, Rushing E, Scheurlen W, Geisenberger C, Rodriguez FJ, Becker A, Preusser M, Haberler C, Bjerkvig R, Cryan J, Farrell M, Deckert M, Hench J, Frank S, Serrano J, Kannan K, Tsigos A, Brück W, Hofer S, Brehmer S, Seiz-Rosenhagen M, Hanggi D, Hans V, Rozsnoki S, Hansford JR, Kohlhof P, Kristensen BW, Lechner M, Lopes B, Mawrin C, Ketter R, Kulozik A, Khatib Z, Heppner F, Koch A, Jouvet A, Keohane C, Mühleisen H, Mueller W, Pohl U, Prinz M, Benner A, Zapatka M, Gottardo NG, Driever PH, Kramm CM, Müller HL, Rutkowski S, von Hoff K, Frühwald MC, Gnekow A, Fleischhack G, Tippelt S, Calaminus G, Monoranu CM, Perry A, Jones C, Jacques TS, Radlwimmer B, Gessi M, Pietsch T, Schramm J, Schackert G, Westphal M, Reifenberger G, Wesseling P, Weller M, Collins VP, Blümcke I, Bendszus M, Debus J, Huang A, Jabado N, Northcott PA, Paulus W, Gajjar A, Robinson GW, Taylor MD, Jaunmuktane Z, Ryzhova M, Platten M, Unterberg A, Wick W, Karajannis MA, Mittelbronn M, Acker T, Hartmann C, Aldape K, Schuller U, Buslei R, Lichter P, Kool M, Herold-Mende C, Ellison DW, Hasselblatt M, Snuderl M, Brandner S, Korshunov A, von Deimling A, Pfister SM. DNA methylation-based classification of central nervous system tumours. *Nature.* 2018;555(7697):469-474.
47. McLendon R, Friedman A, Bigner D, Van Meir EG, Brat DJ, Mastrogiannis GM, Olson JJ, Mikkelsen T, Lehman N, Aldape K, Yung WK, Bogler O, Weinstein JN, VandenBerg S, Berger M, Prados M, Muzny D, Morgan M, Scherer S, Sabo A, Nazareth L, Lewis L, Hall O, Zhu Y, Ren Y, Alvi O, Yao J, Hawes A, Jhangiani S, Fowler G, San Lucas A, Kovar C, Cree A, Dinh H, Santibanez J, Joshi V, Gonzalez-Garay ML, Miller CA, Milosavljevic A, Donehower L, Wheeler DA, Gibbs RA, Cibulskis K, Sougnez C, Fennell T, Mahan S, Wilkinson J, Ziaugra L, Onofrio R, Bloom T, Nicol R, Ardlie K, Baldwin J, Gabriel S, Lander ES, Ding L, Fulton RS, McLellan MD, Wallis J, Larson DE, Shi X, Abbott R, Fulton L, Chen K, Koboldt DC, Wendl MC, Meyer R, Tang Y, Lin L, Osborne JR, Dunford-Shore BH, Miner TL, Delehaunty K, Markovic C, Swift G, Courtney W, Pohl C, Abbott S, Hawkins A, Leong S, Haipok C, Schmidt H, Wiechert M, Vickery T, Scott S, Dooling DJ, Chinwalla A, Weinstock GM, Mardis ER, Wilson RK, Getz G, Winckler W, Verhaak RG, Lawrence MS, O'Kelly M, Robinson J, Alexe G, Beroukhir R, Carter S, Chiang D, Gould J, Gupta S, Korn J, Mermel C, Mesirov J, Monti S, Nguyen H, Parkin M, Reich M, Stransky N, Weir BA, Garraway L, Golub T, Meyerson M, Chin L, Protopopov A, Zhang J, Perna I, Aronson S, Sathiamoorthy N, Ren G, Yao J, Wiedemeyer WR, Kim H, Kong SW, Xiao Y, Kohane IS, Seidman J, Park PJ, Kucherlapati R, Laird PW, Cope L, Herman JG, Weisenberger DJ, Pan F, Van den Berg D, Van Neste L, Yi JM, Schuebel KE, Baylin SB, Absher DM, Li JZ, Southwick A, Brady S, Aggarwal A, Chung T, Sherlock G, Brooks JD, Myers RM, Spellman PT, Purdom E, Jakkula LR, Lapuk AV, Marr H, Dorton S, Choi Y, Han J, Ray A, Wang V, Durinck S, Robinson M, Wang NJ, Vranizan K, Peng V, Van Name E, Fontenay GV, Ngai J, Conboy JG, Parvin B, Feiler HS, Speed TP, Gray JW, Brennan C, Socci ND, Olshen A, Taylor BS, Lash A, Schultz N, Reva B, Antipin Y, Stukalov A, Gross B, Cerami E, Wang WQ, Qin LX, Seshan VE, Villafania L, Cavatore M, Borsu L, Viale A, Gerald W, Sander C, Ladanyi M, Perou CM, Hayes DN, Topal MD, Hoadley KA, Qi Y, Balu S, Shi Y, Wu J, Penny R, Bittner M, Shelton T, Lenkiewicz E, Morris S, Beasley D, Sanders S, Kahn A, Sfeir R, Chen J, Nassau D, Feng L, Hickey E, Barker A, Gerhard DS, Vockley J, Compton C, Vaught J, Fielding P, Ferguson ML, Schaefer C, Zhang J, Madhavan S, Buetow KH, Collins F, Good P, Guyer M, Ozenberger B, Peterson J, Thomson E. Corrigendum: Comprehensive genomic characterization defines human glioblastoma genes and core pathways. *Nature.* 2013;494(7438):506.
48. Turcan S, Rohle D, Goenka A, Walsh LA, Fang F, Yilmaz E, Campos C, Fabius AW, Lu C, Ward PS, Thompson CB, Kaufman A, Guryanova O, Levine R, Heguy A, Viale A, Morris LG, Huse JT, Mellinghoff IK, Chan TA. IDH1 mutation is sufficient to establish the glioma hypermethylator phenotype. *Nature.* 2012;483(7390):479-483.
49. Mohme M, Neidert MC, Regli L, Weller M, Martin R. Immunological challenges for peptide-based immunotherapy in glioblastoma. *Cancer Treat Rev.* 2014;40(2):248-258.
50. Goodenberger ML, Jenkins RB. Genetics of adult glioma. *Cancer Genet.* 2012;205(12):613-621.
51. Noushmehr H, Weisenberger DJ, Diefes K, Phillips HS, Pujara K, Berman BP, Pan F, Pelloski CE, Sulman EP, Bhat KP, Verhaak RG, Hoadley KA, Hayes DN, Perou CM, Schmidt HK, Ding L, Wilson RK, Van Den Berg D, Shen H, Bengtsson H, Neuvial P, Cope LM, Buckley J, Herman JG, Baylin SB, Laird PW, Aldape K. Identification of a CpG island methylator phenotype that defines a distinct subgroup of glioma. *Cancer Cell.* 2010;17(5):510-522.
52. Stupp R, Hegi ME, Mason WP, van den Bent MJ, Taphoorn MJ, Janzer RC, Ludwin SK, Allgeier A, Fisher B, Belanger K, Hau P, Brandes AA, Gijtenbeek J, Marosi C, Vecht CJ, Mokhtari K, Wesseling P, Villa S,

Chapter 1: References

- Eisenhauer E, Gorlia T, Weller M, Lacombe D, Cairncross JG, Mirimanoff RO. Effects of radiotherapy with concomitant and adjuvant temozolomide versus radiotherapy alone on survival in glioblastoma in a randomised phase III study: 5-year analysis of the EORTC-NCIC trial. *Lancet Oncol.* 2009;10(5):459-466.
53. Esteller M, Garcia-Foncillas J, Andion E, Goodman SN, Hidalgo OF, Vanaclocha V, Baylin SB, Herman JG. Inactivation of the DNA-repair gene MGMT and the clinical response of gliomas to alkylating agents. *N Engl J Med.* 2000;343(19):1350-1354.
54. Hegi ME, Diserens AC, Godard S, Dietrich PY, Regli L, Ostermann S, Otten P, Van Melle G, de Tribolet N, Stupp R. Clinical trial substantiates the predictive value of O-6-methylguanine-DNA methyltransferase promoter methylation in glioblastoma patients treated with temozolomide. *Clin Cancer Res.* 2004;10(6):1871-1874.
55. Hegi ME, Diserens AC, Gorlia T, Hamou MF, de Tribolet N, Weller M, Kros JM, Hainfellner JA, Mason W, Mariani L, Bromberg JE, Hau P, Mirimanoff RO, Cairncross JG, Janzer RC, Stupp R. MGMT gene silencing and benefit from temozolomide in glioblastoma. *N Engl J Med.* 2005;352(10):997-1003.
56. Weller M, Felsberg J, Hartmann C, Berger H, Steinbach JP, Schramm J, Westphal M, Schackert G, Simon M, Tonn JC, Heese O, Krex D, Ninkhah G, Pietsch T, Wiestler O, Reifenberger G, von Deimling A, Loeffler M. Molecular predictors of progression-free and overall survival in patients with newly diagnosed glioblastoma: a prospective translational study of the German Glioma Network. *J Clin Oncol.* 2009;27(34):5743-5750.
57. Weller M, Stupp R, Reifenberger G, Brandes AA, van den Bent MJ, Wick W, Hegi ME. MGMT promoter methylation in malignant gliomas: ready for personalized medicine? *Nat Rev Neurol.* 2010;6(1):39-51.
58. Lacroix M, Abi-Said D, Fourney DR, Gokaslan ZL, Shi W, DeMonte F, Lang FF, McCutcheon IE, Hassenbusch SJ, Holland E, Hess K, Michael C, Miller D, Sawaya R. A multivariate analysis of 416 patients with glioblastoma multiforme: prognosis, extent of resection, and survival. *J Neurosurg.* 2001;95(2):190-198.
59. Walker MD, Green SB, Byar DP, Alexander E, Jr., Batzdorf U, Brooks WH, Hunt WE, MacCarty CS, Mahaley MS, Jr., Mealey J, Jr., Owens G, Ransohoff J, 2nd, Robertson JT, Shapiro WR, Smith KR, Jr., Wilson CB, Strike TA. Randomized comparisons of radiotherapy and nitrosoureas for the treatment of malignant glioma after surgery. *N Engl J Med.* 1980;303(23):1323-1329.
60. Villano JL, Seery TE, Bressler LR. Temozolomide in malignant gliomas: current use and future targets. *Cancer Chemother Pharmacol.* 2009;64(4):647-655.
61. Stupp R, Mason WP, van den Bent MJ, Weller M, Fisher B, Taphoorn MJ, Belanger K, Brandes AA, Marosi C, Bogdahn U, Curschmann J, Janzer RC, Ludwin SK, Gorlia T, Allgeier A, Lacombe D, Cairncross JG, Eisenhauer E, Mirimanoff RO. Radiotherapy plus concomitant and adjuvant temozolomide for glioblastoma. *N Engl J Med.* 2005;352(10):987-996.
62. Weller M, Stupp R, Wick W. Epilepsy meets cancer: when, why, and what to do about it? *Lancet Oncol.* 2012;13(9):e375-382.
63. Rossetti AO, Stupp R. Epilepsy in brain tumor patients. *Curr Opin Neurol.* 2010;23(6):603-609.
64. Qiu ZK, Shen D, Chen YS, Yang QY, Guo CC, Feng BH, Chen ZP. Enhanced MGMT expression contributes to temozolomide resistance in glioma stem-like cells. *Chin J Cancer.* 2014;33(2):115-122.
65. Bonavia R, Inda MM, Cavenee WK, Furnari FB. Heterogeneity maintenance in glioblastoma: a social network. *Cancer Res.* 2011;71(12):4055-4060.
66. Gorlia T, Stupp R, Brandes AA, Rampling RR, Fumoleau P, Dittich C, Campone MM, Twelves CC, Raymond E, Hegi ME, Lacombe D, van den Bent MJ. New prognostic factors and calculators for outcome prediction in patients with recurrent glioblastoma: a pooled analysis of EORTC Brain Tumour Group phase I and II clinical trials. *Eur J Cancer.* 2012;48(8):1176-1184.
67. Hunter C, Smith R, Cahill DP, Stephens P, Stevens C, Teague J, Greenman C, Edkins S, Bignell G, Davies H, O'Meara S, Parker A, Avis T, Barthorpe S, Brackenbury L, Buck G, Butler A, Clements J, Cole J, Dicks E, Forbes S, Gorton M, Gray K, Halliday K, Harrison R, Hills K, Hinton J, Jenkinson A, Jones D, Kosmidou V, Laman R, Lugg R, Menzies A, Perry J, Petty R, Raine K, Richardson D, Shepherd R, Small A, Solomon H, Tofts C, Varian J, West S, Widaa S, Yates A, Easton DF, Riggins G, Roy JE, Levine KK, Mueller W, Batchelor TT, Louis DN, Stratton MR, Futreal PA, Wooster R. A hypermutation phenotype and somatic MSH6 mutations in recurrent human malignant gliomas after alkylator chemotherapy. *Cancer Res.* 2006;66(8):3987-3991.
68. Karran P, Offman J, Bignami M. Human mismatch repair, drug-induced DNA damage, and secondary cancer. *Biochimie.* 2003;85(11):1149-1160.
69. Hickman MJ, Samson LD. Role of DNA mismatch repair and p53 in signaling induction of apoptosis by alkylating agents. *Proc Natl Acad Sci U S A.* 1999;96(19):10764-10769.
70. Weller M, van den Bent M, Hopkins K, Tonn JC, Stupp R, Falini A, Cohen-Jonathan-Moyal E, Frappaz D, Henriksson R, Balana C, Chinot O, Ram Z, Reifenberger G, Soffietti R, Wick W. EANO guideline for the diagnosis and treatment of anaplastic gliomas and glioblastoma. *Lancet Oncol.* 2014;15(9):e395-403.
71. Erdem-Eraslan L, van den Bent MJ, Hoogstrate Y, Naz-Khan H, Stubbs A, van der Spek P, Bottcher R, Gao Y, de Wit M, Taal W, Oosterkamp HM, Walenkamp A, Beerepoot LV, Hanse MC, Buter J, Honkoop AH, van der Holt B, Vernhout RM, Sillevius Smitt PA, Kros JM, French PJ. Identification of Patients with Recurrent Glioblastoma Who May Benefit from Combined Bevacizumab and CCNU Therapy: A Report from the BELOB Trial. *Cancer Res.* 2016;76(3):525-534.
72. Stupp R, Taillibert S, Kanner AA, Kesari S, Steinberg DM, Toms SA, Taylor LP, Lieberman F, Silvani A, Fink KL, Barnett GH, Zhu JJ, Henson JW, Engelhard HH, Chen TC, Tran DD, Sroubek J, Tran ND, Hottinger AF, Landolfi J, Desai R, Caroli M, Kew Y, Honnorat J, Idbaih A, Kirson ED, Weinberg U, Palti Y, Hegi ME, Ram Z. Maintenance Therapy With Tumor-Treating Fields Plus Temozolomide vs Temozolomide Alone for Glioblastoma: A Randomized Clinical Trial. *Jama.* 2015;314(23):2535-2543.

Chapter 1: References

73. Stupp R, Wong ET, Kanner AA, Steinberg D, Engelhard H, Heidecke V, Kirson ED, Taillibert S, Liebermann F, Dbalý V, Ram Z, Villano JL, Rainov N, Weinberg U, Schiff D, Kunschner L, Raizer J, Honnorat J, Sloan A, Malkin M, Landolfi JC, Payer F, Mehdorn M, Weil RJ, Pannullo SC, Westphal M, Smrcka M, Chin L, Kostron H, Hofer S, Bruce J, Cosgrove R, Paleologous N, Palti Y, Gutin PH. NovoTTF-100A versus physician's choice chemotherapy in recurrent glioblastoma: a randomised phase III trial of a novel treatment modality. *Eur J Cancer*. 2012;48(14):2192-2202.
74. Swanson KD, Lok E, Wong ET. An Overview of Alternating Electric Fields Therapy (NovoTTF Therapy) for the Treatment of Malignant Glioma. *Curr Neurol Neurosci Rep*. 2016;16(1):8.
75. Weller M, Cloughesy T, Perry JR, Wick W. Standards of care for treatment of recurrent glioblastoma-are we there yet? *Neuro Oncol*. 2013;15(1):4-27.
76. Friedman HS, Prados MD, Wen PY, Mikkelsen T, Schiff D, Abrey LE, Yung WK, Paleologos N, Nicholas MK, Jensen R, Vredenburgh J, Huang J, Zheng M, Cloughesy T. Bevacizumab alone and in combination with irinotecan in recurrent glioblastoma. *J Clin Oncol*. 2009;27(28):4733-4740.
77. Kreisl TN, Kim L, Moore K, Duic P, Royce C, Stroud I, Garren N, Mackey M, Butman JA, Camphausen K, Park J, Albert PS, Fine HA. Phase II trial of single-agent bevacizumab followed by bevacizumab plus irinotecan at tumor progression in recurrent glioblastoma. *J Clin Oncol*. 2009;27(5):740-745.
78. Miller JJ, Wen PY. Emerging targeted therapies for glioma. *Expert Opin Emerg Drugs*. 2016;21(4):441-452.
79. Sathornsumetee S, Reardon DA, Desjardins A, Quinn JA, Vredenburgh JJ, Rich JN. Molecularly targeted therapy for malignant glioma. *Cancer*. 2007;110(1):13-24.
80. Batchelor TT, Sorensen AG, di Tomaso E, Zhang WT, Duda DG, Cohen KS, Kozak KR, Cahill DP, Chen PJ, Zhu M, Ancukiewicz M, Mrugala MM, Plotkin S, Drappatz J, Louis DN, Ivy P, Scadden DT, Benner T, Loeffler JS, Wen PY, Jain RK. AZD2171, a pan-VEGF receptor tyrosine kinase inhibitor, normalizes tumor vasculature and alleviates edema in glioblastoma patients. *Cancer Cell*. 2007;11(1):83-95.
81. Waszak SM, Northcott PA, Buchhalter I, Robinson GW, Sutter C, Groebner S, Grund KB, Brugières L, Jones DTW, Pajtler KW, Morrissy AS, Kool M, Sturm D, Chavez L, Ernst A, Brabetz S, Hain M, Zichner T, Segura-Wang M, Weischenfeldt J, Rausch T, Mardin BR, Zhou X, Baciu C, Lawerenz C, Chan JA, Varlet P, Guerrini-Rousseau L, Fults DW, Grajkowska W, Hauser P, Jabado N, Ra YS, Zitterbart K, Shringarpure SS, De La Vega FM, Bustamante CD, Ng HK, Perry A, MacDonald TJ, Hernáiz Driever P, Bendel AE, Bowers DC, McCowage G, Chintagumpala MM, Cohn R, Hassall T, Fleischhack G, Eggen T, Wesenberg F, Feychting M, Lannering B, Schüz J, Johansen C, Andersen TV, Rööslö M, Kuehni CE, Grotzer M, Kjaerheim K, Monoranu CM, Archer TC, Duke E, Pomeroy SL, Shelagh R, Frank S, Sumerauer D, Scheurlen W, Ryzhova MV, Milde T, Kratz CP, Samuel D, Zhang J, Solomon DA, Marra M, Eils R, Bartram CR, von Hoff K, Rutkowski S, Ramaswamy V, Gilbertson RJ, Korshunov A, Taylor MD, Lichter P, Malkin D, Gajjar A, Korbel JO, Pfister SM. Spectrum and prevalence of genetic predisposition in medulloblastoma: a retrospective genetic study and prospective validation in a clinical trial cohort. *Lancet Oncol*. 2018;19(6):785-798.
82. Northcott PA, Jones DT, Kool M, Robinson GW, Gilbertson RJ, Cho YJ, Pomeroy SL, Korshunov A, Lichter P, Taylor MD, Pfister SM. Medulloblastomics: the end of the beginning. *Nat Rev Cancer*. 2012;12(12):818-834.
83. Hortal AM, Vermeulen JF, Van Hecke W, Bovenschen N. Oncogenic role of cytomegalovirus in medulloblastoma? *Cancer Lett*. 2017;408:55-59.
84. Barreda Costa C, Chu Revollar L, Herrera Alzamora A. Medulloblastoma and recurrent meningioma in association with colonic polyposis: an unusual presentation of Turcot syndrome. *Rev Gastroenterol Peru*. 2019;39(3):280-283.
85. Northcott PA, Buchhalter I, Morrissy AS, Hovestadt V, Weischenfeldt J, Ehrenberger T, Grobner S, Segura-Wang M, Zichner T, Rudneva VA, Warnatz HJ, Sidiropoulos N, Phillips AH, Schumacher S, Kleinheinz K, Waszak SM, Erkek S, Jones DTW, Worst BC, Kool M, Zapatka M, Jäger N, Chavez L, Hutter B, Bieg M, Paramasivam N, Heinold M, Gu Z, Ishaque N, Jäger-Schmidt C, Imbusch CD, Jugold A, Hübschmann D, Risch T, Amstislavskiy V, Gonzalez FGR, Weber UD, Wolf S, Robinson GW, Zhou X, Wu G, Finkelstein D, Liu Y, Cavalli FMG, Luu B, Ramaswamy V, Wu X, Koster J, Ryzhova M, Cho YJ, Pomeroy SL, Herold-Mende C, Schuhmann M, Ebinger M, Liau LM, Mora J, McLendon RE, Jabado N, Kumabe T, Chuah E, Ma Y, Moore RA, Mungall AJ, Mungall KL, Thiessen N, Tse K, Wong T, Jones SJM, Witt O, Milde T, Von Deimling A, Capper D, Korshunov A, Yaspo ML, Kriwacki R, Gajjar A, Zhang J, Beroukhi R, Fraenkel E, Korbel JO, Brors B, Schlesner M, Eils R, Marra MA, Pfister SM, Taylor MD, Lichter P. The whole-genome landscape of medulloblastoma subtypes. *Nature*. 2017;547(7663):311-317.
86. UniProt: the universal protein knowledgebase. *Nucleic Acids Res*. 2017;45(D1):D158-d169.
87. Ramaswamy V, Remke M, Bouffet E, Bailey S, Clifford SC, Doz F, Kool M, Dufour C, Vassal G, Milde T, Witt O, von Hoff K, Pietsch T, Northcott PA, Gajjar A, Robinson GW, Padovani L, André N, Massimino M, Pizer B, Packer R, Rutkowski S, Pfister SM, Taylor MD, Pomeroy SL. Risk stratification of childhood medulloblastoma in the molecular era: the current consensus. *Acta Neuropathol*. 2016;131(6):821-831.
88. Perreault S, Ramaswamy V, Achrol AS, Chao K, Liu TT, Shih D, Remke M, Schubert S, Bouffet E, Fisher PG, Partap S, Vogel H, Taylor MD, Cho YJ, Yeom KW. MRI surrogates for molecular subgroups of medulloblastoma. *AJNR Am J Neuroradiol*. 2014;35(7):1263-1269.
89. Wilne S, Collier J, Kennedy C, Jenkins A, Grout J, Mackie S, Koller K, Grundy R, Walker D. Progression from first symptom to diagnosis in childhood brain tumours. *Eur J Pediatr*. 2012;171(1):87-93.
90. Martin AM, Raabe E, Eberhart C, Cohen KJ. Management of pediatric and adult patients with medulloblastoma. *Curr Treat Options Oncol*. 2014;15(4):581-594.

Chapter 1: References

91. Spiegler BJ, Bouffet E, Greenberg ML, Rutka JT, Mabbott DJ. Change in neurocognitive functioning after treatment with cranial radiation in childhood. *J Clin Oncol.* 2004;22(4):706-713.
92. Mabbott DJ, Penkman L, Witol A, Strother D, Bouffet E. Core neurocognitive functions in children treated for posterior fossa tumors. *Neuropsychology.* 2008;22(2):159-168.
93. Robinson GW, Orr BA, Wu G, Gururangan S, Lin T, Qaddoumi I, Packer RJ, Goldman S, Prados MD, Desjardins A, Chintagumpala M, Takebe N, Kaste SC, Rusch M, Allen SJ, Onar-Thomas A, Stewart CF, Fouladi M, Boyett JM, Gilbertson RJ, Curran T, Ellison DW, Gajjar A. Vismodegib Exerts Targeted Efficacy Against Recurrent Sonic Hedgehog-Subgroup Medulloblastoma: Results From Phase II Pediatric Brain Tumor Consortium Studies PBTC-025B and PBTC-032. *J Clin Oncol.* 2015;33(24):2646-2654.
94. Phillips LE, Koepsell TD, van Belle G, Kukull WA, Gehrels JA, Longstreth WT, Jr. History of head trauma and risk of intracranial meningioma: population-based case-control study. *Neurology.* 2002;58(12):1849-1852.
95. Riemenschneider MJ, Perry A, Reifenberger G. Histological classification and molecular genetics of meningiomas. *Lancet Neurol.* 2006;5(12):1045-1054.
96. Bickerstaff ER, Small JM, Guest IA. The relapsing course of certain meningiomas in relation to pregnancy and menstruation. *J Neurol Neurosurg Psychiatry.* 1958;21(2):89-91.
97. Koenig MA, Geocadin RG, Kulesza P, Olivi A, Brem H. Rhabdoid meningioma occurring in an unrelated resection cavity with leptomeningeal carcinomatosis. Case report. *J Neurosurg.* 2005;102(2):371-375.
98. Evans DG. Neurofibromatosis type 2. *Handb Clin Neurol.* 2015;132:87-96.
99. Kerr K, Qualmann K, Esquenazi Y, Hagan J, Kim DH. Familial Syndromes Involving Meningiomas Provide Mechanistic Insight Into Sporadic Disease. *Neurosurgery.* 2018;83(6):1107-1118.
100. Asgharian B, Chen YJ, Patronas NJ, Peghini PL, Reynolds JC, Vortmeyer A, Zhuang Z, Venzon DJ, Gibril F, Jensen RT. Meningiomas may be a component tumor of multiple endocrine neoplasia type 1. *Clin Cancer Res.* 2004;10(3):869-880.
101. Mortimer PS, Geaney DP, Liddell K, Dawber RP. Basal cell naevus syndrome and intracranial meningioma. *J Neurol Neurosurg Psychiatry.* 1984;47(2):210-212.
102. Yakubov E, Ghochani A, Buslei R, Buchfelder M, Eyüpoglu IY, Savaskan N. Hidden association of Cowden syndrome, PTEN mutation and meningioma frequency. *Oncoscience.* 2016;3(5-6):149-155.
103. Goto M, Miller RW, Ishikawa Y, Sugano H. Excess of rare cancers in Werner syndrome (adult progeria). *Cancer Epidemiol Biomarkers Prev.* 1996;5(4):239-246.
104. Abdel-Rahman MH, Pilarski R, Cebulla CM, Massengill JB, Christopher BN, Boru G, Hovland P, Davidorf FH. Germline BAP1 mutation predisposes to uveal melanoma, lung adenocarcinoma, meningioma, and other cancers. *J Med Genet.* 2011;48(12):856-859.
105. Leblanc R. Familial adenomatous polyposis and benign intracranial tumors: a new variant of Gardner's syndrome. *Can J Neurol Sci.* 2000;27(4):341-346.
106. Kanno H, Yamamoto I, Yoshida M, Kitamura H. Meningioma showing VHL gene inactivation in a patient with von Hippel-Lindau disease. *Neurology.* 2003;60(7):1197-1199.
107. Gerkes EH, Fock JM, den Dunnen WF, van Belzen MJ, van der Lans CA, Hoving EW, Fakkert IE, Smith MJ, Evans DG, Olderode-Berends MJ. A heritable form of SMARCE1-related meningiomas with important implications for follow-up and family screening. *Neurogenetics.* 2016;17(2):83-89.
108. Bacci C, Sestini R, Provenzano A, Paganini I, Mancini I, Porfirio B, Vivarelli R, Genuardi M, Papi L. Schwannomatosis associated with multiple meningiomas due to a familial SMARCB1 mutation. *Neurogenetics.* 2010;11(1):73-80.
109. Rutledge MH, Sarrazin J, Rangaratnam S, Phelan CM, Twist E, Merel P, Delattre O, Thomas G, Nordenskjöld M, Collins VP, Dumanski JP, Rouleau GA. Evidence for the complete inactivation of the NF2 gene in the majority of sporadic meningiomas. *Nat Genet.* 1994;6(2):180-184.
110. Bi WL, Greenwald NF, Abedalthagafi M, Wala J, Gibson WJ, Agarwalla PK, Horowitz P, Schumacher SE, Esaulova E, Mei Y, Chevalier A, Ducar M, Thorner AR, van Hummelen P, Stemmer-Rachamimov A, Artyomov M, Al-Mefty O, Dunn GP, Santagata S, Dunn IF, Beroukheim R. Genomic landscape of high-grade meningiomas. *NPJ Genom Med.* 2017;2.
111. Rutledge MH, Xie YG, Han FY, Peyrard M, Collins VP, Nordenskjöld M, Dumanski JP. Deletions on chromosome 22 in sporadic meningioma. *Genes Chromosomes Cancer.* 1994;10(2):122-130.
112. Abedalthagafi M, Bi WL, Aizer AA, Merrill PH, Brewster R, Agarwalla PK, Listewnik ML, Dias-Santagata D, Thorner AR, Van Hummelen P, Brastianos PK, Reardon DA, Wen PY, Al-Mefty O, Ramkissoon SH, Folkerth RD, Ligon KL, Ligon AH, Alexander BM, Dunn IF, Beroukheim R, Santagata S. Oncogenic PI3K mutations are as common as AKT1 and SMO mutations in meningioma. *Neuro Oncol.* 2016;18(5):649-655.
113. Brastianos PK, Horowitz PM, Santagata S, Jones RT, McKenna A, Getz G, Ligon KL, Palesscandolo E, Van Hummelen P, Ducar MD, Raza A, Sunkavalli A, Macconail LE, Stemmer-Rachamimov AO, Louis DN, Hahn WC, Dunn IF, Beroukheim R. Genomic sequencing of meningiomas identifies oncogenic SMO and AKT1 mutations. *Nat Genet.* 2013;45(3):285-289.
114. Shankar GM, Abedalthagafi M, Vaubel RA, Merrill PH, Nayyar N, Gill CM, Brewster R, Bi WL, Agarwalla PK, Thorner AR, Reardon DA, Al-Mefty O, Wen PY, Alexander BM, van Hummelen P, Batchelor TT, Ligon KL, Ligon AH, Meyerson M, Dunn IF, Beroukheim R, Louis DN, Perry A, Carter SL, Giannini C, Curry WT, Jr., Cahill DP, Barker FG, 2nd, Brastianos PK, Santagata S. Germline and somatic BAP1 mutations in high-grade rhabdoid meningiomas. *Neuro Oncol.* 2017;19(4):535-545.
115. Goutagny S, Nault JC, Mallet M, Henin D, Rossi JZ, Kalamirides M. High incidence of activating TERT promoter mutations in meningiomas undergoing malignant progression. *Brain Pathol.* 2014;24(2):184-189.

Chapter 1: References

116. Clark VE, Erson-Omay EZ, Serin A, Yin J, Cotney J, Özduman K, Avşar T, Li J, Murray PB, Henegariu O, Yilmaz S, Günel JM, Carrión-Grant G, Yilmaz B, Grady C, Tanrikulu B, Bakircioğlu M, Kaymakçalan H, Caglayan AO, Sencar L, Ceyhun E, Atik AF, Bayri Y, Bai H, Kolb LE, Hebert RM, Omay SB, Mishra-Gorur K, Choi M, Overton JD, Holland EC, Mane S, State MW, Bilgüvar K, Baehring JM, Gutin PH, Piepmeier JM, Vortmeyer A, Brennan CW, Pamir MN, Kiliç T, Lifton RP, Noonan JP, Yasuno K, Günel M. Genomic analysis of non-NF2 meningiomas reveals mutations in TRAF7, KLF4, AKT1, and SMO. *Science*. 2013;339(6123):1077-1080.
117. Clark VE, Harmancı AS, Bai H, Youngblood MW, Lee TI, Baranoski JF, Ercan-Sencicek AG, Abraham BJ, Weintraub AS, Hnisz D, Simon M, Kirschek B, Erson-Omay EZ, Henegariu O, Carrión-Grant G, Mishra-Gorur K, Durán D, Goldmann JE, Schramm J, Goldbrunner R, Piepmeier JM, Vortmeyer AO, Günel JM, Bilgüvar K, Yasuno K, Young RA, Günel M. Recurrent somatic mutations in POLR2A define a distinct subset of meningiomas. *Nat Genet*. 2016;48(10):1253-1259.
118. Wils G, Lammens M, Marchal G, Van Calenbergh F, Plets C, Van Fraeyenhoven L, Baert AL. Thickening of dura surrounding meningiomas: MR features. *J Comput Assist Tomogr*. 1989;13(5):763-768.
119. Wen M, Jung S, Moon KS, Pei J, Lee KH, Jin SG, Li SY, Ryu HH. Immunohistochemical profile of the dural tail in intracranial meningiomas. *Acta Neurochir (Wien)*. 2014;156(12):2263-2273.
120. Kessler RA, Garzon-Muvdi T, Yang W, Weingart J, Olivi A, Huang J, Brem H, Lim M. Metastatic Atypical and Anaplastic Meningioma: A Case Series and Review of the Literature. *World Neurosurg*. 2017;101:47-56.
121. Perry A, Scheithauer BW, Stafford SL, Lohse CM, Wollan PC. "Malignancy" in meningiomas: a clinicopathologic study of 116 patients, with grading implications. *Cancer*. 1999;85(9):2046-2056.
122. Ito K, Imagama S, Ando K, Kobayashi K, Shido Y, Go Y, Arima H, Kanbara S, Hirose T, Matsuyama Y, Nishida Y, Ishiguro N. Intraspinal meningioma with malignant transformation and distant metastasis. *Nagoya J Med Sci*. 2017;79(1):97-102.
123. van Alkemade H, de Leau M, Dieleman EM, Kardaun JW, van Os R, Vandertop WP, van Furth WR, Stalpers LJ. Impaired survival and long-term neurological problems in benign meningioma. *Neuro Oncol*. 2012;14(5):658-666.
124. Apra C, Peyre M, Kalamarides M. Current treatment options for meningioma. *Expert Rev Neurother*. 2018;18(3):241-249.
125. Hasan S, Young M, Albert T, Shah AH, Okoye C, Bregy A, Lo SS, Ishkanian F, Komotar RJ. The role of adjuvant radiotherapy after gross total resection of atypical meningiomas. *World Neurosurg*. 2015;83(5):808-815.
126. Patibandla MR, Lee CC, Sheehan J. Stereotactic Radiosurgery of Central Skull Base Meningiomas-Volumetric Evaluation and Long-Term Outcomes. *World Neurosurg*. 2017;108:176-184.
127. Patibandla MR, Lee CC, Tata A, Addagada GC, Sheehan JP. Stereotactic radiosurgery for WHO grade I posterior fossa meningiomas: long-term outcomes with volumetric evaluation. *J Neurosurg*. 2018;129(5):1249-1259.
128. Durand A, Labrousse F, Jouvét A, Bauchet L, Kalamaridès M, Menei P, Deruty R, Moreau JJ, Fèvre-Montange M, Guyotat J. WHO grade II and III meningiomas: a study of prognostic factors. *J Neurooncol*. 2009;95(3):367-375.
129. Rapp C, Dettling S, Liu F, Ull AT, Warta R, Jungk C, Roesch S, Mock A, Sahm F, Schmidt M, Jungwirth G, Zweckberger K, Lamszus K, Gousias K, Kessler AF, Grabe N, Loehr M, Ketter R, Urbschat S, Senft C, Westphal M, Abdollahi A, Debus J, von Deimling A, Unterberg A, Simon M, Herold-Mende CC. Cytotoxic T Cells and their Activation Status are Independent Prognostic Markers in Meningiomas. *Clin Cancer Res*. 2019;25(17):5260-5270.
130. Perry A, Stafford SL, Scheithauer BW, Suman VJ, Lohse CM. Meningioma grading: an analysis of histologic parameters. *Am J Surg Pathol*. 1997;21(12):1455-1465.
131. Mason WP, Gentili F, Macdonald DR, Hariharan S, Cruz CR, Abrey LE. Stabilization of disease progression by hydroxyurea in patients with recurrent or unresectable meningioma. *J Neurosurg*. 2002;97(2):341-346.
132. Ji Y, Rankin C, Grunberg S, Sherrod AE, Ahmadi J, Townsend JJ, Feun LG, Fredericks RK, Russell CA, Kabbavar FF, Stelzer KJ, Schott A, Verschraegen C. Double-Blind Phase III Randomized Trial of the Antiprogestin Agent Mifepristone in the Treatment of Unresectable Meningioma: SWOG S9005. *J Clin Oncol*. 2015;33(34):4093-4098.
133. Graillon T, Romano D, Defilles C, Saveanu A, Mohamed A, Figarella-Branger D, Roche PH, Fuentes S, Chinot O, Dufour H, Barlier A. Octreotide therapy in meningiomas: in vitro study, clinical correlation, and literature review. *J Neurosurg*. 2017;127(3):660-669.
134. Graillon T, Defilles C, Mohamed A, Lisbonis C, Germanetti AL, Chinot O, Figarella-Branger D, Roche PH, Adetchessi T, Fuentes S, Metellus P, Dufour H, Enjalbert A, Barlier A. Combined treatment by octreotide and everolimus: Octreotide enhances inhibitory effect of everolimus in aggressive meningiomas. *J Neurooncol*. 2015;124(1):33-43.
135. Kaley TJ, Wen P, Schiff D, Ligon K, Haidar S, Karimi S, Lassman AB, Nolan CP, DeAngelis LM, Gavrilovic I, Norden A, Drappatz J, Lee EQ, Purow B, Plotkin SR, Batchelor T, Abrey LE, Omuro A. Phase II trial of sunitinib for recurrent and progressive atypical and anaplastic meningioma. *Neuro Oncol*. 2015;17(1):116-121.
136. Nayak L, Iwamoto FM, Rudnick JD, Norden AD, Lee EQ, Drappatz J, Omuro A, Kaley TJ. Atypical and anaplastic meningiomas treated with bevacizumab. *J Neurooncol*. 2012;109(1):187-193.
137. Medzhitov R, Janeway C, Jr. Innate immune recognition: mechanisms and pathways. *Immunol Rev*. 2000;173:89-97.

Chapter 1: References

138. Medzhitov R, Janeway CA, Jr. Innate immunity: impact on the adaptive immune response. *Curr Opin Immunol*. 1997;9(1):4-9.
139. Delves PJ, Roitt IM. The immune system. Second of two parts. *N Engl J Med*. 2000;343(2):108-117.
140. Sakaguchi S, Sakaguchi N, Asano M, Itoh M, Toda M. Immunologic self-tolerance maintained by activated T cells expressing IL-2 receptor alpha-chains (CD25). Breakdown of a single mechanism of self-tolerance causes various autoimmune diseases. *J Immunol*. 1995;155(3):1151-1164.
141. MacLennan ICM, Gulbranson-Judge A, Toellner KM, Casamayor-Palleja M, Chan E, Sze DMY, Luther SA, Orbea HA. The changing preference of T and B cells for partners as T-dependent antibody responses develop. *Immunol Rev*. 1997;156:53-66.
142. Delves PJ, Roitt IM. The immune system. First of two parts. *N Engl J Med*. 2000;343(1):37-49.
143. Boniface JJ, Davis MM. T-cell recognition of antigen. A process controlled by transient intermolecular interactions. *Ann N Y Acad Sci*. 1995;766:62-69.
144. Gruen JR, Weissman SM. Evolving views of the major histocompatibility complex. *Blood*. 1997;90(11):4252-4265.
145. Goldberg AC, Rizzo LV. MHC structure and function - antigen presentation. Part 1. *Einstein (Sao Paulo)*. 2015;13(1):153-156.
146. Beck S, Trowsdale J. Sequence organisation of the class II region of the human MHC. *Immunol Rev*. 1999;167:201-210.
147. Kambayashi T, Laufer TM. Atypical MHC class II-expressing antigen-presenting cells: can anything replace a dendritic cell? *Nat Rev Immunol*. 2014;14(11):719-730.
148. Dengjel J, Nastke MD, Gouttefangeas C, Gitsioudis G, Schoor O, Altenberend F, Muller M, Kramer B, Missiou A, Sauter M, Hennenlotter J, Wernet D, Stenzl A, Rammensee HG, Klingel K, Stevanović S. Unexpected abundance of HLA class II presented peptides in primary renal cell carcinomas. *Clin Cancer Res*. 2006;12(14 Pt 1):4163-4170.
149. Neidert MC, Kowalewski DJ, Silginer M, Kapolou K, Backert L, Freudenmann LK, Peper JK, Marcu A, Wang SS, Walz JS, Wolpert F, Rammensee HG, Henschler R, Lamszus K, Westphal M, Roth P, Regli L, Stevanović S, Weller M, Eisele G. The natural HLA ligandome of glioblastoma stem-like cells: antigen discovery for T cell-based immunotherapy. *Acta Neuropathol*. 2018;135(6):923-938.
150. Boehm U, Klamp T, Groot M, Howard JC. Cellular responses to interferon-gamma. *Annu Rev Immunol*. 1997;15:749-795.
151. Robinson J, Halliwell JA, Hayhurst JD, Flicek P, Parham P, Marsh SG. The IPD and IMGT/HLA database: allele variant databases. *Nucleic Acids Res*. 2015;43(Database issue):D423-431.
152. Bhagavan NV, Ha C-E. Essentials of Medical Biochemistry: With Clinical Cases, 1 ed.: Waltham: Academic Press; 2011.
153. Goldberg AC, Rizzo LV. MHC structure and function - antigen presentation. Part 2. *Einstein (Sao Paulo)*. 2015;13(1):157-162.
154. Finley D. Recognition and processing of ubiquitin-protein conjugates by the proteasome. *Annu Rev Biochem*. 2009;78:477-513.
155. Parcej D, Tampe R. ABC proteins in antigen translocation and viral inhibition. *Nat Chem Biol*. 2010;6(8):572-580.
156. Adiko AC, Babdor J, Gutierrez-Martinez E, Guernonprez P, Saveanu L. Intracellular Transport Routes for MHC I and Their Relevance for Antigen Cross-Presentation. *Front Immunol*. 2015;6:335.
157. Madden DR, Garboczi DN, Wiley DC. The antigenic identity of peptide-MHC complexes: a comparison of the conformations of five viral peptides presented by HLA-A2. *Cell*. 1993;75(4):693-708.
158. Rammensee HG. Chemistry of peptides associated with MHC class I and class II molecules. *Curr Opin Immunol*. 1995;7(1):85-96.
159. Guo HC, Jardetzky TS, Garrett TP, Lane WS, Strominger JL, Wiley DC. Different length peptides bind to HLA-Aw68 similarly at their ends but bulge out in the middle. *Nature*. 1992;360(6402):364-366.
160. Falk K, Rötzschke O, Stevanović S, Jung G, Rammensee HG. Allele-specific motifs revealed by sequencing of self-peptides eluted from MHC molecules. *Nature*. 1991;351(6324):290-296.
161. Rammensee HG, Friede T, Stevanović S. MHC ligands and peptide motifs: first listing. *Immunogenetics*. 1995;41(4):178-228.
162. Kobayashi KS, van den Elsen PJ. NLRC5: a key regulator of MHC class I-dependent immune responses. *Nat Rev Immunol*. 2012;12(12):813-820.
163. Roche PA, Furuta K. The ins and outs of MHC class II-mediated antigen processing and presentation. *Nat Rev Immunol*. 2015;15(4):203-216.
164. Wolf PR, Ploegh HL. How MHC class II molecules acquire peptide cargo: biosynthesis and trafficking through the endocytic pathway. *Annu Rev Cell Dev Biol*. 1995;11:267-306.
165. Dengjel J, Schoor O, Fischer R, Reich M, Kraus M, Muller M, Kreymborg K, Altenberend F, Brandenburg J, Kalbacher H, Brock R, Driessen C, Rammensee HG, Stevanovic S. Autophagy promotes MHC class II presentation of peptides from intracellular source proteins. *Proc Natl Acad Sci U S A*. 2005;102(22):7922-7927.
166. Cresswell P. Assembly, transport, and function of MHC class II molecules. *Annu Rev Immunol*. 1994;12:259-293.
167. Lippolis JD, White FM, Marto JA, Luckey CJ, Bullock TN, Shabanowitz J, Hunt DF, Engelhard VH. Analysis of MHC class II antigen processing by quantitation of peptides that constitute nested sets. *J Immunol*. 2002;169(9):5089-5097.

Chapter 1: References

168. Stern LJ, Brown JH, Jardetzky TS, Gorga JC, Urban RG, Strominger JL, Wiley DC. Crystal structure of the human class II MHC protein HLA-DR1 complexed with an influenza virus peptide. *Nature*. 1994;368(6468):215-221.
169. Chicz RM, Urban RG, Gorga JC, Vignali DA, Lane WS, Strominger JL. Specificity and promiscuity among naturally processed peptides bound to HLA-DR alleles. *J Exp Med*. 1993;178(1):27-47.
170. Rötzschke O, Falk K. Origin, structure and motifs of naturally processed MHC class II ligands. *Curr Opin Immunol*. 1994;6(1):45-51.
171. Sinigaglia F, Hammer J. Defining rules for the peptide-MHC class II interaction. *Curr Opin Immunol*. 1994;6(1):52-56.
172. Rock KL, Shen L. Cross-presentation: underlying mechanisms and role in immune surveillance. *Immunol Rev*. 2005;207:166-183.
173. Parish CR. Cancer immunotherapy: the past, the present and the future. *Immunol Cell Biol*. 2003;81(2):106-113.
174. Coulie PG, Van den Eynde BJ, van der Bruggen P, Boon T. Tumour antigens recognized by T lymphocytes: at the core of cancer immunotherapy. *Nat Rev Cancer*. 2014;14(2):135-146.
175. Coley WB. The treatment of malignant tumors by repeated inoculations of erysipelas. With a report of ten original cases. *Am J Med Sci*. 1893;105:487-511.
176. Urban JL, Schreiber H. Tumor antigens. *Annu Rev Immunol*. 1992;10:617-644.
177. Freudenmann LK, Marcu A, Stevanović S. Mapping the tumour human leukocyte antigen (HLA) ligandome by mass spectrometry. *Immunology*. 2018;154(3):331-345.
178. Weinzierl AO, Maurer D, Altenberend F, Schneiderhan-Marra N, Klingel K, Schoor O, Wernet D, Joos T, Rammensee HG, Stevanović S. A cryptic vascular endothelial growth factor T-cell epitope: identification and characterization by mass spectrometry and T-cell assays. *Cancer Res*. 2008;68(7):2447-2454.
179. Laumont CM, Daouda T, Laverdure JP, Bonneil É, Caron-Lizotte O, Hardy MP, Granados DP, Durette C, Lemieux S, Thibault P, Perreault C. Global proteogenomic analysis of human MHC class I-associated peptides derived from non-canonical reading frames. *Nat Commun*. 2016;7:10238.
180. Cobbold M, De La Peña H, Norris A, Polefrone JM, Qian J, English AM, Cummings KL, Penny S, Turner JE, Cottine J, Abelin JG, Malaker SA, Zarlino AL, Huang HW, Goodyear O, Freeman SD, Shabanowitz J, Pratt G, Craddock C, Williams ME, Hunt DF, Engelhard VH. MHC class I-associated phosphopeptides are the targets of memory-like immunity in leukemia. *Sci Transl Med*. 2013;5(203):203ra125.
181. Mishto M, Liepe J. Post-Translational Peptide Splicing and T Cell Responses. *Trends Immunol*. 2017;38(12):904-915.
182. Liepe J, Marino F, Sidney J, Jeko A, Bunting DE, Sette A, Kloetzel PM, Stumpf MP, Heck AJ, Mishto M. A large fraction of HLA class I ligands are proteasome-generated spliced peptides. *Science*. 2016;354(6310):354-358.
183. DeLong T, Wiles TA, Baker RL, Bradley B, Barbour G, Reisdorph R, Armstrong M, Powell RL, Reisdorph N, Kumar N, Elso CM, DeNicola M, Bottino R, Powers AC, Harlan DM, Kent SC, Mannering SI, Haskins K. Pathogenic CD4 T cells in type 1 diabetes recognize epitopes formed by peptide fusion. *Science*. 2016;351(6274):711-714.
184. Duvall E, Boulpicante M, Yamazaki T, Daskalogianni C, Prado Martins R, Baconnais S, Manoury B, Fahraeus R, Apcher S. Exosome-driven transfer of tumor-associated Pioneer Translation Products (TA-PTPs) for the MHC class I cross-presentation pathway. *Oncoimmunology*. 2016;5(9):e1198865.
185. Obeid J, Hu Y, Slingluff CL, Jr. Vaccines, Adjuvants, and Dendritic Cell Activators-Current Status and Future Challenges. *Semin Oncol*. 2015;42(4):549-561.
186. Ouspenskaia T, Law T, Clauser KR, Klaeger S, Sarkizova S, Aguet F, Li B, Christian E, Knisbacher BA, Le PM, Hartigan CR, Keshishian H, Appfel A, Oliveira G, Zhang W, Chow YT, Ji Z, Shukla SA, Bachireddy P, Getz G, Hacohen N, Keskin DB, Carr SA, Wu CJ, Regev A. Thousands of novel unannotated proteins expand the MHC I immunopeptidome in cancer. *bioRxiv*. 2020:2020.2002.2012.945840.
187. van der Bruggen P, Traversari C, Chomez P, Lurquin C, De Plaen E, Van den Eynde B, Knuth A, Boon T. A gene encoding an antigen recognized by cytolytic T lymphocytes on a human melanoma. *Science*. 1991;254(5038):1643-1647.
188. Brichard V, Van Pel A, Wölfel T, Wölfel C, De Plaen E, Lethe B, Coulie P, Boon T. The tyrosinase gene codes for an antigen recognized by autologous cytolytic T lymphocytes on HLA-A2 melanomas. *J Exp Med*. 1993;178(2):489-495.
189. Cox AL, Skipper J, Chen Y, Henderson RA, Darrow TL, Shabanowitz J, Engelhard VH, Hunt DF, Slingluff CL, Jr. Identification of a peptide recognized by five melanoma-specific human cytotoxic T cell lines. *Science*. 1994;264(5159):716-719.
190. Topalian SL, Gonzales MI, Parkhurst M, Li YF, Southwood S, Sette A, Rosenberg SA, Robbins PF. Melanoma-specific CD4+ T cells recognize nonmutated HLA-DR-restricted tyrosinase epitopes. *J Exp Med*. 1996;183(5):1965-1971.
191. Vigneron N, Stroobant V, Van den Eynde BJ, van der Bruggen P. Database of T cell-defined human tumor antigens: the 2013 update. *Cancer Immun*. 2013;13:15.
192. Klein G, Klein E. Immune surveillance against virus-induced tumors and nonrejectability of spontaneous tumors: contrasting consequences of host versus tumor evolution. *Proc Natl Acad Sci U S A*. 1977;74(5):2121-2125.
193. Levy JP, Leclerc JC. The murine sarcoma virus-induced tumor: exception or general model in tumor immunology? *Adv Cancer Res*. 1977;24:1-66.

Chapter 1: References

194. van der Burg SH, Melief CJ. Therapeutic vaccination against human papilloma virus induced malignancies. *Curr Opin Immunol*. 2011;23(2):252-257.
195. Fisk B, Blevins TL, Wharton JT, Ioannides CG. Identification of an immunodominant peptide of HER-2/neu protooncogene recognized by ovarian tumor-specific cytotoxic T lymphocyte lines. *J Exp Med*. 1995;181(6):2109-2117.
196. Gouttefangeas C, Rammensee HG. Personalized cancer vaccines: adjuvants are important, too. *Cancer Immunol Immunother*. 2018;67(12):1911-1918.
197. Gotter J, Brors B, Hergenbahn M, Kyewski B. Medullary epithelial cells of the human thymus express a highly diverse selection of tissue-specific genes colocalized in chromosomal clusters. *J Exp Med*. 2004;199(2):155-166.
198. Ochs K, Ott M, Bunse T, Sahm F, Bunse L, Deumelandt K, Sonner JK, Keil M, von Deimling A, Wick W, Platten M. K27M-mutant histone-3 as a novel target for glioma immunotherapy. *Oncoimmunology*. 2017;6(7):e1328340.
199. Hanahan D, Weinberg RA. Hallmarks of cancer: the next generation. *Cell*. 2011;144(5):646-674.
200. Dunn GP, Old LJ, Schreiber RD. The immunobiology of cancer immunosurveillance and immunoediting. *Immunity*. 2004;21(2):137-148.
201. Dunn GP, Old LJ, Schreiber RD. The three Es of cancer immunoediting. *Annu Rev Immunol*. 2004;22:329-360.
202. Curiel TJ. Tregs and rethinking cancer immunotherapy. *J Clin Invest*. 2007;117(5):1167-1174.
203. Velcheti V, Schalper K. Basic Overview of Current Immunotherapy Approaches in Cancer. *Am Soc Clin Oncol Educ Book*. 2016;35:298-308.
204. Schreiber RD, Old LJ, Smyth MJ. Cancer immunoediting: integrating immunity's roles in cancer suppression and promotion. *Science*. 2011;331(6024):1565-1570.
205. Domogalla MP, Rostan PV, Raker VK, Steinbrink K. Tolerance through Education: How Tolerogenic Dendritic Cells Shape Immunity. *Front Immunol*. 2017;8:1764.
206. Rozali EN, Hato SV, Robinson BW, Lake RA, Lesterhuis WJ. Programmed death ligand 2 in cancer-induced immune suppression. *Clin Dev Immunol*. 2012;2012:656340.
207. Mapara MY, Sykes M. Tolerance and cancer: mechanisms of tumor evasion and strategies for breaking tolerance. *J Clin Oncol*. 2004;22(6):1136-1151.
208. Palena C, Schlom J. Vaccines against human carcinomas: strategies to improve antitumor immune responses. *J Biomed Biotechnol*. 2010;2010:380697.
209. Schaller TH, Sampson JH. Advances and challenges: dendritic cell vaccination strategies for glioblastoma. *Expert Rev Vaccines*. 2017;16(1):27-36.
210. Kantoff PW, Higano CS, Shore ND, Berger ER, Small EJ, Penson DF, Redfern CH, Ferrari AC, Dreicer R, Sims RB, Xu Y, Frohlich MW, Schellhammer PF. Sipuleucel-T immunotherapy for castration-resistant prostate cancer. *N Engl J Med*. 2010;363(5):411-422.
211. van der Burg SH, Kalos M, Gouttefangeas C, Janetzki S, Ottensmeier C, Welters MJ, Romero P, Britten CM, Hoos A. Harmonization of immune biomarker assays for clinical studies. *Sci Transl Med*. 2011;3(108):108ps144.
212. Rammensee HG, Weinschenk T, Gouttefangeas C, Stevanovic S. Towards patient-specific tumor antigen selection for vaccination. *Immunol Rev*. 2002;188:164-176.
213. Rosenberg SA, Yang JC, Restifo NP. Cancer immunotherapy: moving beyond current vaccines. *Nat Med*. 2004;10(9):909-915.
214. Aucouturier J, Dupuis L, Deville S, Ascarateil S, Ganne V. Montanide ISA 720 and 51: a new generation of water in oil emulsions as adjuvants for human vaccines. *Expert Rev Vaccines*. 2002;1(1):111-118.
215. Parmiani G, Castelli C, Pilla L, Santinami M, Colombo MP, Rivoltini L. Opposite immune functions of GM-CSF administered as vaccine adjuvant in cancer patients. *Ann Oncol*. 2007;18(2):226-232.
216. Speiser DE, Liénard D, Rufer N, Rubio-Godoy V, Rimoldi D, Lejeune F, Krieg AM, Cerottini JC, Romero P. Rapid and strong human CD8+ T cell responses to vaccination with peptide, IFA, and CpG oligodeoxynucleotide 7909. *J Clin Invest*. 2005;115(3):739-746.
217. Rammensee HG, Wiesmüller KH, Chandran PA, Zelba H, Rusch E, Gouttefangeas C, Kowalewski DJ, Di Marco M, Haen SP, Walz JS, Gloria YC, Bödder J, Schertel JM, Tunger A, Müller L, Kiessler M, Wehner R, Schmitz M, Jakobi M, Schneiderhan-Marra N, Klein R, Laske K, Artzner K, Backert L, Schuster H, Schwenck J, Weber ANR, Pichler BJ, Kneilling M, la Fougère C, Forchhammer S, Metzler G, Bauer J, Weide B, Schippert W, Stevanović S, Löffler MW. A new synthetic toll-like receptor 1/2 ligand is an efficient adjuvant for peptide vaccination in a human volunteer. *J Immunother Cancer*. 2019;7(1):307.
218. Berraondo P, Sanmamed MF, Ochoa MC, Etxeberria I, Aznar MA, Pérez-Gracia JL, Rodríguez-Ruiz ME, Ponz-Sarvisé M, Castañón E, Melero I. Cytokines in clinical cancer immunotherapy. *Br J Cancer*. 2019;120(1):6-15.
219. Begley CG, Burton JD, Tsudo M, Brownstein BH, Ambrus JL, Jr., Waldmann TA. Human B lymphocytes express the p75 component of the interleukin 2 receptor. *Leuk Res*. 1990;14(3):263-271.
220. McNally A, Hill GR, Sparwasser T, Thomas R, Steptoe RJ. CD4+CD25+ regulatory T cells control CD8+ T-cell effector differentiation by modulating IL-2 homeostasis. *Proc Natl Acad Sci U S A*. 2011;108(18):7529-7534.
221. Herndon TM, Demko SG, Jiang X, He K, Gootenberg JE, Cohen MH, Keegan P, Pazdur R. U.S. Food and Drug Administration Approval: peginterferon-alfa-2b for the adjuvant treatment of patients with melanoma. *Oncologist*. 2012;17(10):1323-1328.

Chapter 1: References

222. Spaapen RM, Leung MY, Fuertes MB, Kline JP, Zhang L, Zheng Y, Fu YX, Luo X, Cohen KS, Gajewski TF. Therapeutic activity of high-dose intratumoral IFN-beta requires direct effect on the tumor vasculature. *J Immunol.* 2014;193(8):4254-4260.
223. Hervas-Stubbs S, Perez-Gracia JL, Rouzaut A, Sanmamed MF, Le Bon A, Melero I. Direct effects of type I interferons on cells of the immune system. *Clin Cancer Res.* 2011;17(9):2619-2627.
224. Fioravanti J, Medina-Echeverez J, Ardaiz N, Gomar C, Parra-Guillén ZP, Prieto J, Berraondo P. The fusion protein of IFN-alpha and apolipoprotein A-I crosses the blood-brain barrier by a saturable transport mechanism. *J Immunol.* 2012;188(8):3988-3992.
225. Cauwels A, Van Lint S, Paul F, Garcin G, De Koker S, Van Parys A, Wueest T, Gerlo S, Van der Heyden J, Bordat Y, Catteeuw D, Rogge E, Verhee A, Vandekerckhove B, Kley N, Uzé G, Tavernier J. Delivering Type I Interferon to Dendritic Cells Empowers Tumor Eradication and Immune Combination Treatments. *Cancer Res.* 2018;78(2):463-474.
226. Kennedy MK, Glaccum M, Brown SN, Butz EA, Viney JL, Embers M, Matsuki N, Charrier K, Sedger L, Willis CR, Brasel K, Morrissey PJ, Stocking K, Schuh JC, Joyce S, Peschon JJ. Reversible defects in natural killer and memory CD8 T cell lineages in interleukin 15-deficient mice. *J Exp Med.* 2000;191(5):771-780.
227. Di Scala M, Gil-Fariña I, Olagüe C, Vales A, Sobrevals L, Fortes P, Corbacho D, González-Asequinolaza G. Identification of IFN-gamma-producing T cells as the main mediators of the side effects associated to mouse interleukin-15 sustained exposure. *Oncotarget.* 2016;7(31):49008-49026.
228. Marshall D, Sinclair C, Tung S, Seddon B. Differential requirement for IL-2 and IL-15 during bifurcated development of thymic regulatory T cells. *J Immunol.* 2014;193(11):5525-5533.
229. Conlon KC, Lugli E, Welles HC, Rosenberg SA, Fojo AT, Morris JC, Fleisher TA, Dubois SP, Perera LP, Stewart DM, Goldman CK, Bryant BR, Decker JM, Chen J, Worthy TA, Figg WD, Sr., Peer CJ, Sneller MC, Lane HC, Yovandich JL, Creekmore SP, Roederer M, Waldmann TA. Redistribution, hyperproliferation, activation of natural killer cells and CD8 T cells, and cytokine production during first-in-human clinical trial of recombinant human interleukin-15 in patients with cancer. *J Clin Oncol.* 2015;33(1):74-82.
230. Mortier E, Quémener A, Vusio P, Lorenzen I, Boublik Y, Grötzing J, Plet A, Jacques Y. Soluble interleukin-15 receptor alpha (IL-15R alpha)-sushi as a selective and potent agonist of IL-15 action through IL-15R beta/gamma. Hyperagonist IL-15 x IL-15R alpha fusion proteins. *J Biol Chem.* 2006;281(3):1612-1619.
231. Ochoa MC, Melero I, Berraondo P. High-density lipoproteins delivering interleukin-15. *Oncoimmunology.* 2013;2(4):e23410.
232. Nobel Media AB 2019. NobelPrize.org. The Nobel Prize in Physiology or Medicine 2018. [Internet]. Available from: <https://www.nobelprize.org/prizes/medicine/2018/summary/>, accessed on 2019/11/21.
233. Greenfield EA, Nguyen KA, Kuchroo VK. CD28/B7 costimulation: a review. *Crit Rev Immunol.* 1998;18(5):389-418.
234. O'Day SJ, Hamid O, Urba WJ. Targeting cytotoxic T-lymphocyte antigen-4 (CTLA-4): a novel strategy for the treatment of melanoma and other malignancies. *Cancer.* 2007;110(12):2614-2627.
235. Simpson TR, Li F, Montalvo-Ortiz W, Sepulveda MA, Bergerhoff K, Arce F, Roddie C, Henry JY, Yagita H, Wolchok JD, Peggs KS, Ravetch JV, Allison JP, Quezada SA. Fc-dependent depletion of tumor-infiltrating regulatory T cells co-defines the efficacy of anti-CTLA-4 therapy against melanoma. *J Exp Med.* 2013;210(9):1695-1710.
236. Wing K, Onishi Y, Prieto-Martin P, Yamaguchi T, Miyara M, Fehervari Z, Nomura T, Sakaguchi S. CTLA-4 control over Foxp3+ regulatory T cell function. *Science.* 2008;322(5899):271-275.
237. Romano E, Kusio-Kobialka M, Foukas PG, Baumgaertner P, Meyer C, Ballabeni P, Michielin O, Weide B, Romero P, Speiser DE. Ipilimumab-dependent cell-mediated cytotoxicity of regulatory T cells ex vivo by nonclassical monocytes in melanoma patients. *Proc Natl Acad Sci U S A.* 2015;112(19):6140-6145.
238. Keir ME, Liang SC, Guleria I, Latchman YE, Qipo A, Albacker LA, Koulmanda M, Freeman GJ, Sayegh MH, Sharpe AH. Tissue expression of PD-L1 mediates peripheral T cell tolerance. *J Exp Med.* 2006;203(4):883-895.
239. Yearley JH, Gibson C, Yu N, Moon C, Murphy E, Juco J, Lunceford J, Cheng J, Chow LQM, Seiwert TY, Handa M, Tomassini JE, McClanahan T. PD-L2 Expression in Human Tumors: Relevance to Anti-PD-1 Therapy in Cancer. *Clin Cancer Res.* 2017;23(12):3158-3167.
240. Lesterhuis WJ, Steer H, Lake RA. PD-L2 is predominantly expressed by Th2 cells. *Mol Immunol.* 2011;49(1-2):1-3.
241. Buder-Bakhaya K, Hassel JC. Biomarkers for Clinical Benefit of Immune Checkpoint Inhibitor Treatment-A Review From the Melanoma Perspective and Beyond. *Front Immunol.* 2018;9:1474.
242. Hamid O, Robert C, Daud A, Hodi FS, Hwu WJ, Kefford R, Wolchok JD, Hersey P, Joseph RW, Weber JS, Dronca R, Gangadhar TC, Patnaik A, Zarour H, Joshua AM, Gergich K, Elassaiss-Schaap J, Algazi A, Mateus C, Boasberg P, Tumeh PC, Chmielowski B, Ebbinghaus SW, Li XN, Kang SP, Ribas A. Safety and tumor responses with lambrolizumab (anti-PD-1) in melanoma. *N Engl J Med.* 2013;369(2):134-144.
243. Wolchok JD, Kluger H, Callahan MK, Postow MA, Rizvi NA, Lesokhin AM, Segal NH, Ariyan CE, Gordon RA, Reed K, Burke MM, Caldwell A, Kronenberg SA, Agunwamba BU, Zhang X, Lowy I, Inzunza HD, Feely W, Horak CE, Hong Q, Korman AJ, Wigginton JM, Gupta A, Sznol M. Nivolumab plus ipilimumab in advanced melanoma. *N Engl J Med.* 2013;369(2):122-133.
244. Topalian SL, Hodi FS, Brahmer JR, Gettinger SN, Smith DC, McDermott DF, Powderly JD, Carvajal RD, Sosman JA, Atkins MB, Leming PD, Spigel DR, Antonia SJ, Horn L, Drake CG, Pardoll DM, Chen L, Sharfman WH, Anders RA, Taube JM, McMiller TL, Xu H, Korman AJ, Jure-Kunkel M, Agrawal S, McDonald D, Kollia

Chapter 1: References

- GD, Gupta A, Wigginton JM, Sznol M. Safety, activity, and immune correlates of anti-PD-1 antibody in cancer. *N Engl J Med*. 2012;366(26):2443-2454.
245. Ferris RL, Blumenschein G, Jr., Fayette J, Guigay J, Colevas AD, Licitra L, Harrington K, Kasper S, Vokes EE, Even C, Worden F, Saba NF, Iglesias Docampo LC, Haddad R, Rordorf T, Kiyota N, Tahara M, Monga M, Lynch M, Geese WJ, Kopit J, Shaw JW, Gillison ML. Nivolumab for Recurrent Squamous-Cell Carcinoma of the Head and Neck. *N Engl J Med*. 2016;375(19):1856-1867.
246. McDermott DF, Sosman JA, Sznol M, Massard C, Gordon MS, Hamid O, Powderly JD, Infante JR, Fasso M, Wang YV, Zou W, Hegde PS, Fine GD, Powles T. Atezolizumab, an Anti-Programmed Death-Ligand 1 Antibody, in Metastatic Renal Cell Carcinoma: Long-Term Safety, Clinical Activity, and Immune Correlates From a Phase Ia Study. *J Clin Oncol*. 2016;34(8):833-842.
247. Powles T, Eder JP, Fine GD, Braiteh FS, Loriot Y, Cruz C, Bellmunt J, Burris HA, Petrylak DP, Teng SL, Shen X, Boyd Z, Hegde PS, Chen DS, Vogelzang NJ. MPDL3280A (anti-PD-L1) treatment leads to clinical activity in metastatic bladder cancer. *Nature*. 2014;515(7528):558-562.
248. Markham A, Duggan S. Cemiplimab: First Global Approval. *Drugs*. 2018;78(17):1841-1846.
249. Qin S, Xu L, Yi M, Yu S, Wu K, Luo S. Novel immune checkpoint targets: moving beyond PD-1 and CTLA-4. *Mol Cancer*. 2019;18(1):155.
250. Aspeslagh S, Postel-Vinay S, Rusakiewicz S, Soria JC, Zitvogel L, Marabelle A. Rationale for anti-OX40 cancer immunotherapy. *Eur J Cancer*. 2016;52:50-66.
251. Chester C, Sanmamed MF, Wang J, Melero I. Immunotherapy targeting 4-1BB: mechanistic rationale, clinical results, and future strategies. *Blood*. 2018;131(1):49-57.
252. Zappasodi R, Sirard C, Li Y, Budhu S, Abu-Akeel M, Liu C, Yang X, Zhong H, Newman W, Qi J, Wong P, Schaer D, Koon H, Velcheti V, Hellmann MD, Postow MA, Callahan MK, Wolchok JD, Merghoub T. Rational design of anti-GITR-based combination immunotherapy. *Nat Med*. 2019;25(5):759-766.
253. Vonderheide RH, Glennie MJ. Agonistic CD40 antibodies and cancer therapy. *Clin Cancer Res*. 2013;19(5):1035-1043.
254. Pastor F. Aptamers: A New Technological Platform in Cancer Immunotherapy. *Pharmaceuticals (Basel)*. 2016;9(4).
255. Hoffman LM, Gore L. Blinatumomab, a Bi-Specific Anti-CD19/CD3 BiTE® Antibody for the Treatment of Acute Lymphoblastic Leukemia: Perspectives and Current Pediatric Applications. *Front Oncol*. 2014;4:63.
256. Oates J, Hassan NJ, Jakobsen BK. ImmTACs for targeted cancer therapy: Why, what, how, and which. *Mol Immunol*. 2015;67(2 Pt A):67-74.
257. Dudley ME, Wunderlich JR, Shelton TE, Even J, Rosenberg SA. Generation of tumor-infiltrating lymphocyte cultures for use in adoptive transfer therapy for melanoma patients. *J Immunother*. 2003;26(4):332-342.
258. Rosenberg SA, Packard BS, Aebersold PM, Solomon D, Topalian SL, Toy ST, Simon P, Lotze MT, Yang JC, Seipp CA. Use of tumor-infiltrating lymphocytes and interleukin-2 in the immunotherapy of patients with metastatic melanoma. A preliminary report. *N Engl J Med*. 1988;319(25):1676-1680.
259. Rosenberg SA, Yang JC, Sherry RM, Kammula US, Hughes MS, Phan GQ, Citrin DE, Restifo NP, Robbins PF, Wunderlich JR, Morton KE, Laurencot CM, Steinberg SM, White DE, Dudley ME. Durable complete responses in heavily pretreated patients with metastatic melanoma using T-cell transfer immunotherapy. *Clin Cancer Res*. 2011;17(13):4550-4557.
260. Gattinoni L, Finkelstein SE, Klebanoff CA, Antony PA, Palmer DC, Spiess PJ, Hwang LN, Yu Z, Wrzesinski C, Heimann DM, Surh CD, Rosenberg SA, Restifo NP. Removal of homeostatic cytokine sinks by lymphodepletion enhances the efficacy of adoptively transferred tumor-specific CD8+ T cells. *J Exp Med*. 2005;202(7):907-912.
261. Williams KM, Hakim FT, Gress RE. T cell immune reconstitution following lymphodepletion. *Semin Immunol*. 2007;19(5):318-330.
262. Ng SSM, Nagy BA, Jensen SM, Hu X, Alicea C, Fox BA, Felber BK, Bergamaschi C, Pavlakis GN. Heterodimeric IL15 Treatment Enhances Tumor Infiltration, Persistence, and Effector Functions of Adoptively Transferred Tumor-specific T Cells in the Absence of Lymphodepletion. *Clin Cancer Res*. 2017;23(11):2817-2830.
263. Morgan RA, Dudley ME, Wunderlich JR, Hughes MS, Yang JC, Sherry RM, Royal RE, Topalian SL, Kammula US, Restifo NP, Zheng Z, Nahvi A, de Vries CR, Rogers-Freezer LJ, Mavroukakis SA, Rosenberg SA. Cancer regression in patients after transfer of genetically engineered lymphocytes. *Science*. 2006;314(5796):126-129.
264. Dotti G, Gottschalk S, Savoldo B, Brenner MK. Design and development of therapies using chimeric antigen receptor-expressing T cells. *Immunol Rev*. 2014;257(1):107-126.
265. Zhao Z, Condomines M, van der Stegen SJC, Perna F, Kloss CC, Gunset G, Plotkin J, Sadelain M. Structural Design of Engineered Costimulation Determines Tumor Rejection Kinetics and Persistence of CAR T Cells. *Cancer Cell*. 2015;28(4):415-428.
266. Kuhn NF, Purdon TJ, van Leeuwen DG, Lopez AV, Curran KJ, Daniyan AF, Brentjens RJ. CD40 Ligand-Modified Chimeric Antigen Receptor T Cells Enhance Antitumor Function by Eliciting an Endogenous Antitumor Response. *Cancer Cell*. 2019;35(3):473-488.e476.
267. Brudno JN, Kochenderfer JN. Recent advances in CAR T-cell toxicity: Mechanisms, manifestations and management. *Blood Rev*. 2019;34:45-55.
268. Orlando D, Miele E, De Angelis B, Guercio M, Boffa I, Sinibaldi M, Po A, Caruana I, Abballe L, Carai A, Caruso S, Camera A, Moseley A, Hagedoorn RS, Heemskerk MHM, Giangaspero F, Mastronuzzi A, Ferretti E,

Chapter 1: References

- Locatelli F, Quintarelli C. Adoptive Immunotherapy Using PRAME-Specific T Cells in Medulloblastoma. *Cancer Res.* 2018;78(12):3337-3349.
269. Straathof KC, Pule MA, Yotnda P, Dotti G, Vanin EF, Brenner MK, Heslop HE, Spencer DM, Rooney CM. An inducible caspase 9 safety switch for T-cell therapy. *Blood.* 2005;105(11):4247-4254.
270. Kao RL, Truscott LC, Chiou TT, Tsai W, Wu AM, De Oliveira SN. A Cetuximab-Mediated Suicide System in Chimeric Antigen Receptor-Modified Hematopoietic Stem Cells for Cancer Therapy. *Hum Gene Ther.* 2019;30(4):413-428.
271. Kahlon KS, Brown C, Cooper LJ, Raubitschek A, Forman SJ, Jensen MC. Specific recognition and killing of glioblastoma multiforme by interleukin 13-zetakine redirected cytolytic T cells. *Cancer Res.* 2004;64(24):9160-9166.
272. Lupton SD, Brunton LL, Kalberg VA, Overell RW. Dominant positive and negative selection using a hygromycin phosphotransferase-thymidine kinase fusion gene. *Mol Cell Biol.* 1991;11(6):3374-3378.
273. Budde LE, Mardiros A, Chang W-C, Wang X, Berger C, Brown C, Riddell SR, Press OW, Forman SJ. Truncated Cell-Surface CD19 As a Conditional Suicide Switch For Adoptive T Cell Immunotherapy. *Blood.* 2013;122(21):1660-1660.
274. Chmielewski M, Abken H. TRUCKs: the fourth generation of CARs. *Expert Opin Biol Ther.* 2015;15(8):1145-1154.
275. Chmielewski M, Abken H. CAR T Cells Releasing IL-18 Convert to T-Bet(high) FoxO1(low) Effectors that Exhibit Augmented Activity against Advanced Solid Tumors. *Cell Rep.* 2017;21(11):3205-3219.
276. Klinger M, Benjamin J, Kischel R, Stienen S, Zugmaier G. Harnessing T cells to fight cancer with BiTE® antibody constructs-past developments and future directions. *Immunol Rev.* 2016;270(1):193-208.
277. Raja J, Ludwig JM, Gettinger SN, Schalper KA, Kim HS. Oncolytic virus immunotherapy: future prospects for oncology. *J Immunother Cancer.* 2018;6(1):140.
278. Orange M, Reuter U, Hobohm U. Coley's Lessons Remembered: Augmenting Mistletoe Therapy. *Integr Cancer Ther.* 2016;15(4):502-511.
279. Bartlett DL, Liu Z, Sathaiah M, Ravindranathan R, Guo Z, He Y, Guo ZS. Oncolytic viruses as therapeutic cancer vaccines. *Mol Cancer.* 2013;12(1):103.
280. Chiocca EA, Rabkin SD. Oncolytic viruses and their application to cancer immunotherapy. *Cancer Immunol Res.* 2014;2(4):295-300.
281. Andbacka RH, Kaufman HL, Collichio F, Amatruda T, Senzer N, Chesney J, Delman KA, Spitler LE, Puzanov I, Agarwala SS, Milhem M, Cranmer L, Curti B, Lewis K, Ross M, Guthrie T, Linette GP, Daniels GA, Harrington K, Middleton MR, Miller WH, Jr., Zager JS, Ye Y, Yao B, Li A, Doleman S, VanderWalde A, Gansert J, Coffin RS. Talimogene Laherparepvec Improves Durable Response Rate in Patients With Advanced Melanoma. *J Clin Oncol.* 2015;33(25):2780-2788.
282. Alvarez-Breckenridge C, Kaur B, Chiocca EA. Pharmacologic and chemical adjuvants in tumor virotherapy. *Chem Rev.* 2009;109(7):3125-3140.
283. Russell SJ, Peng KW, Bell JC. Oncolytic virotherapy. *Nat Biotechnol.* 2012;30(7):658-670.
284. Kaufman HL, Kim DW, DeRaffele G, Mitcham J, Coffin RS, Kim-Schulze S. Local and distant immunity induced by intralesional vaccination with an oncolytic herpes virus encoding GM-CSF in patients with stage IIIc and IV melanoma. *Ann Surg Oncol.* 2010;17(3):718-730.
285. Medawar PB. Immunity to homologous grafted skin; the fate of skin homografts transplanted to the brain, to subcutaneous tissue, and to the anterior chamber of the eye. *Br J Exp Pathol.* 1948;29(1):58-69.
286. Harling-Berg CJ, Park TJ, Knopf PM. Role of the cervical lymphatics in the Th2-type hierarchy of CNS immune regulation. *J Neuroimmunol.* 1999;101(2):111-127.
287. Scheinberg LC, Kotsilimbas DG, Karpf R, Mayer N. Is the brain "an immunologically privileged site"? 3. Studies based on homologous skin grafts to the brain and subcutaneous tissues. *Arch Neurol.* 1966;15(1):62-67.
288. Goldmann J, Kwidzinski E, Brandt C, Mahlo J, Richter D, Bechmann I. T cells traffic from brain to cervical lymph nodes via the cribroid plate and the nasal mucosa. *J Leukoc Biol.* 2006;80(4):797-801.
289. Tsugawa T, Kuwashima N, Sato H, Fellows-Mayle WK, Dusak JE, Okada K, Papworth GD, Watkins SC, Gambotto A, Yoshida J, Pollack IF, Okada H. Sequential delivery of interferon-alpha gene and DCs to intracranial gliomas promotes an effective antitumor response. *Gene Ther.* 2004;11(21):1551-1558.
290. Louveau A, Smirnov I, Keyes TJ, Eccles JD, Rouhani SJ, Peske JD, Derecki NC, Castle D, Mandell JW, Lee KS, Harris TH, Kipnis J. Structural and functional features of central nervous system lymphatic vessels. *Nature.* 2015;523(7560):337-341.
291. Aspelund A, Antila S, Proulx ST, Karlsen TV, Karaman S, Detmar M, Wiig H, Alitalo K. A dural lymphatic vascular system that drains brain interstitial fluid and macromolecules. *J Exp Med.* 2015;212(7):991-999.
292. Kulprathipanja NV, Kruse CA. Microglia phagocytose alloreactive CTL-damaged 9L gliosarcoma cells. *J Neuroimmunol.* 2004;153(1-2):76-82.
293. Carson MJ, Sutcliffe JG, Campbell IL. Microglia stimulate naive T-cell differentiation without stimulating T-cell proliferation. *J Neurosci Res.* 1999;55(1):127-134.
294. De Simone R, Giampaolo A, Giometto B, Gallo P, Levi G, Peschle C, Aloisi F. The costimulatory molecule B7 is expressed on human microglia in culture and in multiple sclerosis acute lesions. *J Neuropathol Exp Neurol.* 1995;54(2):175-187.
295. Aloisi F, Ria F, Penna G, Adorini L. Microglia are more efficient than astrocytes in antigen processing and in Th1 but not Th2 cell activation. *J Immunol.* 1998;160(10):4671-4680.
296. Hickey WF, Kimura H. Perivascular microglial cells of the CNS are bone marrow-derived and present antigen in vivo. *Science.* 1988;239(4837):290-292.

Chapter 1: References

297. Lowe J, MacLennan KA, Powe DG, Pound JD, Palmer JB. Microglial cells in human brain have phenotypic characteristics related to possible function as dendritic antigen presenting cells. *J Pathol.* 1989;159(2):143-149.
298. Ulvestad E, Williams K, Bjerkvig R, Tiekotter K, Antel J, Matre R. Human microglial cells have phenotypic and functional characteristics in common with both macrophages and dendritic antigen-presenting cells. *J Leukoc Biol.* 1994;56(6):732-740.
299. Gehrman J, Banati RB, Kreutzberg GW. Microglia in the immune surveillance of the brain: human microglia constitutively express HLA-DR molecules. *J Neuroimmunol.* 1993;48(2):189-198.
300. Williams K, Jr., Ulvestad E, Cragg L, Blain M, Antel JP. Induction of primary T cell responses by human glial cells. *J Neurosci Res.* 1993;36(4):382-390.
301. Masson F, Calzascia T, Di Bernardino-Besson W, de Tribolet N, Dietrich PY, Walker PR. Brain microenvironment promotes the final functional maturation of tumor-specific effector CD8+ T cells. *J Immunol.* 2007;179(2):845-853.
302. Sampson JH, Archer GE, Ashley DM, Fuchs HE, Hale LP, Dranoff G, Bigner DD. Subcutaneous vaccination with irradiated, cytokine-producing tumor cells stimulates CD8+ cell-mediated immunity against tumors located in the "immunologically privileged" central nervous system. *Proc Natl Acad Sci U S A.* 1996;93(19):10399-10404.
303. Herrlinger U, Kramm CM, Johnston KM, Louis DN, Finkelstein D, Reznikoff G, Dranoff G, Breakefield XO, Yu JS. Vaccination for experimental gliomas using GM-CSF-transduced glioma cells. *Cancer Gene Ther.* 1997;4(6):345-352.
304. Prins RM, Shu CJ, Radu CG, Vo DD, Khan-Farooqi H, Soto H, Yang MY, Lin MS, Shelly S, Witte ON, Ribas A, Liao LM. Anti-tumor activity and trafficking of self, tumor-specific T cells against tumors located in the brain. *Cancer Immunol Immunother.* 2008;57(9):1279-1289.
305. Ransohoff RM, Kivisakk P, Kidd G. Three or more routes for leukocyte migration into the central nervous system. *Nat Rev Immunol.* 2003;3(7):569-581.
306. Irani DN, Lin KI, Griffin DE. Regulation of brain-derived T cells during acute central nervous system inflammation. *J Immunol.* 1997;158(5):2318-2326.
307. Hickey WF, Hsu BL, Kimura H. T-lymphocyte entry into the central nervous system. *J Neurosci Res.* 1991;28(2):254-260.
308. Hong JJ, Rosenberg SA, Dudley ME, Yang JC, White DE, Butman JA, Sherry RM. Successful treatment of melanoma brain metastases with adoptive cell therapy. *Clin Cancer Res.* 2010;16(19):4892-4898.
309. Muldoon LL, Alvarez JI, Begley DJ, Boado RJ, Del Zoppo GJ, Doolittle ND, Engelhardt B, Hallenbeck JM, Lonser RR, Ohlfest JR, Prat A, Scarpa M, Smeyne RJ, Drewes LR, Neuwelt EA. Immunologic privilege in the central nervous system and the blood-brain barrier. *J Cereb Blood Flow Metab.* 2013;33(1):13-21.
310. Engelhardt B, Coisne C. Fluids and barriers of the CNS establish immune privilege by confining immune surveillance to a two-walled castle moat surrounding the CNS castle. *Fluids Barriers CNS.* 2011;8(1):4.
311. Wilson EH, Weninger W, Hunter CA. Trafficking of immune cells in the central nervous system. *J Clin Invest.* 2010;120(5):1368-1379.
312. Wakim LM, Woodward-Davis A, Bevan MJ. Memory T cells persisting within the brain after local infection show functional adaptations to their tissue of residence. *Proc Natl Acad Sci U S A.* 2010;107(42):17872-17879.
313. Bhowmik A, Khan R, Ghosh MK. Blood brain barrier: a challenge for effectual therapy of brain tumors. *Biomed Res Int.* 2015;2015:320941.
314. Hilf N, Kutruff-Coqui S, Frenzel K, Bukur V, Stevanović S, Gouttefangeas C, Platten M, Tabatabai G, Dutoit V, van der Burg SH, Thor Straten P, Martínez-Ricarte F, Ponsati B, Okada H, Lassen U, Admon A, Ottensmeier CH, Ulges A, Kreiter S, von Deimling A, Skardelly M, Migliorini D, Kroep JR, Idorn M, Rodon J, Piró J, Poulsen HS, Shraibman B, McCann K, Mendrzyk R, Löwer M, Stieglbauer M, Britten CM, Capper D, Welters MJ, Sahuquillo J, Kiesel K, Derhovanessian E, Rusch E, Bunse L, Song C, Heesch S, Wagner C, Kemmer-Brück A, Ludwig J, Castle JC, Schoor O, Tadmor AD, Green E, Fritsche J, Meyer M, Pawlowski N, Dorner S, Hoffgaard F, Rössler B, Maurer D, Weinschenk T, Reinhardt C, Huber C, Rammensee HG, Singh-Jasuja H, Sahin U, Dietrich PY, Wick W. Actively personalized vaccination trial for newly diagnosed glioblastoma. *Nature.* 2019;565(7738):240-245.
315. Keskin DB, Anandappa AJ, Sun J, Tirosh I, Mathewson ND, Li S, Oliveira G, Giobbie-Hurder A, Felt K, Gjini E, Shukla SA, Hu Z, Li L, Le PM, Allesøe RL, Richman AR, Kowalczyk MS, Abdelrahman S, Geduldig JE, Charbonneau S, Pelton K, Iorgulescu JB, Elagina L, Zhang W, Olive O, McCluskey C, Olsen LR, Stevens J, Lane WJ, Salazar AM, Daley H, Wen PY, Chiocca EA, Harden M, Lennon NJ, Gabriel S, Getz G, Lander ES, Regev A, Ritz J, Neuberg D, Rodig SJ, Ligon KL, Suvà ML, Wucherpennig KW, Hacohen N, Fritsch EF, Livak KJ, Ott PA, Wu CJ, Reardon DA. Neoantigen vaccine generates intratumoral T cell responses in phase Ib glioblastoma trial. *Nature.* 2019;565(7738):234-239.
316. Bodey B, Siegel SE, Kaiser HE. Immunocytochemical detection of members of the caspase cascade of apoptosis in childhood medulloblastomas. *In Vivo.* 2005;19(4):749-760.
317. Vermeulen JF, Van Hecke W, Adriaansen EJM, Jansen MK, Bouma RG, Villacorta Hidalgo J, Fisch P, Broekhuizen R, Spliet WGM, Kool M, Bovenschen N. Prognostic relevance of tumor-infiltrating lymphocytes and immune checkpoints in pediatric medulloblastoma. *Oncoimmunology.* 2018;7(3):e1398877.
318. Han S, Zhang C, Li Q, Dong J, Liu Y, Huang Y, Jiang T, Wu A. Tumour-infiltrating CD4(+) and CD8(+) lymphocytes as predictors of clinical outcome in glioma. *Br J Cancer.* 2014;110(10):2560-2568.

Chapter 1: References

319. Pardridge WM. Drug transport across the blood-brain barrier. *J Cereb Blood Flow Metab.* 2012;32(11):1959-1972.
320. Geletneky K, Hajda J, Angelova AL, Leuchs B, Capper D, Bartsch AJ, Neumann JO, Schöning T, Husing J, Beelte B, Kiprianova I, Roscher M, Bhat R, von Deimling A, Brück W, Just A, Frehtman V, Löbhard S, Terletskaia-Ladwig E, Fry J, Jochims K, Daniel V, Krebs O, Dahm M, Huber B, Unterberg A, Rommelaere J. Oncolytic H-1 Parvovirus Shows Safety and Signs of Immunogenic Activity in a First Phase I/IIa Glioblastoma Trial. *Mol Ther.* 2017;25(12):2620-2634.
321. Galstyan A, Markman JL, Shatalova ES, Chiechi A, Korman AJ, Patil R, Klymyshyn D, Tourtellotte WG, Israel LL, Braubach O, Ljubimov VA, Mashouf LA, Ramesh A, Grodzinski ZB, Penichet ML, Black KL, Holler E, Sun T, Ding H, Ljubimov AV, Ljubimova JY. Blood-brain barrier permeable nano immunoconjugates induce local immune responses for glioma therapy. *Nat Commun.* 2019;10(1):3850.
322. Villaseñor R, Ozmen L, Messaddeq N, Grüninger F, Loetscher H, Keller A, Betsholtz C, Freskgård PO, Collin L. Trafficking of Endogenous Immunoglobulins by Endothelial Cells at the Blood-Brain Barrier. *Sci Rep.* 2016;6:25658.
323. Niewoehner J, Bohrmann B, Collin L, Urich E, Sade H, Maier P, Rueger P, Stracke JO, Lau W, Tissot AC, Loetscher H, Ghosh A, Freskgård PO. Increased brain penetration and potency of a therapeutic antibody using a monovalent molecular shuttle. *Neuron.* 2014;81(1):49-60.
324. Alexandrov LB, Nik-Zainal S, Wedge DC, Aparicio SA, Behjati S, Biankin AV, Bignell GR, Bolli N, Borg A, Børresen-Dale AL, Burkhardt S, Burkhardt B, Butler AP, Caldas C, Davies HR, Desmedt C, Eils R, Eyfjörd JE, Foekens JA, Greaves M, Hosoda F, Hutter B, Ilicic T, Imbeaud S, Imielinski M, Jäger N, Jones DT, Jones D, Knappskog S, Kool M, Lakhani SR, López-Otín C, Martin S, Munshi NC, Nakamura H, Northcott PA, Pajic M, Papaemmanuil E, Paradiso A, Pearson JV, Puente XS, Raine K, Ramakrishna M, Richardson AL, Richter J, Rosenstiel P, Schlesner M, Schumacher TN, Span PN, Teague JW, Totoki Y, Tutt AN, Valdés-Mas R, van Buuren MM, van 't Veer L, Vincent-Salomon A, Waddell N, Yates LR, Zucman-Rossi J, Futreal PA, McDermott U, Lichten P, Meyerson M, Grimmond SM, Siebert R, Campo E, Shibata T, Pfister SM, Campbell PJ, Stratton MR. Signatures of mutational processes in human cancer. *Nature.* 2013;500(7463):415-421.
325. Snyder A, Makarov V, Merghoub T, Yuan J, Zaretsky JM, Desrichard A, Walsh LA, Postow MA, Wong P, Ho TS, Hollmann TJ, Bruggeman C, Kannan K, Li Y, Elipenahli C, Liu C, Harbison CT, Wang L, Ribas A, Wolchok JD, Chan TA. Genetic basis for clinical response to CTLA-4 blockade in melanoma. *N Engl J Med.* 2014;371(23):2189-2199.
326. Rizvi NA, Hellmann MD, Snyder A, Kvistborg P, Makarov V, Havel JJ, Lee W, Yuan J, Wong P, Ho TS, Miller ML, Rekhtman N, Moreira AL, Ibrahim F, Bruggeman C, Gasmi B, Zappasodi R, Maeda Y, Sander C, Garon EB, Merghoub T, Wolchok JD, Schumacher TN, Chan TA. Cancer immunology. Mutational landscape determines sensitivity to PD-1 blockade in non-small cell lung cancer. *Science.* 2015;348(6230):124-128.
327. Van Allen EM, Miao D, Schilling B, Shukla SA, Blank C, Zimmer L, Sucker A, Hillen U, Foppen MHG, Goldinger SM, Utikal J, Hassel JC, Weide B, Kaehler KC, Loquai C, Mohr P, Gutzmer R, Dummer R, Gabriel S, Wu CJ, Schadendorf D, Garraway LA. Genomic correlates of response to CTLA-4 blockade in metastatic melanoma. *Science.* 2015;350(6257):207-211.
328. Berghoff AS, Kiesel B, Widhalm G, Rajky O, Ricken G, Wöhrer A, Dieckmann K, Filipits M, Brandstetter A, Weller M, Kurscheid S, Hegi ME, Zielinski CC, Marosi C, Hainfellner JA, Preusser M, Wick W. Programmed death ligand 1 expression and tumor-infiltrating lymphocytes in glioblastoma. *Neuro Oncol.* 2015;17(8):1064-1075.
329. Johnson MD. PD-L1 expression in meningiomas. *J Clin Neurosci.* 2018;57:149-151.
330. Rampling R, Peoples S, Mulholland PJ, James A, Al-Salihi O, Twelves CJ, McBain C, Jefferies S, Jackson A, Stewart W, Lindner J, Kutscher S, Hilf N, McGuigan L, Peters J, Hill K, Schoor O, Singh-Jasuja H, Halford SE, Ritchie JW. A Cancer Research UK First Time in Human Phase I Trial of IMA950 (Novel Muropeptide Therapeutic Vaccine) in Patients with Newly Diagnosed Glioblastoma. *Clin Cancer Res.* 2016;22(19):4776-4785.
331. Publications listed in PubMed dealing with immunotherapy in glioblastoma, meningioma, or medulloblastoma. [Internet]. Available from: <https://www.ncbi.nlm.nih.gov/pubmed/?term=glioblastoma+AND+immunotherapy>, <https://www.ncbi.nlm.nih.gov/pubmed/?term=medulloblastoma+AND+immunotherapy>, and <https://www.ncbi.nlm.nih.gov/pubmed/?term=meningioma+AND+immunotherapy>, accessed on 2019/12/03.
332. Clinical trials of immunotherapeutic intervention in glioblastoma, meningioma, or medulloblastoma registered at ClinicalTrials.gov. [Internet]. Available from: https://clinicaltrials.gov/ct2/results?cond=glioblastoma&term=&type=&rslt=&age_v=&gndr=&intr=immunotherapy&titles=&outc=&spons=&lead=&id=&cntry=&state=&city=&dist=&locn=&strd_s=&strd_e=&prcd_s=&prcd_e=&sfpd_s=&sfpd_e=&lupd_s=&lupd_e=&sort=, https://clinicaltrials.gov/ct2/results?cond=medulloblastoma&term=&type=&rslt=&age_v=&gndr=&intr=immunotherapy&titles=&outc=&spons=&lead=&id=&cntry=&state=&city=&dist=&locn=&strd_s=&strd_e=&prcd_s=&prcd_e=&sfpd_s=&sfpd_e=&lupd_s=&lupd_e=&sort=, and https://clinicaltrials.gov/ct2/results?cond=meningioma&term=&type=&rslt=&age_v=&gndr=&intr=immunotherapy&titles=&outc=&spons=&lead=&id=&cntry=&state=&city=&dist=&locn=&strd_s=&strd_e=&prcd_s=&prcd_e=&sfpd_s=&sfpd_e=&lupd_s=&lupd_e=&sort=, accessed on 2019/12/03.
333. Ahmed N, Brawley V, Hegde M, Bielamowicz K, Kalra M, Landi D, Robertson C, Gray TL, Diouf O, Wakefield A, Ghazi A, Gerken C, Yi Z, Ashoori A, Wu MF, Liu H, Rooney C, Dotti G, Gee A, Su J, Kew Y, Baskin D, Zhang YJ, New P, Grilley B, Stojakovic M, Hicks J, Powell SZ, Brenner MK, Heslop HE, Grossman R, Wels

Chapter 1: References

- WS, Gottschalk S. HER2-Specific Chimeric Antigen Receptor-Modified Virus-Specific T Cells for Progressive Glioblastoma: A Phase 1 Dose-Escalation Trial. *JAMA Oncol.* 2017;3(8):1094-1101.
334. Phuphanich S, Wheeler CJ, Rudnick JD, Mazer M, Wang H, Nuno MA, Richardson JE, Fan X, Ji J, Chu RM, Bender JG, Hawkins ES, Patil CG, Black KL, Yu JS. Phase I trial of a multi-epitope-pulsed dendritic cell vaccine for patients with newly diagnosed glioblastoma. *Cancer Immunol Immunother.* 2013;62(1):125-135.
335. Brown CE, Badie B, Barish ME, Weng L, Ostberg JR, Chang WC, Naranjo A, Starr R, Wagner J, Wright C, Zhai Y, Bading JR, Ressler JA, Portnow J, D'Apuzzo M, Forman SJ, Jensen MC. Bioactivity and Safety of IL13Ralpha2-Redirected Chimeric Antigen Receptor CD8+ T Cells in Patients with Recurrent Glioblastoma. *Clin Cancer Res.* 2015;21(18):4062-4072.
336. Oji Y, Hashimoto N, Tsuboi A, Murakami Y, Iwai M, Kagawa N, Chiba Y, Izumoto S, Elisseeva O, Ichinohasama R, Sakamoto J, Morita S, Nakajima H, Takashima S, Nakae Y, Nakata J, Kawakami M, Nishida S, Hosen N, Fujiki F, Morimoto S, Adachi M, Iwamoto M, Oka Y, Yoshimine T, Sugiyama H. Association of WT1 IgG antibody against WT1 peptide with prolonged survival in glioblastoma multiforme patients vaccinated with WT1 peptide. *Int J Cancer.* 2016;139(6):1391-1401.
337. Freitas M, Malheiros S, Stavale JN, Biassi TP, Zamuner FT, de Souza Begnami M, Soares FA, Vettore AL. Expression of cancer/testis antigens is correlated with improved survival in glioblastoma. *Oncotarget.* 2013;4(4):636-646.
338. Liu G, Ying H, Zeng G, Wheeler CJ, Black KL, Yu JS. HER-2, gp100, and MAGE-1 are expressed in human glioblastoma and recognized by cytotoxic T cells. *Cancer Res.* 2004;64(14):4980-4986.
339. Komata T, Kanzawa T, Kondo Y, Kondo S. Telomerase as a therapeutic target for malignant gliomas. *Oncogene.* 2002;21(4):656-663.
340. Wykosky J, Gibo DM, Stanton C, Debinski W. EphA2 as a novel molecular marker and target in glioblastoma multiforme. *Mol Cancer Res.* 2005;3(10):541-551.
341. Azad TD, Razavi SM, Jin B, Lee K, Li G. Glioblastoma antigen discovery-foundations for immunotherapy. *J Neurooncol.* 2015;123(3):347-358.
342. Heimberger AB, Hlatky R, Suki D, Yang D, Weinberg J, Gilbert M, Sawaya R, Aldape K. Prognostic effect of epidermal growth factor receptor and EGFRvIII in glioblastoma multiforme patients. *Clin Cancer Res.* 2005;11(4):1462-1466.
343. Tang X, Zhao S, Zhang Y, Wang Y, Zhang Z, Yang M, Zhu Y, Zhang G, Guo G, Tong A, Zhou L. B7-H3 as a Novel CAR-T Therapeutic Target for Glioblastoma. *Mol Ther Oncolytics.* 2019;14:279-287.
344. Targeting IDH1R132H in WHO Grade III-IV IDH1R132H-mutated Gliomas by a Peptide Vaccine - a Phase I Safety, Tolerability and Immunogenicity Multicenter Trial (NOA-16). [Internet]. Available from: <https://clinicaltrials.gov/>, NCT02454634, accessed on 2019/12/02.
345. Balsl J, Meyer J, Mueller W, Korshunov A, Hartmann C, von Deimling A. Analysis of the IDH1 codon 132 mutation in brain tumors. *Acta Neuropathol.* 2008;116(6):597-602.
346. Sturm D, Witt H, Hovestadt V, Khuong-Quang DA, Jones DT, Konermann C, Pfaff E, Tönjes M, Sill M, Bender S, Kool M, Zapatka M, Becker N, Zucknick M, Hielscher T, Liu XY, Fontebasso AM, Ryzhova M, Albrecht S, Jacob K, Wolter M, Ebinger M, Schuhmann MU, van Meter T, Frühwald MC, Hauch H, Pekrun A, Radlwimmer B, Niehues T, von Komorowski G, Dürken M, Kulozik AE, Madden J, Donson A, Foreman NK, Drissi R, Fouladi M, Scheurlen W, von Deimling A, Monoranu C, Roggendorf W, Herold-Mende C, Unterberg A, Kramm CM, Felsberg J, Hartmann C, Wiestler B, Wick W, Milde T, Witt O, Lindroth AM, Schwartzentruber J, Faury D, Fleming A, Zakrzewska M, Liberski PP, Zakrzewski K, Hauser P, Garami M, Klekner A, Bogner L, Morrissy S, Cavalli F, Taylor MD, van Sluis P, Koster J, Versteeg R, Volckmann R, Mikkelsen T, Aldape K, Reifenberger G, Collins VP, Majewski J, Korshunov A, Lichter P, Plass C, Jabado N, Pfister SM. Hotspot mutations in H3F3A and IDH1 define distinct epigenetic and biological subgroups of glioblastoma. *Cancer Cell.* 2012;22(4):425-437.
347. PEP-CMV in Recurrent MEDulloblastoma/Malignant Glioma (PRiME). [Internet]. Available from: <https://clinicaltrials.gov/>, NCT03299309, accessed on 2019/12/02.
348. Nair SK, De Leon G, Boczkowski D, Schmittling R, Xie W, Staats J, Liu R, Johnson LA, Weinhold K, Archer GE, Sampson JH, Mitchell DA. Recognition and killing of autologous, primary glioblastoma tumor cells by human cytomegalovirus pp65-specific cytotoxic T cells. *Clin Cancer Res.* 2014;20(10):2684-2694.
349. Ferguson SD, Srinivasan VM, Ghali MG, Heimberger AB. Cytomegalovirus-targeted immunotherapy and glioblastoma: hype or hope? *Immunotherapy.* 2016;8(4):413-423.
350. Schuessler A, Smith C, Beagley L, Boyle GM, Rehan S, Matthews K, Jones L, Crough T, Dasari V, Klein K, Smalley A, Alexander H, Walker DG, Khanna R. Autologous T-cell therapy for cytomegalovirus as a consolidative treatment for recurrent glioblastoma. *Cancer Res.* 2014;74(13):3466-3476.
351. Oba-Shinjo SM, Caballero OL, Jungbluth AA, Rosemberg S, Old LJ, Simpson AJ, Marie SK. Cancer-testis (CT) antigen expression in medulloblastoma. *Cancer Immun.* 2008;8:7.
352. Phase III: Decitabine/Vaccine Therapy in Relapsed/Refractory Pediatric High Grade Gliomas/Medulloblastomas/CNS PNETs. [Internet]. Available from: <https://clinicaltrials.gov/>, NCT02332889, accessed on 2020/01/05.
353. HER2-specific CAR T Cell Locoregional Immunotherapy for HER2-positive Recurrent/Refractory Pediatric CNS Tumors. [Internet]. Available from: <https://clinicaltrials.gov/>, NCT03500991, accessed on 2019/12/03.
354. Bosse KR, Raman P, Zhu Z, Lane M, Martinez D, Heitzeneder S, Rathi KS, Kendersky NM, Randall M, Donovan L, Morrissy S, Sussman RT, Zhelev DV, Feng Y, Wang Y, Hwang J, Lopez G, Harenza JL, Wei JS, Pawel B, Bhatti T, Santi M, Ganguly A, Khan J, Marra MA, Taylor MD, Dimitrov DS, Mackall CL, Maris JM.

Chapter 1: References

- Identification of GPC2 as an Oncoprotein and Candidate Immunotherapeutic Target in High-Risk Neuroblastoma. *Cancer Cell*. 2017;32(3):295-309.e212.
355. Kramer K, Pandit-Taskar N, Humm JL, Zanzonico PB, Haque S, Dunkel IJ, Wolden SL, Donzelli M, Goldman DA, Lewis JS, Lyashchenko SK, Khakoo Y, Carrasquillo JA, Souweidane MM, Greenfield JP, Lyden D, De Braganca KD, Gilheaney SW, Larson SM, Cheung NV. A phase II study of radioimmunotherapy with intraventricular (131) I-3F8 for medulloblastoma. *Pediatr Blood Cancer*. 2018;65(1).
 356. EGFR806-specific CAR T Cell Locoregional Immunotherapy for EGFR-positive Recurrent or Refractory Pediatric CNS Tumors. [Internet]. Available from: <https://clinicaltrials.gov/>, NCT03638167, accessed on 2019/12/03.
 357. Majzner RG, Theruvath JL, Nellan A, Heitzeneder S, Cui Y, Mount CW, Rietberg SP, Linde MH, Xu P, Rota C, Sotillo E, Labanieh L, Lee DW, Orentas RJ, Dimitrov DS, Zhu Z, Croix BS, Delaidelli A, Sekunova A, Bonvini E, Mitra SS, Quezado MM, Majeti R, Monje M, Sorensen PHB, Maris JM, Mackall CL. CAR T Cells Targeting B7-H3, a Pan-Cancer Antigen, Demonstrate Potent Preclinical Activity Against Pediatric Solid Tumors and Brain Tumors. *Clin Cancer Res*. 2019;25(8):2560-2574.
 358. Blaeschke F, Paul MC, Schuhmann MU, Rabsteyn A, Schroeder C, Casadei N, Matthes J, Mohr C, Lotfi R, Wagner B, Kaeuferle T, Feucht J, Willier S, Handgretinger R, Stevanović S, Lang P, Feuchtinger T. Low mutational load in pediatric medulloblastoma still translates into neoantigens as targets for specific T-cell immunotherapy. *Cytotherapy*. 2019;21(9):973-986.
 359. Deng J, Ma M, Wang D, Zhu H, Hua L, Sun S, Chen H, Cheng H, Qian ZR, Xie Q, Zhang T, Gong Y. Expression and Clinical Significance of Immune Checkpoint Regulator B7-H3 (CD276) in Human Meningioma. *World Neurosurg*. 2019.
 360. Syed ON, Mandigo CE, Killory BD, Canoll P, Bruce JN. Cancer-testis and melanocyte-differentiation antigen expression in malignant glioma and meningioma. *J Clin Neurosci*. 2012;19(7):1016-1021.
 361. T Cell Receptor Immunotherapy Targeting NY-ESO-1 for Patients With NY-ESO-1 Expressing Cancer. [Internet]. Available from: <https://clinicaltrials.gov/>, NCT01967823, accessed on 2019/12/03.
 362. Baia GS, Caballero OL, Ho JS, Zhao Q, Cohen T, Binder ZA, Salmasi V, Gallia GL, Quinones-Hinojosa A, Olivi A, Brem H, Burger P, Strausberg RL, Simpson AJ, Eberhart CG, Riggins GJ. NY-ESO-1 expression in meningioma suggests a rationale for new immunotherapeutic approaches. *Cancer Immunol Res*. 2013;1(5):296-302.
 363. Phase I Study of Cellular Immunotherapy for Recurrent/Refractory Malignant Glioma Using Intratumoral Infusions of GRm13Z40-2, An Allogeneic CD8+ Cytolytic T-Cell Line Genetically Modified to Express the IL 13-Zetakine and HyTK and to be Resistant to Glucocorticoids, in Combination With Interleukin-2. [Internet]. Available from: <https://clinicaltrials.gov/>, NCT01082926, accessed on 2019/12/03.
 364. Katoh M, Wilmotte R, Belkouch MC, de Tribolet N, Pizzolato G, Dietrich PY. Survivin in brain tumors: an attractive target for immunotherapy. *J Neurooncol*. 2003;64(1-2):71-76.
 365. Barresi V, Caffo M, Branca G, Vitarelli E, Tuccari G. The density of microvessels positive for Wilms' tumour-1 protein (WT-1) is an independent predictor of recurrence risk in meningiomas. *Brain Tumor Pathol*. 2015;32(3):202-209.
 366. Sahin U, Koslowski M, Türeci O, Eberle T, Zwick C, Romeike B, Moringlane JR, Schwechheimer K, Feiden W, Pfreundschuh M. Expression of cancer testis genes in human brain tumors. *Clin Cancer Res*. 2000;6(10):3916-3922.
 367. Lukas RV, Rodon J, Becker K, Wong ET, Shih K, Touat M, Fasso M, Osborne S, Molinero L, O'Hear C, Grossman W, Baehring J. Clinical activity and safety of atezolizumab in patients with recurrent glioblastoma. *J Neurooncol*. 2018;140(2):317-328.
 368. Omuro A, Vlahovic G, Lim M, Sahebjam S, Baehring J, Cloughesy T, Voloschin A, Ramkissoon SH, Ligon KL, Latek R, Zwirter R, Strauss L, Paliwal P, Harbison CT, Reardon DA, Sampson JH. Nivolumab with or without ipilimumab in patients with recurrent glioblastoma: results from exploratory phase I cohorts of CheckMate 143. *Neuro Oncol*. 2018;20(5):674-686.
 369. Cloughesy TF, Mochizuki AY, Orpilla JR, Hugo W, Lee AH, Davidson TB, Wang AC, Ellingson BM, Rytlewski JA, Sanders CM, Kawaguchi ES, Du L, Li G, Yong WH, Gaffey SC, Cohen AL, Mellinghoff IK, Lee EQ, Reardon DA, O'Brien BJ, Butowski NA, Nghiemphu PL, Clarke JL, Arrillaga-Romany IC, Colman H, Kaley TJ, de Groot JF, Liau LM, Wen PY, Prins RM. Neoadjuvant anti-PD-1 immunotherapy promotes a survival benefit with intratumoral and systemic immune responses in recurrent glioblastoma. *Nat Med*. 2019;25(3):477-486.
 370. Immune Checkpoint Inhibitor Nivolumab in People With Select Rare CNS Cancers. [Internet]. Available from: <https://clinicaltrials.gov/>, NCT03173950, accessed on 2019/12/03.
 371. Neoadjuvant Avelumab and Hypofractionated Proton Radiation Therapy Followed by Surgery for Recurrent Radiation-refractory Meningioma. [Internet]. Available from: <https://clinicaltrials.gov/>, NCT03267836, accessed on 2019/12/03.
 372. Gilbert MR, Dignam JJ, Armstrong TS, Wefel JS, Blumenthal DT, Vogelbaum MA, Colman H, Chakravarti A, Pugh S, Won M, Jeraj R, Brown PD, Jaeckle KA, Schiff D, Stieber VW, Brachman DG, Werner-Wasik M, Tremont-Lukats IW, Sulman EP, Aldape KD, Curran WJ, Jr., Mehta MP. A randomized trial of bevacizumab for newly diagnosed glioblastoma. *N Engl J Med*. 2014;370(8):699-708.
 373. Aguilera D, Mazewski C, Fangusaro J, MacDonald TJ, McNall-Knapp RY, Hayes LL, Kim S, Castellino RC. Response to bevacizumab, irinotecan, and temozolomide in children with relapsed medulloblastoma: a multi-institutional experience. *Childs Nerv Syst*. 2013;29(4):589-596.

Chapter 1: References

374. Shih KC, Chowdhary S, Rosenblatt P, Weir AB, 3rd, Shepard GC, Williams JT, Shastry M, Burris HA, 3rd, Hainsworth JD. A phase II trial of bevacizumab and everolimus as treatment for patients with refractory, progressive intracranial meningioma. *J Neurooncol.* 2016;129(2):281-288.
375. The Breston Robert Tisch Brain Tumor Center - Pediatric Clinical Trials. [Internet]. Available from: <https://tischbraintumorcenter.duke.edu/pediatric-clinical-trials>, accessed on 2019/12/02.
376. Bota DA, Chung J, Dandekar M, Carrillo JA, Kong XT, Fu BD, Hsu FP, Schonthal AH, Hofman FM, Chen TC, Zidovetzki R, Pretto C, Strik A, Schijns VE, Stathopoulos A. Phase II study of ERC1671 plus bevacizumab versus bevacizumab plus placebo in recurrent glioblastoma: interim results and correlations with CD4(+) T-lymphocyte counts. *CNS Oncol.* 2018;7(3):Cns22.
377. Ishikawa E, Muragaki Y, Yamamoto T, Maruyama T, Tsuboi K, Ikuta S, Hashimoto K, Uemae Y, Ishihara T, Matsuda M, Matsutani M, Karasawa K, Nakazato Y, Abe T, Ohno T, Matsumura A. Phase I/IIa trial of fractionated radiotherapy, temozolomide, and autologous formalin-fixed tumor vaccine for newly diagnosed glioblastoma. *J Neurosurg.* 2014;121(3):543-553.
378. Chemotherapy and Vaccine Therapy Followed by Bone Marrow or Peripheral Stem Cell Transplantation and Interleukin-2 in Treating Patients With Recurrent or Refractory Brain Cancer. [Internet]. Available from: <https://clinicaltrials.gov/>, NCT00014573, accessed on 2019/12/03.
379. Liao LM, Ashkan K, Tran DD, Campian JL, Trusheim JE, Cobbs CS, Heth JA, Salacz M, Taylor S, D'Andre SD, Iwamoto FM, Dropcho EJ, Moshel YA, Walter KA, Pillainayagam CP, Aiken R, Chaudhary R, Goldlust SA, Bota DA, Duic P, Grewal J, Elinzano H, Toms SA, Lillehei KO, Mikkelsen T, Walbert T, Abram SR, Brenner AJ, Brem S, Ewend MG, Khagi S, Portnow J, Kim LJ, Loudon WG, Thompson RC, Avigan DE, Fink KL, Geoffroy FJ, Lindhorst S, Lutzky J, Sloan AE, Schackert G, Krex D, Meisel HJ, Wu J, Davis RP, Duma C, Etame AB, Mathieu D, Kesari S, Piccioni D, Westphal M, Baskin DS, New PZ, Lacroix M, May SA, Pluard TJ, Tse V, Green RM, Villano JL, Pearlman M, Petrecca K, Schulder M, Taylor LP, Maida AE, Prins RM, Cloughesy TF, Mulholland P, Bosch ML. First results on survival from a large Phase 3 clinical trial of an autologous dendritic cell vaccine in newly diagnosed glioblastoma. *J Transl Med.* 2018;16(1):142.
380. Buchroithner J, Erhart F, Pichler J, Widhalm G, Preusser M, Stockhammer G, Nowosielski M, Iglseider S, Freyschlag CF, Oberndorfer S, Bordihn K, von Campe G, Hofferlmann M, Ruckser R, Rössler K, Spiegl-Kreinecker S, Fischer MB, Czech T, Visus C, Krumpal G, Felzmann T, Marosi C. Audencel Immunotherapy Based on Dendritic Cells Has No Effect on Overall and Progression-Free Survival in Newly Diagnosed Glioblastoma: A Phase II Randomized Trial. *Cancers (Basel).* 2018;10(10).
381. Erhart F, Buchroithner J, Reitermaier R, Fischhuber K, Klingensbrunner S, Sloma I, Hibsh D, Kozol R, Efroni S, Ricken G, Wöhrer A, Haberler C, Hainfellner J, Krumpal G, Felzmann T, Dohnal AM, Marosi C, Visus C. Immunological analysis of phase II glioblastoma dendritic cell vaccine (Audencel) trial: immune system characteristics influence outcome and Audencel up-regulates Th1-related immunovariabiles. *Acta Neuropathol Commun.* 2018;6(1):135.
382. Vaccination With Dendritic Cells Loaded With Brain Tumor Stem Cells for Progressive Malignant Brain Tumor. [Internet]. Available from: <https://clinicaltrials.gov/>, NCT01171469, accessed on 2019/12/02.
383. Ardon H, De Vleeschouwer S, Van Calenbergh F, Claes L, Kramm CM, Rutkowski S, Wolff JE, Van Gool SW. Adjuvant dendritic cell-based tumour vaccination for children with malignant brain tumours. *Pediatr Blood Cancer.* 2010;54(4):519-525.
384. Brown CE, Alizadeh D, Starr R, Weng L, Wagner JR, Naranjo A, Ostberg JR, Blanchard MS, Kilpatrick J, Simpson J, Kurien A, Priceman SJ, Wang X, Harshbarger TL, D'Apuzzo M, Ressler JA, Jensen MC, Barish ME, Chen M, Portnow J, Forman SJ, Badie B. Regression of Glioblastoma after Chimeric Antigen Receptor T-Cell Therapy. *N Engl J Med.* 2016;375(26):2561-2569.
385. Genetically Modified T-cells in Treating Patients With Recurrent or Refractory Malignant Glioma. [Internet]. Available from: <https://clinicaltrials.gov/>, NCT02208362, accessed on 2020/01/02.
386. A Phase I Study to Investigate Tolerability and Efficacy of ALECSAT Administered to Glioblastoma Multiforme Patients (ALECSAT-GBM). [Internet]. Available from: <https://clinicaltrials.gov/>, NCT01588769, accessed on 2020/01/02.
387. Vaccine Immunotherapy for Recurrent Medulloblastoma and Primitive Neuroectodermal Tumor (Re-MATCH). [Internet]. Available from: <https://clinicaltrials.gov/>, NCT01326104, accessed on 2019/12/02.
388. Geletneký K, Huesing J, Rommelaere J, Schlehofer JR, Leuchs B, Dahm M, Krebs O, von Knebel Doeberitz M, Huber B, Hajda J. Phase I/IIa study of intratumoral/intracerebral or intravenous/intracerebral administration of Parvovirus H-1 (ParvOryx) in patients with progressive primary or recurrent glioblastoma multiforme: ParvOryx01 protocol. *BMC Cancer.* 2012;12:99.
389. Markert JM, Liechty PG, Wang W, Gaston S, Braz E, Karrasch M, Nabors LB, Markiewicz M, Lakeman AD, Palmer CA, Parker JN, Whitley RJ, Gillespie GY. Phase Ib trial of mutant herpes simplex virus G207 inoculated pre-and post-tumor resection for recurrent GBM. *Mol Ther.* 2009;17(1):199-207.
390. Safety Study of Replication-competent Adenovirus (Delta-24-rgd) in Patients With Recurrent Glioblastoma. [Internet]. Available from: <https://clinicaltrials.gov/>, NCT01582516, accessed on 2019/12/09.
391. HSV G207 in Children With Recurrent or Refractory Cerebellar Brain Tumors. [Internet]. Available from: <https://clinicaltrials.gov/>, NCT03911388, accessed on 2019/12/02.
392. Phase 1b Study PVSRIPO for Recurrent Malignant Glioma in Children. [Internet]. Available from: <https://clinicaltrials.gov/>, NCT03043391, accessed on 2019/12/02.
393. Weinzierl AO, Lemmel C, Schoor O, Müller M, Krüger T, Wernet D, Hennenlotter J, Stenzl A, Klingel K, Rammensee HG, Stevanović S. Distorted relation between mRNA copy number and corresponding major histocompatibility complex ligand density on the cell surface. *Mol Cell Proteomics.* 2007;6(1):102-113.

Chapter 1: References

394. Fortier MH, Caron É, Hardy MP, Voisin G, Lemieux S, Perreault C, Thibault P. The MHC class I peptide repertoire is molded by the transcriptome. *J Exp Med*. 2008;205(3):595-610.
395. Bassani-Sternberg M, Pletscher-Frankild S, Jensen LJ, Mann M. Mass spectrometry of human leukocyte antigen class I peptidomes reveals strong effects of protein abundance and turnover on antigen presentation. *Mol Cell Proteomics*. 2015;14(3):658-673.
396. Shraibman B, Barnea E, Kadosh DM, Haimovich Y, Slobodin G, Rosner I, López-Larrea C, Hilf N, Kuttruff S, Song C, Britten C, Castle J, Kreiter S, Frenzel K, Tatagiba M, Tabatabai G, Dietrich PY, Dutoit V, Wick W, Platten M, Winkler F, von Deimling A, Kroep J, Sahuquillo J, Martinez-Ricarte F, Rodon J, Lassen U, Ottensmeier C, van der Burg SH, Thor Straten P, Poulsen HS, Ponsati B, Okada H, Rammensee HG, Sahin U, Singh H, Admon A. Identification of Tumor Antigens Among the HLA Peptidomes of Glioblastoma Tumors and Plasma. *Mol Cell Proteomics*. 2019;18(6):1255-1268.
397. Bassani-Sternberg M, Bräunlein E, Klar R, Engleitner T, Sinitcyn P, Audehm S, Straub M, Weber J, Slotta-Huspenina J, Specht K, Martignoni ME, Werner A, Hein R, Busch DH, Peschel C, Rad R, Cox J, Mann M, Krackhardt AM. Direct identification of clinically relevant neoepitopes presented on native human melanoma tissue by mass spectrometry. *Nat Commun*. 2016;7:13404.
398. Müller M, Gfeller D, Coukos G, Bassani-Sternberg M. 'Hotspots' of Antigen Presentation Revealed by Human Leukocyte Antigen Ligandomics for Neoantigen Prioritization. *Front Immunol*. 2017;8:1367.
399. Jappe EC, Kringelum J, Trolle T, Nielsen M. Predicted MHC peptide binding promiscuity explains MHC class I 'hotspots' of antigen presentation defined by mass spectrometry eluted ligand data. *Immunology*. 2018;154(3):407-417.
400. Pearson H, Daouda T, Granados DP, Durette C, Bonneil E, Courcelles M, Rodenbrock A, Laverdure JP, Côté C, Mader S, Lemieux S, Thibault P, Perreault C. MHC class I-associated peptides derive from selective regions of the human genome. *J Clin Invest*. 2016;126(12):4690-4701.
401. Murphy JP, Konda P, Kowalewski DJ, Schuster H, Clements D, Kim Y, Cohen AM, Sharif T, Nielsen M, Stevanovic S, Lee PW, Gujar S. MHC-I ligand discovery using targeted database searches of mass spectrometry data: Implications for T cell immunotherapies. *J Proteome Res*. 2017.
402. Stickel JS, Stickel N, Hennenlotter J, Klingel K, Stenzl A, Rammensee HG, Stevanović S. Quantification of HLA class I molecules on renal cell carcinoma using Edman degradation. *BMC Urol*. 2011;11:1.
403. Berlin C, Kowalewski DJ, Schuster H, Mirza N, Walz S, Handel M, Schmid-Horch B, Salih HR, Kanz L, Rammensee HG, Stevanović S, Stickel JS. Mapping the HLA ligandome landscape of acute myeloid leukemia: a targeted approach toward peptide-based immunotherapy. *Leukemia*. 2015;29(3):647-659.
404. Walz S, Stickel JS, Kowalewski DJ, Schuster H, Weisel K, Backert L, Kahn S, Nelde A, Stroth T, Handel M, Kohlbacher O, Kanz L, Salih HR, Rammensee HG, Stevanović S. The antigenic landscape of multiple myeloma: mass spectrometry (re)defines targets for T-cell-based immunotherapy. *Blood*. 2015;126(10):1203-1213.
405. Kowalewski DJ, Schuster H, Backert L, Berlin C, Kahn S, Kanz L, Salih HR, Rammensee HG, Stevanovic S, Stickel JS. HLA ligandome analysis identifies the underlying specificities of spontaneous antileukemia immune responses in chronic lymphocytic leukemia (CLL). *Proc Natl Acad Sci U S A*. 2015;112(2):E166-175.
406. Kalaora S, Barnea E, Merhavi-Shoham E, Qutob N, Teer JK, Shimony N, Schachter J, Rosenberg SA, Besser MJ, Admon A, Samuels Y. Use of HLA peptidomics and whole exome sequencing to identify human immunogenic neo-antigens. *Oncotarget*. 2016;7(5):5110-5117.
407. Bassani-Sternberg M, Barnea E, Beer I, Avivi I, Katz T, Admon A. Soluble plasma HLA peptidome as a potential source for cancer biomarkers. *Proc Natl Acad Sci U S A*. 2010;107(44):18769-18776.
408. Synowsky SA, Shirran SL, Cooke FGM, Antoniou AN, Botting CH, Powis SJ. The major histocompatibility complex class I immunopeptidome of extracellular vesicles. *J Biol Chem*. 2017;292(41):17084-17092.
409. Löffler MW, Mohr C, Bichmann L, Freudenmann LK, Walzer M, Schroeder CM, Trautwein N, Hilke FJ, Zinser RS, Mühlenbruch L, Kowalewski DJ, Schuster H, Sturm M, Matthes J, Riess O, Czernel S, Nahnsen S, Königsrainer I, Thiel K, Nadalin S, Beckert S, Bösmüller H, Fend F, Velic A, Maček B, Haen SP, Buonaguro L, Kohlbacher O, Stevanović S, Königsrainer A, Rammensee HG. Multi-omics discovery of exome-derived neoantigens in hepatocellular carcinoma. *Genome Med*. 2019;11(1):28.
410. Marcu A, Bichmann L, Kuchenbecker L, Backert L, Kowalewski DJ, Freudenmann LK, Löffler MW, Lübke M, Walz JS, Velz J, Moch H, Regli L, Silgner M, Weller M, Schlosser A, Kohlbacher O, Stevanović S, Rammensee H-G, Neidert MC. The HLA Ligand Atlas. A resource of natural HLA ligands presented on benign tissues. *bioRxiv*. 2019:778944.
411. Neidert MC, Schoor O, Trautwein C, Trautwein N, Christ L, Melms A, Honegger J, Rammensee HG, Herold-Mende C, Dietrich PY, Stevanović S. Natural HLA class I ligands from glioblastoma: extending the options for immunotherapy. *J Neurooncol*. 2013;111(3):285-294.
412. Gfeller D, Guillaume P, Michaux J, Pak HS, Daniel RT, Racle J, Coukos G, Bassani-Sternberg M. The Length Distribution and Multiple Specificity of Naturally Presented HLA-I Ligands. *J Immunol*. 2018;201(12):3705-3716.
413. Barnstable CJ, Bodmer WF, Brown G, Galfre G, Milstein C, Williams AF, Ziegler A. Production of monoclonal antibodies to group A erythrocytes, HLA and other human cell surface antigens-new tools for genetic analysis. *Cell*. 1978;14(1):9-20.
414. Shackelford DA, Lampson LA, Strominger JL. Separation of three class II antigens from a homozygous human B cell line. *J Immunol*. 1983;130(1):289-296.

Chapter 1: References

415. Ødum N, Ledbetter JA, Martin P, Geraghty D, Tsu T, Hansen JA, Gladstone P. Homotypic aggregation of human cell lines by HLA class II-, class Ia- and HLA-G-specific monoclonal antibodies. *Eur J Immunol.* 1991;21(9):2121-2131.
416. González-Galarza FF, Takeshita LY, Santos EJ, Kempson F, Maia MH, da Silva AL, Teles e Silva AL, Ghattaoraya GS, Alfirevic A, Jones AR, Middleton D. Allele frequency net 2015 update: new features for HLA epitopes, KIR and disease and HLA adverse drug reaction associations. *Nucleic Acids Res.* 2015;43(Database issue):D784-788.
417. Hulsen T, de Vlieg J, Alkema W. BioVenn - a web application for the comparison and visualization of biological lists using area-proportional Venn diagrams. *BMC Genomics.* 2008;9:488.
418. Tate JG, Bamford S, Jubb HC, Sondka Z, Beare DM, Bindal N, Boutselakis H, Cole CG, Creatore C, Dawson E, Fish P, Harsha B, Hathaway C, Jupe SC, Kok CY, Noble K, Ponting L, Ramshaw CC, Rye CE, Speedy HE, Stefancsik R, Thompson SL, Wang S, Ward S, Campbell PJ, Forbes SA. COSMIC: the Catalogue Of Somatic Mutations In Cancer. *Nucleic Acids Res.* 2019;47(D1):D941-d947.
419. Huang da W, Sherman BT, Lempicki RA. Systematic and integrative analysis of large gene lists using DAVID bioinformatics resources. *Nat Protoc.* 2009;4(1):44-57.
420. Jiao X, Sherman BT, Huang da W, Stephens R, Baseler MW, Lane HC, Lempicki RA. DAVID-WS: a stateful web service to facilitate gene/protein list analysis. *Bioinformatics.* 2012;28(13):1805-1806.
421. Sherry ST, Ward MH, Kholodov M, Baker J, Phan L, Smigielski EM, Sirotkin K. dbSNP: the NCBI database of genetic variation. *Nucleic Acids Res.* 2001;29(1):308-311.
422. The GTEx Consortium. The Genotype-Tissue Expression (GTEx) project. *Nat Genet.* 2013;45(6):580-585.
423. Di Marco M, Schuster H, Backert L, Ghosh M, Rammensee HG, Stevanovic S. Unveiling the Peptide Motifs of HLA-C and HLA-G from Naturally Presented Peptides and Generation of Binding Prediction Matrices. *J Immunol.* 2017;199(8):2639-2651.
424. Vita R, Overton JA, Greenbaum JA, Ponomarenko J, Clark JD, Cantrell JR, Wheeler DK, Gabbard JL, Hix D, Sette A, Peters B. The immune epitope database (IEDB) 3.0. *Nucleic Acids Res.* 2015;43(Database issue):D405-412.
425. Bardou P, Mariette J, Escudie F, Djemiel C, Klopp C. jvenn: an interactive Venn diagram viewer. *BMC Bioinformatics.* 2014;15:293.
426. Cheever MA, Allison JP, Ferris AS, Finn OJ, Hastings BM, Hecht TT, Mellman I, Prindiville SA, Viner JL, Weiner LM, Matrisian LM. The prioritization of cancer antigens: a national cancer institute pilot project for the acceleration of translational research. *Clin Cancer Res.* 2009;15(17):5323-5337.
427. Almeida LG, Sakabe NJ, deOliveira AR, Silva MC, Mundstein AS, Cohen T, Chen YT, Chua R, Gurung S, Gnjatc S, Jungbluth AA, Caballero OL, Bairoch A, Kiesler E, White SL, Simpson AJ, Old LJ, Camargo AA, Vasconcelos AT. CTdatabase: a knowledge-base of high-throughput and curated data on cancer-testis antigens. *Nucleic Acids Res.* 2009;37(Database issue):D816-819.
428. Rapin N, Hoof I, Lund O, Nielsen M. MHC motif viewer. *Immunogenetics.* 2008;60(12):759-765.
429. Andreatta M, Nielsen M. Gapped sequence alignment using artificial neural networks: application to the MHC class I system. *Bioinformatics.* 2016;32(4):511-517.
430. Nielsen M, Andreatta M. NetMHCpan-3.0: improved prediction of binding to MHC class I molecules integrating information from multiple receptor and peptide length datasets. *Genome Med.* 2016;8(1):33.
431. Hoof I, Peters B, Sidney J, Pedersen LE, Sette A, Lund O, Buus S, Nielsen M. NetMHCpan, a method for MHC class I binding prediction beyond humans. *Immunogenetics.* 2009;61(1):1-13.
432. Jurtz V, Paul S, Andreatta M, Marcatili P, Peters B, Nielsen M. NetMHCpan-4.0: Improved Peptide-MHC Class I Interaction Predictions Integrating Eluted Ligand and Peptide Binding Affinity Data. *J Immunol.* 2017;199(9):3360-3368.
433. Keshava Prasad TS, Goel R, Kandasamy K, Keerthikumar S, Kumar S, Mathivanan S, Telikicherla D, Raju R, Shafreen B, Venugopal A, Balakrishnan L, Marimuthu A, Banerjee S, Somanathan DS, Sebastian A, Rani S, Ray S, Harrys Kishore CJ, Kanth S, Ahmed M, Kashyap MK, Mohmood R, Ramachandra YL, Krishna V, Rahiman BA, Mohan S, Ranganathan P, Ramabadran S, Chaerkady R, Pandey A. Human Protein Reference Database-2009 update. *Nucleic Acids Res.* 2009;37(Database issue):D767-772.
434. Eng JK, McCormack AL, Yates JR. An approach to correlate tandem mass spectral data of peptides with amino acid sequences in a protein database. *J Am Soc Mass Spectrom.* 1994;5(11):976-989.
435. MacLean B, Tomazela DM, Shulman N, Chambers M, Finney GL, Frewen B, Kern R, Tabb DL, Liebler DC, MacCoss MJ. Skyline: an open source document editor for creating and analyzing targeted proteomics experiments. *Bioinformatics.* 2010;26(7):966-968.
436. Rammensee HG, Bachmann J, Emmerich NP, Bachor OA, Stevanović S. SYFPEITHI: database for MHC ligands and peptide motifs. *Immunogenetics.* 1999;50(3-4):213-219.
437. Kowalewski DJ, Stevanovic S. Biochemical large-scale identification of MHC class I ligands. *Methods Mol Biol.* 2013;960:145-157.
438. Röttschke O, Falk K, Wallny HJ, Faath S, Rammensee HG. Characterization of naturally occurring minor histocompatibility peptides including H-4 and H-Y. *Science.* 1990;249(4966):283-287.
439. Merck Millipore. [Internet]. Available from: <http://www.merckmillipore.com/>, accessed on 2017/03/30.
440. Zhang N, Li L. Effects of common surfactants on protein digestion and matrix-assisted laser desorption/ionization mass spectrometric analysis of the digested peptides using two-layer sample preparation. *Rapid Commun Mass Spectrom.* 2004;18(8):889-896.

CHAPTER 2



Multi-omics analysis identifies novel antigens for glioblastoma immunotherapy and delineates dynamics during progression from primary to recurrent disease

Lena Katharina Freudenmann (L.K.F.) planned and performed all HLA peptidome analyses excepting HLA-IP of ZH613, ZH616, ZH617, and ZH631, which had been part of a pilot experiment by Ana Marcu. L.K.F. analyzed the entire immunopeptidomic dataset and contributed all figures and texts. Acquisition and analysis of exome and transcriptome data including variant calling as well as calculation of allele frequencies and expression values was conducted at CeGaT GmbH and at the Quantitative Biology Center, University of Tübingen. Initial search for neo-antigens was performed by Leon Bichmann, whereas L.K.F. validated candidates and conducted all downstream analyses. HLA allotypes were determined by HistoGenetics or by the Quantitative Biology Center, University of Tübingen. Samples along with clinical metadata were provided by collaborating physicians and analyzed by L.K.F.

1 Abstract

Glioblastoma is the most aggressive and most frequent primary CNS tumor. Despite extensive research, patients have not sufficiently benefited from recent scientific developments including immune checkpoint inhibitors. However, glioblastoma has been shown to be vulnerable to T cells targeting non-mutated peptides presented on HLA molecules. Immunotherapeutic intervention is typically administered subsequent to standard radiochemotherapy contributing to potential hypermutation and clonal evolution perhaps drastically altering the antigenic repertoire. Thus, we have for the first time investigated the immunopeptidomic landscape of 24 recurrent glioblastomas in comparison with 38 primary tumors, including 22 autologous pairs of samples, to define tumor antigens robustly presented at both recurrent and primary disease, while addressing not only HLA class I- but also HLA class II-restricted peptides. Relative quantitation of HLA ligand abundances, comparative profiling, and functional annotation clustering further delineated antigenic profiles and features associated with primary or recurrent glioblastoma, respectively. Moreover, this multi-omics approach provides the first evidence for natural HLA presentation of two neo-antigenic peptides in human brain tumors. Taken together, we defined a set of glioblastoma-associated antigens representing prime candidates to be pursued in the development of future immunotherapies as being naturally, exclusively, and frequently presented on both primary and recurrent neoplasias. This may contribute to improve the therapeutic situation in recurrent glioblastoma lacking evidence-based protocols.

2 Introduction

Glioblastoma represents the most frequent and most aggressive primary CNS neoplasia accounting for a 5-year relative survival rate of only 6.8%.¹ Extensive research has been conducted, however, a sufficient translation of scientific knowledge into clinical benefit has so far stayed out. The standard-of-care still comprises surgery and adjuvant radiochemotherapy according to the Stupp protocol and evidence-based therapeutic regimens to manage disease recurrence do not exist.²⁻⁶ Glioblastoma recurrence is inevitable, as these diffusely growing tumors deeply infiltrate into surrounding benign brain tissue rendering complete surgical resection virtually impossible.^{2-4,7} Radio- and especially adjuvant and concomitant chemotherapy are expected to significantly alter the repertoire of potential targets by clonal evolution and, in a fraction of patients, by somatic hypermutation.^{8,9} Although few datasets investigating the antigenic landscape of glioblastoma have been published, none has so far addressed recurrent tumors despite this is the condition, in which experimental therapies are initially applied to be evaluated for clinical effectiveness. Likewise, HLA class II-restricted targets have been inadequately examined by previous studies.¹⁰⁻¹⁴

We employ a multi-omics approach comprising HLA peptidome analyses, whole exome and transcriptome sequencing, and DNA methylation profiling. Comparison with a large dataset of benign immunopeptidomes enabled the definition of glioblastoma-associated antigens and peptides as candidate targets for cancer immunotherapy. Antigens were reviewed for CTA-like expression profiles by querying the GTEx database, which contains RNA expression data acquired across a large set of benign human tissues.¹⁵ This also allowed excluding such with

CNS-specific expression and to identify antigens not known to be expressed in any tissue. Moreover, exome sequencing of tumors and autologous blood cells may allow the identification of neo-antigenic HLA ligands, especially in hypermutated recurrent tumors, in a fully individualized setting or disprove the efficient translation of non-synonymous mutations into peptides naturally presented on HLA, as already done for several cancer entities including primary glioblastoma.^{12,16-19} Besides yielding candidate targets for immunotherapy, this study provides a deep insight into glioblastoma biology during progression from primary to recurrent disease. To address this, we compared the immunopeptidomic landscape of primary and recurrent tumors in a predominantly autologous setting, whereby mutational, transcriptional, and DNA methylation profiling will follow.

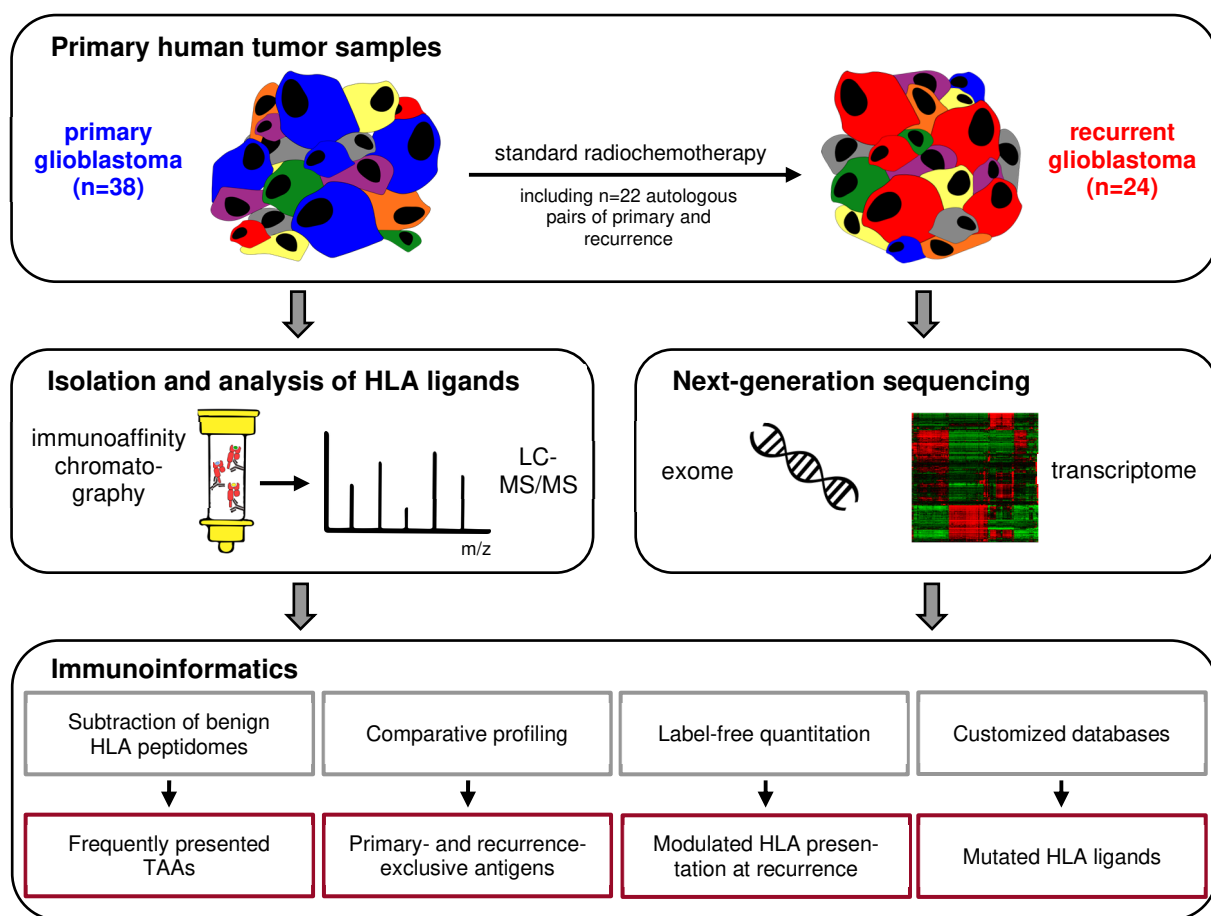


Figure 8. Multi-omics analysis of glioblastoma with a particular focus on the similarities and differences between primary and recurrent disease. While the analysis of immunopeptidomic data has been completed, the investigation of whole exome and transcriptome data as well as integration with LC-MS/MS data has been performed for n=13 primary tumors and is currently being extended to all patients with paired primary and recurrent glioblastomas being available. The two middle panels of the figure were kindly provided by PD Dr. med. Marian Christoph Neidert.

3 Methods

Patient collective

Written informed consent of the 40 patients included in the present study was obtained in accordance with the Declaration of Helsinki protocol and the local review boards (Kantonale Ethikkommission Zürich / KEK-ZH-Nr. 2015-0163; Ethik-Kommission der Ärztekammer

Hamburg / PV4904) before surgery. Patients underwent surgery at the Department of Neurosurgery of the University Hospital Zürich or of the University Medical Center Hamburg-Eppendorf. Tissue samples were snap frozen in liquid nitrogen and stored at -80°C until use. All patients had histopathologically confirmed glioblastoma and specimens along with clinical metadata were kindly provided by PD Dr. med. Marian Christoph Neidert and Dr. med. Julia Velz (University Hospital Zürich, Department of Neurosurgery), Dr. Konstantina Kapolou (University Hospital and University of Zürich, Department of Neurology, Laboratory for Molecular Neuro-Oncology) as well as by Prof. Dr. med. Manfred Westphal and Dr. med. Malte Mohme (University Medical Center Hamburg-Eppendorf, Department of Neurosurgery).

All patients had histopathologically confirmed glioblastoma (all IDH1^{WT} excepting n=2 lacking IDH1-status and n=1 IDH1^{mut} at recurrence; n=17 MGMT⁺ / n=20 MGMT⁻ / n=3 lacking MGMT-status) with 38 and 24 samples obtained during surgery at primary or recurrent disease, respectively. The present study population had a female-to-male ratio of 4:5 and a median age of onset of 67 [33-86] years. Autologous primary and recurrent tumors enabling LFQ of relative HLA class I and II ligand abundances were available from 22 patients. The median amount of tissue subjected to HLA-IP accounted to 893 [119-2759] mg for primary and to 451 [35-5834] mg for recurrent glioblastomas. Individual patient and sample characteristics are given in Table 6 and Figure 9, whereby a closer look on HLA allotype frequencies in the study cohort is provided in CHAPTER 5.

Table 6. Study cohort comprising 40 glioblastoma patients (n=38 primary and n=24 recurrent tumors). Age of onset was defined as the age at initial diagnosis. The MGMT-status differentiates tumors into such with (+) and without (-) MGMT promoter methylation, whereas the IDH1-status distinguishes glioblastomas lacking a mutation of the IDH1 gene (WT) from those with mutant IDH1 (mut). HLA class II allotypes were only available for samples sequenced at HistoGenetics. Abbreviations not introduced in the text above: primary glioblastoma (P), recurrent glioblastoma (R), not determined (n.d.). #Sample mass not used for further calculations (part of sample lost during HLA-IP).

Internal sample ID	Gender	Age of onset [years]	IDH1-status	MGMT-status	PFS from primary [months]	Time from P to R surgery [months]	OS from primary [months]	HLA typing	Sample mass HLA-IP [mg] P / R	Direct injection P / R	Relative quantitation HLA class I / II
Autologous pairs of primary and recurrent glioblastoma											
GBM2	♂		WT		n.d.	10	n.d.	A*02:01;A*03:01;B*07:02;B*15:01;C*07:02;C*03:04			+ / +
P N1-06		67		+					978	-	
R N162-06									526	-	
GBM3	♂		WT		n.d.	11	n.d.	A*02:01;A*01:01;B*27:05;B*18:01;C*02:02;C*07:01			- / +
P N82-12		68		-					1862	-	
R N56-13									174	-	
GBM4	♂		WT		n.d.	10	n.d.	A*03:01;A*03:01;B*07:02;B*07:02;C*07:02;C*07:02			+ / -
P N119-08		65		-					332	-	
R N73-09									534	-	
GBM5	♀		WT		n.d.	12	n.d.	A*01:01;A*01:01;B*13:02;B*15:01;C*03:03;C*06:02			+ / +
P N12-05		66		+					729	-	
R N108-06									375	-	
GBM6	♀		WT		n.d.	12	n.d.	A*02:05;A*03:01;B*35:01;B*15:03;C*04:01;C*12:03			+ / -
P N156-08		63		-					1258	-	
R N146-09									253	-	
GBM7	♀		WT / mut		n.d.	46	n.d.	A*11:01;A*02:01;B*07:02;B*56:01;C*01:02;C*02:02			+ / +
P N163-07		47		+					893	-	
R N182-10									566	-	
GBM8	♀		n.d.		n.d.	24	n.d.	A*68:01;A*03:01;B*07:02;B*44:02;C*07:02;C*07:04			- / -
P N122/07		40		n.d.					119	+	
R N131/09									82	+	
GBM9	♀		WT		n.d.	7	n.d.	A*33:05;A*01:01;B*08:01;B*14:02;C*07:01;C*08:02			+ / +
P N45/14		40		+					1471	+	
R N203/14									917	+	
GBM10	♂		n.d.		n.d.	60	n.d.	A*02:01;A*03:01;B*07:02;B*07:02;C*07:02;C*07:02			- / -
P N207/10		52		-					252	+	
R N476/15									1167	+	

Chapter 2: Methods

GBM11	♂	WT	n.d.	20	n.d.	A*02:05;A*02:01;B*41:01;B*07:02;C*07:01;C*07:02			+ / +
P N138/15	74	+					663	+	
R N546/15							310	+	
GBM12	♂	WT	6	6	9	A*11:01;A*02:01;B*35:01;B*15:01;C*01:02;C*04:01			+ / +
P ZH560	54	-					206	+	
R ZH588							5834	-	
GBM13	♀	WT	15	15	n.d.	A*01:01;A*02:01;B*08:01;B*13:02;C*06:02;C*07:01			- / -
P ZH794	72	n.d.				DRB1*03:01;DRB1*07:01;DRB3*01:01;DRB4*01:01;	734	-	
R ZH917						DQB1*02:01;DQB1*02:01;DQA1*02:01;DQA1*05:01	546	+	
GBM14	♂	WT	6	13	18	A*33:01;A*02:01;B*35:03;B*14:02;C*08:02;C*04:01			+ / +
P ZH301	68	n.d.					250	+	
R ZH384							2784 [#]	-	
GBM15	♂	WT	5	16	n.d.	A*24:02;A*02:01;B*44:02;B*44:03;C*05:01;C*02:02			- / +
P ZH399	54	-					348	+	
R ZH535							95	+	
GBM16	♂	WT	3	36	41	A*03:01;A*01:01;B*07:02;B*08:01;C*07:01;C*07:02			+ / +
P ZH415	59	+					893	+	
R ZH622							344	+	
GBM17	♂	WT	9	10	19	A*01:01;A*03:01;B*44:03;B*57:01;C*04:01;C*06:02			- / -
P ZH746	72	-				DRB1*07:01;DRB1*13:05;DRB3*02:02;DRB4*01:01;	922	-	
R ZH855						DQB1*02:01;DQB1*03:01;DQA1*02:01;DQA1*05:01	735	+	
GBM18	♀	WT	10	11	n.d.	A*03:01;A*11:01;B*07:02;B*08:01;C*07:01;C*07:02			- / -
P ZH813	57	-				DRB1*03:01;DRB1*04:04;DRB3*01:01;DRB4*01:01;	1655	-	
R ZH895						DQB1*02:01;DQB1*03:02;DQA1*03:01;DQA1*05:01	2147	-	
GBM19	♂	WT	11	11	n.d.	A*02:01;A*24:02;B*40:02;B*44:02;C*01:02;C*05:01			- / -
P ZH818	68	-				DRB1*01:01;DRB1*13:01;DRB3*02:02;DQB1*05:01;	662	-	
R ZH904						DQB1*06:03;DQA1*01:03;DQA1*01:01	40	+	
GBM20	♀	WT	19	23	n.d.	A*29:02;A*02:01;B*44:03;B*44:02;C*05:01;C*16:01			+ / +
P ZH669	69	-					140	+	
R ZH909							35	+	
GBM21	♀	WT	38	38	n.d.	A*02:01;A*02:01;B*35:03;B*44:02;C*12:03;C*07:04			- / +
P ZH561	33	+					310	+	
R ZH862							215	+	
GBM22	♀	WT	7	20	23	A*03:01;A*24:02;B*35:03;B*40:01;C*03:04;C*12:03			- / -
P ZH736	76	+				DRB1*09:01;DRB1*11:01;DRB3*02:02;DRB4*01:01;	1074	-	
R ZH736R						DQB1*03:03;DQB1*03:01;DQA1*03:01;DQA1*05:01	3714	-	
GBM23	♀	WT	20	21	24	A*03:01;A*23:01;B*35:02;B*47:01;C*04:01;C*06:02			- / -
P ZH763	70	+				DRB1*07:01;DRB1*11:04;DRB3*02:02;DRB4*01:01;	1981	-	
R ZH945						DQB1*02:01;DQB1*03:01;DQA1*02:01;DQA1*05:01	542	+	
Unpaired tumor samples									
P ZH613	♂	WT	n.d.	n.d.	n.d.	A*02:05;A*31:01;B*51:01;B*58:01;C*05:01;C*07:01	840	-	
	74	-				DRB1*13:01;DRB1*13:02;DRB3*02:02;DRB3*03:01;			
						DQB1*06:09;DQB1*06:03;DQA1*01:03;DQA1*01:02			
P ZH616	♀	WT	n.d.	n.d.	n.d.	A*02:01;A*29:02;B*07:02;B*44:02;C*05:01;C*07:02	1160	-	
	86	-				DRB1*12:01;DRB1*15:01;DRB3*02:02;DRB5*01:01;			
						DQB1*03:01;DQB1*06:02;DQA1*01:02;DQA1*05:01			
P ZH617	♀	WT	n.d.	n.d.	n.d.	A*01:01;A*02:01;B*08:01;B*44:02;C*05:01;C*07:01	600	-	
	74	+				DRB1*03:01;DRB1*03:01;DRB3*01:01;DRB3*01:01;			
						DQB1*02:01;DQB1*02:01;DQA1*05:01;DQA1*05:01			
P ZH631	♂	WT	n.d.	n.d.	n.d.	A*11:01;A*32:01;B*44:02;B*51:01;C*03:03;C*07:04	370	-	
	60	+				DRB1*01:01;DRB1*08:01;DQB1*04:02;DQB1*05:01;			
						DQA1*01:01;DQA1*04:01			
P ZH645	♂	WT	n.d.	n.d.	n.d.	A*01:01;A*02:01;B*49:01;B*51:01;C*01:02;C*07:01	1037	-	
	66	-				DRB1*07:01;DRB1*13:02;DRB3*03:01;DRB4*01:01;			
						DQB1*02:01;DQB1*06:04;DQA1*01:02;DQA1*02:01			
P ZH654	♂	WT	n.d.	n.d.	n.d.	A*01:01;A*31:01;B*51:01;B*57:01;C*06:02;C*15:06	2759	-	
	72	+				DRB1*04:04;DRB1*07:01;DRB4*01:03;DRB4*01:01;			
						DQB1*03:03;DQB1*03:02;DQA1*02:01;DQA1*03:01			
P ZH678	♂	WT	n.d.	n.d.	n.d.	A*02:01;A*11:01;B*44:03;B*51:01;C*04:01;C*15:02	2619	-	
	66	-				DRB1*11:01;DRB1*11:01;DRB3*02:02;DRB3*02:02;			
						DQB1*03:01;DQB1*03:01;DQA1*05:01;DQA1*05:01			
P ZH681	♂	WT	n.d.	n.d.	n.d.	A*02:01;A*02:01;B*07:02;B*57:01;C*06:02;C*07:02	1244	-	
	78	+				DRB1*07:01;DRB1*13:02;DRB3*03:01;DRB4*01:03;			
						DQB1*03:03;DQB1*06:04;DQA1*01:02;DQA1*02:01			
P ZH720	♂	WT	n.d.	n.d.	n.d.	A*02:01;A*02:01;B*18:01;B*39:10;C*07:01;C*12:03	960	-	
	70	-				DRB1*13:01;DRB1*13:01;DRB3*01:01;DRB3*01:01;			
						DQB1*06:03;DQB1*06:03;DQA1*01:03;DQA1*01:03			
P ZH750	♀	WT	n.d.	n.d.	n.d.	A*02:01;A*24:02;B*15:17;B*44:02;C*07:01;C*07:04	1019	-	
	60	-				DRB1*11:01;DRB1*13:02;DRB3*02:02;DRB3*03:01;			
						DQB1*03:01;DQB1*06:04;DQA1*01:02;DQA1*05:01			
P ZH757	♂	WT	n.d.	n.d.	n.d.	A*02:01;A*02:01;B*07:02;B*27:05;C*01:02;C*07:02	645	-	
	70	-				DRB1*08:01;DRB1*15:01;DRB5*01:01;DQB1*04:02;			
						DQB1*06:02;DQA1*01:02;DQA1*04:01			
P ZH761	♂	WT	n.d.	n.d.	n.d.	A*02:01;A*03:01;B*44:02;B*51:26;C*01:02;C*16:01	1193	-	
	80	+				DRB1*01:01;DRB1*12:01;DRB3*02:02;DQB1*03:01;			
						DQB1*05:01;DQA1*01:01;DQA1*05:01			
P ZH791	♂	WT	n.d.	n.d.	n.d.	A*03:01;A*11:01;B*07:02;B*13:02;C*06:02;C*07:02	751	-	
	63	-				DRB1*11:01;DRB1*15:01;DRB3*02:02;DRB5*01:01;			
						DQB1*03:01;DQB1*06:02;DQA1*01:02;DQA1*05:01			
P ZH802	♀	WT	n.d.	n.d.	n.d.	A*31:01;A*33:01;B*14:02;B*44:02;C*05:01;C*08:02	1712	-	
	70	-				DRB1*04:04;DRB1*13:02;DRB3*03:01;DRB4*01:01;			
						DQB1*03:02;DQB1*06:04:01;DQA1*01:02;DQA1*03:01			
P ZH810	♀	WT	n.d.	n.d.	n.d.	A*24:02;A*24:02;B*44:03;B*57:01;C*04:01;C*06:02	1158	-	
	53	+				DRB1*07:01;DRB1*11:01;DRB3*02:02;DRB4*01:01;			
						DQB1*03:03;DQB1*03:01;DQA1*02:01;DQA1*05:01			

Chapter 2: Methods

P ZH829	♀ 70	WT -	n.d.	n.d.	n.d.	A*02:01;A*02:01;B*44:05;B*55:01;C*01:02;C*02:02 DRB1*13:01;DRB1*16:01;DRB3*02:02;DRB5*02:02; DQB1*05:02;DQB1*06:03;DQA1*01:03;DQA1*01:02	276	-
R ZH753	♀ 59	WT +	n.d.	n.d.	n.d.	A*02:01;A*02:01;B*08:01;B*51:01;C*07:01;C*15:02 DRB1*01:01;DRB1*03:01;DRB3*01:01;DQB1*02:01; DQB1*05:01;DQA1*01:01;DQA1*05:01	2483	-
R ZH784	♂ 63	WT +	n.d.	n.d.	n.d.	A*01:01;A*02:01;B*07:02;B*08:01;C*07:01;C*07:02 DRB1*11:01;DRB1*15:01;DRB3*02:02;DRB5*01:01; DQB1*03:01;DQB1*06:02;DQA1*01:02;DQA1*05:01	287	-

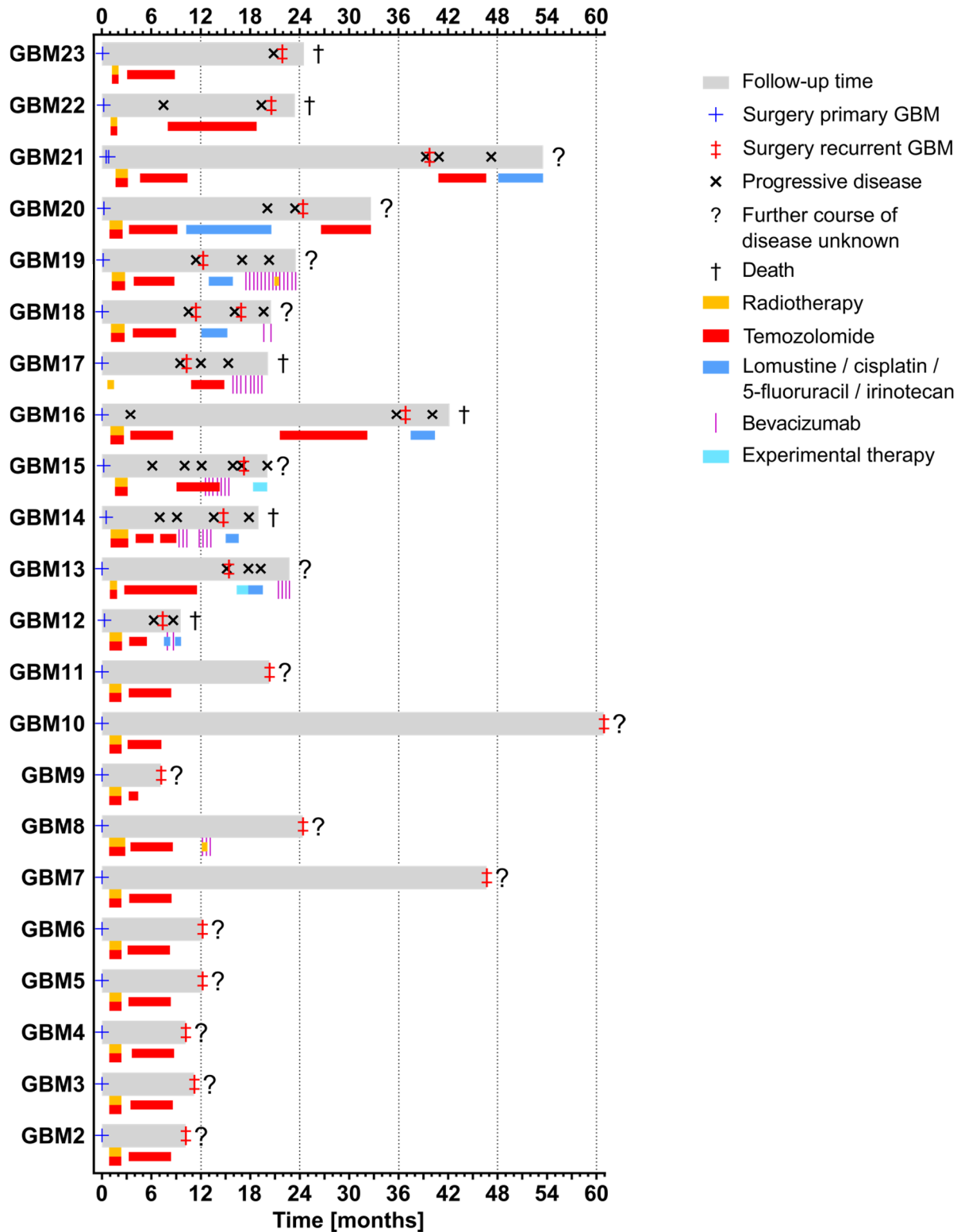


Figure 9. Clinical timeline for the 22 glioblastoma patients with both primary and recurrent tumors being analyzed. Median follow-up time accounted for 20 [7-61] months with patients 2-11

lacking clinical information subsequent to surgery for recurrent glioblastoma. All patients excepting GBM17 received radiochemotherapy and adjuvant temozolomide following surgical resection of primary glioblastoma. The time between surgery of primary and recurrent glioblastoma came up to 14 [6-60] months in median. Experimental therapies as part of clinical trials comprise the CDK2 / Janus kinase 2 (JAK2) / FMS-like tyrosine kinase 3 (FLT3) inhibitor TG02 (EORTC-1608; GBM13) and the fibroblast growth factor receptor inhibitor BGJ398 (CBGJ398X2201; GBM15). Prior to surgical resection of recurrent tumors, patients GBM4 and GBM10 were treated with an anti-EGFR antibody or bevacizumab (AVAglio study), respectively – precise dates of treatments were, however, not available.

HLA-IP and subsequent LC-MS/MS to identify HLA-presented peptides

HLA class I- and II-presented peptides were isolated from primary human tissue and analyzed by LC-MS/MS as described in 3.2. To handle the pronounced high degree of intratumoral heterogeneity characteristic of glioblastoma, a pool of frozen chopped tissue was created from which samples for HLA-IP, whole exome, and RNA sequencing were gathered. All peptide eluates were analyzed in three technical replicates each consuming 20% sample share on an Orbitrap Fusion Lumos. From autologous pairs of primary and recurrent tumors suitable for LFQ-MS, five adjusted technical replicates starting with 17% sample share in the dose-finding run were acquired. Two additional technical replicates consuming 17% sample share each were measured of samples heavily diluted for relative quantitation purposes. The maximum available number of LC-MS/MS runs were subjected to comparative profiling upon co-processing. Direct injection of several peptide eluates was performed as indicated in Table 6.

HLA typing, whole exome, and RNA sequencing

HLA class I and II allotypes of all primary glioblastomas without autologous recurrent tumors being available as well as of ZH753, ZH784, and patients GBM13, 17, 18, 19, 22, and 23 were determined on 4-digit level by next-generation sequencing at HistoGenetics (New York, USA). For remaining patients, 4-digit HLA class I typing was retrieved from whole exome sequencing data of genomic DNA isolated from blood or PBMCs using the OptiType²⁰ algorithm by Marie Gauder and Dr. Stefan Czernmel (Quantitative Biology Center, University of Tübingen).

Whole exome and RNA sequencing was performed for all 22 patients with paired primary and recurrent glioblastoma as well as for ZH613, ZH616, ZH654, ZH681, ZH720, ZH750, ZH753, ZH757, and ZH802 at CeGaT GmbH (Tübingen). Genomic DNA was isolated from PBMCs using the DNeasy 96 Blood & Tissue Kit (Qiagen). For patients GBM2-11, isolated genomic DNA had already been provided by Dr. med. Malte Mohme. DNA and RNA were isolated from fresh frozen tumor tissue using the AllPrep DNA/RNA Mini Kit (Qiagen). Whole exome sequencing libraries were prepared from 50 ng DNA using the Twist Human Core Exome Kit (Twist Bioscience) and subsequent data acquisition was performed by paired-end sequencing and at 100 bp read length on a NovaSeq 6000 sequencing system (Illumina). For genomic DNA, 10 giga bases (Gb) were acquired per sample, whereas sequencing depth of tumor samples came up to 18 Gb. RNA was only isolated from tumor tissues. Following quality control for RNA integrity, sequencing libraries were prepared from 10 ng RNA using the SMARTer Stranded Total RNA-Seq Kit v2 - Pico Input Mammalian (Takara Bio), whereby ribosomal RNA was removed. Paired-end sequencing at 100 bp read length was performed for 10 Gb on a NovaSeq 6000. Sequencing reads were demultiplexed employing the Illumina bcl2fastq 2.19 followed by Adapter trimming with Skewer 0.2.2²¹ (exome sequencing) or cutadapt 1.12²²

(RNA sequencing). FASTQ²³-formatted files were uploaded to qPortal²⁴ (Quantitative Biology Center, University of Tübingen) for further data analysis.

Variant calling and calculation of expression values at a time when only 13 primary tumors had been sequenced, was performed by Christopher Mohr and Silvia Morini (Quantitative Biology Center, University of Tübingen). BWA v0.7.17-r1188²⁵ was employed to map exomic reads to the human reference genome GRCh37 (Ensembl release 75). Somatic variants comprising insertions or deletions (indels) as well as single nucleotide variants (SNVs) were called separately by Strelka v2.9.3²⁶ with variants being annotated with SnpEff v4.3t²⁷. Variant allele frequencies (VAFs) representing the percentage of glioblastoma cells harboring the respective mutation were computed by division of the number of variant reads by the number of WT reads acquired from the same genomic region. Of note, this calculation assumes relatively high tumor cell content in the glioblastoma sample from which DNA was extracted.²⁸ Reported mutational loads (both indels and SNVs) refer to variants passing confidence filtering criteria of the variant caller Strelka v2.9.3 (filter 'PASS'). The probability p of an incorrect variant call is calculated from a phred-scale empirical variant scoring (EVS) step: $p = 10^{-\frac{\text{--somaticEVS}}{10}}$. The EVS model is based on a supervised random forest classifier and provides a quality score for every variant.^{29,30} This quality score takes into account '(1) the genotype probability computed by the core variant probability model, (2) root-mean-square mapping quality, (3) strand bias, (4) the fraction of reads consistent with locus haplotype model, and (5) the complexity of the reference context as measured by metrics such as homopolymer length and compressibility'²⁹. Applying the 'PASS' filter to variants excludes variants with a read depth < 2 in the glioblastoma sample and sets an EVS threshold of ≥ 7 (equivalent to $p < 20\%$) or of ≥ 6 (equivalent to $p < 25\%$) for SNVs and indels, respectively.^{29,30} Finer selection for confident somatic variants was based on filtering for mutations with an EVS ≥ 13 corresponding to a probability of $\leq 5\%$ that the respective variant is incorrect.

Analysis of RNA data was based on the Nextflow pipeline release 1.3³¹ and the Sarek pipeline release 2.3³². Quality control of FASTQ files was accomplished by FASTQC³³, whereas MultiQC v1.73³⁴ aggregated the Bioinformatic workflow. Before read alignment to the human reference genome GRCh37 (Ensembl release 75) with STAR v2.6.1d³⁵, another adapter trimming step was conducted *via* Trim Galore v0.5.05³⁶. RNA sequencing data was evaluated using RSeQC v3.0.0³⁷ with features (transcripts) being counted by featureCounts v1.6.4³⁸. Besides reporting raw counts per gene, reads per kilobase per million mapped reads (RPKM) were calculated as a measure of expression strength³⁹ by (1) dividing the total number of reads in the respective sample by 1,000,000, (2) normalizing the read counts of a gene by the factor calculated in (1), and (3) dividing the result of (2) by the number of kilobases spanned by the respective gene.

For GBM 17, 18, 22, and 23, whole exome and RNA sequencing data of primary tumors and genomic DNA will be re-analyzed by Marie Gauder and Dr. Stefan Czernmel to ensure comparability with data obtained from autologous tumor recurrence.

Search for neo-antigenic HLA-presented peptides

From the initial unfiltered variant calling performed for 13 primary glioblastomas, FASTA-formatted files were computed by translation of whole exome data with FRED²⁴⁰. Patient-

specific proteomes including mutated protein sequences arising from SNVs concatenated with a human reference proteome (Swiss-Prot release UP000005640, 20,416 reviewed protein sequences) as well as common laboratory contaminants served as database for annotation of MS² spectra using the MHCquant pipeline⁴¹. MHCquant was built within the OpenMS 2.4 framework⁴² employing the search engine Comet 2016.01 rev. 3⁴³ for peptide identification and Percolator 3.1.1⁴⁴ for FDR estimation. The FDR threshold was set to $\leq 5\%$ on peptide level and only the best sequence annotation (rank 1) was reported per fragment spectrum. Oxidation of methionine residues was the only permitted dynamic modification and no enzymatic restriction was set. Database search was performed at 5 ppm precursor ion and 0.02 Da fragment ion tolerance. HLA class I ligands were restricted to span 8 to 12 AA, to have a molecular weight of 800 to 2,500 Da, and to carry two or three positive charges. In contrast, the search space for HLA class II-restricted peptides was set to a length of 8 to 25 AA, a precursor mass of 800 to 5,000 Da, and a number of 2 to 5 positive charges. Identifications mapping to common laboratory contaminants were automatically excluded from reported peptide lists. Neo-antigenic peptides were predicted by shifting a window of 8 to 12 AA (HLA class I) or 8 to 25 AA (HLA class II) around the mutated amino acid, whereby no prediction of HLA binding probability was performed. Peptides identified by the MHCquant pipeline were designated as mutated when uniquely mapping to the list of predicted mutated 8- to 12-mers or 8- to 25-mers, respectively.

Potential neo-epitopes as identified by Leon Bichmann using the MHCquant pipeline underwent an in-house validation step by standard data processing with the SEQUEST search engine embedded in Proteome Discoverer 1.4 against patient-specific customized databases. This especially allowed assessing the spectral quality by viewing fragment spectra and corresponding scores. Moreover, a prediction of binding to the patient's HLA class I allotypes was performed as described in 3.2.2 and peptide sequences (with all possible exchanges of the isobaric AAs leucine and isoleucine) were queried against the UniProt⁴⁵ and dbSNP⁴⁶ databases to exclude that the identified peptide mapped to a WT sequence or a single nucleotide polymorphism. The VAF of the mutation-of-interest was reviewed with VAFs $\geq 5\%$ being considered as confident. In addition, the expression of the corresponding gene (independent of whether WT or variant transcripts were sequenced) was verified based on RNA data, whereby a minimum of 10 raw counts was set as threshold. Finally, heavy isotope-labeled peptides were synthesized by solid-phase peptide synthesis (Wirkstoffpeptidlabor, Department of Immunology, University of Tübingen), whereby heavy isotope-labeled isoleucine [$I(^{13}C_6; ^{15}N)$] was incorporated at one position each. Peptides were first completely dissolved in 100% DMSO, facilitated by vortexing, with subsequent addition of MS grade H₂O. Peptides were diluted with A_{Load} and spiked at ~ 100 fmol/ μ l into a complex matrix of HLA class I peptides eluted from JY cells. Following LC-MS/MS (standard HLA class I method as described in 3.2.2) on an Orbitrap Fusion Lumos, raw files were processed using a concatenated FASTA-formatted file consisting of the Swiss-Prot release from September 27th 2013 (20,279 reviewed protein sequences) and the mutant protein sequences. Heavy isotope labels (+7.017 Da) were permitted as additional dynamic modification for isoleucine residues and processing was otherwise performed as described in 3.2.2 for HLA class I peptidome data.

Somatic mutations of confirmed HLA-presented neo-antigenic peptides were queried against the COSMIC database⁴⁷ to investigate whether these are recurrent or even known driver mutations. In addition, effects of these mutations on protein phosphorylation were assessed using the PhosphoMotif Finder of the Human Protein Reference Database⁴⁸. To search for threonine and tyrosine phosphorylation within the confirmed mutated peptide of ZH681, phosphorylation (+79.966 Da) was permitted as dynamic modification at these residues for standard data processing with the SEQUEST search engine against the patient-specific customized database.

4 Results

4.1 Peptide yields of HLA-IPs and HLA class I allotype coverage

To define candidate targets for glioblastoma immunotherapy naturally presented on HLA, we analyzed 38 primary and 24 recurrent tumor specimens derived from 40 different patients. The study cohort included 55 distinct HLA class I allotypes covering 99.95% of the world population, whereby 92.17% of all individuals are expected to be positive for at least three allotypes (Supplementary Figure 1). The most frequent allotypes among glioblastoma patients were HLA-A*02:01 (63%), -A*03:01 (28%), -A*01:01 (25%), -B*07:02 (33%), -B*44:02 (28%), -B*08:01 (15%), -B*51:01 (9%), -C*07:01 (30%), -C*07:02 (30%), -C*01:02 (20%), and -C*06:02 (20%) (Supplementary Table 1).

A median of 3742 [450-7007] and 3710 [65-6333] HLA class I ligands were identified from primary or recurrent glioblastomas, respectively. All HLA class I peptide eluates except that of GBM5R exhibited a purity of at least 80% and none of the samples were censored for low peptide yield or low percentage of HLA class I ligands. Concerning HLA class II, median peptide yields came up to 2527 [293-8812] and 3203 [333-8287]. The total number of unique HLA class I and II peptides, HLA class I ligands as well as the purity of HLA class I peptide eluates are given in Figure 10 A for every specimen. The length distribution of HLA class I ligands clearly peaked at 9 AA length, whereas HLA class II-presented peptides were typically 13- to 18-mers. A fraction of samples showed a broadened length distribution curve elevated either for shorter (≤ 12 AA) or longer (≥ 19 AA) peptides, whereby no difference between primary and recurrent tumors was observed (Figure 10 B). Taking tissue masses subjected to HLA-IP into account (Table 6), enabled us to investigate whether peptide yields correlate with sample quantities used. The amount of glioblastoma tissue correlated with the number of HLA class I ligand identifications, whereas this was not the case for HLA class II-presented peptides (Figure 10 C). Considering the relative number of identified unique peptides per one mg of tissue input revealed a slightly increased yield of HLA class I as compared with HLA class II peptides eluted from primary glioblastomas and of HLA class II-restricted peptides identified on recurrent *versus* primary tumors (Figure 10 D).

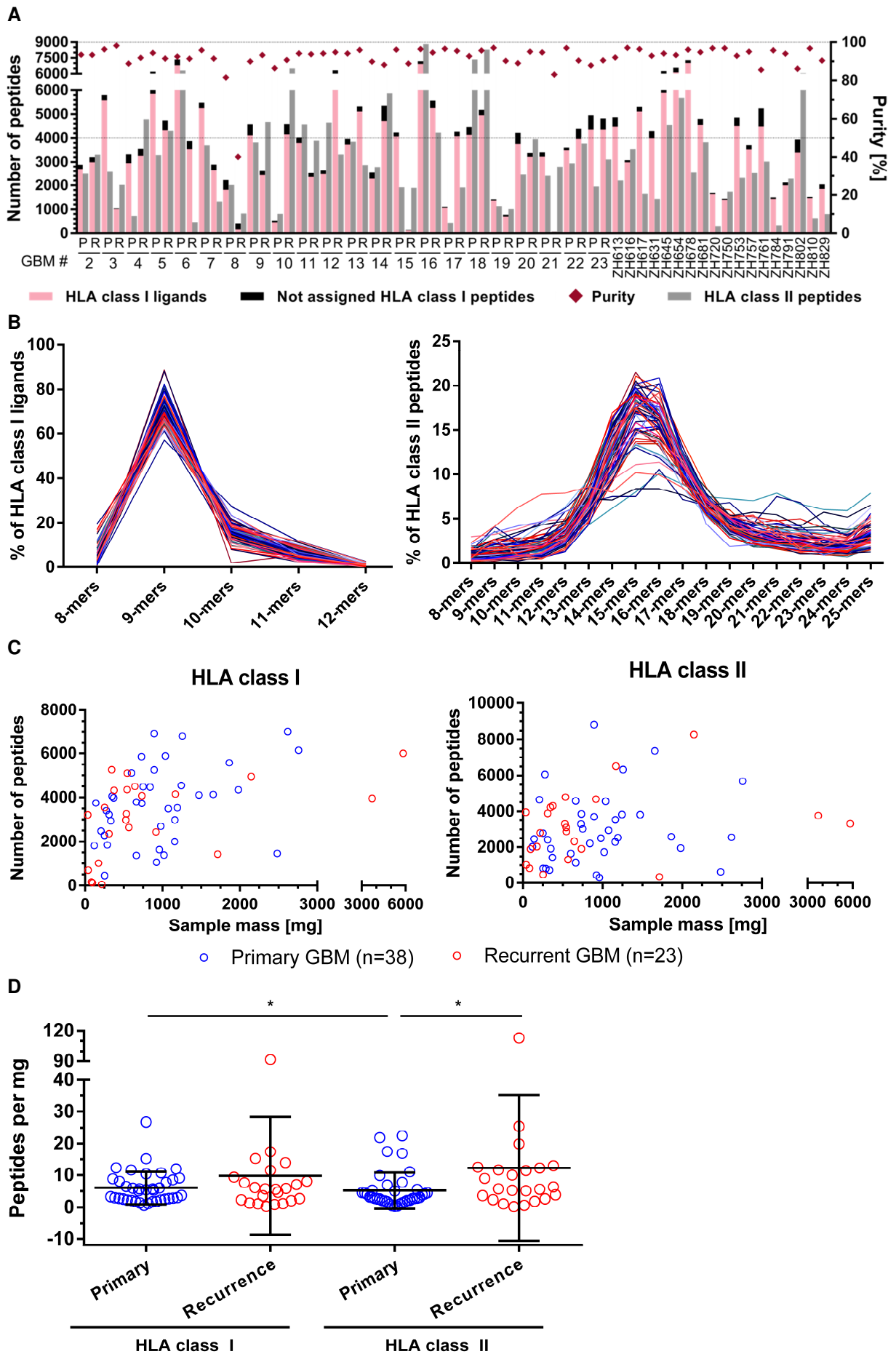


Figure 10. Number and length distribution of identified HLA class I- and II-presented peptides.

(A) HLA class I and II peptide yields of primary and recurrent glioblastomas. Calculated purities refer to the proportion of HLA class I peptides annotated to an HLA allotype of the respective patient.

(B) Length distribution of HLA class I ligands and HLA class II peptides. Across the entire dataset, 9-mers constituted 71% of HLA class I ligands, whereas 73% of HLA class II-presented peptides had a length between 13 and 18 AA. Each line represents data of one sample with primary and recurrent tumors being illustrated in blueish and redish shades, respectively. While the entire HLA class II dataset included 9% of peptides with ≤ 12 AA and 19% of peptides with ≥ 19 AA, these shares were distorted in a fraction of patients (GBM2R, GBM4P, GBM8P, GBM8R, GBM17R, ZH720, and ZH802: 16-28% 8- to 12-mers; GBM4P, GBM6R, GBM10P, ZH679, ZH720, and ZH829: 30-49% 19- to 25-mers).

(C) Unique peptides per sample versus amount of tissue subjected to HLA-IP. The total amount of unique HLA class I ligands or HLA class II-restricted peptides was set in relation to the amount of tissue subjected to HLA-IP, whereby GBM14R was excluded owing to sample loss during HLA-IP. By non-linear regression (one-phase association) exponential functions with a forced y-intercept of 0 (internal data created by Daniel Kowalewski at the Department of Immunology, University of Tübingen indicate that subjecting cell-free lysis buffer to HLA-IP does not result in peptide identifications) were fitted. The goodness of fit was poor for all these models: $R^2 = 0.13$ (primary HLA class I) / 0.40 (recurrence HLA class I) / 0.02 (primary HLA class II) / 0.09 (recurrence HLA class II). However, a correlation analysis across normally distributed HLA class I ligand identifications (according to D'Agostino & Pearson omnibus normality test) identified a significant correlation of sample quantities used and the number of identified HLA class I-restricted peptides: two-tailed p -values = 0.0169 (primary) / 0.0222 (recurrence). In turn, HLA class II peptide yields were not found to correlate with sample masses subjected to HLA-IP: two-tailed p -values = 0.1854 (primary HLA class I; Spearman correlation for non-Gaussian data) / 0.2840 (recurrence HLA class I; Pearson correlation for parametric data).

(D) Peptide yields normalized to one mg of tissue input. To investigate, whether the relative number of peptide identifications differs between primary and recurrent glioblastomas (21/23 recurrent samples are autologous to primary tumors) as well as between HLA class I- and II-IPs of the same sample, Wilcoxon matched-pairs signed rank tests were performed (normalized peptide yields – excepting recurrence HLA class II – did not have Gaussian distributions according to D'Agostino & Pearson omnibus normality test). Narrowly significant differences were observed between the number of HLA class I and II peptides eluted from primary tumors (two-tailed p -value = 0.0429) as well as between the number of HLA class II-presented peptides on primary versus recurrent glioblastomas (two-tailed p -value = 0.0290). One outlier, GBM20R, showed both increased relative HLA class I and II peptide yields.

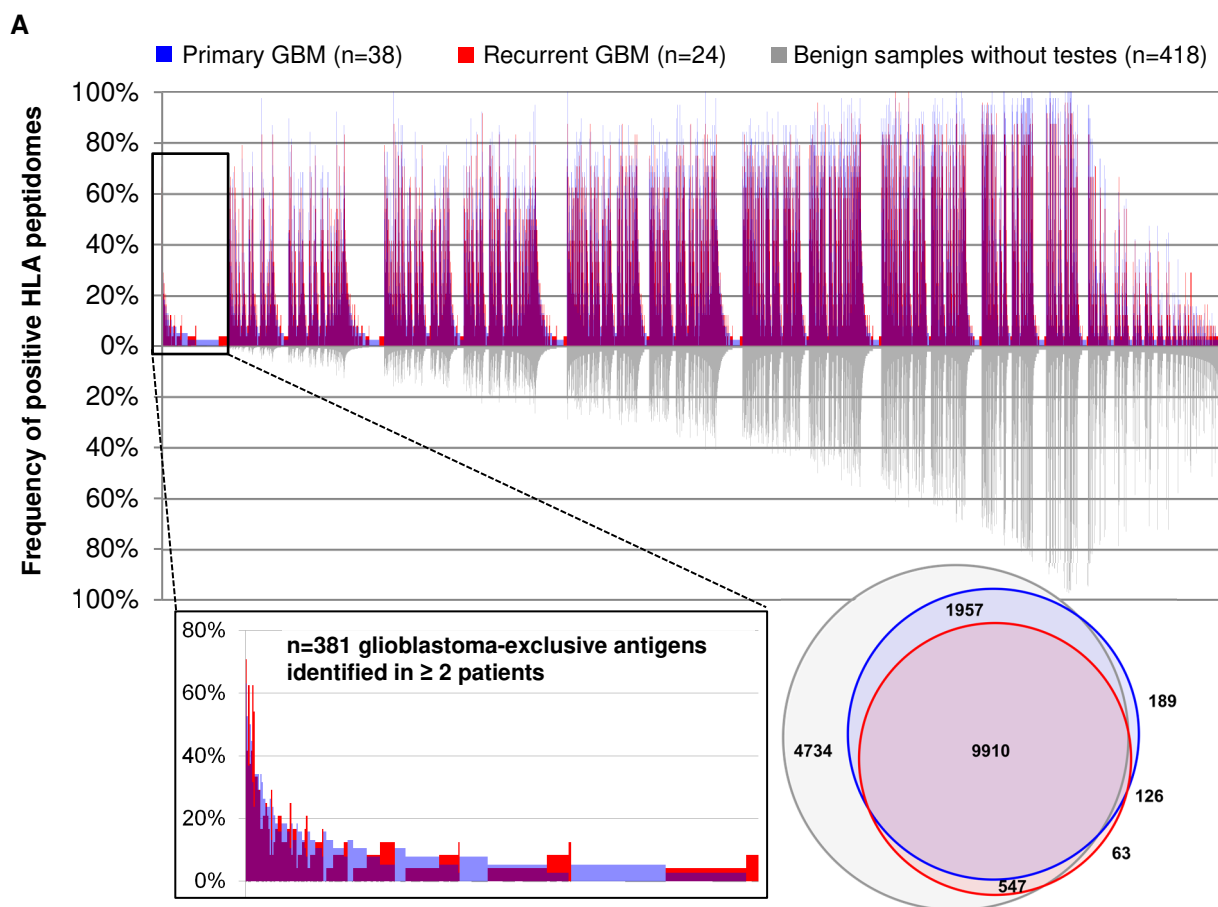
4.2 Definition of glioblastoma-associated antigens

By immunoaffinity chromatography and LC-MS/MS, the repertoire of HLA class I and II peptides and corresponding antigens naturally presented on 62 glioblastomas was mapped. To define glioblastoma-associated antigens and peptides, an in-house benign database comprising 30 distinct primary human organs ($n=418$ HLA class I and $n=364$ HLA class II datasets) was subtracted. The term glioblastoma-associated was assigned to peptides and antigens that were never identified on CNS-related tissues (brain, cerebellum, and spinal cord) and for which a maximum of one non-CNS-related sample was positive. Moreover, the robust presentation on both primary and recurrent tumors was defined as a prerequisite for all candidate immunotherapeutic targets reported herein. The frequency of positive primary human malignancies other than glioblastoma ($n=824$ samples for HLA class I; $n=585$ samples for HLA class II) encompassing 36 cancer entities was evaluated as well. As additional criterium to select targets for cancer immunotherapies, RNA expression data acquired across a large set of benign human tissues and deposited in the GTEx database¹⁵ was reported for every candidate antigen. Further, this allowed the identification of antigens not known to be expressed in any tissue (defined as less than ten transcripts per million (TPM) in any tissue), such with a classical CTA-like expression profile (not exceeding ten TPM in other organs than

testis) as well as to exclude antigens with brain-specific expression representing the tissue of tumor origin.

Glioblastoma-associated HLA class I-presented antigens and peptides

HLA class I peptidome analyses of primary (n=38) and recurrent glioblastoma (n=24) allowed the identification of 12,182 and 10,646 distinct source proteins represented by HLA class I ligands on primary or recurrent tumor tissue, respectively. These represent between 92% (recurrence) and 96% (primary) of the estimated maximum attainable amount of distinct source proteins (Figure 11 C). Despite the vast overlap of glioblastomas with benign samples, 381 antigens were exclusively presented on tumors of at least two different patients (Figure 11 A). Following manual curation of the underlying peptides for HLA motifs as well as multi-mapping to several source proteins, a set of 62 glioblastoma-associated antigens and corresponding peptides naturally presented on 5-50% of primary as well as on 4-63% of recurrent tumors was created. Among these, TANC2, FA2H, and BEST1 were the most frequent ones. Despite being shared by primary and recurrent glioblastomas, several antigens were rather associated with primary tumors (e.g. SHISA4), while others were preferentially presented at disease recurrence (e.g. LHFPLS; Figure 11 B). Peptide sequences and their HLA restriction, a listing of positive samples, and the GTEx profile of the corresponding source protein can be retrieved from Supplementary Table 2. It is noteworthy that two of these tumor-associated HLA class I antigens (HSF2BP, E2F1) exhibited a CTA-like expression profile and were not listed in the CTDDatabase⁴⁹.



B

G patch domain-containing protein 11 (GPATCH11)
 growth arrest and DNA damage-inducible proteins-interacting protein 1 (GADD45GIP1) T-box transcription factor TBX15 (TBX15)
 85/88 kDa calcium-independent phospholipase A2 (PLA2G6) uncharacterized protein C7orf50 (C7orf50)
 CMP-N-acetylneuraminase-beta-galactosamide-alpha-2,3-sialyltransferase 4 (ST3GAL4) IGF-like family receptor 1 (IGFLR1)
 lipoma HMGIC fusion partner-like 2 protein (LHFPL2) mitochondrial 39S ribosomal protein L35 (MRPL35)
 zinc finger and BTB domain-containing protein 47 (ZBTB47) cannabinoid receptor 1 (CNR1) glycosyltransferase-like domain-containing protein 2 (GTDC2)
 protein shisa-4 (SHISA4) transmembrane protein 255A (TMEM255A)
 5'-AMP-activated protein kinase subunit beta-2 (PRKAB2) neuronal migration protein doublecortin (DCX)
 SAC3 domain-containing protein 1 (SAC3D1) protein shisa-9 (SHISA9) lysyl oxidase homolog 2 (LOXL2)
 collagen alpha-2 (IX) chain (COL9A2) sugar phosphate exchanger 3 (SLC37A3)
 insulin-like growth factor-binding protein 2 (IGFBP2) transmembrane protein 87A (TMEM87A)
 solute carrier family 15 member 2 (SLC15A2)
 fatty acid 2-hydroxylase (FA2H)
 transcription factor SOX-21 (SOX21) transcription factor HES-4 (HES4)
 protein Wnt-5a (WNT5A) protein TANC2 (TANC2)
 transcription factor SOX-2 (SOX2) heat shock factor 2-binding protein (HSF2BP)
 uroporphyrinogen-III synthase (UROS)
 6-pyruvoyl tetrahydrobiopterin synthase (PTS) Bestrophin-1 (BEST1)
 T-box transcription factor TBX18 (TBX18)
 embryonal Fyn-associated substrate (EF3) protein pitchfork (PIFO) probable G-protein coupled receptor 75 (GPR75)
 NADH dehydrogenase [ubiquinone] 1 alpha transcription factor E2F1 (E2F1)
 protein Dos (DOS) transmembrane protein 237 (TMEM237)
 Frizzled-3 (FZD3) subcomplex subunit 4-like 2 (NDUFA4L2) peroxisome biogenesis factor 10 (PEX10)
 POU domain, class 3, transcription factor 3 (POU3F3) leucine-rich repeat neuronal protein 3 (LRRN3)
 blood vessel epicardial substance (BVES)
 uncharacterized protein C2orf72 (C2orf27) transcription factor E2F7 (E2F7)
 sodium- and chloride-dependent creatine transporter 1 (SLC6A8) uncharacterized protein C21orf62 (C21orf62) olfactory receptor 51A7 (OR51A7)
 immunoglobulin superfamily member 11 (IGSF11) integral membrane protein DGCR2/IDD (DGCR2)
 uncharacterized aarF domain-containing protein kinase 1 (ADCK1) solute carrier family 25 member 53 (SLC25A53)
 exostosin-like 3 (EXTL3) low-density lipoprotein receptor class A domain-containing protein 3 (LDLRAD3)
 leucine-rich repeats and immunoglobulin-like domains protein 1 (LRIG1) BTB/POZ domain-containing protein 17 (BTBD17)
 oligodendrocyte transcription factor 3 (OLIG3)

C

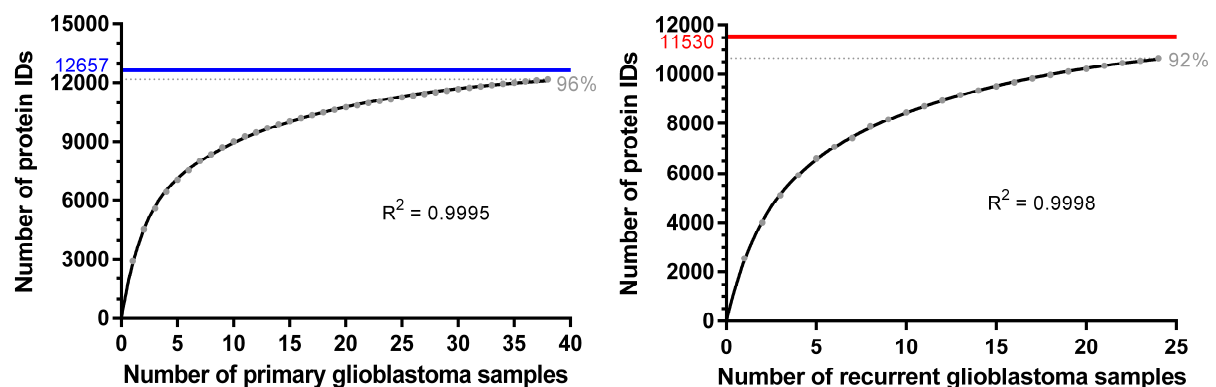
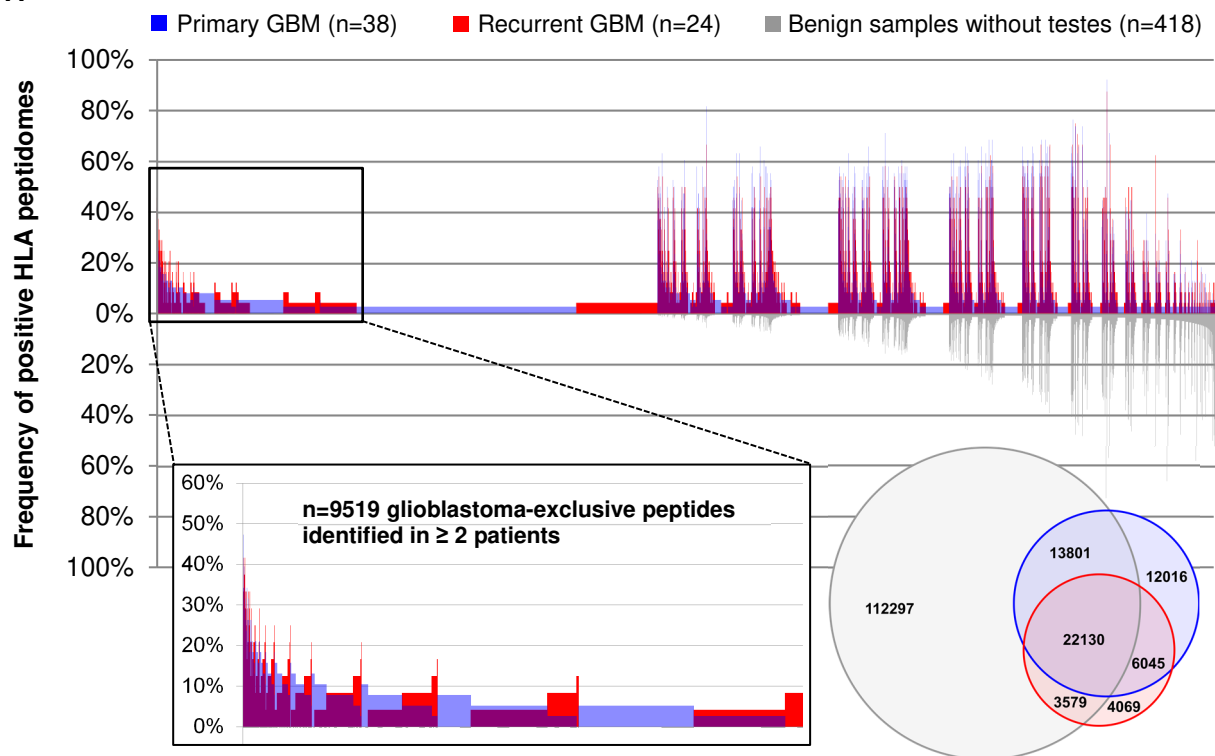


Figure 11. Definition of glioblastoma-associated antigens based on class I immunopeptidome analyses. (A) Comparative profiling of the HLA class I peptidome of glioblastoma *versus* an in-house benign database. Each bar in this waterfall plot (associated with the x-axis) represents a single source protein, whereas the frequency of positive HLA peptidomes is shown on the y-axis, separately

Chapter 2: Results

for primary glioblastoma (n=38), recurrent glioblastoma (n=24), and benign samples without testes (n=418 covering 29 different human tissues). Those source proteins detected on a maximum of one non-CNS-related tissue were designated as glioblastoma-exclusive, whereby n=361 were identified on primary and/or recurrent tumors of at least two patients (highlighted as enlarged view on the left). The Venn diagram on the right illustrates the number of distinct HLA class I-presented antigens per group, however, the overlaps cannot map the permission of one positive non-CNS-related sample within the benign dataset. **(B) Word cloud of glioblastoma-associated antigens.** Based on comparative profiling and subsequent quality control of underlying peptides (HLA motifs as well as multi-mapping to several source proteins), a set of 62 glioblastoma-associated antigens naturally presented on 5-50% of primary as well as on 4-63% of recurrent tumors was defined. The font size in the word cloud is proportional to the frequency of positive primary (blue) and recurrent (red) glioblastomas. **(C) Saturation analysis for the identification of antigens represented by HLA class I ligands on primary or recurrent glioblastoma tissue.** For each source count, the mean number of antigens was calculated by 1,000 random samplings. Using non-linear regression, exponential functions with a forced y-intercept of 0 (internal data created by Daniel Kowalewski at the Department of Immunology, University of Tübingen indicate that subjecting cell-free lysis buffer to HLA-IP does not result in peptide identifications) were fitted. For both models, the goodness of fit was in the uppermost range ($R^2 = 0.9995$ and $R^2 = 0.9998$). Based on these curves, the maximum attainable number of distinct source proteins was estimated (highlighted as solid lines). With the available number of 38 primary and 24 recurrence samples, 96% or 92% of the estimated maximum attainable amount of unique HLA class I-presented proteins had been identified, respectively. Considering primary and recurrent tumors jointly as 62 glioblastomas, these achieve 98% coverage of the estimated maximum attainable number of distinct source proteins (Supplementary Figure 2).

A



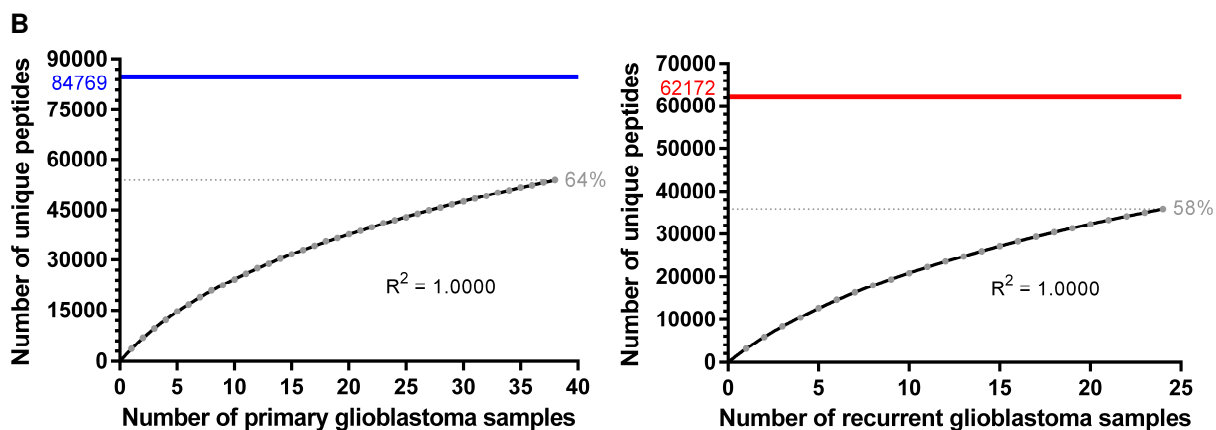


Figure 12. HLA class I peptidomics to define glioblastoma-associated peptides. (A) Comparative profiling of HLA class I ligands presented on glioblastoma versus an in-house benign database. Every peptide evaluated for tumor association is represented by a bar in the waterfall plot (associated with the x-axis), whereas the y-axis shows the frequency of positive HLA peptidomes, separately for primary glioblastoma ($n=38$), recurrent glioblastoma ($n=24$), and benign samples without testes ($n=418$ covering 29 different human tissues). Peptides were designated as glioblastoma-exclusive, when detected on a maximum of one non-CNS-related tissue, whereby $n=9,519$ were identified on primary and/or recurrent tumors of at least two patients (highlighted as enlarged view on the left). The number of distinct HLA class I ligands per group is illustrated by the Venn diagram on the right, whereby the overlaps cannot map the permission of one positive non-CNS-related sample within the benign dataset. **(B) Saturation analysis for the identification of HLA class I ligands in primary or recurrent glioblastoma tissue.** For each source count, the mean number of peptides was calculated by 1,000 random samplings. Using non-linear regression, exponential functions with a forced y-intercept of 0 (internal data created by Daniel Kowalewski at the Department of Immunology, University of Tübingen indicate that subjecting cell-free lysis buffer to HLA-IP does not result in peptide identifications) were fitted. For both models, the goodness of fit was in the uppermost range ($R^2 = 1.0000$). Based on these curves, the maximum attainable number of distinct peptides was estimated (highlighted as solid lines). With the available number of 38 primary and 24 recurrence samples, 64% and 58% of the estimated maximum attainable amount of unique HLA class I ligands had been identified, respectively. Considering primary and recurrent tumors jointly as 62 glioblastomas, these achieve 74% coverage of the estimated maximum attainable number of distinct peptides (Supplementary Figure 2).

On the peptide level, 53,992 and 35,823 distinct HLA class I ligands were eluted from primary ($n=38$) and recurrent glioblastoma ($n=24$), obtaining 64% and 58% of the estimated maximum attainable coverage, respectively (Figure 12 B). Comparative profiling identified 9,519 glioblastoma-exclusive peptides presented on primary and/or recurrent tumors of at least two different patients (Figure 12 A). Subsequent to manual curation, a set of 155 peptides derived from 158 antigens and presented on 16-55% of primary as well as on 17-46% of recurrent tumors was defined. Among these, HLA ligands derived from GFAP, CERS1, CARNS1, CHI3L2, and PTPRZ were the most frequent ones. Peptide sequences and their HLA restriction, a listing of positive samples, and the corresponding source protein are given in Supplementary Table 3.

Combining the list of peptides derived from HLA class I-presented glioblastoma-associated antigens (Supplementary Table 2) with that of HLA class I ligands designated as glioblastoma-associated (Supplementary Table 3) gave $n=357$ candidate target peptides for cancer immunotherapy. These cover 99.93% of the world population (Supplementary Figure 3), whereby an average of 84 peptides are expected to match per patient. The population coverage on a per-country basis is shown in Figure 13.

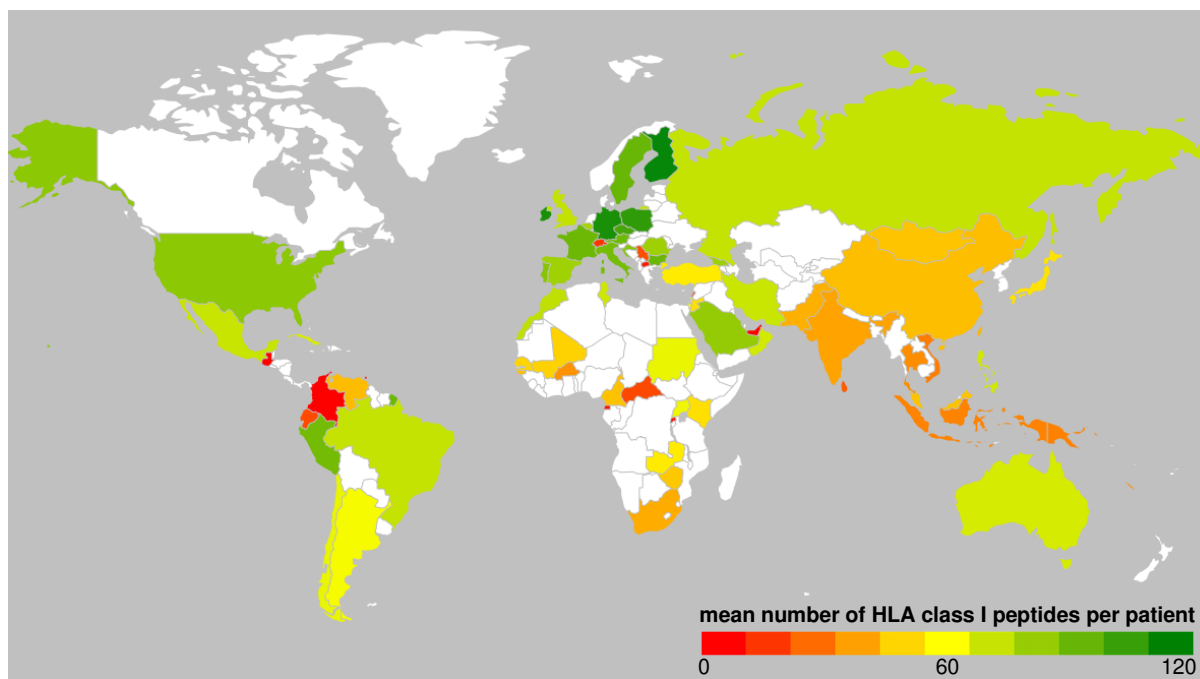


Figure 13. Population coverage of glioblastoma-associated HLA class I peptides. Using the population coverage tool provided by the IEDB Analysis Resource⁵⁰, the population coverage of the n=357 candidate target peptides for glioblastoma immunotherapy was calculated on a per-country basis. On average, 84 HLA class I peptides match per patient worldwide. For visualization of the United Kingdom, the individual values of England, Northern Ireland, Scotland, and Wales were multiplied with the relative area portion. Countries not included in the IEDB tool or not covered by the geographic heat map add-on of Microsoft Excel are colorless.

Glioblastoma-associated HLA class II antigens

HLA class II peptidome analyses of primary (n=38) and recurrent tumors (n=24) allowed the identification of 7,792 and 7,225 distinct source proteins giving rise to HLA class II-restricted peptides on glioblastoma tissue, respectively. These represent between 72% (recurrent glioblastoma) and 79% (primary glioblastoma) of the estimated maximum attainable amount of distinct source proteins (Figure 14 C). Despite the vast overlap of glioblastomas with benign samples, 413 antigens were exclusively presented on primary and/or recurrent tumors of at least two different patients (Figure 14 A). Following manual curation of the underlying peptides for peptide length and the presence of length variants as well as multi-mapping to several source proteins, a set of 26 glioblastoma-associated antigens and corresponding peptides naturally presented on 5-32% of primary as well as on 4-46% of recurrent tumors was created. Among these, GPC5, COLGALT2, NOP16, ESCO1, and BBOX1 were the most frequent ones. Despite being shared by primary and recurrent glioblastomas, several antigens were rather associated with primary tumors (e.g. NOP16), while others were preferentially presented at disease recurrence (e.g. CDC26; Figure 14 B). Peptide sequences, a listing of positive patients, and the GTE_x profile of the corresponding source protein can be retrieved from Supplementary Table 2. Of note, one of these glioblastoma-associated HLA class II antigens (RAD51) exhibited a CTA-like expression profile and was not listed in the CTDatabase⁴⁹.

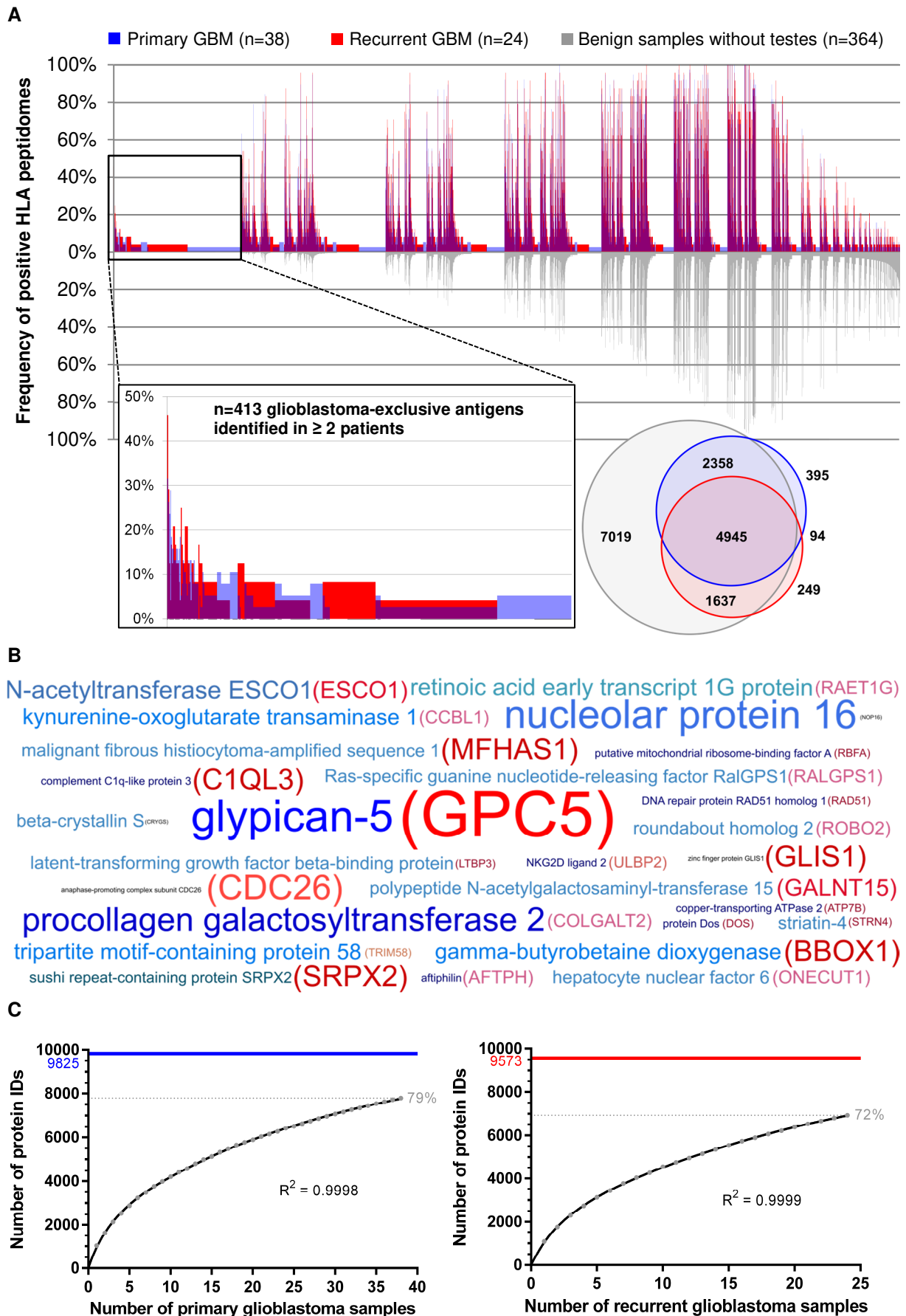


Figure 14. Definition of glioblastoma-associated antigens based on class II immunopeptidome analyses. (A) Comparative profiling of the HLA class II peptidome of glioblastoma versus an in-

house benign database. Each bar in this waterfall plot (associated with the x-axis) represents a single source protein, whereas the frequency of positive HLA peptidomes is shown on the y-axis, separately for primary glioblastoma (n=38), recurrent glioblastoma (n=24), and benign samples without testes (n=364 covering 30 different human tissues). Those source proteins detected on a maximum of one non-CNS-related tissue were designated as glioblastoma-exclusive, whereby n=413 were identified on primary and/or recurrent tumors of at least two patients (highlighted as enlarged view on the left). The Venn diagram on the right illustrates the number of distinct HLA class II-presented antigens per group, however, the overlaps cannot map the permission of one positive non-CNS-related sample within the benign dataset. **(B) Word cloud of glioblastoma-associated antigens.** Based on comparative profiling and subsequent quality control of underlying peptides (peptide length and/or presence of length variants as well as multi-mapping to several source proteins), a set of 26 glioblastoma-associated antigens naturally presented on 5-32% of primary as well as on 4-46% of recurrent tumors was defined. The font size in the word cloud is proportional to the frequency of positive primary (blue) and recurrent (red) glioblastomas. **(C) Saturation analysis for the identification of antigens represented by HLA class II peptides on primary or recurrent glioblastoma tissue.** For each source count, the mean number of antigens was calculated by 1,000 random samplings. Using non-linear regression, exponential functions with a forced y-intercept of 0 (internal data created by Daniel Kowalewski at the Department of Immunology, University of Tübingen indicate that subjecting cell-free lysis buffer to HLA-IP does not result in peptide identifications) were fitted. For both models, the goodness of fit was in the uppermost range ($R^2 = 0.9998$ and $R^2 = 0.9999$). Based on these curves, the maximum attainable number of distinct source proteins was estimated (highlighted as solid lines). With the available number of 38 primary and 24 recurrence samples, 79% or 72% of the estimated maximum attainable amount of distinct HLA class II-presented proteins had been identified, respectively. Considering primary and recurrent tumors jointly as 62 glioblastomas, these achieve 83% coverage of the estimated maximum attainable number of distinct source proteins (Supplementary Figure 2).

On the peptide level, 48,149 and 40,375 distinct HLA class II-presented peptides were eluted from primary (n=38) and recurrent glioblastoma (n=24), obtaining 59% (primary) and 47% (recurrence) of the estimated maximum attainable coverage (Figure 15 B). Subsequent to comparative profiling, all antigens represented by at least one glioblastoma-exclusive HLA class II-presented peptide were subjected to hotspot analysis (Figure 15 A). Glioblastoma-associated HLA class II presentation hotspots were defined to have a minimum length of eight AA and to be covered by peptides identified in at least six primary as well as four recurrent tumors of a minimum of eight different patients, while not having matching sequences in benign samples. This identified a set of 21 antigens harboring regions uniquely presented on malignant tissue with peptide-specific frequencies reaching up to 39% and 29% of positive HLA peptidomes for primary and recurrent glioblastomas, respectively. Peptide sequences, a listing of positive patients, and the corresponding source protein are given in Supplementary Table 4.

Comparing glioblastoma-associated HLA class I- (n=62) and II-presented antigens (n=26) as well as glioblastoma-associated HLA class I- (n=158 source proteins) and II-restricted peptides (n=21 source proteins) delineated seven antigens (DOS, COLGALT2, PTPRZ1, NRCAM, LRP1, TNC, and CHI3L1) represented on both HLA class I and II molecules. Remaining glioblastoma-associated candidate target antigens and peptides were uniquely identified *via* either HLA class I or II peptidome analysis.

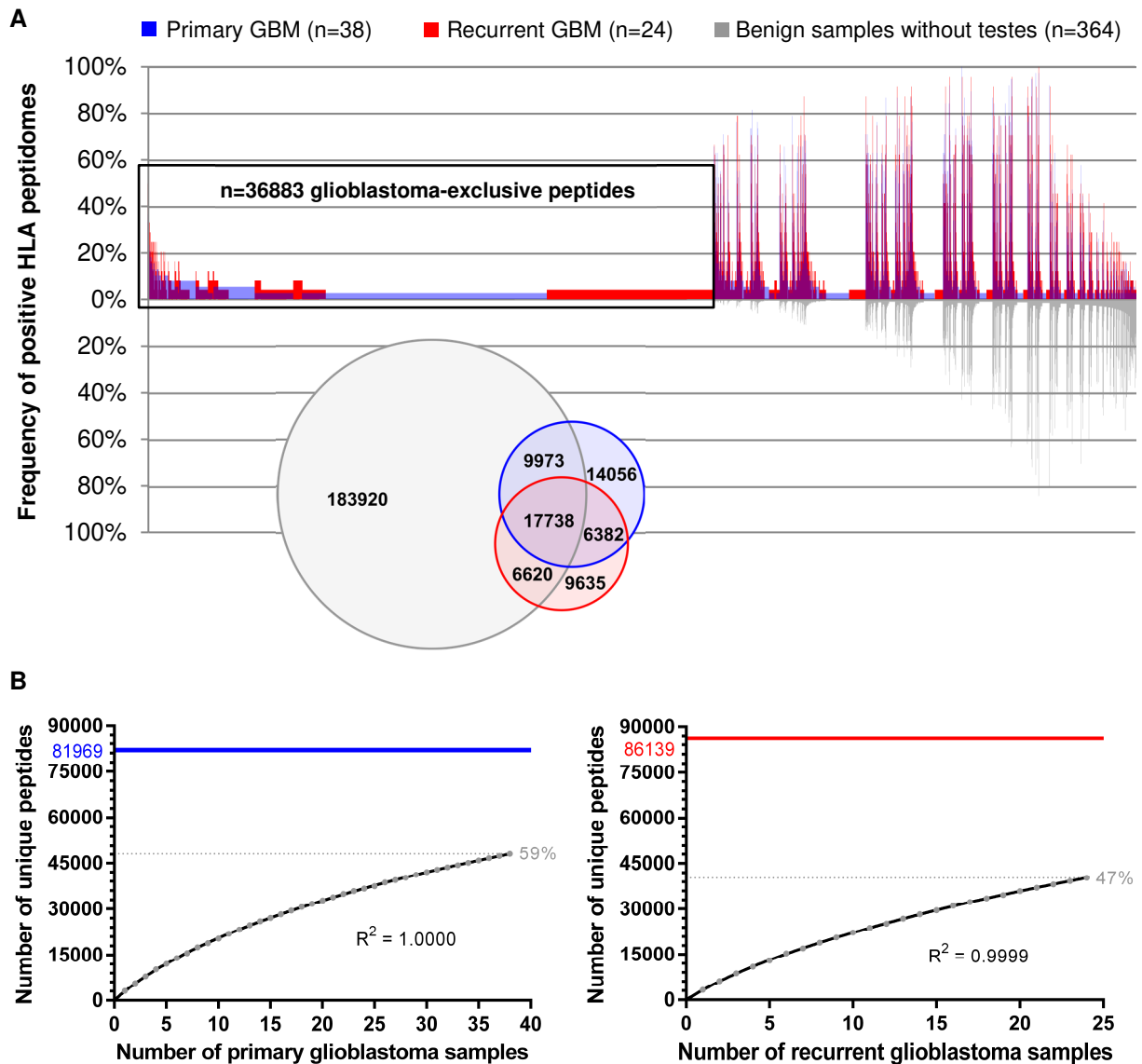
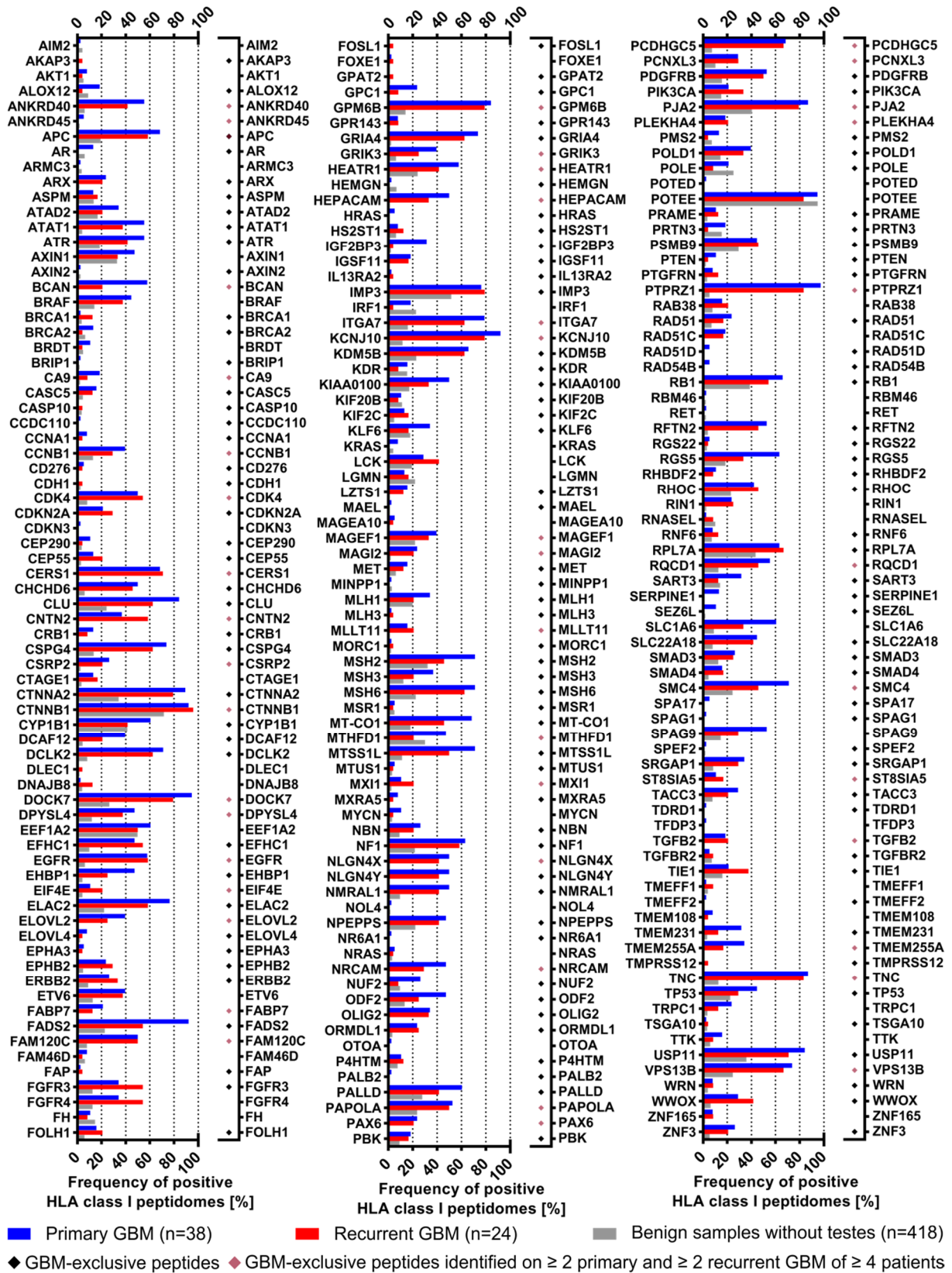


Figure 15. HLA class II peptidomics to define glioblastoma-associated peptides (A) Comparative profiling of HLA class II peptides presented on glioblastoma versus an in-house benign database. Every peptide evaluated for tumor association is represented by a bar in the waterfall plot (associated with the x-axis), whereas the y-axis shows the frequency of positive HLA peptidomes, separately for primary glioblastoma (n=38), recurrent glioblastoma (n=24), and benign samples without testes (n=364 covering 30 different human tissues). Being detected on a maximum of one non-CNS-related tissue, n=36,883 peptides were designated as glioblastoma-exclusive. Corresponding source proteins were subjected to hotspot analysis. The number of distinct HLA class II-restricted peptides per group is illustrated by the Venn diagram on the left, whereby the overlaps cannot map the permission of one positive non-CNS-related sample within the benign dataset. **(B) Saturation analysis for the identification of HLA class II-presented peptides in primary or recurrent glioblastoma tissue.** For each source count, the mean number of peptides was calculated by 1,000 random samplings. Using non-linear regression, exponential functions with a forced y-intercept of 0 (internal data created by Daniel Kowalewski at the Department of Immunology, University of Tübingen indicate that subjecting cell-free lysis buffer to HLA-IP does not result in peptide identifications) were fitted. For both models, the goodness of fit was in the uppermost range ($R^2 = 1.0000$ and $R^2 = 0.9999$). Based on these curves, the maximum attainable number of distinct peptides was estimated (highlighted as solid lines). With the available number of 38 primary and 24 recurrence samples, 59% or 47% of the estimated maximum attainable amount of unique HLA class II-presented peptides had been identified, respectively. Considering primary and recurrent tumors jointly as 62 glioblastomas, these achieve 63% coverage of the estimated maximum attainable number of distinct peptides (Supplementary Figure 2).

HLA ligands derived from established CTAs and TAAs

A



B

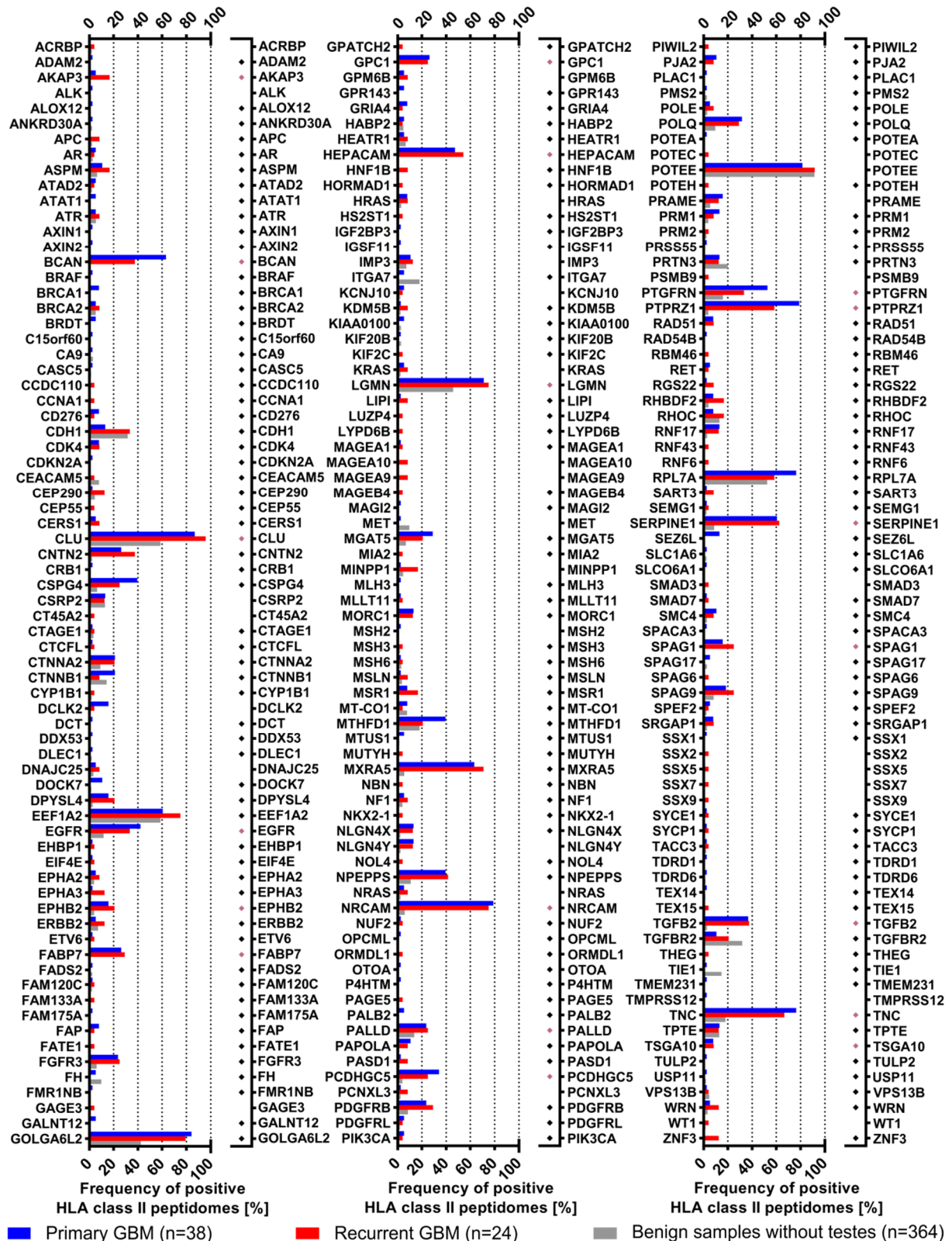


Figure 16. Identification of established TAAs, CTAs, and glioblastoma-associated antigens across the present HLA peptidome dataset. While peptides mapping to multiple source proteins were considered to calculate the frequency of positive HLA peptidomes, these were excluded to report the representation by glioblastoma-exclusive peptides. CTAs and TAAs exclusively identified on benign samples were not listed. (A) CTAs and TAAs naturally presented on HLA class I molecules of

human primary and/or recurrent glioblastoma tissue. The present immunopeptidomic dataset included HLA class I ligands derived from 217 TAAs and CTAs, with 44 sharing tumor-exclusive peptides in a minimum of two primary and two recurrent glioblastomas of at least four different patients (highlighted with red diamonds). The frequency of positive HLA peptidomes was assessed based on HLA class I ligands for tumor samples, whereby benign hits were reported independent of HLA binding probabilities of the underlying peptide identifications. **(B) TAAs and CTAs represented in the HLA class II peptidomes of primary and/or recurrent glioblastoma tissue.** Among 216 naturally presented CTAs and TAAs, 19 were represented by glioblastoma-exclusive peptides on at least two primary as well as two recurrent tumors of a minimum of four different patients (highlighted with red diamonds).

Considering a total number of 366 established CTAs and TAAs (3.2.1) as well as 83 antigens reported to be associated with glioblastoma (2.3.2; n=16 overlapped with the general list of CTAs and TAAs), the present HLA peptidome dataset acquired from primary and recurrent tumors was screened for previously published tumor antigens. Of these, n=217 and n=216 were represented by HLA class I ligands and HLA class II-presented peptides, respectively. Despite these high identification rates, presentation frequencies of CTAs and TAAs were in general low, especially of those exclusively identified on malignant tissues. Among 16 HLA class I-presented TAAs and CTAs fulfilling the aforementioned criteria to be designated as glioblastoma-exclusive antigen, OLIG2, TMEM255A, and PAX6 were the most frequent ones (24-34% positive primary as well as 17-33% positive recurrent tumors). 41 additional TAAs and CTAs were represented by tumor-exclusive HLA class I ligands on at least two primary as well as on two recurrent glioblastomas obtained from a minimum of four different patients (Figure 16 A, Supplementary Table 5). On HLA class II, 44 antigens were exclusively identified in the peptidome of glioblastomas, with FABP7, CDK4, RAD51, and CERS1 being the most frequent ones (5-26% positive primary as well as 5-29% positive recurrent tumors). 18 further CTAs and TAAs were represented by glioblastoma-exclusive HLA class II-restricted peptides eluted from at least two primary as well as two recurrent neoplastic specimens originating from a minimum of four different patients (Figure 16 B, Supplementary Table 5).

4.3 The HLA peptidome of primary *versus* recurrent glioblastoma

Primary- and recurrence-exclusive antigens

Using the same HLA class I and II peptidome datasets as in 4.2 while applying a different evaluation enabled the identification of fundamental differences of the antigenic landscape of glioblastoma presented at primary or recurrent disease, respectively. A total of 2,146 HLA class I- and 2,753 HLA class II-presented antigens were identified in primary tumors only, whereas these numbers came up to 610 and 1,886 recurrence-exclusive antigens, respectively (Figure 17 A and B). It was striking that the number of primary- and recurrence-exclusive antigens was inverse for HLA class I and II: at a frequency threshold of 17%, a total of three (HLA class I) and 15 (HLA class II) recurrence-exclusive antigens were identified while 20 (HLA class I) and five (HLA class II) antigens were exclusively presented on $\geq 18\%$ of primary glioblastomas. This distorted ratio was maintained at lower thresholds (e.g. $\geq 13\%$ of positive HLA peptidomes: 19/52 recurrence-exclusive and 122/29 primary-exclusive HLA class I/II antigens). Subsequent to manual curation of the corresponding peptides including multi-mapping to multiple source proteins, HLA class I binding motifs as well as the length and the presence of length variants of HLA class II-restricted peptides, a set of 19/5 and 3/14 HLA

class I/II antigens associated with primary or recurrent disease in glioblastoma was defined. PDZD2, ROBO1, and PTPRG constituted the most frequent primary-associated antigens, whereas THY1 and HEATR3 were highly associated with recurrent glioblastoma (Supplementary Table 6).

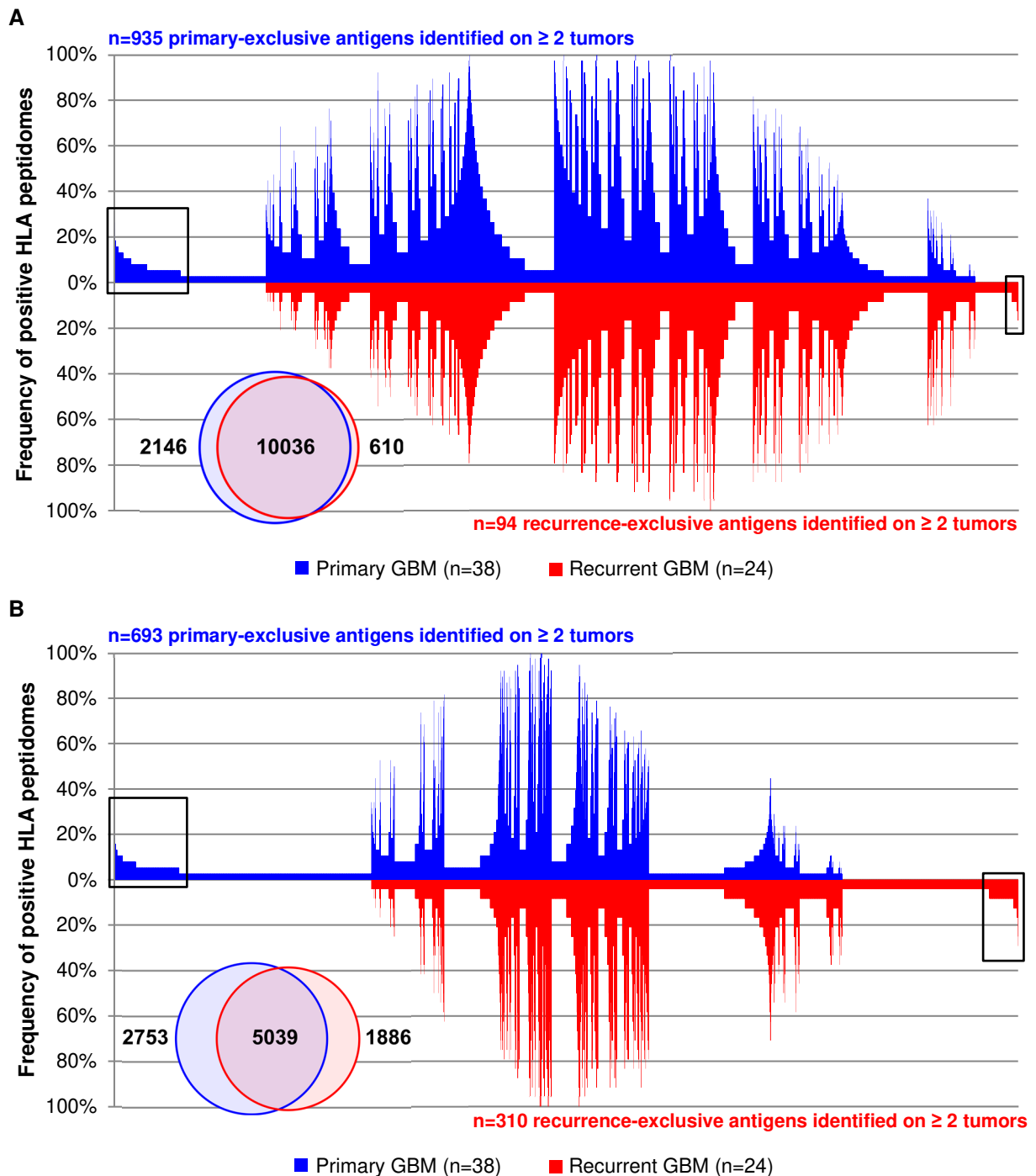
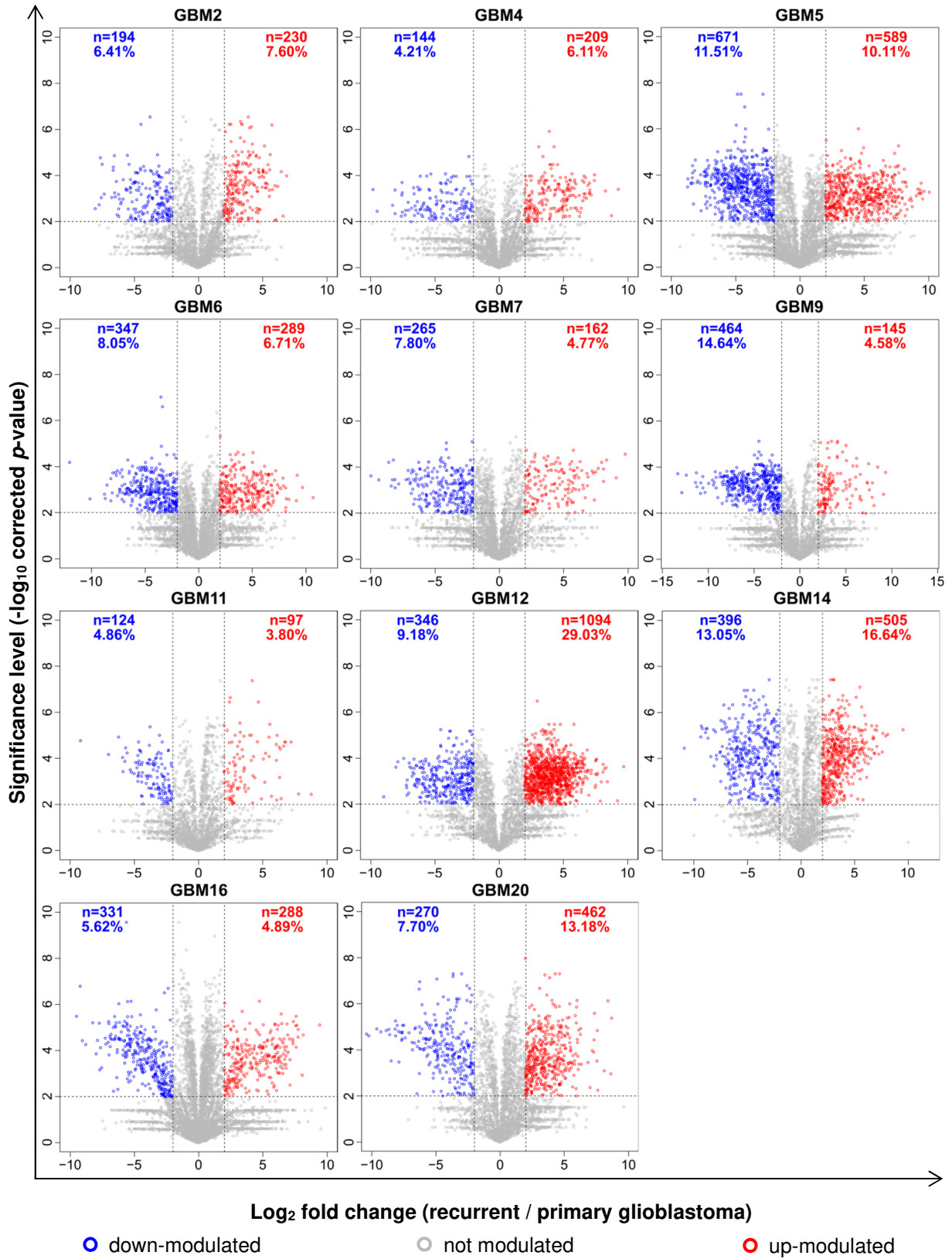


Figure 17. (A) HLA class I- and (B) HLA class II-presented antigens associated with primary or recurrent disease in glioblastoma. Each protein evaluated by comparative profiling is represented by a bar in the waterfall plots, whereas the frequency of positive HLA peptidomes is shown on the y-axis, separately for primary (n=38; blue) and recurrent glioblastoma (n=24; red). Primary- and recurrence-exclusive antigens detected on at least two tumors each are highlighted with boxes. The Venn diagrams in the left lower corner of the waterfall plots illustrate the number of unique antigens per group and the overlap between the two groups.

Relative HLA ligand abundances on primary versus recurrent glioblastoma

LFQ-MS to identify HLA class I ligands significantly up- and down-modulated at disease recurrence was possible for eleven glioblastoma patients and based on a mean number of $3,809 \pm 1,056$ peptides evaluated for relative abundance per patient. On average, $9.76 \pm 7.19\%$ and $8.46 \pm 3.21\%$ of the patients' HLA class I peptidomes were subject to significant up- and down-modulation, respectively (Figure 18 A). Comparative profiling to identify common patterns of modulated HLA presentation was performed on source protein level. In total, 260 and 259 antigens were exclusively represented by up- or down-modulated peptides, respectively. Following manual curation of the underlying peptides for HLA motifs as well as multi-mapping to several source proteins, a set of nine antigens represented by up-modulated peptides on recurrent *versus* primary glioblastoma in two out of eleven of patients was defined. Conversely, 21 proteins were under-represented in the HLA class I peptidome acquired from recurrent as compared with autologous primary disease (18-27% of patients). Among these, SEZ6 was the most frequent one (Figure 18 B, Supplementary Table 7).

A



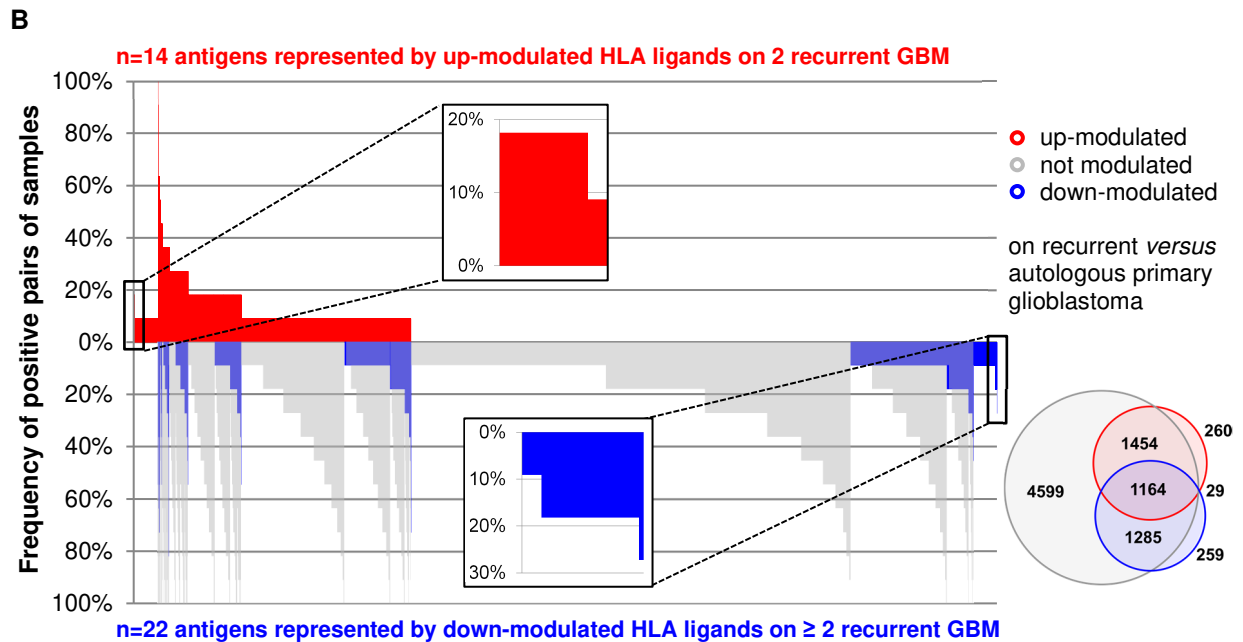
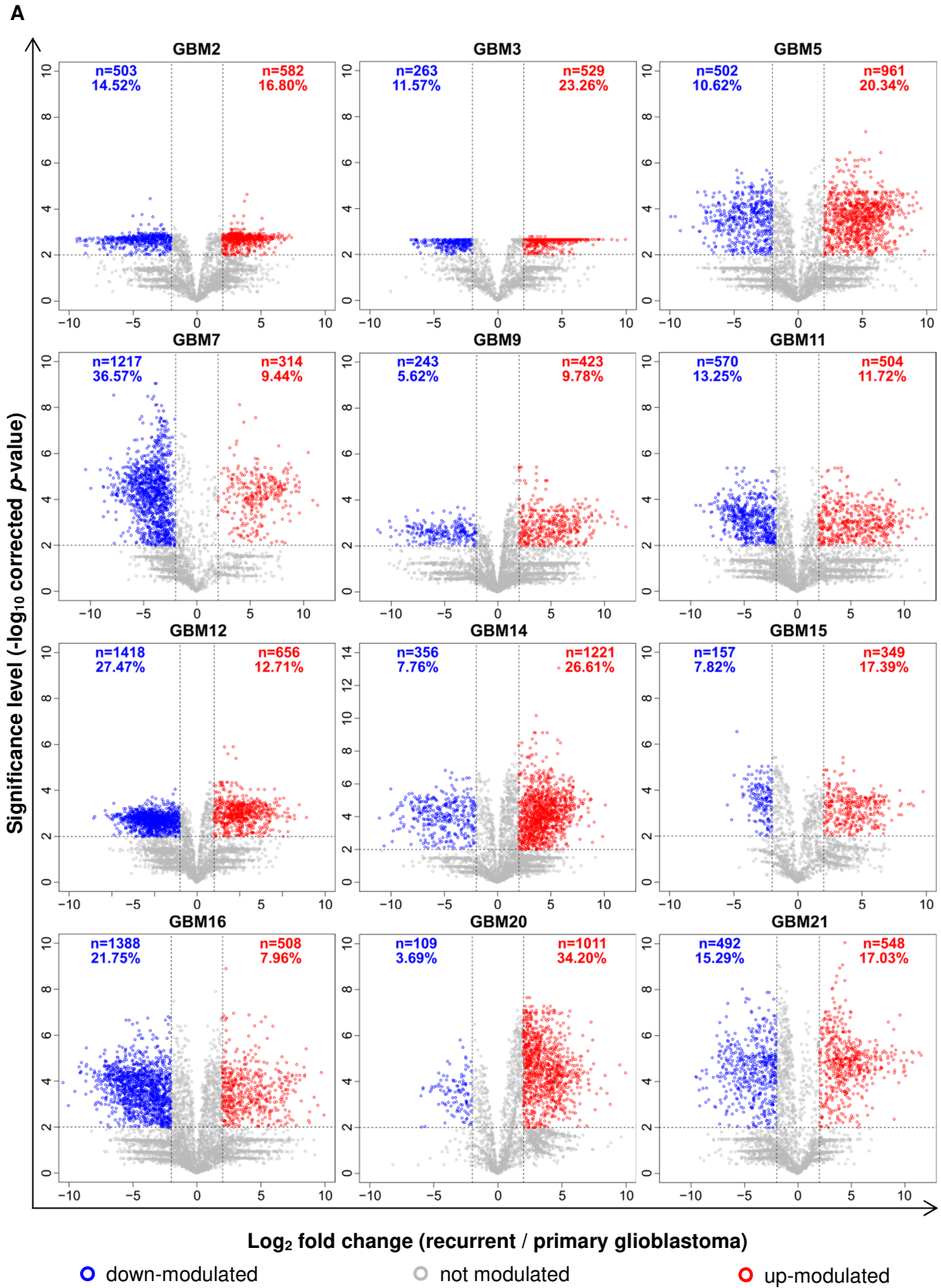


Figure 18. Patterns of modulated HLA class I presentation in glioblastoma across eleven patients. (A) Volcano plots of relative HLA ligand abundances on recurrent *versus* autologous primary glioblastoma. By LFQ-MS, relative abundances of HLA class I ligands, each of which is represented by a dot, were compared. The x-axis indicates changes of abundance as \log_2 fold change and corresponding significance levels (after BH correction for multiple testing) are associated with the y-axis. Significant modulation was defined by a corrected p -value ≤ 0.01 and a fold change of mean AUC in (recurrence / primary) ≥ 4 or ≤ 0.25 regarding up- (highlighted in red) or down-modulated (highlighted in blue) peptides, respectively. The total number of up- and down-modulated peptides as well as their proportion in the patient's HLA class I peptidome are indicated in quadrants of each Volcano plot. **(B) Comparative profiling of antigens corresponding to peptides displayed in Volcano plots.** Each bar in this waterfall plot (associated with the x-axis) represents a single protein, whereas the frequency of positive pairs of samples is shown on the y-axis. Comparing the source proteins of peptides underlying significant up- or down-modulation as well as of those not being modulated allowed the identification of exclusively and recurrently over- ($n=14$) or under-represented ($n=22$) antigens across eleven LFQ datasets acquired from primary and autologous recurrent glioblastoma.

In twelve glioblastoma patients, a mean number of $3,894 \pm 1,202$ HLA class II-presented peptides were evaluated for relative abundance on recurrent *versus* primary tumors by LFQ-MS. On average, $14.66 \pm 9.22\%$ and $17.27 \pm 7.50\%$ of the patients' HLA class II peptidomes were subject to significant up- or down-modulation, respectively (Figure 19 A). Comparative profiling to identify common patterns of modulated HLA presentation was performed on source protein level, since length variants with common core sequences cannot be adequately addressed across patients. In total, $n=194$ and $n=256$ antigens were exclusively represented by up- or down-modulated peptides, respectively. Subsequent to manual curation of multi-mapping peptides, 8 and 12 antigens were found to be over-represented in the HLA class II peptidome of recurrent or primary glioblastoma (Figure 19 B, Supplementary Table 7).



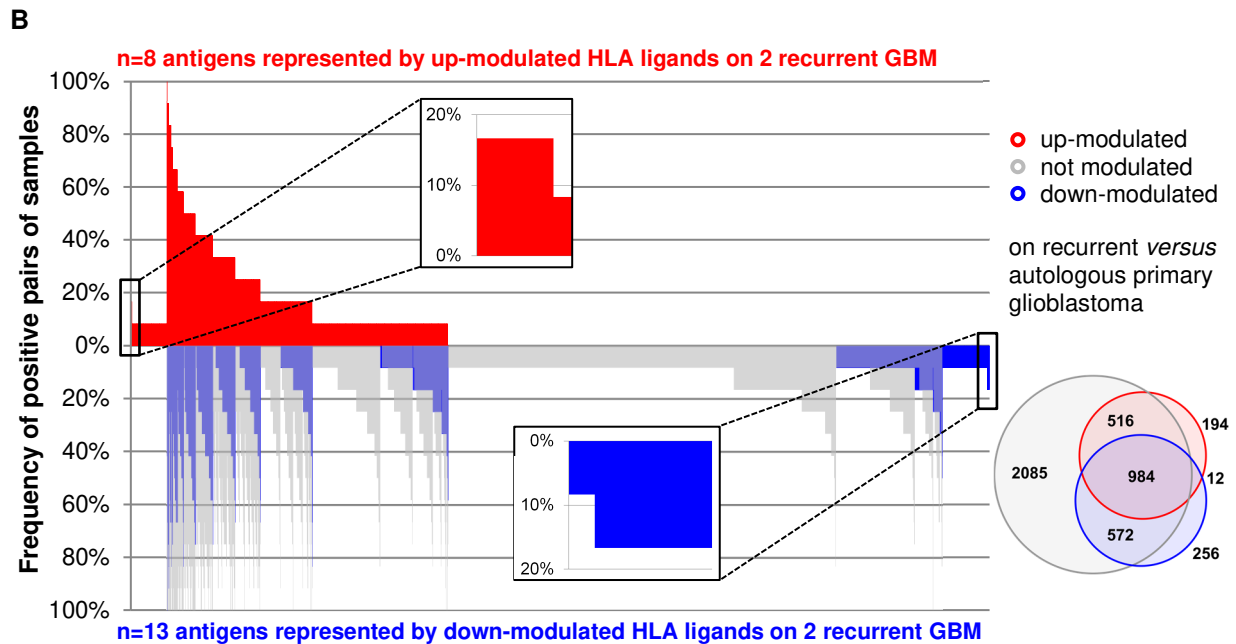
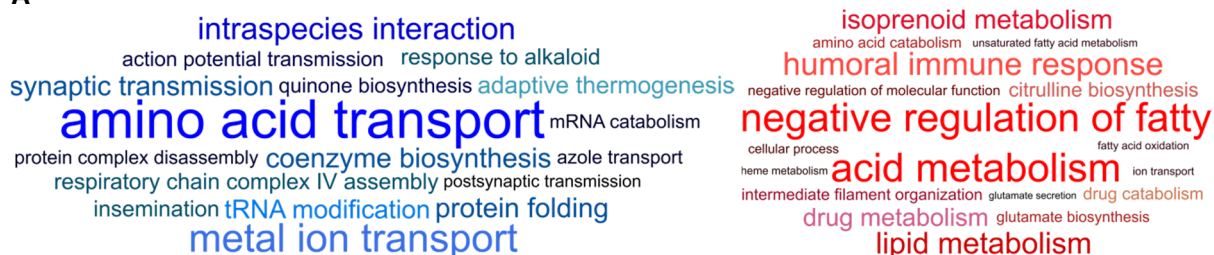


Figure 19. Patterns of modulated HLA class II presentation in glioblastoma across twelve patients. (A) Volcano plots of relative HLA class II-presented peptide abundances on recurrent *versus* autologous primary glioblastoma. By LFQ-MS, relative abundances of HLA class II-restricted peptides, each of which is represented by a dot, were compared. The x-axis indicates changes of abundance as \log_2 fold change and corresponding significance levels (after BH correction for multiple testing) are associated with the y-axis. Significant modulation was defined by a corrected p-value ≤ 0.01 and a fold change of mean AUC in (recurrence / primary) ≥ 4 or ≤ 0.25 regarding up- (highlighted in red) or down-modulated (highlighted in blue) peptides, respectively. The total number of up- and down-modulated peptides as well as their proportion in the patient's HLA class II peptidome are indicated in quadrants of each Volcano plot. **(B) Comparative profiling of antigens corresponding to peptides displayed in Volcano plots.** Each bar in this waterfall plot (associated with the x-axis) represents a single protein, whereas the frequency of positive pairs of samples is shown on the y-axis. Comparing the source proteins of peptides underlying significant up- or down-modulation as well as of those not being modulated allowed the identification of exclusively and recurrently over- (n=8) or under-represented (n=13) antigens across twelve LFQ datasets acquired from primary and autologous recurrent glioblastoma.

Functional annotation of antigens associated with primary and recurrent disease

All proteins exclusively identified on primary or recurrent tumors as well as antigens exclusively represented by down- or up-modulated peptides at disease recurrence were subjected to functional annotation clustering, separately for HLA class I and II. Top three clusters associated with primary disease comprised amino acid transport, metal ion transport, and intraspecies interaction for antigens presented on HLA class I as well as organelle organization, microtubule cytoskeleton organization, and histone H4 acetylation for antigens presented on HLA class II molecules. Conversely, source proteins associated with tumor recurrence were mainly involved in the negative regulation of fatty acid metabolism, humoral immune response, and lipid metabolism or in the positive regulation of hydrolase activity, gene expression, and mitotic cell cycle considering HLA class I- or II-presented antigens, respectively.

A



B

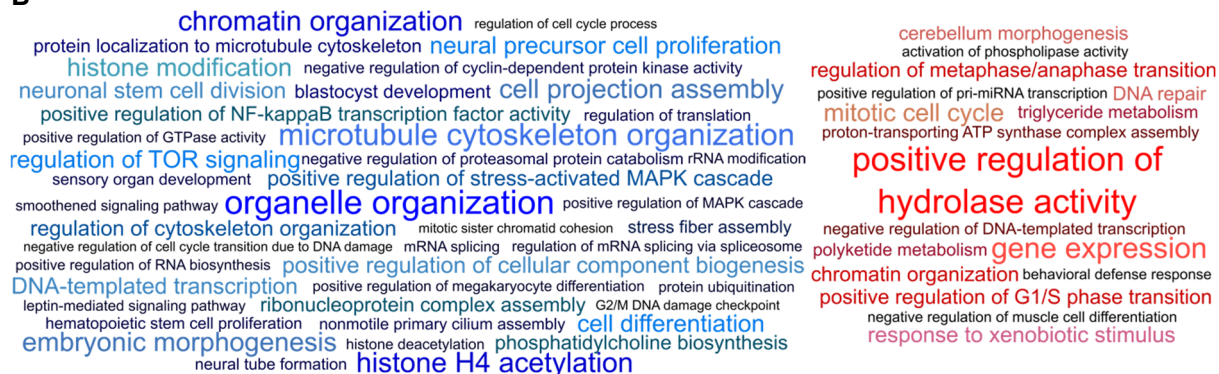


Figure 20. Functional annotation of (A) HLA class I- and (B) HLA class II-presented antigens associated with primary (blue) and recurrent disease (red). All proteins exclusively identified on primary or recurrent tumors as well as antigens exclusively represented by down- or up-modulated peptides at disease recurrence were subjected to functional annotation clustering. Enrichment scores are proportional to the font size in the word clouds.

4.4 Natural HLA presentation of neo-antigens

Mutational burden of primary glioblastomas

From a total of 13 primary glioblastomas, somatic variants comprising insertions, deletions, and single nucleotide alterations were determined. Primary glioblastomas carried a median of 409 [175-3,417] SNVs as well as 1 [0-8] indels. Intronic variants constituted the majority of SNVs, which is why the median number of non-synonymous mutations was drastically smaller than that of SNVs (52 [16-772]; Figure 21). All indels were located up- or downstream of genes, in intergenic regions or introns, as well as in splice regions of non-coding transcripts.

One patient, ZH613, with strongly elevated mutational load was found to carry a missense mutation affecting the MMR protein MLH1 (ENST00000231790 / ENSG00000076242 c.1643A>G; ENSP00000231790 p.548 Y>C). The COSMIC database included two entries of missense mutations affecting the identical AA position (glioblastoma: c.1643A>T / p.548 Y>F; endometrioid carcinoma c.1643A>G / p.548 Y>C).

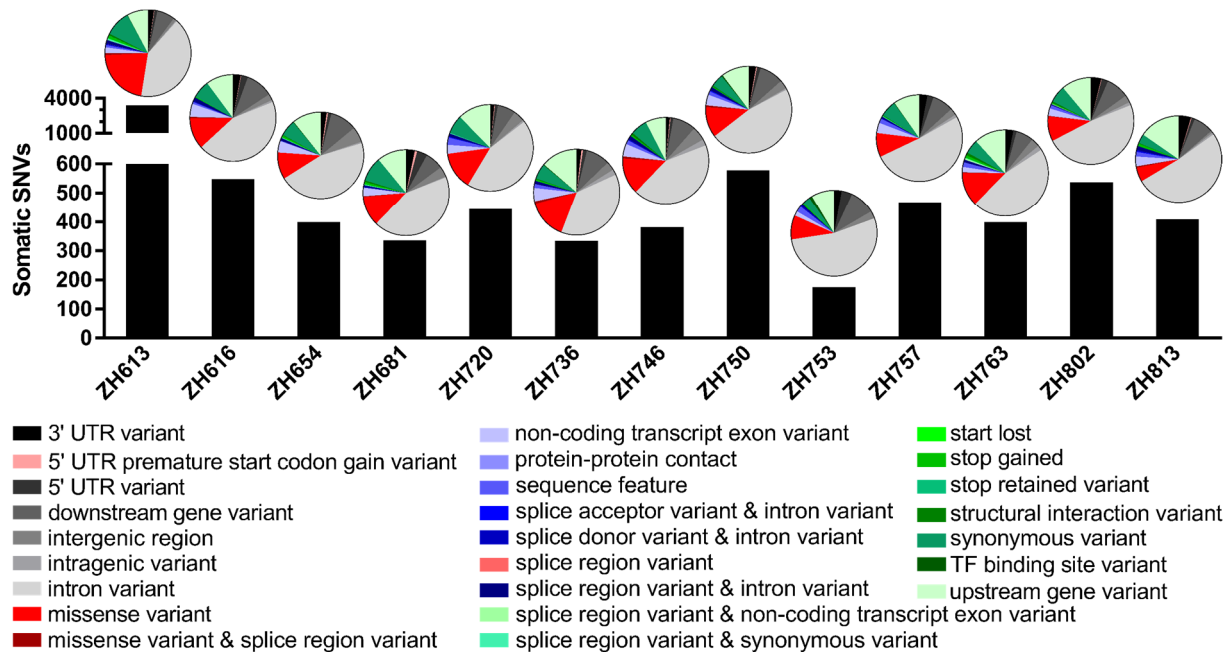


Figure 21. Composition of SNVs in primary glioblastomas. While the majority of SNVs affected non-coding regions such as introns, non-synonymous mutations (5' UTR premature start codon gain variants, splice region variants, missense variants, missense and splice region variants; marked in red) constituted on average only $13 \pm 4\%$ of SNVs. The SNV load of ZH613 (3,417 SNVs) was eightfold increased as compared with the average number of SNVs in ZH616-813 (417 SNVs).

Identification of mutated HLA ligands

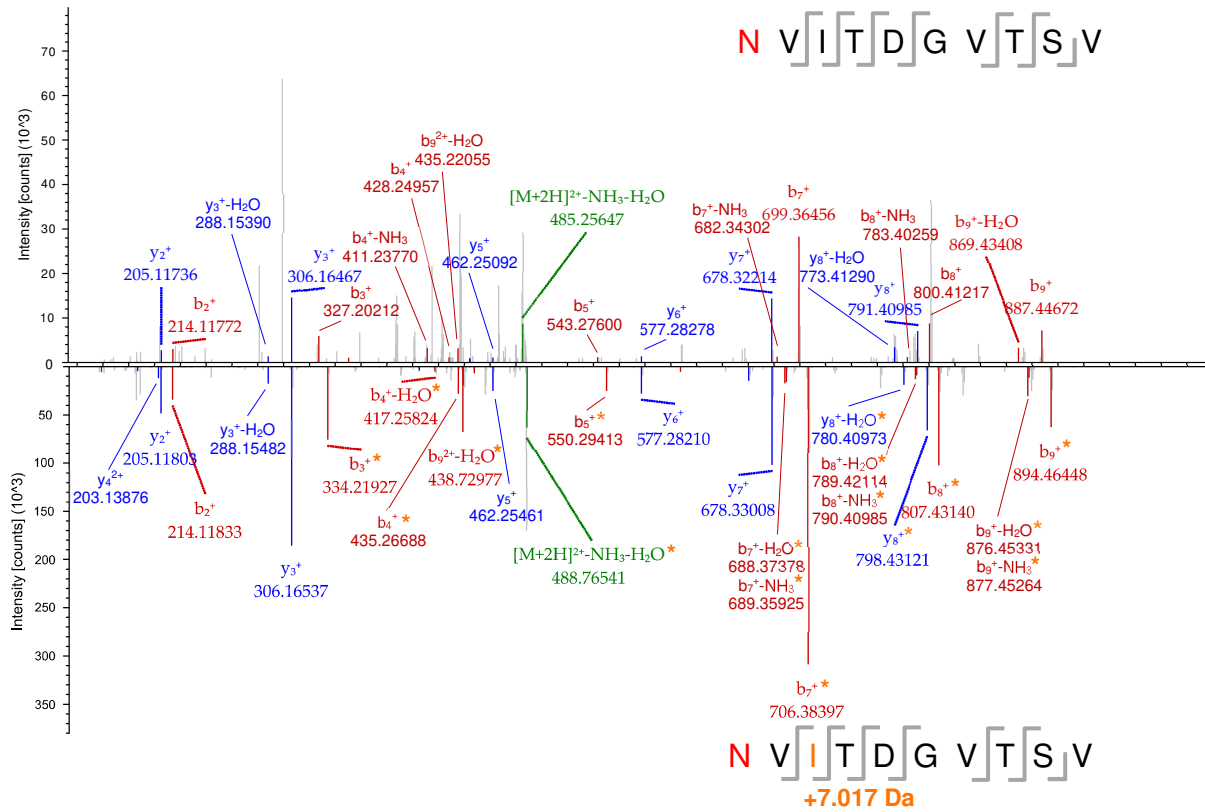
Unfiltered SNVs served as base to search immunopeptidomic data for neo-antigenic HLA ligands. For HLA class I, this search yielded one candidate each for patient ZH613 and ZH681 – two samples with pronounced high peptide yields (4,474 and 4,546 annotated ligands). The HLA-A*02:05 ligand NVITDGVTSV derived from the SZT2 subunit of KICSTOR complex (ENST00000562955 / ENSG00000198198 c.779T>A; ENSP00000457168 p.260I>N) had promising spectrum-specific scores (based on SEQUEST and MHCquant database search; 0.1 – 1.5% FDR) and middle-range spectral quality by means of manual assessment (Figure 22 A). Further, the mutation had a pronounced high VAF of 71.90% and the gene was expressed at 10.97 RPKM (5,568 raw counts). A total of five (four by both search engines) WT HLA class I ligands derived from other positions within the source protein SZT2 were detected within the immunopeptidome of this patient: SSNPALALR (HLA-A*31:01), RLFNEHLVSA (HLA-A*02:05), GQAGPEITDEL (annotated to HLA-A*02:05), FQPEIYVTI (HLA-A*02:05), and YQSLIKVLL (HLA-A*02:05). The HLA-B*57:01 ligand RAYTPPRISW arising from mutant PDGFR α (ENST00000257290 / ENSG00000134853 c.1027C>A; ENSP00000257290 p.343P>T) was identified at 2.5% FDR using the MHCquant pipeline, but at > 20% FDR by SEQUEST. Despite poor spectral quality according to SEQUEST scores and manual assessment (Figure 22 B), this peptide underwent validation by a synthetic heavy isotope-labeled peptide due to strong expression (35,434 raw counts equivalent to 98.65 RPKM) and a VAF of 15.27%. Moreover, eight HLA class I-presented non-mutated peptides derived from PDGFR α were identified within the same sample both by MHCquant and SEQUEST: KYSDIQRSL (HLA-C*07:02), TRSYVILSF (HLA-C*06:02; -C*07:02), SQLEAVNLHEV (annotated to HLA-A*02:01), KQADTTQYV (HLA-A*02:01), STFLPVKW (HLA-B*57:01),

GSTFLPVKW (HLA-B*57:01), TLIENLTEI (HLA-A*02:01), and RPASYKKKSML (HLA-B*07:02). Both candidates were included in filtered high confidence somatic variant lists and were validated by searching the dbSNP database and querying the sequences (with all possible exchanges of the isobaric AAs leucine and isoleucine) against the UniProt database. Synthesis of heavy isotope-labeled peptides spiked into a complex matrix of HLA class I peptides eluted from JY cells and subsequent LC-MS/MS finally proved the neo-antigenic sequence identity by comparison of experimental and synthetic peptide fragment spectra (Figure 22).

Interestingly, the position 343 of PDGFR α was found to be affected by recurrent mutations in glioblastoma. Two different patients were listed with p.343P>S mutations in the COSMIC database, whereby the mutation to serine generates – like the mutation to threonine of patient ZH681 – a phosphorylatable AA. Both mutations were found to alter the phosphorylation state of PDGFR α by generating one neo-phosphorylation motif each for tyrosine residues as well as eight (p.343P>T) or 13 (p.343P>S) neo-phosphorylation motifs for serine or threonine residues. As a consequence, both the mutated AAs themselves and the tyrosine residue at p.342 may become phosphorylated creating binding motifs for protein domains. One and two neo-phospho-serine/threonine binding motifs recognized by WW or 14-3-3 domains were identified for p.343P>T and p.343P>S, respectively. Remarkably, the two neo-phospho-tyrosine binding motifs identified in both protein variants represent binding sites for Src homology 2 (SH2) domains of the Crk adapter molecule and for the C-terminal SH2 domain of the Ras GTPase activating protein (RasGAP; Supplementary Table 9). RAYTPPRISW, the neo-antigenic HLA-B*57:01 ligand verified in ZH681, was not found to carry a tyrosine or threonine phosphorylation. The SZT2 p.260I>N variant was neither listed in the COSMIC database nor found to have a direct impact on SZT2 protein phosphorylation.

For HLA class II, a single candidate was identified in patient ZH750: SARGPSTPGVLSNCTSPLPG derived from autophagy-related protein 9 (ATG9B) ENST00000377974 / ENSG00000181652 c.2294A>G; UPI00015E055A p.756E>G. However, this peptide did not undergo further validation, since the fragment spectrum was annotated with better scores to another WT protein by SEQUEST (Supplementary Figure 5).

A



B

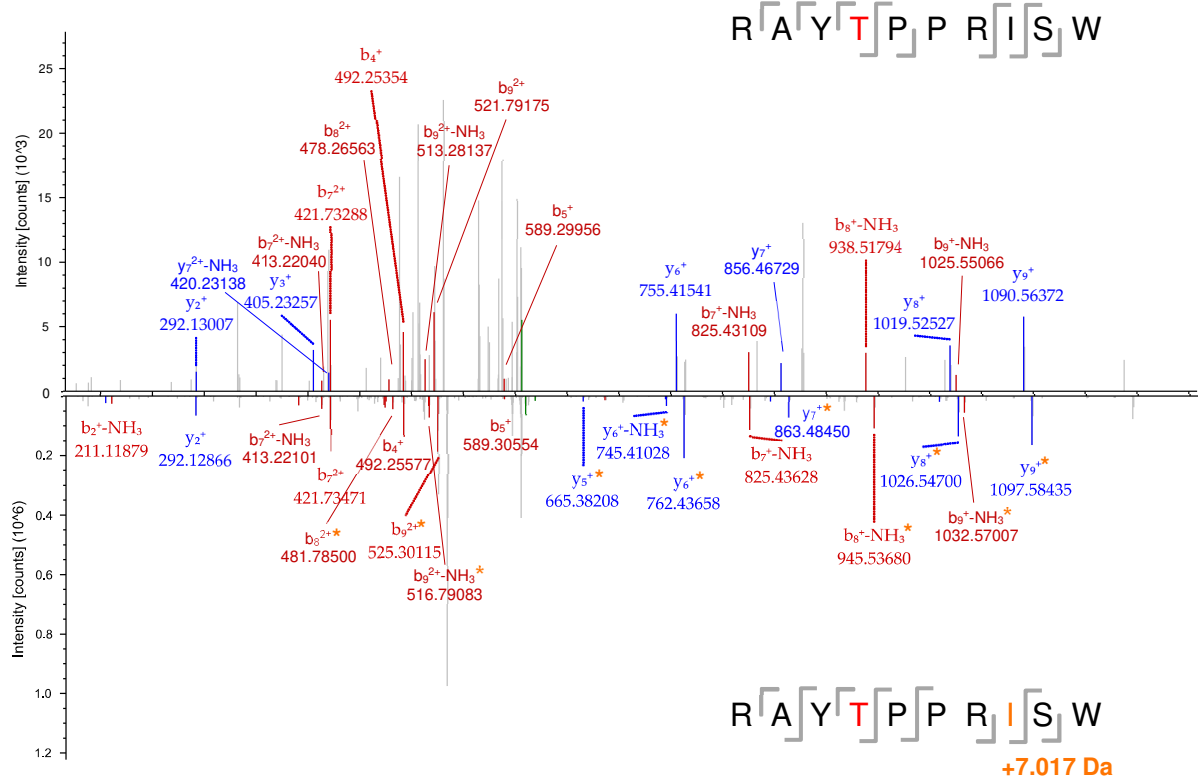


Figure 22. Fragment spectra of neo-antigenic HLA class I ligands identified in primary glioblastomas. The upper spectrum per panel was acquired from glioblastoma tissue, whereas the lower one represents the validation spectrum of a heavy isotope-labeled synthetic peptide. Mutated amino acids are marked in red within the sequence, b and y ions are indicated as red and blue peaks

in fragment spectra, and fragments harboring heavy isotope-labeled isoleucine (+7.017 Da) are marked with an orange asterisk. **(A) HLA-A*02:05-restricted peptide derived from SZT2 subunit of KICSTOR complex (ENST00000562955 / ENSG00000198198 c.779T>A; ENSP00000457168 p.260I>N) detected in ZH613.** NVITDGVTSV was identified at -1.2 ppm precursor mass deviation, 1.5% FDR (q value = 0.015; MHCquant: 0.1% FDR / q value = 0.001), and a cross-correlation of theoretical and measured spectrum of 1.44 (XCorr = 1.44). Despite several interfering signals, the entire sequence was covered by a sufficient number of both b and y ions. The second-best sequence annotated to this spectrum by SEQUEST scored 38.89% worse (dScore = 0.3889). The experimental fragment spectrum is mirrored by that of the synthetic peptide with most peaks being shared. **(B) HLA-B*57:01-restricted peptide arising from mutant PDGFR α (ENST00000257290 / ENSG00000134853 c.1027C>A; ENSP00000257290 p.343P>T) detected in patient ZH681.** RAYTPPRISW was identified at 2.41 ppm precursor mass deviation, 21.3% FDR (q value = 0.213; MHCquant: 2.5% FDR / q value = 0.025), and poor spectral correlation (XCorr = 0.96). Despite poor signal-to-noise ratio, more than ten b and y ions contributed to sequence annotation. The next-best sequence annotation by SEQUEST fitted only 8.33% worse (dScore 0.0833). The experimental fragment spectrum is mirrored by that of the synthetic peptide with most peaks being shared.

The number of unique HLA class I peptides, non-synonymous mutational loads, and the amount of validated neo-antigenic peptide identifications obtained from 13 primary glioblastomas were supplemented with comparable published HLA class I peptidome datasets. Taking all samples presented in Figure 23 into account, one neo-antigenic peptide identification resulted on average from 5.7×10^5 unique HLA class I peptides and 1.2×10^3 non-synonymous mutations, respectively. For the calculation of mutated peptides in relation to the number of non-synonymous mutations, 15 glioblastoma patients of the GAPVAC-101 trial¹² were considered additionally. From these, no neo-antigenic peptides could be verified with mutational loads being available while lacking peptide yields.

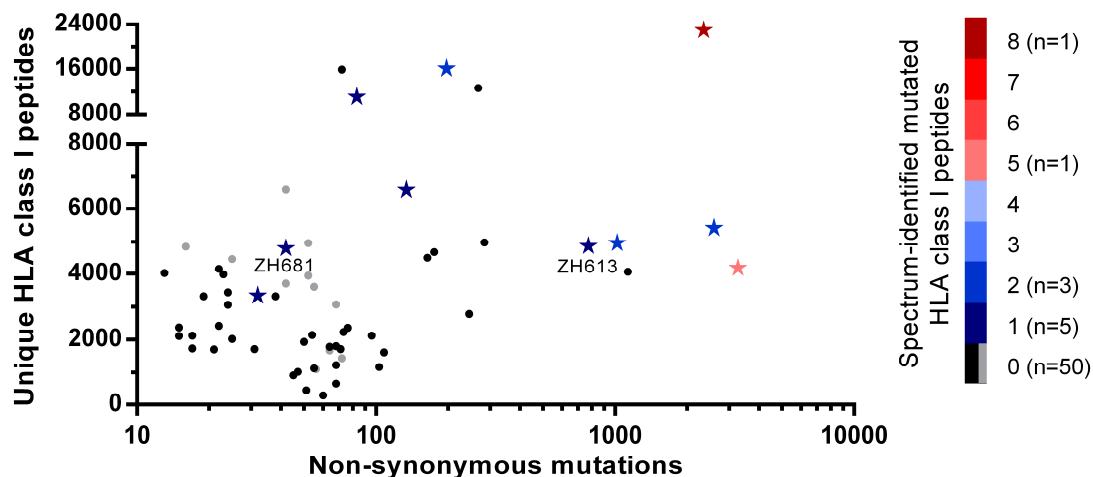


Figure 23. Identification of neo-antigenic peptides naturally presented on HLA class I by LC-MS/MS. The number of unique HLA class I peptides was plotted against the number of non-synonymous mutations on a per-sample basis (n=60). Data as shown in Freudenmann *et al.*⁵¹ was complemented by that of the 13 glioblastoma patients presented herein (marked in grey), by hepatocellular carcinomas (n=16) published by Löffler *et al.*¹⁶, as well as by colorectal cancer organoids (n=5) analyzed by Newey *et al.*⁵² Color-coded stars depict validated mutated peptide identifications, whereby those samples with more than one neo-antigenic peptide are clearly separated from those devoid of mutated HLA ligands.

5 Discussion

Glioblastoma is the most aggressive and most frequent malignant brain tumor accounting for an average annual incidence of almost 12,000 cases in the US. Despite extensive research, prognosis has remained poor with a 5-year relative survival rate of only 6.8%.¹ Cancer immunotherapy may meet the urgent demand for innovative treatments.²⁻⁶ Few studies addressing the naturally presented antigenic landscape of glioblastoma have already been published, however, none has focused on disease recurrence. Likewise, HLA class II-restricted targets have not been covered sufficiently.¹⁰⁻¹⁴ Herein, we present a large-scale multi-omics study with immunopeptidomics as core element examining the similarities and differences of primary and recurrent glioblastomas and defining candidate targets for immunotherapeutic intervention compatible with both disease conditions.

The present study population comprising 40 glioblastoma patients had a representative age distribution from 33 to 86 years with a median age of onset of 67 years and a slightly increased proportion of females (male : female ratio of 1.22).¹ The cohort included 55 distinct HLA class I allotypes covering 99.95% of the world population, whereby 92.17% of all individuals are expected to be positive for at least three allotypes. HLA class I and II ligands were isolated in considerable numbers from a total of 38 primary and 24 recurrent – almost exclusively IDH1^{WT} – tumors. This large immunopeptidomic dataset strongly refutes significant down-regulation or even loss of HLA expression to be a common phenomenon in glioblastoma, which is in line with findings in many other cancer entities.^{10,51,53-55} Nevertheless, there were two recurrent tumor specimens (GBM15R, GBM21R) with low HLA class I ligand identifications while yielding remarkable numbers of HLA class II-restricted peptides. In these selected cases, reduced HLA expression appears plausible, since technical artefacts affecting lysate preparation, peptide purification, or mass spectrometry can be ruled out. We observed marginally increased yields of HLA class I as compared with HLA class II peptides eluted from primary glioblastomas and of HLA class II-restricted peptides identified on recurrent *versus* primary tumors. The fact that the two compared groups had overlapping error bars each, however, weakens the confidence of the underlying statistical calculation. High numbers of HLA class II peptide identifications can originate from tumor cells themselves, but also from infiltrating macrophages and microglia.^{10,56-58} The latter have been postulated to constitute 30-50% of bulk tumor mass in glioma^{56,58-60} and to be tumor-supportive by creating an immunosuppressive microenvironment, releasing cytokines and growth factors thus promoting glioma cell migration, proliferation, and survival.^{56,57,61-63}

On the basis of the present dataset comprising 38 primary and 24 recurrent tumors with 22 representing autologous pairs gathered from the same patient, we have learned that the HLA peptidome of glioblastoma undoubtedly underlies significant dynamics during the progression from primary to recurrent disease. At recurrence, 20-30% of the patients' HLA class I and II peptidomes were subject to modulated HLA presentation as compared with autologous primary disease. Moreover, almost 5,000 and 2,500 antigens including tumor-exclusive ones were only presented on primary or recurrent neoplasms, respectively. Thus, we draw the conclusion that radiochemotherapy and clonal evolution during disease progression^{8,9} drastically alter the antigenic landscape, which has to be considered when defining targets for glioblastoma immunotherapy. Consequently, we focused on those antigens and peptides

exhibiting robust and frequent presentation independent of disease state. This not only renders them broadly applicable to a large number of patients, but also reduces the risk of lacking clinical efficacy when targeting antigens lost following initial surgical resection and radiochemotherapy.

We found glioblastoma to be a pronounced rich source of candidate targets for cancer immunotherapy. With the currently available number of 23 benign brain and cerebellum samples, we expect to achieve less than 100% saturation of HLA class I and II protein identifications. Transcriptome data acquired from a large set of benign human tissues were therefore integrated as orthogonal level into target selection to exclude antigens with a highly CNS-associated expression profile. This way, we aim at minimizing on-target off-tumor toxicities, which is of utmost importance as antigen-specific T cells directed against glioblastoma cross the blood-brain barrier.⁶⁴⁻⁶⁷ Nevertheless, all candidate targets reported herein require a strict immunological validation process to warrant a good safety profile. Despite selecting tumor-exclusive antigens with a non-CNS-specific expression profile, it is conceivable that antigens such as GFAP – a prominent astrocytic marker⁶⁸ – may not be unrestrictedly specific for malignant cells. The search for glioblastoma-associated antigens frequently and robustly presented on both primary and recurrent neoplasms uncovered 62 and 26 for HLA class I and II, respectively. Among these, TANC2, FA2H, BEST1, GPC5, COLGALT2, NOP16, ESCO1, and BBOX1 were the most frequent ones. TANC2 has been described as driver gene amplified and overexpressed in breast cancer. In such cells, TANC2 knockdown induces cell cycle arrest resulting in halving of cell viability.⁶⁹ The synthesis of sphingolipids including 2-hydroxy fatty acids, which are ubiquitous in the CNS as they are an essential component of myelin, is catalyzed by FA2H.^{70,71} Upregulation of FA2H and aberrant sphingolipid composition have been reported for several cancer entities including ovarian and lung carcinoma, neuroblastoma, and schwannoma.^{70,72-74} In the latter, a cell cycle inhibitory function has been attributed to FA2H, but the tumor-promoting function of this enzyme has so far not been clarified.^{70,72} The calcium-activated chloride channel BEST1 is expressed in epithelial and nervous cells.⁷⁵⁻⁷⁸ Besides fulfilling physiological functions, BEST1 is also involved in tumorigenesis by promoting EMT and cancer cell proliferation upon overexpression.⁷⁶⁻⁷⁹ Glioma cells hijack the calcium-chloride axis *via* BEST1 to induce regulatory volume decrease as survival mechanism and to promote infiltration.⁸⁰ Glypicans (GPC1-6) are cell surface-resident heparan sulfate proteoglycans with multifaceted roles in growth factor signaling and neoplastic cell proliferation.^{81,82} Members of the glypican family have already been identified as oncoproteins and suggested as targets for glioblastoma (GPC1), neuroblastoma (GPC2), and hepatocellular carcinoma (GPC3) immunotherapy.^{10,83,84} COLGALT2 accomplishes glycosylation of collagen⁸⁵ and is strongly expressed in glioma, but also in healthy brain tissue.⁸⁶ Extracellular matrix modification is a key process in the course of cancer progression facilitating tumor cell migration and proliferation as well as establishment of a tumor-protective niche.⁸⁷ Little is known about the nucleolar protein 16 (five PubMed entries⁸⁸), which exhibits estrogen- and c-Myc-responsive expression and is associated with poor prognosis in breast cancer.^{86,89} Glioblastoma cells may benefit from expressing the acetyltransferase ESCO1 at high levels, as it promotes DNA replication by establishing sister chromatid cohesion.⁹⁰⁻⁹² BBOX1 catalyzes L-carnitine synthesis, which is essential for fatty acid oxidation.^{93,94} Besides that, BBOX1 antisense RNA 1 binds and inhibits the tumor-

suppressive microRNA miR-3940-3p resulting in up-regulation of Survivin thus inhibiting apoptosis and enhancing proliferation.⁹⁵ Of note, this set of HLA class I- and II-presented antigens comprised three with CTA-like expression profiles (HSF2BP, E2F1, RAD51), which had so far not been listed in the CTDatabase⁴⁹. When targeting glioblastoma-associated proteins by peptide-specific immunotherapy, one would – if possible – preferentially select such peptides presented on both primary and recurrent tumors or in accordance with the patient's indication (e.g. APFDGSRLVF derived from FA2H was eluted from recurrent glioblastomas only).

Apart from defining targets being tumor-exclusive on the level of the entire protein, we have also focused on glioblastoma-associated peptides which are shared by specimens gathered at primary and recurrent disease and potentially arise from differential antigen processing in malignant cells. This unveiled a set of 155 HLA class I ligands derived from 158 antigens presented on 16-55% of primary as well as on 17-46% of recurrent tumors and of 21 antigens harboring glioblastoma-associated HLA class II presentation hotspots giving rise to peptides naturally presented on up to 15 primary and seven recurrent malignant samples. Taking together glioblastoma-associated antigens and peptides presented on HLA class I molecules (n=357 candidate target peptides), these achieve a world population coverage of 99.93% with an average number of 84 peptides matching per patient. Assuming that two third of these candidates will be excluded during the course of immunogenicity testing, which appears overestimated according to our previous experience with immunopeptidomics-based target definition approaches,⁹⁶ the number of peptides would still be enough to achieve sufficient coverage of the world population. Overlapping glioblastoma-associated HLA class I- and II-presented antigens as well as glioblastoma-associated HLA class I- and II-restricted peptides with each other, it become evident that each HLA class presents a unique repertoire of tumor antigens to T cells. This warrants HLA class I and II to be considered as equal partners in comprehensive target definition approaches. The present immunopeptidomic dataset comprising 62 primary human glioblastoma samples has, moreover, demonstrated once more that established TAAs and CTAs are not prime targets for cancer immunotherapy as being either broadly presented across both malignant and benign tissues or lacking frequent presentation on HLA molecules.⁹⁶ Hereby, we did not observe a fundamental difference between primary and recurrent glioblastomas.

Neo-epitopes arising from mutant proteins are designated as ideal tumor antigens offering maximum tumor specificity.^{51,97,98} However, proving these to be naturally presented on HLA in native human tumor tissue has remained a major obstacle questioning their clinical relevance when contributing in amounts below the detection limit of modern highly resolving LC-MS/MS systems to the tumor HLA peptidome.^{12,16,17,51} In a recent clinical trial, GAPVAC-101, tissues of 15 primary glioblastomas were evaluated for naturally presented neo-antigens – without any hit.¹² We performed whole exome sequencing from 13 primary glioblastomas unveiling a mutational burden comparable to that of the GAPVAC-101 patients with the exception of one patient, ZH613, with strongly elevated mutational load reasoned by a mutation of the MMR protein MLH1. Indeed, we here provide the first evidence of two neo-antigenic HLA class I ligands to be naturally presented on glioblastoma cells: NVITDGVTSV (HLA-A*02:05) derived from SZT2 subunit of KICSTOR complex (p.260I>N) in ZH613 and RAYTPPRISW (HLA-

B*57:01) derived from PDGFR α (p.343P>T) in ZH681. From both antigens, we also eluted five (SZT2) or eight (PDGFR α) different WT sequence peptides, which might be a general indicator for the presence of mutated peptides in malignancies ensuring presentability of the antigen of interest. Remarkably, the position 343 of PDGFR α was found to be recurrently mutated in glioblastoma creating both a neo-phosphorylation site and neo-phosphorylation motifs within this growth factor receptor. This allows the presumption that the p.343P>T and p.343P>S mutations take part in rendering the growth factor receptor constitutively active thus promoting tumor cell proliferation.^{47,48} PDGFR α is known to drive glioblastoma cell proliferation and small molecules for the treatment of PDGFR α -activated glioblastoma are currently being developed.^{8,99-101} Hence, we speculate that we might even have detected a mutated peptide suitable not only for fully individualized application but for a larger number of patients carrying the respective mutation. Immunological characterization of both neo-antigenic peptides including T-cell priming and/or IFN- γ enzyme-linked immunospot assay (ELISpot) employing PBMCs and TILs of the patients and – if possible – killing assays with autologous tumor cell lines is currently being performed by Dr. med. Julia Velz and Gioele Medici in the Laboratory for Molecular Neuro-Oncology at the University of Zürich. Despite proving natural HLA presentation of mutated peptides in brain tumors for the first time, we conclude that the translation of non-synonymous mutations into neo-antigenic HLA ligands remains inefficient. Considering 60 class I immunopeptidome datasets acquired from various cancer entities, one neo-antigenic peptide identification resulted on average from 5.7×10^5 unique HLA class I peptides and 1.2×10^3 non-synonymous mutations. Thus, we are convinced that, for the large majority of glioblastoma patients, detection of neo-epitopes remains impossible rendering non-mutated antigens the first choice for antigen-specific immunotherapies.

Once analysis of RNA and whole exome sequencing as well as DNA methylation data has been completed for all patients with both primary and recurrent tumors being available, we aim to evaluate expression levels of defined candidate target antigens, to screen the cohort for tumors exhibiting a hypermutation phenotype following radiochemotherapy, and to search for neo-antigenic HLA ligands in this extended dataset. A pilot dataset acquired from GBM3 on a meanwhile obsolete sequencing system indicated a vast increase in the proportion of missense mutations in the hypermutated recurrent as compared with the autologous primary tumor (GBM3P: n=21 / 6%; GBM3R: n=4,569 / 38%; data not shown). This might identify a small subset of patients in which the search for mutated peptides is more promising paving the way for stratified target discovery and treatment attempts in recurrent glioblastoma. Most importantly, these data will provide a deeper insight into clonal evolution and transcriptional changes during glioblastoma progression. We aim to map quantitative changes in primary *versus* recurrent glioblastoma with a special focus on immunobiological markers (e.g. CTLA4, PD1/PDL1, FOXP3, CD3, CD4, CD8, CD68, CD70, CD163)¹⁰² as well as the entire antigen processing machinery. Transcriptional, mutational, and DNA methylation phenotypes as well as the repertoire of presented antigens will be evaluated for correlation with each other and with clinical parameters (e.g. MGMT promotor methylation, progression-free or overall survival).

Herein, we investigated the immunopeptidomic landscape of glioblastoma in an unprecedented depth addressing for the first time both primary and recurrent tumors as well

as HLA class I- and II-presented targets. We defined a large, novel set of non-mutated tumor antigens robustly presented at primary and recurrent disease and provide the first evidence for two neo-antigens naturally presented on HLA molecules of brain tumor cells. This study paves the way for future antigen-specific immunotherapies including DC or peptide vaccination as well as T cell-based concepts which may contribute to meet the urgent need for therapeutic options to manage disease recurrence and to improve dismal survival rates.

6 References

1. Ostrom QT, Cioffi G, Gittleman H, Patil N, Waite K, Kruchko C, Barnholtz-Sloan JS. CBTRUS Statistical Report: Primary Brain and Other Central Nervous System Tumors Diagnosed in the United States in 2012-2016. *Neuro Oncol.* 2019;21(Supplement_5):v1-v100.
2. Stupp R, Brada M, van den Bent MJ, Tonn JC, Pentheroudakis G. High-grade glioma: ESMO Clinical Practice Guidelines for diagnosis, treatment and follow-up. *Ann Oncol.* 2014;25 Suppl 3:iii93-101.
3. Alifieris C, Trafalis DT. Glioblastoma multiforme: Pathogenesis and treatment. *Pharmacol Ther.* 2015;152:63-82.
4. Mohme M, Neidert MC, Regli L, Weller M, Martin R. Immunological challenges for peptide-based immunotherapy in glioblastoma. *Cancer Treat Rev.* 2014;40(2):248-258.
5. Weller M, van den Bent M, Hopkins K, Tonn JC, Stupp R, Falini A, Cohen-Jonathan-Moyal E, Frappaz D, Henriksson R, Balana C, Chinot O, Ram Z, Reifenberger G, Soffiatti R, Wick W. EANO guideline for the diagnosis and treatment of anaplastic gliomas and glioblastoma. *Lancet Oncol.* 2014;15(9):e395-403.
6. Erdem-Eraslan L, van den Bent MJ, Hoogstrate Y, Naz-Khan H, Stubbs A, van der Spek P, Bottcher R, Gao Y, de Wit M, Taal W, Oosterkamp HM, Walenkamp A, Beerepoot LV, Hanse MC, Buter J, Honkoop AH, van der Holt B, Vernhout RM, Sillevius Smitt PA, Kros JM, French PJ. Identification of Patients with Recurrent Glioblastoma Who May Benefit from Combined Bevacizumab and CCNU Therapy: A Report from the BELOB Trial. *Cancer Res.* 2016;76(3):525-534.
7. Gorlia T, Stupp R, Brandes AA, Rampling RR, Fumoleau P, Ditttrich C, Campone MM, Twelves CC, Raymond E, Hegi ME, Lacombe D, van den Bent MJ. New prognostic factors and calculators for outcome prediction in patients with recurrent glioblastoma: a pooled analysis of EORTC Brain Tumour Group phase I and II clinical trials. *Eur J Cancer.* 2012;48(8):1176-1184.
8. McLendon R, Friedman A, Bigner D, Van Meir EG, Brat DJ, Mastrogianakis GM, Olson JJ, Mikkelsen T, Lehman N, Aldape K, Yung WK, Bogler O, Weinstein JN, Vandenberg S, Berger M, Prados M, Muzny D, Morgan M, Scherer S, Sabo A, Nazareth L, Lewis L, Hall O, Zhu Y, Ren Y, Alvi O, Yao J, Hawes A, Jhangiani S, Fowler G, San Lucas A, Kovar C, Cree A, Dinh H, Santibanez J, Joshi V, Gonzalez-Garay ML, Miller CA, Milosavljevic A, Donehower L, Wheeler DA, Gibbs RA, Cibulskis K, Sougnez C, Fennell T, Mahan S, Wilkinson J, Ziaugra L, Onofrio R, Bloom T, Nicol R, Ardlie K, Baldwin J, Gabriel S, Lander ES, Ding L, Fulton RS, McLellan MD, Wallis J, Larson DE, Shi X, Abbott R, Fulton L, Chen K, Koboldt DC, Wendl MC, Meyer R, Tang Y, Lin L, Osborne JR, Dunford-Shore BH, Miner TL, Delehaunty K, Markovic C, Swift G, Courtney W, Pohl C, Abbott S, Hawkins A, Leong S, Haipok C, Schmidt H, Wiechert M, Vickery T, Scott S, Dooling DJ, Chinwalla A, Weinstock GM, Mardis ER, Wilson RK, Getz G, Winckler W, Verhaak RG, Lawrence MS, O'Kelly M, Robinson J, Alexe G, Beroukhi R, Carter S, Chiang D, Gould J, Gupta S, Korn J, Mermel C, Mesirov J, Monti S, Nguyen H, Parkin M, Reich M, Stransky N, Weir BA, Garraway L, Golub T, Meyerson M, Chin L, Protopopov A, Zhang J, Perna I, Aronson S, Sathiamoorthy N, Ren G, Yao J, Wiedemeyer WR, Kim H, Kong SW, Xiao Y, Kohane IS, Seidman J, Park PJ, Kucherlapati R, Laird PW, Cope L, Herman JG, Weisenberger DJ, Pan F, Van den Berg D, Van Neste L, Yi JM, Schuebel KE, Bayliss SB, Absher DM, Li JZ, Southwick A, Brady S, Aggarwal A, Chung T, Sherlock G, Brooks JD, Myers RM, Spellman PT, Purdom E, Jakkula LR, Lapuk AV, Marr H, Dorton S, Choi Y, Han J, Ray A, Wang V, Durinck S, Robinson M, Wang NJ, Vranizan K, Peng V, Van Name E, Fontenay GV, Ngai J, Conboy JG, Parvin B, Feiler HS, Speed TP, Gray JW, Brennan C, Socci ND, Olshen A, Taylor BS, Lash A, Schultz N, Reva B, Antipin Y, Stukalov A, Gross B, Cerami E, Wang WQ, Qin LX, Seshan VE, Villafania L, Cavatore M, Borsu L, Viale A, Gerald W, Sander C, Ladanyi M, Perou CM, Hayes DN, Topal MD, Hoadley KA, Qi Y, Balu S, Shi Y, Wu J, Penny R, Bittner M, Shelton T, Lenkiewicz E, Morris S, Beasley D, Sanders S, Kahn A, Sfeir R, Chen J, Nassau D, Feng L, Hickey E, Barker A, Gerhard DS, Vockley J, Compton C, Vaught J, Fielding P, Ferguson ML, Schaefer C, Zhang J, Madhavan S, Buetow KH, Collins F, Good P, Guyer M, Ozenberger B, Peterson J, Thomson E. Comprehensive genomic characterization defines human glioblastoma genes and core pathways. *Nature.* 2008;455(7216):1061-1068.
9. Hunter C, Smith R, Cahill DP, Stephens P, Stevens C, Teague J, Greenman C, Edkins S, Bignell G, Davies H, O'Meara S, Parker A, Avis T, Barthorpe S, Brackenbury L, Buck G, Butler A, Clements J, Cole J, Dicks E, Forbes S, Gorton M, Gray K, Halliday K, Harrison R, Hills K, Hinton J, Jenkinson A, Jones D, Kosmidou V, Laman R, Lugg R, Menzies A, Perry J, Petty R, Raine K, Richardson D, Shepherd R, Small A, Solomon H, Tofts C, Varian J, West S, Widaa S, Yates A, Easton DF, Riggins G, Roy JE, Levine KK, Mueller W, Batchelor TT, Louis DN, Stratton MR, Futreal PA, Wooster R. A hypermutation phenotype and somatic MSH6 mutations in recurrent human malignant gliomas after alkylator chemotherapy. *Cancer Res.* 2006;66(8):3987-3991.

Chapter 2: References

10. Neidert MC, Kowalewski DJ, Silginer M, Kapolou K, Backert L, Freudenmann LK, Peper JK, Marcu A, Wang SS, Walz JS, Wolpert F, Rammensee HG, Henschler R, Lamszus K, Westphal M, Roth P, Regli L, Stevanović S, Weller M, Eisele G. The natural HLA ligandome of glioblastoma stem-like cells: antigen discovery for T cell-based immunotherapy. *Acta Neuropathol.* 2018;135(6):923-938.
11. Neidert MC, Schoor O, Trautwein C, Trautwein N, Christ L, Melms A, Honegger J, Rammensee HG, Herold-Mende C, Dietrich PY, Stevanović S. Natural HLA class I ligands from glioblastoma: extending the options for immunotherapy. *J Neurooncol.* 2013;111(3):285-294.
12. Hilf N, Kuttruff-Coqui S, Frenzel K, Bukur V, Stevanović S, Gouttefangeas C, Platten M, Tabatabai G, Dutoit V, van der Burg SH, Thor Straten P, Martínez-Ricarte F, Ponsati B, Okada H, Lassen U, Admon A, Ottensmeier CH, Ulges A, Kreiter S, von Deimling A, Skardelly M, Migliorini D, Kroep JR, Idorn M, Rodon J, Piró J, Poulsen HS, Shraibman B, McCann K, Mendrzyk R, Löwer M, Stieglbauer M, Britten CM, Capper D, Welters MJP, Sahuquillo J, Kiesel K, Derhovanessian E, Rusch E, Bunse L, Song C, Heesch S, Wagner C, Kemmer-Brück A, Ludwig J, Castle JC, Schoor O, Tadmor AD, Green E, Fritsche J, Meyer M, Pawlowski N, Dorner S, Hoffgaard F, Rössler B, Maurer D, Weinschenk T, Reinhardt C, Huber C, Rammensee HG, Singh-Jasuja H, Sahin U, Dietrich PY, Wick W. Actively personalized vaccination trial for newly diagnosed glioblastoma. *Nature.* 2019;565(7738):240-245.
13. Shraibman B, Barnea E, Kadosh DM, Haimovich Y, Slobodin G, Rosner I, López-Larrea C, Hilf N, Kuttruff S, Song C, Britten C, Castle J, Kreiter S, Frenzel K, Tatagiba M, Tabatabai G, Dietrich PY, Dutoit V, Wick W, Platten M, Winkler F, von Deimling A, Kroep J, Sahuquillo J, Martínez-Ricarte F, Rodon J, Lassen U, Ottensmeier C, van der Burg SH, Thor Straten P, Poulsen HS, Ponsati B, Okada H, Rammensee HG, Sahin U, Singh H, Admon A. Identification of Tumor Antigens Among the HLA Peptidomes of Glioblastoma Tumors and Plasma. *Mol Cell Proteomics.* 2019;18(6):1255-1268.
14. Dutoit V, Herold-Mende C, Hilf N, Schoor O, Beckhove P, Bucher J, Dorsch K, Flohr S, Fritsche J, Lewandowski P, Lohr J, Rammensee HG, Stevanovic S, Trautwein C, Vass V, Walter S, Walker PR, Weinschenk T, Singh-Jasuja H, Dietrich PY. Exploiting the glioblastoma peptidome to discover novel tumour-associated antigens for immunotherapy. *Brain.* 2012;135(Pt 4):1042-1054.
15. The GTEx Consortium. The Genotype-Tissue Expression (GTEx) project. *Nat Genet.* 2013;45(6):580-585.
16. Löffler MW, Mohr C, Bichmann L, Freudenmann LK, Walzer M, Schroeder CM, Trautwein N, Hilke FJ, Zinser RS, Mühlenbruch L, Kowalewski DJ, Schuster H, Sturm M, Matthes J, Riess O, Czernmel S, Nahnsen S, Königsrainer I, Thiel K, Nadalin S, Beckert S, Bösmüller H, Fend F, Velic A, Maček B, Haen SP, Buonaguro L, Kohlbacher O, Stevanović S, Königsrainer A, Rammensee HG. Multi-omics discovery of exome-derived neoantigens in hepatocellular carcinoma. *Genome Med.* 2019;11(1):28.
17. Bassani-Sternberg M, Bräunlein E, Klar R, Engleitner T, Sinitcyn P, Audehm S, Straub M, Weber J, Slotta-Huspenina J, Specht K, Martignoni ME, Werner A, Hein R, Busch DH, Peschel C, Rad R, Cox J, Mann M, Krackhardt AM. Direct identification of clinically relevant neoepitopes presented on native human melanoma tissue by mass spectrometry. *Nat Commun.* 2016;7:13404.
18. Khodadoust MS, Olsson N, Wagar LE, Haabeth OA, Chen B, Swaminathan K, Rawson K, Liu CL, Steiner D, Lund P, Rao S, Zhang L, Marceau C, Stehr H, Newman AM, Czerwinski DK, Carlton VE, Moorhead M, Faham M, Kohrt HE, Carette J, Green MR, Davis MM, Levy R, Elias JE, Alizadeh AA. Antigen presentation profiling reveals recognition of lymphoma immunoglobulin neoantigens. *Nature.* 2017;543(7647):723-727.
19. Singh-Jasuja H, Emmerich NP, Rammensee HG. The Tübingen approach: identification, selection, and validation of tumor-associated HLA peptides for cancer therapy. *Cancer Immunol Immunother.* 2004;53(3):187-195.
20. Szolek A, Schubert B, Mohr C, Sturm M, Feldhahn M, Kohlbacher O. OptiType: precision HLA typing from next-generation sequencing data. *Bioinformatics.* 2014;30(23):3310-3316.
21. Jiang H, Lei R, Ding SW, Zhu S. Skewer: a fast and accurate adapter trimmer for next-generation sequencing paired-end reads. *BMC Bioinformatics.* 2014;15:182.
22. Kechin A, Boyarskikh U, Kel A, Filipenko M. cutPrimers: A New Tool for Accurate Cutting of Primers from Reads of Targeted Next Generation Sequencing. *J Comput Biol.* 2017;24(11):1138-1143.
23. Cock PJ, Fields CJ, Goto N, Heuer ML, Rice PM. The Sanger FASTQ file format for sequences with quality scores, and the Solexa/Illumina FASTQ variants. *Nucleic Acids Res.* 2010;38(6):1767-1771.
24. Mohr C, Friedrich A, Wojnar D, Kenar E, Polatkan AC, Codrea MC, Czernmel S, Kohlbacher O, Nahnsen S. qPortal: A platform for data-driven biomedical research. *PLoS One.* 2018;13(1):e0191603.
25. Li H, Durbin R. Fast and accurate short read alignment with Burrows-Wheeler transform. *Bioinformatics.* 2009;25(14):1754-1760.
26. Saunders CT, Wong WS, Swamy S, Becq J, Murray LJ, Cheetham RK. Strelka: accurate somatic small-variant calling from sequenced tumor-normal sample pairs. *Bioinformatics.* 2012;28(14):1811-1817.
27. Cingolani P, Platts A, Wang le L, Coon M, Nguyen T, Wang L, Land SJ, Lu X, Ruden DM. A program for annotating and predicting the effects of single nucleotide polymorphisms, SnpEff: SNPs in the genome of *Drosophila melanogaster* strain w1118; iso-2; iso-3. *Fly (Austin).* 2012;6(2):80-92.
28. Sallman DA, Padron E. Integrating mutation variant allele frequency into clinical practice in myeloid malignancies. *Hematol Oncol Stem Cell Ther.* 2016;9(3):89-95.
29. Kim S, Scheffler K, Halpern AL, Bekritsky MA, Noh E, Källberg M, Chen X, Kim Y, Beyter D, Krusche P, Saunders CT. Strelka2: fast and accurate calling of germline and somatic variants. *Nat Methods.* 2018;15(8):591-594.
30. Ewing B, Green P. Base-calling of automated sequencer traces using phred. II. Error probabilities. *Genome Res.* 1998;8(3):186-194.

Chapter 2: References

31. Nextflow pipeline. [Internet]. Available from: <https://github.com/nf-core/maseq>.
32. Sarek pipeline. [Internet]. Available from: <https://github.com/SciLifeLab/Sarek>.
33. Andrews S. FastQC: A Quality Control Tool for High Throughput Sequence Data. [Internet]. Available from: <http://www.bioinformatics.babraham.ac.uk/projects/fastqc/>. 2010.
34. Ewels P, Magnusson M, Lundin S, Käller M. MultiQC: summarize analysis results for multiple tools and samples in a single report. *Bioinformatics*. 2016;32(19):3047-3048.
35. Dobin A, Davis CA, Schlesinger F, Drenkow J, Zaleski C, Jha S, Batut P, Chaisson M, Gingeras TR. STAR: ultrafast universal RNA-seq aligner. *Bioinformatics*. 2013;29(1):15-21.
36. Krueger F. Trim Galore: A Wrapper Tool Around Cutadapt and Fastqc to Consistently Apply Quality and Adapter Trimming to Fastq Files, with Some Extra Functionality for Mspi-Digested Rrbs-Type (Reduced Representation Bisulfite-Seq) Libraries. [Internet]. Available from: http://www.bioinformatics.babraham.ac.uk/projects/trim_galore/, accessed on 2016/04/28. 2012.
37. Wang L, Wang S, Li W. RSeQC: quality control of RNA-seq experiments. *Bioinformatics*. 2012;28(16):2184-2185.
38. Liao Y, Smyth GK, Shi W. featureCounts: an efficient general purpose program for assigning sequence reads to genomic features. *Bioinformatics*. 2014;30(7):923-930.
39. Mortazavi A, Williams BA, McCue K, Schaeffer L, Wold B. Mapping and quantifying mammalian transcriptomes by RNA-Seq. *Nat Methods*. 2008;5(7):621-628.
40. Schubert B, Walzer M, Brachvogel HP, Szolek A, Mohr C, Kohlbacher O. FRED 2: an immunoinformatics framework for Python. *Bioinformatics*. 2016;32(13):2044-2046.
41. Bichmann L, Nelde A, Ghosh M, Heumos L, Mohr C, Peltzer A, Kuchenbecker L, Sachsenberg T, Walz JS, Stevanović S, Rammensee HG, Kohlbacher O. MHCquant: Automated and Reproducible Data Analysis for Immunopeptidomics. *J Proteome Res*. 2019;18(11):3876-3884.
42. Röst HL, Sachsenberg T, Aiche S, Bielow C, Weisser H, Aicheler F, Andreotti S, Ehrlich HC, Gutenbrunner P, Kenar E, Liang X, Nahnsen S, Nilse L, Pfeuffer J, Rosenberger G, Rurik M, Schmitt U, Veit J, Walzer M, Wojnar D, Wolski WE, Schilling O, Choudhary JS, Malmstrom L, Aebersold R, Reinert K, Kohlbacher O. OpenMS: a flexible open-source software platform for mass spectrometry data analysis. *Nat Methods*. 2016;13(9):741-748.
43. Eng JK, Hoopmann MR, Jahan TA, Egertson JD, Noble WS, MacCoss MJ. A deeper look into Comet-implementation and features. *J Am Soc Mass Spectrom*. 2015;26(11):1865-1874.
44. The M, MacCoss MJ, Noble WS, Käll L. Fast and Accurate Protein False Discovery Rates on Large-Scale Proteomics Data Sets with Percolator 3.0. *J Am Soc Mass Spectrom*. 2016;27(11):1719-1727.
45. UniProt: the universal protein knowledgebase. *Nucleic Acids Res*. 2017;45(D1):D158-d169.
46. Sherry ST, Ward MH, Kholodov M, Baker J, Phan L, Smigielski EM, Sirotkin K. dbSNP: the NCBI database of genetic variation. *Nucleic Acids Res*. 2001;29(1):308-311.
47. Tate JG, Bamford S, Jubb HC, Sondka Z, Beare DM, Bindal N, Boutselakis H, Cole CG, Creatore C, Dawson E, Fish P, Harsha B, Hathaway C, Jupe SC, Kok CY, Noble K, Ponting L, Ramshaw CC, Rye CE, Speedy HE, Stefancsik R, Thompson SL, Wang S, Ward S, Campbell PJ, Forbes SA. COSMIC: the Catalogue Of Somatic Mutations In Cancer. *Nucleic Acids Res*. 2019;47(D1):D941-d947.
48. Keshava Prasad TS, Goel R, Kandasamy K, Keerthikumar S, Kumar S, Mathivanan S, Telikicherla D, Raju R, Shafreen B, Venugopal A, Balakrishnan L, Marimuthu A, Banerjee S, Somanathan DS, Sebastian A, Rani S, Ray S, Harrys Kishore CJ, Kanth S, Ahmed M, Kashyap MK, Mohmood R, Ramachandra YL, Krishna V, Rahiman BA, Mohan S, Ranganathan P, Ramabadran S, Chaerkady R, Pandey A. Human Protein Reference Database-2009 update. *Nucleic Acids Res*. 2009;37(Database issue):D767-772.
49. Almeida LG, Sakabe NJ, deOliveira AR, Silva MC, Mundstein AS, Cohen T, Chen YT, Chua R, Gurung S, Gnjatic S, Jungbluth AA, Caballero OL, Bairoch A, Kiesler E, White SL, Simpson AJ, Old LJ, Camargo AA, Vasconcelos AT. CTdatabase: a knowledge-base of high-throughput and curated data on cancer-testis antigens. *Nucleic Acids Res*. 2009;37(Database issue):D816-819.
50. Vita R, Overton JA, Greenbaum JA, Ponomarenko J, Clark JD, Cantrell JR, Wheeler DK, Gabbard JL, Hix D, Sette A, Peters B. The immune epitope database (IEDB) 3.0. *Nucleic Acids Res*. 2015;43(Database issue):D405-412.
51. Freudenmann LK, Marcu A, Stevanović S. Mapping the tumour human leukocyte antigen (HLA) ligandome by mass spectrometry. *Immunology*. 2018;154(3):331-345.
52. Newey A, Griffiths B, Michaux J, Pak HS, Stevenson BJ, Woolston A, Semiannikova M, Spain G, Barber LJ, Matthews N, Rao S, Watkins D, Chau I, Coukos G, Racle J, Gfeller D, Starling N, Cunningham D, Bassani-Sternberg M, Gerlinger M. Immunopeptidomics of colorectal cancer organoids reveals a sparse HLA class I neoantigen landscape and no increase in neoantigens with interferon or MEK-inhibitor treatment. *J Immunother Cancer*. 2019;7(1):309.
53. Kowalewski DJ, Schuster H, Backert L, Berlin C, Kahn S, Kanz L, Salih HR, Rammensee HG, Stevanovic S, Stickel JS. HLA ligandome analysis identifies the underlying specificities of spontaneous antileukemia immune responses in chronic lymphocytic leukemia (CLL). *Proc Natl Acad Sci U S A*. 2015;112(2):E166-175.
54. Stickel JS, Stickel N, Hennenlotter J, Klingel K, Stenzl A, Rammensee HG, Stevanović S. Quantification of HLA class I molecules on renal cell carcinoma using Edman degradation. *BMC Urol*. 2011;11:1.
55. Keskin DB, Anandappa AJ, Sun J, Tirosh I, Mathewson ND, Li S, Oliveira G, Giobbie-Hurder A, Felt K, Gjini E, Shukla SA, Hu Z, Li L, Le PM, Allesøe RL, Richman AR, Kowalczyk MS, Abdelrahman S, Geduldig JE, Charbonneau S, Pelton K, Iorgulescu JB, Elagina L, Zhang W, Olive O, McCluskey C, Olsen LR, Stevens J, Lane WJ, Salazar AM, Daley H, Wen PY, Chiocca EA, Harden M, Lennon NJ, Gabriel S, Getz G, Lander ES,

Chapter 2: References

- Regev A, Ritz J, Neuberger D, Rodig SJ, Ligon KL, Suvà ML, Wucherpennig KW, Hacohen N, Fritsch EF, Livak KJ, Ott PA, Wu CJ, Reardon DA. Neoantigen vaccine generates intratumoral T cell responses in phase Ib glioblastoma trial. *Nature*. 2019;565(7738):234-239.
56. Hambardzumyan D, Gutmann DH, Kettenmann H. The role of microglia and macrophages in glioma maintenance and progression. *Nat Neurosci*. 2016;19(1):20-27.
 57. Li W, Graeber MB. The molecular profile of microglia under the influence of glioma. *Neuro Oncol*. 2012;14(8):958-978.
 58. Rossi ML, Hughes JT, Esiri MM, Coakham HB, Brownell DB. Immunohistological study of mononuclear cell infiltrate in malignant gliomas. *Acta Neuropathol*. 1987;74(3):269-277.
 59. Morantz RA, Wood GW, Foster M, Clark M, Gollahon K. Macrophages in experimental and human brain tumors. Part 2: studies of the macrophage content of human brain tumors. *J Neurosurg*. 1979;50(3):305-311.
 60. Badie B, Scharfner JM. Flow cytometric characterization of tumor-associated macrophages in experimental gliomas. *Neurosurgery*. 2000;46(4):957-961; discussion 961-952.
 61. Wesolowska A, Kwiatkowska A, Slomnicki L, Dembinski M, Master A, Sliwa M, Franciszkiwicz K, Chouaib S, Kaminska B. Microglia-derived TGF-beta as an important regulator of glioblastoma invasion-an inhibition of TGF-beta-dependent effects by shRNA against human TGF-beta type II receptor. *Oncogene*. 2008;27(7):918-930.
 62. Markovic DS, Vinnakota K, Chirasani S, Synowitz M, Raguet H, Stock K, Sliwa M, Lehmann S, Kálin R, van Rooijen N, Holmbeck K, Heppner FL, Kiwit J, Matyash V, Lehnardt S, Kaminska B, Glass R, Kettenmann H. Gliomas induce and exploit microglial MT1-MMP expression for tumor expansion. *Proc Natl Acad Sci U S A*. 2009;106(30):12530-12535.
 63. Coniglio SJ, Eugenin E, Dobrenis K, Stanley ER, West BL, Symons MH, Segall JE. Microglial stimulation of glioblastoma invasion involves epidermal growth factor receptor (EGFR) and colony stimulating factor 1 receptor (CSF-1R) signaling. *Mol Med*. 2012;18(1):519-527.
 64. Wilson EH, Weninger W, Hunter CA. Trafficking of immune cells in the central nervous system. *J Clin Invest*. 2010;120(5):1368-1379.
 65. Dettori P, Bradac GB, Scialfa G. Selective angiography of the external and internal carotid arteries in the diagnosis of supra-tentorial meningiomas. *Neuroradiology*. 1970;1(3):166-172.
 66. Manaka H, Sakata K, Tatezaki J, Shinohara T, Shimohigoshi W, Yamamoto T. Safety and Efficacy of Preoperative Embolization in Patients with Meningioma. *J Neurol Surg B Skull Base*. 2018;79(Suppl 4):S328-s333.
 67. Bhowmik A, Khan R, Ghosh MK. Blood brain barrier: a challenge for effectual therapy of brain tumors. *Biomed Res Int*. 2015;2015:320941.
 68. Middeldorp J, Hol EM. GFAP in health and disease. *Prog Neurobiol*. 2011;93(3):421-443.
 69. Mahmood SF, Gruel N, Chapeaublanc E, Lescure A, Jones T, Reyat F, Vincent-Salomon A, Raynal V, Pierron G, Perez F, Camonis J, Del Nery E, Delattre O, Radvanyi F, Bernard-Pierrot I. A siRNA screen identifies RAD21, EIF3H, CHRAC1 and TANC2 as driver genes within the 8q23, 8q24.3 and 17q23 amplicons in breast cancer with effects on cell growth, survival and transformation. *Carcinogenesis*. 2014;35(3):670-682.
 70. Alderson NL, Hama H. Fatty acid 2-hydroxylase regulates cAMP-induced cell cycle exit in D6P2T schwannoma cells. *J Lipid Res*. 2009;50(6):1203-1208.
 71. Eckhardt M, Yaghootfam A, Fewou SN, Zöller I, Gieselmann V. A mammalian fatty acid hydroxylase responsible for the formation of alpha-hydroxylated galactosylceramide in myelin. *Biochem J*. 2005;388(Pt 1):245-254.
 72. Lemay AM, Courtemanche O, Couttas TA, Jamsari G, Gagné A, Bossé Y, Joubert P, Don AS, Marsolais D. High FA2H and UGT8 transcript levels predict hydroxylated hexosylceramide accumulation in lung adenocarcinoma. *J Lipid Res*. 2019;60(10):1776-1786.
 73. Ladisch S, Sweeley CC, Becker H, Gage D. Aberrant fatty acyl alpha-hydroxylation in human neuroblastoma tumor gangliosides. *J Biol Chem*. 1989;264(20):12097-12105.
 74. Kiguchi K, Takamatsu K, Tanaka J, Nozawa S, Iwamori M, Nagai Y. Glycosphingolipids of various human ovarian tumors: a significantly high expression of I3SO3GalCer and Lewis antigen in mucinous cystadenocarcinoma. *Cancer Res*. 1992;52(2):416-421.
 75. Sun H, Tsunenari T, Yau KW, Nathans J. The vitelliform macular dystrophy protein defines a new family of chloride channels. *Proc Natl Acad Sci U S A*. 2002;99(6):4008-4013.
 76. Barro Soria R, Spitzner M, Schreiber R, Kunzelmann K. Bestrophin-1 enables Ca²⁺-activated Cl⁻ conductance in epithelia. *J Biol Chem*. 2009;284(43):29405-29412.
 77. Spitzner M, Martins JR, Soria RB, Ousingsawat J, Scheidt K, Schreiber R, Kunzelmann K. Eag1 and Bestrophin 1 are up-regulated in fast-growing colonic cancer cells. *J Biol Chem*. 2008;283(12):7421-7428.
 78. Oh SJ, Lee CJ. Distribution and Function of the Bestrophin-1 (Best1) Channel in the Brain. *Exp Neurobiol*. 2017;26(3):113-121.
 79. Aldehni F, Spitzner M, Martins JR, Barro-Soria R, Schreiber R, Kunzelmann K. Bestrophin 1 promotes epithelial-to-mesenchymal transition of renal collecting duct cells. *J Am Soc Nephrol*. 2009;20(7):1556-1564.
 80. Saberbaghi T, Wong R, Rutka JT, Wang GL, Feng ZP, Sun HS. Role of Cl⁻ channels in primary brain tumour. *Cell Calcium*. 2019;81:1-11.
 81. Filmus J, Capurro M, Rast J. Glypicans. *Genome Biol*. 2008;9(5):224.
 82. Matas-Rico E, van Veen M, Leyton-Puig D, van den Berg J, Koster J, Kedziora KM, Molenaar B, Weerts MJ, de Rink I, Medema RH, Giepmans BN, Perrakis A, Jalink K, Versteeg R, Moolenaar WH.

Chapter 2: References

- Glycerophosphodiesterase GDE2 Promotes Neuroblastoma Differentiation through Glypican Release and Is a Marker of Clinical Outcome. *Cancer Cell*. 2016;30(4):548-562.
83. Bosse KR, Raman P, Zhu Z, Lane M, Martinez D, Heitzeneder S, Rathi KS, Kendersky NM, Randall M, Donovan L, Morrissy S, Sussman RT, Zhelev DV, Feng Y, Wang Y, Hwang J, Lopez G, Harenza JL, Wei JS, Pawel B, Bhatti T, Santi M, Ganguly A, Khan J, Marra MA, Taylor MD, Dimitrov DS, Mackall CL, Maris JM. Identification of GPC2 as an Oncoprotein and Candidate Immunotherapeutic Target in High-Risk Neuroblastoma. *Cancer Cell*. 2017;32(3):295-309.e212.
 84. Gao W, Tang Z, Zhang YF, Feng M, Qian M, Dimitrov DS, Ho M. Immunotoxin targeting glypican-3 regresses liver cancer via dual inhibition of Wnt signalling and protein synthesis. *Nat Commun*. 2015;6:6536.
 85. Hennes T. Collagen glycosylation. *Curr Opin Struct Biol*. 2019;56:131-138.
 86. Smith RN, Aleksic J, Butano D, Carr A, Contrino S, Hu F, Lyne M, Lyne R, Kalderimis A, Rutherford K, Stepan R, Sullivan J, Wakeling M, Watkins X, Micklem G. InterMine: a flexible data warehouse system for the integration and analysis of heterogeneous biological data. *Bioinformatics*. 2012;28(23):3163-3165.
 87. Pickup MW, Mouw JK, Weaver VM. The extracellular matrix modulates the hallmarks of cancer. *EMBO Rep*. 2014;15(12):1243-1253.
 88. Publications listed in PubMed dealing with the nucleolar protein 16. [Internet]. Available from: <https://pubmed.ncbi.nlm.nih.gov/?term=NOP16>, accessed on 2020/05/29.
 89. Butt AJ, Sergio CM, Inman CK, Anderson LR, McNeil CM, Russell AJ, Nusch M, Preiss T, Biankin AV, Sutherland RL, Musgrove EA. The estrogen and c-Myc target gene HSPC111 is over-expressed in breast cancer and associated with poor patient outcome. *Breast Cancer Res*. 2008;10(2):R28.
 90. Zhang J, Shi X, Li Y, Kim BJ, Jia J, Huang Z, Yang T, Fu X, Jung SY, Wang Y, Zhang P, Kim ST, Pan X, Qin J. Acetylation of Smc3 by Eco1 is required for S phase sister chromatid cohesion in both human and yeast. *Mol Cell*. 2008;31(1):143-151.
 91. Rivera-Colón Y, Maguire A, Liszczak GP, Olia AS, Marmorstein R. Molecular Basis for Cohesin Acetylation by Establishment of Sister Chromatid Cohesion N-Acetyltransferase ESCO1. *J Biol Chem*. 2016;291(51):26468-26477.
 92. Terret ME, Sherwood R, Rahman S, Qin J, Jallepalli PV. Cohesin acetylation speeds the replication fork. *Nature*. 2009;462(7270):231-234.
 93. McGarry JD, Brown NF. The mitochondrial carnitine palmitoyltransferase system. From concept to molecular analysis. *Eur J Biochem*. 1997;244(1):1-14.
 94. Rigault C, Le Borgne F, Demarquoy J. Genomic structure, alternative maturation and tissue expression of the human BBOX1 gene. *Biochim Biophys Acta*. 2006;1761(12):1469-1481.
 95. Yang Y, Yu Q, Li B, Guan R, Huang C, Yang X. BBOX1-AS1 Accelerates Gastric Cancer Proliferation by Sponging miR-3940-3p to Upregulate BIRC5 Expression. *Dig Dis Sci*. 2020.
 96. Bilich T, Nelde A, Bichmann L, Roerden M, Salih HR, Kowalewski DJ, Schuster H, Tsou CC, Marcu A, Neidert MC, Lübke M, Rieth J, Schemionek M, Brümmendorf TH, Vucinic V, Niederwieser D, Bauer J, Märklin M, Peper JK, Klein R, Kohlbacher O, Kanz L, Rammensee HG, Stevanović S, Walz JS. The HLA ligandome landscape of chronic myeloid leukemia delineates novel T-cell epitopes for immunotherapy. *Blood*. 2019;133(6):550-565.
 97. Coulie PG, Van den Eynde BJ, van der Bruggen P, Boon T. Tumour antigens recognized by T lymphocytes: at the core of cancer immunotherapy. *Nat Rev Cancer*. 2014;14(2):135-146.
 98. Urban JL, Schreiber H. Tumor antigens. *Annu Rev Immunol*. 1992;10:617-644.
 99. Sang Y, Hou Y, Cheng R, Zheng L, Alvarez AA, Hu B, Cheng SY, Zhang W, Li Y, Feng H. Targeting PDGFR α -activated glioblastoma through specific inhibition of SHP-2-mediated signaling. *Neuro Oncol*. 2019;21(11):1423-1435.
 100. Verhaak RG, Hoadley KA, Purdom E, Wang V, Qi Y, Wilkerson MD, Miller CR, Ding L, Golub T, Mesirov JP, Alexe G, Lawrence M, O'Kelly M, Tamayo P, Weir BA, Gabriel S, Winckler W, Gupta S, Jakkula L, Feiler HS, Hodgson JG, James CD, Sarkaria JN, Brennan C, Kahn A, Spellman PT, Wilson RK, Speed TP, Gray JW, Meyerson M, Getz G, Perou CM, Hayes DN. Integrated genomic analysis identifies clinically relevant subtypes of glioblastoma characterized by abnormalities in PDGFRA, IDH1, EGFR, and NF1. *Cancer Cell*. 2010;17(1):98-110.
 101. Tan FH, Putoczki TL, Stylli SS, Luwor RB. Ponatinib: a novel multi-tyrosine kinase inhibitor against human malignancies. *Onco Targets Ther*. 2019;12:635-645.
 102. Rahman M, Kresak J, Yang C, Huang J, Hiser W, Kubilis P, Mitchell D. Analysis of immunobiologic markers in primary and recurrent glioblastoma. *J Neurooncol*. 2018;137(2):249-257.

CHAPTER 3



HLA peptidome analysis of medulloblastoma uncovers potential targets for cancer immunotherapy

Lena Katharina Freudenmann (L.K.F.) planned and performed all HLA peptidome analyses, analyzed the entire immunopeptidomic dataset, and contributed all figures and texts. Acquisition and analysis of RNA sequencing data including HLA typing was conducted at CeGaT GmbH and at the Quantitative Biology Center, University of Tübingen. Samples along with clinical metadata were provided by collaborating physicians.

1 Abstract

Neoplasms of the brain and CNS are the most common pediatric tumors – with medulloblastoma representing the malignant entity with the highest incidence – and the leading cause of cancer-related mortality in children. Multimodal therapy achieves cure rates of up to 75%, whereas recurrent medulloblastoma remains largely incurable. Conversely, those patients surviving face severe long-term sequelae in consequence of irradiation of the developing brain. Cancer immunotherapy may contribute to the development of innovative therapeutic regimens, whereby the definition of appropriate targets represents a fundamental pillar. Herein, we present the first investigation of the immunopeptidomic landscape of 28 medulloblastomas for target antigens and peptides naturally presented on HLA class I and II molecules. While established tumor-associated and cancer-testis antigens did not fulfill the requirement of both frequent and tumor-exclusive presentation, immunopeptidome analysis unveiled a novel set medulloblastoma-associated antigens and peptides. Remarkably, a significant fraction was shared by childhood and adult medulloblastomas and, most importantly, identified across WNT-activated, non-WNT/non-SHH, and SHH-activated tumors. In conclusion, we defined a set of tumor-associated antigens and peptides characterized by natural, frequent, and exclusive HLA presentation on native medulloblastoma tissue. These represent prime candidates for application in antigen-specific immunotherapeutic approaches, which may replace radiotherapy in multimodal therapeutic regimens and represent an option for the management of disease recurrence.

2 Introduction

Brain and CNS tumors are the most common pediatric neoplasms, the leading cause of death due to pediatric cancer, and the seventh most common cause of child mortality in general.^{1,2} Medulloblastoma is *per se* graded with WHO grade IV and constitutes the most frequent intracranial malignancy in children, whereas only around 7% of total cases occur in adults older than 40 years.^{1,3} Therapeutic regimens for medulloblastomas are guided by both the age and the present subgroup, whereby radiotherapy is standard-of-care in patients older than three to five years and in infants suffering from high- or very high-risk tumors.^{4,5} Overall, multimodal therapy comprising surgical resection, chemotherapy, and radiotherapy – when indicated – achieves good cure rates of 70-75%.^{4,6} Management of disease recurrence is still an open question and recurrent medulloblastoma has remained largely incurable.^{4,7} Those patients surviving face long-term sequelae predominantly caused by irradiation of the developing brain. These comprise neurological, developmental, psychosocial, and neuroendocrine deficits, or even secondary neoplasms such as glioblastoma or meningioma.^{4,6,8,9} Hence, the development of novel therapies offering therapeutic options for recurrent medulloblastomas and, most importantly, replacing radiotherapy in the treatment of primary tumors is urgently required.

The antigenic landscape of medulloblastoma has never been investigated and this tumor entity is characterized by a profound lack of potential targets for cancer immunotherapy. Consequently, we aimed to define tumor-associated peptides and antigens that are naturally presented on HLA class I or II molecules of primary medulloblastomas, but not on benign

human tissues. In addition, candidate target antigens were queried against the GTEx database containing RNA expression data acquired across a large set of benign human tissues in order to examine whether they exhibit CTA-like expression profiles, to exclude such with brain- or cerebellum-specific expression, and to identify antigens not known to be expressed in any tissue.¹⁰

3 Methods

Patient collective

Written informed consent of the 28 patients included in the present study and/or their legal representative was obtained in accordance with the Declaration of Helsinki protocol and the local review boards (Kantonale Ethikkommission Zürich / KEK-ZH-Nr. 2015-0163; Ethik-Kommission der Ärztekammer Hamburg / PV4904; authorized vote-free usage of residual tissue collected for other purposes in Sankt Augustin and Würzburg) before surgery. Patients underwent surgery at the Department of Neurosurgery of the University Hospital Zürich, Asklepios Hospital Sankt Augustin, Altona Children's Hospital, or at the University Children's Hospital Würzburg. Tissue samples were snap frozen in liquid nitrogen, Bambanker medium, or Tissue-Tek® O.C.T.™ and stored at -80°C until use. Medulloblastoma specimens along with clinical metadata were kindly provided by PD Dr. med. Marian Christoph Neidert and Dr. med. Julia Velz (University Hospital Zürich, Department of Neurosurgery), Prof. Dr. med. Matthias Eyrich (University Children's Hospital Würzburg, Department of Pediatric Oncology), Prof. Dr. med. Manfred Westphal and Dr. med. Malte Mohme (University Medical Center Hamburg-Eppendorf, Department of Neurosurgery) as well as by Prof. Dr. med. Martina Messing-Jünger, PD Dr. med. Harald Reinhard, and Dr. med. Andreas Röhrig (Asklepios Hospital Sankt Augustin). All patients had histopathologically confirmed medulloblastoma, whereby the collective comprised tumors of all subgroups: n=4 WNT-activated, n=7 SHH-activated, n=2 Group 3, n=2 Group 4, n=8 non-WNT/non-SHH (not differentiated into Group 3 and Group 4), and n=5 without annotation to a subgroup. Two samples were obtained during surgery at disease recurrence. The present study population had a female-to-male ratio of 2:3 and a median age of onset of 8 [1-37] years including two cases of adolescent and adult medulloblastoma each. The median available amount of tissue for HLA-IP accounted to 320 [120-1511] mg. Individual patient and sample characteristics are listed in Table 7, whereby a closer look on HLA allotype frequencies in the study cohort is provided in CHAPTER 5.

Table 7. Clinical and experimental metadata of the 28 medulloblastoma patients included in the present study. Letters in internal sample IDs indicate the location, where patients underwent surgery: HH – Altona Children's Hospital, SA – Asklepios Hospital Sankt Augustin, Wü – University Children's Hospital Würzburg, ZH – University Hospital Zürich. Age of onset was defined as the age at initial diagnosis, whereby two cases of adolescent and adult medulloblastoma each were included in the study cohort (marked in grey). Several Non-WNT/non-SHH tumors were not differentiated into Group 3 and Group 4 medulloblastomas. Abbreviation not introduced in the text above: not determined (n.d.). #Sample mass contains few Bambanker medium or Tissue-Tek® O.C.T.™ and is considered separately for calculations of e.g. median amount of available tissue or relative peptide yields.

Internal sample ID	Gender Age of onset [years]	Subgroup	HLA typing	Sample mass HLA-IP [mg]
HH-01	♀ 7	SHH	A*02:01;A*32:01;B*13:02;B*27:02;C*02:02;C*06:02	345

Chapter 3: Methods

HH-02	♂ 13	Group 3	A*02:05;A*11:01;B*35:03;B*50:01;C*06:02;C*12:03	207
HH-03	♂ 4	Non-WNT/non-SHH	A*02:01;A*68:01;B*51:01;B*51:01;C*14:02;C*15:02	209
HH-04	♂ 12	WNT	A*03:01;A*24:02;B*07:02;B*44:02;C*07:02;C*16:04	167
HH-05	♀ 11	WNT	A*11:01;A*24:02;B*35:01;B*44:02;C*04:01;C*05:01	178
HH-06	♂ 5	Non-WNT/non-SHH	A*11:01;A*68:01;B*41:02;B*52:01;C*12:02;C*17:01	386
SA1 Tissue from 1 st recurrence at 4 years after initial diagnosis	♀ 4	Most likely Non-WNT/non-SHH	A*02:01;A*68:01;B*15:01;B*51:01;C*03:03;C*15:02	186
SA2	♂ 7	n.d.	A*01:01;A*11:01;B*07:02;B*08:01;C*07:01;C*07:02	290
SA3 Tissue from 1 st recurrence at 1 year after initial diagnosis	♀ 8	n.d.	A*02:01;A*32:01;B*57:01;B*40:02;C*02:02;C*06:02	222
SA4	♂ 9	n.d.	A*01:01;A*02:01;B*07:02;B*37:01;C*06:02;C*07:02	120
SA5	♀ 1	n.d.	A*11:01;A*26:01;B*15:08;B*27:05;C*01:02;C*02:02	295
Wü-N391/17	♂ 19	n.d.	A*02:01;A*02:11;B*41:01;B*52:01;C*07:01;C*12:02	776#
Wü-N526/17	♀ 12	Group 4	A*03:01;A*26:01;B*44:03;B*50:01;C*04:01;C*06:02	513#
Wü-N998/13	♂ 2	WNT	A*03:01;A*29:02;B*44:03;B*51:01;C*14:02;C*16:01	1066#
ZH513	♂ 8	Non-WNT/non-SHH	A*03:01;A*11:01;B*27:05;B*35:01;C*01:02;C*04:01	1461
ZH680	♀ 7	Non-WNT/non-SHH	A*25:01;A*31:01;B*15:18;B*27:05;C*01:02;C*07:04	1554#
ZH703	♂ 4	Group 4	A*02:02;A*03:01;B*13:02;B*18:01;C*06:02;C*07:04	1302
ZH713	♂ 3	Group 3	A*03:01;A*26:01;B*38:01;B*49:01;C*07:01;C*12:03	932#
ZH718	♂ 1	SHH/TP53 ^{WT}	A*02:01;A*25:01;B*44:02;B*18:01;C*05:01;C*05:01	823#
ZH732	♂ 5	Non-WNT/non-SHH	A*03:01;A*80:01;B*40:02;B*58:01;C*02:02;C*07:01	607
ZH741	♀ 8	WNT	A*02:01;A*24:02;B*18:01;B*44:05;C*02:02;C*07:01	1668#
ZH859	♂ 16	SHH/TP53 ^{mut}	A*03:01;A*24:02;B*35:01;B*35:02;C*04:01;C*04:01	863
ZH868	♀ 2	SHH/TP53 ^{WT}	A*01:01;A*02:01;B*44:02;B*57:01;C*05:01;C*06:02	1165
ZH872	♂ 6	SHH/TP53 ^{mut}	A*03:01;A*68:02;B*44:02;B*57:01;C*06:02;C*07:04	1511
ZH890	♀ 9	Non-WNT/non-SHH	A*01:01;A*31:01;B*08:01;B*35:03;C*04:01;C*07:01	3218#
ZH913	♂ 29	SHH/TP53 ^{WT}	A*29:02;A*68:01;B*44:02;B*44:03;C*07:04;C*16:01	869
ZH919	♀ 8	Non-WNT/non-SHH	A*02:01;A*02:01;B*35:08;B*51:01;C*04:01;C*15:02	402
ZH937	♂ 37	Most likely SHH/TP53 ^{WT}	A*02:01;A*30:01;B*13:02;B*44:02;C*05:01;C*06:02	278

HLA typing and RNA sequencing

HLA class I allotypes were retrieved from whole RNA sequencing using the OptiType¹¹ algorithm by Dr. Gurpreet Kaur, whereas HLA class II allotypes are currently being determined by Marie Gauder and Dr. Stefan Czernel (Quantitative Biology Center, University of Tübingen).

RNA sequencing was performed for all 28 patients at CeGaT GmbH (Tübingen). Since genomic DNA was not available, we forewent whole exome or genome sequencing. However, DNA was isolated from tumor tissue as well for future DNA methylation profiling. RNA and DNA were isolated from fresh frozen tumor tissue (≥ 20 mg) – containing residual Bamberker medium or Tissue-Tek[®] O.C.T.[™] in some cases – using the AllPrep DNA/RNA Mini Kit (Qiagen). Following quality control for RNA integrity, sequencing libraries were prepared from

78 ng RNA using the KAPA RNA HyperPrep Kit with RiboErase (HMR; Roche), whereby ribosomal RNA was depleted. Paired-end sequencing at 100 bp read length was performed on a NovaSeq 6000 sequencing system (Illumina). Sequencing reads were demultiplexed employing the Illumina bcl2fastq 2.20 and untrimmed FASTQ¹²-formatted files were uploaded to qPortal¹³ (Quantitative Biology Center, University of Tübingen) for further evaluation. Analysis of transcriptome data beyond HLA typing has not yet been completed, but is currently being performed by Marie Gauder and Dr. Stefan Czernmel (Quantitative Biology Center, University of Tübingen).

HLA-IP and subsequent LC-MS/MS to identify HLA-presented peptides

HLA class I- and II-presented peptides were isolated from primary human tissue and analyzed by LC-MS/MS as described in 3.2. As far as possible, Tissue-Tek[®] O.C.T.[™] and Bambanker medium were cut off from embedded samples, while keeping specimens frozen during this step. Both HLA-IP and RNA sequencing were performed from cleaned up tissue to reduce interferences with embedding material during experimental sample processing. All peptide eluates were analyzed in four technical replicates each consuming 14% sample share on an Orbitrap Fusion Lumos. Direct injection was performed for all samples excepting HH-01, HH-02, ZH513, ZH680, ZH703, ZH718, and ZH732.

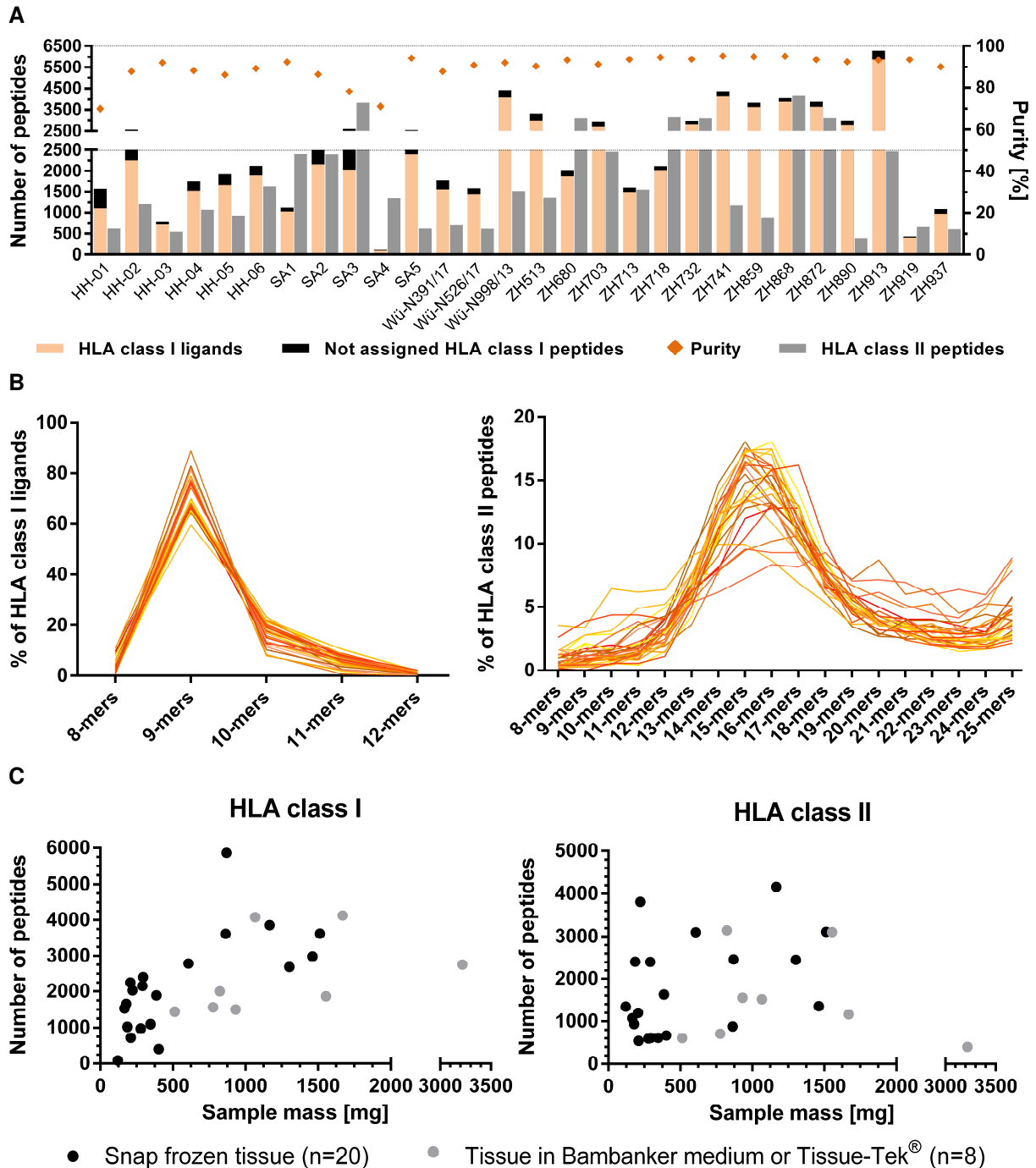
4 Results

4.1 HLA class I allotype coverage and peptide yields of HLA-IPs

Aimed at defining medulloblastoma-associated antigens naturally presented on HLA as candidate targets for cancer immunotherapy, 28 primary tumors were analyzed. The study cohort comprised 60 different HLA class I allotypes with HLA-A*02:01 (39%), -A*03:01 (32%), -A*11:01 (21%), -B*44:02 (25%), -B*51:01 (14%), -B*07:02 (11%), -B*13:02 (11%), -B*18:01 (11%), -B*27:05 (11%), -B*35:01 (11%), -B*44:03 (11%), -B*57:01 (11%), -C*06:02 (32%), -C*04:01 (21%), -C*07:01 (21%), and -C*02:02 (18%) being the most frequent ones (Supplementary Table 10). All HLA class I allotypes cover 99.95% of the world population, whereby 92.08% of all individuals are expected to be positive for at least three allotypes (Supplementary Figure 6).

A median of 2016 [88-5867] HLA class I ligands and 1347 [400-4164] HLA class II-presented peptides were identified from medulloblastoma samples. HLA class I peptide eluates exhibited a purity of at least 70% and none of the samples were censored for low peptide yield or low percentage of HLA class I ligands. It was striking that the average purity of samples collected in Zürich ($93.3 \pm 1.6\%$; n=14) was superior compared to tissue specimens received from Hamburg ($85.6 \pm 7.2\%$; n=6) or Sankt Augustin ($84.4 \pm 8.8\%$; n=5) and slightly increased in comparison with tissues from Würzburg ($90.3 \pm 1.8\%$; n=3). The total number of unique HLA class I and II peptides, HLA class I ligands as well as the purity of HLA class I peptide eluates are given in Figure 24 A for every specimen. The length distribution of HLA class I ligands clearly peaked at 9 AA length, whereas HLA class II-presented peptides were typically 13- to 18-mers. A fraction of patients showed a broadened length distribution curve elevated either for shorter (≤ 12 AA) or longer (≥ 19 AA) peptides (Figure 24 B). Taking tissue masses

subjected to HLA-IP into account (Table 7), enabled us to investigate whether peptide yields correlate with sample quantities used. This revealed a significant or indicated correlation of the amount of snap frozen medulloblastoma tissue with the number of identified HLA class I ligands or HLA class II-restricted peptides, respectively. In turn, no correlation of employed sample quantities and peptide yields was observed for tissues that had previously been embedded in Bamberker medium or Tissue-Tek® O.C.T.™ (Figure 24 C). Considering the relative number of identified unique peptides per one mg of tissue input revealed a significantly increased yield of HLA class I and HLA class II peptides eluted from snap frozen *versus* embedded tissues (Figure 24 D).



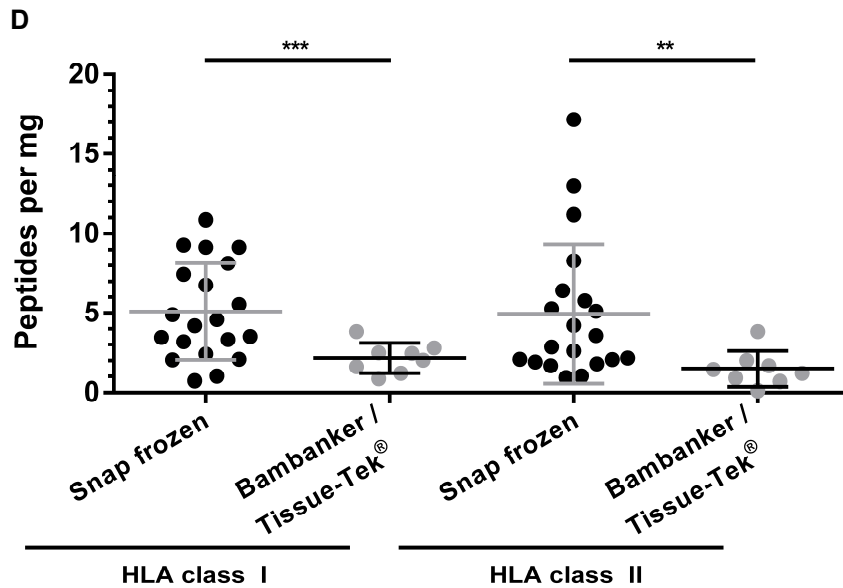


Figure 24. Number and length distribution of identified HLA class I- and II-presented peptides. (A) HLA class I and II peptide yields obtained from medulloblastoma tissue. Calculated purities refer to the proportion of HLA class I peptides annotated to an HLA allotype of the respective patient. **(B) Length distribution of HLA class I ligands and HLA class II peptides.** Across the entire dataset, 9-mers constituted 71% of HLA class I ligands, whereas 67% of HLA class II-presented peptides had a length between 13 and 18 AA. Each line represents data of a single sample. While the entire HLA class II dataset included 9% of peptides with ≤ 12 AA and 24% of peptides with ≥ 19 AA, these shares were distorted in a fraction of patients (HH-02, Wü-N998/13, ZH713, and ZH937: 13-26% 8- to 12-mers; HH-04, HH-05, and ZH919: 39-48% 19- to 25-mers). **(C) Unique peptides per sample versus amount of tissue subjected to HLA-IP.** The total amount of unique HLA class I ligands or HLA class II-restricted peptides identified by analyzing four technical replicates was set in relation to the amount of tissue subjected to HLA-IP. For this purpose, samples were differentiated into snap frozen tissues and such embedded in Bambanker medium or Tissue-Tek® O.C.T.™. By non-linear regression (one-phase association) exponential functions with a forced y-intercept of 0 (internal data created by Daniel Kowalewski at the Department of Immunology, University of Tübingen indicate that subjecting cell-free lysis buffer to HLA-IP does not result in peptide identifications) were fitted. However, the goodness of fit was poor for all models with the exception of HLA class I ligands eluted from snap frozen tissue: $R^2 = 0.5527$ (snap frozen HLA class I) / 0.2888 (embedded HLA class I) / 0.1328 (snap frozen HLA class II) / 0.03929 (embedded HLA class II). A correlation analysis across these normally distributed data (according to D'Agostino & Pearson omnibus normality test) identified a significant correlation of snap frozen sample quantities and the number of identified HLA class I ligands (two-tailed p -value = 0.0011) and an indicated correlation with the number of HLA class II-restricted peptides not reaching statistical significance (two-tailed p -value = 0.0639). The amount of tissue obtained after cutting off Tissue-Tek® O.C.T.™ and removing Bambanker medium as far as possible did neither correlate with the number HLA class I nor with HLA class II peptide identifications: two-tailed p -values = 0.3662 (HLA class I) / 0.5748 (HLA class II). **(D) Peptide yields normalized to one mg of tissue input.** It was intended to investigate, whether the relative number of peptide identifications differs between snap frozen samples and tissues embedded in Bambanker medium or Tissue-Tek® O.C.T.™ as well as between HLA class I- and II-IPs. An unpaired t test (normalized HLA class I ligand yields had Gaussian distributions according to D'Agostino & Pearson omnibus normality test) with Welch's correction for unequal standard deviation (according to F test, p -value = 0.0042) revealed a significant difference between relative HLA class I ligand yields obtained from snap frozen *versus* embedded tissues (two-tailed p -value = 0.0007). Likewise, a significantly increased number of HLA class II peptides was isolated from snap frozen in comparison to embedded tissues (two-tailed p -value = 0.0026), as identified by Mann-Whitney testing for unpaired non-parametric data. In turn, no significant differences were observed between relative HLA class I and II peptide yields obtained from the same type of sample: two-tailed p -values = 0.2774 (snap frozen tissues) / 0.2500 (embedded tissues); Wilcoxon matched-

pairs signed rank tests for paired non-Gaussian data (according to D'Agostino & Pearson omnibus normality test).

4.2 Identification of medulloblastoma-associated antigens

Employing immunoaffinity chromatography and subsequent LC-MS/MS, we mapped the antigenic repertoire naturally presented on HLA class I and II molecules of 28 medulloblastomas. To define medulloblastoma-associated antigens and peptides, an in-house benign database comprising 30 distinct primary human organs (n=418 HLA class I and n=364 HLA class II datasets) was subtracted. The term medulloblastoma-associated was assigned to peptides and antigens that were never identified on CNS-related tissues (brain, cerebellum, and spinal cord) and for which a maximum of one non-CNS-related sample was positive. Moreover, the frequency of positive primary human malignancies other than medulloblastoma (n=874 samples for HLA class I; n=626 samples for HLA class II) encompassing 37 cancer entities was evaluated. As additional criterium to select targets for cancer immunotherapies, RNA expression data acquired across a large set of benign human tissues and deposited in the GTEx database¹⁰ was reported for every candidate antigen. Further, this allowed the identification of antigens not known to be expressed in any tissue (defined as less than ten TPM in any tissue), such with a classical CTA-like expression profile (not exceeding ten TPM in other organs than testis) as well as to exclude antigens specifically expressed in the brain and/or cerebellum, which represent the tissue of tumor origin.

Medulloblastoma-associated HLA class I-presented antigens and peptides

HLA class I peptidome analysis of medulloblastoma (n=28) allowed the identification of 9,821 distinct source proteins represented by HLA class I ligands on native tumor tissue. These represent 91% of the estimated maximum attainable amount of distinct source proteins (Figure 25 C). Despite the vast overlap of medulloblastomas with benign samples, 77 antigens were exclusively presented on at least two neoplasms (Figure 25 A). Following manual curation of the underlying peptides for HLA motifs as well as multi-mapping to several source proteins, a set of 15 medulloblastoma-associated antigens and corresponding peptides naturally presented on 11-29% of tumors was created. Among these, SPINK8, WNT5A, and SHISA9 were the most frequent ones (Figure 25 B). We found a total of seven medulloblastoma-associated antigens to be presented by both childhood and adult tumors (WNT5A, INSM2, NDUFA4L2, OLIG3, BTBD17, EFS, SERTAD4) as well as five presented across all subgroups (SPINK8, WNT5A, NDUFA4L2, BTBD17, EFS). Three antigens were exclusively identified in the non-WNT/non-SHH subgroup, whereas five and two ones were shared by non-WNT/non-SHH and SHH-activated (INSM2, HES4, IGFBPL1, DCX, OLIG3) or by WNT- and SHH-activated neoplasms (VMA21, SERTAD4), respectively. Peptide sequences and their HLA restriction, a listing of positive patients, and the GTEx profile of the corresponding source protein can be retrieved from Supplementary Table 11. Of note, none of these medulloblastoma-associated HLA class I antigens exhibited a CTA-like expression profile.

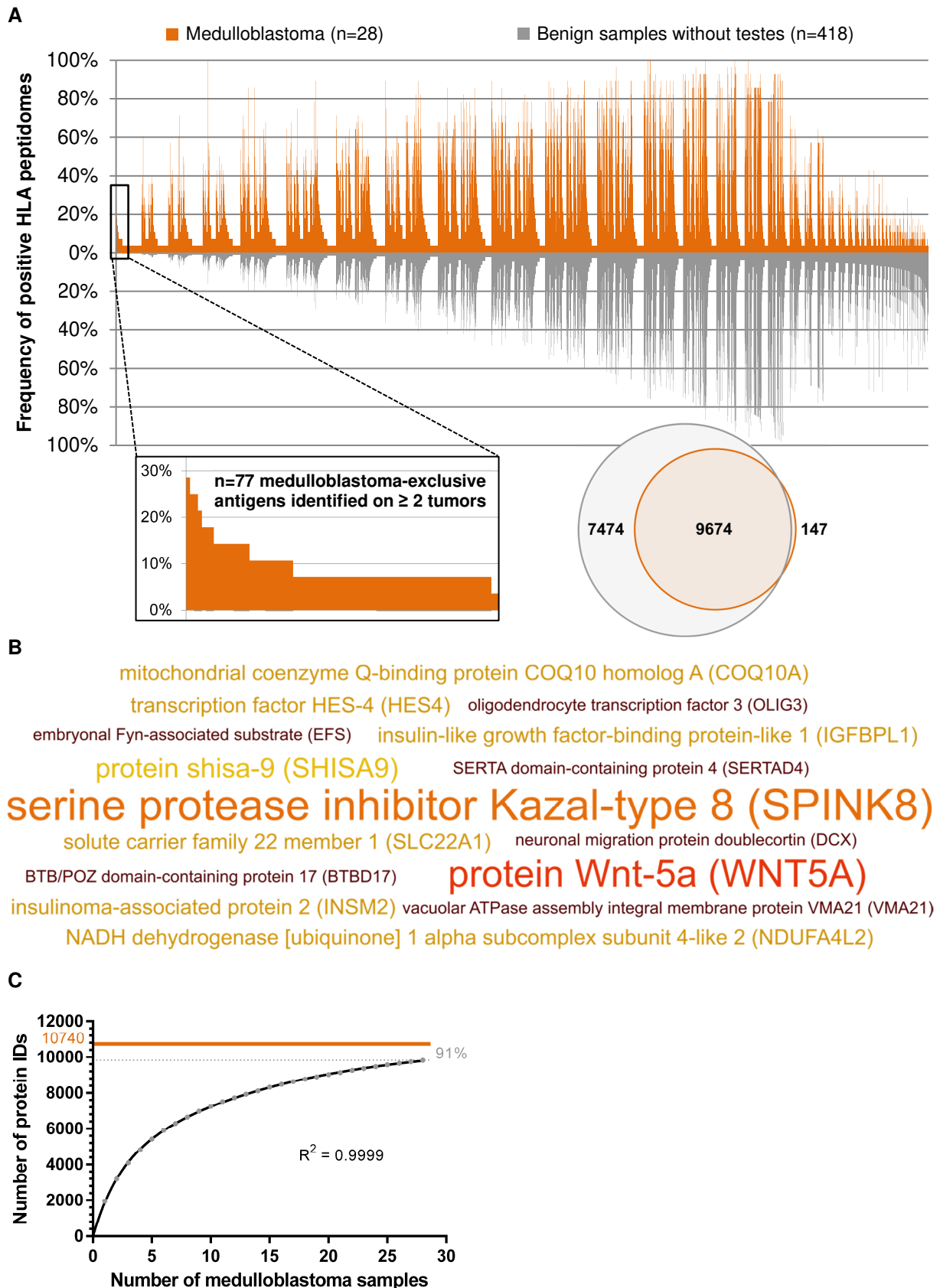


Figure 25. Definition of medulloblastoma-associated antigens based on class I immunopeptidome analyses. (A) Comparative profiling of the HLA class I peptidome of medulloblastoma versus an in-house benign database. Each bar in this waterfall plot (associated with the x-axis) represents a single source protein, whereas the frequency of positive HLA peptidomes is shown on the y-axis, separately for medulloblastoma (n=28) and benign samples without testes

(n=418 covering 29 different human tissues). Those source proteins detected on a maximum of one non-CNS-related tissue were designated as medulloblastoma-exclusive, whereby n=77 were identified on at least two tumors (highlighted as enlarged view on the left). The Venn diagram on the right illustrates the number of distinct HLA class I-presented antigens per group, however, the overlap cannot map the permission of one positive non-CNS-related sample within the benign dataset. **(B) Word cloud of medulloblastoma-associated antigens.** Based on comparative profiling and subsequent quality control of underlying peptides (HLA motifs as well as multi-mapping to several source proteins), a set of 15 medulloblastoma-associated antigens naturally presented on 11-29% of tumors was defined. The font size in the word cloud is proportional to the frequency of positive specimens. **(C) Saturation analysis for the identification of antigens represented by HLA class I ligands on medulloblastoma tissue.** For each source count, the mean number of antigens was calculated by 1,000 random samplings. Using non-linear regression, an exponential function with a forced y-intercept of 0 (internal data created by Daniel Kowalewski at the Department of Immunology, University of Tübingen indicate that subjecting cell-free lysis buffer to HLA-IP does not result in peptide identifications) was fitted. The goodness of fit was in the uppermost range ($R^2 = 0.9999$). Based on this curve, the maximum attainable number of distinct source proteins was estimated (highlighted as solid line). With the available number of 28 medulloblastoma samples, 91% of the estimated maximum attainable amount of distinct HLA class I-presented proteins had been identified.

On the peptide level, 32,199 distinct HLA class I ligands were eluted from medulloblastomas (n=28), obtaining 75% of the estimated maximum attainable coverage (Figure 26 B). Although the HLA class I peptidome of medulloblastoma showed a pronounced high overlap with that of benign samples, 1,963 medulloblastoma-exclusive peptides presented on at least two tumors were identified (Figure 26 A). Subsequent to manual curation, a set of 34 peptides derived from 38 antigens and presented on 18-29% of tumors was defined. Among these, HLA ligands derived from GFAP, HNRNPK, SNX14, AGRN, DNMT3A, KIF1A, and GABRG2 were the most frequent ones. Although only two adults were part of the cohort, twelve medulloblastoma-associated peptides were eluted from both childhood and adult tumors. Considering the different subgroups, 13 peptides proved to be pan-medulloblastoma targets, whereas WNT- and SHH-activated or WNT-activated and non-WNT/non-SHH shared two peptides each. One HLA class I ligand was exclusively part of the immunopeptidome of non-WNT/non-SHH medulloblastomas. Peptide sequences and their HLA restriction, a listing of positive patients, and the corresponding source protein are given in Supplementary Table 12.

Combining the list of peptides derived from HLA class I-presented medulloblastoma-associated antigens (Supplementary Table 11) with that of HLA class I ligands designated as medulloblastoma-associated (Supplementary Table 12) gave n=66 candidate target peptides for cancer immunotherapy. These cover 98.64% of the world population (Supplementary Figure 7), whereby an average of 14 peptides are expected to match per patient. The population coverage on a per-country basis is shown in Figure 27.

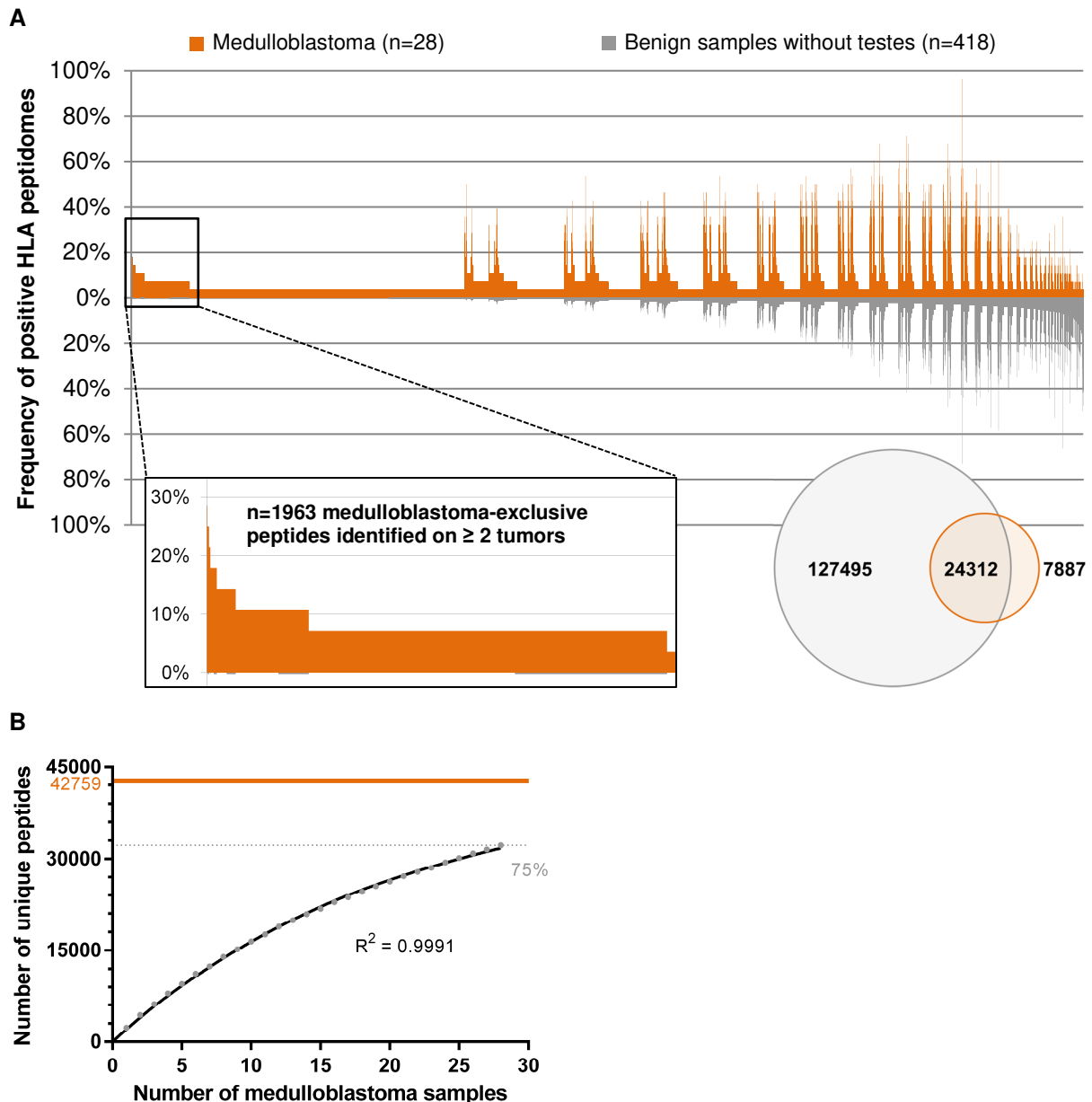


Figure 26. HLA class I peptidomics to define medulloblastoma-associated peptides. (A) Comparative profiling of HLA class I ligands presented on medulloblastoma versus an in-house benign database. Every peptide evaluated for tumor association is represented by a bar in the waterfall plot (associated with the x-axis), whereas the y-axis shows the frequency of positive HLA peptidomes, separately for medulloblastoma (n=28) and benign samples without testes (n=418 covering 29 different human tissues). Peptides were designated as medulloblastoma-exclusive, when detected on a maximum of one non-CNS-related tissue, whereby n=1,963 were identified on at least two neoplasms (highlighted as enlarged view on the left). The number of distinct HLA class I ligands per group is illustrated by the Venn diagram on the right, whereby the overlap cannot map the permission of one positive non-CNS-related sample within the benign dataset. **(B) Saturation analysis for the identification of HLA class I ligands in medulloblastoma tissue.** For each source count, the mean number of peptides was calculated by 1,000 random samplings. Using non-linear regression, an exponential function with a forced y-intercept of 0 (internal data created by Daniel Kowalewski at the Department of Immunology, University of Tübingen indicate that subjecting cell-free lysis buffer to HLA-IP does not result in peptide identifications) was fitted. The goodness of fit was in the uppermost range ($R^2 = 0.9991$). Based on this curve, the maximum attainable number of distinct peptides was estimated (highlighted as solid lines). With the available number of 28 medulloblastoma samples, 75% of the estimated maximum attainable amount of distinct HLA class I ligands had been identified.

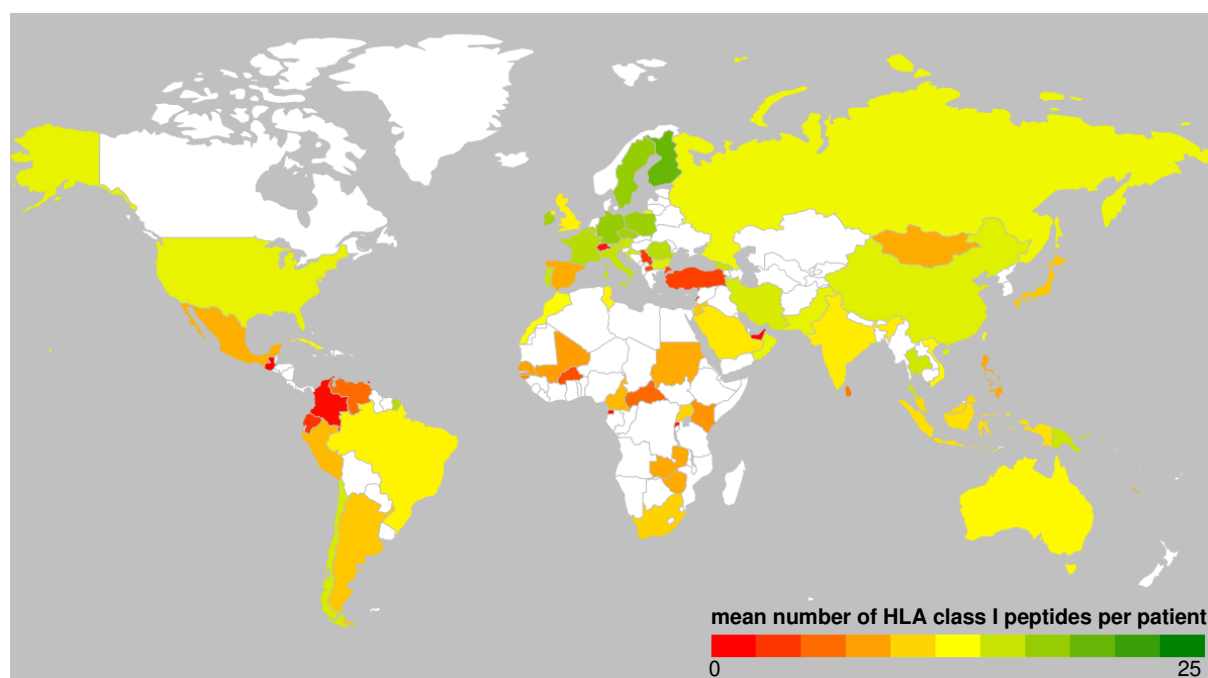
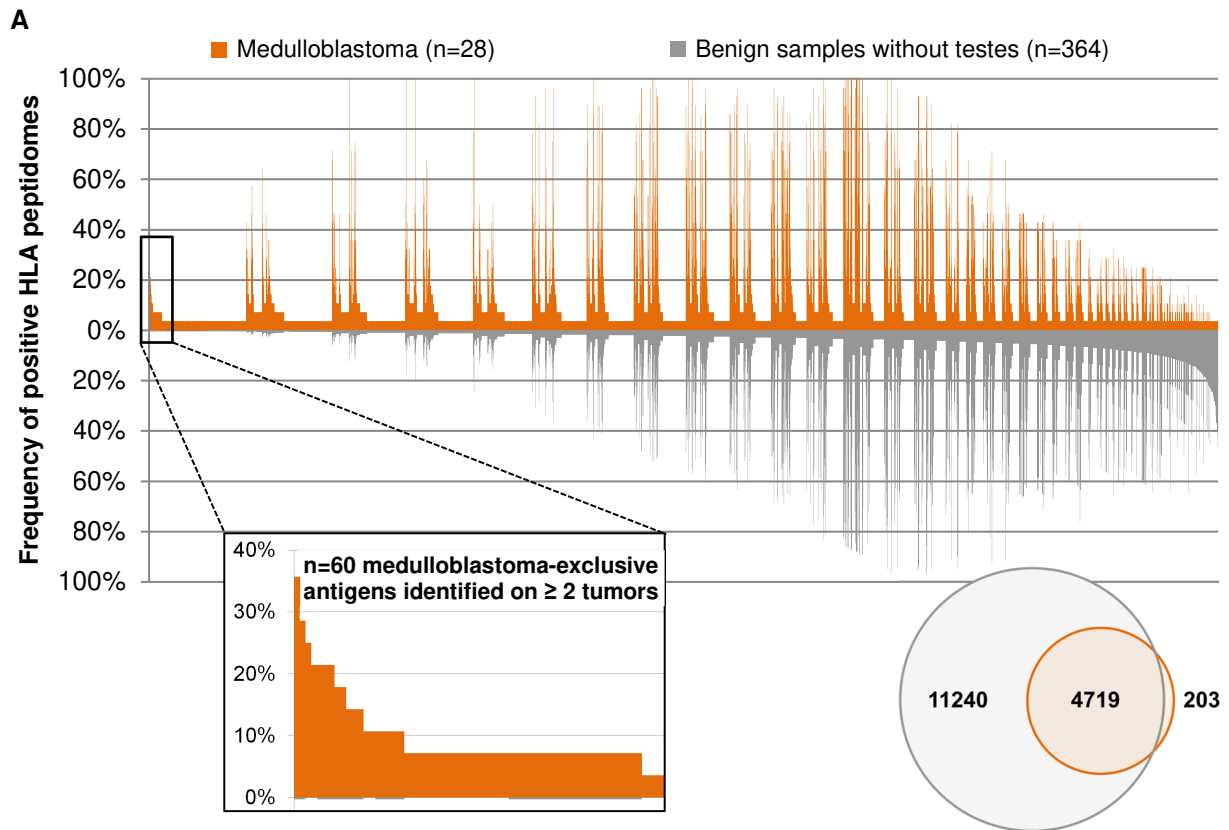


Figure 27. Population coverage of medulloblastoma-associated HLA class I peptides. Using the population coverage tool provided by the IEDB Analysis Resource¹⁴, the population coverage of the n=66 candidate target peptides for medulloblastoma immunotherapy was calculated on a per-country basis. On average, 14 HLA class I peptides match per patient worldwide. For visualization of the United Kingdom, the individual values of England, Northern Ireland, Scotland, and Wales were multiplied with the relative area portion. Countries not included in the IEDB tool or not covered by the geographic heat map add-on of Microsoft Excel are colorless.

Medulloblastoma-associated HLA class II antigens

HLA class II peptidome analyses of medulloblastoma allowed the identification of 4,922 distinct source proteins giving rise to HLA class II-restricted peptides. These represent 71% of the estimated maximum attainable amount of distinct antigens (Figure 28 C). Although medulloblastomas largely overlapped with benign samples, 60 antigens were exclusively presented by at least two tumors (Figure 28 A). Following manual curation of the underlying peptides for peptide length and the presence of length variants as well as multi-mapping to several source proteins, a set of ten medulloblastoma-associated antigens and corresponding peptides naturally presented on 11-36% of tumors was created. Among these, IGFBPL1, CBX4, ESCO1, SYCP3, and CCDC59 were the most frequent ones (Figure 28 B). Three of the medulloblastoma-associated antigens were identified across all subgroups (CBX4, ESCO1, LLPH) and five ones were shared by non-WNT/non-SHH and SHH-activated tumors (IGFBPL1, SYCP3, PLA2G7, PCDH20, CGGBP1). WNT- and SHH-activated neoplasias or WNT-activated and non-SHH/non-WNT tumors had one antigen each in common. Six out of ten tumor-associated antigens were found to be presented on HLA class II in both adult and childhood medulloblastomas (IGFBPL1, CBX4, ESCO1, CCDC59, PCDH20, CGGBP1), although the present study population included only two adults. Peptide sequences, a listing of positive patients, and the GTEx profile of the corresponding source protein can be retrieved from Supplementary Table 11. It is noteworthy that one of these tumor-associated HLA class II antigens (SYCP3) exhibited a CTA-like expression profile with the related SYCP1 being listed in the CTDatabase¹⁵.



B

E3 SUMO-protein ligase CBX4 (CBX4) CGG triplet repeat-binding protein 1 (CGGBP1)
 something about silencing protein 10 (UTP3) **synaptonemal complex protein 3 (SYCP3)**
insulin-like growth factor-binding protein-like 1 (IGFBPL1)
 protein LLP homolog (LLPH) protocadherin-20 (PCDH20)
thyroid transcription factor 1-associated protein 26 (CCDC59)
 platelet-activating factor acetylhydrolase (PLA2G7) **N-acetyltransferase ESCO1 (ESCO1)**

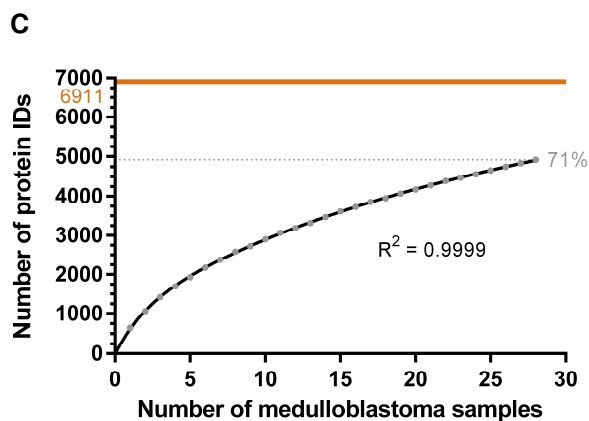


Figure 28. Definition of medulloblastoma-associated antigens based on class II immunopeptidome analyses. (A) Comparative profiling of the HLA class II peptidome of medulloblastoma versus an in-house benign database. Each bar in this waterfall plot (associated with the x-axis) represents a single source protein, whereas the frequency of positive HLA peptidomes is shown on the y-axis, separately for medulloblastoma (n=28) and benign samples without testes

(n=364 covering 30 different human tissues). Those source proteins detected on a maximum of one non-CNS-related tissue were designated as medulloblastoma-exclusive, whereby n=60 were identified on at least two neoplasms (highlighted as enlarged view on the left). The Venn diagram on the right illustrates the number of distinct HLA class II-presented antigens per group, however, the overlap cannot map the permission of one positive non-CNS-related sample within the benign dataset. **(B) Word cloud of medulloblastoma-associated antigens.** Based on comparative profiling and subsequent quality control of underlying peptides (peptide length and/or presence of length variants as well as multi-mapping to several source proteins), a set of ten tumor-associated antigens naturally presented on 11-36% of medulloblastomas was defined. The font size in the word cloud is proportional to the frequency of positive tumors. **(C) Saturation analysis for the identification of antigens represented by HLA class II peptides on medulloblastoma tissue.** For each source count, the mean number of antigens was calculated by 1,000 random samplings. Using non-linear regression, an exponential function with a forced y-intercept of 0 (internal data created by Daniel Kowalewski at the Department of Immunology, University of Tübingen indicate that subjecting cell-free lysis buffer to HLA-IP does not result in peptide identifications) was fitted. The goodness of fit was in the uppermost range ($R^2 = 0.9999$). Based on this curve, the maximum attainable number of distinct source proteins was estimated (highlighted as solid line). With the available number of 28 medulloblastoma samples, 71% of the estimated maximum attainable amount of distinct HLA class II-presented proteins had been identified.

On the peptide level, 25,076 distinct HLA class II-presented peptides were eluted from medulloblastomas (n=28), obtaining 66% of the estimated maximum attainable coverage (Figure 29 B). Subsequent to comparative profiling, all antigens represented by at least one tumor-exclusive HLA class II-presented peptide were subjected to hotspot analysis (Figure 29 A). Medulloblastoma-associated HLA class II presentation hotspots were defined to have a minimum length of eight AA and to be covered by peptides identified in at least five patients, while not having matching sequences in benign samples. This identified a set of eleven antigens harboring regions uniquely presented on tumor tissue with peptide-specific frequencies reaching up to 43% of positive HLA peptidomes. Half of these hotspot targets were represented within the immunopeptidome of all medulloblastoma subgroups or of both adult and childhood tumors, respectively. One hotspot target each was exclusively presented by non-SHH/non-WNT and SHH-activated tumors each, whereas non-SHH/non-WNT and SHH-activated medulloblastomas had two proteins harboring HLA class II presentation hotspots in common. Furthermore, SHH- and WNT-activated or non-SHH/non-WNT and WNT-activated neoplasms shared one protein with hotspot-derived peptides each, respectively. Peptide sequences, a listing of positive patients, and the corresponding source protein are given in Supplementary Table 13.

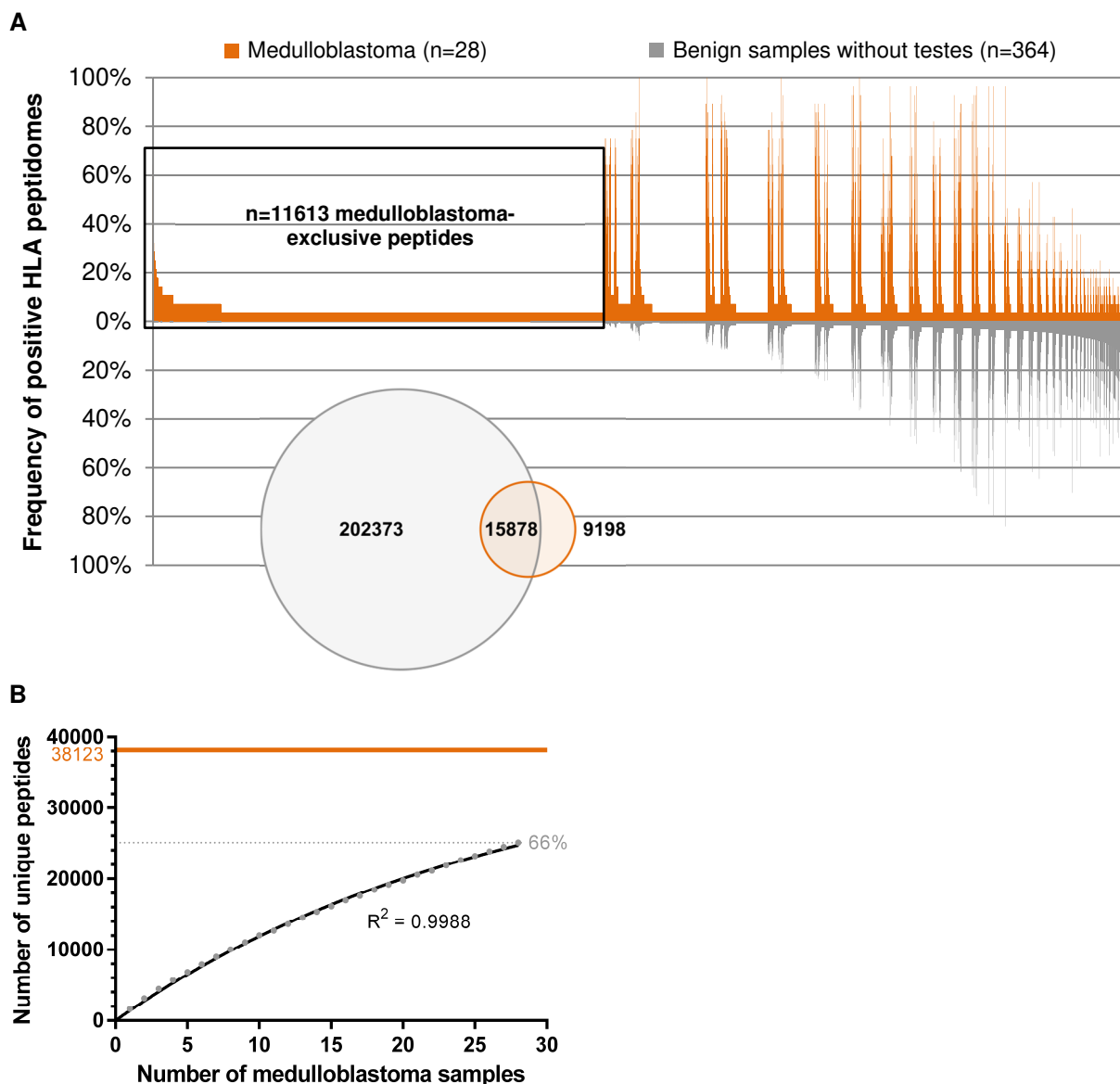


Figure 29. HLA class II peptidomics to define medulloblastoma-associated peptides (A) Comparative profiling of HLA class II peptides presented on medulloblastoma versus an in-house benign database. Every peptide evaluated for tumor association is represented by a bar in the waterfall plot (associated with the x-axis), whereas the y-axis shows the frequency of positive HLA peptidomes, separately for medulloblastoma (n=28) and benign samples without testes (n=364 covering 30 different human tissues). Being detected on a maximum of one non-CNS-related tissue, n=11,613 peptides were designated as medulloblastoma-exclusive. Corresponding source proteins were subjected to hotspot analysis. The number of distinct HLA class II-restricted peptides per group is illustrated by the Venn diagram on the left, whereby the overlap cannot map the permission of one positive non-CNS-related sample within the benign dataset. **(B) Saturation analysis for the identification of HLA class II-presented peptides in medulloblastoma tissue.** For each source count, the mean number of peptides was calculated by 1,000 random samplings. Using non-linear regression, an exponential function with a forced y-intercept of 0 (internal data created by Daniel Kowalewski at the Department of Immunology, University of Tübingen indicate that subjecting cell-free lysis buffer to HLA-IP does not result in peptide identifications) was fitted. The goodness of fit was in the uppermost range ($R^2 = 0.9988$). Based on this curve, the maximum attainable number of distinct peptides was estimated (highlighted as solid line). With the available number of 28 malignant samples, 66% of the estimated maximum attainable amount of distinct HLA class II-presented peptides had been identified.

Comparing medulloblastoma-associated HLA class I- (n=15) and II-presented antigens (n=10) as well as medulloblastoma-associated HLA class I- (n=38 source proteins) and II-restricted peptides (n=11 source proteins), revealed a largely unique antigenic repertoire inherent to HLA class I and II peptidomes. However, IGFBPL1, INSM1, and INSM2 yielded both HLA class I- and II-presented target peptides.

Established CTAs and TAAs naturally presented on medulloblastoma

Considering a total number of 366 established CTAs and TAAs (3.2.1) as well as 16 antigens reported to be associated with medulloblastoma (2.3.2; n=15 overlapped with the general list of CTAs and TAAs), the present HLA peptidome dataset acquired from medulloblastomas was screened for previously published tumor antigens. Of these, n=117 and n=84 were represented by HLA class I ligands and HLA class II-presented peptides, respectively. Although identification rates were comparatively high, CTAs and TAAs were basically presented at low frequency, especially those exclusively identified on medulloblastoma. While none of the HLA class I-presented TAAs and CTAs fulfilling the aforementioned criteria to be designated as tumor-exclusive antigen were identified on more than one specimen, 16 ones were represented by medulloblastoma-exclusive HLA class I ligands on at least two and a maximum of four tumors. On HLA class II, 13 antigens were exclusively identified in the peptidome of medulloblastomas, with RAD51 and GPC2 being the only ones reaching a total of two positive tumors. Eight further CTAs and TAAs were represented by tumor-exclusive HLA class II-presented peptides on 7-14% of neoplasms (Figure 30, Supplementary Table 14).

Chapter 3: Results

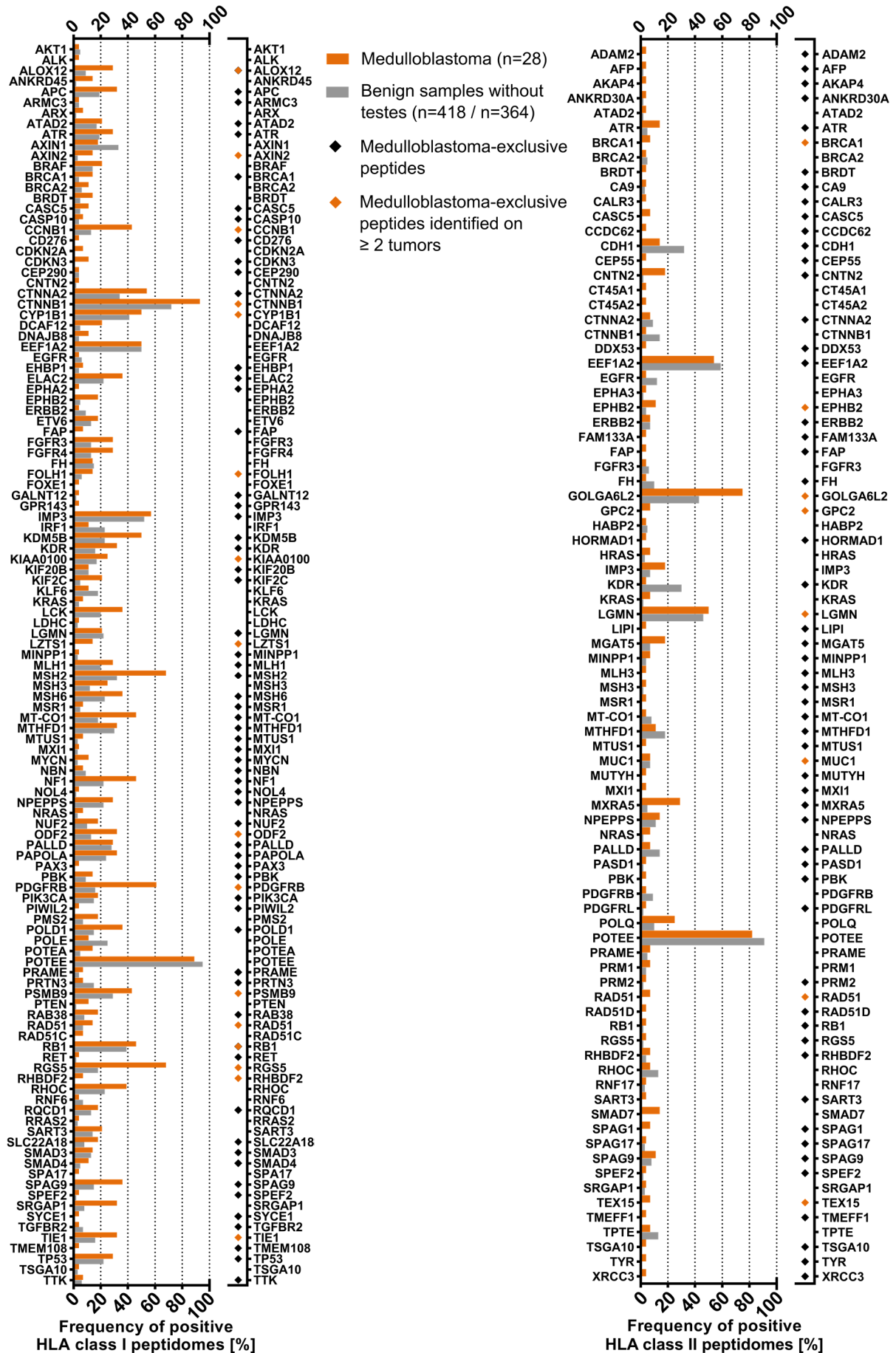


Figure 30. Identification of established TAAs, CTAs, and medulloblastoma-associated antigens across the present HLA peptidome dataset. The present immunopeptidomic dataset included HLA class I ligands derived from 116 TAAs and CTAs (left panel), with 16 being represented by medulloblastoma-exclusive peptides on at least two tumors (highlighted with orange diamonds). The frequency of positive HLA peptidomes was assessed based on HLA class I ligands for tumor samples, whereby benign hits were reported independent of HLA binding probabilities of the underlying peptide identifications. Concerning HLA class II (right panel), a total of 85 TAAs and CTAs were found to be naturally presented on medulloblastoma. Among these, eight yielded tumor-exclusive peptides attaining a presentation frequency of $\geq 7\%$ (highlighted with orange diamonds). While peptides mapping to multiple source proteins were considered to calculate the frequency of positive HLA peptidomes, these were excluded to report the representation by medulloblastoma-exclusive peptides. CTAs and TAAs exclusively identified on benign samples were not listed.

5 Discussion

Medulloblastoma is the most common pediatric malignancy of the CNS, which represents the top-ranking localization of childhood tumors and the leading cause of death due to cancer in children.¹⁻³ Surgery, chemotherapy, and radiotherapy achieve cure rates of up to 75%, however, radiation of the developing brain causes severe long-term sequelae and recurrent medulloblastoma has remained largely incurable.⁴⁻⁹ Cancer immunotherapy may replace radiotherapy in multimodal therapeutic regimens and represent an option to manage disease recurrence. Herein, we present the first investigation of the immunopeptidomic landscape of medulloblastoma to define HLA class I- and II-restricted candidate targets.

Both HLA class I- and II-presented peptides were eluted in considerable amounts from 28 primary medulloblastoma samples proving this cancer entity to be well suitable for studies of the HLA peptidome. Expression of HLA molecules and presentation of a manifold repertoire of peptides, which seems to apply for medulloblastoma, does also represent a prerequisite for immunotherapeutic intervention. This result was actually not expected, since several components of the antigen processing machinery (e.g. HLA-A, -B, and -C, calnexin, β_2m , LMP2, LMP7) have previously been reported to be down-regulated in medulloblastoma.¹⁶ We could only observe the apparent down-modulation of HLA expression when analyzing the medulloblastoma cell lines MM8A, D341, D283 Med, and DAOY (800-2,200 μ l cell pellet volumes) yielding 32-772 HLA class I and 98-354 HLA class II peptides when acquiring two technical replicates consuming 14% sample share each on an Orbitrap Fusion Lumos (data not shown). This again emphasizes that the use of cell lines represents an inferior substitute for primary human tumor samples.¹⁷ Nevertheless, there were obvious hints of reduced HLA class I expression in specimen SA4. We ruled out poor quality of the tissue lysate or W6/32 antibody, failure during ZipTip_{C18}[®] purification, and technical issues during LC-MS/MS, as HLA class II peptide yields were fine, the identical W6/32 batch passed quality control and was employed for several samples with high numbers of HLA class I peptide identifications, direct injection was performed, and as the HLA class I peptide eluate was measured prior to that of HLA class II, while the LC-MS/MS system ran at good performance. This presumption will be validated, once analysis of RNA expression data has been completed. Relative HLA class I and II peptide yields obtained from fresh frozen tissue were significantly higher as compared with samples previously embedded in Bamberker medium or Tissue-Tek[®] O.C.T.[™]. This may, on the one hand, be reasoned by remnants of embedding material falsifying determined

sample weights and, on the other hand, by interferences to antibody binding efficiency during HLA-IP and/or also during MS. The latter appears very plausible as samples previously embedded in Tissue-Tek® O.C.T.™ showed a large number of interfering peaks in the total ion chromatogram (from minute 80 of the LC gradient) comparable in height to the typical CHAPS peak observed around minute 105 to 110. It turned out that these were series of peaks of the positively charged PEG with a distance of 44 m/z. PEG is – like CHAPS – known to cause ion suppression (and isobaric interference) in LC-MS/MS.¹⁸⁻²⁰ A different average purity of HLA class I peptide eluates was observed across the four different institutions, which can be reasoned by discrepancies in sample collection. In Zürich, sample collection for immunopeptidomics has been a well-established routine process since many years, whereas surgical staff in Hamburg, Sankt Augustin, and Würzburg has far less experience with sample requirements for HLA peptidomics. This problem could be addressed by transferring standard operating procedures of sample collection with the purpose to isolate HLA ligands from Zürich, providing samples with the best purities, to other institutions.

The present study population having a female-to-male ratio of 2:3 and a median age of onset of eight years constituted a representative cohort of medulloblastoma patients.¹ In total, n=4 WNT-activated (14%), n=7 SHH-activated (25%), n=2 Group 3, n=2 Group 4, n=8 non-WNT/non-SHH (not differentiated into Group 3 and Group 4), and n=5 without annotation to a subgroup were analyzed including two cases of adult medulloblastoma. The 60 distinct HLA class I allotypes cover 99.95% of the world population, whereby 92.08% of all individuals are expected to be positive for at least three allotypes. We found medulloblastoma to be a – albeit rather sparse – source of candidate targets for cancer immunotherapy. Antigens appearing tumor-exclusive in the analysis but showing a highly CNS-associated expression profile were excluded since we do not expect to achieve 100% saturation of HLA class I and II protein identifications with the currently available number of 23 benign brain and cerebellum samples. Thus, it is conceivable that brain-specific proteins appear as false-positive tumor-exclusive antigens in comparative profiling. In contrast to other tumors including meningioma, T cells targeting medulloblastoma cross the blood-brain barrier and may then cause on-target off-tumor toxicities in cells presenting CNS-specific antigens.²¹⁻²⁴ The search for frequently presented medulloblastoma-associated antigens uncovered 15 and ten for HLA class I and II, respectively. Among these, IGFBPL1 (36%), SPINK8 (29%), WNT5A (25%), CBX4 (21%), ESCO1 (21%), SHISA9 (18%), SYCP3 (18%), and CCDC59 (18%) were the most frequent ones. The neurotrophic insulin-like growth factor axis has a prominent role in regulating CNS development and promoting the growth of tumor cells, including medulloblastoma, ependymoma, meningioma, and glioma, *via* anti-apoptotic and mitogenic peptides.²⁵⁻²⁸ Several members of the insulin-like growth factor binding protein family have been associated with ependymomas and medulloblastomas by being elevated in comparison with control cerebella and indicating poor prognosis when expressed at high levels.²⁹ SPINK8, spanning only 97 AA,³⁰ is not expressed above background levels (10 TPM) in benign human tissues and has been suggested to be epididymis-specific.^{10,31,32} Other Kazal-type serine peptidase inhibitors such as SPINK1, also called secretory tumor-associated trypsin inhibitor, have been found to be over-expressed in various cancer entities, to promote tumor progression, and to correlate with adverse prognosis.³³⁻³⁷ In colorectal carcinoma, SPINK1 has been suggested to act by inhibiting Metallothionein tumor suppressors.³⁴ A member of the oncogenic WNT protein

family was identified with WNT5A, which is renowned for tumor-associated elevated expression.^{38,39} WNT5A was, however, not specific for tumors of the WNT-activated subgroup, but identified in SHH-activated and non-WNT/non-SHH medulloblastomas as well. Furthermore, HLA class I-presented peptides derived from WNT5A were identified in 51 malignant samples other than medulloblastoma. An oncogenic function exerted by activation of Notch1 signaling has also been attributed to CBX4.⁴⁰ Moreover, CBX4-mediated sumoylation activates the oncogenic DNA repair protein BMI-1, which has been implied for targeted therapy in pediatric diffuse intrinsic pontine glioma.⁴¹⁻⁴⁵ Besides promoting cell cycle progression as well as cancer cell migration and metastasis,^{40,41,45} CBX4 is also angiogenic by promoting VEGF expression and governing the hypoxia-inducible factor 1- α .⁴⁶ The acetyltransferase ESCO1 accomplishes sister chromatid cohesion during the S phase of DNA replication facilitating and speeding the traverse of replication forks – a beneficial feature for malignant cells.⁴⁷⁻⁴⁹ In turn, little is known about SHISA9 (seven PubMed entries⁵⁰), which is not expressed with more than 7 TPM in any benign human tissue.¹⁰ SHISA9, also named CKAMP44, is a subunit of synaptic glutamatergic α -amino-3-hydroxy-5-methyl-4-isoxazolepropionic acid (AMPA) receptors with regulatory functions in neurotransmission and synaptic plasticity.⁵¹⁻⁵³ SYCP3 did not only exhibit a CTA-like expression profile,¹⁰ but is also described as testis-specific protein regulating sister chromosome segregation during meiosis with aberrant expression in malignant – including brain tumor – cells.⁵⁴⁻⁵⁸ Since the related SYCP1 is listed in the CTDDatabase,¹⁵ it appears obvious that SYCP3 represents a novel CTA naturally presented on HLA class II molecules. CCDC59, referred to as thyroid transcription factor 1-associated protein 26, is a poorly studied protein (seven PubMed entries⁵⁹) with reported function in the regulation of surfactant protein synthesis in the lung.⁶⁰⁻⁶²

Investigating acquired immunopeptidomic data for medulloblastoma-associated peptides unveiled a set of 34 HLA class I ligands derived from 38 antigens presented on 18-29% of tumors as well as of eleven antigens harboring medulloblastoma-associated HLA class II presentation hotspots giving rise to naturally presented peptides across at least five patients. It was conspicuous that the two most frequent medulloblastoma-associated HLA class I ligands were 10-mers, which is not the typical length of HLA class I-presented peptides, annotated to multiple HLA allotypes not perfectly matching the motif. Moreover, we observed a large number of HLA-A*25:01 and -A*26:01 ligands among both medulloblastoma-associated and CTA- or TAA-derived tumor-exclusive peptides. A total of 17 samples included in the benign dataset were positive for HLA-A*25:01 and/or -A*26:01 with none of them representing a CNS-related tissue. This implies an insufficient coverage of the tissue of tumor origin regarding these HLA allotypes and all tumor-exclusive peptides binding to HLA-A*25:01 or -A*26:01 were consequently excluded from candidate target lists. Conversely, the benign dataset of CNS-related samples covered twelve HLA-A allotypes (A*01:01, A*02:01, A*02:05, A*03:01, A*11:01, A*23:01, A*24:02, A*30:01, A*32:01, A*68:01, A*68:02, A*69:01), 16 HLA-B allotypes (B*07:02, B*08:01, B*13:02, B*14:02, B*15:01, B*27:05, B*35:01, B*35:03, B*35:08, B*37:01, B*40:02, B*44:02, B*45:01, B*49:01, B*50:01, B*58:01), and 10 HLA-C allotypes (C*02:02, C*03:03, C*03:04, C*04:01, C*06:02, C*07:01, C*07:02, C*07:04, C*08:02, C*16:01). Medulloblastoma-exclusive peptide hits were only pursued when the corresponding HLA class I allotype was contained in the CNS subset of the benign reference peptidome database. It was striking that overlapping medulloblastoma-associated HLA class I- and II-presented

antigens (n=10) as well as tumor-associated HLA class I- and II-restricted peptides, revealed a largely unique antigenic repertoire inherent to HLA class I and II peptidomes with only three antigens (IGFBPL1, INSM1, INSM2) yielding both HLA class I- and II-presented target peptides. This underlines the necessity to respect both HLA classes on both antigen and peptide level for comprehensive target discovery approaches. Besides that, we found a significant proportion of candidate targets to be pan-medulloblastoma peptides or antigens as being coincidentally eluted from WNT-activated, non-WNT/non-SHH, and SHH-activated neoplasms (n=5 / n=13 HLA class I antigen / peptide targets, n=3 / n=5 HLA class II antigen / hotspot targets). Likewise, almost half of all medulloblastoma-associated antigens and peptides was shared by childhood and adult tumors (n=7 / n=12 HLA class I antigen / peptide targets, n=6 / n=6 HLA class II antigen / hotspot targets). In this context, it should be added that the number of targets presented independent of patient age is expected to be even higher, as only two cases of adult medulloblastoma were included in the present cohort. This allows the conclusion that medulloblastoma subgroups exhibit a common antigenic signature promising that defined targets are broadly applicable in medulloblastoma immunotherapy. Combining the list of medulloblastoma-associated antigens and peptides presented on HLA class I (n=66 candidate target peptides for cancer immunotherapy), these achieve a world population coverage of 98.64% whereby an average of 14 peptides are expected to match per patient. Established CTAs and TAAs failed to fulfil the requirements of frequent and tumor-exclusive presentation as being either anecdotally detected in very few tumors or being broadly identified on both malignant and benign tissues. Considering these turned out to be no valuable contribution to defining candidate targets for medulloblastoma immunotherapy. This strongly advises against basing target discovery approaches solely on RNA expression, protein, or immunohistochemistry data, as the HLA peptidome represents an autonomous layer molded by the antigen processing machinery.^{17,63-66}

Once analysis of transcriptome and DNA methylation profiling data has been completed, we aim to investigate whether an imprint of the present subgroup manifests at these levels. Moreover, we selected a set of 15 HLA class I-restricted peptides covering 14 antigens and common HLA allotypes (HLA-A*01, -A*02, -A*03, -A*11, -A*68, -B*35) to undergo immunogenicity testing. This will include priming of naïve T cells from healthy donors and – if possible – medulloblastoma patients and will be performed by Dr. med. Julia Velz and Gioele Medici in the Laboratory for Molecular Neuro-Oncology at the University of Zürich.

In conclusion, the data presented demonstrate that medulloblastoma is eligible for immunotherapeutic intervention. We mapped the antigenic landscape of medulloblastoma in an unprecedented depth unveiling a novel set of canonical non-mutated tumor-associated peptides and antigens with natural and frequent presentation on HLA class I and II molecules. These may guide the development of peptide-specific immunotherapies such as vaccination with DCs and peptides or T cell-based strategies which may eventually represent an option to manage disease recurrence and replace radiotherapy in multimodal therapeutic regimens.

6 References

1. Ostrom QT, Cioffi G, Gittleman H, Patil N, Waite K, Kruchko C, Barnholtz-Sloan JS. CBTRUS Statistical Report: Primary Brain and Other Central Nervous System Tumors Diagnosed in the United States in 2012-2016. *Neuro Oncol.* 2019;21(Supplement 5):v1-v100.
2. de Blank PM, Ostrom QT, Rouse C, Wolinsky Y, Kruchko C, Salcido J, Barnholtz-Sloan JS. Years of life lived with disease and years of potential life lost in children who die of cancer in the United States, 2009. *Cancer Med.* 2015;4(4):608-619.
3. Louis DN, Perry A, Reifenberger G, von Deimling A, Figarella-Branger D, Cavenee WK, Ohgaki H, Wiestler OD, Kleihues P, Ellison DW. The 2016 World Health Organization Classification of Tumors of the Central Nervous System: a summary. *Acta Neuropathol.* 2016;131(6):803-820.
4. Massimino M, Biassoni V, Gangola L, Garre ML, Gatta G, Giangaspero F, Poggi G, Rutkowski S. Childhood medulloblastoma. *Crit Rev Oncol Hematol.* 2016;105:35-51.
5. Martin AM, Raabe E, Eberhart C, Cohen KJ. Management of pediatric and adult patients with medulloblastoma. *Curr Treat Options Oncol.* 2014;15(4):581-594.
6. Johnsen JI, Kogner P, Albiñá A, Henriksson MA. Embryonal neural tumours and cell death. *Apoptosis.* 2009;14(4):424-438.
7. Packer RJ, Gajjar A, Vezina G, Rorke-Adams L, Burger PC, Robertson PL, Bayer L, LaFond D, Donahue BR, Marymont MH, Muraszko K, Langston J, Spoto R. Phase III study of craniospinal radiation therapy followed by adjuvant chemotherapy for newly diagnosed average-risk medulloblastoma. *J Clin Oncol.* 2006;24(25):4202-4208.
8. Spiegler BJ, Bouffet E, Greenberg ML, Rutka JT, Mabbott DJ. Change in neurocognitive functioning after treatment with cranial radiation in childhood. *J Clin Oncol.* 2004;22(4):706-713.
9. Mabbott DJ, Penkman L, Witol A, Strother D, Bouffet E. Core neurocognitive functions in children treated for posterior fossa tumors. *Neuropsychology.* 2008;22(2):159-168.
10. The GTEx Consortium. The Genotype-Tissue Expression (GTEx) project. *Nat Genet.* 2013;45(6):580-585.
11. Szolek A, Schubert B, Mohr C, Sturm M, Feldhahn M, Kohlbacher O. OptiType: precision HLA typing from next-generation sequencing data. *Bioinformatics.* 2014;30(23):3310-3316.
12. Cock PJ, Fields CJ, Goto N, Heuer ML, Rice PM. The Sanger FASTQ file format for sequences with quality scores, and the Solexa/Illumina FASTQ variants. *Nucleic Acids Res.* 2010;38(6):1767-1771.
13. Mohr C, Friedrich A, Wojnar D, Kenar E, Polatkan AC, Codrea MC, Czernemmel S, Kohlbacher O, Nahnsen S. qPortal: A platform for data-driven biomedical research. *PLoS One.* 2018;13(1):e0191603.
14. Vita R, Overton JA, Greenbaum JA, Ponomarenko J, Clark JD, Cantrell JR, Wheeler DK, Gabbard JL, Hix D, Sette A, Peters B. The immune epitope database (IEDB) 3.0. *Nucleic Acids Res.* 2015;43(Database issue):D405-412.
15. Almeida LG, Sakabe NJ, deOliveira AR, Silva MC, Mundstein AS, Cohen T, Chen YT, Chua R, Gurung S, Gnajatic S, Jungbluth AA, Caballero OL, Bairoch A, Kiesler E, White SL, Simpson AJ, Old LJ, Camargo AA, Vasconcelos AT. CTdatabase: a knowledge-base of high-throughput and curated data on cancer-testis antigens. *Nucleic Acids Res.* 2009;37(Database issue):D816-819.
16. Raffaghello L, Nozza P, Morandi F, Camoriano M, Wang X, Garrè ML, Cama A, Basso G, Ferrone S, Gambini C, Pistoia V. Expression and functional analysis of human leukocyte antigen class I antigen-processing machinery in medulloblastoma. *Cancer Res.* 2007;67(11):5471-5478.
17. Freudenmann LK, Marcu A, Stevanović S. Mapping the tumour human leukocyte antigen (HLA) ligandome by mass spectrometry. *Immunology.* 2018;154(3):331-345.
18. Zhang N, Li L. Effects of common surfactants on protein digestion and matrix-assisted laser desorption/ionization mass spectrometric analysis of the digested peptides using two-layer sample preparation. *Rapid Commun Mass Spectrom.* 2004;18(8):889-896.
19. Temesi D, Law B, Howe N. Synthesis and evaluation of PEG414, a novel formulating agent that avoids analytical problems associated with polydisperse vehicles such as PEG400. *J Pharm Sci.* 2003;92(12):2512-2518.
20. Tong XS, Wang J, Zheng S, Pivnichny JV, Griffin PR, Shen X, Donnelly M, Vakerich K, Nunes C, Fenyk-Melody J. Effect of signal interference from dosing excipients on pharmacokinetic screening of drug candidates by liquid chromatography/mass spectrometry. *Anal Chem.* 2002;74(24):6305-6313.
21. Wilson EH, Weninger W, Hunter CA. Trafficking of immune cells in the central nervous system. *J Clin Invest.* 2010;120(5):1368-1379.
22. Dettori P, Bradac GB, Scialfa G. Selective angiography of the external and internal carotid arteries in the diagnosis of supra-tentorial meningiomas. *Neuroradiology.* 1970;1(3):166-172.
23. Manaka H, Sakata K, Tatezaki J, Shinohara T, Shimohigoshi W, Yamamoto T. Safety and Efficacy of Preoperative Embolization in Patients with Meningioma. *J Neuro Surg B Skull Base.* 2018;79(Suppl 4):S328-s333.
24. Bhowmik A, Khan R, Ghosh MK. Blood brain barrier: a challenge for effectual therapy of brain tumors. *Biomed Res Int.* 2015;2015:320941.
25. Russo VC, Gluckman PD, Feldman EL, Werther GA. The insulin-like growth factor system and its pleiotropic functions in brain. *Endocr Rev.* 2005;26(7):916-943.


Chapter 3: References

26. Wang JY, Del Valle L, Gordon J, Rubini M, Romano G, Croul S, Peruzzi F, Khalili K, Reiss K. Activation of the IGF-IR system contributes to malignant growth of human and mouse medulloblastomas. *Oncogene*. 2001;20(29):3857-3868.
27. Zumkeller W, Westphal M. The IGF/IGFBP system in CNS malignancy. *Mol Pathol*. 2001;54(4):227-229.
28. Samani AA, Yakar S, LeRoith D, Brodt P. The role of the IGF system in cancer growth and metastasis: overview and recent insights. *Endocr Rev*. 2007;28(1):20-47.
29. de Bont JM, van Doorn J, Reddingius RE, Graat GH, Passier MM, den Boer ML, Pieters R. Various components of the insulin-like growth factor system in tumor tissue, cerebrospinal fluid and peripheral blood of pediatric medulloblastoma and ependymoma patients. *Int J Cancer*. 2008;123(3):594-600.
30. UniProt: the universal protein knowledgebase. *Nucleic Acids Res*. 2017;45(D1):D158-d169.
31. Jalkanen J, Kotimäki M, Huhtaniemi I, Poutanen M. Novel epididymal protease inhibitors with Kazal or WAP family domain. *Biochem Biophys Res Commun*. 2006;349(1):245-254.
32. Jeong J, Lee B, Kim J, Kim J, Hong SH, Kim D, Choi S, Cho BN, Cho C. Expressional and functional analyses of epididymal SPINKs in mice. *Gene Expr Patterns*. 2019;31:18-25.
33. Marshall A, Lukk M, Kutter C, Davies S, Alexander G, Odom DT. Global gene expression profiling reveals SPINK1 as a potential hepatocellular carcinoma marker. *PLoS One*. 2013;8(3):e59459.
34. Tiwari R, Pandey SK, Goel S, Bhatia V, Shukla S, Jing X, Dhanasekaran SM, Ateeq B. SPINK1 promotes colorectal cancer progression by downregulating Metallothioneins expression. *Oncogenesis*. 2015;4:e162.
35. Kelloniemi E, Rintala E, Finne P, Stenman UH. Tumor-associated trypsin inhibitor as a prognostic factor during follow-up of bladder cancer. *Urology*. 2003;62(2):249-253.
36. Tomlins SA, Rhodes DR, Yu J, Varambally S, Mehra R, Perner S, Demichelis F, Helgeson BE, Laxman B, Morris DS, Cao Q, Cao X, Andrén O, Fall K, Johnson L, Wei JT, Shah RB, Al-Ahmadie H, Eastham JA, Eggener SE, Fine SW, Hotakainen K, Stenman UH, Tsodikov A, Gerald WL, Lilja H, Reuter VE, Kantoff PW, Scardino PT, Rubin MA, Bjartell AS, Chinnaiyan AM. The role of SPINK1 in ETS rearrangement-negative prostate cancers. *Cancer Cell*. 2008;13(6):519-528.
37. Paju A, Vartiainen J, Haglund C, Itkonen O, von Boguslawski K, Leminen A, Wahlström T, Stenman UH. Expression of trypsinogen-1, trypsinogen-2, and tumor-associated trypsin inhibitor in ovarian cancer: prognostic study on tissue and serum. *Clin Cancer Res*. 2004;10(14):4761-4768.
38. Howng SL, Wu CH, Cheng TS, Sy WD, Lin PC, Wang C, Hong YR. Differential expression of Wnt genes, beta-catenin and E-cadherin in human brain tumors. *Cancer Lett*. 2002;183(1):95-101.
39. Smalley MJ, Dale TC. Wnt signalling in mammalian development and cancer. *Cancer Metastasis Rev*. 1999;18(2):215-230.
40. Zeng JS, Zhang ZD, Pei L, Bai ZZ, Yang Y, Yang H, Tian QH. CBX4 exhibits oncogenic activities in breast cancer via Notch1 signaling. *Int J Biochem Cell Biol*. 2018;95:1-8.
41. Hu C, Zhang Q, Tang Q, Zhou H, Liu W, Huang J, Liu Y, Wang Q, Zhang J, Zhou M, Sheng F, Lai W, Tian J, Li G, Zhang R. CBX4 promotes the proliferation and metastasis via regulating BMI-1 in lung cancer. *J Cell Mol Med*. 2020;24(1):618-631.
42. Kumar SS, Sengupta S, Lee K, Hura N, Fuller C, DeWire M, Stevenson CB, Fouladi M, Drissi R. BMI-1 is a potential therapeutic target in diffuse intrinsic pontine glioma. *Oncotarget*. 2017;8(38):62962-62975.
43. Ismail IH, Gagné JP, Caron MC, McDonald D, Xu Z, Masson JY, Poirier GG, Hendzel MJ. CBX4-mediated SUMO modification regulates BMI1 recruitment at sites of DNA damage. *Nucleic Acids Res*. 2012;40(12):5497-5510.
44. Qiu M, Liang Z, Chen L, Tan G, Liu L, Wang K, Chen H, Liu J. MicroRNA-200c suppresses cell growth and metastasis by targeting Bmi-1 and E2F3 in renal cancer cells. *Exp Ther Med*. 2017;13(4):1329-1336.
45. Zhang Z, Bu X, Chen H, Wang Q, Sha W. Bmi-1 promotes the invasion and migration of colon cancer stem cells through the downregulation of E-cadherin. *Int J Mol Med*. 2016;38(4):1199-1207.
46. Li J, Xu Y, Long XD, Wang W, Jiao HK, Mei Z, Yin QQ, Ma LN, Zhou AW, Wang LS, Yao M, Xia Q, Chen GQ. Cbx4 governs HIF-1 α to potentiate angiogenesis of hepatocellular carcinoma by its SUMO E3 ligase activity. *Cancer Cell*. 2014;25(1):118-131.
47. Zhang J, Shi X, Li Y, Kim BJ, Jia J, Huang Z, Yang T, Fu X, Jung SY, Wang Y, Zhang P, Kim ST, Pan X, Qin J. Acetylation of Smc3 by Eco1 is required for S phase sister chromatid cohesion in both human and yeast. *Mol Cell*. 2008;31(1):143-151.
48. Rivera-Colón Y, Maguire A, Liszczak GP, Olia AS, Marmorstein R. Molecular Basis for Cohesin Acetylation by Establishment of Sister Chromatid Cohesion N-Acetyltransferase ESCO1. *J Biol Chem*. 2016;291(51):26468-26477.
49. Terret ME, Sherwood R, Rahman S, Qin J, Jallepalli PV. Cohesin acetylation speeds the replication fork. *Nature*. 2009;462(7270):231-234.
50. Publications listed in PubMed dealing with the protein shisa-9. [Internet]. Available from: <https://www.ncbi.nlm.nih.gov/pubmed/?term=shisa9>, accessed on 2020/04/04.
51. Kunde SA, Rademacher N, Zieger H, Shoichet SA. Protein kinase C regulates AMPA receptor auxiliary protein Shisa9/CKAMP44 through interactions with neuronal scaffold PICK1. *FEBS Open Bio*. 2017;7(9):1234-1245.
52. Karataeva AR, Klaassen RV, Ströder J, Ruiperez-Alonso M, Hjorth JJ, van Nierop P, Spijker S, Mansvelter HD, Smit AB. C-terminal interactors of the AMPA receptor auxiliary subunit Shisa9. *PLoS One*. 2014;9(2):e87360.
53. von Engelhardt J, Mack V, Sprengel R, Kavenstock N, Li KW, Stern-Bach Y, Smit AB, Seeburg PH, Monyer H. CKAMP44: a brain-specific protein attenuating short-term synaptic plasticity in the dentate gyrus. *Science*. 2010;327(5972):1518-1522.

Chapter 3: References

54. Mobasheri MB, Jahanzad I, Mohagheghi MA, Aarabi M, Farzan S, Modarressi MH. Expression of two testis-specific genes, TSGA10 and SYCP3, in different cancers regarding to their pathological features. *Cancer Detect Prev*. 2007;31(4):296-302.
55. Parra MT, Viera A, Gómez R, Page J, Benavente R, Santos JL, Rufas JS, Suja JA. Involvement of the cohesin Rad21 and SCP3 in monopolar attachment of sister kinetochores during mouse meiosis I. *J Cell Sci*. 2004;117(Pt 7):1221-1234.
56. Aarabi M, Modarressi MH, Soltanghoreae H, Behjati R, Amirjannati N, Akhondi MM. Testicular expression of synaptonemal complex protein 3 (SYCP3) messenger ribonucleic acid in 110 patients with nonobstructive azoospermia. *Fertil Steril*. 2006;86(2):325-331.
57. Niemeyer P, Türeci Ö, Eberle T, Graf N, Pfreundschuh M, Sahin U. Expression of serologically identified tumor antigens in acute leukemias. *Leuk Res*. 2003;27(7):655-660.
58. Yuan L, Pelttari J, Brundell E, Björkroth B, Zhao J, Liu JG, Brismar H, Daneholt B, Höög C. The synaptonemal complex protein SCP3 can form multistranded, cross-striated fibers in vivo. *J Cell Biol*. 1998;142(2):331-339.
59. Publications listed in PubMed dealing with the thyroid transcription factor 1-associated protein 26. [Internet]. Available from: <https://www.ncbi.nlm.nih.gov/pubmed/?term=ccdc59> and <https://www.ncbi.nlm.nih.gov/pubmed/?term=thyroid+transcription+factor+1-associated+protein+26>, accessed on 2020/04/04.
60. Yang YS, Yang MC, Wang B, Weissler JC. BR22, a novel protein, interacts with thyroid transcription factor-1 and activates the human surfactant protein B promoter. *Am J Respir Cell Mol Biol*. 2001;24(1):30-37.
61. Yang MC, Guo Y, Liu CC, Weissler JC, Yang YS. The TTF-1/TAP26 complex differentially modulates surfactant protein-B (SP-B) and -C (SP-C) promoters in lung cells. *Biochem Biophys Res Commun*. 2006;344(2):484-490.
62. Boggaram V, Chandru H, Gottipati KR, Thakur V, Das A, Berhane K. Transcriptional regulation of SP-B gene expression by nitric oxide in H441 lung epithelial cells. *Am J Physiol Lung Cell Mol Physiol*. 2010;299(2):L252-262.
63. Weinzierl AO, Lemmel C, Schoor O, Müller M, Krüger T, Wernet D, Hennenlotter J, Stenzl A, Klingel K, Rammensee HG, Stevanović S. Distorted relation between mRNA copy number and corresponding major histocompatibility complex ligand density on the cell surface. *Mol Cell Proteomics*. 2007;6(1):102-113.
64. Fortier MH, Caron É, Hardy MP, Voisin G, Lemieux S, Perreault C, Thibault P. The MHC class I peptide repertoire is molded by the transcriptome. *J Exp Med*. 2008;205(3):595-610.
65. Bassani-Sternberg M, Pletscher-Frankild S, Jensen LJ, Mann M. Mass spectrometry of human leukocyte antigen class I peptidomes reveals strong effects of protein abundance and turnover on antigen presentation. *Mol Cell Proteomics*. 2015;14(3):658-673.
66. Shraibman B, Barnea E, Kadosh DM, Haimovich Y, Slobodin G, Rosner I, López-Larrea C, Hilf N, Kuttruff S, Song C, Britten C, Castle J, Kreiter S, Frenzel K, Tatagiba M, Tabatabai G, Dietrich PY, Dutoit V, Wick W, Platten M, Winkler F, von Deimling A, Kroep J, Sahuquillo J, Martinez-Ricarte F, Rodon J, Lassen U, Ottensmeier C, van der Burg SH, Thor Straten P, Poulsen HS, Ponsati B, Okada H, Rammensee HG, Sahin U, Singh H, Admon A. Identification of Tumor Antigens Among the HLA Peptidomes of Glioblastoma Tumors and Plasma. *Mol Cell Proteomics*. 2019;18(6):1255-1268.

CHAPTER 4



The immunopeptidome of meningioma reveals candidate targets for immunotherapies and delineates modulated presentation of HLA ligands in comparison with autologous dura

Lena Katharina Freudenmann (L.K.F.) planned and performed all HLA peptidome analyses, whereby Lena Mühlenbruch supported HLA-IP of 14/42 samples during the training period in the course of her master thesis. L.K.F. analyzed the entire immunopeptidomic dataset and contributed all figures and texts. HLA allotypes were determined by HistoGenetics and Nagarajan Paramasivam and samples along with clinical metadata were provided by collaborating physicians.

1 Abstract

Meningiomas are the most common neoplasms of the brain and CNS. Tumor localization and disease recurrence exacerbate the therapeutic situation with surgery and radiotherapy representing the only established therapy regimens. Cancer immunotherapy may meet the high demand for contemporary treatments, however, little is known about the antigens to be targeted. Herein, we present the first investigation of the immunopeptidomic landscape of 33 meningiomas for naturally presented target antigens for application in antigen-specific immunotherapeutic approaches. Meningeal neoplasias proved to be a rich source of novel tumor-associated peptides and antigens presented on HLA class I and II molecules. Remarkably, a large fraction were pan-meningioma targets presented across all WHO grades. Established cancer-testis and tumor-associated antigens, however, lacked frequent and/or meningioma-exclusive HLA presentation. In a subset of patients with autologous tumor-free dura being available, relative quantitation of HLA class I- and II-restricted peptide abundances delineated common patterns of modulated peptide presentation. In conclusion, the defined set of meningioma-associated antigens and peptides provides prime candidates to be pursued in the development of future immunotherapies as being naturally, exclusively, and frequently presented on native meningioma tissue. This may contribute to overcome the lack of therapeutic options for non-resectable and recurrent, especially high-grade, meningiomas.

2 Introduction

Meningeal tumors constitute the most frequent brain and CNS neoplasms accounting for an average annual incidence of 30,551 in the US. Despite being diagnosed as non-malignant in almost 99% of cases, these tumors nevertheless cause severe health issues including, among others, seizures and focal neurological deficits.¹⁻⁴ Complete surgical resection of meningiomas localized at the skull base, which is rich in neurovascular structures and where 38% of WHO grade I tumors arise, can be challenging and tumor recurrence of those meningiomas with a more malignant behavior despite multiple resections and radiotherapy is a common clinical problem. Poor progression-free and overall survival rates in particular affect those patients with subtotal resection.^{5,6} So far, no chemotherapy with meningioma as indication has been approved by the FDA and no standard-of-care for the management of recurrent meningiomas has been established.^{5,7} Consequently, there is a high demand for contemporary treatment strategies supplementing surgery and radiotherapy – a demand that could be elegantly serviced by cancer immunotherapy.

One additional reason for investigating T cell-based immunotherapy in meningioma is the fact that the tumor is supplied by vascular branches of the external carotid artery.^{8,9} This is a major difference to the other brain tumor entities discussed previously (glioblastoma and medulloblastoma) which arise within the brain parenchyma itself. The latter (so-called intra-axial) lesions are supplied by branches of the internal carotid artery.¹⁰⁻¹² Within this vascular territory, the actively controlled and dynamic blood-brain barrier (neurovascular unit) creates a partially immunoprivileged niche within the brain parenchyma, but also within the tumor niche and thereby counteracts the entrance of T cells.¹³⁻¹⁵

Potential T-cell targets are underinvestigated in meningiomas and no studies have been conducted to investigate the antigenic repertoire naturally presented on native tumor tissue. We employed an immunopeptidome-centric approach to define meningioma-associated peptides and antigens. For comparative profiling, the in-house benign HLA peptidome database was complemented with autologous tumor-free dura, which was available from nine patients and represents the tissue of tumor origin. Moreover, relative quantitation of HLA class I and II ligand abundances on tumor *versus* autologous non-neoplastic dura was performed delineating HLA ligands with either significant over- or under-representation in tumor HLA peptidomes. Candidate target antigens were queried against the GTEx database, in which RNA expression data acquired across a large set of benign human tissues are made publicly available, to identify such with a CTA-like expression profile as well as proteins with no confirmed expression in any tissue.¹⁶

3 Methods

Patient collective

Written informed consent of the 33 patients included in the present study was obtained in accordance with the Declaration of Helsinki protocol and the local review board (Kantonale Ethikkommission Zürich; KEK-ZH-Nr. 2015-0163) before surgery. All patients underwent surgery at the Department of Neurosurgery of the University Hospital Zürich, whereby tissue samples were snap frozen in liquid nitrogen and stored at -80°C until use. Meningioma and autologous tumor-free dura specimens along with clinical metadata were kindly provided by Dr. med. Julia Velz, Dr. med. Sophie Shi-Yüing Wang, and PD Dr. med. Marian Christoph Neidert (University Hospital Zürich, Department of Neurosurgery).

All patients had histopathologically confirmed meningioma (n=22 WHO grade I, n=9 WHO grade II, and n=2 WHO grade III) with three samples obtained during surgery at disease recurrence. The present study population had a female-to-male ratio of 2:1 and a median age of onset of 59 [34-83] years. Autologous tumor-free dura supplementing the in-house benign HLA peptidome dataset with the tissue of tumor origin to define meningioma-associated antigens was available from nine patients. Further, this enabled LFQ of relative HLA class I and II ligand abundances on meningioma *versus* autologous dura for five or six patients, respectively. The median available amount of tissue for HLA-IP accounted to 1448 [249-3372] mg for meningioma and to 974 [300-2355] mg for dura samples. Individual patient and sample characteristics are listed in Table 8, whereby a closer look on HLA allotype frequencies in the study cohort is provided in CHAPTER 5.

Table 8. Clinical and experimental metadata of the 33 meningioma patients included in the present study. Age of onset was defined as the age at initial diagnosis. HLA class II allotypes were only available for those samples sequenced at HistoGenetics. Nine meningiomas with available autologous tumor-free dura are marked in grey.

Internal sample ID	Gender	WHO grade	HLA typing	Sample mass HLA-IP [mg]	Relative quantitation HLA class I / II
MNG1 Tissue from 1 st recurrence at 4.7 years after initial diagnosis	♀ 68	II	A*24:02;A*29:02;B*18:01;B*44:03;C*16:01;C*07:01	1075	
MNG2	♀ 57	I	A*30:01;A*03:01;B*13:02;B*07:02;C*07:02;C*06:02	684	
MNG3	♀ 46	I	A*01:01;A*68:01;B*40:01;B*57:01;C*03:04;C*06:02	1002	
MNG4	♀ 81	I	A*01:01;A*03:01;B*07:02;B*51:08;C*16:02;C*07:02	3683	
MNG5	♀ 43	I	A*01:01;A*24:02;B*08:01;B*13:02;C*06:02;C*07:01	1275	
MNG6	♀ 67	I	A*02:01;A*68:01;B*18:01;B*35:03;C*04:01;C*07:01	1536	
MNG7	♀ 78	I	A*30:02;A*01:01;B*08:01;B*07:02;C*07:01;C*07:01	1530	
MNG499	♂ 69	I	A*11:01;A*68:01;B*51:01;B*51:02;C*15:02;C*15:02 DRB1*04:04;DRB1*04:04;DRB4*01:01;DRB4*01:01; DQB1*03:02;DQB1*03:02;DQA1*03:01;DQA1*03:01	1827	
MNG501	♀ 72	II	A*02:01;A*02:01;B*15:01;B*51:01;C*03:03;C*15:02 DRB1*13:01;DRB1*15:01;DRB3*02:02;DRB5*01:01; DQB1*06:02;DQB1*06:03;DQA1*01:03;DQA1*01:02	1355	
MNG612 Tissue from 2 nd recurrence at 10.9 years after initial diagnosis	♀ 34	III	A*32:01;A*02:01;B*51:01;B*27:05;C*14:02;C*01:02	4858	
MNG623	♀ 64	I	A*29:02;A*31:01;B*18:01;B*44:03;C*07:01;C*16:01 DRB1*07:01;DRB1*11:04;DRB3*02:02;DRB4*01:01; DQB1*02:01;DQB1*03:01;DQA1*02:01;DQA1*05:01	522 300	– –
MNG624	♀ 74	I	A*01:01;A*01:01;B*08:01;B*35:01;C*04:01;C*07:01 DRB1*01:01;DRB1*03:01;DRB3*01:01;DQB1*02:01; DQB1*05:01;DQA1*01:01;DQA1*05:01	581	
MNG628	♂ 65	II	A*02:01;A*24:02;B*18:01;B*35:01;C*04:01;C*12:03 DRB1*11:04;DRB1*14:01;DRB3*02:01;DRB3*02:02; DQB1*03:01;DQB1*05:03;DQA1*01:01;DQA1*05:01	1167 473	– –
MNG632	♂ 42	I	A*30:02;A*68:01;B*35:01;B*35:01;C*04:01;C*04:01	1637	
MNG634 Tissue from 1 st recurrence at 7.3 years after initial diagnosis	♂ 49	I	A*24:02;A*31:01;B*13:02;B*55:01;C*06:02;C*01:02	915	
MNG635	♀ 59	II	A*24:02;A*31:01;B*13:02;B*55:01;C*06:02;C*01:02	249	
MNG636	♀ 59	I	A*03:01;A*33:01;B*38:01;B*44:03;C*02:02;C*12:03	1613	
MNG637	♀ 37	I	A*02:01;A*02:01;B*18:01;B*55:01;C*03:03;C*12:03	3021	
MNG638	♀ 57	II	A*24:02;A*02:01;B*18:01;B*14:02;C*08:02;C*07:01	1171	
MNG641	♀ 59	II	A*02:01;A*03:01;B*07:02;B*41:01;C*07:02;C*17:01 DRB1*11:04;DRB1*16:01;DRB3*02:02;DRB5*02:02; DQB1*03:01;DQB1*05:02;DQA1*01:02;DQA1*05:01	3372	
MNG642	♂ 56	II	A*11:01;A*34:01;B*15:35;B*51:01;C*04:01;C*07:02 DRB1*04:05;DRB1*15:02;DRB4*01:01;DRB5*01:01; DQB1*04:01;DQB1*05:02;DQA1*01:02;DQA1*03:01	1769	
MNG646	♀ 63	I	A*01:01;A*03:01;B*08:01;B*40:02;C*02:02;C*07:01 DRB1*03:01;DRB1*04:01;DRB3*01:01;DRB4*01:01; DQB1*02:01;DQB1*03:02;DQA1*03:01;DQA1*05:01	3025	
MNG661	♂ 42	I	A*24:02;A*30:02;B*18:01;B*49:01;C*03:03;C*12:03 DRB1*04:05;DRB1*11:04;DRB3*02:02;DRB4*01:01; DQB1*03:01;DQB1*03:02;DQA1*03:01;DQA1*05:01	1454 974	– –
MNG666	♀ 67	I	A*02:01;A*03:01;B*07:02;B*39:01;C*07:02;C*12:03 DRB1*11:01;DRB1*13:01;DRB3*02:02;DRB3*02:02; DQB1*03:01;DQB1*06:03;DQA1*01:03;DQA1*05:01	2339	
MNG673	♀ 44	I	A*02:01;A*29:02;B*44:03;B*57:01;C*03:04;C*16:01 DRB1*07:01;DRB1*13:01;DRB3*02:02;DRB4*01:01; DQB1*02:01;DQB1*06:03;DQA1*01:03;DQA1*02:01	2658	
MNG679	♀ 49	I	A*23:01;A*29:02;B*44:03;B*44:03;C*04:01;C*16:01 DRB1*07:01;DRB1*07:01;DRB4*01:01;DRB4*01:01; DQB1*02:01;DQB1*02:01;DQA1*02:01;DQA1*02:01	1135 605	+ +
MNG682	♀ 72	I	A*26:01;A*29:02;B*15:01;B*35:01;C*04:01;C*04:01 DRB1*01:01;DRB1*14:01;DRB3*02:02;DQB1*05:03; DQB1*05:01;DQA1*01:01;DQA1*01:01	1346	

Chapter 4: Results

MNG700	♂	I	A*02:01;A*32:01;B*27:05;B*44:02;C*02:02;C*05:01	874	-
MNG700 Dura	44		DRB1*04:01;DRB1*09:01;DRB4*01:01;DRB4*01:01; DQB1*03:01;DQB1*03:03;DQA1*03:01;DQA1*03:01	380	+
MNG702	♂	I	A*01:01;A*02:01;B*37:01;B*51:01;C*02:02;C*06:02	1441	+
MNG702 Dura	41		DRB1*11:01;DRB1*13:01;DRB3*01:01;DRB3*02:02; DQB1*03:01;DQB1*06:03;DQA1*01:03;DQA1*05:01	2355	+
MNG734	♂	III	A*02:01;A*66:01;B*39:31;B*40:02;C*02:02;C*12:03	1259	
	54		DRB1*12:01;DRB1*16:02;DRB3*02:02;DRB5*02:02; DQB1*03:01;DQB1*05:02;DQA1*01:02;DQA1*05:01		
MNG814	♂	II	A*03:01;A*68:01;B*07:02;B*07:02;C*07:02;C*07:02	896	+
MNG814 Dura	83		DRB1*14:01;DRB1*04:04;DRB3*02:02;DRB4*01:01; DQB1*03:02;DQB1*05:03;DQA1*01:01;DQA1*03:01	1324	+
MNG819	♀	I	A*02:01;A*23:01;B*15:01;B*50:01;C*03:03;C*06:02	1543	+
MNG819 Dura	70		DRB1*03:01;DRB1*04:01;DRB3*02:02;DRB4*01:01; DQB1*02:01;DQB1*03:02;DQA1*03:01;DQA1*05:01	988	+
MNG833	♂	II	A*24:02;A*24:02;B*35:01;B*51:01;C*01:02;C*04:01	1735	+
MNG833 Dura	63		DRB1*11:01;DRB1*13:01;DRB3*02:02;DRB3*02:02; DQB1*03:01;DQB1*06:03;DQA1*01:03;DQA1*05:01	1689	+

HLA typing

HLA class I and II allotypes of MNG499, MNG501, MNG623, MNG624, MNG628, MNG641, MNG642, MNG646, MNG661, MNG666, MNG673, MNG679, MNG682, MNG700, MNG702, MNG734, MNG814, MNG819, and MNG833 were determined on 4-digit level by next-generation sequencing of tumor tissue at HistoGenetics (New York, USA). For remaining patients, 4-digit HLA class I typing was kindly provided by Nagarajan Paramasivam (German Cancer Research Center, Division of Theoretical Bioinformatics and Heidelberg Center for Personalized Oncology) as retrieved from whole genome sequencing using the Polysolver¹⁷ algorithm. A detailed description on whole genome sequencing of meningioma and matched blood as control was performed can be retrieved from Paramasivam *et al.*¹⁸

HLA-IP and subsequent LC-MS/MS to identify HLA-presented peptides

HLA class I- and II-presented peptides were isolated from primary human tissue and analyzed by LC-MS/MS as described in 3.2. All peptide eluates were analyzed on an LTQ Orbitrap XL, whereby residual sample volume was subjected to measurement on an Orbitrap Fusion Lumos. For those samples acquired on both devices (Figure 31 A), peptide and protein lists were merged manually with peptide-specific scores being reported for every LC-MS/MS system.

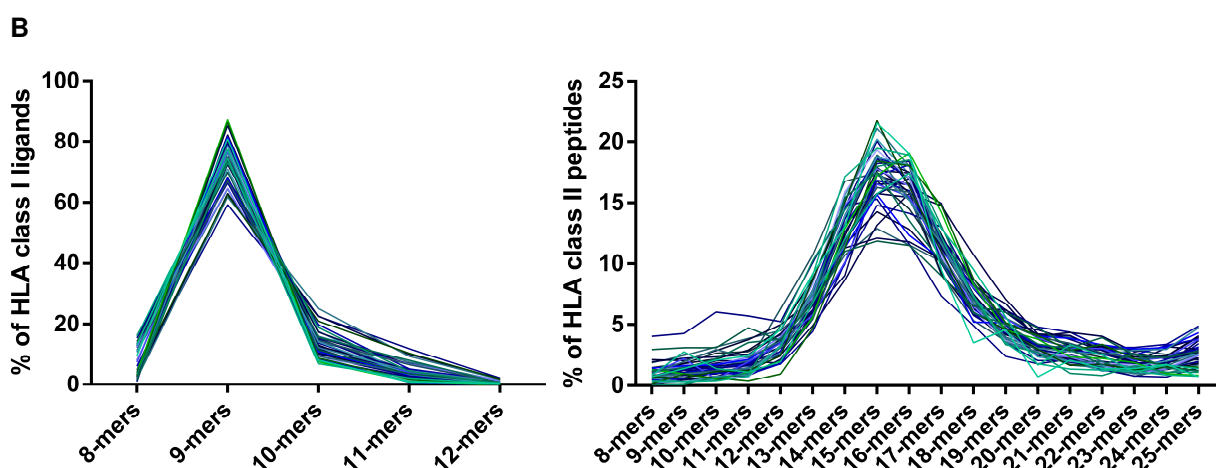
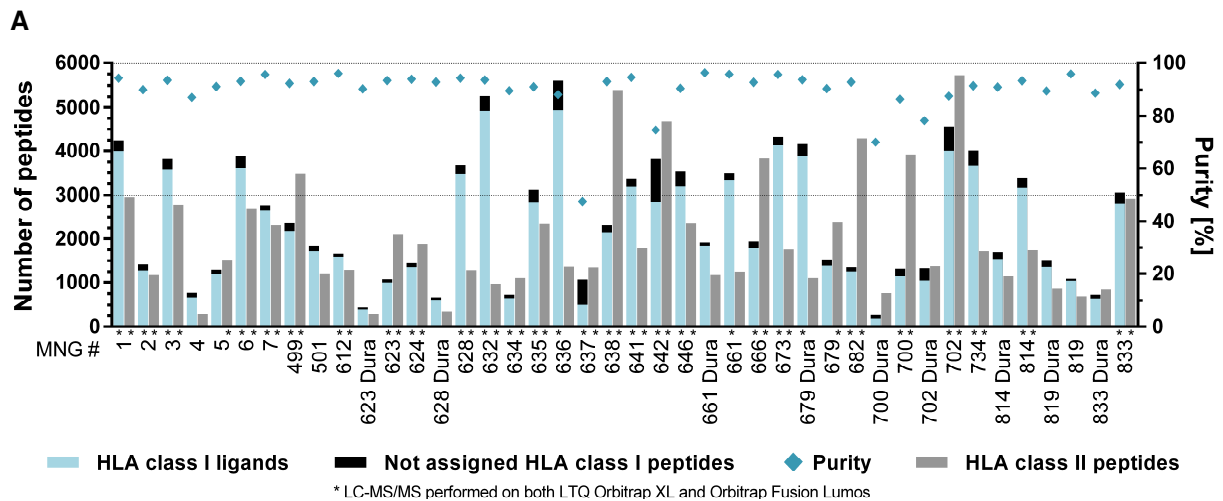
4 Results

4.1 Peptide yields of HLA-IPs and HLA class I allotype coverage

To define candidate targets for meningioma immunotherapy naturally presented on HLA, we analyzed 33 primary tumor and nine autologous tumor-free dura specimens. The meningioma cohort included 58 distinct HLA class I allotypes covering 99.98% of the world population, whereby 94.60% of all individuals are expected to be positive for at least three allotypes (Supplementary Figure 8). The most frequent allotypes among meningioma patients were HLA-A*02:01 (20%), -A*03:01 (12%), -A*01:01 (11%), -A*24:02 (11%), -B*18:01 (11%), -B*07:02 (9%), -B*35:01 (9%), -B*51:01 (9%), -C*04:01 (14%), -C*07:01 (12%), and -C*06:02 (11%) (Supplementary Table 15).

A median of 2649 [505-4939] and 1038 [185-3891] HLA class I ligands were identified from meningioma or dura samples, respectively. All HLA class I peptide eluates except that of

MNG637 exhibited a purity of at least 70% and none of the samples were censored for low peptide yield or low percentage of HLA class I ligands. Concerning HLA class II, median peptide yields came up to 1882 [301-5720] and 852 [283-1371]. The total number of unique HLA class I and II peptides, HLA class I ligands as well as the purity of HLA class I peptide eluates are given in Figure 31 A for every specimen. The length distribution of HLA class I ligands clearly peaked at 9 AA length, whereas HLA class II-presented peptides were typically 13- to 18-mers. All investigated samples had comparable length distribution profiles independent of dignity or peptide yield (Figure 31 B). Taking tissue masses subjected to HLA-IP into account (Table 8), enabled us to investigate whether peptide yields correlate with sample quantities used. However, the amount of dura or meningioma tissue did neither correlate with the number of HLA class I nor with the number HLA class II peptide identifications per technical replicate (Figure 31 C). Considering the relative number of identified unique peptides per technical replicate and per one mg of tissue input revealed a significantly increased yield of HLA class I as compared with HLA class II peptides eluted from meningioma tissues (Figure 31 D).



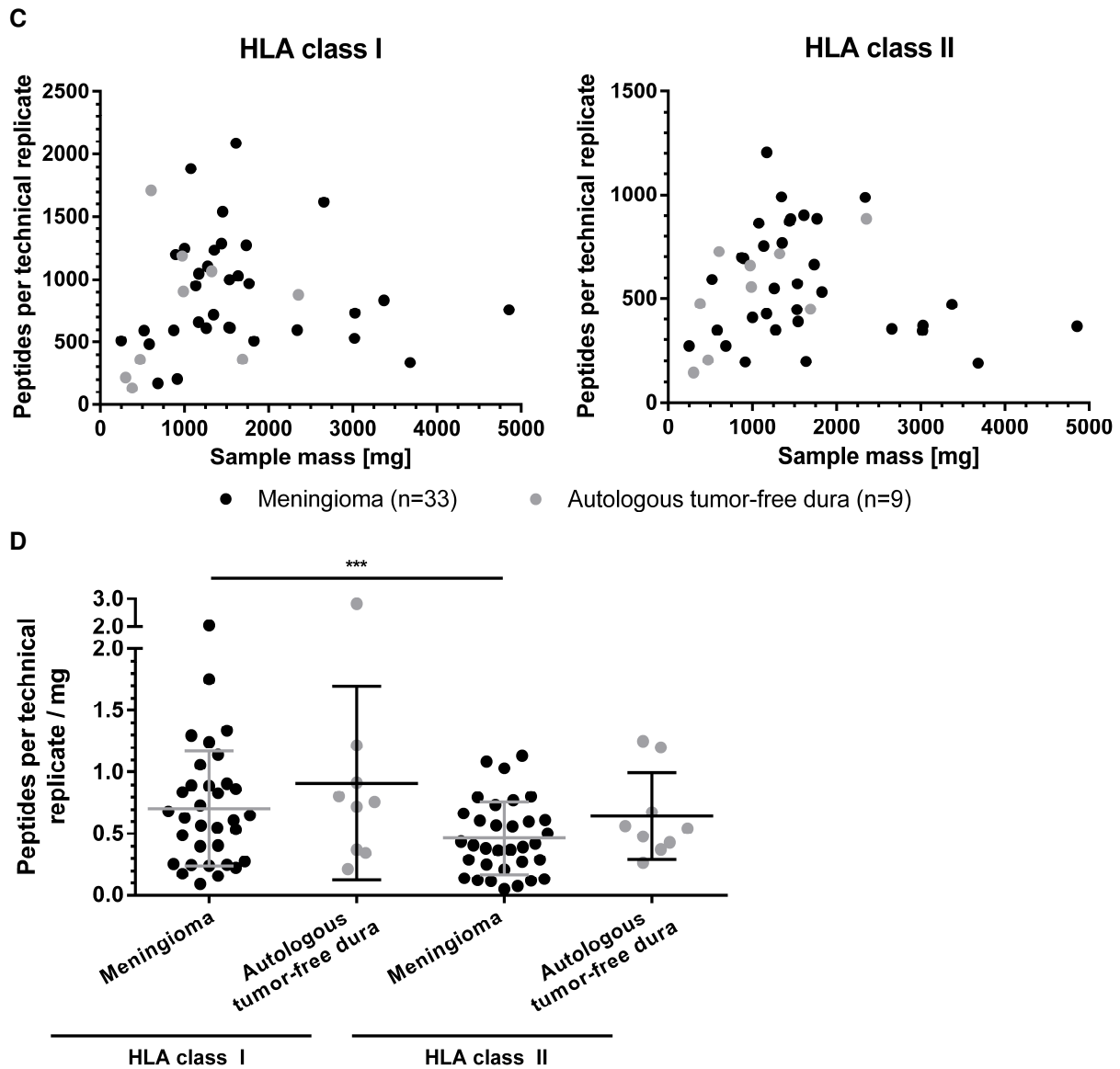


Figure 31. Number and length distribution of identified HLA class I- and II-presented peptides. (A) HLA class I and II peptide yields of meningioma and autologous tumor-free dura tissue. Calculated purities refer to the proportion of HLA class I peptides annotated to an HLA allotype of the respective patient. Asterisks indicate data acquisition on both LC-MS/MS systems. **(B) Length distribution of HLA class I ligands and HLA class II peptides.** Across the entire dataset, 9-mers constituted 72% of HLA class I ligands, whereas 71% of HLA class II-presented peptides had a length between 13 and 18 AA. Each line represents data of one sample with tumors being illustrated in blueish and dura samples in greenish shades. **(C) Unique peptides per sample and technical replicate versus amount of tissue subjected to HLA-IP.** To exclude device artefacts, only measurements acquired on an LTQ Orbitrap XL were evaluated. Likewise, only technical replicates consuming 20% sample share each were considered and such diluted for relative quantitation of peptide abundances in paired meningioma and tumor-free dura were excluded from this analysis. By non-linear regression (one-phase association) exponential functions with a forced y-intercept of 0 (internal data created by Daniel Kowalewski at the Department of Immunology, University of Tübingen indicate that subjecting cell-free lysis buffer to HLA-IP does not result in peptide identifications) were fitted. However, the goodness of fit was poor for all these models: $R^2 = 0.08$ (meningioma HLA class I) / 0.20 (dura HLA class I) / 0.05 (meningioma HLA class II) / 0.50 (dura HLA class II). Similarly, a correlation analysis across these normally distributed data (according to D'Agostino & Pearson omnibus normality test) did not identify a significant correlation of sample quantities used and the number of peptides identified: two-tailed p -values = 0.8875 (meningioma HLA class I) / 0.6039 (dura HLA class I) / 0.2862 (meningioma

HLA class II) / 0.0542 (dura HLA class II). **(D) Peptide yields per technical replicate normalized to one mg of tissue input.** To investigate, whether the relative number of peptide identifications differs between meningioma and autologous tumor-free dura as well as between HLA class I- and II-IPs of the same sample, Wilcoxon matched-pairs signed rank tests were performed (normalized peptide yields did not have Gaussian distributions according to D'Agostino & Pearson omnibus normality test). The only significant difference was observed between the number of HLA class I and II peptides eluted from meningeal tumors (two-tailed p -value = 0.0001).

4.2 Definition of meningioma-associated antigens

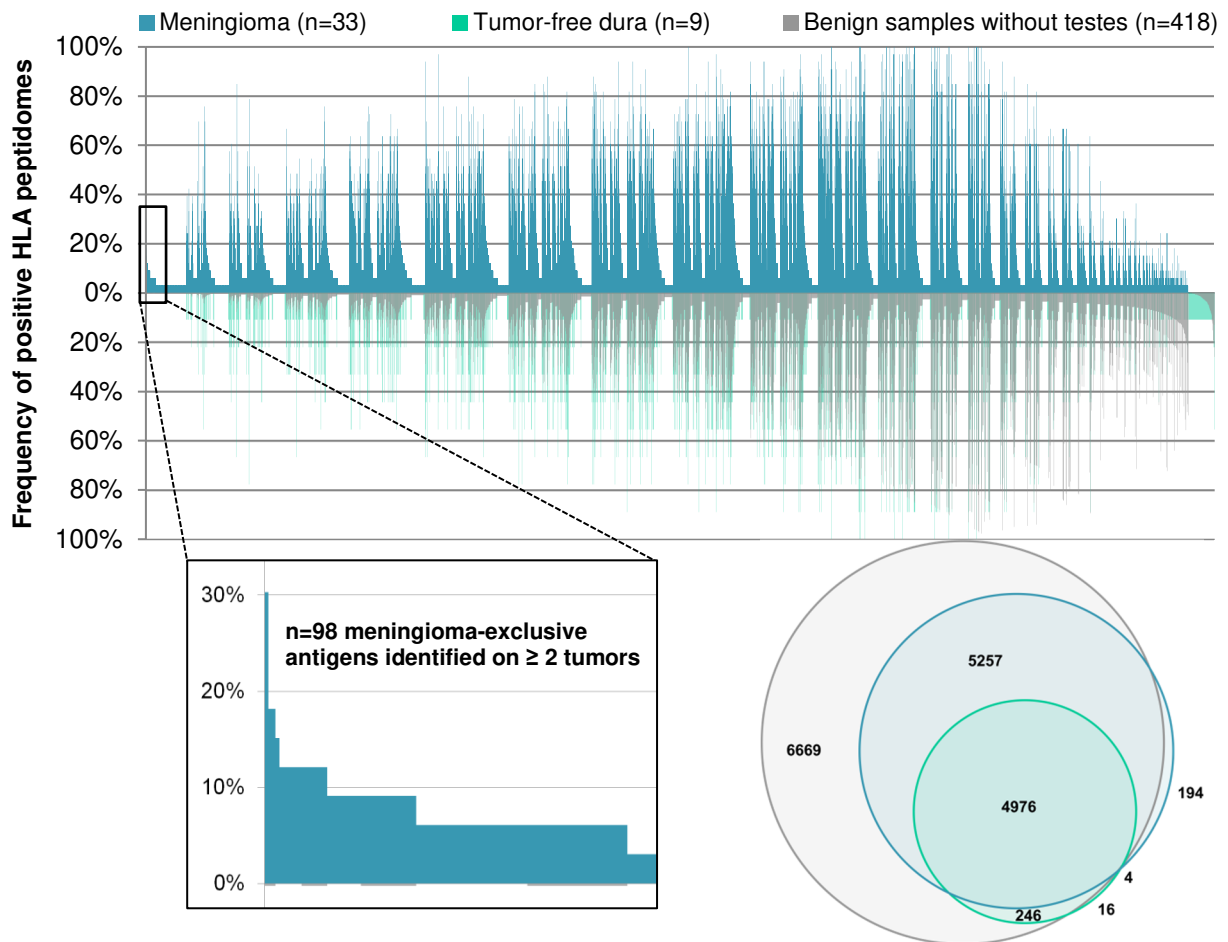
By immunoaffinity chromatography and LC-MS/MS, the repertoire of HLA class I and II peptides and corresponding antigens naturally presented on 33 meningiomas was mapped. To define meningioma-associated antigens and peptides, an in-house benign database comprising 30 distinct primary human organs (n=418 HLA class I and n=364 HLA class II peptidome datasets) supplemented with nine autologous tumor-free dura samples representing the tissue of tumor origin was subtracted. The term meningioma-associated was assigned to peptides and antigens that were never identified on CNS-related tissues (brain, cerebellum, spinal cord, and dura) and for which a maximum of one non-CNS-related sample was positive. Moreover, the frequency of positive primary non-meningeal human malignancies (n=841 samples for HLA class I; n=593 samples for HLA class II) encompassing 36 cancer entities was evaluated. As additional criterium to select targets for cancer immunotherapies, RNA expression data acquired across a large set of benign human tissues and deposited in the GTEx database¹⁶ was reported for every candidate antigen. Further, this allowed the identification of antigens not known to be expressed in any tissue (defined as less than ten TPM in any tissue) as well as such with a classical CTA-like expression profile (not exceeding ten TPM in other organs than testis).

Meningioma-associated HLA class I-presented antigens and peptides

HLA class I peptidome analyses of meningioma (n=33) and autologous tumor-free dura (n=9) allowed the identification of 10,431 and 5,242 distinct source proteins represented by HLA class I ligands on neoplastic or tumor-free meningeal tissue, respectively. These represent between 82% (dura) and 93% (meningioma) of the estimated maximum attainable amount of distinct source proteins (Figure 32 C). Despite the vast overlap of meningiomas with benign samples and/or autologous tumor-free dura, 98 antigens were exclusively presented by at least two meningeal tumors (Figure 32 A). Following manual curation of the underlying peptides for HLA motifs as well as multi-mapping to several source proteins, a set of 28 meningioma-associated antigens and corresponding peptides naturally presented on 9-30% of tumors was created. Among these, NMNA2, WNT5A, TBX15/18, and OSR1 were the most frequent ones (Figure 32 B). Despite only two WHO grade III tumors being included in the present dataset, seven of the meningioma-associated antigens were identified across all WHO grades (NMNA2, TBX15/18, XXLT1, SLC25A44, RHOD, CREBL2, PLCD4) and one each was shared by WHO grade I and III (NINJ2) or WHO grade II and III tumors (TMEM87A), respectively. WHO grade I and II meningiomas had 16 antigens in common and three antigens were exclusively part of the immunopeptidome of WHO grade I meningeal neoplasias (TC1D2, B4GALT4, MTU1). Peptide sequences and their HLA restriction, a listing of positive patients, and the GTEx profile of the corresponding source protein can be retrieved from Supplementary

Table 16. Of note, none of these meningioma-associated HLA class I antigens exhibited a CTA-like expression profile.

A



B

protein Wnt-5a (WNT5A) forkhead box protein (FOX) E3, D4-like 1/2/3/5/6
 insulin-like growth factor-binding protein 6 (IGFBP6) folate receptor gamma (FOLR3) sterol O-acyltransferase 2 (SOAT2)
 Rho-related GTP-binding protein RhoD (RHOD) protein odd-skipped-related 1 (OSR1)
 solute carrier family 25 member 44 (SLC25A44) cAMP-responsive element-binding protein-like 2 (CREBL2)
 transmembrane protein 87A (TMEM87A) NKG2-C type II integral membrane protein (NKG2C) / NKG2-E type II integral membrane protein (NKG2E)
 protein AF-9 (AF-9) **nicotinamide mononucleotide** protein SSX5/9 (SSX5/9)
 cadherin-3 (CDH3)
 ninjurin-2 (NINJ2) **adenylyltransferase 2 (NMNA2)** Frizzled-7 (FZD7)
 globoside alpha-1,3-N-acetylgalactosaminyltransferase 1 (GBGT1) mitochondrial tRNA-specific 2-thiouridylase 1 (MTU1)
 1-phosphatidylinositol 4,5-bisphosphate phosphodiesterase delta-4 (PLCD4) beta-1,4-galactosyltransferase 4 (B4GALT4)
 E3 ubiquitin-protein ligase ZNRF2 (ZNRF2) paraneoplastic antigen Ma2 (PNMA2) xyloside xylosyltransferase 1 (XXLT1)
 transmembrane protein 255B (TMEM255B) Tctex1 domain-containing protein 2 (TC1D2)
 uncharacterized protein C8orf34 (C8orf34) T-box transcription factor TBX15/18 (TBX15/18)

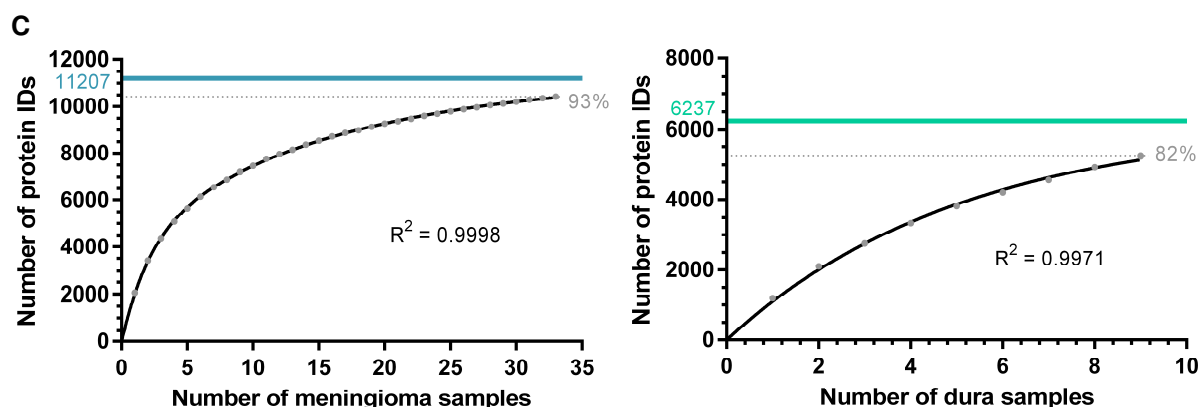


Figure 32. Definition of meningioma-associated antigens based on class I immunopeptidome analyses. (A) Comparative profiling of the HLA class I peptidome of meningioma versus an in-house benign database complemented by tumor-free dura. Each bar in this waterfall plot (associated with the x-axis) represents a single source protein, whereas the frequency of positive HLA peptidomes is shown on the y-axis, separately for meningioma ($n=33$), tumor-free dura ($n=9$), and benign samples without testes ($n=418$ covering 29 different human tissues). Those source proteins detected on a maximum of one non-CNS-related tissue were designated as meningioma-exclusive, whereby $n=98$ were identified on at least two meningeal tumors (highlighted as enlarged view on the left). The Venn diagram on the right illustrates the number of distinct HLA class I-presented antigens per group, however, the overlaps cannot map the permission of one positive non-CNS-related sample within the benign dataset. **(B) Word cloud of meningioma-associated antigens.** Based on comparative profiling and subsequent quality control of underlying peptides (HLA motifs as well as multi-mapping to several source proteins), a set of 28 meningioma-associated antigens naturally presented on 9-30% of meningeal tumors was defined. The font size in the word cloud is proportional to the frequency of positive meningeal tumors. **(C) Saturation analysis for the identification of antigens represented by HLA class I ligands on meningioma or tumor-free dura tissue.** For each source count, the mean number of antigens was calculated by 1,000 random samplings. Using non-linear regression, exponential functions with a forced y-intercept of 0 (internal data created by Daniel Kowalewski at the Department of Immunology, University of Tübingen indicate that subjecting cell-free lysis buffer to HLA-IP does not result in peptide identifications) were fitted. For both models, the goodness of fit was in the uppermost range ($R^2 = 0.9998$ and $R^2 = 0.9971$). Based on these curves, the maximum attainable number of distinct source proteins was estimated (highlighted as solid lines). With the available number of 33 meningioma and nine tumor-free dura samples, 93% or 82% of the estimated maximum attainable amount of distinct HLA class I-presented proteins had been identified, respectively.

On the peptide level, 38,038 and 9,170 distinct HLA class I ligands were eluted from meningeal neoplasms ($n=33$) and tumor-free dura ($n=9$), obtaining 77% (meningioma) and 38% (dura) of the estimated maximum attainable coverage (Figure 33 B). Although the HLA class I peptidome of meningioma showed a pronounced high overlap with that of benign samples and/or autologous tumor-free dura, 2,515 meningioma-exclusive peptides presented on at least two tumors were identified (Figure 33 A). Subsequent to manual curation, a set of 74 peptides derived from 68 antigens and presented on 15-30% of tumors was defined. Among these, HLA ligands derived from OGN, FOXC2, and IFI44L were the most frequent ones. Overall, 31 peptides were presented across all WHO grades, 36 were shared by WHO grade I and II tumors, and two peptides were eluted from both WHO grade I and III meningiomas. One and four peptides were exclusively identified from WHO grade III or I meningeal neoplasms, respectively. Peptide sequences and their HLA restriction, a listing of positive patients, and the corresponding source protein are given in Supplementary Table 17.

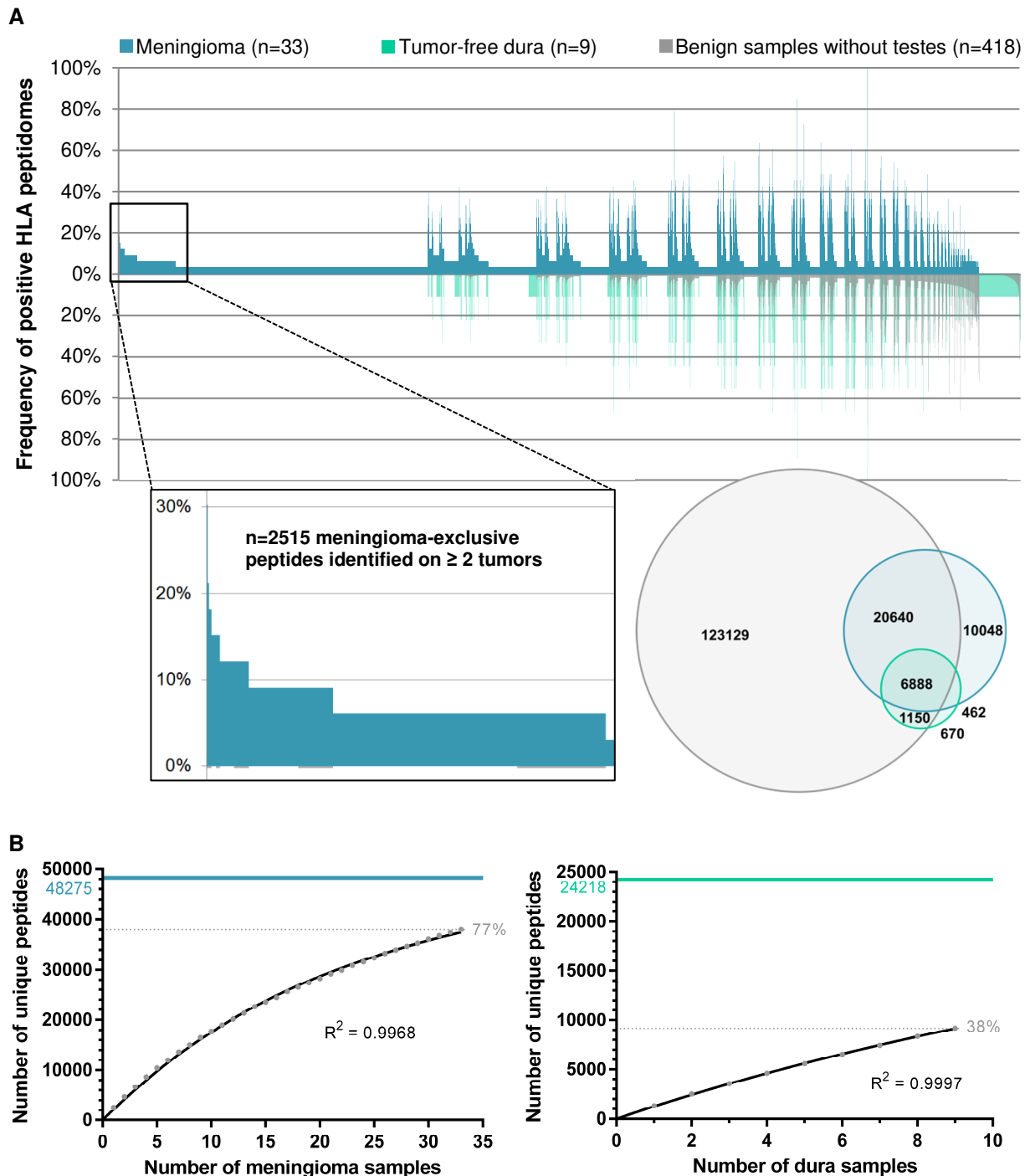


Figure 33. HLA class I peptidomics to define meningioma-associated peptides. (A) Comparative profiling of HLA class I ligands presented on meningioma versus an in-house benign database supplemented with tumor-free dura. Every peptide evaluated for tumor association is represented by a bar in the waterfall plot (associated with the x-axis), whereas the y-axis shows the frequency of positive HLA peptidomes, separately for meningioma (n=33), tumor-free dura (n=9), and benign samples without testes (n=418 covering 29 different human tissues). Peptides were designated as meningioma-exclusive, when detected on a maximum of one non-CNS-related tissue, whereby n=2,515 were identified on at least two meningeal tumors (highlighted as enlarged view on the left). The number of distinct HLA class I ligands per group is illustrated by the Venn diagram on the right, whereby the overlaps cannot map the permission of one positive non-CNS-related sample within the benign dataset. **(B) Saturation analysis for the identification of HLA class I ligands in meningioma or tumor-free dura tissue.** For each source count, the mean number of peptides was calculated by 1,000 random samplings. Using non-linear regression, exponential functions with a forced y-intercept of 0 (internal

data created by Daniel Kowalewski at the Department of Immunology, University of Tübingen indicate that subjecting cell-free lysis buffer to HLA-IP does not result in peptide identifications) were fitted. For both models, the goodness of fit was in the uppermost range ($R^2 = 0.9968$ and $R^2 = 0.9997$). Based on these curves, the maximum attainable number of distinct peptides was estimated (highlighted as solid lines). With the available number of 33 meningioma and nine tumor-free dura samples, 77% or 38% of the estimated maximum attainable amount of distinct HLA class I ligands had been identified, respectively.

Combining the list of peptides derived from HLA class I-presented meningioma-associated antigens (Supplementary Table 16) with that of HLA class I ligands designated as meningioma-associated (Supplementary Table 17) gave $n=141$ candidate target peptides for cancer immunotherapy. These cover 99.57% of the world population (Supplementary Figure 9), whereby an average of 21 peptides are expected to match per patient. The population coverage on a per-country basis is shown in Figure 34.

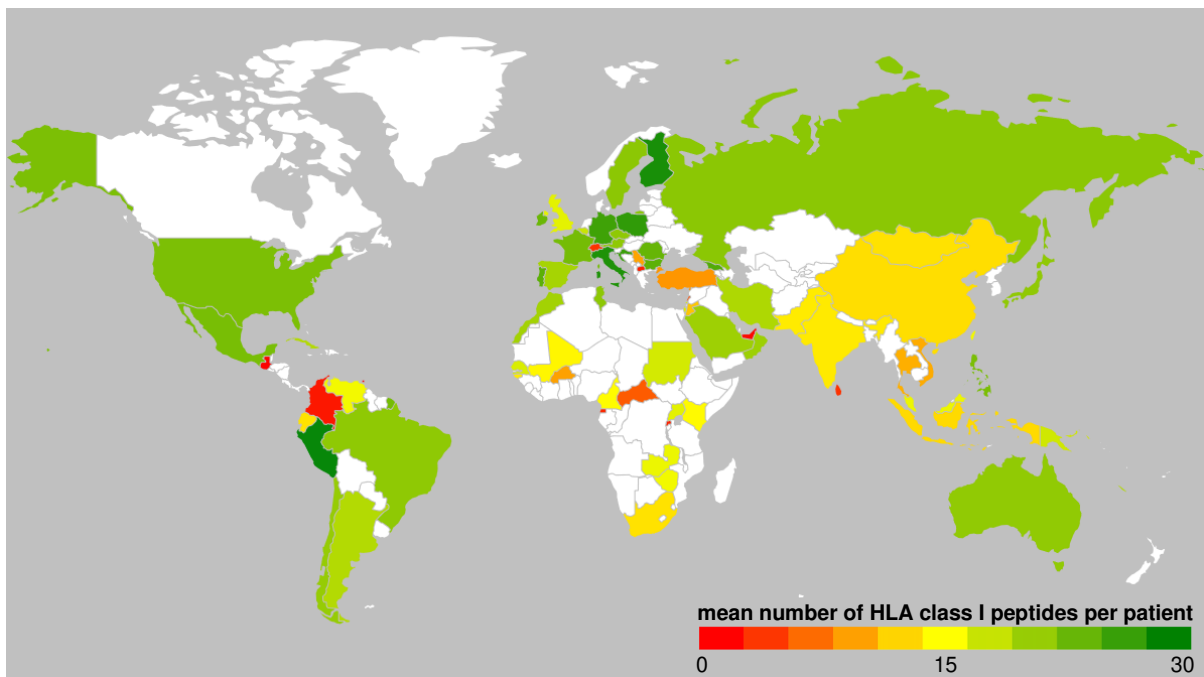
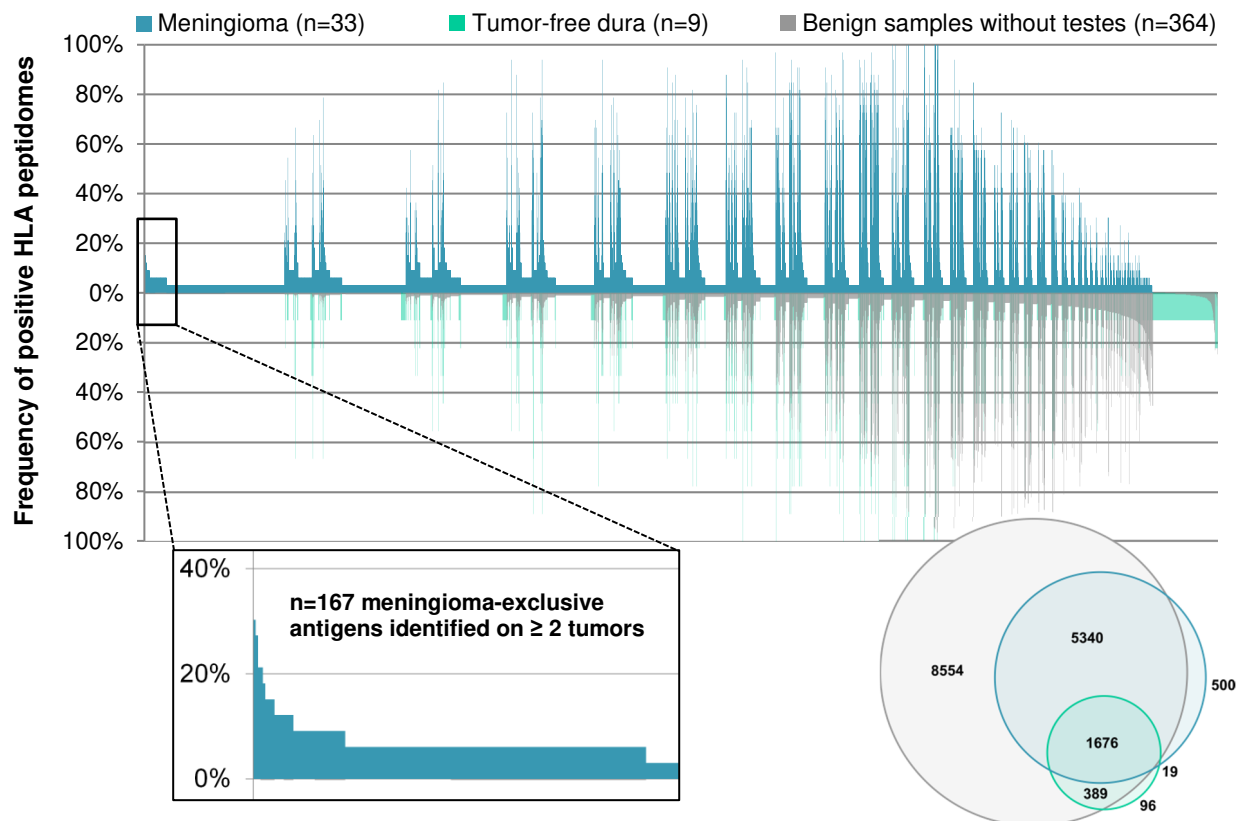


Figure 34. Population coverage of meningioma-associated HLA class I peptides. Using the population coverage tool provided by the IEDB Analysis Resource¹⁹, the population coverage of the $n=141$ candidate target peptides for meningioma immunotherapy was calculated on a per-country basis. On average, 21 HLA class I peptides match per patient worldwide. For visualization of the United Kingdom, the individual values of England, Northern Ireland, Scotland, and Wales were multiplied with the relative area portion. Countries not included in the IEDB tool or not covered by the geographic heat map add-on of Microsoft Excel are colorless.

Meningioma-associated HLA class II antigens

HLA class II peptidome analyses of meningioma (n=33) and autologous tumor-free dura (n=9) allowed the identification of 7,535 and 2,180 distinct source proteins giving rise to HLA class II-restricted peptides on neoplastic or tumor-free meningeal tissue, respectively. These represent between 70% (dura) and 72% (meningioma) of the estimated maximum attainable amount of distinct source proteins (Figure 35 C). Despite the vast overlap of meningiomas with benign samples and/or autologous tumor-free dura, 167 antigens were exclusively presented by at least two meningioma tumors (Figure 35 A). Following manual curation of the underlying peptides for peptide length and the presence of length variants as well as multi-mapping to several source proteins, a set of 37 meningioma-associated antigens and corresponding peptides naturally presented on 9-30% of tumors was created. Among these, PRSS35, A4GALT, FBN2, and SNED1 were the most frequent ones (Figure 35 B). Six of the meningioma-associated antigens were identified across all WHO grades (A4GALT, FBN2, SNED1, MPP6, PCED1B, ANGEL2) and 24 ones were shared by WHO grade I and II tumors. Six antigens were exclusively part of the immunopeptidome of WHO grade I meningeal neoplasias (CAPN14, KIR2DS4, TIMM44, ECD, CD86, RFWD3), whereas WHO grade I and III meningiomas had one antigen in common (KLC2). Peptide sequences, a listing of positive patients, and the GTEx profile of the corresponding source protein can be retrieved from Supplementary Table 16. Of note, three of these meningioma-associated HLA class II antigens (C1orf112, SIRPD, TTLL6) exhibited a CTA-like expression profile and were not listed in the CTDDatabase²⁰.

A



B

serine/threonine-protein kinase Sgk3 (SGK3) **MAGUK p55 subfamily member 6 (MPP6)**
lactosylceramide 4-alpha-uncharacterized protein KIAA1586 (KIAA1586)
galactosyltransferase (A4GALT) highly divergent homeobox (HDX) calpain-14 (CAPN14)
 probable allantoinase (ALLC) nucleoporin GLE1 (GLE1)
 bone morphogenetic protein 5 (BMP5) nuclear factor of activated T-cells, cytoplasmic 2 (NFATC2)
fibrillin-2 (FBN2) methylenetetrahydrofolate reductase (MTHFR) transcription factor SOX-6 (SOX6)
 T-lymphocyte activation antigen CD86 (CD86) uncharacterized protein C1orf112 (C1orf112) PC-esterase domain-containing protein 1B (PCED1B)
 protein SGT1 (ECD) mucin-4 (MUC4) **inactive serine protease 35 (PRSS35)**
 melanoma-associated antigen 10 (MAGEA10) mitochondrial import inner membrane translocase subunit TIM44 (TIMM44)
 N-acetyltransferase ESCO1 (ESCO1) zinc finger E-box-binding homeobox 2 (ZEB2) tubulin polyglutamylase TTL6 (TLL6)
ZAR1-like protein (ZAR1L) killer cell immunoglobulin-like receptor 2DS4 (KIR2DS4) calcium-binding protein 39-like (CAB39L)
 protein angel homolog 2 (ANGEL2) dorsal root ganglia homeobox protein (DRGX) signal-regulatory protein delta (SIRPD)
G protein-regulated inducer of neurite outgrowth 2 (GPRIN2) meteorin-like protein (METRNL) kinesin light chain 2 (KLC2)
 signal transducer and activator of transcription 5B (STAT5B) E3 ubiquitin-protein ligase RFW3 (RFWD3) ubiquitin conjugation factor E4 B (UBE4B)
sushi, nidogen and EGF-like domain-containing protein 1 (SNED1)

C

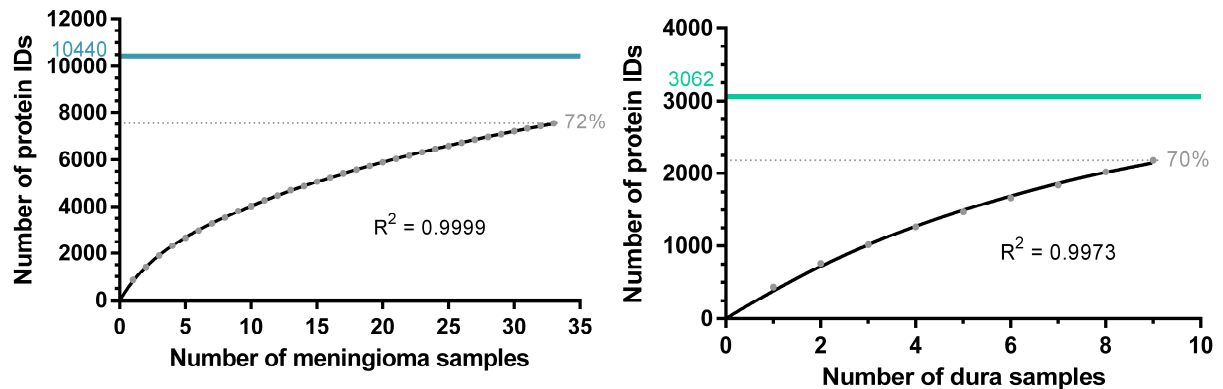
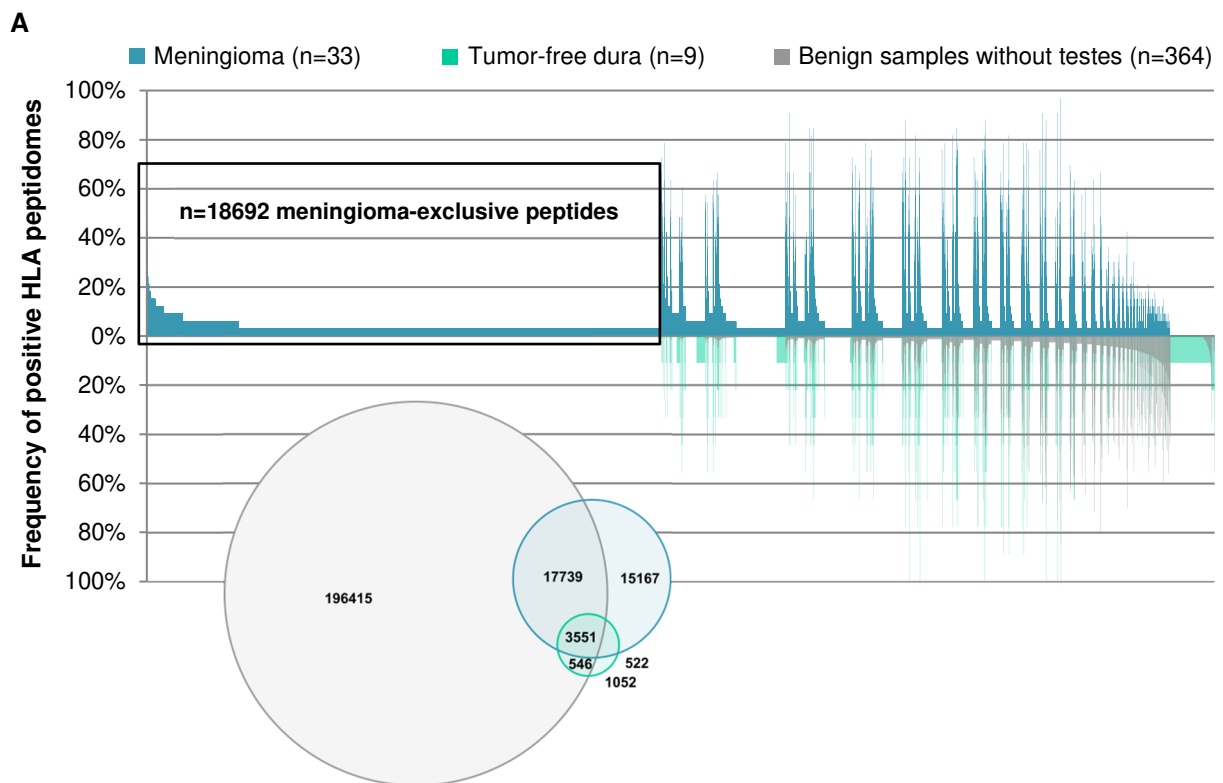


Figure 35. Definition of meningioma-associated antigens based on class II immunopeptidome analyses. (A) Comparative profiling of the HLA class II peptidome of meningioma versus an in-house benign database supplemented with tumor-free dura. Each bar in this waterfall plot (associated with the x-axis) represents a single source protein, whereas the frequency of positive HLA peptidomes is shown on the y-axis, separately for meningioma (n=33), tumor-free dura (n=9), and benign samples without testes (n=364 covering 30 different human tissues). Those source proteins detected on a maximum of one non-CNS-related tissue were designated as meningioma-exclusive, whereby n=167 were identified on at least two meningeal tumors (highlighted as enlarged view on the left). The Venn diagram on the right illustrates the number of distinct HLA class II-presented antigens per group, however, the overlaps cannot map the permission of one positive non-CNS-related sample within the benign dataset. **(B) Word cloud of meningioma-associated antigens.** Based on comparative profiling and subsequent quality control of underlying peptides (peptide length and/or presence of length variants as well as multi-mapping to several source proteins), a set of 37 meningioma-associated antigens naturally presented on 9-30% of meningeal tumors was defined. The font size in the word cloud is proportional to the frequency of positive meningeal tumors. **(C) Saturation analysis for the identification of antigens represented by HLA class II peptides on meningioma or tumor-free dura tissue.** For each source count, the mean number of antigens was calculated by 1,000 random samplings. Using non-linear regression, exponential functions with a forced y-intercept of 0 (internal data created by Daniel Kowalewski at the Department of Immunology, University of Tübingen indicate that subjecting cell-free lysis buffer to HLA-IP does not result in peptide identifications) were fitted. For both models, the goodness of fit was in the uppermost range ($R^2 = 0.9999$ and $R^2 = 0.9973$). Based on these curves, the maximum attainable number of distinct source proteins was estimated (highlighted as solid lines). With the available number of 33 meningioma and nine tumor-free dura

samples, 72% or 70% of the estimated maximum attainable amount of distinct HLA class II-presented proteins had been identified, respectively.

On the peptide level, 36,979 and 9,170 distinct HLA class II-presented peptides were eluted from meningeal neoplasms (n=33) and tumor-free dura (n=9), obtaining 54% (meningioma) and 50% (dura) of the estimated maximum attainable coverage (Figure 36 B). Subsequent to comparative profiling, all antigens represented by at least one meningioma-exclusive HLA class II-presented peptide were subjected to hotspot analysis (Figure 36 A). Meningioma-associated HLA class II presentation hotspots were defined to have a minimum length of eight AA and to be covered by peptides identified in at least five patients, while not having matching sequences in benign samples. This identified a set of 44 antigens harboring regions uniquely presented on tumor tissue with peptide-specific frequencies reaching up to 45% of positive HLA peptidomes. A total of 15 proteins were represented with hotspot-derived peptides across all WHO grades, whereas presentation hotspots within 26 proteins were shared by WHO grade I and II tumors. Further, one meningioma-associated HLA class II presentation hotspot was exclusively detected in WHO grade I meningeal neoplasms, whereas WHO grade I and III tumors had two hotspot targets in common. Peptide sequences, a listing of positive patients, and the corresponding source protein are given in Supplementary Table 18.

Comparing meningioma-associated HLA class I- (n=36) and II-presented antigens (n=37) as well as meningioma-associated HLA class I- (n=68 source proteins) and II-restricted peptides (n=44 source proteins), revealed a unique antigenic repertoire inherent to HLA class I and II peptidomes. STAB1 represented the only shared antigen yielding both meningioma-associated HLA class I and II ligands.



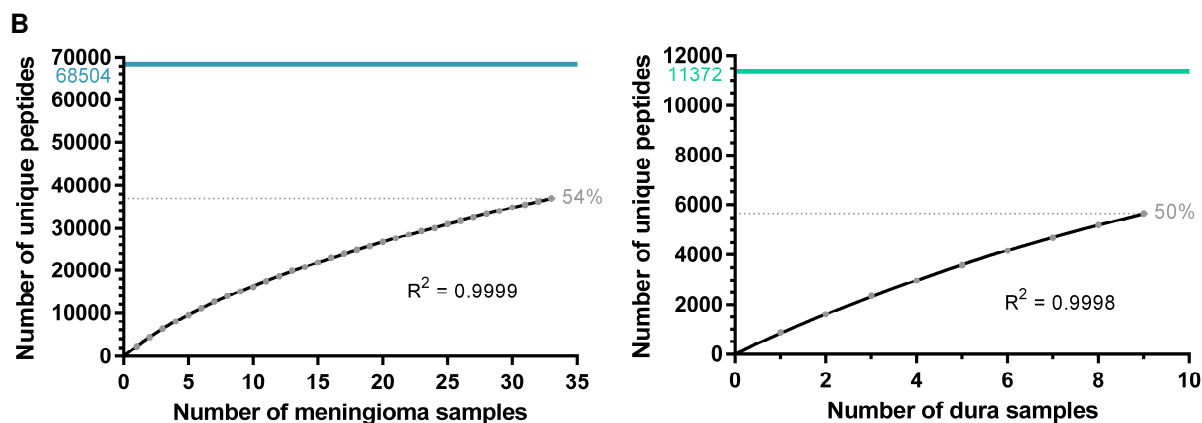
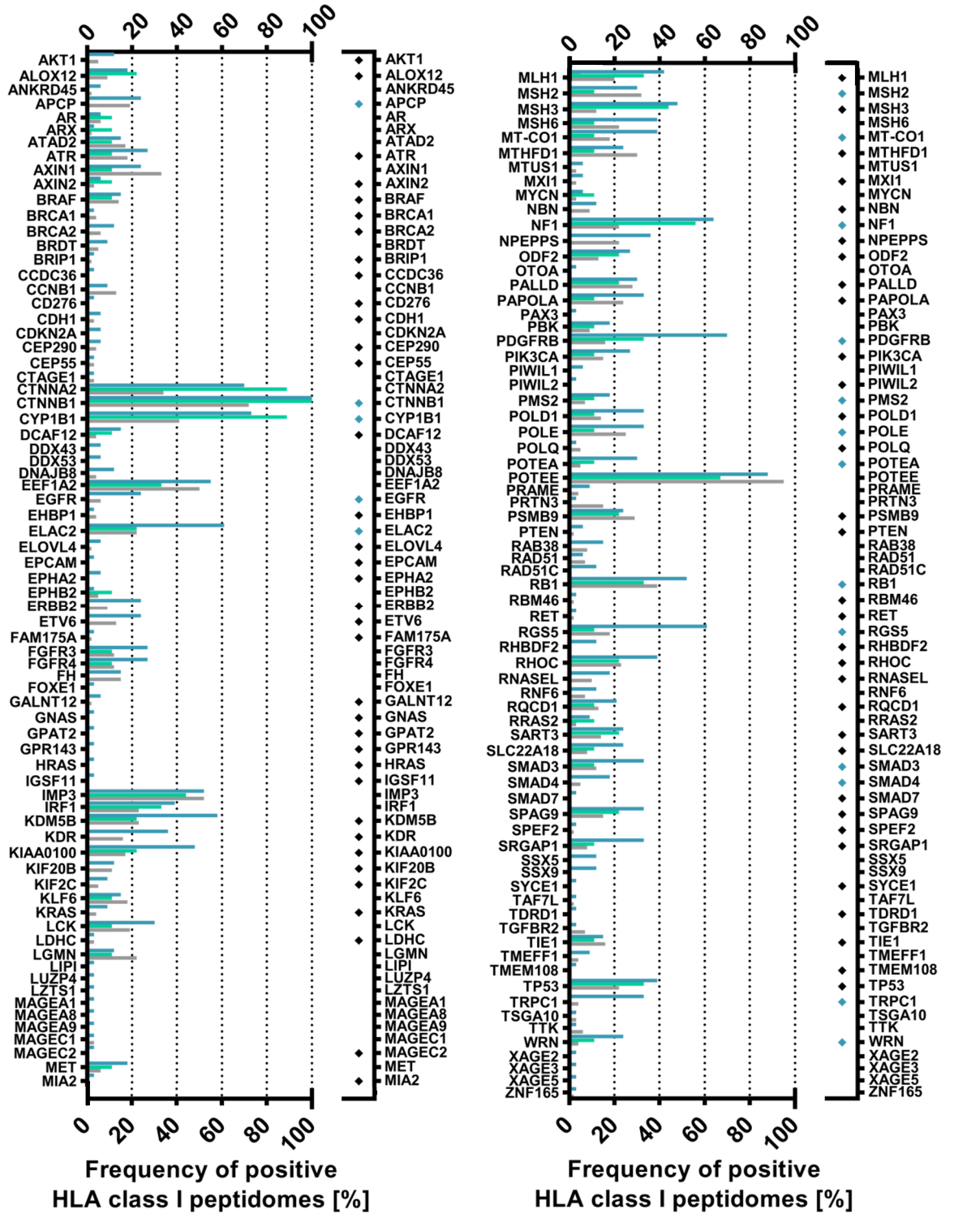


Figure 36. HLA class II peptidomics to define meningioma-associated peptides (A) Comparative profiling of HLA class II peptides presented on meningioma versus an in-house benign database supplemented with tumor-free dura. Every peptide evaluated for tumor association is represented by a bar in the waterfall plot (associated with the x-axis), whereas the y-axis shows the frequency of positive HLA peptidomes, separately for meningioma ($n=33$), tumor-free dura ($n=9$), and benign samples without testes ($n=364$ covering 30 different human tissues). Being detected on a maximum of one non-CNS-related tissue, $n=18,692$ peptides were designated as meningioma-exclusive. Corresponding source proteins were subjected to hotspot analysis. The number of distinct HLA class II-restricted peptides per group is illustrated by the Venn diagram on the left, whereby the overlaps cannot map the permission of one positive non-CNS-related sample within the benign dataset. **(B) Saturation analysis for the identification of HLA class II-presented peptides in meningioma or tumor-free dura tissue.** For each source count, the mean number of peptides was calculated by 1,000 random samplings. Using non-linear regression, exponential functions with a forced y-intercept of 0 (internal data created by Daniel Kowalewski at the Department of Immunology, University of Tübingen indicate that subjecting cell-free lysis buffer to HLA-IP does not result in peptide identifications) were fitted. For both models, the goodness of fit was in the uppermost range ($R^2 = 0.9999$ and $R^2 = 0.9998$). Based on these curves, the maximum attainable number of distinct peptides was estimated (highlighted as solid lines). With the available number of 33 meningioma and nine tumor-free dura samples, 54% or 50% of the estimated maximum attainable amount of distinct HLA class II-presented peptides had been identified, respectively.

Natural HLA presentation of established CTAs and TAAs

Considering a total number of 366 established CTAs and TAAs (3.2.1) as well as 15 antigens reported to be associated with meningeal neoplasias (2.3.2; $n=10$ overlapped with the general list of CTAs and TAAs), the present HLA peptidome dataset acquired from meningiomas was screened for previously published tumor antigens. Of these, $n=145$ and $n=126$ were represented by HLA class I ligands and HLA class II-presented peptides, respectively. Despite these high identification rates, presentation frequencies of CTAs and TAAs were in general low, especially of those exclusively identified on meningeal tumors. Among 23 HLA class I-presented TAAs and CTAs fulfilling the aforementioned criteria to be designated as meningioma-exclusive antigen, SSX5, SSX9, DDX43, and DDX53 were the most frequent ones (6-12% positive tumors). 18 additional TAAs and CTAs were represented by meningioma-exclusive HLA class I ligands on at least two and a maximum of four meningiomas (Figure 37 A, Supplementary Table 19). On HLA class II, 26 antigens were exclusively identified in the peptidome of meningiomas, with MAGEA10, MUTYH, and CABYR being the most frequent ones (6-15% positive tumors). 20 further CTAs and TAAs were represented by meningioma-exclusive HLA class II-presented peptides on at least two and a maximum of five neoplasms (Figure 37 B, Supplementary Table 19).

A



B

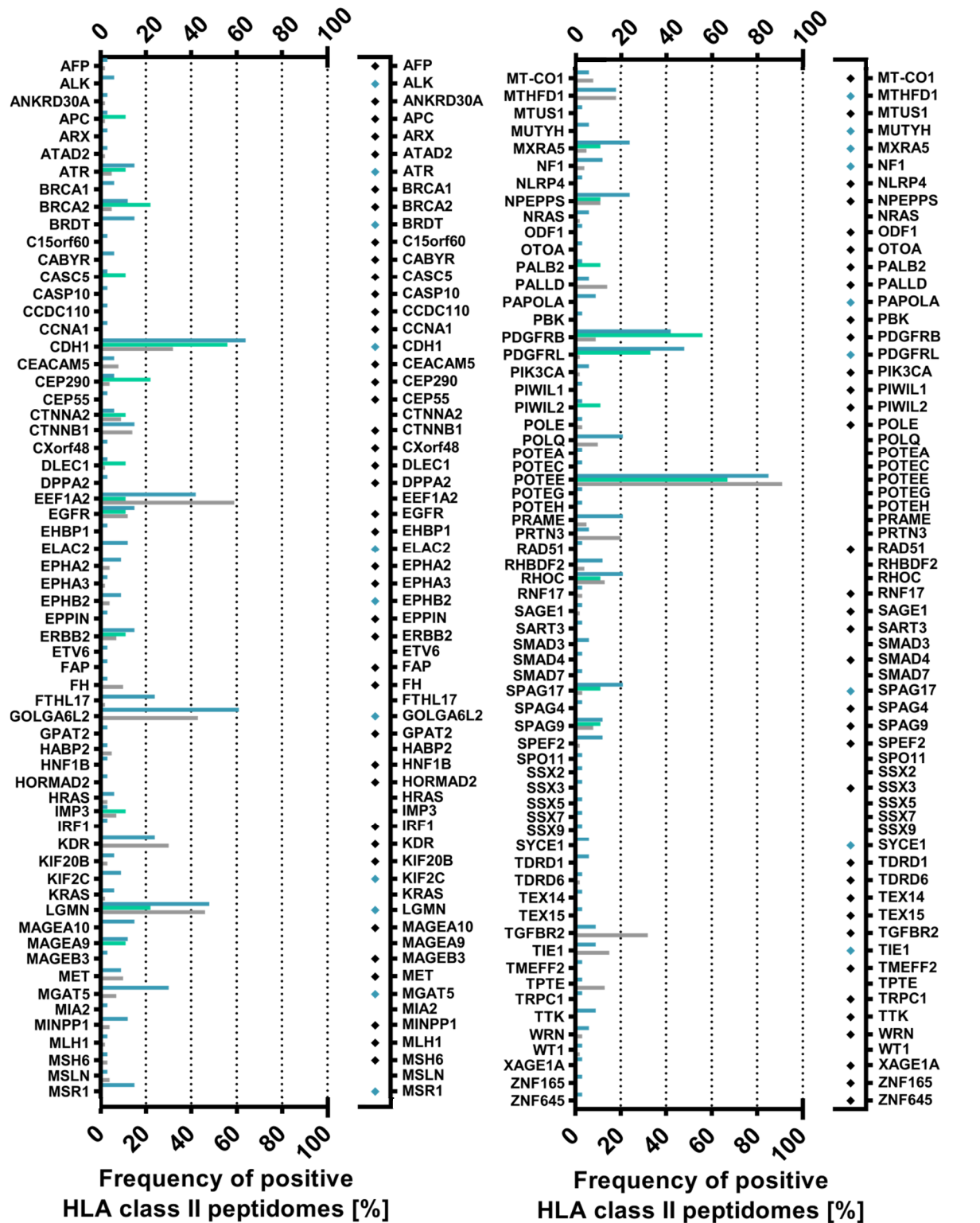


Figure 37. Identification of established TAAs, CTAs, and meningioma-associated antigens across the present HLA peptidome dataset. While peptides mapping to multiple source proteins were considered to calculate the frequency of positive HLA peptidomes, these were excluded to report the representation by meningioma-exclusive peptides. CTAs and TAAs exclusively identified on benign samples were not listed. (A) CTAs and TAAs naturally presented on HLA class I molecules of

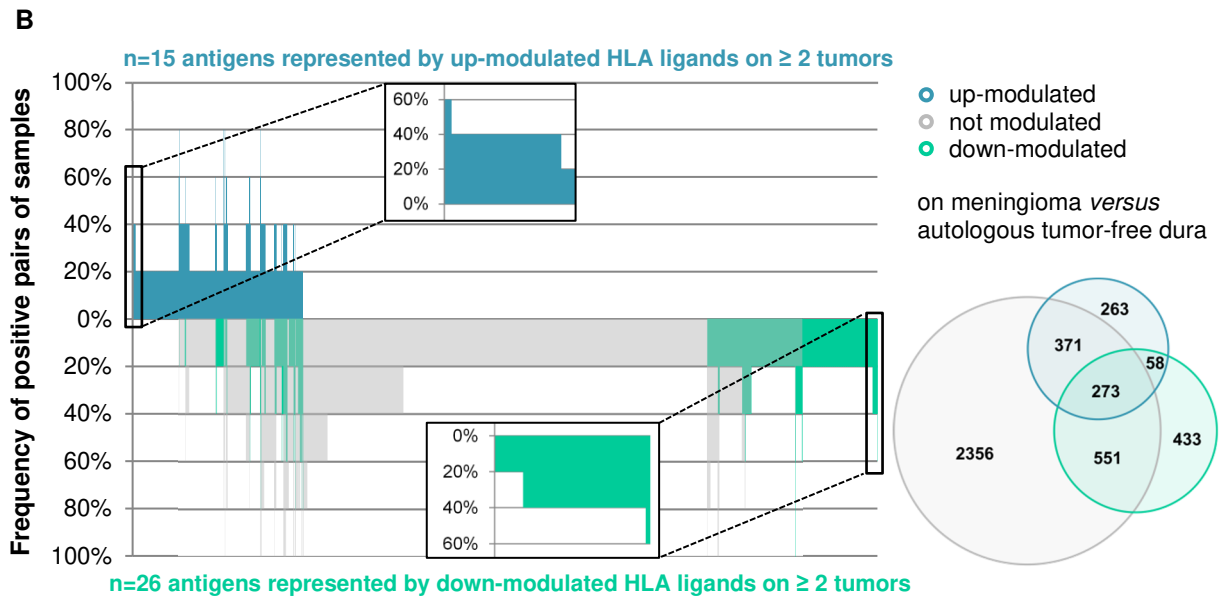
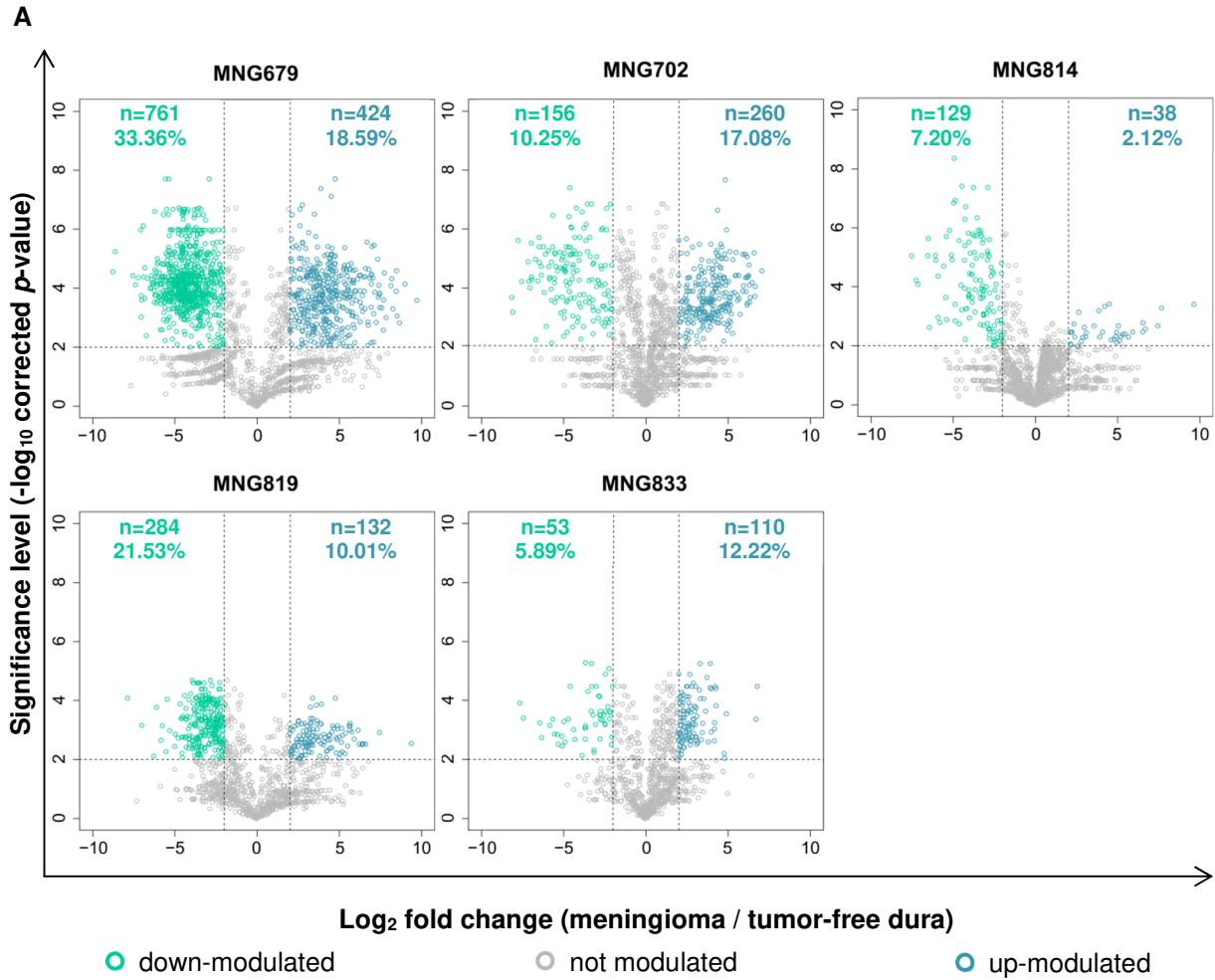
human meningioma and/or tumor-free dura tissue. The present immunopeptidomic dataset included HLA class I ligands derived from 145 TAAs and CTAs, with 18 being represented by meningioma-exclusive peptides on at least two tumors (highlighted with blue diamonds). The frequency of positive HLA peptidomes was assessed based on HLA class I ligands for meningioma and dura samples, whereby benign hits were reported independent of HLA binding probabilities of the underlying peptide identifications. **(B) TAAs and CTAs represented in the HLA class II peptidomes of human meningioma and/or tumor-free dura tissue.** Among 126 naturally presented CTAs and TAAs, 20 were represented by meningioma-exclusive peptides on at least two tumors (highlighted with blue diamonds).

4.3 Relative HLA ligand abundances on meningioma *versus* dura

From nine meningioma patients not only tumor tissue, but also autologous tumor-free dura was available enabling relative quantitation of HLA ligand abundances. Significant modulation was defined by a corrected p -value ≤ 0.01 and a fold change of mean AUC in (meningioma / dura) ≥ 4 or ≤ 0.25 regarding up- or down-modulated peptides, respectively. To obtain a deeper insight into general patterns of modulated HLA presentation on meningioma *versus* non-neoplastic dura, significantly modulated peptides were assigned to the source proteins they originated from. These protein lists were combined for all patients and subjected to comparative profiling unveiling HLA class I and II antigens recurrently represented by up- or down-modulated peptides, respectively. Moreover, functional annotation clustering identified biological processes in which antigens underlying modulated HLA presentation across meningioma patients were involved.

Significantly modulated HLA class I ligands

LFQ-MS to identify significantly up- and down-modulated HLA class I ligands was possible for five meningioma patients and based on a mean number of $1,563 \pm 462$ HLA class I ligands evaluated for relative abundance per patient. On average, $12.00 \pm 5.85\%$ and $15.65 \pm 10.43\%$ of the patients' HLA class I peptidomes were subject to significant up- and down-modulation, respectively (Figure 38 A). Since these five patients shared a maximum of two HLA-A, -B, or -C allotypes, comparative profiling to identify common patterns of modulated HLA presentation was performed on source protein level. In total, 263 and 433 antigens were exclusively represented by up- or down-modulated peptides, respectively (Figure 38 B). Functional annotation clustering identified the up-modulated ones to be mainly involved in organelle organization, cellular protein localization, ribosome biogenesis, DNA-templated transcription, and histone modification, whereas the down-modulated ones play a role in antigen processing and presentation, intracellular signal transduction, negative regulation of signal transduction, membrane protein localization, and viral processes (Figure 38 C, Supplementary Table 21). Following manual curation of the underlying peptides for HLA motifs as well as multi-mapping to several source proteins, a set of 13 antigens represented by up-modulated peptides on meningioma *versus* autologous tumor-free dura in 40-60% of patients was defined. Among these, RLA2 was the most frequent one. Conversely, 18 proteins were under-represented in the HLA class I peptidome of meningioma as compared with autologous non-neoplastic dura (40-60% of patients). PRC2C was represented by down-modulated HLA-A*23:01 and -A*24:02 ligands on three out of five meningiomas (Figure 38 B, Supplementary Table 20).



C

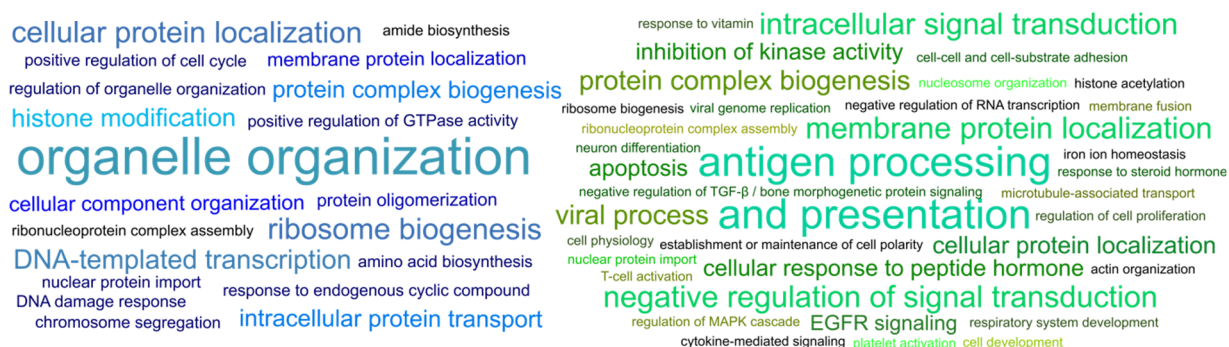
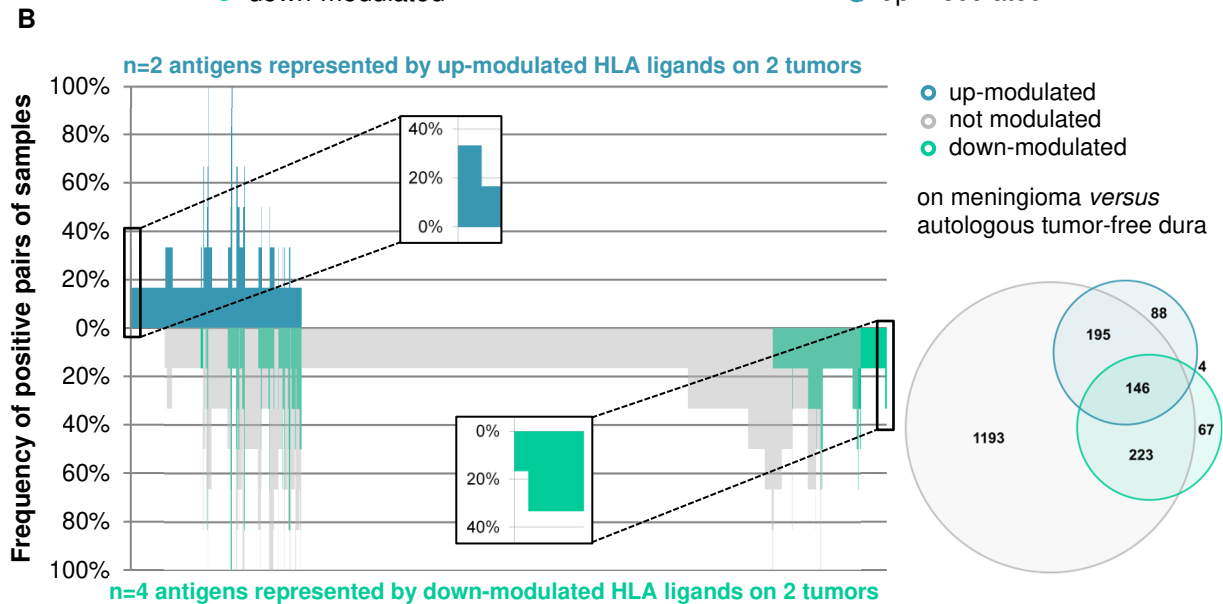
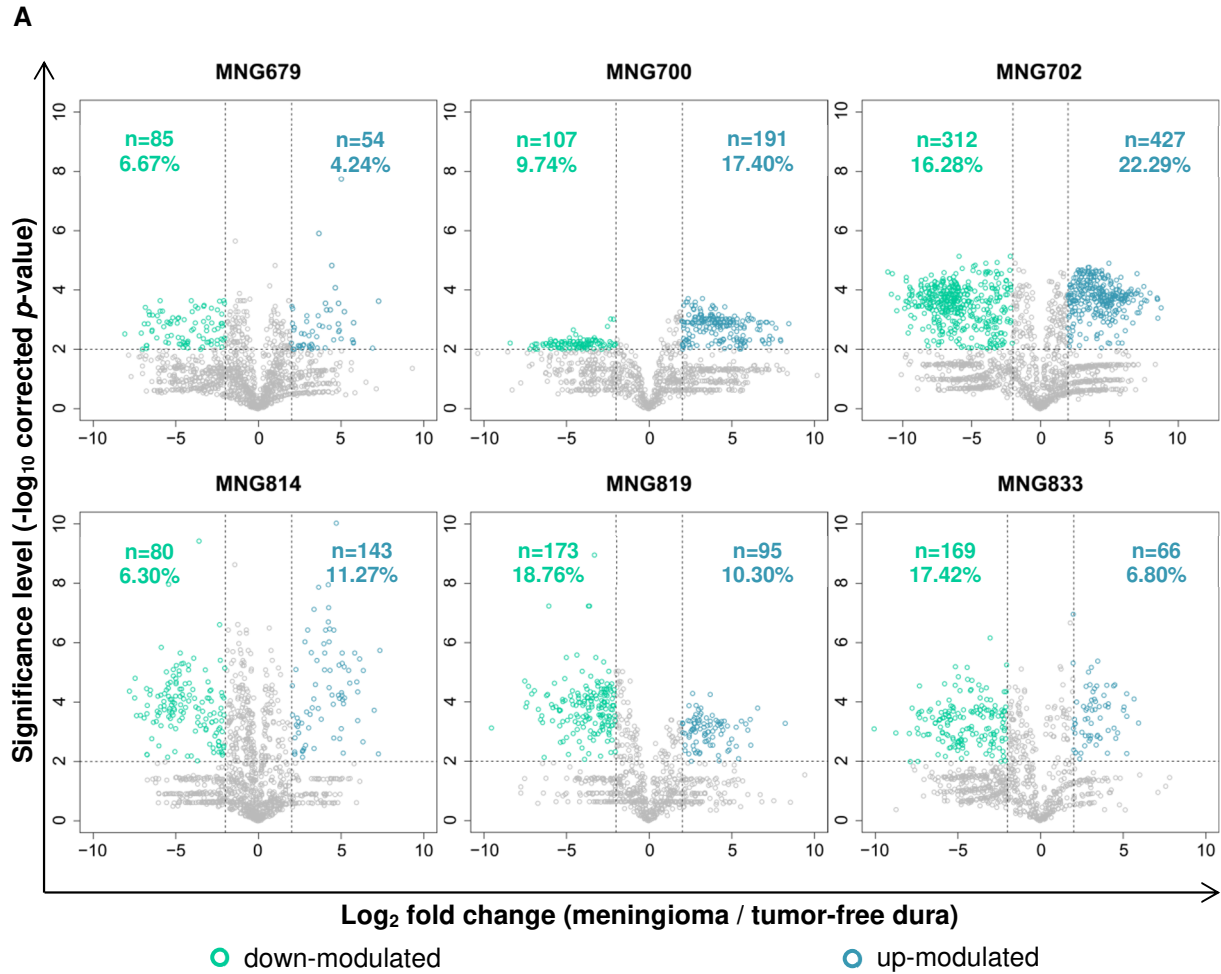


Figure 38. Patterns of modulated HLA class I presentation in meningioma across five patients. (A) Volcano plots of relative HLA ligand abundances on meningioma versus autologous tumor-free dura. By LFQ-MS, relative abundances of HLA class I ligands, each of which is represented by a dot, were compared. The x-axis indicates changes of abundance as \log_2 fold change and corresponding significance levels (after BH correction for multiple testing) are associated with the y-axis. Significant modulation was defined by a corrected p -value ≤ 0.01 and a fold change of mean AUC in (meningioma / dura) ≥ 4 or ≤ 0.25 regarding up- (highlighted in blue) or down-modulated (highlighted in green) peptides, respectively. The total number of up- and down-modulated peptides as well as their proportion in the patient's HLA class I peptidome are indicated in quadrants of each Volcano plot. Only four technical replicates were available from both dura and tumor tissue of patient MNG819. **(B) Comparative profiling of antigens corresponding to peptides displayed in Volcano plots.** Each bar in this waterfall plot (associated with the x-axis) represents a single protein, whereas the frequency of positive pairs of samples is shown on the y-axis. Comparing the source proteins of peptides underlying significant up- or down-modulation as well as of those not being modulated allowed the identification of exclusively and recurrently over- ($n=15$) or under-represented ($n=26$) antigens across five LFQ datasets acquired from meningioma and autologous tumor-free dura. **(C) Functional annotation of antigens exclusively represented by up- or down-modulated peptides.** Modulation-exclusive source proteins ($n=263$ over-represented antigens shown in the left and $n=433$ under-represented antigens shown in the right panel) were clustered for functional annotation with enrichment scores being proportional to the font size in the word clouds.

HLA class II-presented peptides with significant modulation

LFQ-MS to identify significantly up- and down-modulated HLA class II-restricted peptides was possible for six meningioma patients and based on a mean number of $1,242 \pm 330$ HLA class II-presented peptides evaluated for relative abundance per patient. On average, $12.05 \pm 6.13\%$ and $12.53 \pm 5.13\%$ of the patients' HLA class II peptidomes were subject to significant up- and down-modulation, respectively (Figure 39 A). Comparative profiling to identify common patterns of modulated HLA presentation was performed on source protein level, since length variants with common core sequences cannot be adequately addressed across patients. In total, $n=88$ and $n=67$ antigens were exclusively represented by up- or down-modulated peptides, respectively (Figure 39 B). Annotating these to biological functions did only identify three clusters for over-represented antigens (cell-cell adhesion, ribonucleoside metabolism, actin organization) and two clusters for under-represented antigens (response to oxidative stress, protein catabolism; Figure 39 C, Supplementary Table 21). No common signature of modulated HLA class II presentation was identified across the six patients, with only two (VQA1, QCR8) and four (CATF, ACH10, BROMI, NSF) antigens being represented by up- or down-modulated peptides in two patients, respectively (Figure 39 B, Supplementary Table 20).



C

actin organization
 cell-cell adhesion
 ribonucleoside metabolism

protein catabolism
 response to oxidative stress

Figure 39. Patterns of modulated HLA class II presentation in meningioma across six patients. (A) Volcano plots of relative HLA class II-presented peptide abundances on meningioma *versus* autologous tumor-free dura. By LFQ-MS, relative abundances of HLA class II-restricted peptides,

each of which is represented by a dot, were compared. The x-axis indicates changes of abundance as \log_2 fold change and corresponding significance levels (after BH correction for multiple testing) are associated with the y-axis. Significant modulation was defined by a corrected p -value ≤ 0.01 and a fold change of mean AUC in (meningioma / dura) ≥ 4 or ≤ 0.25 regarding up- (highlighted in blue) or down-modulated (highlighted in green) peptides, respectively. The total number of up- and down-modulated peptides as well as their proportion in the patient's HLA class II peptidome are indicated in quadrants of each Volcano plot. **(B) Comparative profiling of antigens corresponding to peptides displayed in Volcano plots.** Each bar in this waterfall plot (associated with the x-axis) represents a single protein, whereas the frequency of positive pairs of samples is shown on the y-axis. Comparing the source proteins of peptides underlying significant up- or down-modulation as well as of those not being modulated allowed the identification of exclusively and recurrently over- ($n=2$) or under-represented ($n=4$) antigens across six LFQ datasets acquired from meningioma and autologous tumor-free dura. **(C) Functional annotation of antigens exclusively represented by up- or down-modulated peptides.** Modulation-exclusive source proteins ($n=88$ over-represented antigens shown in the left and $n=67$ under-represented antigens shown in the right panel) were clustered for functional annotation with enrichment scores being proportional to the font size in the word clouds.

5 Discussion

Neoplasms of the meninges constitute more than one third of all brain and CNS tumors. Despite being largely non-malignant, meningiomas cause severe health issues and impossibility of complete surgical resection owing to localization and tumor recurrence despite surgery and radiation apply to a significant fraction.¹⁻⁶ Cancer immunotherapy may complement surgery and radiotherapy as well as meet the high demand for therapeutic regimens to manage disease recurrence.^{5,7} The natural presentation of candidate target antigens on HLA molecules has so far not been investigated. Herein, we present a large-scale immunopeptidomic study defining meningioma-associated HLA class I- and II-restricted peptides.

Meningioma proved to be suitable for HLA peptidomic efforts, yielding considerable numbers of HLA class I- and II-presented peptides from a total of 33 primary tumor samples. Furthermore, HLA expression and presentation of a manifold repertoire of peptides is a prerequisite for immunotherapeutic approaches. Likewise, several thousands of distinct HLA class I- and II-restricted peptides were eluted from autologous tumor-free dura being available from nine patients. Non-neoplastic dura was analyzed to supplement an in-house benign database already covering 30 distinct human tissues with that of tumor origin to define meningioma-associated antigens and peptides. There was no indication for decreased HLA expression on meningioma *versus* tumor-free dura yielding comparable amounts of HLA class I and II peptides per mg of tissue input. However, this comparison cannot delineate peptide identifications on tumor cells and such on stromal or infiltrating immune cells, which are part of bulk tumor tissue.²¹ Moreover, it is conceivable that cellular density varies between neoplastic and tumor-free meningeal tissue. A significant difference was observed between the relative number of HLA class I ligands and HLA class II-presented peptides identified per technical replicate and mg of meningioma tissue. The fact that the two compared groups had overlapping error bars, however, weakens the confidence of the underlying statistical calculation.

The present study population having a female-to-male ratio of 2:1 and a median age of onset of 59 constituted a representative cohort of meningioma patients.¹ In total, n=22 WHO grade I, n=9 WHO grade II, and n=2 WHO grade III tumors were analyzed. The 58 distinct HLA class I allotypes cover 99.98% of the world population, whereby 94.60% of all individuals are expected to be positive for at least three allotypes. The search for frequently presented meningioma-associated antigens revealed 28 and 37 for HLA class I and II, respectively. Among these, NMNA2 (30%), PRSS35 (30%), A4GALT (27%), FBN2 (21%), SNED1 (21%) WNT5A (18%), TBX15/18 (18%), and OSR1 (15%) were the most frequent ones. NMNA2 catalyzes nicotinamide adenine dinucleotide biosynthesis reflecting high energy consumption, accelerating glycolysis, and promoting cancer cell survival.²²⁻²⁵ WNT5A is a member of the oncogenic WNT protein family, which is known to be expressed in meningioma and many other tumors.^{26,27} In turn, little is known about the inactive serine protease PRSS35 (twelve PubMed entries²⁸), which has been reported to be expressed in ovaries²⁹ as well as in the context of renal fibrosis,³⁰ oocyte maturation,³¹ and epithelial-to-mesenchymal transition (EMT) of ovarian cancer cells.³² The latter acts *via* activation of the SMAD pathway and can be induced by WNT proteins,^{32,33} which is in line with the detection of up-modulated SMAD2-derived HLA class I ligands on two out of five meningiomas, 16 unique (non-multi-mapping) HLA class I ligands originating from WNT1, WNT2B, WNT5A, WNT6, or wntless homolog in 19 out of 33 tumors, 30 HLA class I ligands derived from FZD1, FZD2, FZD4, FZD6, FZD7, FZD8, and secreted frizzled related protein 2 across 25 out of 33 meningiomas as well as 42 unique (non-multi-mapping) CTNNB1-derived HLA class I ligands presented on every of the 33 analyzed tumors. These findings may indicate that activation of WNT signaling pathways in meningeal neoplasms is reflected by the immunopeptidome. With A4GALT, a meningioma-associated antigen acting as key regulator of both epithelial-to-mesenchymal and mesenchymal-to-epithelial transition of cancer cells was identified.³⁴ EMT can not only be induced by WNT, but also upon TGF- β stimulation.³³ Extracellular TGF- β is sequestered in microfibrils by FBN1 and FBN2, whereby the TGF- β capacity of FBN1 is higher. FBN1 has been reported to be down-regulated in tumor endothelial cells shifting the FBN1/FBN2 ratio in microfibrils towards FBN2. This causes a locally increased concentration of active TGF- β in the tumor microenvironment promoting not only EMT of tumor cells, but also angiogenesis.^{33,35} SNED1 is described to be up-regulated in several tumor entities including meningioma³⁶, to promote tumor invasiveness and metastasis formation, and to correlate with poor outcomes of estrogen- and progesterone-receptor-negative breast cancer patients when expressed at high levels.³⁷ T-box transcription factors such as TBX15 and TBX18 play a pivotal role in embryonic development and are hijacked by tumor cells.³⁸⁻⁴¹ OSR1, a serine/threonine protein kinase of the WNK pathway, participates in increasing the metastatic potential and proliferation rate of tumor cells as well as in promoting angiogenesis by interfering with PI3K-AKT, TGF- β , and nuclear factor kappa-light-chain-enhancer of activated B cells (NF- κ B) signaling networks.^{42,43}

Besides meningioma-associated antigens, meningioma-associated peptides potentially arising from differential antigen processing in tumor cells were defined. The applied threshold of five positive samples for reported meningioma-exclusive HLA class I ligands is for certain biased towards the most frequent HLA class I allotypes within the cohort. However, this also increases the confidence of meningioma exclusivity by ensuring sufficient coverage by HLA peptidomes included in the benign dataset supplemented with tumor-free dura specimens. In

addition, meningioma-exclusive targets from frequent allotypes have the advantage of being relevant for a large proportion of the potential patient population. Searching acquired HLA class I and II peptidome data for meningioma-associated peptides unveiled a set of 74 HLA class I ligands derived from 68 antigens presented on 15-30% of tumors as well as 44 antigens harboring meningioma-associated HLA class II presentation hotspots giving rise to naturally presented peptides across at least five patients. Remarkably, comparison of meningioma-associated HLA class I- and II-presented antigens as well as meningioma-associated HLA class I- and II-restricted peptides revealed a unique antigenic repertoire inherent to HLA class I and II peptidomes. Thus, it is inevitable to consider both HLA classes on both antigen and peptide level for comprehensive target discovery approaches. It is noteworthy that among the defined meningioma-associated peptides and proteins, seven HLA class I-presented antigens, 31 HLA class I ligands, six HLA class II-presented antigens, and 15 source proteins harboring hotspot regions proved to be pan-meningioma antigens or peptides presented across all WHO grades. Those tumor-associated antigens and peptides uniquely identified in tumors of the same WHO grade represented a clear minority within each of the four candidate target groups. This indicates that there are common antigenic signatures across differently graded meningiomas and promises broad application of defined targets for the immunotherapy of meningioma. Taking together meningioma-associated antigens and peptides presented on HLA class I molecules (n=141 candidate target peptides), these achieve a world population coverage of 99.57% with an average number of 21 peptides matching per patient. Assuming that half of these candidates will be excluded during the course of immunogenicity testing, which appears overestimated according to our previous experience with immunopeptidomics-based target definition approaches,⁴⁴ the number of peptides would still be enough to achieve sufficient coverage of the world population.

The HLA class II dataset contained three meningioma-associated CTAs (C1orf112, SIRPD, TTL6), which have so far not been listed in the CTDDatabase²⁰, whereas none of the HLA class I-presented meningioma-associated antigens exhibited a CTA-like RNA expression profile. Screening the present HLA peptidomes for 369 established CTAs, TAAs, or antigens reported to be meningioma-associated resulted in high overall identification rates. However, most antigens were also presented on tumor-free dura or benign tissues. SSX5/SSX9 and MAGEA10 had already been identified as meningioma-associated antigens *via* comparative profiling. Remaining meningioma-exclusive antigens and peptides derived from established TAAs and CTAs were characterized by infrequent HLA presentation refuting these as prime targets for cancer immunotherapies. This again emphasizes that the immunopeptidome represents an autonomous layer strongly influenced by the antigen processing machinery and cannot be expected to mirror the proteome or even the transcriptome.⁴⁵⁻⁴⁹ Thus, target definition for immunotherapeutic approaches is not recommended to be solely based on immunohistochemistry, protein, or RNA expression data, but calls for investigating the antigenic repertoire naturally presented on HLA molecules instead.

Moreover, relative quantitation of HLA-presented peptide abundances on meningioma *versus* autologous tumor-free dura was performed. 13 antigens were recurrently and exclusively represented by up-modulated HLA class I ligands with the ribosomal protein RLA2³⁶ being the most frequent one (60% of patients). This is in line with the finding that source proteins of up-

modulated HLA class I ligands functionally clustered for involvement in anabolic processes, especially RNA transcription and protein biosynthesis. Likewise, 18 proteins were frequently under-represented in tumor HLA class I peptidomes. Among these, PRC2C, which is involved in hematopoietic cell differentiation,³⁶ was the most frequent one (60% of tumors). Antigen processing and presentation, the functional annotation of under-represented source proteins with the highest enrichment score, can, however, be designated as an artefact arising from few peptides mapping to a large number of protein accessions annotated to HLA class II molecules. Besides that, many antigens represented by down-modulated HLA class I ligands were associated with cellular signal transduction and protein localization. While proteins promoting cell cycle progression were over-represented, such involved in apoptosis or the regulation of cell proliferation were under-represented in the HLA class I peptidome of meningiomas. This may indicate that increased proliferative activity and concomitant inhibition of apoptosis are reflected by quantitative changes in the immunopeptidome. In turn, modulation of HLA class II peptide presentation did not show a common signature across patients, with only six antigens underlying the same modulation of presentation in two patients. Likewise, only few clusters of functional annotation were identified among over- and under-represented antigens.

HLA-A*02:01 was not only the most frequent HLA class I allotype in the meningioma cohort, but also has a pronounced high allele frequency across the world (meningioma cohort: 23%; China: 13-19%; Germany: 12-27%; Japan 12%; Russia: 30%; USA: 4-28%).⁵⁰ Thus, all HLA-A*02:01-restricted peptides derived from meningioma-associated antigens as well as meningioma-associated HLA-A*02:01 ligands presented on at least 18% of tumors were selected for synthesis. Immunogenicity testing including priming of naïve T cells from healthy donors and – if possible – meningioma patients will be performed by Dr. med. Julia Velz and Gioele Medici in the Laboratory for Molecular Neuro-Oncology at the University of Zürich.

Taken together, our study demonstrates that meningioma is suited for immunotherapeutic intervention. The unprecedented investigation of the antigenic repertoire of meningeal neoplasms delineated a novel set of non-mutated meningioma-associated antigens and peptides naturally presented on HLA class I and II molecules. These enable developing peptide-specific immunotherapies such as peptide and DC vaccination or T cell-based approaches which may ultimately contribute to overcome the lack of therapeutic options for non-resectable and recurrent meningiomas.

6 References

1. Ostrom QT, Cioffi G, Gittleman H, Patil N, Waite K, Kruchko C, Barnholtz-Sloan JS. CBTRUS Statistical Report: Primary Brain and Other Central Nervous System Tumors Diagnosed in the United States in 2012-2016. *Neuro Oncol.* 2019;21(Supplement_5):v1-v100.
2. Riemenschneider MJ, Perry A, Reifenberger G. Histological classification and molecular genetics of meningiomas. *Lancet Neurol.* 2006;5(12):1045-1054.
3. Bickerstaff ER, Small JM, Guest IA. The relapsing course of certain meningiomas in relation to pregnancy and menstruation. *J Neurol Neurosurg Psychiatry.* 1958;21(2):89-91.
4. Koenig MA, Geocadin RG, Kulesza P, Olivi A, Brem H. Rhabdoid meningioma occurring in an unrelated resection cavity with leptomeningeal carcinomatosis. Case report. *J Neurosurg.* 2005;102(2):371-375.
5. Apra C, Peyre M, Kalamirides M. Current treatment options for meningioma. *Expert Rev Neurother.* 2018;18(3):241-249.

Chapter 4: References

6. van Alkemade H, de Leau M, Dieleman EM, Kardaun JW, van Os R, Vandertop WP, van Furth WR, Stalpers LJ. Impaired survival and long-term neurological problems in benign meningioma. *Neuro Oncol.* 2012;14(5):658-666.
7. Kessler RA, Garzon-Muvdi T, Yang W, Weingart J, Olivi A, Huang J, Brem H, Lim M. Metastatic Atypical and Anaplastic Meningioma: A Case Series and Review of the Literature. *World Neurosurg.* 2017;101:47-56.
8. Dettori P, Bradac GB, Scialfa G. Selective angiography of the external and internal carotid arteries in the diagnosis of supra-tentorial meningiomas. *Neuroradiology.* 1970;1(3):166-172.
9. Manaka H, Sakata K, Tatezaki J, Shinohara T, Shimohigoshi W, Yamamoto T. Safety and Efficacy of Preoperative Embolization in Patients with Meningioma. *J Neurol Surg B Skull Base.* 2018;79(Suppl 4):S328-s333.
10. Louis DN, Perry A, Reifenberger G, von Deimling A, Figarella-Branger D, Cavenee WK, Ohgaki H, Wiestler OD, Kleihues P, Ellison DW. The 2016 World Health Organization Classification of Tumors of the Central Nervous System: a summary. *Acta Neuropathol.* 2016;131(6):803-820.
11. Malhotra M, Toulouse A, Godinho BM, Mc Carthy DJ, Cryan JF, O'Driscoll CM. RNAi therapeutics for brain cancer: current advancements in RNAi delivery strategies. *Mol Biosyst.* 2015;11(10):2635-2657.
12. Purves D, Augustine GJ, Fitzpatrick D, Katz LC, LaMantia AS, McNamara JO, Williams SM. Neuroscience. 2nd edition. Sunderland (MA): Sinauer Associates; 2001. The Blood Supply of the Brain and Spinal Cord. Available from: <https://www.ncbi.nlm.nih.gov/books/NBK11042/>, accessed on 2020/03/31.
13. Bhowmik A, Khan R, Ghosh MK. Blood brain barrier: a challenge for effectual therapy of brain tumors. *Biomed Res Int.* 2015;2015:320941.
14. Wilson EH, Weninger W, Hunter CA. Trafficking of immune cells in the central nervous system. *J Clin Invest.* 2010;120(5):1368-1379.
15. Mohme M, Neidert MC, Regli L, Weller M, Martin R. Immunological challenges for peptide-based immunotherapy in glioblastoma. *Cancer Treat Rev.* 2014;40(2):248-258.
16. The GTEx Consortium. The Genotype-Tissue Expression (GTEx) project. *Nat Genet.* 2013;45(6):580-585.
17. Shukla SA, Rooney MS, Rajasagi M, Tiao G, Dixon PM, Lawrence MS, Stevens J, Lane WJ, Dellagatta JL, Steelman S, Sougnez C, Cibulskis K, Kiezun A, Hacohen N, Brusic V, Wu CJ, Getz G. Comprehensive analysis of cancer-associated somatic mutations in class I HLA genes. *Nat Biotechnol.* 2015;33(11):1152-1158.
18. Paramasivam N, Hübschmann D, Toprak UH, Ishaque N, Neidert M, Schrimpf D, Stichel D, Reuss D, Sievers P, Reinhardt A, Wefers AK, Jones DTW, Gu Z, Werner J, Uhrig S, Wirsching HG, Schick M, Bewerunge-Hudler M, Beck K, Brehmer S, Urbschat S, Seiz-Rosenhagen M, Hänggi D, Herold-Mende C, Ketter R, Eils R, Ram Z, Pfister SM, Wick W, Weller M, Grossmann R, von Deimling A, Schlesner M, Sahm F. Mutational patterns and regulatory networks in epigenetic subgroups of meningioma. *Acta Neuropathol.* 2019;138(2):295-308.
19. Vita R, Overton JA, Greenbaum JA, Ponomarenko J, Clark JD, Cantrell JR, Wheeler DK, Gabbard JL, Hix D, Sette A, Peters B. The immune epitope database (IEDB) 3.0. *Nucleic Acids Res.* 2015;43(Database issue):D405-412.
20. Almeida LG, Sakabe NJ, deOliveira AR, Silva MC, Mundstein AS, Cohen T, Chen YT, Chua R, Gurung S, Gnjatich S, Jungbluth AA, Caballero OL, Bairoch A, Kiesler E, White SL, Simpson AJ, Old LJ, Camargo AA, Vasconcelos AT. CTdatabase: a knowledge-base of high-throughput and curated data on cancer-testis antigens. *Nucleic Acids Res.* 2009;37(Database issue):D816-819.
21. Murphy JP, Konda P, Kowalewski DJ, Schuster H, Clements D, Kim Y, Cohen AM, Sharif T, Nielsen M, Stevanovic S, Lee PW, Gujar S. MHC-I ligand discovery using targeted database searches of mass spectrometry data: Implications for T cell immunotherapies. *J Proteome Res.* 2017.
22. Jayaram HN, Kusumanchi P, Yalowitz JA. NMNAT expression and its relation to NAD metabolism. *Curr Med Chem.* 2011;18(13):1962-1972.
23. Qi J, Cui C, Deng Q, Wang L, Chen R, Zhai D, Xie L, Yu J. Downregulated SIRT6 and upregulated NMNAT2 are associated with the presence, depth and stage of colorectal cancer. *Oncol Lett.* 2018;16(5):5829-5837.
24. Buonvicino D, Mazzola F, Zamporlini F, Resta F, Ranieri G, Camaioni E, Muzzi M, Zecchi R, Pieraccini G, Dölle C, Calamante M, Bartolucci G, Ziegler M, Stecca B, Raffaelli N, Chiarugi A. Identification of the Nicotinamide Salvage Pathway as a New Toxication Route for Antimetabolites. *Cell Chem Biol.* 2018;25(4):471-482.e477.
25. Cairns RA, Harris IS, Mak TW. Regulation of cancer cell metabolism. *Nat Rev Cancer.* 2011;11(2):85-95.
26. Howng SL, Wu CH, Cheng TS, Sy WD, Lin PC, Wang C, Hong YR. Differential expression of Wnt genes, beta-catenin and E-cadherin in human brain tumors. *Cancer Lett.* 2002;183(1):95-101.
27. Smalley MJ, Dale TC. Wnt signalling in mammalian development and cancer. *Cancer Metastasis Rev.* 1999;18(2):215-230.
28. Publications listed in PubMed dealing with the inactive serine protease 35. [Internet]. Available from: <https://www.ncbi.nlm.nih.gov/pubmed/?term=prss35>, accessed on 2020/03/17.
29. Miyakoshi K, Murphy MJ, Yeoman RR, Mitra S, Dubay CJ, Hennebold JD. The identification of novel ovarian proteases through the use of genomic and bioinformatic methodologies. *Biol Reprod.* 2006;75(6):823-835.
30. LeBleu VS, Teng Y, O'Connell JT, Charytan D, Müller GA, Müller CA, Sugimoto H, Kalluri R. Identification of human epididymis protein-4 as a fibroblast-derived mediator of fibrosis. *Nat Med.* 2013;19(2):227-231.
31. Li SH, Lin MH, Hwu YM, Lu CH, Yeh LY, Chen YJ, Lee RK. Correlation of cumulus gene expression of GJA1, PRSS35, PTX3, and SERPINE2 with oocyte maturation, fertilization, and embryo development. *Reprod Biol Endocrinol.* 2015;13:93.

Chapter 4: References

32. Paullin T, Powell C, Menzie C, Hill R, Cheng F, Martyniuk CJ, Westerheide SD. Spheroid growth in ovarian cancer alters transcriptome responses for stress pathways and epigenetic responses. *PLoS One*. 2017;12(8):e0182930.
33. Moustakas A, Heldin CH. Signaling networks guiding epithelial-mesenchymal transitions during embryogenesis and cancer progression. *Cancer Sci*. 2007;98(10):1512-1520.
34. Jacob F, Alam S, Konantz M, Liang CY, Kohler RS, Everest-Dass AV, Huang YL, Rimmer N, Fedier A, Schötzau A, Lopez MN, Packer NH, Lengerke C, Heinzelmann-Schwarz V. Transition of Mesenchymal and Epithelial Cancer Cells Depends on alpha1-4 Galactosyltransferase-Mediated Glycosphingolipids. *Cancer Res*. 2018;78(11):2952-2965.
35. van Loon K, Yemelyanenko-Lyalenko J, Margadant C, Griffioen AW, Huijbers EJM. Role of fibrillin-2 in the control of TGF-beta activation in tumor angiogenesis and connective tissue disorders. *Biochim Biophys Acta Rev Cancer*. 2020;1873(2):188354.
36. Smith RN, Aleksic J, Butano D, Carr A, Contrino S, Hu F, Lyne M, Lyne R, Kalderimis A, Rutherford K, Stepan R, Sullivan J, Wakeling M, Watkins X, Micklem G. InterMine: a flexible data warehouse system for the integration and analysis of heterogeneous biological data. *Bioinformatics*. 2012;28(23):3163-3165.
37. Naba A, Clauser KR, Lamar JM, Carr SA, Hynes RO. Extracellular matrix signatures of human mammary carcinoma identify novel metastasis promoters. *Elife*. 2014;3:e01308.
38. Wansleben S, Peres J, Hare S, Goding CR, Prince S. T-box transcription factors in cancer biology. *Biochim Biophys Acta*. 2014;1846(2):380-391.
39. Douglas NC, Papaioannou VE. The T-box transcription factors TBX2 and TBX3 in mammary gland development and breast cancer. *J Mammary Gland Biol Neoplasia*. 2013;18(2):143-147.
40. Willmer T, Cooper A, Peres J, Omar R, Prince S. The T-Box transcription factor 3 in development and cancer. *Biosci Trends*. 2017;11(3):254-266.
41. Papaioannou VE. T-box genes in development: from hydra to humans. *Int Rev Cytol*. 2001;207:1-70.
42. Gallolu Kankanamalage S, Karra AS, Cobb MH. WNK pathways in cancer signaling networks. *Cell Commun Signal*. 2018;16(1):72.
43. Sie ZL, Li RY, Sampurna BP, Hsu PJ, Liu SC, Wang HD, Huang CL, Yuh CH. WNK1 Kinase Stimulates Angiogenesis to Promote Tumor Growth and Metastasis. *Cancers (Basel)*. 2020;12(3).
44. Bilich T, Nelde A, Bichmann L, Roerden M, Salih HR, Kowalewski DJ, Schuster H, Tsou CC, Marcu A, Neidert MC, Lübke M, Rieth J, Schemionek M, Brümmendorf TH, Vucinic V, Niederwieser D, Bauer J, Märklin M, Peper JK, Klein R, Kohlbacher O, Kanz L, Rammensee HG, Stevanović S, Walz JS. The HLA ligandome landscape of chronic myeloid leukemia delineates novel T-cell epitopes for immunotherapy. *Blood*. 2019;133(6):550-565.
45. Weinzierl AO, Lemmel C, Schoor O, Müller M, Krüger T, Wernet D, Hennenlotter J, Stenzl A, Klingel K, Rammensee HG, Stevanović S. Distorted relation between mRNA copy number and corresponding major histocompatibility complex ligand density on the cell surface. *Mol Cell Proteomics*. 2007;6(1):102-113.
46. Fortier MH, Caron É, Hardy MP, Voisin G, Lemieux S, Perreault C, Thibault P. The MHC class I peptide repertoire is molded by the transcriptome. *J Exp Med*. 2008;205(3):595-610.
47. Bassani-Sternberg M, Pletscher-Frankild S, Jensen LJ, Mann M. Mass spectrometry of human leukocyte antigen class I peptidomes reveals strong effects of protein abundance and turnover on antigen presentation. *Mol Cell Proteomics*. 2015;14(3):658-673.
48. Shraibman B, Barnea E, Kadosh DM, Haimovich Y, Slobodin G, Rosner I, López-Larrea C, Hilf N, Kuttruff S, Song C, Britten C, Castle J, Kreiter S, Frenzel K, Tatagiba M, Tabatabai G, Dietrich PY, Dutoit V, Wick W, Platten M, Winkler F, von Deimling A, Kroep J, Sahuquillo J, Martinez-Ricarte F, Rodon J, Lassen U, Ottensmeier C, van der Burg SH, Thor Straten P, Poulsen HS, Ponsati B, Okada H, Rammensee HG, Sahin U, Singh H, Admon A. Identification of Tumor Antigens Among the HLA Peptidomes of Glioblastoma Tumors and Plasma. *Mol Cell Proteomics*. 2019;18(6):1255-1268.
49. Freudenmann LK, Marcu A, Stevanović S. Mapping the tumour human leukocyte antigen (HLA) ligandome by mass spectrometry. *Immunology*. 2018;154(3):331-345.
50. González-Galarza FF, Takeshita LY, Santos EJ, Kempson F, Maia MH, da Silva AL, Teles e Silva AL, Ghattaoraya GS, Alfirevic A, Jones AR, Middleton D. Allele frequency net 2015 update: new features for HLA epitopes, KIR and disease and HLA adverse drug reaction associations. *Nucleic Acids Res*. 2015;43(Database issue):D784-788.

CHAPTER 5



A meta-analysis comparing the immunopeptidomic landscape of intracranial neoplasms

Lena Katharina Freudenmann created and analyzed all HLA peptidomic datasets as indicated in previous chapters, performed the meta-analysis, and contributed all figures and texts.

1 Abstract

Intracranial neoplasias are among the most common and most severe tumor diseases in both children and adults. We performed a large meta-analysis including 123 HLA class I and II peptidome datasets acquired from n=40 glioblastoma, n=28 medulloblastoma, and n=33 meningioma patients. Each of these neoplasms is characterized by a unique underlying cellular background suggesting that there might be – besides similarities – also profound differences in the antigenic landscape of these brain tumors. Specific HLA genotypes are associated with increased or decreased susceptibility to autoimmune and infectious diseases and have recently been found to coin response to cancer immunotherapy. This encouraged us to screen the three cohorts for altered HLA allotype frequencies. We found six HLA class I allotypes to be significantly enriched among patients suffering from intracranial neoplasias. Additionally, we identified WNT5A and ESCO1 as pan-brain tumor antigens, while other candidate targets for cancer immunotherapy exhibited largely entity-specific HLA presentation. Taken together, we demonstrated that immunopeptidomics-based target definition inevitably has to be performed for every tumor entity individually and that intracranial neoplasias are associated with cumulative occurrence of particular HLA allomorphs.

2 Introduction

The intracranial neoplasms glioblastoma, medulloblastoma, and meningioma originate from different cell types, namely glial, embryonal neuroepithelial / cerebellar granule neural precursor, and meningeal cells.¹⁻⁵ To investigate, whether this difference in cellular origin is reflected by the antigenic landscape of these three tumors, the repertoires of HLA class I- and II-presented peptides were searched for similarities and differences. Linus Backert, a former colleague, tried to identify antigens shared between four hematological malignancies based on HLA peptidome data. However, multiple myeloma, acute myeloid, chronic myeloid, and chronic lymphocytic leukemias essentially had entity-specific tumor-associated antigens.⁶ The immunopeptidomic datasets acquired during the course of this thesis were searched for pan-brain tumor antigens shared between glioblastoma, medulloblastoma, and meningioma.

The development and course of various autoimmune and infectious diseases has been associated with specific HLA class I and II alleles.⁷⁻¹⁰ A cohort of 22 ependymoma patients has recently been found to have a significantly increased allotype frequency of HLA-A*26:01 as compared with the German population (internal data created by Lena Mühlenbruch at the Department of Immunology, University of Tübingen). Hence, the HLA class I allotype frequencies within the glioblastoma, medulloblastoma, and meningioma cohort were compared with the distribution in the German population.

3 Methods

Acquisition of HLA peptidome data and definition of candidate target antigens

Peptides presented on HLA class I and II molecules were isolated and analyzed as described previously (CHAPTER 1 / 3.2; CHAPTER 2-4 / 3). Definition of candidate targets for cancer immunotherapy was performed as reported in CHAPTER 2-4.

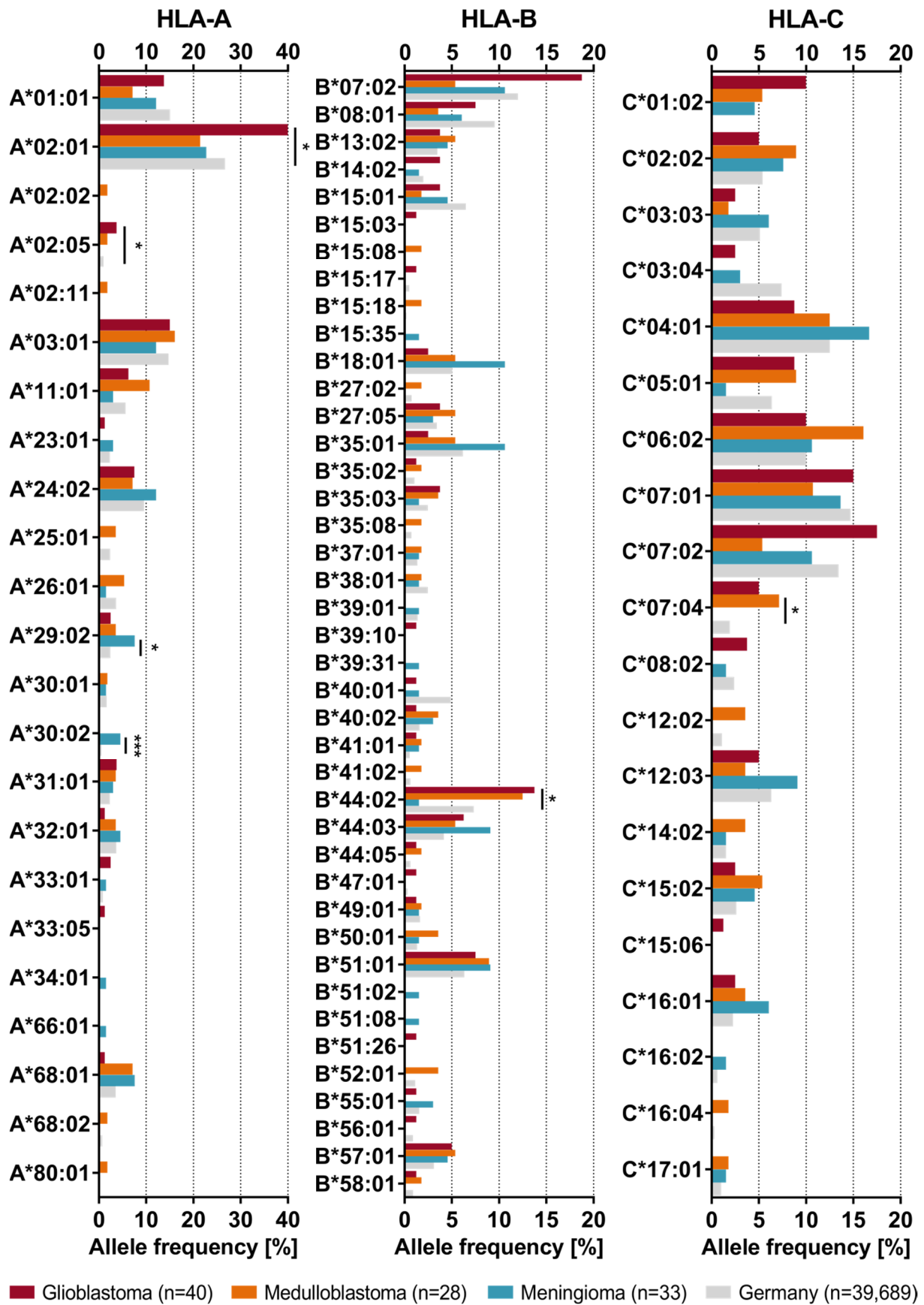
HLA class I allele frequencies

Tumor samples were collected during surgical resections performed in Switzerland and Germany and HLA typing was conducted as reported previously (CHAPTER 2-4 / 3). For each of the three patient cohorts, HLA class I allele frequencies were calculated (Supplementary Table 1, Supplementary Table 10, Supplementary Table 15). Owing to the poor data availability from Switzerland, allele frequencies calculated for each patient cohort were only set in relation to a large German reference population as retrieved from the Allele Frequency Net Database (Germany pop 8; n=39,689).¹¹ One-hit wonders (n=1 positive patient) were not considered for statistical evaluation employing Yates's continuity corrected χ^2 tests.

4 Results

4.1 HLA class I allotypes associated with intracranial neoplasia

We investigated the HLA class I allele frequencies observed among glioblastoma, medulloblastoma, or meningioma patients in comparison with a large German reference population. HLA-A*02:01, -A*02:05, and -B*44:02 were found to be significantly enriched in glioblastoma, whereas increased allele frequencies of HLA-C*07:04 or HLA-A*29:02 and -A*30:02 were identified among medulloblastoma and meningioma patients, respectively (Figure 40).



Tumor entity	HLA allotype	n alleles (allele frequency) in patient / reference cohort	Two-tailed p-value	χ^2	OR (95% CI)
Glioblastoma	A*02:01	32 (40.0%) / 21,170 (26.7%)	0.0102	6.594	1.8 (1.2-2.9)
	A*02:05	3 (3.8%) / 738 (0.9%)	0.0412	4.166	4.2 (1.3-13.2)
	B*44:02	11 (13.8%) / 5,810 (7.3%)	0.0464	3.967	2.0 (1.1-3.8)
Medulloblastoma	C*07:04	4 (7.1%) / 1,524 (1.9%)	0.0184	5.560	3.9 (1.4-10.9)
Meningioma	A*29:02	3 (4.6%) / 437 (0.6%)	0.0187	5.532	3.3 (1.3-8.3)
	A*30:02	5 (7.6%) / 1,897 (2.4%)	0.0004	12.54	8.6 (2.7-27.5)

Figure 40. Association of HLA class I allotypes with intracranial neoplasias. Using the Yates's continuity corrected χ^2 test HLA class I allele frequencies among glioblastoma, medulloblastoma, and meningioma patients were compared with that of a large German population (upper panel). This identified a significantly increased allele frequency of three, one, and two HLA class I allotypes among glioblastoma, medulloblastoma, or meningioma patients, respectively (lower panel). Reference data for HLA-A*02:02, -A*66:02, and -C*01:02 were not available. Abbreviations not introduced in the text above: odds ratio (OR), confidence interval (CI).

4.2 The immunopeptidome of intracranial neoplasia in comparison

Considerable numbers of both HLA class I- and II-restricted peptides were eluted from glioblastomas (n=62), medulloblastomas (n=28), and meningiomas (n=33). Simple overlap analysis delineated only a small fraction of antigens to be entity-specific neither being identified in benign samples nor in any of the respective two other tumor types. The proportion of entity-specific proteins came up to 0.51-1.99% for HLA class I (Figure 41 A) and to 2.09-5.40% for HLA class II peptidomes (Figure 41 B) being highest for glioblastoma and lowest for medulloblastoma in each case. From a total of 12,792 HLA class I- and 9,678 HLA class II-presented antigens 260 ones were glioblastoma-associated on the peptide or protein level, respectively. For medulloblastoma, these numbers came up to 9,821 HLA class I- and 4,922 HLA class II- presented antigens comprising 71 tumor-associated ones. Immunopeptidome analysis of meningioma uncovered 10,431 and 7,535 proteins to be naturally presented on HLA class I and II molecules, whereby 184 yielded tumor-associated HLA ligands.

Comparing candidate targets of cancer immunotherapy defined for glioblastoma, medulloblastoma, and meningioma delineated an entity-specific repertoire of TAAs naturally presented on HLA molecules. However, WNT5A and ESCO1 proved to be pan-tumor antigens frequently and tumor-exclusively presented on all three intracranial neoplasms. Another 13 antigens each were shared by medulloblastomas and glioblastomas (OLIG3, NDUFA4L2, SHISA9, DCX, BTBD17, EFS, HES4, GFAP, PTPRZ1, KIF1A, CRMP1, AKAP9, NCAM1) or by meningiomas and glioblastomas (TMEM87A, TBX15, TBX18, SESN3, LRP1, FMNL2, STAB1, GRAMD3, OSGIN2, SERPINC1, FN1, COL5A2, SCG2), respectively (Figure 41 C, Supplementary Table 2-4, Supplementary Table 11-13, Supplementary Table 16-18).

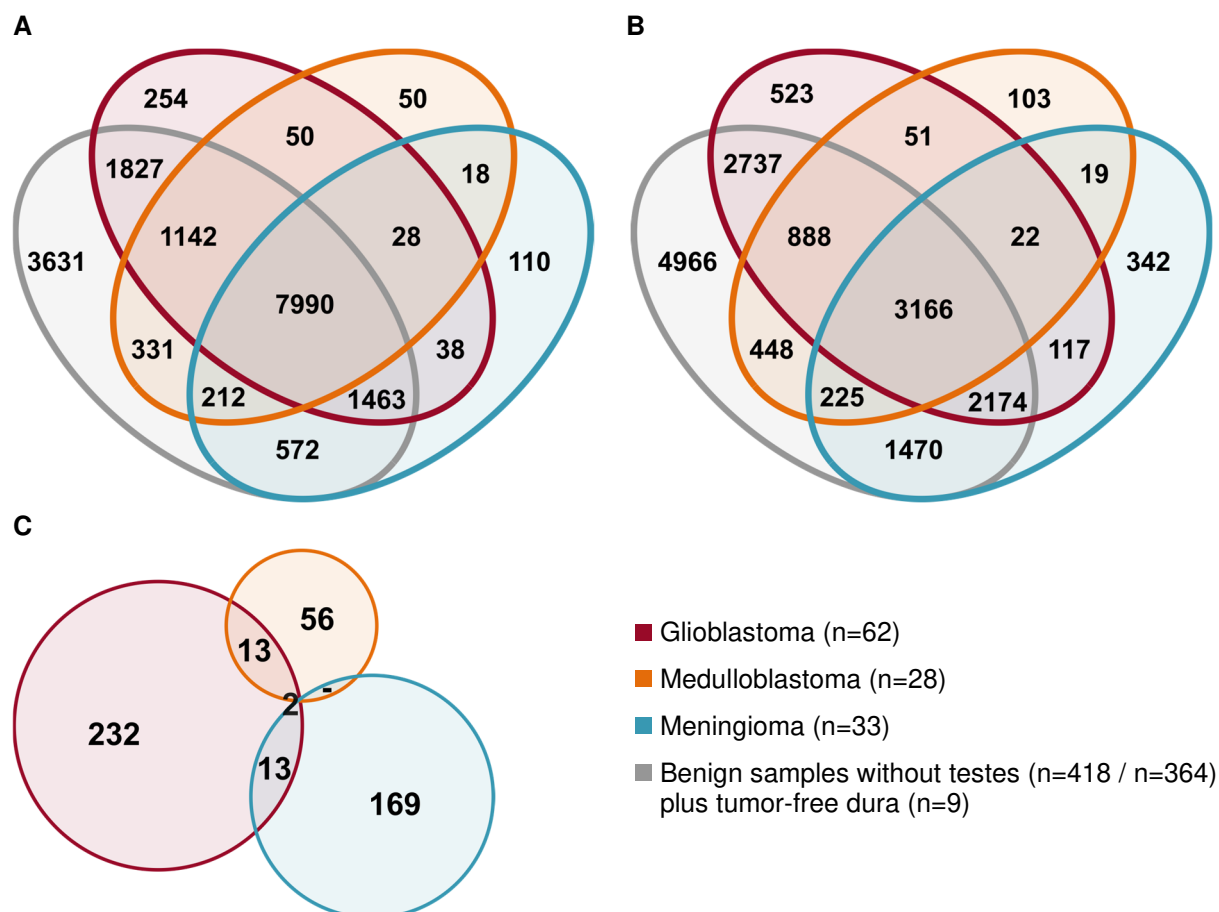


Figure 41. Similarities and differences of the immunopeptidomic landscape of glioblastoma, medulloblastoma, and meningioma. Overlap of (A) HLA class I- and (B) HLA class II-presented antigens. It should be noted that Venn diagrams cannot illustrate that tumor-exclusive proteins were permitted to be identified in one non-CNS-related sample within the benign dataset. **(C) Identification of shared and unique brain tumor antigens.** Combining the lists of HLA class I- and II-presented candidate targets for each tumor uncovered a small but notable overlap between the three entities. While 26 source proteins were tumor-exclusive or yielded tumor-associated peptides in two tumor types each, all investigated intracranial neoplasias had two tumor-associated antigens in common: WNT5A and ESCO1.

5 Discussion

Glial, embryonal neuroepithelial / cerebellar granule neural precursor, and meningeal cells represent the cellular origin of glioblastomas, medulloblastomas, and meningiomas.¹⁻⁵ We aimed at investigating whether the immunopeptidome and, most importantly, the repertoire of candidate targets for immunotherapy is imprinted by the cell lineage from which neoplastic transformation once started. Besides that, we evaluated the three patient cohorts presented herein for an association of intracranial neoplasias with specific HLA class I allomorphs.

Genetic predisposition represents a common element of multifactorial disease development. This encloses, among many others, the individual composition of HLA class I and II alleles. Autoimmune disorders, for instance, have a long history of HLA association including, for instance, ankylosing spondylitis (HLA-B*27), type 1 diabetes (HLA-DRB1*04:01–DQB1*03:02), narcolepsy (HLA-DQB1*06:02), and celiac disease (HLA-DQA1*05:01–DQB1*02:01 or HLA-DQA1*03:01–DQB1*03:02).⁷ The individual HLA genotype does not only

influence the observed immune phenotype, the susceptibility for, and the course of autoimmune and infectious diseases, but also the response to cancer immunotherapy.^{7-10,12} Maximal heterozygosity of HLA-A, -B, and -C alleles has been found to favor response to checkpoint inhibition thereby improving overall survival. In turn, HLA-B*15:01 has been suggested to impair neo-antigen-directed CD8⁺ T-cell responses.¹² Moreover, a cohort of 22 ependymoma patients has recently been found to have a significantly increased allotype frequency of HLA-A*26:01 as compared with the German population (internal data created by Lena Mühlenbruch at the Department of Immunology, University of Tübingen). Hence, the HLA class I allotype frequencies within the glioblastoma, medulloblastoma, and meningioma cohort were compared with the distribution in the German population. A significant fraction of tumor samples originated from surgeries performed in Switzerland, however, hardly any data on HLA allele frequencies had been available from this country. Assuming that the ethnic background and composition of the Swiss population is comparable to that of the German population, we used solely data from Germany for the comparison of HLA class I allotype frequencies. We found HLA-A*02:01, -A*02:05, and -B*44:02 to be significantly enriched among glioblastoma patients. The heavily elevated allele frequency of HLA-A*02:01 (40.0% *versus* 26.7%) might reason why previous immunotherapeutic efforts have focused on this allotype¹³⁻¹⁵ representing not only an overall common HLA allomorph, but being naturally enriched in glioblastoma patient collectives. Conversely, increased allele frequencies of HLA-C*07:04 or HLA-A*29:02 and -A*30:02 were identified within the cohort of medulloblastoma or meningioma patients, respectively. Once HLA class II allotypes have been successfully imputed from whole exome and RNA sequencing data, we aim to investigate whether there are also HLA class II alleles associated with intracranial neoplasias.

The immunopeptidomic datasets acquired during the course of this thesis were compared with each other and searched for pan-brain tumor antigens shared between glioblastoma, medulloblastoma, and meningioma. Despite high peptide yields per sample as well as a large total amount of unique peptide and protein identifications, the number of candidate targets defined for medulloblastoma (n=71) was considerably smaller as compared with the other two tumor types (glioblastoma: n=260 / meningioma: n=184). This may indicate that the antigenic landscape of medulloblastomas resembles that of benign tissues more than meningeal tumors and glioblastomas do. We found the repertoire of HLA-presented antigens, especially of those with tumor association, to be shaped by the cellular origin of neoplastic cells. Apart from WNT5A and ESCO1 proven to be pan-brain tumor antigens, candidate targets exhibited entity-specific HLA presentation. This is in line with previous findings in hematological malignancies, namely multiple myeloma, acute myeloid, chronic myeloid, and chronic lymphocytic leukemia, strongly encouraging and requiring immunopeptidomic studies to be performed for every tumor entity individually.⁶

The yield of HLA class I and II peptides per mg of tissue is representative of the cellular density, HLA expression, and to some extent also of the degree of immune infiltration.¹⁶⁻¹⁹ For both glioblastoma and medulloblastoma RNA sequencing was performed, which permits comparing the expression of all components of the antigen processing machinery including HLA class I and II molecules between these two tumor types. Subsequent to completion of transcriptome analysis, we aim to compare the number of peptide identifications relative to the amount of

tissue input and HLA expression between these two intracranial neoplasias. Including the meningioma dataset in this analysis is, however, not possible, as RNA sequencing data is lacking and data acquisition on another less sensitive LC-MS/MS system would introduce a technical bias.

In conclusion, we found six HLA class I allotypes to be associated with intracranial neoplasias as being significantly enriched among glioblastoma, medulloblastoma, or meningioma patients. Comparison of naturally presented candidate targets for cancer immunotherapy unveiled a unique repertoire of HLA-presented peptides inherent to every tumor entity as well as two pan-brain tumor antigens: WNT5A and ESCO1.


6 References

1. Ostrom QT, Cioffi G, Gittleman H, Patil N, Waite K, Kruchko C, Barnholtz-Sloan JS. CBTRUS Statistical Report: Primary Brain and Other Central Nervous System Tumors Diagnosed in the United States in 2012-2016. *Neuro Oncol.* 2019;21(Supplement_5):v1-v100.
2. Louis DN, Perry A, Reifenberger G, von Deimling A, Figarella-Branger D, Cavenee WK, Ohgaki H, Wiestler OD, Kleihues P, Ellison DW. The 2016 World Health Organization Classification of Tumors of the Central Nervous System: a summary. *Acta Neuropathol.* 2016;131(6):803-820.
3. Jäkel S, Dimou L. Glial Cells and Their Function in the Adult Brain: A Journey through the History of Their Ablation. *Front Cell Neurosci.* 2017;11:24.
4. Johnsen JI, Kogner P, Albiñá A, Henriksson MA. Embryonal neural tumours and cell death. *Apoptosis.* 2009;14(4):424-438.
5. Schüller U, Heine VM, Mao J, Kho AT, Dillon AK, Han YG, Huillard E, Sun T, Ligon AH, Qian Y, Ma Q, Alvarez-Buylla A, McMahon AP, Rowitch DH, Ligon KL. Acquisition of granule neuron precursor identity is a critical determinant of progenitor cell competence to form Shh-induced medulloblastoma. *Cancer Cell.* 2008;14(2):123-134.
6. Backert L, Kowalewski DJ, Walz S, Schuster H, Berlin C, Neidert MC, Schemionek M, Brummendorf TH, Vucinic V, Niederwieser D, Kanz L, Salih HR, Kohlbacher O, Weisel K, Rammensee HG, Stevanovi AS, Walz JS. A meta-analysis of HLA peptidome composition in different hematological entities: Entity-specific dividing lines and "pan-leukemia" antigens. *Oncotarget.* 2017.
7. Caillat-Zucman S. Molecular mechanisms of HLA association with autoimmune diseases. *Tissue Antigens.* 2009;73(1):1-8.
8. Trachtenberg E, Korber B, Sollars C, Kepler TB, Hraber PT, Hayes E, Funkhouser R, Fugate M, Theiler J, Hsu YS, Kunstman K, Wu S, Phair J, Erlich H, Wolinsky S. Advantage of rare HLA supertype in HIV disease progression. *Nat Med.* 2003;9(7):928-935.
9. The International HIV Controllers Study. The major genetic determinants of HIV-1 control affect HLA class I peptide presentation. *Science.* 2010;330(6010):1551-1557.
10. Hill AV, Allsopp CE, Kwiatkowski D, Anstey NM, Twumasi P, Rowe PA, Bennett S, Brewster D, McMichael AJ, Greenwood BM. Common west African HLA antigens are associated with protection from severe malaria. *Nature.* 1991;352(6336):595-600.
11. González-Galarza FF, Takeshita LY, Santos EJ, Kempson F, Maia MH, da Silva AL, Teles e Silva AL, Ghattaoraya GS, Alfirevic A, Jones AR, Middleton D. Allele frequency net 2015 update: new features for HLA epitopes, KIR and disease and HLA adverse drug reaction associations. *Nucleic Acids Res.* 2015;43(Database issue):D784-788.
12. Chowell D, Morris LGT, Grigg CM, Weber JK, Samstein RM, Makarov V, Kuo F, Kendall SM, Requena D, Riaz N, Greenbaum B, Carroll J, Garon E, Hyman DM, Zehir A, Solit D, Berger M, Zhou R, Rizvi NA, Chan TA. Patient HLA class I genotype influences cancer response to checkpoint blockade immunotherapy. *Science.* 2018;359(6375):582-587.
13. Hilf N, Kuttruff-Coqui S, Frenzel K, Bukur V, Stevanović S, Gouttefangeas C, Platten M, Tabatabai G, Dutoit V, van der Burg SH, Thor Straten P, Martínez-Ricarte F, Ponsati B, Okada H, Lassen U, Admon A, Ottensmeier CH, Ulges A, Kreiter S, von Deimling A, Skardelly M, Migliorini D, Kroep JR, Idorn M, Rodon J, Piró J, Poulsen HS, Shraibman B, McCann K, Mendrzyk R, Löwer M, Stieglbauer M, Britten CM, Capper D, Welters MJP, Sahuquillo J, Kiesel K, Derhovanessian E, Rusch E, Bunse L, Song C, Heesch S, Wagner C, Kemmer-Brück A, Ludwig J, Castle JC, Schoor O, Tadmor AD, Green E, Fritsche J, Meyer M, Pawlowski N, Dorner S, Hoffgaard F, Rössler B, Maurer D, Weinschenk T, Reinhardt C, Huber C, Rammensee HG, Singh-Jasuja H, Sahin U, Dietrich PY, Wick W. Actively personalized vaccination trial for newly diagnosed glioblastoma. *Nature.* 2019;565(7738):240-245.

Chapter 5: References

14. Phuphanich S, Wheeler CJ, Rudnick JD, Mazer M, Wang H, Nuno MA, Richardson JE, Fan X, Ji J, Chu RM, Bender JG, Hawkins ES, Patil CG, Black KL, Yu JS. Phase I trial of a multi-epitope-pulsed dendritic cell vaccine for patients with newly diagnosed glioblastoma. *Cancer Immunol Immunother.* 2013;62(1):125-135.
15. Dutoit V, Herold-Mende C, Hilf N, Schoor O, Beckhove P, Bucher J, Dorsch K, Flohr S, Fritsche J, Lewandrowski P, Lohr J, Rammensee HG, Stevanovic S, Trautwein C, Vass V, Walter S, Walker PR, Weinschenk T, Singh-Jasuja H, Dietrich PY. Exploiting the glioblastoma peptidome to discover novel tumour-associated antigens for immunotherapy. *Brain.* 2012;135(Pt 4):1042-1054.
16. Rossi ML, Hughes JT, Esiri MM, Coakham HB, Brownell DB. Immunohistological study of mononuclear cell infiltrate in malignant gliomas. *Acta Neuropathol.* 1987;74(3):269-277.
17. Hambardzumyan D, Gutmann DH, Kettenmann H. The role of microglia and macrophages in glioma maintenance and progression. *Nat Neurosci.* 2016;19(1):20-27.
18. Li W, Graeber MB. The molecular profile of microglia under the influence of glioma. *Neuro Oncol.* 2012;14(8):958-978.
19. Neidert MC, Kowalewski DJ, Silginer M, Kopolou K, Backert L, Freudenmann LK, Peper JK, Marcu A, Wang SS, Walz JS, Wolpert F, Rammensee HG, Henschler R, Lamszus K, Westphal M, Roth P, Regli L, Stevanović S, Weller M, Eisele G. The natural HLA ligandome of glioblastoma stem-like cells: antigen discovery for T cell-based immunotherapy. *Acta Neuropathol.* 2018;135(6):923-938.

CHAPTER 6



Implementation of a mix of ten synthetic heavy isotope-labeled peptides as retention time standard

Lena Katharina Freudenmann (L.K.F.) planned and performed mass spectrometry and data analysis for all titration experiments. Standardized HLA class I peptide eluates of JY cells were prepared by L.K.F. and Lena Mühlenbruch (JY17#3 and JY17#4) and by Jens Bauer (JY19#1), whereby ready-to-use RT peptides as well as JY19#1 with spiked RT peptides were frozen by L.K.F. and Jens Bauer. Data acquisition for performance monitoring using JY19#1 was conducted as routine procedure by the mass spectrometry team of the Department of Immunology at the University of Tübingen (Jens Bauer, L.K.F., Ana Marcu, Lena Mühlenbruch, and Annika Nelde) with data being analyzed and presented by L.K.F. Samples for the comparison of five LC-MS/MS systems were prepared by Ana Marcu and L.K.F. and measured by the respective companies or collaborators, respectively. These data were analyzed by Ana Marcu and Bruker Daltonics. Figure 49 was adapted from Ana Marcu's presentation of the data. All texts and remaining figures were contributed by L.K.F.

1 Abstract

Synthetic peptide spike-ins have been established as part of good proteomic practice, but have so far not been implemented for immunopeptidomics. These offer tremendous potential not only for constant monitoring of chromatographic and mass spectrometric performance, but also for contemporary data acquisition strategies and quantitative approaches with enhanced identification and reproducibility rate, which depend on retention time (RT) alignment between measurements to be compared with each other. We implemented a set of ten heavy isotope-labeled RT peptides that are compatible with immunopeptidomic requirements. Following titration to determine the optimal concentration for each peptide, these served as base for performance monitoring of two liquid chromatography-coupled tandem mass spectrometry (LC-MS/MS) systems over half a year. During the course of a procurement measure, the mix of ten RT peptides was used to compare five LC-MS/MS systems – especially regarding sensitivity – thus guiding device selection. Moreover, these RT peptides will enable deeper exploration of immunopeptidomes by data-independent acquisition and more accurate quantification strategies. Further, they will represent an essential tool in method development including optimization of collision energies for new LC-MS/MS systems used for immunopeptidomic research.

2 Introduction

Observed peptide retention times (RT) vary not only across different chromatographic systems, but also within the same system over time. Main influencing factors are solvent composition and solvent exchanges (mobile phase), flow rate, gradient settings, column material and column exchanges (stationary phase), and the volume comprised by the LC system. A standardized set of synthetic spike-in peptides enables indexing of RTs, monitoring of chromatographic performance, as well as comparison and calibration of collision energies between two mass spectrometers.¹ In relation to spike-in peptide RTs, peptide-specific RT indexes are calculated, represented by the dimensionless variable *iRT*, to align multiple LC-MS/MS runs.² RT alignment of LC-MS/MS measurements is of utmost importance when performing data-independent acquisition (DIA). Here, not only the most intense precursor ions are selected for fragmentation (as in case of DDA), but comprehensive sampling and fragmentation of peptide features is performed. This increases the identification rate as well as the reproducibility and quantifiability by eliminating the semi-stochastic process of peptide selection inherent to DDA. However, this results in chimeric fragment spectra that are difficult to demultiplex and impede assigning the correct chromatographic peak, which can be facilitated by spike-in RT standard peptides.^{1,3-6}

Previous attempts employing *iRT* peptides (Biognosys)² had failed, as these proteomic RT standards were not compatible with immunopeptidomic LC-MS/MS methods (internal data created at the Department of Immunology, University of Tübingen). ProteomeTools Calibration Standard (PROCAL) was developed by JPT Peptide Technologies for proteomic purposes with tryptic digests as analyte as well. However, several of the contained peptides lie as doubly or triply positive precursor ions within the *m/z* window applied for HLA peptidome analyses.¹ After a pilot experiment using the entire mix of 40 peptides, the ten best peptides were synthesized

in-house. The PROCAL sequences are arbitrary and do not occur in any proteome according to present knowledge. However, when facing the emerging field of cryptic and neo-antigenic peptides with many sequences having remained unknown so far, we decided to use heavy isotope labels nevertheless. These ten RT peptides were titrated for optimal concentration in both LC-MS/MS systems currently operated at the Department of Immunology, University of Tübingen for immunopeptidomic studies.

3 Methods

LC-MS/MS to detect PROCAL spike-in peptides

The commercially available PROCAL kit containing 40 RT peptides (JPT Peptide Technologies; Table 9) was dissolved in 100 μ l A_{Load} followed by vortexing and sonicating for 60 and 30 s, respectively. This yielded a stock solution containing 100 fmol/peptide/ μ l that was subsequently serially diluted with A_{Load} (1:2 / 1:4 / 1:8) to a concentration of 50 / 25 / 12.5 fmol/peptide/ μ l. Synthetic peptides were diluted 1:5 with a standardized HLA class I peptide eluate prepared from JY cells (JY17#3) so that spike-in peptides had a concentration of 20 / 10 / 5 / 2.5 fmol/peptide/ μ l (equivalent to 100 / 50 / 25 / 12.5 fmol/peptide/measurement). Data were acquired on an Orbitrap Fusion Lumos with the standard method for HLA class I peptides (3.2.2) For data base search, a concatenated FASTA-formatted file consisting of the Swiss-Prot release from September 27th 2013 (20,279 reviewed protein sequences) and 40 PROCAL sequences was used.

Table 9. PROCAL peptides with annotation of molecular weight and m/z values of doubly and triply positively charged precursor ions. Precursor ions not detectable with the standard HLA class I LC-MS/MS method covering a mass range of 400-650 m/z are marked in red. Information were retrieved from Zolg *et al.*¹

Accession	Sequence	M [Da = g/mol]	[M+2H] ⁺⁺ [M+3H] ⁺⁺⁺	Accession	Sequence	M [Da = g/mol]	[M+2H] ⁺⁺ [M+3H] ⁺⁺⁺
RT0001	YSAHEEHYDK	1414.5902	708.30 472.54	RT0021	HFALFSTDVTK	1264.6452	633.33 422.56
RT0002	HEHISSDYAGK	1242.5629	622.29 415.19	RT0022	TFTGTTDSFFK	1250.5819	626.30 417.87
RT0003	TFAHTESHISK	1256.6149	629.31 419.88	RT0023	VSGFSDISIYK	1214.6183	608.32 405.88
RT0004	ISLGEHEGGGK	1082.5356	542.28 361.85	RT0024	TFGTETFDTFK	1292.5925	647.30 431.87
RT0005	LSSGYDGTSYK	1176.5299	589.27 393.18	RT0025	TSIDSFIDSYK	1274.6030	638.31 425.87
RT0006	FGTGTYAGGEK	1086.4982	544.26 363.17	RT0026	ASDLLSGYYIK	1228.6339	615.32 410.55
RT0007	VGASTGYSGLK	1038.5346	520.27 347.19	RT0027	FLFTGYDTSVK	1276.6339	639.32 426.55
RT0008	TASGVGGFSTK	1010.5033	506.26 337.84	RT0028	GIFGAFTDDYK	1232.5713	617.29 411.86
RT0009	SYASDFGSSAK	1118.4880	560.25 373.84	RT0029	VYAETLSGFIK	1226.6547	614.33 409.89
RT0010	LYSYSSSTESK	1326.5980	664.31 443.21	RT0030	GFVIDDGLITK	1176.6390	589.33 393.22
RT0011	LYTGAGYDEVK	1214.5819	608.30 405.87	RT0031	GASDFLSFAVK	1140.5815	571.30 381.20

Chapter 6: Methods

RT0012	TLIAYDDSSSTK	1212.5874	607.30	RT0032	FFLTGTSTIFVK	1258.6961	630.36
			405.20				420.57
RT0013	HLTGLTFDITYK	1294.6557	648.34	RT0033	VSSIFFDTFDK	1304.6289	653.32
			432.56				435.88
RT0014	FLASSEGGFTK	1142.5608	572.29	RT0034	GDFTFFIDTFK	1336.6339	669.32
			381.86				446.55
RT0015	GFLDYESTGAK	1186.5506	594.28	RT0035	LFISALVDFFK	1298.7274	650.37
			396.52				433.92
RT0016	ALFSSITDSEK	1196.5925	599.30	RT0036	SLFFIIDGFVK	1284.7118	643.36
			399.87				429.24
RT0017	FVGTEYDGLAK	1198.5870	600.30	RT0037	IDVYILALLLK	1272.8057	637.41
			400.54				425.28
RT0018	YALDSYSLSSK	1232.5925	617.30	RT0038	SILAFLYLYFK	1376.7744	689.39
			411.87				459.93
RT0019	HDTVFGSYLYK	1328.6401	665.33	RT0039	SLIFFLSTLLK	1280.7744	641.39
			443.89				427.93
RT0020	YFGYTSDFGK	1284.5663	643.29	RT0040	FLISLLEEFVK	1400.7591	701.39
			429.20				467.93

Selection of RT peptides for in-house synthesis

Mean RTs from up to four LC-MS/MS runs (2.5-20 fmol/peptide/ μ l) were calculated for each PROCAL peptide. The 90 min LC gradient was divided up into bins of 10 min, whereby between one and two RT peptides were chosen per bin. Criteria for RT peptide selection were (1) detection at 2.5-5 fmol/ μ l and (2) one labelable amino acid that is shared with all other RT peptides. The latter is important to reduce the number of dynamic modifications in raw data processing thus preventing an increase in FDR. In total, a set of twelve peptides were subjected to solid-phase peptide synthesis (Wirkstoffpeptidlabor, Department of Immunology, University of Tübingen), whereby heavy isotope-labeled leucine [L($^{13}\text{C}_6$; ^{15}N)] was incorporated at one position each. The synthesis of RT005 and RT0030 failed for three times, thus reducing the set of RT peptides to ten.

Titration of RT peptide mixes for two LC-MS/MS systems

To avoid overdosing of spike-in peptides which may interfere with detection of (low abundant) native peptides and to establish a sensitive performance monitoring method, RT peptides were titrated for each LC-MS/MS system. Synthetic peptides were weighed in and dissolved at 1 mg/ml. For this purpose, peptides were first completely dissolved in 100% DMSO, facilitated by vortexing, with subsequent addition of MS grade H_2O . Peptides were diluted with A_{Load} to a concentration of 10 pmol/ μ l. The dilution factor (Table 10) was calculated from the peptide-specific molecular weight, the peptide purity as determined by analytical high-performance liquid chromatography (HPLC), and a peptide content of 75%, which is a reference value obtained by nitrogen determination (20% TFA and 5-10% H_2O content in peptide powders produced in-house; internal data of the Wirkstoffpeptidlabor, Department of Immunology, University of Tübingen). By serial dilution with A_{Load} , peptides were adjusted to 50 / 10 / 5 / 2.5 / 1 / 0.5 / 0.1 fmol/peptide/ μ l followed by 1:10 dilution with JY-derived HLA class I peptides (Orbitrap Fusion Lumos JY17#3; LTQ Orbitrap XL: JY17#4). Data acquisition was performed with standard LC-MS/MS methods for HLA class I peptides (400-650 m/z), whereby the highest (5 fmol/peptide/ μ l) and lowest (0.01 fmol/peptide/ μ l) concentration was only measured on the LTQ Orbitrap XL or the Orbitrap Fusion Lumos, respectively. For data analysis, heavy isotope

labels (+7.017 Da) were permitted as additional dynamic modification for leucine residues and the Swiss-Prot release from September 27th 2013 (20,279 reviewed protein sequences) concatenated with ten RT peptide sequences was used as reference database.

Table 10. Ten heavy isotope-labeled peptides synthesized as RT standard. M/z values of doubly and triply positively charged precursor ions were retrieved from Skyline. Precursors not detectable with the standard HLA class I LC-MS/MS method covering a mass range of 400-650 m/z are marked in red. The penultimate column gives molarities of peptide solutions obtained by dissolving 1 mg peptide powder in 1 ml solvent; calculated from molecular weight, synthetic peptide purity, and a peptide content of 75%. Dilution factors to adjust peptide solutions to 10 pmol/μl are given in the last column.

Accession	Sequence	M [Da = g/mol]	[M+2H] ⁺⁺ [M+3H] ⁺⁺⁺	Peptide purity [%]	1 mg/ml = X nmol/μl	Dilution factor > 10 pmol/μl
RT0004	IS[L(¹³ C ₆ ; ¹⁵ N)]GEHEGGGK	1089.5357	545.7837 364.1915	87.18	0.6001	60.01
RT0007	VGASTGYSG[L(¹³ C ₆ ; ¹⁵ N)]K	1045.5346	523.7831 349.5245	86.83	0.6229	62.29
RT0012	T[L(¹³ C ₆ ; ¹⁵ N)]IAYDDSSTK	1219.5874	610.8096 407.5421	65.67	0.4038	40.38
RT0014	F[L(¹³ C ₆ ; ¹⁵ N)]ASSEGGFTK	1149.5608	575.7963 384.1999	83.18	0.5427	54.27
RT0015	GF[L(¹³ C ₆ ; ¹⁵ N)]DYESTGAK	1193.5507	597.7912 398.8632	88.7	0.5574	55.74
RT0016	A[L(¹³ C ₆ ; ¹⁵ N)]FSSITDSEK	1203.5925	602.8121 402.2105	88.78	0.5532	55.32
RT0021	HFA[L(¹³ C ₆ ; ¹⁵ N)]FSTDVTK	1271.6452	636.8385 424.8947	82.68	0.4876	48.76
RT0029	VYAET[L(¹³ C ₆ ; ¹⁵ N)]SGFIK	1233.6547	617.8432 412.2310	81.54	0.4957	49.57
RT0031	GASDF[L(¹³ C ₆ ; ¹⁵ N)]SFAVK	1147.5816	574.8066 383.5402	67.51	0.4412	44.12
RT0032	FF[L(¹³ C ₆ ; ¹⁵ N)]TGTSIFVK	1265.6962	633.8639 422.9117	71.08	0.4212	42.12

Comparison of five LC-MS/MS systems

During the course of a procurement measure for a new LC-MS/MS system, standardized samples of JY-derived HLA class I peptides and ten heavy isotope-labeled RT peptides were measured on five devices coming into question. For this purpose, equimolar concentrations of ten heavy isotope-labeled RT peptides were spiked into a complex matrix of HLA class I peptides eluted from JY cells. Following serial 1:2 dilution from 0.2 fmol/peptide/μl to 0.1 / 0.05 / 0.025 / 0.0125 fmol/peptide/μl, samples were acquired on an Orbitrap Fusion Lumos (Thermo Fisher Scientific; Department of Immunology, University of Tübingen; 90 min gradient), an Orbitrap Fusion (Thermo Fisher Scientific; Immatics Biotechnologies GmbH; 70 min gradient), a Q Exactive HF (Thermo Fisher Scientific; Proteome Center Tübingen, University of Tübingen; 90 min gradient), a TimsTOF Pro with Parallel Accumulation Serial Fragmentation acquisition (Bruker Daltonics; 30 / 60 / 100 min gradient), and on a TripleTOF 6600 (AB SCIEX; 90 min gradient). M/z windows and gradient designs were attuned to immunopeptidomic demands as far as possible. Data was analyzed by Bruker Daltonics (TimsTOF Pro) and by Ana Marcu (Department of Immunology, University of Tübingen) employing the PEAKS 8.5 software (Bioinformatics Solutions Inc.), as this was compatible with all raw file formats. In brief, the fragmentation type was set to CID and database search against the Swiss-Prot release from September 27th 2013 (20,279 reviewed protein sequences)

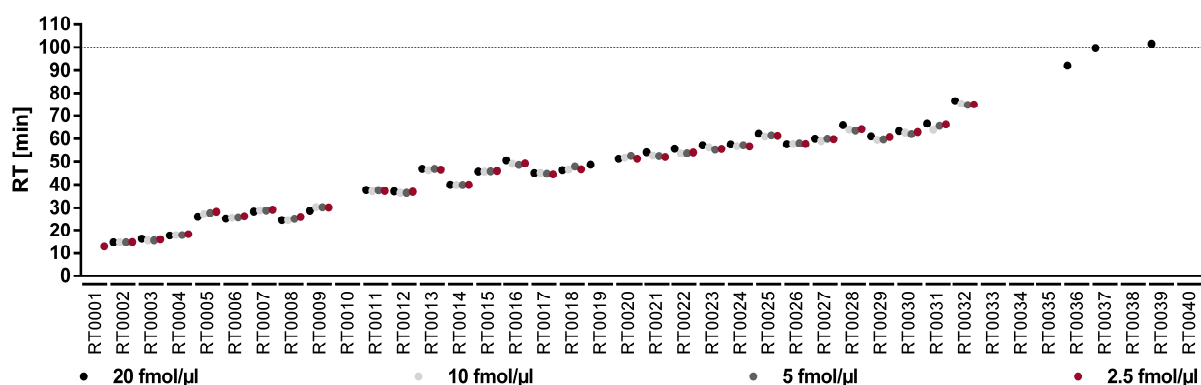
concatenated with the sequences of ten RT peptides was performed at a precursor mass tolerance of 5 (Thermo Fisher Scientific instruments) or 10 ppm (TripleTOF 6600), a fragment mass tolerance of 0.02 (Thermo Fisher Scientific instruments) or 0.5 Da (TripleTOF 6600), and a FDR of 5% estimated by target-decoy database search ('decoy-fusion'). A maximum number of three variable modifications, comprising oxidation of methionine (+15.995 Da) and heavy isotope-labeled leucine (+7.017 Da), were permitted per peptide.

4 Results

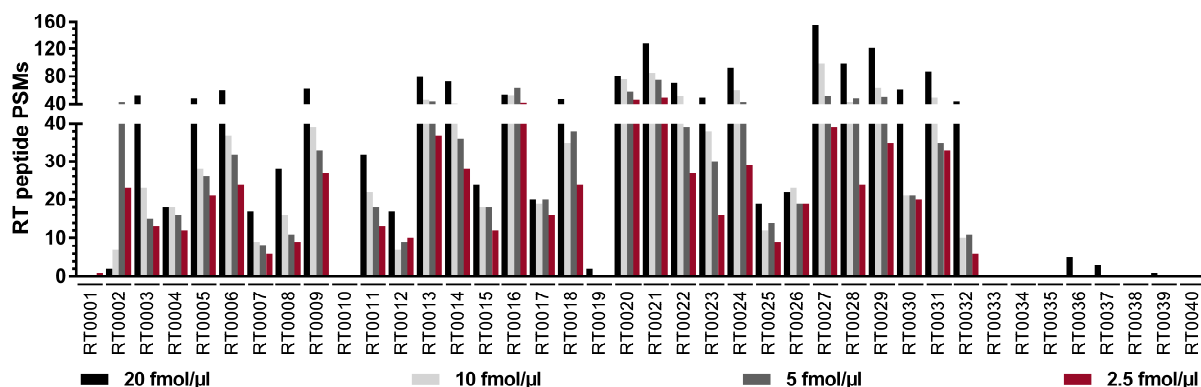
4.1 Compatibility of PROCAL peptides with immunopeptidomics

PROCAL peptides were spiked at 20 / 10 / 5 / 2.5 fmol/peptide/ μ l into a matrix of HLA class I peptides eluted from JY cells and acquired on an Orbitrap Fusion Lumos. 34 out of 40 peptides were detectable in full length in at least one measurement, whereby the limit of detection was not reached with 2.5 fmol/ μ l for 29 peptides (Figure 42). These were distributed across the entire 90 min gradient (Figure 42 A). Of note, spike-in PROCAL peptides did not severely impede the detection of JY-derived peptides as visible by a constant number of unique peptide identifications across the titration series (Supplementary Table 22).

A



B



C

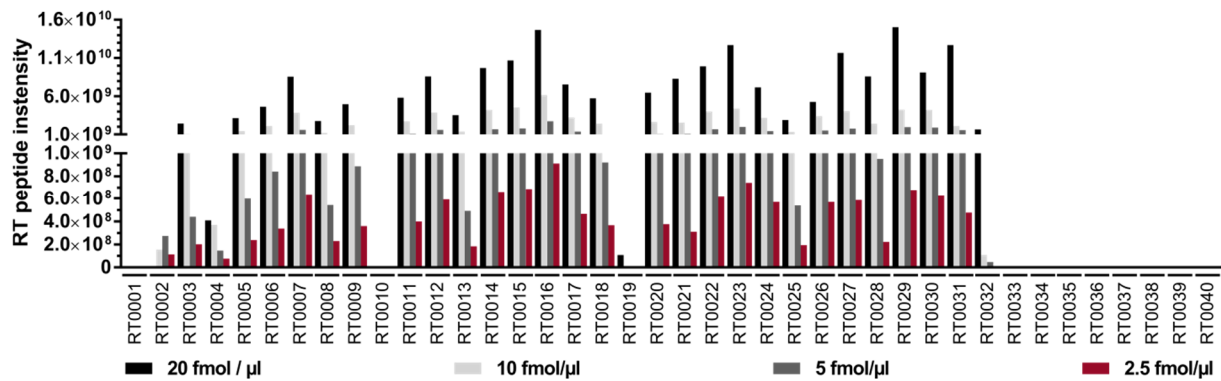
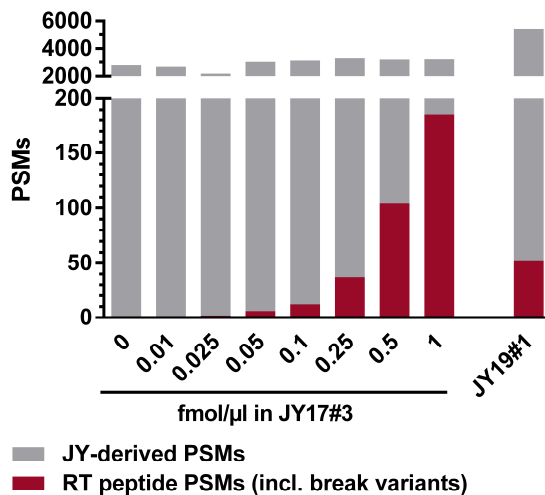


Figure 42. Identification of PROCAL peptides titrated in a complex matrix of HLA class I peptides [2.5-20 fmol/peptide/μl]. RT peptide intensities (AUC), PSMs, and RTs were reported for the best scoring PSM detected in full length. Of note, the number of break variants increased with mounting peptide concentration. **(A) Observed RTs of RT0001-RT0040.** The dashed line indicates the end of the 90 min gradient. **(B) Number of PSMs identified per RT peptide** and **(C) RT peptide intensities.** RT0036, RT0037, and RT0039 eluted at the end of or after the 90 min gradient and had very low intensities < 8 × 10⁵ at 20 fmol/μl. RT0010, RT0033, RT0034, RT0035, RT0038, and RT0040 were not detected at all.

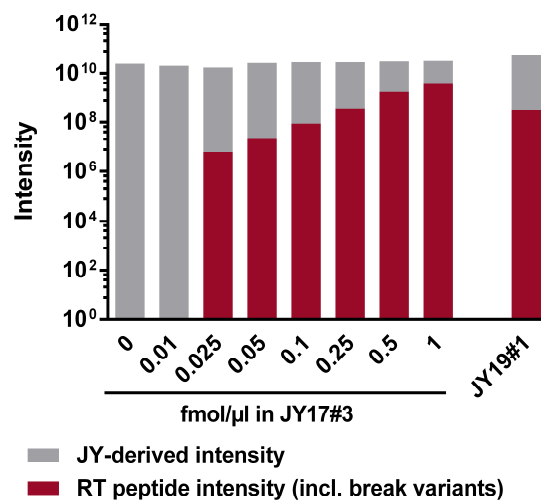
4.2 Titration of in-house heavy isotope-labeled RT peptides

Heavy isotope-labeled RT peptides were spiked at 0.01-1 fmol/peptide/μl or at 0.025-5 fmol/peptide/μl in a complex matrix of HLA class I ligands for the Orbitrap Fusion Lumos (Figure 43, Figure 44) and the LTQ Orbitrap XL (Figure 45, Figure 46), respectively. As already observed for PROCAL peptides, high concentrations of spike-in RT peptides did not affect the number of unique peptide identifications (Supplementary Table 22). Criteria to determine optimal concentrations were ≥ 2 PSMs (Figure 43, Figure 45) and an AUC comparable to JY-derived precursors of medium intensity (Figure 44, Figure 46).

A



C



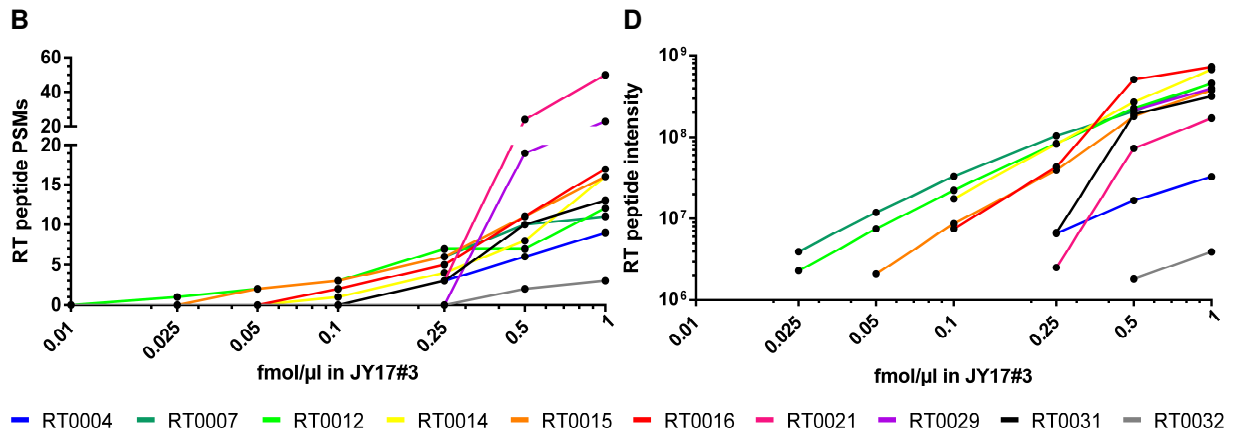
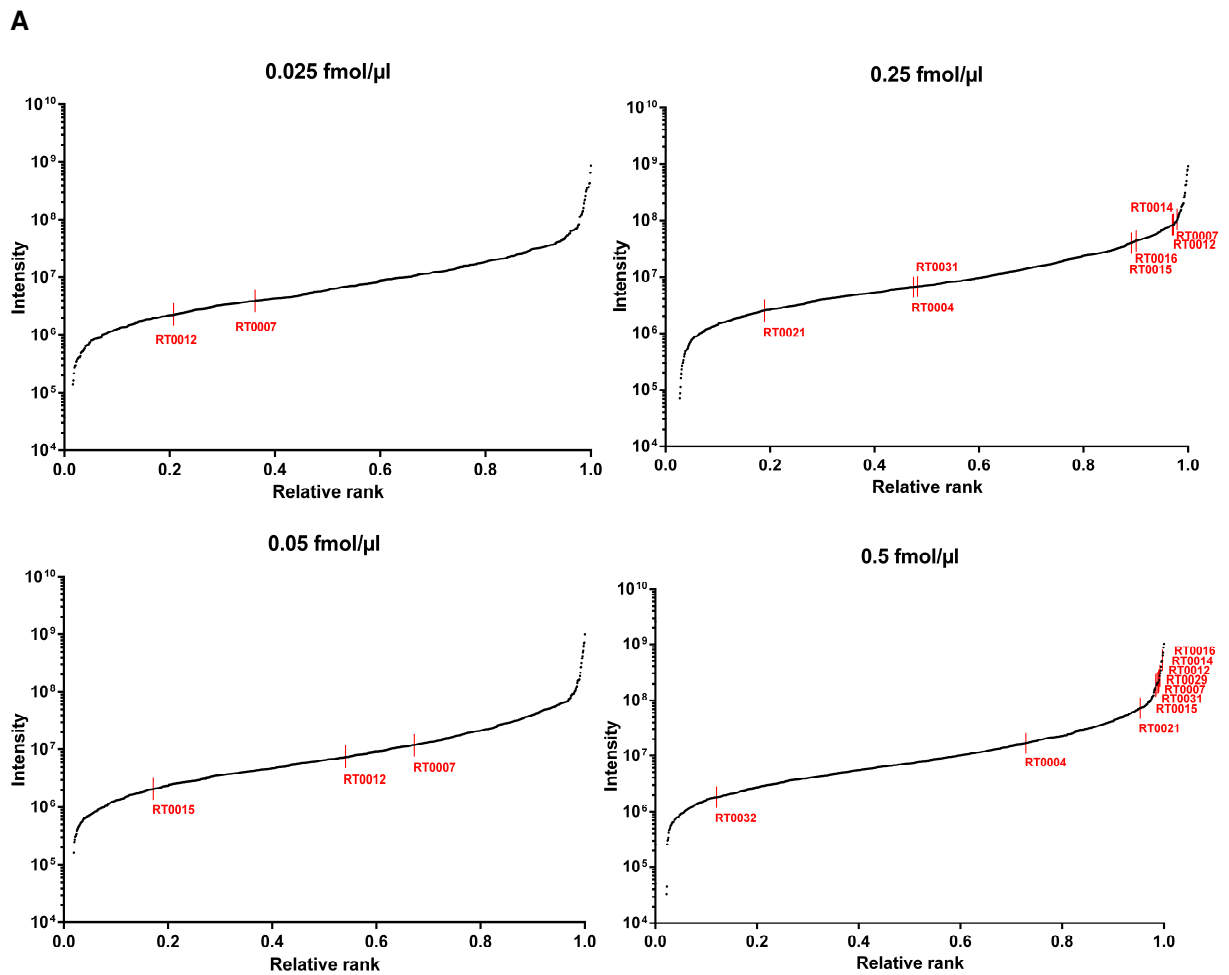


Figure 43. Titration of RT peptides in JY17#3 for the Orbitrap Fusion Lumos. Panel (A) and (C) include PSMs and intensities of both full-length and break variants, whereas (B) and (D) report dose-dependent PSM numbers and intensities for full-length peptides only.



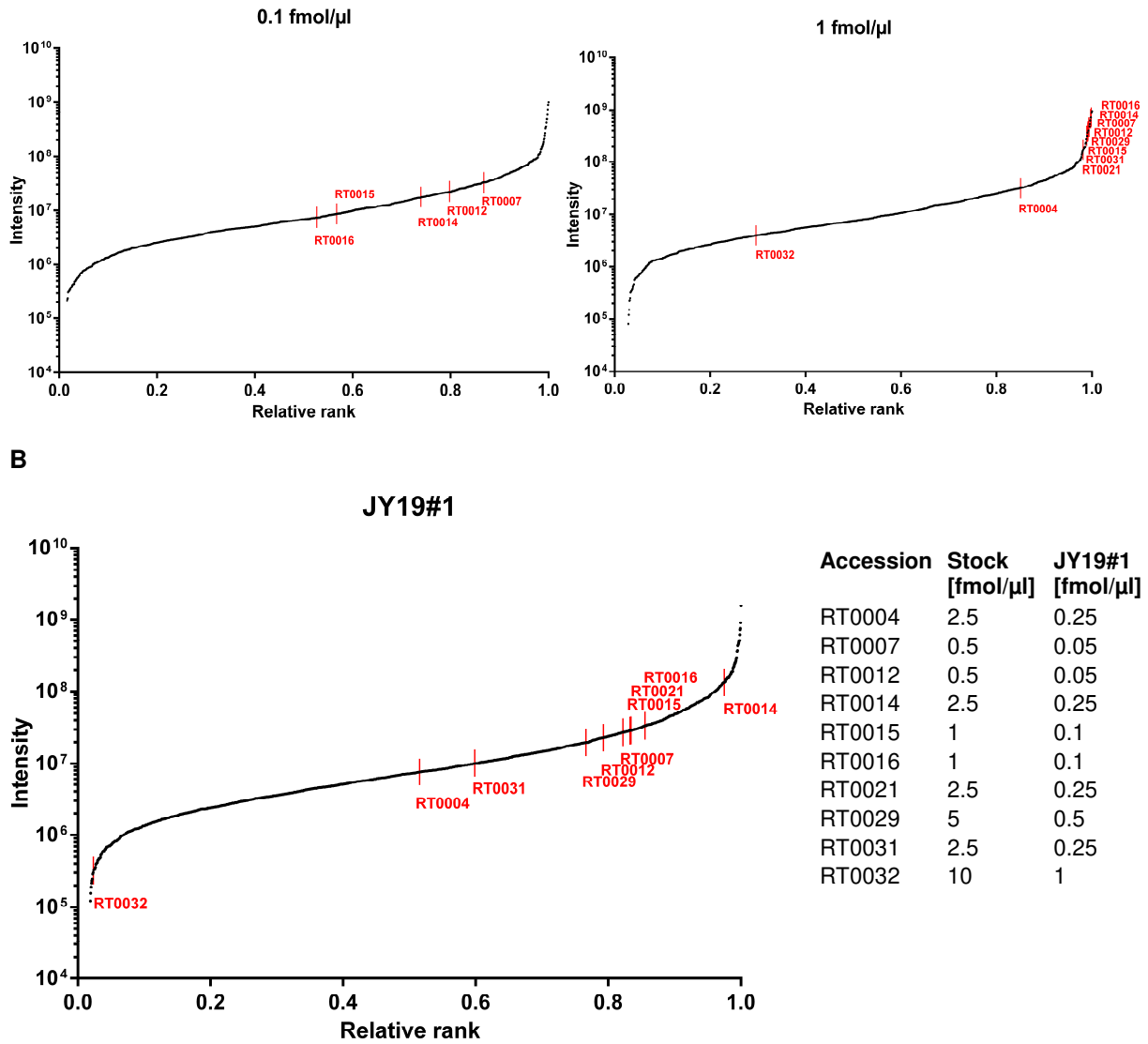


Figure 44. Relative rank of full-length RT peptides in comparison with JY17#3-derived peptides (Orbitrap Fusion Lumos). Best scoring PSMs were sorted by intensities and ranked according to their AUCs. RT peptides are marked in red for **(A) titration series** and **(B) titrated RT peptide mix spiked into the newly synthesized LC-MS/MS standard JY19#1**. RT peptide concentrations of ready-to-use stocks (to be diluted 1:10 with sample of interest) and in JY19#1 are listed on the right.

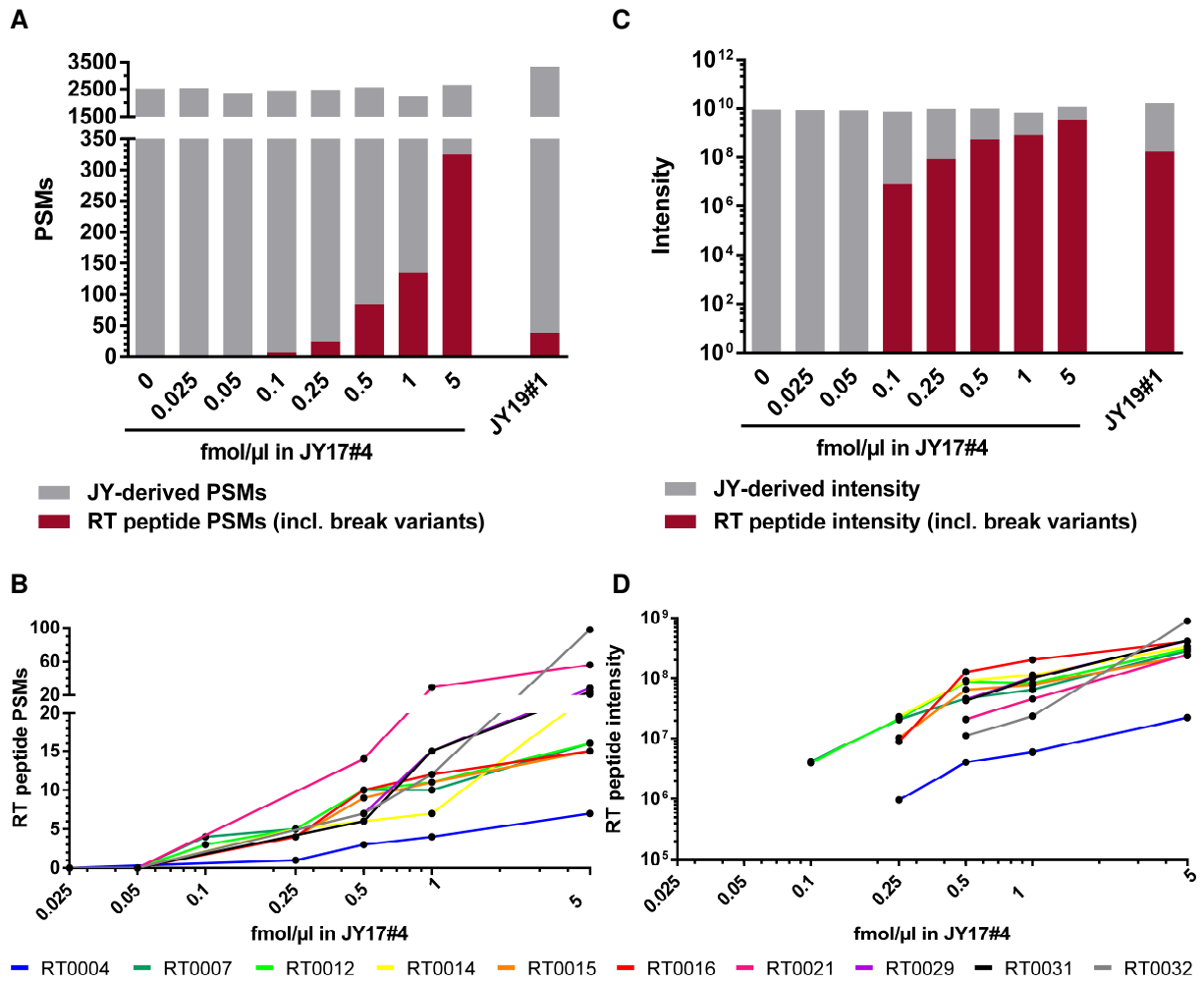
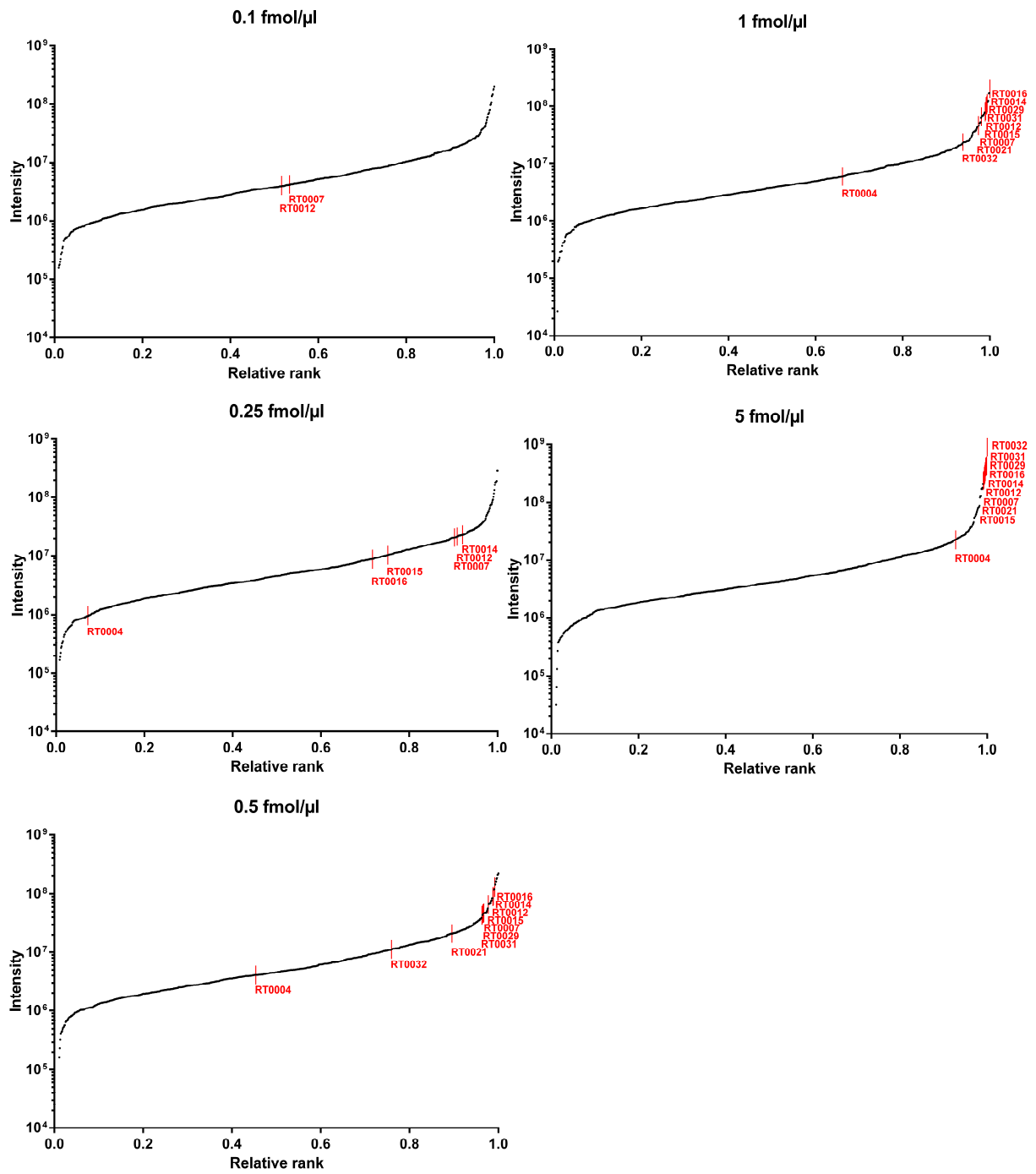


Figure 45. Titration of RT peptides in JY17#4 for the LTQ Orbitrap XL. Panel (A) and (C) include PSMs and intensities of both full length and break variants, whereas (B) and (D) report dose-dependent PSM numbers and intensities for full length peptides only.

Chapter 6: Results

A



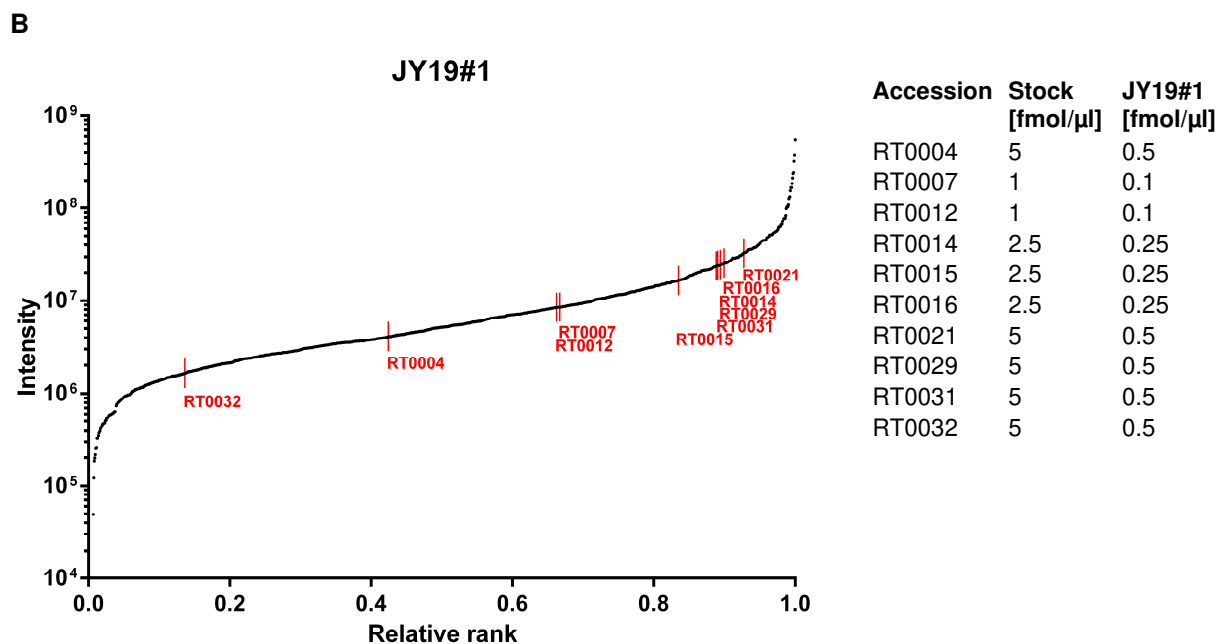


Figure 46. Relative rank of full-length RT peptides in comparison with JY17#4-derived peptides (LTQ Orbitrap XL). Best scoring PSMs were sorted by intensities and ranked according to their AUCs. RT peptides are marked in red for (A) titration series and (B) titrated RT peptide mix spiked into the newly synthesized LC-MS/MS standard JY19#1. RT peptide concentrations of ready-to-use stocks (to be diluted 1:10 with sample of interest) and in JY19#1 are listed on the right.

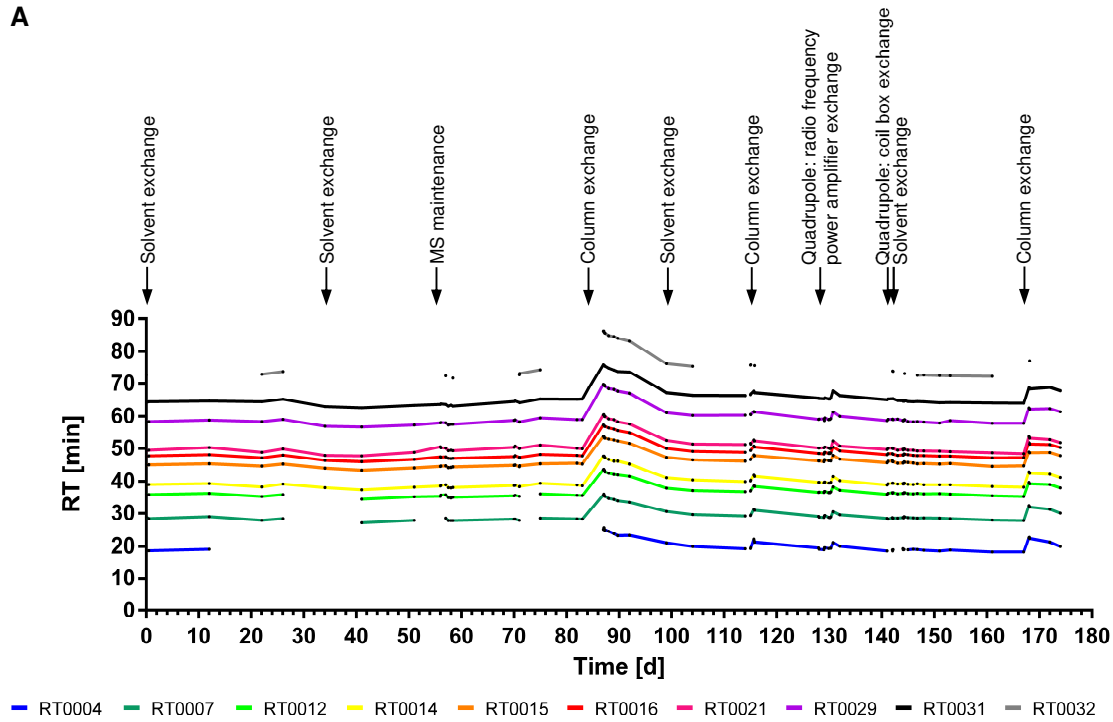
The LC-MS/MS standard JY19#1 composed of HLA class I ligands eluted from JY cells was prepared by Jens Bauer (Department of Immunology, University of Tübingen). Upon spike-in of ten RT peptides almost 500 vials of the lower concentrated and 300 vials of the higher concentrated standard each containing 25 μl sample (5 technical replicates) were filled for the Orbitrap Fusion Lumos and the LTQ Orbitrap XL, respectively. Moreover, almost 200 ready-to-use aliquots of 1000 μl RT peptide mix to be diluted 1:10 with sample were frozen for each LC-MS/MS system. Highly concentrated stocks of 1 mg/ml are available for every single RT peptide as well.

4.3 Performance monitoring of LC-MS/MS systems by RT peptides

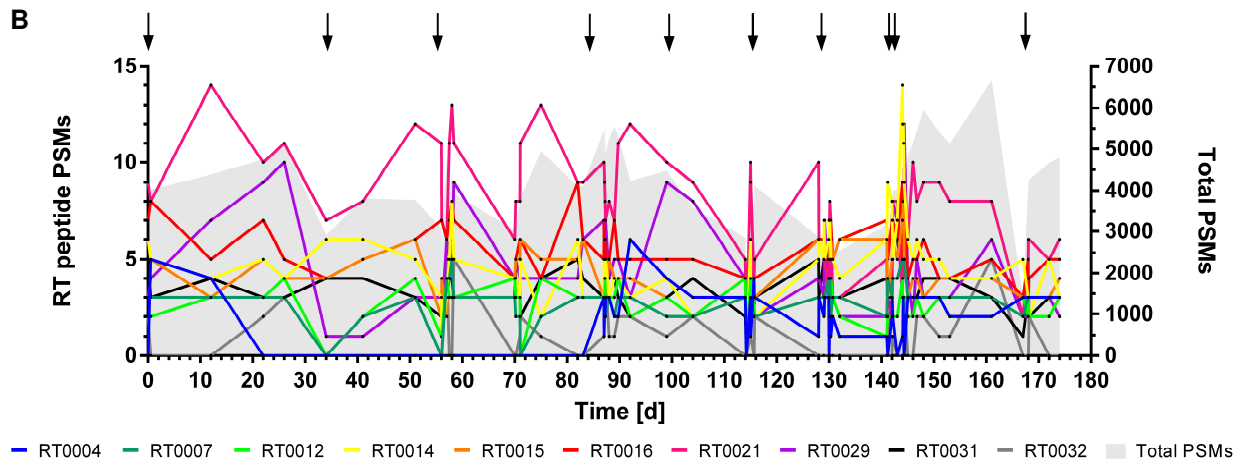
The performance of the two LC-MS/MS systems at the Department of Immunology, University of Tübingen is constantly monitored by means of standardized HLA class I peptide eluates. Since implementation of RT peptides and manufacturing of the JY19#1 standard containing ten RT peptides, performance monitoring was significantly improved. RTs were largely stable over time and only changed upon technical intervention. In contrast, RT peptides and JY-derived peptides were subject to strong fluctuations on the level of both PSMs and intensities that could not be explained. Renewal of solvents (mobile phase), trapping and/or separation columns (stationary phase) were identified as major factors influencing the performance of both the Orbitrap Fusion Lumos (Figure 47) and the LTQ Orbitrap XL (Figure 48). Detection of RT0032 evolved as marker of top performance for both devices, as this peptide was only present when the other nine were as well.

Chapter 6: Results

A



B



C

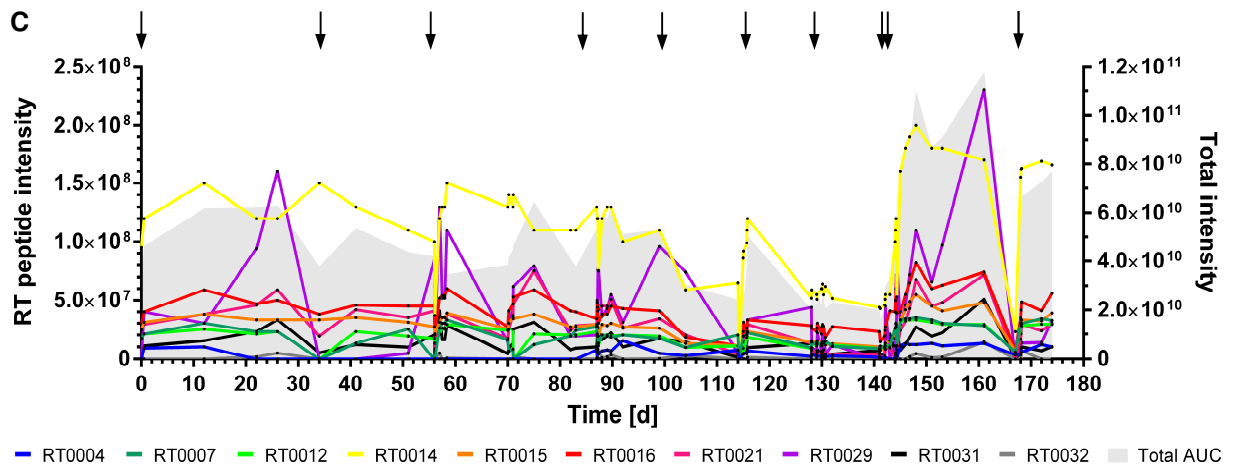
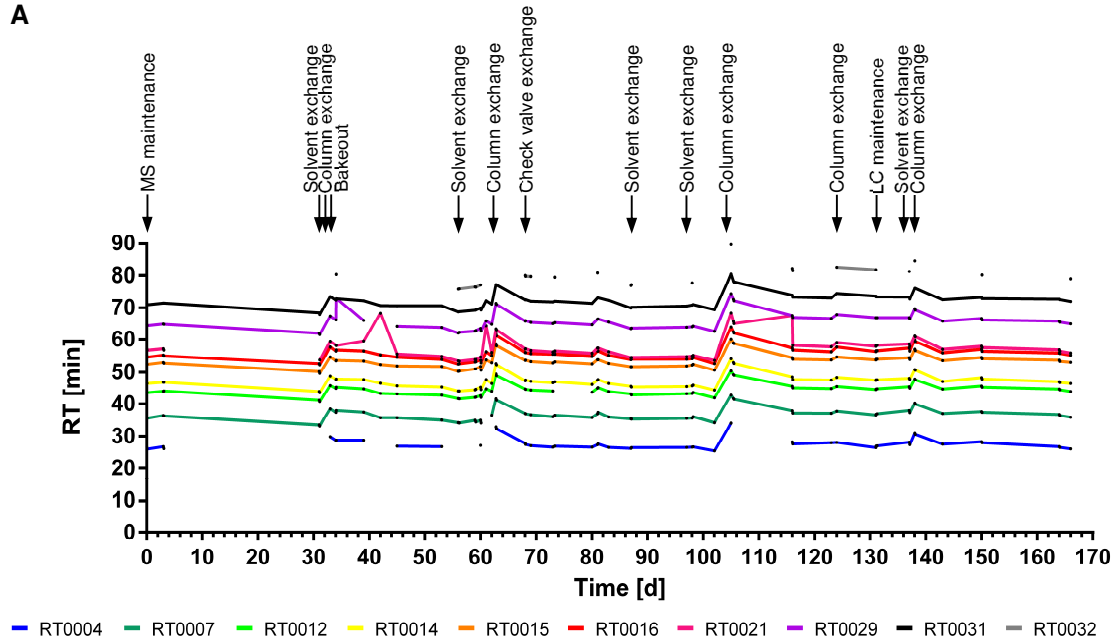
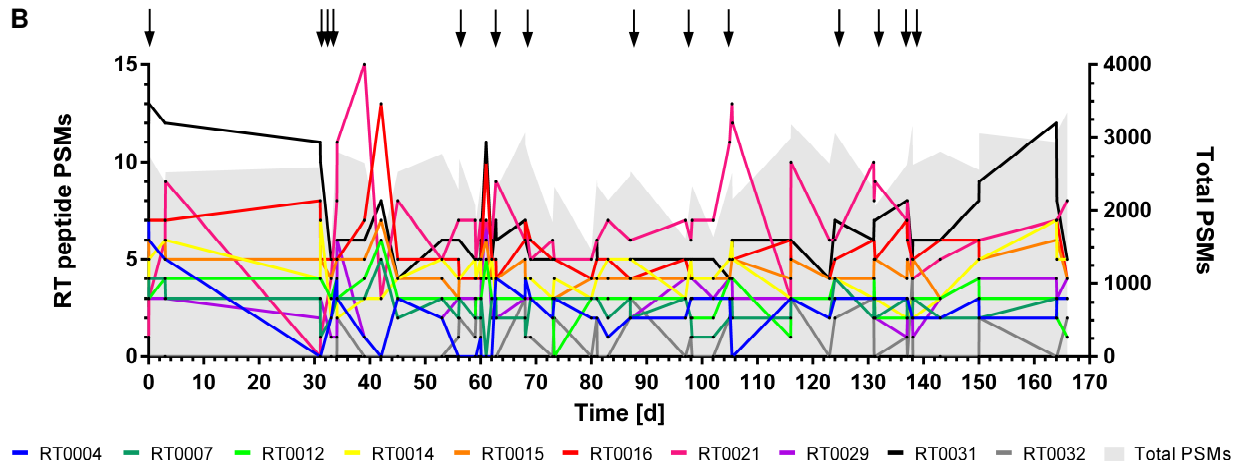


Figure 47. Performance of the Orbitrap Fusion Lumos. LC-MS/MS performance was monitored over almost half a year (19.06.2019 – 09.12.2019) by analyzing (A) RTs of spike-in peptides, (B) total and RT peptide-derived PSMs, and (C) intensities of RT peptides and summed AUC of all peptide identifications. Reported RTs and intensities refer to the best scoring PSM each.

A



B



C

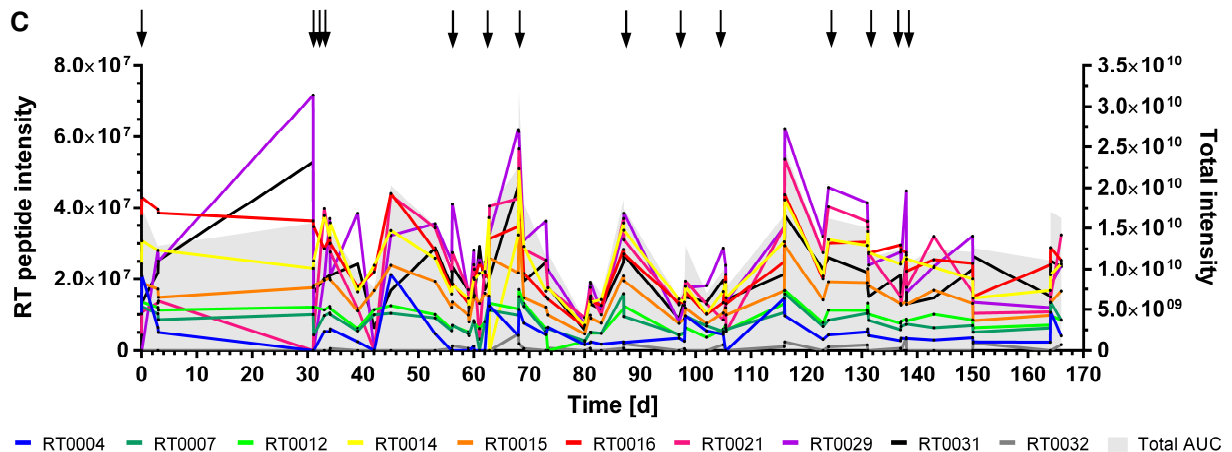
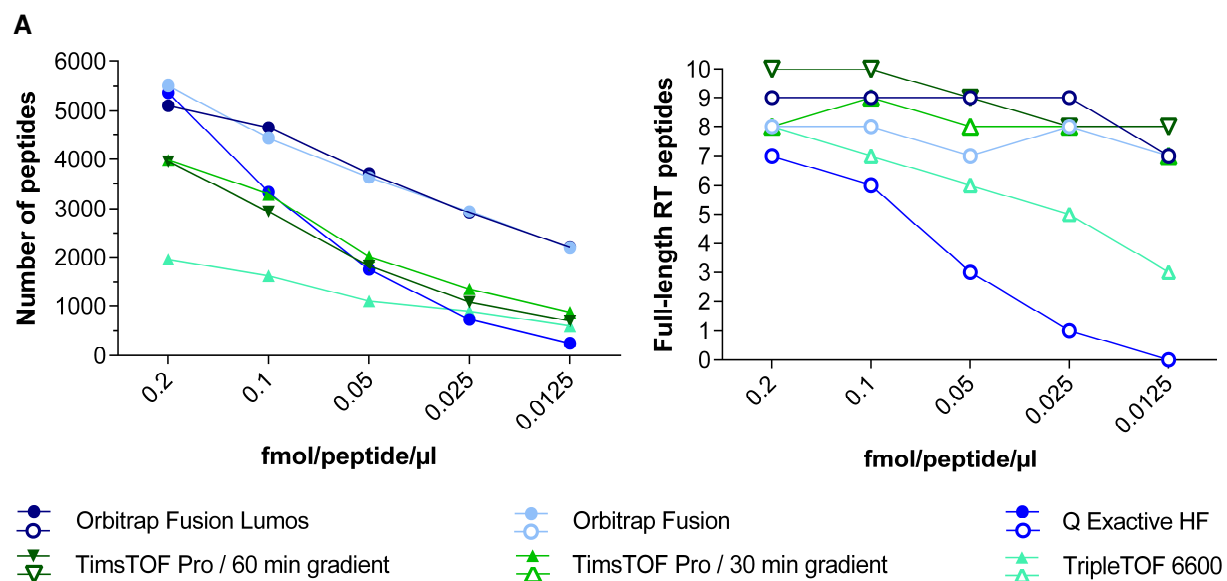


Figure 48. Performance of the LTQ Orbitrap XL. LC-MS/MS performance was monitored over almost half a year (14.06.2019 – 27.11.2019) by analyzing (A) RTs of spike-in peptides, (B) total and RT peptide-derived PSMs, and (C) intensities of RT peptides and summed AUC of all peptide identifications. Reported RTs and intensities refer to the best scoring PSM each.

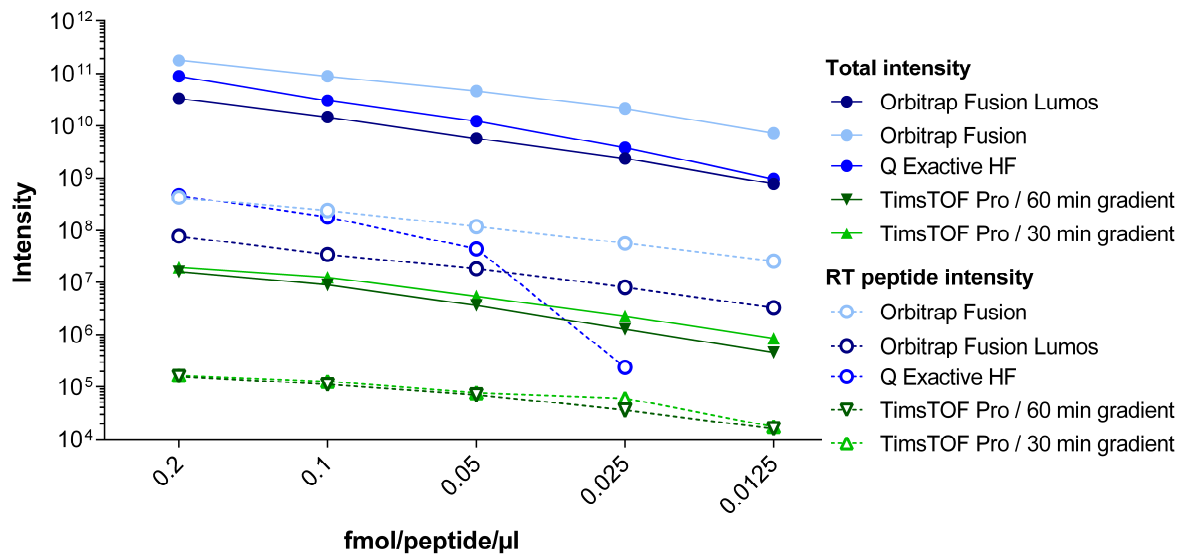
4.4 Comparison of LC-MS/MS systems for a procurement measure

In the course of a procurement measure for a new LC-MS/MS system, standardized samples of JY-derived HLA class I peptides and ten heavy isotope-labeled RT peptides were measured on five devices coming into question. The highest concentrated sample contained 0.2 fmol/peptide/ μ l and was serially diluted with A_{Load} to 0.1 / 0.05 / 0.025 / 0.0125 fmol/peptide/ μ l. Data acquisition was performed on an Orbitrap Fusion Lumos, an Orbitrap Fusion, a Q Exactive HF, a TimsTOF Pro with Parallel Accumulation Serial Fragmentation acquisition, and on a TripleTOF 6600. Overall, the Orbitrap Fusion Lumos and the Orbitrap Fusion, which are both operated in immunopeptidomic laboratories, performed best for the titration series. On the level of unique peptide identifications, data generated by the Q Exactive HF or by the TimsTOF Pro were comparable, whereby RT peptides were identified more reliably by the TimsTOF Pro (all 10 RT peptides at the two highest and 8 RT peptides at the two lowest concentration). The sensitivity of the Orbitrap Fusion was similar to the Orbitrap Fusion Lumos, both detecting 7 RT peptides at 12.5 amol/ μ l (Figure 49 A). From the third titration stage, the Q Exactive HF showed a clear decline in performance. The TripleTOF 6600 performed relatively well in RT peptide detection at high concentrations, whereas JY-derived HLA class I ligand identification and annotation of peptide intensities was severely impaired or even impossible. Peptide intensities were highest for the three Orbitrap instruments and reported reliably up to the lowest concentration stage (Figure 49 B and C).

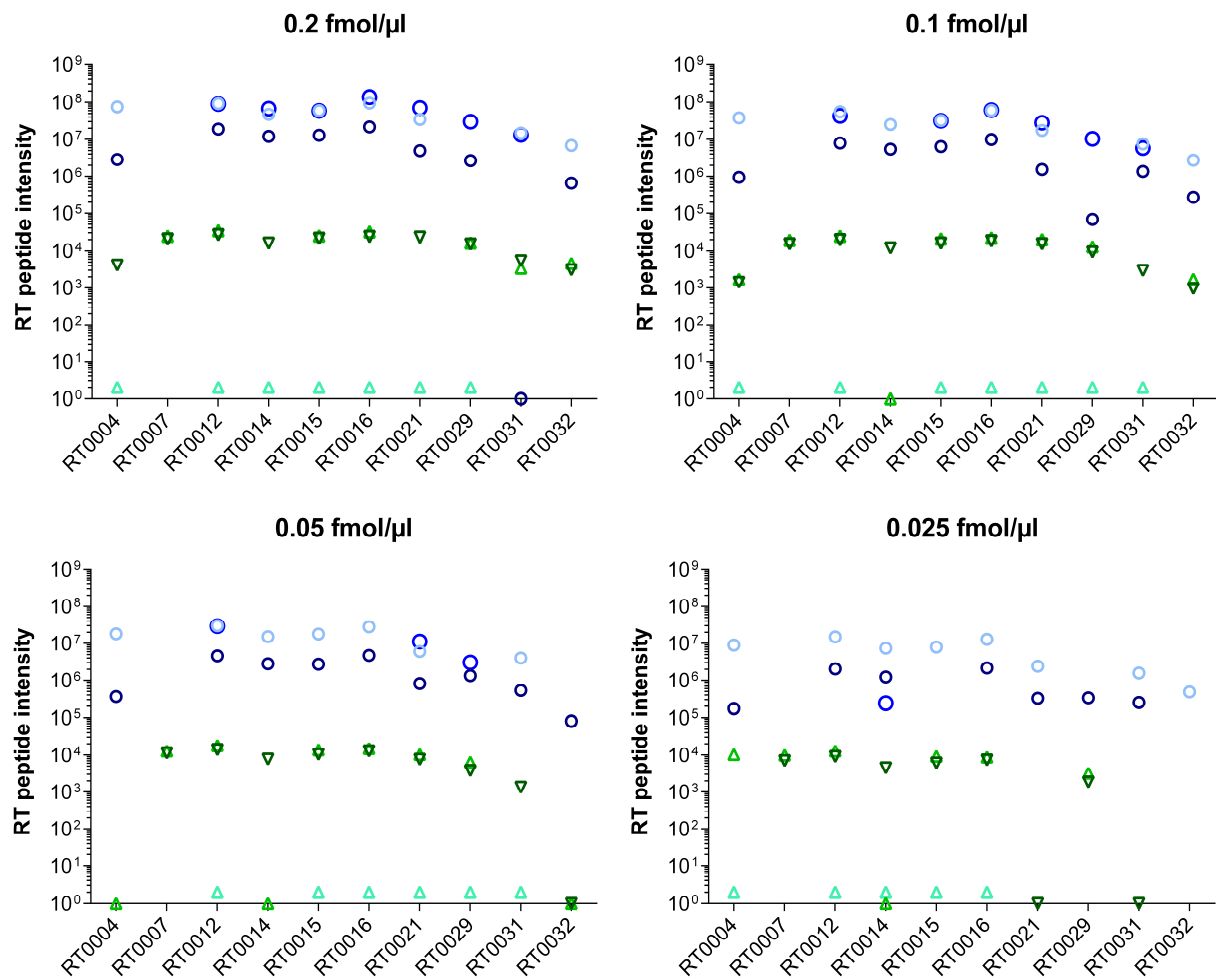


Chapter 6: Results

B



C



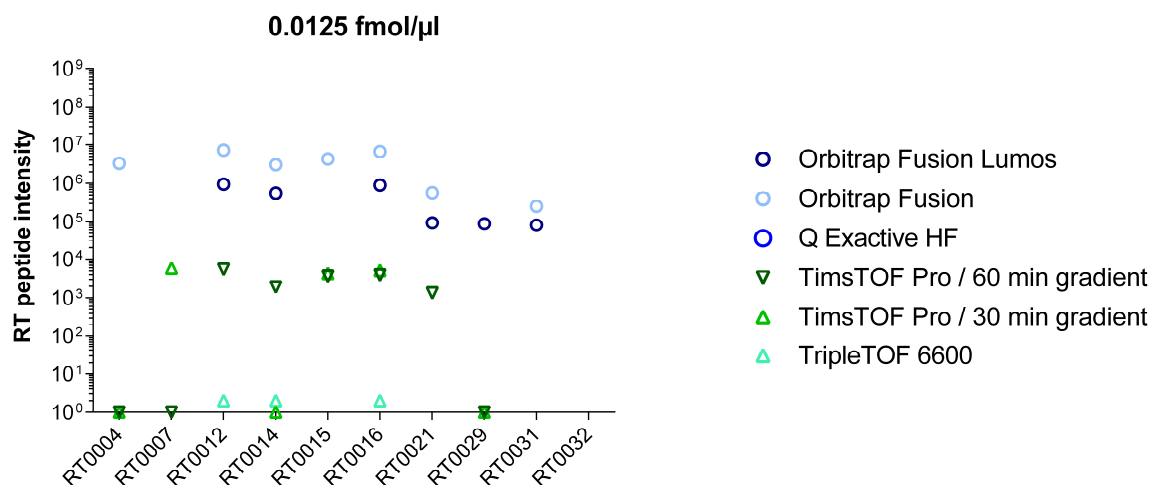


Figure 49. Performance of five LC-MS/MS systems with immunopeptidomic samples. LC-MS/MS systems coming into question in the course of a procurement measure were evaluated by data acquisition from a standardized titration series of RT peptides spiked into a matrix of HLA class I peptides eluted from JY cells. Raw data were kindly analyzed by Ana Marcu (Department of Immunology, University of Tübingen) and by Bruker Daltonics (TimsTOF Pro) using the PEAKS software. Overall, the Orbitrap Fusion Lumos and the Orbitrap Fusion, which are both operated in immunopeptidomic laboratories, performed best for the titration series. **(A) Total number of unique peptide identifications and number of identified RT peptides.** Even at the highest concentration, the TripleTOF 6600 reached less than 40% of the peptide identification rate achieved by Thermo Fisher Scientific instruments. Of note, gradient duration hardly affected the peptide yields achieved by the TimsTOF Pro, whereas RT peptide identification benefited from using the longer gradient. **Intensities (B) summed for all peptides or RT peptides and (C) of every individual RT peptide across all concentration stages.** Recorded intensities were largely comparable for the three Orbitrap instruments, followed by the TimsTOF Pro. At the lowest concentration of 12.5 amol/ μ l, the detection rate of the TimsTOF Pro was best, whereby the Orbitrap Fusion and the Orbitrap Fusion Lumos were superior regarding annotation of peptide intensities. Since corresponding peptide intensities could not be retrieved from TripleTOF 6600 data, intensities were not reported in (B) and with a value of 2 in (C).

5 Discussion

Synthetic peptide spike-ins have a wide range of applications including constant monitoring of chromatographic and mass spectrometric performance, contemporary data acquisition strategies and quantitative approaches with enhanced identification and reproducibility rates, as well as comparison and calibration of collision energies between two mass spectrometers.^{1,3,4,6} However, such standardized peptide mixtures have so far not been introduced to immunopeptidomics. PROCAL, a mix of 40 synthetic peptides, was developed for proteomic purposes with tryptic digests as analyte. We found 34 of these peptides to be detectable with our LC-MS/MS method for HLA class I ligands. According to the manufacturer's instructions, the six most hydrophobic peptides elute at 33.7-39.9% AcN from the columns. Thus, these were not expected to elute over the course of the applied 90 min gradient ranging from 3 to 40% nano pump solvent B (equal to 2.4-32% AcN), but only during the wash peak reaching 95% solvent B (76% AcN) in min 106. In addition, the manufacturer's instructions claim that dissolution of the peptide mix in aqueous solvents other than 100% DMSO or 30% AcN results in loss of the six most hydrophobic peptides.¹ To evaluate the compatibility of PROCAL peptides with immunopeptidomic LC-MS/MS data acquisition, we deliberately

dissolved the peptides in A_{Load} , the standard solvent for HLA ligand extracts. Hence, this represents another reason for losing some of the PROCAL peptides. However, failure to detect RT0010 and (almost) RT0019 can neither be explained by inadequate dissolution nor by an insufficient AcN content of nano pump solvents. Both of these peptides were not within the applied mass window of 400-650 m/z when having two positive charges. This allows the presumption that present solvent compositions in combination with the peptide's ability to take up protons did not favor the formation of detectable triply positively charged precursor ions.

Based on this pilot experiments employing PROCAL peptides, 12 sequences were selected for in-house synthesis with heavy isotope-labeled leucine. Two of these were not synthesizable reducing the number to ten RT peptides. These were titrated for both LC-MS/MS systems currently operated at the Department of Immunology at the University of Tübingen. Following titration, ready-to-use standards composed of a complex matrix of HLA class I peptides eluted from JY cells as well as ten spike-in RT peptides were manufactured. These standards are constantly used to monitor chromatographic and mass spectrometric performance and are sufficient for a total of 2,500 and 1,500 standard injections on the Orbitrap Fusion Lumos or the LTQ Orbitrap XL, respectively. During the course of almost half a year, LC-MS/MS performance was shown to be significantly influenced by renewal of solvents (mobile phase) as well as of trapping and/or separation columns (stationary phase). However, major fluctuations affecting peptide intensities and the number of PSMs, but not retention times, appeared independent of any technical intervention on both devices and can so far not be explained. Besides performance monitoring, RT peptides are of great value for troubleshooting by revealing e.g. retention time shifts, selective loss of peptide identifications at a specific retention time, reduced peptide intensities, impaired fragmentation quality, or a decrease in mass accuracy.

During the course of a procurement measure, the mix of ten RT peptides was used to compare five LC-MS/MS systems coming into question – especially regarding sensitivity – thus guiding device selection. Overall, the Orbitrap Fusion Lumos and the Orbitrap Fusion performed best for the entire dilution series of HLA class I ligands eluted from JY cells with spike-in RT peptides at equal concentration. These results are to some extent biased, as both machines were operated in immunopeptidomic laboratories with highly optimized LC-MS/MS methods for the detection of HLA-presented peptides. Assuming that the performance of non-immunopeptidomic LC-MS/MS systems can be enhanced by optimizing methods to this special kind of analytes, the TimsTOF Pro offers promising prospects by introducing the trapped ion mobility separation-based detection technology which is complementary to our present Orbitrap instruments.⁷ Regarding the detection of RT peptides, the TimsTOF Pro even outperformed all other LC-MS/MS systems with a detection limit of < 12.5 amol/μl for eight spike-in peptides. At the highest concentration, the number of unique peptide identifications achieved by the Q Exactive HF was comparable to the Orbitrap Fusion and the Orbitrap Fusion Lumos. For subsequent dilution stages, a clear decline in performance was observed, whereby technical issues during acquisition appear the most probable cause. The Q Exactive HF is nearly identical in construction with the Orbitrap Fusion and the Orbitrap Fusion Lumos, while being less expensive.⁸ Hence, it should be possible to push it at the same performance level by strictly optimizing both chromatographic and mass spectrometric parameters.

The implemented set of ten heavy isotope-labeled RT peptides represents an essential tool in method development including optimization of collision energies for these newly acquired LC-MS/MS systems used for immunopeptidomic research. Further, these RT peptides open up new avenues to innovative data acquisition strategies in the field of immunopeptidomics. Data-independent acquisition and more accurate quantification strategies will enable deeper explorations of immunopeptidomes comprising so far underrepresented species such as neo-antigenic or cryptic epitopes. RT peptides may also facilitate the transfer of spectral libraries required for the analysis of data-independently acquired MS/MS spectra from one to another platform by allowing a comparison of fragmentation characteristics.^{1,3,4,6} Of note, all RT peptides are also covered by the mass window applied to HLA class II peptide eluates.

6 References

1. Zolg DP, Wilhelm M, Yu P, Knaute T, Zerweck J, Wenschuh H, Reimer U, Schnatbaum K, Kuster B. PROCAL: A Set of 40 Peptide Standards for Retention Time Indexing, Column Performance Monitoring, and Collision Energy Calibration. *Proteomics*. 2017;17(21).
2. Escher C, Reiter L, MacLean B, Ossola R, Herzog F, Chilton J, MacCoss MJ, Rinner O. Using iRT, a normalized retention time for more targeted measurement of peptides. *Proteomics*. 2012;12(8):1111-1121.
3. Amodei D, Egertson J, MacLean BX, Johnson R, Merrihew GE, Keller A, Marsh D, Vitek O, Mallick P, MacCoss MJ. Improving Precursor Selectivity in Data-Independent Acquisition Using Overlapping Windows. *J Am Soc Mass Spectrom*. 2019;30(4):669-684.
4. Michalski A, Cox J, Mann M. More than 100,000 detectable peptide species elute in single shotgun proteomics runs but the majority is inaccessible to data-dependent LC-MS/MS. *J Proteome Res*. 2011;10(4):1785-1793.
5. Venable JD, Dong MQ, Wohlschlegel J, Dillin A, Yates JR. Automated approach for quantitative analysis of complex peptide mixtures from tandem mass spectra. *Nat Methods*. 2004;1(1):39-45.
6. Weisbrod CR, Eng JK, Hoopmann MR, Baker T, Bruce JE. Accurate peptide fragment mass analysis: multiplexed peptide identification and quantification. *J Proteome Res*. 2012;11(3):1621-1632.
7. Bruker Daltonics TimsTOF Pro. [Internet]. Available from: <https://www.bruker.com/products/mass-spectrometry-and-separations/lc-ms/o-tof/timstof-pro.html>, accessed on 2020/02/02.
8. Thermo Fisher Scientific Mass Spectrometers. [Internet]. Available from: <https://www.thermofisher.com/search/browse/category/de/en/602508/Mass+Spectrometry+Systems+&>, accessed on 2020/02/02.

CHAPTER 7



General discussion and perspective

1 General discussion and perspective

With the great success of checkpoint inhibitors, cancer immunotherapy has started to evolve as novel pillar in multimodal anti-tumor therapies.¹⁻⁴ Immune checkpoint blockade appears effective in metastatic melanoma or non-small cell lung carcinoma,⁵⁻⁸ while patients suffering from other types of tumors including intracranial neoplasia do not clinically benefit.^{9,10} The reason for this was found out later when response to checkpoint inhibition was shown to positively correlate with mutational burden,^{7,11,12} which is low among brain tumors excepting MMR-deficient ones and recurrent glioblastomas exhibiting a hypermutation phenotype¹³⁻¹⁶ Cancer immunotherapy aims at breaking immune evasion by provision of the (appropriate) antigen (1), supply of T-cell co-stimulation or blockade of T-cell co-inhibition (2), and transfer of effector cells (3).^{17,18} As the second strategy alone has shown to be ineffective in tumors with low mutational burden and lacking pre-existing immunity, one should go for providing the appropriate antigen activating the patient's T cells or directly providing (antigen-specific) effector cells. Combined with checkpoint inhibition this might then elicit clinically relevant anti-tumoral immune responses.^{2,17,19} In the case of glioblastoma, concomitant administration of anti-PD-1 or anti-PD-L1 antibodies might be promising, as PD-L1 is expressed in 72% of recurrent and 88% of primary glioblastomas.²⁰ Medulloblastomas and meningiomas, in turn, are rarely PD-L1 positive,^{21,22} suggesting to target the PD-1–PD-L1 axis only *via* PD-1 or to use other checkpoint antibodies blocking e.g. CTLA4, TIGIT, LAG-3, and VISTA on T cells or B7-H3 expressed on tumor cells.^{2,23,24}

Immunopeptidomics has proven as state-of-the art and method of choice to define candidate targets for cancer immunotherapy as it offers an unbiased and comprehensive view on the pathophysiologically relevant antigenic landscape.²⁵ We proved glioblastoma and, most importantly, also medulloblastoma and meningioma to be compatible with HLA peptidome-centric target definition yielding both HLA class I- and II-restricted peptides in considerable numbers. Remarkably, even with scarce amounts of tissue being available (less than 100 mg), we achieved several thousand peptide identifications (e.g. GBM20R: 3,213 HLA class I ligands and 3,957 HLA class II-restricted peptides isolated from 35 mg of tissue) using an optimized protocol including consequent avoidance of sample loss during lysate preparation and HLA-IP as well as direct injection, for LC-MS/MS. Future approaches may even encompass the analysis of circulating neoplastic cells as well as brain tumor-derived soluble HLA-peptide complexes and extracellular vesicles isolated from blood or CSF. Besides representing a substitute when patient-derived tumor tissue is not available or facilitating the investigation of subclones and their effusions, these may serve as liquid biopsy to diagnose and monitor disease or even as predictive biomarker for response to therapy and prognosis.²⁵⁻³³ The repertoire of HLA-presented antigens, which have so far been exploited for immunotherapeutic approaches comprises viral antigens, non-mutated differentiation antigens, TAAs, and CTAs as well as neo-antigens arising from non-synonymous mutations.^{25,34-41} Epitopes derived from oncogenic viruses or mutation-bearing proteins represent prime candidates for antigen-specific immunotherapies as they offer maximum tumor specificity and do not underlie central tolerance to self-antigens that has to be overcome for anti-tumor responses.⁴² A viral etiology of common intracranial neoplasms has, however, remained under controversial discussion.⁴³⁻⁴⁶ Although we succeeded in proving two neo-antigenic peptides to be naturally presented on

HLA molecules of glioblastoma cells for the first time, the verification of mutated peptides by LC-MS/MS has remained anecdotally – even in tumors with higher mutational burden as compared with brain tumors. In addition to extremely low confirmation rates of predicted neo-epitopes, around 99% of somatic mutations are not being recognized by T cells greatly supporting to target non-mutated tumor-associated and tumor-specific antigens by immunotherapy instead.^{14,25,47-51}

During the course of this thesis, I analyzed 123 brain tumor specimens gaining a deep insight into the immunopeptidomic landscape of intracranial neoplasms. We identified a total of 485 candidate target antigens exploitable for immunotherapeutic efforts. Among these, two proved to be pan-brain tumor antigens (WNT5A and ESCO1) characterized by frequent and tumor-exclusive HLA presentation on glioblastomas, medulloblastomas, and meningiomas. This is in line with previous findings in hematological malignancies (multiple myeloma, acute myeloid, chronic myeloid, and chronic lymphocytic leukemia)⁵² and strongly emphasizes that the repertoire of naturally presented tumor antigens is highly entity-specific encouraging and requiring immunopeptidomic studies of every tumor type individually. In turn, we found a large fraction of meningioma-associated antigens and peptides to be presented across all WHO grades as well as candidate targets for medulloblastoma to be shared by WNT-activated, non-WNT/non-SHH, and SHH-activated as well as by childhood and adult tumors. Moreover, the data presented herein demonstrate that established TAAs and CTAs – independent of whether these are published as pan-tumor or entity-specific antigens – are not recommended for immunotherapeutic purposes as being either broadly presented on both benign and neoplastic tissues or exhibiting infrequent albeit tumor-exclusive HLA presentation. While meningiomas are supplied by vascular branches of the external carotid artery,^{53,54} the blood supply of glioblastomas and medulloblastomas arising within the brain parenchyma itself is accomplished by branches of the internal carotid artery.⁵⁵⁻⁵⁷ Targeting such intra-axial lesions located beyond the blood-brain barrier (neurovascular unit) inevitably requires epitopes to be tumor-specific and not to be presented on other CNS cells.⁵⁸⁻⁶⁰ Although our target discovery approach focused on tumor-exclusively presented antigens lacking CNS-associated expression, an intense validation process is required to warrant an excellent safety profile of selected antigens excluding on-target off-tumor effects within the CNS. This is particularly important as the benign HLA peptidome dataset subtracted during the course of comparative profiling comprising n=12 brains, n=11 cerebella, and n=1 spinal cord neither covers all HLA allotypes nor achieves 100% saturation of the benign CNS peptidome.

Apart from the aforementioned TAAs and TSAs there is another class of HLA ligands, which has so far not been exploited for immunotherapeutic efforts: cryptic peptides. These arise from antisense transcripts, novel unannotated open reading frames, non-coding regions (5' and 3' UTRs, introns, intergenic regions), non-canonical reading frames of protein-coding regions, or unconventional (proteasomal) splicing events. They have been proven to be immunogenic and estimated to contribute with 6.5-13% to the entirety of HLA-presented peptides.^{25,61-64} Thus, the chance to identify tumor-associated cryptic peptides appears a lot more promising than the search for neo-antigenic HLA ligands arising from non-synonymous mutations.⁶⁵⁻⁶⁸ However, cryptic peptides may also be neo-antigenic with the majority of somatic mutations affecting non-coding regions (Figure 21).^{25,64,69} Data-independent acquisition and more accurate

quantification strategies – enabled by the use of retention time standard peptides presented herein – as well as the development and usage of technically complementary LC-MS/MS systems, innovative bioinformatic algorithms, and computational tools will foster deeper explorations of tumor and benign immunopeptidomes.⁶⁵⁻⁶⁸ I am convinced that cryptic peptides will be subject of future target discovery approaches for cancer immunotherapy.^{25,69,70} Addressing non-mutated cryptic peptides in intracranial neoplasias is possible by re-analyzing the acquired LC-MS/MS data using the *de novo* sequencing workflow Peptide-PRISM, which is currently being developed for immunopeptidomic datasets by the group of Andreas Schlosser at the University of Würzburg (unpublished data by Erhard *et al.*, manuscript submitted 2020). In addition, one could re-measure remaining peptide eluates employing more sophisticated protocols such as data-independent acquisition with spiked RT peptides possibly using multiple complementary LC-MS/MS systems to maximize the number of unique peptide identifications per sample. A comprehensive search for mutation-bearing cryptic peptides, however, requires whole genome sequencing.⁶⁴ This is possible for a large fraction of the glioblastoma cohort, while germline DNA essential for somatic variant calling is not available from medulloblastoma and meningioma patients.

As recently shown in the GAPVAC-101 trial, only one out of six WT antigens employed in APVAC2 was immunogenic. This strongly argues against the use of naturally presented tumor-associated peptides without prior evaluation of immunogenicity for vaccination approaches.¹⁴ For a selected set of glioblastoma-, medulloblastoma-, and meningioma-associated peptides presented herein, these experiments are currently being performed by Dr. Konstantina Kapolou, Dr. med. Julia Velz, and Gioele Medici in the Laboratory for Molecular Neuro-Oncology at the University of Zürich. These include IFN- γ ELISpots, naïve T-cell primings, and killing assays – if possible, in an autologous setting using TILs or PBMCs and an established tumor cell line from the same patient. Immunological characterization of TILs isolated from fresh glioblastoma tissue further comprises mass cytometry and ultra-deep TCR sequencing. A research group from the Washington University School of Medicine headed by Robert Schreiber has recently postulated that effective anti-tumor immune responses induced by immunotherapies require one MHC class I- and class II-presented (neo-)antigen each. Of note, this is even the case for MHC class II-negative tumors. In an ideal scenario of peptide vaccination, long peptides harboring both an immunogenic CD8 and CD4 epitope are applied inducing T-cell activation at the site of disease in the TME.⁷¹ However, this conclusion was drawn from a monoclonal sarcoma model, while naturally grown human tumors are constituted of several subclonal populations of neoplastic cells.^{60,71,72} Against the background of intratumoral heterogeneity – which is particularly high in glioblastoma^{60,72} – it is not possible to elicit clinically relevant anti-tumor responses by targeting a single antigen. Instead, a mix of targetable CD4 and CD8 epitopes is required.^{2,71,73} Herein, we provide such a mixture of both HLA class I- and II-restricted candidate target peptides for glioblastoma, medulloblastoma, and meningioma immunotherapy.

Besides target specificity, adaptability and durability of anti-tumor immune responses are crucial for clinical efficacy.⁷⁴ To not only prime, but also amplify tumor-directed immunity, (peptide) vaccines should be administered several times, whereby the exact dosage schedule is subject of ongoing research.⁷³ Moreover, the use of an appropriate adjuvant and

administration route have a decisive impact on the induction of clinically relevant responses which have stayed out in 95% of cancer vaccine administrations.^{73,75,76} The treatment of intracranial neoplasms represents a prime example of needed co-stimulation as T cells have to be empowered to enter the neurovascular unit in addition.⁵⁸⁻⁶⁰ Besides the application of vaccine adjuvants, great potential is seen for the development of combination therapies complementing each other and unleashing synergistic effects. Radiotherapy, for instance, disrupts the blood-brain barrier, induces local neuroinflammation and antigen release thus guiding immune effector cells to the site of disease.⁷⁷⁻⁸⁰ For peptide vaccination in glioblastoma, it has recently been shown that concomitant medication such as dexamethasone shapes and can even impede the response to immunotherapy.⁸¹ Likewise, checkpoint blockade is of different effectiveness when administered in an adjuvant or neoadjuvant setting. It has been suggested that the larger degree of antigenic diversity before surgery for recurrent glioblastoma favors the expansion of (polyclonal) anti-tumor T cells upon checkpoint inhibition.⁸² Consequently, not only the composition, dosage, and timing of antigen-specific immunotherapeutic agents themselves, but also of concomitant medication and therapies have a decisive impact on patient outcomes and should therefore be subject of in-depth investigations.

In conclusion, there is tremendous potential for the implementation of cancer immunotherapy as additional pillar of multimodal therapies for intracranial neoplasias. Being convinced that non-mutated antigens will coin peptide-specific approaches with immunopeptidomics-based target definition in the short to medium term, we defined a large set of naturally, frequently, and tumor-exclusively presented antigens and peptides for glioblastoma, medulloblastoma, and meningioma immunotherapy. Apart from peptide vaccination, these may also guide the development of DC- and T cell-based strategies. With antigen-specific immunotherapy for intracranial neoplasms, we envision to replace radiotherapy in the treatment of childhood tumors thus reducing long-term sequelae, to offer therapeutic options for the management of disease recurrence, and to improve patient outcomes.

2 References

1. Nobel Media AB 2019. NobelPrize.org. The Nobel Prize in Physiology or Medicine 2018. [Internet]. Available from: <https://www.nobelprize.org/prizes/medicine/2018/summary/>, accessed on 2019/11/21.
2. Velcheti V, Schalper K. Basic Overview of Current Immunotherapy Approaches in Cancer. *Am Soc Clin Oncol Educ Book*. 2016;35:298-308.
3. Mapara MY, Sykes M. Tolerance and cancer: mechanisms of tumor evasion and strategies for breaking tolerance. *J Clin Oncol*. 2004;22(6):1136-1151.
4. Parish CR. Cancer immunotherapy: the past, the present and the future. *Immunol Cell Biol*. 2003;81(2):106-113.
5. Hodi FS, O'Day SJ, McDermott DF, Weber RW, Sosman JA, Haanen JB, Gonzalez R, Robert C, Schadendorf D, Hassel JC, Akerley W, van den Eertwegh AJ, Lutzky J, Lorigan P, Vaubel JM, Linette GP, Hogg D, Ottensmeier CH, Lebbé C, Peschel C, Quirt I, Clark JI, Wolchok JD, Weber JS, Tian J, Yellin MJ, Nichol GM, Hoos A, Urba WJ. Improved survival with ipilimumab in patients with metastatic melanoma. *N Engl J Med*. 2010;363(8):711-723.
6. Wolchok JD, Kluger H, Callahan MK, Postow MA, Rizvi NA, Lesokhin AM, Segal NH, Ariyan CE, Gordon RA, Reed K, Burke MM, Caldwell A, Kronenberg SA, Agunwamba BU, Zhang X, Lowy I, Inzunza HD, Feely W, Horak CE, Hong Q, Korman AJ, Wigginton JM, Gupta A, Sznol M. Nivolumab plus ipilimumab in advanced melanoma. *N Engl J Med*. 2013;369(2):122-133.
7. Rizvi NA, Hellmann MD, Snyder A, Kvistborg P, Makarov V, Havel JJ, Lee W, Yuan J, Wong P, Ho TS, Miller ML, Rekhtman N, Moreira AL, Ibrahim F, Bruggeman C, Gasmi B, Zappasodi R, Maeda Y, Sander C, Garon

Chapter 7: References

- EB, Merghoub T, Wolchok JD, Schumacher TN, Chan TA. Cancer immunology. Mutational landscape determines sensitivity to PD-1 blockade in non-small cell lung cancer. *Science*. 2015;348(6230):124-128.
8. Robert C, Long GV, Brady B, Dutriaux C, Maio M, Mortier L, Hassel JC, Rutkowski P, McNeil C, Kalinka-Warzocha E, Savage KJ, Hernberg MM, Lebbé C, Charles J, Mihalciou C, Chiarion-Sileni V, Mauch C, Cognetti F, Arance A, Schmidt H, Schadendorf D, Gogas H, Lundgren-Eriksson L, Horak C, Sharkey B, Waxman IM, Atkinson V, Ascierto PA. Nivolumab in previously untreated melanoma without BRAF mutation. *N Engl J Med*. 2015;372(4):320-330.
 9. Lukas RV, Rodon J, Becker K, Wong ET, Shih K, Touat M, Fasso M, Osborne S, Molinero L, O'Hear C, Grossman W, Baehring J. Clinical activity and safety of atezolizumab in patients with recurrent glioblastoma. *J Neurooncol*. 2018;140(2):317-328.
 10. Omuro A, Vlahovic G, Lim M, Sahebjam S, Baehring J, Cloughesy T, Voloschin A, Ramkissoon SH, Ligon KL, Latek R, Zwirter R, Strauss L, Paliwal P, Harbison CT, Reardon DA, Sampson JH. Nivolumab with or without ipilimumab in patients with recurrent glioblastoma: results from exploratory phase I cohorts of CheckMate 143. *Neuro Oncol*. 2018;20(5):674-686.
 11. Snyder A, Makarov V, Merghoub T, Yuan J, Zaretsky JM, Desrichard A, Walsh LA, Postow MA, Wong P, Ho TS, Hollmann TJ, Bruggeman C, Kannan K, Li Y, Elipenahli C, Liu C, Harbison CT, Wang L, Ribas A, Wolchok JD, Chan TA. Genetic basis for clinical response to CTLA-4 blockade in melanoma. *N Engl J Med*. 2014;371(23):2189-2199.
 12. Van Allen EM, Miao D, Schilling B, Shukla SA, Blank C, Zimmer L, Sucker A, Hillen U, Foppen MHG, Goldinger SM, Utikal J, Hassel JC, Weide B, Kaehler KC, Loquai C, Mohr P, Gutzmer R, Dummer R, Gabriel S, Wu CJ, Schadendorf D, Garraway LA. Genomic correlates of response to CTLA-4 blockade in metastatic melanoma. *Science*. 2015;350(6257):207-211.
 13. Alexandrov LB, Nik-Zainal S, Wedge DC, Aparicio SA, Behjati S, Biankin AV, Bignell GR, Bolli N, Borg A, Børresen-Dale AL, Boyault S, Burkhardt B, Butler AP, Caldas C, Davies HR, Desmedt C, Eils R, Eyfjörd JE, Foekens JA, Greaves M, Hosoda F, Hutter B, Ilicic T, Imbeaud S, Imielinski M, Jäger N, Jones DT, Jones D, Knappskog S, Kool M, Lakhani SR, López-Otín C, Martin S, Munshi NC, Nakamura H, Northcott PA, Pajic M, Papaemmanuil E, Paradiso A, Pearson JV, Puente XS, Raine K, Ramakrishna M, Richardson AL, Richter J, Rosenstiel P, Schlesner M, Schumacher TN, Span PN, Teague JW, Totoki Y, Tutt AN, Valdés-Mas R, van Buuren MM, van 't Veer L, Vincent-Salomon A, Waddell N, Yates LR, Zucman-Rossi J, Futreal PA, McDermott U, Lichter P, Meyerson M, Grimmond SM, Siebert R, Campo E, Shibata T, Pfister SM, Campbell PJ, Stratton MR. Signatures of mutational processes in human cancer. *Nature*. 2013;500(7463):415-421.
 14. Hilf N, Kuttruff-Coqui S, Frenzel K, Bukur V, Stevanović S, Gouttefangeas C, Platten M, Tabatabai G, Dutoit V, van der Burg SH, Thor Straten P, Martínez-Ricarte F, Ponsati B, Okada H, Lassen U, Admon A, Ottensmeier CH, Ulges A, Kreiter S, von Deimling A, Skardelly M, Migliorini D, Kroep JR, Idorn M, Rodon J, Piró J, Poulsen HS, Shraibman B, McCann K, Mendrzyk R, Löwer M, Stieglbauer M, Britten CM, Capper D, Welters MJ, Sahuquillo J, Kiesel K, Derhovanessian E, Rusch E, Bunse L, Song C, Heesch S, Wagner C, Kemmer-Brück A, Ludwig J, Castle JC, Schoor O, Tadmor AD, Green E, Fritsche J, Meyer M, Pawlowski N, Dorner S, Hoffgaard F, Rössler B, Maurer D, Weinschenk T, Reinhardt C, Huber C, Rammensee HG, Singh-Jasuja H, Sahin U, Dietrich PY, Wick W. Actively personalized vaccination trial for newly diagnosed glioblastoma. *Nature*. 2019;565(7738):240-245.
 15. Hunter C, Smith R, Cahill DP, Stephens P, Stevens C, Teague J, Greenman C, Edkins S, Bignell G, Davies H, O'Meara S, Parker A, Avis T, Barthorpe S, Brackenbury L, Buck G, Butler A, Clements J, Cole J, Dicks E, Forbes S, Gorton M, Gray K, Halliday K, Harrison R, Hills K, Hinton J, Jenkinson A, Jones D, Kosmidou V, Laman R, Lugg R, Menzies A, Perry J, Petty R, Raine K, Richardson D, Shepherd R, Small A, Solomon H, Tofts C, Varian J, West S, Widaa S, Yates A, Easton DF, Riggins G, Roy JE, Levine KK, Mueller W, Batchelor TT, Louis DN, Stratton MR, Futreal PA, Wooster R. A hypermutation phenotype and somatic MSH6 mutations in recurrent human malignant gliomas after alkylator chemotherapy. *Cancer Res*. 2006;66(8):3987-3991.
 16. McLendon R, Friedman A, Bigner D, Van Meir EG, Brat DJ, Mastrogianakis GM, Olson JJ, Mikkelsen T, Lehman N, Aldape K, Yung WK, Bogler O, Weinstein JN, VandenBerg S, Berger M, Prados M, Muzny D, Morgan M, Scherer S, Sabo A, Nazareth L, Lewis L, Hall O, Zhu Y, Ren Y, Alvi O, Yao J, Hawes A, Jhangiani S, Fowler G, San Lucas A, Kovar C, Cree A, Dinh H, Santibanez J, Joshi V, Gonzalez-Garay ML, Miller CA, Milosavljevic A, Donehower L, Wheeler DA, Gibbs RA, Cibulskis K, Sougnez C, Fennell T, Mahan S, Wilkinson J, Ziaugra L, Onofrio R, Bloom T, Nicol R, Ardlie K, Baldwin J, Gabriel S, Lander ES, Ding L, Fulton RS, McLellan MD, Wallis J, Larson DE, Shi X, Abbott R, Fulton L, Chen K, Koboldt DC, Wendl MC, Meyer R, Tang Y, Lin L, Osborne JR, Dunford-Shore BH, Miner TL, Delehaanty K, Markovic C, Swift G, Courtney W, Pohl C, Abbott S, Hawkins A, Leong S, Haipok C, Schmidt H, Wiechert M, Vickery T, Scott S, Dooling DJ, Chinwalla A, Weinstock GM, Mardis ER, Wilson RK, Getz G, Winckler W, Verhaak RG, Lawrence MS, O'Kelly M, Robinson J, Alexe G, Beroukhi R, Carter S, Chiang D, Gould J, Gupta S, Korn J, Mermel C, Mesirov J, Monti S, Nguyen H, Parkin M, Reich M, Stransky N, Weir BA, Garraway L, Golub T, Meyerson M, Chin L, Protopopov A, Zhang J, Perna I, Aronson S, Sathiamoorthy N, Ren G, Yao J, Wiedemeyer WR, Kim H, Kong SW, Xiao Y, Kohane IS, Seidman J, Park PJ, Kucherlapati R, Laird PW, Cope L, Herman JG, Weisenberger DJ, Pan F, Van den Berg D, Van Neste L, Yi JM, Schuebel KE, Baylin SB, Absher DM, Li JZ, Southwick A, Brady S, Aggarwal A, Chung T, Sherlock G, Brooks JD, Myers RM, Spellman PT, Purdom E, Jakkula LR, Lapuk AV, Marr H, Dorton S, Choi Y, Han J, Ray A, Wang V, Durinck S, Robinson M, Wang NJ, Vranizan K, Peng V, Van Name E, Fontenay GV, Ngai J, Conboy JG, Parvin B, Feiler HS, Speed TP, Gray JW, Brennan C, Socci ND, Olshen A, Taylor BS, Lash A, Schultz N, Reva B, Antipin Y, Stukalov A, Gross B, Cerami E, Wang WQ, Qin LX, Seshan VE, Villafania L, Cavatore M, Borsu L, Viale A, Gerald W, Sander C, Ladanyi M, Perou CM,

Chapter 7: References

- Hayes DN, Topal MD, Hoadley KA, Qi Y, Balu S, Shi Y, Wu J, Penny R, Bittner M, Shelton T, Lenkiewicz E, Morris S, Beasley D, Sanders S, Kahn A, Sfeir R, Chen J, Nassau D, Feng L, Hickey E, Barker A, Gerhard DS, Vockley J, Compton C, Vaught J, Fielding P, Ferguson ML, Schaefer C, Zhang J, Madhavan S, Buetow KH, Collins F, Good P, Guyer M, Ozenberger B, Peterson J, Thomson E. Comprehensive genomic characterization defines human glioblastoma genes and core pathways. *Nature*. 2008;455(7216):1061-1068.
17. Freudenmann LK. Mapping the HLA Ligandome of Primary versus Recurrent Disease in Glioblastoma Multiforme by Mass Spectrometry. *Master Thesis, Master of Science in Molecular Medicine, Eberhard Karls Universität Tübingen, Faculty of Medicine*. 2017.
 18. Curiel TJ. Tregs and rethinking cancer immunotherapy. *J Clin Invest*. 2007;117(5):1167-1174.
 19. Rampling R, Peoples S, Mulholland PJ, James A, Al-Salihi O, Twelves CJ, McBain C, Jefferies S, Jackson A, Stewart W, Lindner J, Kutscher S, Hilf N, McGuigan L, Peters J, Hill K, Schoor O, Singh-Jasuja H, Halford SE, Ritchie JW. A Cancer Research UK First Time in Human Phase I Trial of IMA950 (Novel Multi-peptide Therapeutic Vaccine) in Patients with Newly Diagnosed Glioblastoma. *Clin Cancer Res*. 2016;22(19):4776-4785.
 20. Berghoff AS, Kiesel B, Widhalm G, Rajky O, Ricken G, Wöhrer A, Dieckmann K, Filipits M, Brandstetter A, Weller M, Kurscheid S, Hegi ME, Zielinski CC, Marosi C, Hainfellner JA, Preusser M, Wick W. Programmed death ligand 1 expression and tumor-infiltrating lymphocytes in glioblastoma. *Neuro Oncol*. 2015;17(8):1064-1075.
 21. Vermeulen JF, Van Hecke W, Adriaansen EJM, Jansen MK, Bouma RG, Villacorta Hidalgo J, Fisch P, Broekhuizen R, Spliet WGM, Kool M, Bovenschen N. Prognostic relevance of tumor-infiltrating lymphocytes and immune checkpoints in pediatric medulloblastoma. *Oncoimmunology*. 2018;7(3):e1398877.
 22. Johnson MD. PD-L1 expression in meningiomas. *J Clin Neurosci*. 2018;57:149-151.
 23. Qin S, Xu L, Yi M, Yu S, Wu K, Luo S. Novel immune checkpoint targets: moving beyond PD-1 and CTLA-4. *Mol Cancer*. 2019;18(1):155.
 24. Majzner RG, Theruvath JL, Nellan A, Heitzeneder S, Cui Y, Mount CW, Rietberg SP, Linde MH, Xu P, Rota C, Sotillo E, Labanieh L, Lee DW, Orentas RJ, Dimitrov DS, Zhu Z, Croix BS, Delaidelli A, Sekunova A, Bonvini E, Mitra SS, Quezado MM, Majeti R, Monje M, Sorensen PHB, Maris JM, Mackall CL. CAR T Cells Targeting B7-H3, a Pan-Cancer Antigen, Demonstrate Potent Preclinical Activity Against Pediatric Solid Tumors and Brain Tumors. *Clin Cancer Res*. 2019;25(8):2560-2574.
 25. Freudenmann LK, Marcu A, Stevanović S. Mapping the tumour human leukocyte antigen (HLA) ligandome by mass spectrometry. *Immunology*. 2018;154(3):331-345.
 26. Bassani-Sternberg M, Barnea E, Beer I, Avivi I, Katz T, Admon A. Soluble plasma HLA peptidome as a potential source for cancer biomarkers. *Proc Natl Acad Sci U S A*. 2010;107(44):18769-18776.
 27. Shraibman B, Barnea E, Kadosh DM, Haimovich Y, Slobodin G, Rosner I, López-Larrea C, Hilf N, Kuttruff S, Song C, Britten C, Castle J, Kreiter S, Frenzel K, Tatagiba M, Tabatabai G, Dietrich PY, Dutoit V, Wick W, Platten M, Winkler F, von Deimling A, Kroep J, Sahuquillo J, Martinez-Ricarte F, Rodon J, Lassen U, Ottensmeier C, van der Burg SH, Thor Straten P, Poulsen HS, Ponsati B, Okada H, Rammensee HG, Sahin U, Singh H, Admon A. Identification of Tumor Antigens Among the HLA Peptidomes of Glioblastoma Tumors and Plasma. *Mol Cell Proteomics*. 2019;18(6):1255-1268.
 28. Synowsky SA, Shirran SL, Cooke FGM, Antoniou AN, Botting CH, Powis SJ. The major histocompatibility complex class I immunopeptidome of extracellular vesicles. *J Biol Chem*. 2017;292(41):17084-17092.
 29. Campoli M, Ferrone S. Tumor escape mechanisms: potential role of soluble HLA antigens and NK cells activating ligands. *Tissue Antigens*. 2008;72(4):321-334.
 30. Andre F, Scharz NE, Movassagh M, Flament C, Pautier P, Morice P, Pomel C, Lhomme C, Escudier B, Le Chevalier T, Tursz T, Amigorena S, Raposo G, Angevin E, Zitvogel L. Malignant effusions and immunogenic tumour-derived exosomes. *Lancet*. 2002;360(9329):295-305.
 31. Chistiakov DA, Chekhonin VP. Circulating tumor cells and their advances to promote cancer metastasis and relapse, with focus on glioblastoma multiforme. *Exp Mol Pathol*. 2018;105(2):166-174.
 32. Garzia L, Kijima N, Morrissy AS, De Antonellis P, Guerreiro-Stucklin A, Holgado BL, Wu X, Wang X, Parsons M, Zayne K, Manno A, Kuzan-Fischer C, Nor C, Donovan LK, Liu J, Qin L, Garancher A, Liu KW, Mansouri S, Luu B, Thompson YY, Ramaswamy V, Peacock J, Farooq H, Skowron P, Shih DJH, Li A, Ensan S, Robbins CS, Cybulsky M, Mitra S, Ma Y, Moore R, Mungall A, Cho YJ, Weiss WA, Chan JA, Hawkins CE, Massimino M, Jabado N, Zapotocky M, Sumerauer D, Bouffet E, Dirks P, Tabori U, Sorensen PHB, Brastianos PK, Aldape K, Jones SJM, Marra MA, Woodgett JR, Wechsler-Reya RJ, Fults DW, Taylor MD. A Hematogenous Route for Medulloblastoma Leptomeningeal Metastases. *Cell*. 2018;172(5):1050-1062.e1014.
 33. Erkan EP, Ströbel T, Dorfer C, Sonntagbauer M, Weinhäusel A, Saydam N, Saydam O. Circulating Tumor Biomarkers in Meningiomas Reveal a Signature of Equilibrium Between Tumor Growth and Immune Modulation. *Front Oncol*. 2019;9:1031.
 34. Coulie PG, Van den Eynde BJ, van der Bruggen P, Boon T. Tumour antigens recognized by T lymphocytes: at the core of cancer immunotherapy. *Nat Rev Cancer*. 2014;14(2):135-146.
 35. Urban JL, Schreiber H. Tumor antigens. *Annu Rev Immunol*. 1992;10:617-644.
 36. van der Bruggen P, Traversari C, Chomez P, Lurquin C, De Plaen E, Van den Eynde B, Knuth A, Boon T. A gene encoding an antigen recognized by cytolytic T lymphocytes on a human melanoma. *Science*. 1991;254(5038):1643-1647.
 37. Brichard V, Van Pel A, Wölfel T, Wölfel C, De Plaen E, Lethe B, Coulie P, Boon T. The tyrosinase gene codes for an antigen recognized by autologous cytolytic T lymphocytes on HLA-A2 melanomas. *J Exp Med*. 1993;178(2):489-495.

Chapter 7: References

38. Cox AL, Skipper J, Chen Y, Henderson RA, Darrow TL, Shabanowitz J, Engelhard VH, Hunt DF, Slingluff CL, Jr. Identification of a peptide recognized by five melanoma-specific human cytotoxic T cell lines. *Science*. 1994;264(5159):716-719.
39. Topalian SL, Gonzales MI, Parkhurst M, Li YF, Southwood S, Sette A, Rosenberg SA, Robbins PF. Melanoma-specific CD4+ T cells recognize nonmutated HLA-DR-restricted tyrosinase epitopes. *J Exp Med*. 1996;183(5):1965-1971.
40. Klein G, Klein E. Immune surveillance against virus-induced tumors and nonrejectability of spontaneous tumors: contrasting consequences of host versus tumor evolution. *Proc Natl Acad Sci U S A*. 1977;74(5):2121-2125.
41. van der Burg SH, Melief CJ. Therapeutic vaccination against human papilloma virus induced malignancies. *Curr Opin Immunol*. 2011;23(2):252-257.
42. Gotter J, Brors B, Hergenbahn M, Kyewski B. Medullary epithelial cells of the human thymus express a highly diverse selection of tissue-specific genes colocalized in chromosomal clusters. *J Exp Med*. 2004;199(2):155-166.
43. Miller G. Brain cancer. A viral link to glioblastoma? *Science*. 2009;323(5910):30-31.
44. Chi J, Gu B, Zhang C, Peng G, Zhou F, Chen Y, Zhang G, Guo Y, Guo D, Qin J, Wang J, Li L, Wang F, Liu G, Xie F, Feng D, Zhou H, Huang X, Lu S, Liu Y, Hu W, Yao K. Human herpesvirus 6 latent infection in patients with glioma. *J Infect Dis*. 2012;206(9):1394-1398.
45. Poltermann S, Schlehofer B, Steindorf K, Schnitzler P, Geletneky K, Schlehofer JR. Lack of association of herpesviruses with brain tumors. *J Neurovirol*. 2006;12(2):90-99.
46. Holdhoff M, Guner G, Rodriguez FJ, Hicks JL, Zheng Q, Forman MS, Ye X, Grossman SA, Meeker AK, Heaphy CM, Eberhart CG, De Marzo AM, Arav-Boger R. Absence of cytomegalovirus in glioblastoma and other high-grade gliomas by real-time PCR, immunohistochemistry and in situ hybridization. *Clin Cancer Res*. 2016.
47. Löffler MW, Mohr C, Bichmann L, Freudenmann LK, Walzer M, Schroeder CM, Trautwein N, Hilke FJ, Zinser RS, Mühlenbruch L, Kowalewski DJ, Schuster H, Sturm M, Matthes J, Riess O, Czemmel S, Nahnsen S, Königsrainer I, Thiel K, Nadalin S, Beckert S, Bösmüller H, Fend F, Velic A, Maček B, Haen SP, Buonaguro L, Kohlbacher O, Stevanović S, Königsrainer A, Rammensee HG. Multi-omics discovery of exome-derived neoantigens in hepatocellular carcinoma. *Genome Med*. 2019;11(1):28.
48. Tran E, Ahmadzadeh M, Lu YC, Gros A, Turcotte S, Robbins PF, Gartner JJ, Zheng Z, Li YF, Ray S, Wunderlich JR, Somerville RP, Rosenberg SA. Immunogenicity of somatic mutations in human gastrointestinal cancers. *Science*. 2015;350(6266):1387-1390.
49. Bassani-Sternberg M, Bräunlein E, Klar R, Engleitner T, Sinitcyn P, Audehm S, Straub M, Weber J, Slotta-Huspénina J, Specht K, Martignoni ME, Werner A, Hein R, Busch DH, Peschel C, Rad R, Cox J, Mann M, Krackhardt AM. Direct identification of clinically relevant neoepitopes presented on native human melanoma tissue by mass spectrometry. *Nat Commun*. 2016;7:13404.
50. Newey A, Griffiths B, Michaux J, Pak HS, Stevenson BJ, Woolston A, Semiannikova M, Spain G, Barber LJ, Matthews N, Rao S, Watkins D, Chau I, Coukos G, Racle J, Gfeller D, Starling N, Cunningham D, Bassani-Sternberg M, Gerlinger M. Immunopeptidomics of colorectal cancer organoids reveals a sparse HLA class I neoantigen landscape and no increase in neoantigens with interferon or MEK-inhibitor treatment. *J Immunother Cancer*. 2019;7(1):309.
51. Khodadoust MS, Olsson N, Wagar LE, Haabeth OA, Chen B, Swaminathan K, Rawson K, Liu CL, Steiner D, Lund P, Rao S, Zhang L, Marceau C, Stehr H, Newman AM, Czerwinski DK, Carlton VE, Moorhead M, Faham M, Kohrt HE, Carette J, Green MR, Davis MM, Levy R, Elias JE, Alizadeh AA. Antigen presentation profiling reveals recognition of lymphoma immunoglobulin neoantigens. *Nature*. 2017;543(7647):723-727.
52. Backert L, Kowalewski DJ, Walz S, Schuster H, Berlin C, Neidert MC, Schemionek M, Brümmendorf TH, Vucinic V, Niederwieser D, Kanz L, Salih HR, Kohlbacher O, Weisel K, Rammensee HG, Stevanović S, Walz JS. A meta-analysis of HLA peptidome composition in different hematological entities: entity-specific dividing lines and "pan-leukemia" antigens. *Oncotarget*. 2017;8(27):43915-43924.
53. Manaka H, Sakata K, Tatezaki J, Shinohara T, Shimohigoshi W, Yamamoto T. Safety and Efficacy of Preoperative Embolization in Patients with Meningioma. *J Neurol Surg B Skull Base*. 2018;79(Suppl 4):S328-s333.
54. Dettori P, Bradac GB, Scialfa G. Selective angiography of the external and internal carotid arteries in the diagnosis of supra-tentorial meningiomas. *Neuroradiology*. 1970;1(3):166-172.
55. Malhotra M, Toulouse A, Godinho BM, Mc Carthy DJ, Cryan JF, O'Driscoll CM. RNAi therapeutics for brain cancer: current advancements in RNAi delivery strategies. *Mol Biosyst*. 2015;11(10):2635-2657.
56. Louis DN, Perry A, Reifenberger G, von Deimling A, Figarella-Branger D, Cavenee WK, Ohgaki H, Wiestler OD, Kleihues P, Ellison DW. The 2016 World Health Organization Classification of Tumors of the Central Nervous System: a summary. *Acta Neuropathol*. 2016;131(6):803-820.
57. Purves D, Augustine GJ, Fitzpatrick D, Katz LC, LaMantia AS, McNamara JO, Williams SM. Neuroscience. 2nd edition. Sunderland (MA): Sinauer Associates; 2001. The Blood Supply of the Brain and Spinal Cord. Available from: <https://www.ncbi.nlm.nih.gov/books/NBK11042/>, accessed on 2020/03/31.
58. Bhowmik A, Khan R, Ghosh MK. Blood brain barrier: a challenge for effectual therapy of brain tumors. *Biomed Res Int*. 2015;2015:320941.
59. Wilson EH, Weninger W, Hunter CA. Trafficking of immune cells in the central nervous system. *J Clin Invest*. 2010;120(5):1368-1379.

Chapter 7: References

60. Mohme M, Neidert MC, Regli L, Weller M, Martin R. Immunological challenges for peptide-based immunotherapy in glioblastoma. *Cancer Treat Rev.* 2014;40(2):248-258.
61. Weinzierl AO, Maurer D, Altenberend F, Schneiderhan-Marra N, Klingel K, Schoor O, Wernet D, Joos T, Rammensee HG, Stevanović S. A cryptic vascular endothelial growth factor T-cell epitope: identification and characterization by mass spectrometry and T-cell assays. *Cancer Res.* 2008;68(7):2447-2454.
62. Laumont CM, Daouda T, Laverdure JP, Bonneil É, Caron-Lizotte O, Hardy MP, Granados DP, Durette C, Lemieux S, Thibault P, Perreault C. Global proteogenomic analysis of human MHC class I-associated peptides derived from non-canonical reading frames. *Nat Commun.* 2016;7:10238.
63. Mishto M, Liepe J. Post-Translational Peptide Splicing and T Cell Responses. *Trends Immunol.* 2017;38(12):904-915.
64. Ouspenskaia T, Law T, Clauser KR, Klaefer S, Sarkizova S, Aguet F, Li B, Christian E, Knisbacher BA, Le PM, Hartigan CR, Keshishian H, Apffel A, Oliveira G, Zhang W, Chow YT, Ji Z, Shukla SA, Bachireddy P, Getz G, Hacohen N, Keskin DB, Carr SA, Wu CJ, Regev A. Thousands of novel unannotated proteins expand the MHC I immunopeptidome in cancer. *bioRxiv.* 2020:2020.2002.2012.945840.
65. Zolg DP, Wilhelm M, Yu P, Knaute T, Zerweck J, Wenschuh H, Reimer U, Schnatbaum K, Kuster B. PROCAL: A Set of 40 Peptide Standards for Retention Time Indexing, Column Performance Monitoring, and Collision Energy Calibration. *Proteomics.* 2017;17(21).
66. Amodei D, Egertson J, MacLean BX, Johnson R, Merrihew GE, Keller A, Marsh D, Vitek O, Mallick P, MacCoss MJ. Improving Precursor Selectivity in Data-Independent Acquisition Using Overlapping Windows. *J Am Soc Mass Spectrom.* 2019;30(4):669-684.
67. Michalski A, Cox J, Mann M. More than 100,000 detectable peptide species elute in single shotgun proteomics runs but the majority is inaccessible to data-dependent LC-MS/MS. *J Proteome Res.* 2011;10(4):1785-1793.
68. Weisbrod CR, Eng JK, Hoopmann MR, Baker T, Bruce JE. Accurate peptide fragment mass analysis: multiplexed peptide identification and quantification. *J Proteome Res.* 2012;11(3):1621-1632.
69. Laumont CM, Perreault C. Exploiting non-canonical translation to identify new targets for T cell-based cancer immunotherapy. *Cell Mol Life Sci.* 2018;75(4):607-621.
70. Laumont CM, Vincent K, Hesnard L, Audemard É, Bonneil É, Laverdure JP, Gendron P, Courcelles M, Hardy MP, Côté C, Durette C, St-Pierre C, Benhammadi M, Lanoix J, Vobecky S, Haddad E, Lemieux S, Thibault P, Perreault C. Noncoding regions are the main source of targetable tumor-specific antigens. *Sci Transl Med.* 2018;10(470).
71. Alspach E, Lussier DM, Miceli AP, Kizhvato I, DuPage M, Luoma AM, Meng W, Lichti CF, Esaulova E, Vomund AN, Runci D, Ward JP, Gubin MM, Medrano RFV, Arthur CD, White JM, Sheehan KCF, Chen A, Wucherpennig KW, Jacks T, Unanue ER, Artyomov MN, Schreiber RD. MHC-II neoantigens shape tumour immunity and response to immunotherapy. *Nature.* 2019;574(7780):696-701.
72. Bonavia R, Inda MM, Cavenee WK, Furnari FB. Heterogeneity maintenance in glioblastoma: a social network. *Cancer Res.* 2011;71(12):4055-4060.
73. Gouttefangeas C, Rammensee HG. Personalized cancer vaccines: adjuvants are important, too. *Cancer Immunol Immunother.* 2018;67(12):1911-1918.
74. Weiss T, Weller M, Roth P. Immunotherapy for glioblastoma: concepts and challenges. *Curr Opin Neurol.* 2015;28(6):639-646.
75. Obeid J, Hu Y, Slingluff CL, Jr. Vaccines, Adjuvants, and Dendritic Cell Activators-Current Status and Future Challenges. *Semin Oncol.* 2015;42(4):549-561.
76. Rosenberg SA, Yang JC, Restifo NP. Cancer immunotherapy: moving beyond current vaccines. *Nat Med.* 2004;10(9):909-915.
77. Arvanitis CD, Ferraro GB, Jain RK. The blood-brain barrier and blood-tumour barrier in brain tumours and metastases. *Nat Rev Cancer.* 2020;20(1):26-41.
78. Warrington JP, Ashpole N, Csiszar A, Lee YW, Ungvari Z, Sonntag WE. Whole brain radiation-induced vascular cognitive impairment: mechanisms and implications. *J Vasc Res.* 2013;50(6):445-457.
79. Teng F, Tsien CI, Lawrence TS, Cao Y. Blood-tumor barrier opening changes in brain metastases from pre to one-month post radiation therapy. *Radiother Oncol.* 2017;125(1):89-93.
80. Demaria S, Golden EB, Formenti SC. Role of Local Radiation Therapy in Cancer Immunotherapy. *JAMA Oncol.* 2015;1(9):1325-1332.
81. Keskin DB, Anandappa AJ, Sun J, Tirosh I, Mathewson ND, Li S, Oliveira G, Giobbie-Hurder A, Felt K, Gjini E, Shukla SA, Hu Z, Li L, Le PM, Allesøe RL, Richman AR, Kowalczyk MS, Abdelrahman S, Geduldig JE, Charbonneau S, Pelton K, Iorgulescu JB, Elagina L, Zhang W, Olive O, McCluskey C, Olsen LR, Stevens J, Lane WJ, Salazar AM, Daley H, Wen PY, Chiocca EA, Harden M, Lennon NJ, Gabriel S, Getz G, Lander ES, Regev A, Ritz J, Neuberg D, Rodig SJ, Ligon KL, Suvà ML, Wucherpennig KW, Hacohen N, Fritsch EF, Livak KJ, Ott PA, Wu CJ, Reardon DA. Neoantigen vaccine generates intratumoral T cell responses in phase Ib glioblastoma trial. *Nature.* 2019;565(7738):234-239.
82. Cloughesy TF, Mochizuki AY, Orpilla JR, Hugo W, Lee AH, Davidson TB, Wang AC, Ellingson BM, Rytlewski JA, Sanders CM, Kawaguchi ES, Du L, Li G, Yong WH, Gaffey SC, Cohen AL, Mellinghoff IK, Lee EQ, Reardon DA, O'Brien BJ, Butowski NA, Nghiemphu PL, Clarke JL, Arrillaga-Romany IC, Colman H, Kaley TJ, de Groot JF, Liau LM, Wen PY, Prins RM. Neoadjuvant anti-PD-1 immunotherapy promotes a survival benefit with intratumoral and systemic immune responses in recurrent glioblastoma. *Nat Med.* 2019;25(3):477-486.

Danksagung

Der Weg bis zum Dokortitel hängt einerseits von persönlichen Ressourcen wie Zielstrebigkeit, Fleiß, Durchhaltevermögen, Wissen und experimentellem Geschick ab. Andererseits leistet auch das wissenschaftliche Netzwerk einen essentiellen Beitrag, ohne den eine Doktorarbeit schlichtweg unmöglich wäre. Daher möchte ich mich zunächst bei meinen Doktorvätern Prof. Dr. Stefan Stevanović und Prof. Dr. Hans-Georg Rammensee dafür bedanken, dass ich meine Doktorarbeit in deren Arbeitsgruppe bzw. Abteilung absolvieren konnte. Ihre Begeisterung für die Immunologie ist unglaublich inspirierend und ich danke ihnen für die herausragende wissenschaftliche Leitung. Gemeinsam mit Prof. Dr. Jürgen Frank, Gerhard Hörr, Lynne Yakes, Carmen Höner und dem Deutschen Konsortium für Translationale Krebsforschung haben sie zudem die Finanzierung meiner Stelle, von Verbrauchsmaterial, Chemikalien und Geräten zu jeder Zeit gewährleistet sowie bürokratische und organisatorische Hürden für mich beseitigt. Die künstlerische Darstellung meines Promotionsthemas auf dem Titelbild dieser Arbeit verdanke ich meinem Patenonkel Martin Schatz.

Meine berufliche Entwicklung wurde entscheidend durch Daniel Kowalewski (inzwischen Immatics Biotechnologies GmbH), meinen Supervisor während der Bachelor- und Masterarbeit, geprägt. Durch ihn habe ich einen Zugang zu der faszinierenden Technologie der Massenspektrometrie gefunden und konnte jederzeit auf sein konstruktives Feedback, substanzielle Diskussionen und kreative Ideen zählen. Ebenso gilt mein Dank dem Massenspektrometrie-Team, unseren Bioinformatikern sowie ehemaligen Doktoranden: Ana Marcu, Dr. Annika Nelde, Daniel Kowalewski, Dr. Heiko Schuster, Jens Bauer, Lena Mühlenbruch, Leon Bichmann, Dr. Léon Kuchenbecker, Dr. Linus Backert, Michael Ghosh, Dr. Moreno DiMarco sowie den Mitarbeitern des QBIC rund um Dr. Sven Nahnsen. Ohne deren Arbeit zur Etablierung von Geräten und Messmethoden, Protokollen, Skripten und Auswertemethoden, dem qPortal und zur Erstellung unserer hausinternen HLA-Peptidom-Datenbank wäre eine Bearbeitung meiner Projekte in dieser Form nicht möglich gewesen. Darüber hinaus konnte ich stets auf ihren Rat zählen und sie haben gemeinsam mit allen anderen Tübinger Immunologen zu einer wirklich angenehmen und harmonischen Arbeitsatmosphäre beigetragen.

Nicht zuletzt möchte ich allen Patienten und deren Angehörigen danken, die trotz der schwierigen Lebenssituation ein offenes Ohr für die Forschung hatten. Nur durch deren Einwilligung zu Gewebe- und Blutproben war es möglich, die Projekte im Rahmen meiner Promotion zu bearbeiten. Dies bedurfte auch der Arbeit gut funktionierender Teams aus Ärzten und Klinikpersonal, die geeignete Patienten gesucht, aufgeklärt und für eine korrekte Asservierung des Probenmaterials gesorgt haben. Besonders das Sammeln von Primär- und Rezidivtumoren der selben Patienten erforderte hierbei einen großen organisatorischen Aufwand. Für die Zusammenstellung des Glioblastom-Kollektivs möchte ich insbesondere Prof. Dr. med. Manfred Westphal (Universitätsklinikum Hamburg-Eppendorf, Klinik für Neurochirurgie), Dr. med. Malte Mohme und seinem Team (Universitätsklinikum Hamburg-Eppendorf, Klinik für Neurochirurgie), PD Dr. med. Marian Christoph Neidert (UniversitätsSpital Zürich, Klinik für Neurochirurgie), Dr. Konstantina Kapolou (UniversitätsSpital und Universität Zürich, Klinik für Neurologie, Labor für Molekulare Neuro-

Danksagung

Onkologie) und Dr. med. Julia Velz (UniversitätsSpital Zürich, Klinik für Neurochirurgie) danken. Dr. med. Sophie Shi-Yüing Wang und PD Dr. med. Marian Christoph Neidert (UniversitätsSpital Zürich, Klinik für Neurochirurgie) stellten freundlicherweise die Proben für das Meningeomprojekt zur Verfügung. Mein Dank gilt Dr. med. Julia Velz und PD Dr. med. Marian Christoph Neidert (UniversitätsSpital Zürich, Klinik für Neurochirurgie) für die Zusammenstellung der Medulloblastom-Kohorte in Zusammenarbeit mit dem Universitäts-Kinderspital und dem UniversitätsSpital Zürich, Prof. Dr. med. Manfred Westphal und Dr. med. Malte Mohme (Universitätsklinikum Hamburg-Eppendorf, Klinik für Neurochirurgie), Prof. Dr. med. Matthias Eyrich (Universitäts-Kinderklinik Würzburg) sowie Prof. Dr. med. Martina Messing-Jünger, PD Dr. med. Harald Reinhard und Dr. med. Andreas Röhrig (Asklepios Klinik Sankt Augustin). Zusätzlich bedanke ich mich bei allen bereits genannten Medizinern sowie bei Dr. med. Markus W. Löffler (Universitätsklinikum Tübingen, Klinik für Allgemeine, Viszeral- und Transplantationschirurgie sowie Abteilung für Klinische Pharmakologie; Universität Tübingen, Interfakultäres Institut für Zellbiologie, Abteilung Immunologie) und Prof. Dr. med. Sebastian P. Haen (Universitätsklinikum Tübingen, Klinik für Innere Medizin, Abteilung für Onkologie, Hämatologie, Immunologie, Rheumatologie und Pulmologie; Interfakultäres Institut für Zellbiologie, Abteilung Immunologie; Universitätsklinikum Hamburg-Eppendorf) für die Bereitstellung klinischer Daten sowie für hilfreiche Erläuterungen und Hintergrundinformationen beispielsweise zum chirurgischen Prozedere oder zu Therapiekonzepten.

Darüber hinaus danke ich Claudia Falkenburger, Beate Pömmerl und Franziska Löwenstein für die Produktion von Antikörpern, die Bereitstellung von allgemeinem Verbrauchsmaterial sowie die Organisation der Spülküche. Für die Produktion synthetischer Peptide für unsere Patienten wie auch für Experimente möchte ich mich bei unserem GMP-Team (Camille Supper, Prof. Dr. Hans-Georg Rammensee, Julia Stuck, Prof. Dr. Jürgen Frank, Marina Martin, Marion Richter, Dr. med. Markus Löffler, Dr. Monika Denk, Michael Ghosh, Mirijam Bohn, Nicole Bauer, Patricia Hrستیć, Prof. Dr. Stefan Stevanović, Ulrich Wulle) bedanken.

Letztendlich verdanke ich meinen beruflichen Erfolg aber nicht nur meinen Kollegen und Kooperationspartnern, sondern in ganz besonderer Weise auch meiner Familie und meinen engsten Freunden. Ihr habt mir in jeder Phase des Studiums und der Promotion den Rücken gestärkt, hattet immer ein offenes Ohr für die beruflichen wie persönlichen Höhen und Tiefen, habt meine Freizeit um unvergessliche Momente bereichert und mein Ziel in gewisser Weise auch zu Eurem eigenen gemacht. Ein erfülltes Privatleben mit Menschen, die man liebt, ist meiner Einschätzung nach die beste Voraussetzung, um beruflich erfolgreich zu sein. Möglicherweise würde ich jetzt nicht an diesem Punkt stehen, wenn ich Euch nicht hätte, und dafür möchte ich Euch von ganzem Herzen danken!

Appendix

Abbreviations

α -KG	α -ketoglutarate
AA	Amino acid
AAST	Anaplastic astrocytoma
AcN	Acetonitrile
ACTL8 / CT57	Actin-like protein 8
ADCC	Antibody-dependent cellular cytotoxicity
AIM2	Absent in melanoma 2
ALECSAT	Autologous Lymphoid Effector Cells Specific Against Tumour Cells
AMPA	α -amino-3-hydroxy-5-methyl-4-isoxazolepropionic acid
ANR40	Ankyrin repeat domain-containing protein 40
APC	Antigen-presenting cell
ARF / p14 ^{ARF}	Alternative open reading frame
ARG1	Arginase-1
ARID1A/2	AT-rich interactive domain-containing protein 1A/2
ASPM	Abnormal spindle-like microcephaly-associated protein
ATAT	Alphatubulin N-acetyltransferase 1
ATG9B	Autophagy-related protein 9
ATRT	Atypical teratoid rhabdoid tumor
AUC	Area under the curve
β_2 m	β_2 microglobulin
B7-H3 / CD276	B7 homolog 3 protein
BAP1	BRCA-associated protein-1
B-FABP	Brain-type fatty acid-binding protein
BH	Benjamini-Hochberg
BIRC5	Baculoviral IAP repeat-containing protein 5 / survivin
BiTe	Bi-specific antibody for T-cell redirection and activation
BRCA2	Breast cancer type 2 susceptibility protein
BRPF1	Peregrin
BSG	Brain stem glioma
BTLA	B- and T-cell lymphocyte attenuator
CAR	Chimeric antigen receptor
CD	Cluster of differentiation
CD19t	Truncated CD19
CDK2/4/6	Cyclin-dependent kinase 4 / 6
CDKN2A / p16 ^{INK4a}	Cyclin-dependent kinase inhibitor 2A
CDKN2B / p15 ^{INK4b}	Cyclin-dependent kinase 4 inhibitor 2B
CerS1	Ceramide synthase 1
CGE	Cobalt gray equivalent
CHAPS	[(3-cholamidopropyl) dimethyl-ammonio]-1-propanesulfonate
CI	Confidence interval
CID	Collision-induced dissociation
CLIP	Class II-associated invariant chain peptide
CLUS	Clusterin
c-Met	Met proto-oncogene / hepatocyte growth factor receptor
CNBr	Cyanogen bromide
CNS	Central nervous system
COSMIC	Catalogue Of Somatic Mutations In Cancer
CpG ODN	Deoxycytidyl-deoxyguanosin oligodeoxynucleotide
CR	Complete response
CREBBP	CREB-binding protein
CRUM1	Protein crumbs homolog 1
CSF	Cerebrospinal fluid
CSF1	Colony stimulating factor 1
CSI	Craniospinal irradiation
CSPG4	Chondroitin sulfate proteoglycan 4
CSPG7	Chondroitin sulfate proteoglycan 7 / brevican core protein
CSRP2	Cysteine and glycine-rich protein 2
CTA	Cancer-testis antigen

Appendix: Abbreviations

CTCF / CT27	Transcriptional repressor CTCFL
CTL	Cytotoxic T lymphocyte
CTLA4	Cytotoxic T-lymphocyte-associated antigen 4
CTNNB1	Catenin beta-1
D2HG	D-2-hydroxyglutarate
DC	Dendritic cell
DCLK2	Serine/threonine-protein kinase DCLK2
DDA	Date-dependent acquisition
DDX3X	X-chromosomal ATP-dependent RNA helicase DEAD box protein 3
DJC25	DnaJ homolog subfamily C member 25
DMSO	Dimethyl sulfoxide
DOCK7	Dedicator of cytokinesis protein 7
DP2.5 / APC	Deleted in polyposis 2.5 / adenomatous polyposis coli protein
DPBS	Dulbecco's phosphate-buffered saline
DRP-4	Dihydropyrimidinase-related protein 4
DTH	Delayed-type hypersensitivity
EAA4	Excitatory amino acid transporter 4
EBV	Epstein-Barr Virus
EFHC1	EF-hand domain-containing protein 1
EGFR	Epidermal growth factor receptor
EGFRt	Truncated EGFR
EGFRvIII	Epidermal growth factor receptor variant III
eIF4E	Eukaryotic translation initiation factor 4E
ELISpot	Enzyme-linked immunospot assay
ELOV2	Elongation of very long chain fatty acids protein 2
EMT	Epithelial-to-mesenchymal transition
EphA2	Ephrin type-A receptor 2
ER	Endoplasmic reticulum
ERAAP	ER aminopeptidase associated with antigen processing
EVS	Empirical variant scoring
F120C	Constitutive coactivator of PPAR-gamma-like protein 2
FA	Formic acid
FADS2	Acyl-CoA 6-desaturase
Fas	Fas cell surface death receptor
FasL	Fas ligand
FBXW7	F-box/WD repeat-containing protein 7
fc	Fold change
FDA	U.S. Food and Drug Administration
FDR	False discovery rate
FLT3	FMS-like tyrosine kinase 3
FPRP	Prostaglandin F2 receptor negative regulator
FTMS	Fourier Transform Mass Spectrometry (refers to Orbitrap detection)
GABA	Gamma-aminobutyric acid
GAGE-1 / CT4.1	G antigen 1
GAPVAC	The Glioma Actively Personalized VAccine Consortium
Gb	Giga base
GBM	Glioblastoma
G-CIMP	Glioma CpG island methylator phenotype
GITR	Glucocorticoid-induced tumor necrosis factor receptor
GluK3	Ionotropic glutamate receptor kainate 3
GluR4	Glutamate receptor 4
GM-CSF	Granulocyte-macrophage colony-stimulating factor
GMP	Good manufacturing practice
GO	Gene Ontology
gp100	Melanocytes lineage-specific antigen gp100
GPC1/2	Glypican-1/2
GPM6B	Neuronal membrane glycoprotein M6-b
GSE1	Genetic suppressor element 1
GTEx	Genotype-Tissue Expression database
HCD	Higher-energy induced dissociation
HCMV	Human cytomegalovirus
HEAT1	HEAT repeat-containing protein 1

Appendix: Abbreviations

HEPACAM	Hepatocyte cell adhesion molecule
HER2	Receptor tyrosine-protein kinase erbB-2
HFE	Human hemochromatosis protein
HHV	Human herpesvirus
HLA	Human leukocyte antigen
HLA-IP	HLA-immunoprecipitation
HO-1	Heme oxygenase-1
HPLC	High-performance liquid chromatography
HS2ST	Heparan sulfate 2-O-sulfotransferase 1
HyTK	Hygromycin phosphotransferase-herpes simplex virus 1 thymidine kinase
i.d.	Intradermal
i.n.	Intranodal
i.t.	Intratumoral
i.v.	Intravenous
IDH1/2	Isocitrate dehydrogenase 1/2
IDH ^{mut}	Mutated IDH1/2 genes
IDH ^{WT}	Non-mutated / wild-type IDH1/2 genes
IDO1	Indoleamine 2,3-dioxygenase-1
IEDB	Immune Epitope Database
IF2BP3	Insulin-like growth factor 2 mRNA binding protein 3
IFN	Interferon
IFN- α	Interferon alpha / Type I interferon
li	Invariant chain
IL13R α 2	IL-13 receptor alpha 2
IL-2/10/12/15/21	Interleukin 2/10/12/15/21
ILT	Inhibitory Ig-like transcript
ImmTAC	Immune-mobilizing monoclonal T-cell receptors against cancer
Indel	Insertion or deletion
iRT	Indexed retention time
ITA7	Integrin alpha-7
JAK2	Janus kinase 2
JY	B-lymphoblastoid cell line
KANSL1	KAT8 regulatory NSL complex subunit 1
KBTBD4	Kelch repeat and BTB domain-containing protein 4
KCJ10	ATP-sensitive inward rectifier potassium channel 10
KDM6A	Lysine-specific demethylase 6A
KLF4	Kruppel-like factor 4
KMT2C/D	Histone-lysine N-methyltransferase 2C/2D
LAG-3	Lymphocyte activation gene-3
LC-MS/MS	(Reversed-phase) Liquid chromatography coupled with tandem mass spectrometry
LFQ	Label-free quantitation
LMP	Low molecular weight protein
LTQ	Linear trap quadrupole
LZTS1	Leucine zipper putative tumor suppressor 1
m/z	Mass-to-charge ratio
MAGE-A1 / CT1.1	Melanoma-associated antigen 1
MAGE-A3 / CT1.3	Melanoma-associated antigen 3
MAGE-A4 / CT1.4	Melanoma-associated antigen 4
MAGE-A6 / CT1.6	Melanoma-associated antigen 6
MAGE-C1 / CT7.1	Melanoma-associated antigen C1
MAGE-C2 / CT10	Melanoma-associated antigen C2
MAGE-F1	Melanoma-associated antigen F1
MAGI2	Membrane-associated guanylate kinase inverted 2
MAPK	Mitogen-activated protein kinase
MB	Medulloblastoma
MDM2	Mouse double minute 2 homolog
MDSC	Myeloid-derived suppressor cells
MGMT	O ⁶ -methylguanine-DNA methyltransferase
MHC	Major histocompatibility complex
MIC	MHC class I polypeptide-related sequence protein
MIC25	MICOS complex subunit MIC25
MiIC	Multivesicular late endosomal-lysosomal MHC class II antigen-processing compartment

Appendix: Abbreviations

MLH1	MutL homolog 1
MMR	Mismatch repair
MNG	Meningioma
MS	Mass spectrometry
MS/MS	Tandem mass spectrometry
MSH2/6	MutS homolog 2/6
MTSS2	Protein MTSS 2
n.a.	Not available
n.d.	Not determined
NF1/2	Neurofibromin-1/-2
NF- κ B	Nuclear factor kappa-light-chain-enhancer of activated B cells
NIC	Nanoscale immunoconjugate
NK cell	Natural killer cell
NLGNX/Y	X-/Y-linked neuroligin-4
NMRL1	NmrA-like family domain-containing protein 1
NRCAM	Neuronal cell adhesion molecule
NY-ESO-1 / CT6.1	New York esophageal squamous cell carcinoma-1
OIP5 / CT86	Opa-interacting protein 5 / protein Mis18-beta
OLIG2	Oligodendrocyte transcription factor 2
OR	Odds ratio
ORML1	ORM1-like protein 1
OS	Overall survival
P4HTM	Transmembrane prolyl 4hydroxylase
PAI1	Plasminogen activator inhibitor 1
PALB2	Partner and localizer of BRCA2
PAX6	Paired box protein Pax6
PBMCs	Peripheral blood mononuclear cell
PBS	Phosphate-buffered saline
PCDGM	Protocadherin gamma-C5
PCX3	Pecanex-like protein 3
PD	Progressive disease
PD-1	Programmed cell death protein 1
PDGFR / PDGFR α	Platelet-derived growth factor receptor / alpha
PD-L1 / PD-L2	Programmed cell death ligand 1 / 2
PEG	Polyethylene glycol
PFS	Progression-free survival
pfu	Plaque-forming units
PI3K	Phosphatidylinositol-3-OH kinase
PJA2	E3 ubiquitin-protein ligase Praja-2
PKHA4	Pleckstrin homology domain-containing family A member 4
PLC	Peptide-loading complex
PMS2	Postmeiotic segregation increased 2
PNET	Primitive neuroectodermal tumor
POLR2A	RNA polymerase II subunit A
Poly-ICLC	Polyinosinic-polycytidylic acid stabilized by polylysine and carboxymethylcellulose
PR	Partial response
PRAME	Melanoma antigen preferentially expressed in tumors
PRiME	PEP-CMV in Recurrent Medulloblastoma/Malignant Glioma
PROCAL	ProteomeTools Calibration Standard
PSM	Peptide spectrum match
PTCH1	Protein patched homolog 1
PTEN	Phosphatase and tensin homolog
PTM	Post-translational modification
PTPRZ	Receptor-type tyrosine-protein phosphatase zeta
RAD54B	DNA repair and recombination protein RAD54B
RasGAP	Ras GTPase activating protein
RFTN2	Raftlin-2
RIN1	Ras and Rab interactor 1
RL7A	60S ribosomal protein L7a
RPKM	Reads per kilobase per million mapped reads
rpm	Revolutions per minute
RR	Radiological response

Appendix: Abbreviations

RT	Retention time
S	Svedberg unit
s.c.	Subcutaneous
S/N	Signal-to-noise ratio
SD	Stable disease
SE6L1	Seizure 6-like protein
SH2	Src homology 2
SHH	Sonic Hedgehog
SIA8E	Alpha-2,8-sialyltransferase 8E
Siglec-15	Sialic acid-binding immunoglobulin-like lectin 15
siRNA	Small interfering RNA
SMARCA4	ATP-dependent helicase SMARCA4
SMARCB1 / SMARCE1	SWI/SNF-related matrix-associated actin-dependent regulator of chromatin subfamily B / E member 1
SMC4	Structural maintenance of chromosomes protein 4
SMO	Smoothed homolog
SNV	Single nucleotide variant
SO6A1 / CT48	Solute carrier organic anion transporter family member 6A1
SPA17 / CT22	Sperm autoangiogenic protein 17
SUFU	Suppressor of fused homolog
SV40	Simian virus 40
SYCP1 / CT8	Synaptonemal complex protein 1
T255A	Transmembrane protein 255A
TAA	Tumor-associated antigen
TACC3	Transforming acidic coiled-coil-containing protein 3
TAP	Transporter associated with antigen processing
TCF4	Transcription factor 4
TCR	T-cell receptor
TERT	Telomerase reverse transcriptase
TET2	Tet methylcytosine dioxygenase 2
TFA	Trifluoroacetic acid
TGFB2	Transforming growth factor beta-2 proprotein
TGF- β	Transforming growth factor β
Th cell	CD4 ⁺ T helper cell
Th1 / Th2	Type 1 / Type 2 CD4 ⁺ T helper cell
TIGIT	T-cell immunoglobulin and ITIM domain
TILs	Tumor-infiltrating lymphocytes
TIM-3	T-cell immunoglobulin and mucin-domain containing-3
TLR1/2/3/7/8/9	Toll-like receptor 1/2/3/7/8/9
TM231	Transmembrane protein 231
TME	Tumor microenvironment
TMZ	Temozolomide
TN-C	Tenascin C
TNF / TNF- α	Tumor necrosis factor / alpha
TP53	Tumor suppressor p53
TRAF7	TNF receptor-associated factor 7
TRAIL	Tumor necrosis factor-related apoptosis inducing ligand
TRAILR	TRAIL receptor
Treg	CD4 ⁺ CD25 ⁺ regulatory T cell
TRP2	Tyrosinase-related protein 2
TSA	Tumor-specific antigen
TTF	Tumor treating fields
TTP	Time to progression
TTRNA	Total tumor RNA
T-Vec	Talimogene laherparepvec
UBP11	Ubiquitin carboxyl-terminal hydrolase 11
US	United States
UTR	Untranslated region
VAF	Variant allele frequency
VEGF	Vascular endothelial growth factor
VEGFR	Vascular endothelial growth factor receptor
VISTA	V-domain immunoglobulin suppressor of T-cell activation
VP13B	Vacuolar protein sorting-associated protein 13B

Appendix: Abbreviations

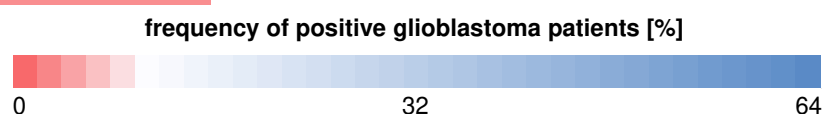
WHO	World Health Organization
Wnt	Wingless and Int-1
WT	Wild-type
WT1	Wilms' tumor gene 1
XAGE3 / CT12.3	X antigen family member 3
xALT	<i>Ex vivo</i> expanded Autologous Lymphocyte Transfer
ZIC1	Zinc finger protein ZIC 1
ZMYM3	Zinc finger MYM-type protein 3
ZNF3	Zinc finger protein 3

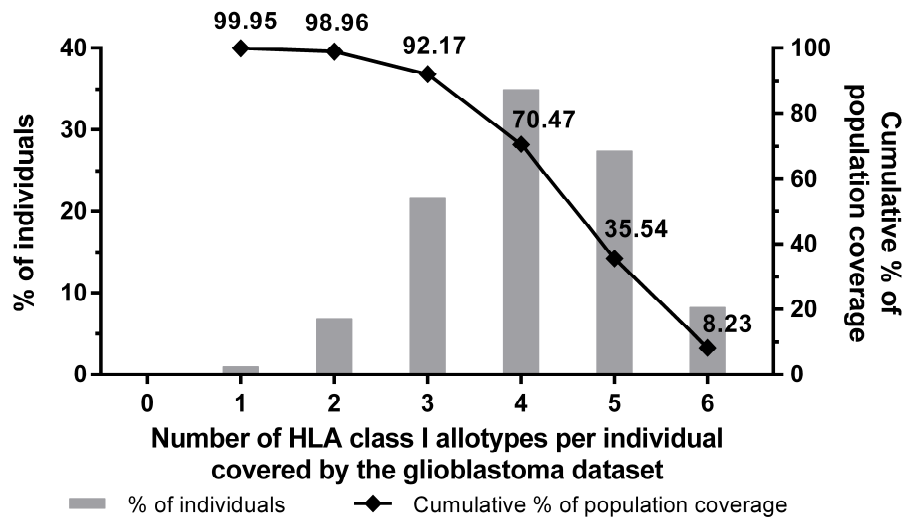
Supplementary Figures and Tables

Supplement of CHAPTER 2

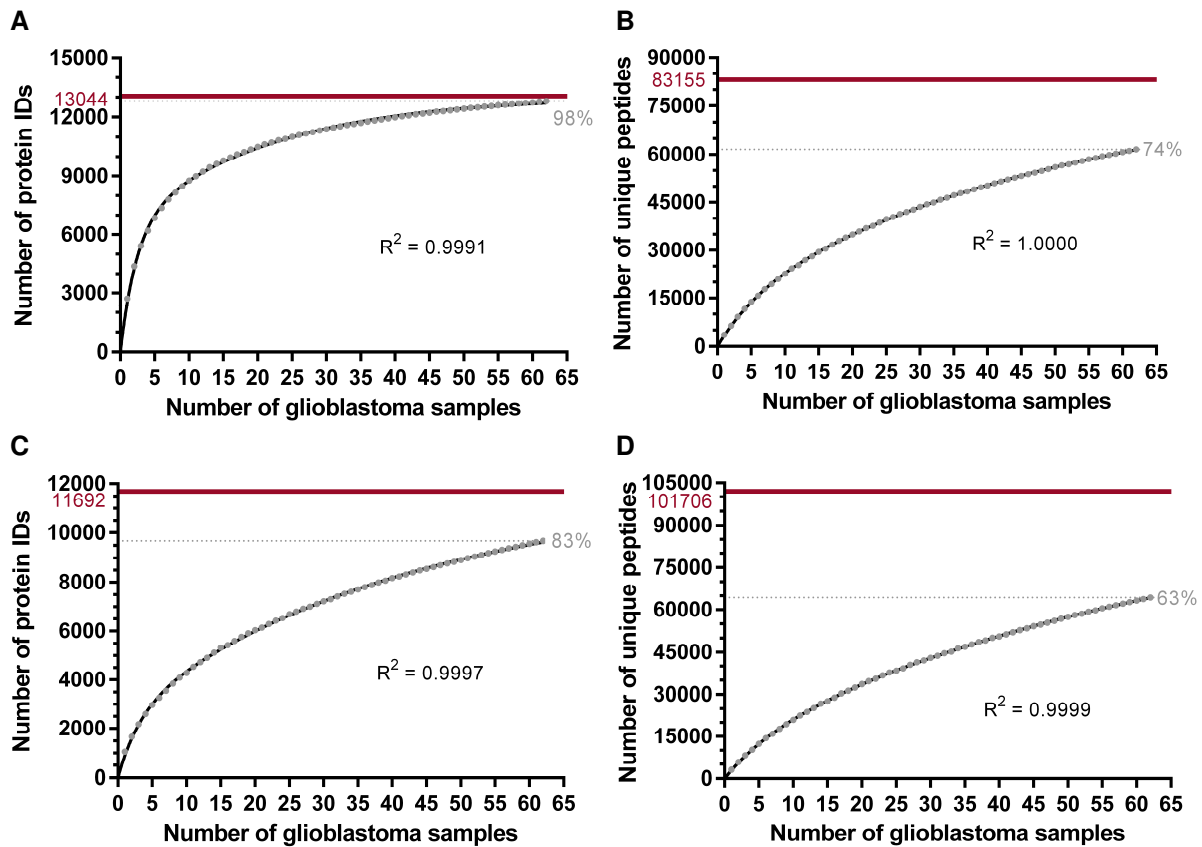
Supplementary Table 1. HLA class I allotype and allele frequencies in the glioblastoma collective comprising n=40 patients. The top three ranking HLA-A, -B, and -C allotypes within the study cohort are marked in bold.

HLA allotype	Positive patients	Allele frequency	HLA allotype	Positive patients	Allele frequency
A*01:01	25%	14%	B*41:01	3%	1%
A*02:01	63%	40%	B*44:02	28%	14%
A*02:05	8%	4%	B*44:03	13%	6%
A*03:01	28%	15%	B*44:05	3%	1%
A*11:01	13%	6%	B*47:01	3%	1%
A*23:01	3%	1%	B*49:01	3%	1%
A*24:02	13%	8%	B*51:01	15%	8%
A*29:02	5%	3%	B*51:26	3%	1%
A*31:01	8%	4%	B*55:01	3%	1%
A*32:01	3%	1%	B*56:01	3%	1%
A*33:01	5%	3%	B*57:01	10%	5%
A*33:05	3%	1%	B*58:01	3%	1%
A*68:01	3%	1%	C*01:02	20%	10%
B*07:02	33%	19%	C*02:02	10%	5%
B*08:01	15%	8%	C*03:03	5%	3%
B*13:02	8%	4%	C*03:04	5%	3%
B*14:02	8%	4%	C*04:01	18%	9%
B*15:01	8%	4%	C*05:01	18%	9%
B*15:03	3%	1%	C*06:02	20%	10%
B*15:17	3%	1%	C*07:01	30%	15%
B*18:01	5%	3%	C*07:02	30%	18%
B*27:05	8%	4%	C*07:04	10%	5%
B*35:01	5%	3%	C*08:02	8%	4%
B*35:02	3%	1%	C*12:03	10%	5%
B*35:03	8%	4%	C*15:02	5%	3%
B*39:10	3%	1%	C*15:06	3%	1%
B*40:01	3%	1%	C*16:01	5%	3%
B*40:02	3%	1%			





Supplementary Figure 1. HLA class I allotype population coverage. Using the population coverage tool provided by the IEDB Analysis Resource, the world population coverage of the 55 distinct HLA-A, -B, and -C allotypes was calculated. The percentage of individuals positive for a specific number of HLA class I allotypes (max. of 6) is indicated by bar charts (associated with the left y-axis). The line diagram (associated with the right y-axis) shows the cumulative percentage of population coverage. The HLA class I allotypes of the glioblastoma cohort cover 99.95% of the world population (first diamond on line diagram counted from the left) meaning that only 0.05% of all individuals are negative for all HLA-A, -B, and -C allotypes included in the present study (first bar counted from the left). 92.17% of all individuals are positive for at least three HLA class I allotypes (third diamond on line diagram counted from the left).



Supplementary Figure 2. Saturation analysis for the identification of HLA-presented antigens and peptides in glioblastoma tissue. For each source count, the mean number of (A) HLA class I-presented antigens, (B) HLA class I ligands, (C) HLA class II-presented antigens, and (D) HLA class II-restricted peptides was calculated by 1,000 random samplings. Using non-linear regression,

exponential functions with a forced y-intercept of 0 (internal data created by Daniel Kowalewski at the Department of Immunology, University of Tübingen indicate that subjecting cell-free lysis buffer to HLA-IP does not result in peptide identifications) were fitted. For all models, the goodness of fit was in the uppermost range ($R^2 = 0.9991$, $R^2 = 1.0000$, $R^2 = 0.9997$ and $R^2 = 0.9999$). Based on these curves, the maximum attainable number of distinct source proteins and peptides was estimated (highlighted as solid lines). With the available number of 62 glioblastoma samples, 98% or 83% of the estimated maximum attainable amount of distinct HLA class I- and II-presented proteins as well as 74% or 63% of the estimated maximum attainable amount of distinct HLA class I- or II-restricted peptides had been identified, respectively.

Supplementary Table 2. Glioblastoma-associated HLA class I- and II-presented antigens identified on both primary and recurrent tumors of at least five different patients. GTEx profiles were assessed from all available datasets excepting EBV-transformed lymphocytes and cultured fibroblasts. Glioblastoma-exclusive antigens with a brain-specific expression profile > 10 TPM were not reported (HLA class I: n=29; HLA class II: n=6) as candidate targets. Color codes were defined as follows: ■ < 10 TPM in any tissue, ◆ > 10 TPM in testes and < 10 TPM in other tissues (CTA-like expression profile), ■ 10-20 TPM in any tissue, ■ 20-30 TPM in any tissue, ■ > 30 TPM in any tissue. The number of positive tumors other than glioblastoma was based on n=824 HLA class I and n=585 HLA class II peptidome datasets. HLA restrictions not passing manual assessment as quality control as well as one highly repetitive sequence annotated to IGFBP2 are indicated in italic. These peptides were excluded from downstream analyses such as calculation of peptides matching per patient worldwide. HLA class II-presented proteins neither identified with peptides exceeding a length of twelve AA nor with different sequences across patients were not considered for this listing of candidate target antigens. NOP16, ESCO1, MFHAS1, TRIM58, CDC26, ONECUT1, AFTPH, and RBFA were detected with only one HLA class II peptide sequence across all patients. Frequencies of positive tumors are given separately for n=38 primary (P) and n=24 recurrent (R) glioblastomas.

Antigen	Frequency of positive tumors	Peptide sequence	HLA restriction	UniProt accession GTEx profile	Positive non-GBM tumors
Glioblastoma-associated HLA class I antigens					
Protein TANC2 (TANC2) 1 peptide multi-maps to non-GBM-exclusive TANC1 (Q9C0D5)	50% P / 38% R GBM3P	ALMDKEGLTAL DEHIFQAI	A*02:01 B*18:01	Q9HCD6 ■	62
	GBM4P	APYRPPDISL	B*07:02		
	GBM4R	APYRPPDISL	B*07:02		
	GBM5P	GIIATLTSY YAGESSKEL YSENVERTKY	B*15:01 C*03:03 A*01:01		
	GBM5R	GIIATLTSY	B*15:01		
	GBM6P	AIISRLVAL LVPEFVHNV MKFPTQSSF	A*02:05 A*02:05 B*15:03		
	GBM7P	APYRPPDISL	B*07:02		
	GBM8P	TTESVFVGR	A*68:01		
	GBM9P	AIISRLVAL DLQAYILHR	B*08:01 A*33:05		
	GBM10R	ALMDKEGLTAL APYRPPDISL RPSQGLPVI	A*02:01 B*07:02 B*07:02		
	GBM11P	ALMDKEGLTAL LVPEFVHNV	A*02:01 A*02:01; A*02:05		
	GBM12R	GIIATLTSY	B*15:01		
	GBM13P	AIISRLVAL	A*02:01; B*08:01		
	GBM16P	AIISRLVAL APYRPPDISL RPSQGLPVI	B*08:01 B*07:02 B*07:02		
	GBM16R	AIISRLVAL APYRPPDISL	B*08:01 B*07:02		
	GBM17R	NEAEFHKPDY SESGLTPLGY	B*44:03 B*44:03		
	GBM18R	AIISRLVAL APYRPPDISL	B*08:01 B*07:02		
	GBM22P	SEIQNNISL	B*40:01		
	GBM22R	SEIQNNISL	B*40:01		
	ZH613	LVPEFVHNV	A*02:05		

Appendix: Supplement of CHAPTER 2

	ZH617	AIISRLVAL	A*02:01; B*08:01	
		YSENVERTKY	A*01:01	
	ZH631	GQQQGVFKK	A*11:01	
		KMIGKFPSW	A*32:01	
	ZH654	RTLPLVAQAY	B*57:01	
		YSENVERTKY	A*01:01	
	ZH678	GQQQGVFKK	A*11:01	
		NEAEFHKPDY	B*44:03	
	ZH681	ALMDKEGLTAL	A*02:01	
		RTLPLVAQAY	B*57:01	
	ZH753	AIISRLVAL	A*02:01; B*08:01	
	ZH761	NEAEFHKPDY	B*44:02	
	ZH802	DLQAYILHR	A*33:01	
Fatty acid 2-hydroxylase (FA2H)	<u>32% P / 63% R</u>			Q7L5A8 ■ 13
	GBM2P	APAPPPAASF	B*07:02	
	GBM2R	APAPPPAASF	B*07:02	
		RLFTSFTTEY	B*15:01	
	GBM4P	APAPPPAASF	B*07:02	
	GBM4R	APAPPPAASF	B*07:02	
		APFDGSRLVF	B*07:02	
	GBM5P	HMKPPSDSY	B*15:01	
	GBM5R	HMKPPSDSY	B*15:01	
		RLFTSFTTEY	B*15:01	
	GBM6R	APAPPPAASF	B*35:01	
		APFDGSRLVF	B*35:01	
		FAQGNVRLF	C*12:03	
		LPEAVGGTVF	B*35:01	
	GBM7P	APAPPPAASF	B*07:02	
		FAQGNVRLF	C*02:02	
	GBM7R	APAPPPAASF	B*07:02	
	GBM10R	APAPPPAASF	B*07:02	
		APFDGSRLVF	B*07:02	
	GBM11R	APAPPPAASF	B*07:02	
	GBM12R	APAPPPAASF	B*35:01	
		APFDGSRLVF	B*35:01	
		HMKPPSDSY	B*15:01	
		LPEAVGGTVF	B*35:01	
		SPHKGSYLY	B*35:01	
	GBM16P	APAPPPAASF	B*07:02	
	GBM16R	APAPPPAASF	B*07:02	
		APFDGSRLVF	B*07:02	
	GBM17R	RTFAQGNVRLF	B*57:01	
	GBM18R	APAPPPAASF	B*07:02	
	GBM22R	FAQGNVRLF	C*12:03	
	GBM23R	LPEAVGGTVF	B*35:02; C*04:01	
	ZH613	RTFAQGNVR	A*31:01	
	ZH654	RTFAQGNVR	A*31:01	
		RTFAQGNVRLF	B*57:01	
	ZH681	APAPPPAASF	B*07:02	
		RTFAQGNVRLF	B*57:01	
	ZH753	FAHQKSGF	B*08:01; C*15:02	
	ZH757	APAPPPAASF	B*07:02	
	ZH761	FAQGNVRLF	C*16:01	
	ZH784	APAPPPAASF	B*07:02	
	ZH791	APAPPPAASF	B*07:02	
	ZH802	RTFAQGNVR	A*31:01	
Bestrophin-1 (BEST1)	<u>24% P / 54% R</u>			O76090 ■ 5
	GBM2P	SPTNIHTTL	B*07:02	
	GBM2R	SPTNIHTTL	B*07:02	
		TQVVTVAVY	B*15:01	
	GBM4P	SPTNIHTTL	B*07:02	
	GBM4R	SPTNIHTTL	B*07:02	
	GBM5R	TQVVTVAVY	B*15:01	
	GBM7P	SPTNIHTTL	B*07:02	
	GBM7R	SPTNIHTTL	B*07:02	
	GBM9R	DAHAGIIGR	A*33:05	
	GBM10P	SPTNIHTTL	B*07:02	
	GBM10R	SPTNIHTTL	B*07:02	
	GBM11R	SPTNIHTTL	B*07:02	
	GBM14R	DAHAGIIGR	A*33:01	
	GBM16P	SPTNIHTTL	B*07:02	
	GBM16R	SPTNIHTTL	B*07:02	
	GBM18R	SPTNIHTTL	B*07:02	
	GBM22R	SPTNIHTTL	B*35:03	
	ZH616	SPTNIHTTL	B*07:02	
	ZH681	SPTNIHTTL	B*07:02	

Appendix: Supplement of CHAPTER 2

	ZH753	ALMEHPEVSQV	A*02:01	
	ZH757	ALMEHPEVSQV	A*02:01	
		SPTNIHTTL	B*07:02	
	ZH784	SPTNIHTTL	B*07:02	
	ZH802	DAHAGIIGR	A*33:01	
		RYANLGNVLILR	A*31:01	
Oligodendrocyte transcription factor 3 (OLIG3)	<u>34% P / 33% R</u>			Q7RTU3 ■ 3
Peptides multi-map to GBM-exclusive OLIG2 (Q13516) with brain-associated expression	GBM2R	MPYAHGPSV	B*07:02	
	GBM4P	MPYAHGPSV	B*07:02	
	GBM4R	MPYAHGPSV	B*07:02	
	GBM6R	MPYAHGPSV	B*35:01	
	GBM7P	MPYAHGPSV	B*07:02;	
			B*56:01	
	GBM7R	MPYAHGPSV	B*07:02;	
			B*56:01	
	GBM8P	EVMPYAHGPSVR	A*68:01	
	GBM10R	MPYAHGPSV	B*07:02	
	GBM16P	MPYAHGPSV	B*07:02	
	GBM16R	MPYAHGPSV	B*07:02	
	GBM18R	MPYAHGPSV	B*07:02	
	ZH613	MPYAHGPSV	B*51:01	
	ZH631	MPYAHGPSV	B*51:01	
	ZH645	MPYAHGPSV	B*51:01	
	ZH654	MPYAHGPSV	B*51:01	
	ZH678	MPYAHGPSV	B*51:01	
	ZH681	MPYAHGPSV	B*07:02	
	ZH753	MPYAHGPSV	B*51:01	
	ZH757	MPYAHGPSV	B*07:02	
	ZH761	LARNYLML	C*16:01	
		MPYAHGPSV	B*51:26	
	ZH829	MPYAHGPSV	B*55:01	
Transcription factor SOX-2/21 (SOX2/21)	<u>34%/26% P</u>			P48431 ■ 5
4 peptides multi-map to GBM-exclusive SOX1 (O00570) and to non-GBM-exclusive SOX14 (O95416)	<u>29%/21% R</u>			Q9Y651 ■ 3
	GBM14R	DEAKRLRAL (SOX1/2)	B*14:02	
	GBM14R	KMAQENPKM (SOX1/2/14/21)	A*02:01	
	GBM20R	SEISKRLGAEW (SOX1/2/14/21)	B*44:02	
	ZH654	ISKRLGAEW (SOX1/2/14/21)	B*57:01	
	ZH681	ISKRLGAEW (SOX1/2/14/21)	B*57:01	
		KMAQENPKM (SOX1/2/14/21)	A*02:01	
	GBM4P	YPQHPLNA (SOX2)	B*07:02	
	GBM4R	YPQHPLNA (SOX2)	B*07:02	
	GBM5P	AQMMPMHRY (SOX2)	B*15:01	
	GBM6P	AQMMPMHRY (SOX2)	B*15:03	
	GBM6R	AQMMPMHRY (SOX2)	B*15:03	
	GBM7P	HPGLNAHGA (SOX2)	B*56:01	
		QPMHRYDVSA (SOX2)	B*07:02;	
			B*56:01	
		YPQHPLNA (SOX2)	B*07:02;	
			B*56:01	
	GBM7R	QPMHRYDVSA (SOX2)	B*07:02;	
			B*56:01	
		YPQHPLNA (SOX2)	B*07:02;	
			B*56:01	
	ZH616	YPQHPLNA (SOX2)	B*07:02	
	ZH681	YPQHPLNA (SOX2)	B*07:02	
	ZH757	YPQHPLNA (SOX2)	B*07:02	
	ZH829	YPQHPLNA (SOX2)	B*55:01	
Uncharacterized protein C2orf72 (C2orf72)	<u>29% P / 29% R</u>			A6NCS6 ■ 8
	GBM2R	RPAEPPFQAL	B*07:02	
	GBM4P	IRSPLVFVL	C*07:02	
		RPAEPPFQAL	B*07:02	
	GBM4R	IRSPLVFVL	C*07:02	
		RPAEPPFQAL	B*07:02	
	GBM7P	RPAEPPFQAL	B*07:02	
	GBM7R	RPAEPPFQAL	B*07:02	
	GBM10R	RPAEPPFQAL	B*07:02	
	GBM11P	RPAEPPFQAL	B*07:02	
	GBM13P	IRSPLVFVL	C*06:02;	
			C*07:01	
	GBM16P	IRSPLVFVL	C*07:01;	
			C*07:02	
		RPAEPPFQAL	B*07:02	
	GBM16R	IRSPLVFVL	C*07:01;	
			C*07:02	
		RPAEPPFQAL	B*07:02	
	GBM18P	RPAEPPFQAL	B*07:02	
	GBM18R	IRSPLVFVL	C*07:01;	
			C*07:02	
		RPAEPPFQAL	B*07:02	
	ZH616	RPAEPPFQAL	B*07:02	

Appendix: Supplement of CHAPTER 2

	ZH654	IRSPLVFVL	C*06:02		
	ZH681	RPAEPPFQAL	B*07:02		
	ZH720	RPAEPPFQAL	B*39:10		
	ZH757	RPAEPPFQAL	B*07:02		
	ZH784	RPAEPPFQAL	B*07:02		
Transmembrane protein 255A (TMEM255A)	<u>34% P / 17% R</u>			Q5JRV8	6
	GBM3P	YAHPQVASY	C*02:02		
	GBM4P	YYPGVILGF	C*07:02		
	GBM6P	ATILNIVGL	A*02:05;		
			C*12:03		
		YAHPQVASY	C*12:03		
	GBM7P	YAHPQVASY	C*02:02		
	GBM9P	DLKPLYANR	A*33:05		
	GBM14R	DLKPLYANR	A*33:01		
	GBM16P	YYPGVILGF	C*07:02		
	GBM16R	YYPGVILGF	C*07:02		
	GBM19P	YYPGVILGF	A*24:02		
	GBM22P	YYPGVILGF	A*24:02		
	GBM22R	YYPGVILGF	A*24:02		
	GBM23P	YYPGVILGF	A*23:01		
	GBM23R	YYPGVILGF	A*23:01		
	ZH613	ATILNIVGL	A*02:05;		
			C*07:01		
	ZH750	YYPGVILGF	A*24:02		
	ZH802	DLKPLYANR	A*33:01		
	ZH810	YYPGVILGF	A*24:02		
G patch domain-containing protein 11 (GPATCH11)	<u>34% P / 17% R</u>			Q8N954	15
	GBM3P	YMSDSFINV	A*02:01		
	GBM6P	YMSDSFINV	A*02:05		
	GBM10R	YMSDSFINV	A*02:01		
	GBM11P	YMSDSFINV	A*02:01;		
			A*02:05		
	GBM11R	YMSDSFINV	A*02:01;		
			A*02:05		
	GBM13P	YMSDSFINV	A*02:01		
	GBM13R	YMSDSFINV	A*02:01		
	GBM14R	YMSDSFINV	A*02:01		
	GBM15P	AEEKAAEQF	B*44:02;		
			B*44:03		
	GBM16P	NLKNRQKSL	B*08:01		
	GBM23P	RDIGLKNAL	B*47:01		
	ZH617	YMSDSFINV	A*02:01		
	ZH645	YMSDSFINV	A*02:01		
	ZH681	YMSDSFINV	A*02:01		
	ZH757	YMSDSFINV	A*02:01		
	ZH829	AEEKAAEQF	B*44:05		
Collagen alpha-2(IX) chain (COL9A2)	<u>24% P / 25% R</u>			Q14055	17
	GBM4P	SPRSLLVLLQ	B*07:02		
	GBM4R	SPRSLLVLLQ	B*07:02		
	GBM7P	SPRSLLVLLQ	B*07:02		
	GBM8P	SPRSLLVLLQ	B*07:02		
	GBM10R	SPRSLLVLLQ	B*07:02		
	GBM16P	SPRSLLVLLQ	B*07:02		
	GBM16R	SPRSLLVLLQ	B*07:02		
	GBM18R	SPRSLLVLLQ	B*07:02		
	ZH613	TASPRSLLV	B*51:01		
	ZH654	TASPRSLLV	B*51:01;		
			C*15:06		
	ZH678	TASPRSLLV	C*15:02		
	ZH681	SPRSLLVLLQ	B*07:02		
	ZH753	TASPRSLLV	C*15:02		
	ZH757	KMLQEQLAEV	A*02:01		
		SPRSLLVLLQ	B*07:02		
	ZH784	SPRSLLVLLQ	B*07:02		
NADH dehydrogenase [ubiquinone] 1 alpha subcomplex subunit 4-like 2 (NDUFA4L2)	<u>26% P / 8% R</u>			Q9NRX3	68
	GBM18P	ASLGARFYR	A*11:01		
	GBM18R	GSAALYLLR	A*11:01		
	GBM20P	GASLGARFY	A*29:02		
	GBM20R	GASLGARFY	A*29:02		
	ZH613	ASLGARFYR	A*31:03		
		DQYKFLAV	B*51:01		
	ZH631	DQYKFLAV	B*51:01		
	ZH645	DQYKFLAV	B*51:01		
	ZH654	DQYKFLAV	B*51:01		
	ZH678	DQYKFLAV	B*51:01		
	ZH761	DQYKFLAV	B*51:01		
	ZH791	GSAALYLLR	A*11:01		
	ZH802	AGASLGARFYR	A*31:01		

Appendix: Supplement of CHAPTER 2

Protein Wnt-5a (WNT5A)	<u>21% P / 13% R</u>			P41221 ■	42
		GBM2P	AMSSKFFLV	A*02:01	
		GBM3P	AMSSKFFLV	A*02:01	
		GBM10R	AMSSKFFLV	A*02:01	
		GBM11R	AMSSKFFLV	A*02:01	
		GBM14R	AMSSKFFLV	A*02:01	
		GBM20P	AMSSKFFLV	A*02:01	
		GBM21P	AMSSKFFLV	A*02:01	
		ZH616	AMSSKFFLV	A*02:01	
		ZH617	AMSSKFFLV	A*02:01	
		ZH681	AMSSKFFLV	A*02:01	
		ZH757	AMSSKFFLV	A*02:01	
	Immunoglobulin superfamily member 11 (IGSF11)	<u>18% P / 17% R</u>			Q5DX21 ■
		GBM4P	SPQPRNIGL	B*07:02	
			VPAQSRAGSLV	B*07:02	
		GBM4R	SPQPRNIGL	B*07:02	
		GBM7P	SPQPRNIGL	B*07:02	
		GBM10R	VPAQSRAGSLV	B*07:02	
		GBM16R	SPQPRNIGL	B*07:02	
		GBM17R	EEGIPRPTY	B*44:03	
		ZH645	SESPGSIQV	B*49:01	
		ZH654	LPDIGGRNI	B*51:01	
		ZH678	EEGIPRPTY	B*44:03	
		ZH761	SEEGIPRPTY	B*44:03	
		ZH802	KTLVVTANR	B*44:02	
			A*31:01		
Mitochondrial 39S ribosomal protein L35 (MRPL35)	<u>18% P / 17% R</u>			Q9NZE8 ■	15
		GBM3P	YVDDPYQKY	A*01:01	
		GBM5P	YVDDPYQKY	A*01:01;	
				B*15:01	
		GBM5R	YVDDPYQKY	A*01:01;	
				B*15:01	
		GBM9P	YVDDPYQKY	A*01:01	
		GBM9R	YVDDPYQKY	A*01:01	
		GBM13P	YVDDPYQKY	A*01:01	
		GBM13R	YVDDPYQKY	A*01:01	
		GBM16P	YVDDPYQKY	A*01:01	
		GBM16R	YVDDPYQKY	A*01:01	
		ZH617	YVDDPYQKY	A*01:01	
	ZH654	YVDDPYQKY	A*01:01		
Transmembrane protein 87A (TMEM87A)	<u>18% P / 13% R</u>			Q8NBN3 ■	33
		GBM7P	HPSPLSFFSA	B*07:02;	
				B*56:01	
		GBM7R	HPSPLSFFSA	B*07:02;	
				B*56:01	
		GBM15P	AELLSAVKR	B*44:03	
		GBM17R	FKAEVELY	C*06:02	
		ZH613	DAPYIFIV	B*51:01	
		ZH645	DAPYIFIV	B*51:01	
		ZH654	DAPYIFIV	B*51:01	
		ZH678	DAPYIFIV	B*51:01	
		ZH753	DAPYIFIV	B*51:01	
		ZH761	AAWLQVLPV	B*51:26;	
			C*16:01		
		DAPYIFIV	B*51:26		
85/88 kDa calcium-independent phospholipase A2 (PLA2G6)	<u>18% P / 13% R</u>			O60733 ■	3
		GBM3P	ALWETEVYI	A*02:01	
		GBM7P	ALWETEVYI	A*02:01	
		GBM7R	ALWETEVYI	A*02:01	
		GBM13R	ALWETEVYI	A*02:01	
		GBM19P	ALWETEVYI	A*02:01	
		GBM22P	LPFYESSPQVL	B*35:03	
		ZH750	ALWETEVYI	A*02:01	
		ZH757	ALWETEVYI	A*02:01	
		ZH784	ALWETEVYI	A*02:01	
		ZH829	ALWETEVYI	A*02:01	
Protein shisa-9 (SHISA9)	<u>18% P / 13% R</u>			B4DS77 ■	4
		GBM7P	KVNDDFYTK	A*11:01	
		GBM10R	KVNDDFYTK	A*03:01	
		GBM16P	KVNDDFYTK	A*03:01	
		GBM16R	KVNDDFYTK	A*03:01	
		GBM18P	KVNDDFYTK	A*03:01;	
				A*11:01	
		GBM18R	KVNDDFYTK	A*03:01;	
				A*11:01	
		ZH631	KVNDDFYTK	A*11:01	
	ZH678	KVNDDFYTK	A*11:01		
	ZH761	KVNDDFYTK	A*03:01		

Appendix: Supplement of CHAPTER 2

	ZH791	KVNDDFYTK	A*03:01; A*11:01		
Leucine-rich repeat neuronal protein 3 (LRRN3) 2 peptides multi-map to non-GBM-exclusive LRRN1 (Q6UXK5)	<u>18% P / 13% R</u> GBM6P	GTIESLPNL	A*02:05; C*12:03	Q9H3W5 ■	5
	GBM6R	GTIESLPNL	A*02:05; C*12:03		
	GBM9P	DMNFKPLINLR	A*33:05		
		DMPLRIHVL	B*08:01		
	GBM16P	DMPLRIHVL	B*08:01		
	GBM16R	DMPLRIHVL	B*08:01		
	GBM19P	LYPPLINLW	A*24:02		
	GBM22P	LYPPLINLW	A*24:02		
	GBM22R	LYPPLINL	A*24:02		
	ZH617	DMPLRIHVL	A*02:01; B*08:01		
			A*24:02		
Neuronal migration protein doublecortin (DCX) Peptides multi-map to non-GBM-exclusive doublecortin-like kinase 1/2 (DCLK1/2; O15075/Q8N568)	<u>16% P / 17% R</u> GBM10R	VLTDITEAI	A*02:01	O43602 ■	8
	GBM13P	VLTDITEAI	A*02:01; B*13:02		
	GBM13R	VLTDITEAI	A*02:01; B*13:02		
	GBM14R	VLTDITEAI	A*02:01		
	GBM23P	TAHSFEQVL	B*35:02		
	GBM23R	TAHSFEQVL	B*35:02		
	ZH645	VLTDITEAI	A*02:01		
	ZH681	VLTDITEAI	A*02:01		
	ZH757	VLTDITEAI	A*02:01		
	ZH761	VLTDITEAI	A*02:01		
			A*02:01		
Protein pitchfork (PIFO)	<u>13% P / 17% R</u> GBM3P	VRFKPIQK	B*27:05	Q8TCI5 ■	1
		VRFKPIQKEM	B*27:05		
	GBM4P	RVAYLSLYY	A*03:01		
	GBM4R	RVAYLSLYY	A*03:01		
	GBM16P	RVAYLSLYY	A*03:01		
	GBM16R	RVAYLSLYY	A*03:01		
	GBM17R	RVAYLSLYY	A*03:01		
	GBM20R	AELSTDKDF	B*44:02; B*44:03		
			B*44:02		
	ZH616	AELSTDKDF	B*44:02		
	ZH617	AELSTDKDF	B*44:02		
Uncharacterized aarF domain-containing protein kinase 1 (ADCK1)	<u>13% P / 17% R</u> GBM5P	TQISFSEAF	B*15:01	Q86TW2 ■	17
	GBM5R	TQISFSEAF	B*15:01		
	GBM9P	DFGAVRVGR	A*33:05		
	GBM9R	DFGAVRVGR	A*33:05		
	GBM13R	LTEEFRLNY	A*01:01		
	GBM14R	DFGAVRVGR	A*33:01		
	GBM16P	LTEEFRLNY	A*01:01		
	GBM23P	NYLPQISHL	A*23:01;		
	ZH802		C*06:02		
		DFGAVRVGR	A*33:01		
			A*33:01		
SAC3 domain-containing protein 1 (SAC3D1)	<u>13% P / 17% R</u> GBM4P	KPRPPPSQL	B*07:02	A6NKF1 ■	14
	GBM4R	KPRPPPSQL	B*07:02		
	GBM7P	KPRPPPSQL	B*07:02		
	GBM10R	KPRPPPSQL	B*07:02		
	GBM16P	KPRPPPSQL	B*07:02		
	GBM16R	KPRPPPSQL	B*07:02		
	GBM18P	KPRPPPSQL	B*07:02		
	GBM18R	KPRPPPSQL	B*07:02		
	ZH681	KPRPPPSQL	B*07:02		
			B*07:02		
			B*07:02		
Low-density lipoprotein receptor class A domain-containing protein 3 (LDLRAD3)	<u>16% P / 8% R</u> GBM5P	ASEVGSPPSY	A*01:01	Q86YD5 ■	2
		LLDQRPAWY	A*01:01; B*15:01		
	GBM9P	ASEVGSPPSY	A*01:01		
	GBM13R	ASEVGSPPSY	A*01:01		
		LLDQRPAWY	A*01:01		
	GBM16P	ASEVGSPPSY	A*01:01		
		LLDQRPAWY	A*01:01		
	GBM16R	LLDQRPAWY	A*01:01		
	ZH617	ASEVGSPPSY	A*01:01;		
	ZH645	ASEVGSPPSY	B*44:02		
			A*01:01		
		A*01:01			
ZH654	LLDQRPAWY	A*01:01			

Appendix: Supplement of CHAPTER 2

6-pyruvoyl tetrahydrobiopterin synthase (PTS)	<u>16% P / 8% R</u>			Q03393 ■	39
	GBM3P	ETDNNIVVY	A*01:01		
	GBM5R	ETDNNIVVY	A*01:01		
	GBM6P	QKVLPGVGLY	B*51:03		
	GBM13R	ETDNNIVVY	A*01:01		
	GBM15P	GEIDPATGM	B*44:02		
	GBM16P	ETDNNIVVY	A*01:01		
	ZH645	ETDNNIVVY	A*01:01		
ZH654	ETDNNIVVY	A*01:01			
Probable G-protein coupled receptor 75 (GPR75)	<u>16% P / 8% R</u>			O95800 ■	2
	GBM4P	TPAASRLQL	B*07:02		
	GBM4R	TPAASRLQL	B*07:02		
	GBM7P	TPAASRLQL	B*07:02		
	GBM16P	TPAASRLQL	B*07:02		
	GBM16R	TPAASRLQL	B*07:02		
	GBM18P	TPAASRLQL	B*07:02		
	ZH613	GLNPFYISR	A*31:01		
ZH654	GLNPFYISR	A*31:01			
POU domain, class 3, transcription factor 3 (POU3F3) 1 peptide multi-maps to GBM-exclusive POU3F2/4 (P20265/P49335)	<u>13% P / 13% R</u>			P20264 ■	6
	GBM4P	NPYLPGNL	B*07:02		
	GBM4R	NPYLPGNL	B*07:02		
	GBM7P	SPTSIDKIAA	B*56:01		
	GBM10R	LVRGDTPEL	A*02:01; B*07:02		
	GBM16P	NPYLPGNL	B*07:02		
	GBM16R	NPYLPGNL	B*07:02		
	ZH613	DVYSQVGTV	B*51:01		
ZH631	DVYSQVGTV	B*51:01			
Integral membrane protein DGCR2/IDD (DGCR2)	<u>13% P / 13% R</u>			P98153 ■	13
	GBM4P	VPKADSGAFL	B*07:02		
	GBM4R	VPKADSGAFL	B*07:02		
	GBM10R	VPKADSGAFL	B*07:02		
	GBM16P	VPKADSGAFL	B*07:02		
	GBM16R	VPKADSGAFL	B*07:02		
	GBM23P	FYDPADDDAF	C*04:01		
	ZH654	DPSHFHAVNV	B*51:01		
ZH681	VPKADSGAFL	B*07:02			
Cannabinoid receptor 1 (CNR1)	<u>11% P / 17% R</u>			P21554 ■	2
	GBM5P	KLGGVTASF	B*15:01		
	GBM12R	FPQKFPLTSF	B*35:01		
	GBM14R	FPHIDETYL	B*35:03		
		FPQKFPLTSF	B*35:03		
		STDTSAEAL	C*08:02		
		TVNPIIYAL	A*02:01; C*08:02		
			B*07:02		
		B*07:02			
		B*35:03			
		A*24:02			
		C*03:04;			
		C*12:03			
		A*02:01			
		A*02:01			
Lipoma HMGIC fusion partner-like 2 protein (LHFPL2)	<u>8% P / 21% R</u>			Q6ZUX7 ■	12
	GBM10R	SPEPYHPTL	B*07:02		
	GBM14R	SPEPYHPTL	B*35:03; C*08:02		
	GBM16P	SPEPYHPTL	B*07:02		
	GBM16R	SPEPYHPTL	B*07:02		
	GBM18R	SPEPYHPTL	B*07:02		
	GBM21P	SPEPYHPTL	B*35:03		
	GBM23P	SPEPYHPTL	B*35:02		
GBM23R	IRNPGVQHF	C*06:02			
GBM23R	SPEPYHPTL	B*35:02			
Insulin-like growth factor-binding protein 2 (IGFBP2)	<u>16% P / 4% R</u>			P18065 ■	8
	GBM7P	LPLPPPPLL	B*56:01		
	GBM12P	YHPGSELPL	B*35:01		
	GBM16P	YHPGSEL	B*07:02		
	GBM18R	YHPGSEL	B*07:02		
	GBM21P	YHPGSEL	B*35:03		
	GBM22P	YHPGSEL	B*35:03; C*03:04		
		YHPGSELPL	B*35:03		
ZH645	AEYGASPEQV	B*49:01			
Protein shisa-4 (SHISA4)	<u>16% P / 4% R</u>			Q96DD7 ■	6
	GBM23R	YPYPQDPKA	B*35:02		
	ZH613	LAFSPKTI	B*51:01		
	ZH631	LAFSPKTI	B*51:01		

Appendix: Supplement of CHAPTER 2

	ZH645	LAFSPKTI	B*51:01		
	ZH678	LAFSPKTI	B*51:01		
	ZH757	AAPLTAIAL	C*01:02		
	ZH761	AAPLTAIAL	C*01:02		
IGF-like family receptor 1 (IGFLR1)	<u>13% P / 8% R</u>			Q9H665 ■	45
	GBM5P	GRADALRVL	C*06:02		
	GBM5R	GRADALRVL	C*06:02		
	GBM13P	GRADALRVL	C*06:02		
	GBM13R	GRADALRVL	C*06:02		
	GBM23P	GRADALRVL	C*06:02		
	ZH654	GRADALRVL	C*06:02		
	ZH681	GRADALRVL	C*06:02		
CMP-N-acetylneuraminat-beta-galactosamide-alpha-2,3-sialyltransferase 4 (ST3GAL4)	<u>13% P / 8% R</u>			Q11206 ■	15
	GBM7P	SIPKNIQSL	C*01:02		
	GBM18R	DLLLRVLAI	B*08:01		
	GBM23R	RDQPIFLRL	B*47:01		
	ZH613	SIPKNIQSL	A*02:05		
	ZH678	AITSSSIPK	A*11:01		
	ZH757	SIPKNIQSL	C*01:02		
	ZH761	SIPKNIQSL	C*01:02		
Solute carrier family 25 member 53 (SLC25A53)	<u>13% P / 8% R</u>			Q5H9E4 ■	7
	GBM7P	STFLTFPIYK	A*11:01		
	GBM7R	STFLTFPIYK	A*11:01		
	GBM18P	STFLTFPIYK	A*11:01		
	GBM18R	STFLTFPIYK	A*11:01		
	ZH631	STFLTFPIYK	A*11:01		
	ZH654	AVSEAVRQLW	B*57:01		
	ZH678	STFLTFPIYK	A*11:01		
Leucine-rich repeats and immunoglobulin-like domains protein 1 (LRIG1)	<u>13% P / 8% R</u>			Q96JA1 ■	10
	GBM3P	ARIHRKGWSF	B*27:05		
	GBM16P	LPRLTQLDL	B*07:02		
	GBM16R	RPVRGGLGA	B*07:02		
	GBM21P	FPEPDTHSV	B*35:03		
	GBM23P	FPEPDTHSV	B*35:02		
	GBM23R	FPEPDTHSV	B*35:02		
	ZH654	AALPGDLPSW	B*57:01		
		AFHPQPVS	A*31:01		
Glycosyltransferase-like domain-containing protein 2 (GTDC2)	<u>11% P / 13% R</u>			Q8NAT1 ■	12
	GBM7P	ILNEAELL	A*02:01		
	GBM10R	AMLPGMDLQYV	A*02:01		
	GBM11P	AMLPGMDLQYV	A*02:01		
	GBM11R	LILNEAELL	A*02:01;		
			A*02:05		
	GBM13R	AMLPGMDLQYV	A*02:01		
	ZH681	AMLPGMDLQYV	A*02:01		
		ILNEAELL	A*02:01		
	ZH757	AMLPGMDLQYV	A*02:01		
Growth arrest and DNA damage-inducible proteins-interacting protein 1 (GADD45GIP1)	<u>11% P / 13% R</u>			Q8TAE8 ■	12
	GBM7P	SLWPSPEQL	A*02:01		
	GBM13R	SLWPSPEQL	A*02:01		
	GBM14R	SLWPSPEQL	A*02:01		
	GBM20R	AEAQELLY	B*44:02;		
			B*44:03		
	ZH617	SLWPSPEQL	A*02:01		
	ZH681	SLWPSPEQL	A*02:01		
	ZH757	SLWPSPEQL	A*02:01		
T-box transcription factor TBX15/18 (TBX15/18)	<u>11%/8% P</u>			Q96SF7 ■	18
	<u>13%/8% R</u>			Q95935 ■	11
1 peptide multi-maps to non-GBM-exclusive TBX20 (Q9UMR3)	GBM3P	GLDPHQYY (TBX15/18)	A*01:01		
	GBM6P	YQNQQITRL (TBX15/18)	A*02:05;		
			C*12:03		
	GBM9P	DIVPVDNKRYR (TBX15/18/20)	A*33:05		
		GLDPHQYY (TBX15/18)	A*01:01		
	GBM9R	GLDPHQYY (TBX15/18)	A*01:01		
	GBM11R	YQNQQITRL (TBX15/18)	A*02:05;		
			B*41:01		
	GBM12R	KTFNFPETVF (TBX15)	B*15:01		
	ZH654	KTFNFPETVF (TBX15)	B*57:01		
Exostosin-like 3 (EXTL3)	<u>11% P / 13% R</u>			Q43909 ■	12
	GBM5P	KSDTQNLLY	A*01:01		
	GBM13P	KSDTQNLLY	A*01:01		
	GBM13R	KSDTQNLLY	A*01:01		
	GBM16P	KSDTQNLLY	A*01:01		
	GBM16R	KSDTQNLLY	A*01:01		
	ZH645	KSDTQNLLY	A*01:01		
	ZH753	LPYLNKVVV	B*51:01		
Uncharacterized protein C7orf50 (C7orf50)	<u>11% P / 13% R</u>			Q9BRJ6 ■	12
	GBM10R	VPDEHFSTL	B*07:02		
	GBM16P	VPDEHFSTL	B*07:02		

Appendix: Supplement of CHAPTER 2

	GBM16R	VPDEHFSTL	B*07:02		
	GBM21P	VPDEHFSTL	B*35:03		
	GBM23P	VPDEHFSTL	B*35:02;		
			C*04:01		
	GBM23R	VPDEHFSTL	B*35:03;		
			C*04:01		
	ZH802	AYLEGLQGR	A*31:01		
Uncharacterized protein C21orf62 (C21orf62)	<u>8% P / 17% R</u>			Q9NYP8 ■	6
	GBM6P	LPLAVERTSY	B*35:01		
	GBM6R	LPLAVERTSY	B*35:01		
	GBM10R	RTFPMPSPNK	A*03:01		
	GBM16P	RTFPMPSPNK	A*03:01		
	GBM22R	SYNGHLTIWF	A*24:02		
	GBM23R	RTFPMPSPNK	A*03:01		
	ZH810	SYNGHLTIWF	A*24:02		
BTB/POZ domain-containing protein 17 (BTBD17)	<u>13% P / 4% R</u>			A6NE02 ■	1
	GBM3P	DELELFHAL	B*18:01		
	GBM4P	AVFDKFIRY	A*03:01		
	GBM7R	AVFDKFIRY	A*11:01;		
			C*02:02		
	ZH616	AVFDKFIRY	A*29:02		
	ZH631	AVFDKFIRY	A*11:01;		
			A*32:01		
	ZH654	NASDVVLRV	B*51:01		
		RARPPPAVAER	A*31:01		
Peroxisome biogenesis factor 10 (PEX10)	<u>13% P / 4% R</u>			O60683 ■	7
	GBM3P	QRARKEWRL	B*27:05;		
			C*07:01		
	GBM6P	AKRLTGITY	B*15:03		
	GBM18R	AVLPYLLDK	A*11:01		
	ZH613	RSLPGEDLRAR	A*31:01		
	ZH654	RSLPGEDLRAR	A*31:01		
	ZH802	RSLPGEDLRAR	A*31:01		
Sodium- and chloride- dependent creatine transporter 1 (SLC6A8)	<u>13% P / 4% R</u>			P48029 ■	20
1 peptide multi-maps to non- GBM-exclusive SLC6A6 (P31641)	GBM5P	LLDLLPASY	A*01:01;		
			B*15:01		
	GBM16P	LLDLLPASY	A*01:01		
	GBM16R	LLDLLPASY	A*01:01		
	ZH616	VVYYEPLVY	A*29:02		
	ZH631	IAYPRAVTL	C*03:03		
	ZH810	VWIDAGTQIFF	A*24:02		
5'-AMP-activated protein kinase subunit beta-2 (PRKAB2)	<u>11% P / 8% R</u>			O43741 ■	9
1 peptide multi-maps to non- GBM-exclusive PRKAB1	GBM6P	GTINNLIHV	A*02:05;		
			C*12:03		
	GBM11P	GTINNLIHV	A*02:05		
	GBM14R	LPEPNHVML	B*35:03;		
			C*04:01		
	GBM23P	LPEPNHVML	B*35:02;		
			C*04:01		
	GBM23R	LPEPNHVML	B*35:02;		
			C*04:01		
	ZH613	GTINNLIHV	A*02:05		
Transcription factor E2F1 (E2F1)	<u>11% P / 8% R</u>			Q01094 ◆	12
	GBM3P	DTDSQRLAY	A*01:01		
	GBM13P	DTDSQRLAY	A*01:01		
	GBM16P	DTDSQRLAY	A*01:01		
	GBM16R	DTDSQRLAY	A*01:01		
	GBM17R	DTDSQRLAY	A*01:01		
	ZH617	DTDSQRLAY	A*01:01		
Solute carrier family 15 member 2 (SLC15A2)	<u>11% P / 8% R</u>			Q16348 ■	17
	GBM4P	APSSMKSVL	B*07:02		
	GBM10R	APSSMKSVL	B*07:02		
	GBM16P	APSSMKSVL	B*07:02		
	GBM23P	VMFSVTGLEF	A*23:01		
	GBM23R	VMFSVTGLEF	A*23:01		
	ZH681	APSSMKSVL	B*07:02		
Sugar phosphate exchanger 3 (SLC37A3)	<u>11% P / 8% R</u>			Q8NCC5 ■	22
	GBM9P	DRLNLRWVL	B*14:02		
	GBM10R	SPNDKSINAL	B*07:02		
	GBM16P	SPNDKSINAL	B*07:02		
	GBM16R	SPNDKSINAL	B*07:02		
	ZH616	SVLQYGYEY	A*29:02		
	ZH761	ALTEWLRFY	A*03:01		
		VAQVKAISF	C*16:01		
Frizzled-3 (FZD3)	<u>11% P / 8% R</u>			Q9NPG1 ■	8
	GBM5P	SRPDLILFL	C*06:02		
	GBM13P	SRPDLILFL	C*06:02		
	GBM16P	SRPDLILFL	C*07:02		
	GBM16R	SRPDLILFL	C*07:02		

Appendix: Supplement of CHAPTER 2

Protein Dos (DOS)	GBM23R	SRPDLILFL	C*06:02	Q8N350 ■	0
	ZH654	SRPDLILFL	C*06:02		
	<u>11% P / 4% R</u>				
	ZH613	LPPLKIVTI	B*51:01		
	ZH631	LPPLKIVTI	B*51:01		
Embryonal Fyn-associated substrate (EFS)	ZH654	LPPLKIVTI	B*51:01	O43281 ■	16
	ZH678	LPPLKIVTI	B*51:01		
	ZH753	LPPLKIVTI	B*51:01		
	<u>11% P / 4% R</u>				
	GBM7P	LPALPVPEA	B*07:02; B*56:01		
Transmembrane protein 17 (TMEM17)	GBM18R	IPRASGTQL	B*07:02	Q86X19 ■	3
	ZH616	IPRASGTQL	B*07:02		
		STGDLQLLY	A*29:02		
	ZH678	AESPQELSF	B*44:03		
	ZH761	AESPQELSF	B*44:02; B*44:03		
Transcription factor E2F7 (E2F7)	<u>11% P / 4% R</u>			Q96AV8 ■	8
	GBM11P	LLFNEGLTNL	A*02:01		
	GBM14R	NLQEKVPEL	A*02:01		
	ZH617	NLQEKVPEL	A*02:01; B*08:01		
	ZH681	NLQEKVPEL	A*02:01		
Transmembrane protein 237 (TMEM237)	ZH761	NLQEKVPEL	A*02:01	Q96Q45 ■	7
	<u>11% P / 4% R</u>				
	GBM5P	LAYPFQSL	C*03:03		
	GBM6P	FQAADRSEL	A*02:05		
		LQPWIVVNL	A*02:05		
Lysyl oxidase homolog 2 (LOXL2)	GBM9P	DVKPSWTTR	A*33:05	Q9Y4K0 ■	26
	GBM14R	DVKPSWTTR	A*33:01		
	ZH802	DVKPSWTTR	A*33:01		
	<u>11% P / 4% R</u>				
	GBM6P	FGFPGERTY	C*12:03		
Heat shock factor 2-binding protein (HSF2BP)	GBM15P	AEMVQTTY	B*44:02	O75031 ◆	13
	GBM18R	RTYNTKVYKM	A*03:01		
	GBM21P	FGFPGERTY	C*12:03		
	ZH613	ASNAFQETW	B*58:01		
	<u>8% P / 8% R</u>				
Transcription factor HES-4 (HES4)	GBM3P	VLLDTILQL	A*02:01	Q9HCC6 ■	13
	GBM7P	VLLDTILQL	A*02:01		
	GBM12R	VLLDTILQL	A*02:01		
	GBM13R	VLLDTILQL	A*02:01		
	ZH750	VLLDTILQL	A*02:01		
Uroporphyrinogen-III synthase (UROS)	<u>8% P / 8% R</u>			P10746 ■	18
	GBM4P	RINESLAQLK	A*03:01		
	GBM10R	RINESLAQLK	A*03:01		
	GBM16R	RINESLAQLK	A*03:01		
	GBM18P	RINESLAQLK	A*03:01		
Blood vessel epicardial substance (BVES)	GBM23P	RINESLAQLK	A*03:01	Q8NE79 ■	5
	<u>5% P / 13% R</u>				
	GBM5P	TAIGFTPEL	C*03:03		
	GBM16R	SPEFRSTQM	B*07:02		
	GBM18R	SPEFRSTQM	B*07:02		
Olfactory receptor 51A7 (OR51A7)	GBM22R	TAIGFTPEL	C*03:04;	Q8NH64 ■	13
	ZH616	SPEFRSTQM	C*12:03		
			B*07:02		
	<u>5% P / 13% R</u>				
	GBM2P	GLILAIRSI	A*02:01		
Transmembrane protein 17 (TMEM17)	GBM13R	ILAIRSILL	A*02:01; B*08:01	Q86X19 ■	3
			B*08:01		
	GBM16P	ILAIRSILL	B*08:01		
	GBM18R	ILAIRSILL	B*08:01		
	ZH753	ILAIRSILL	A*02:01; B*08:01		

Appendix: Supplement of CHAPTER 2

Zinc finger and BTB domain-containing protein 47 (ZBTB47)	<u>5% P / 13% R</u>				
	GBM4P	RPKPPPGVA	B*07:02	Q9UFB7 ■ 10	
	GBM12R	FLLESELLL	A*02:01		
	GBM13R	FLLESELLL	A*02:01;		
			B*13:02		
	GBM14R	FLLESELLL	A*02:01		
GBM16P	RPKPPPGVA	B*07:02			
Glioblastoma-associated HLA class II antigens					
Glypican-5 (GPC5)	<u>32% P / 46% R</u>			P78333 ■ 1	
	GBM2P	LFQWRLLGAVRGLPD			
	GBM2R	KLFQWRLLGAVRGLPD			
		LFQWRLLGAVRGLPD			
		LFQWRLLGAVRGLPDSP			
	GBM6P	LFQWRLLGAVRGLPD			
	GBM6R	LFQWRLLGAVRGLPD			
	GBM7P	INSLRLYRSFYGGL			
		LFQWRLLGAVRGLPD			
	GBM7R	LFQWRLLGAVRGLPD			
	GBM9R	INSLRLYRSFYGGL			
	GBM10R	FINSLRLYRSFYGGLA			
		INSLRLYRSFYGG			
		INSLRLYRSFYGGL			
		INSLRLYRSFYGGLA			
		VNRFFDSLPLVYN			
		VNRFFDSLPLVYNH			
	GBM11P	INSLRLYRSFYGG			
		INSLRLYRSFYGGL			
	GBM11R	INSLRLYRSFYGGL			
	GBM12P	GIDPVINQIIDKCLKH			
		KLFQWRLLGAVRGLPD			
		LFQWRLLGAVRGLPD			
	GBM12R	LFQWRLLGAVRGLPD			
	GBM13P	GIDPVINQIIDKCLKH			
	GBM16P	FINSLRLYRSFYGGLA			
		INSLRLYRSFYGGL			
		VRKLFQWRLLGAVRGLPD			
	GBM18P	IDPVINQIIDKCLKH			
	GBM19R	LFQWRLLGAVRGLPD			
GBM22P	GIDPVINQIIDKCLKH				
	IDPVINQIIDKCLKH				
GBM22R	GIDPVINQIIDKCLKH				
GBM23R	GIDPVINQIIDKCLKH				
ZH616	FINSLRLYRSFYGGLA				
	INSLRLYRSFYGGL				
	INSLRLYRSFYGGLA				
ZH654	GIDPVINQIIDKCLKH				
	IDPVINQIIDKCLKH				
ZH753	LFQWRLLGAVRGLPD				
ZH761	LFQWRLLGAVRGLPD				
Procollagen galactosyltransferase 2 (COLGALT2)	<u>24% P / 13% R</u>			Q8IYK4 ■ 4	
	GBM5P	DLKAFSAEPLLIYPT			
		DLKAFSAEPLLIYPHTY			
	GBM6P	DLKAFSAEPLLIYPHT			
	GBM7P	DLKAFSAEPLLIYPT			
		DLKAFSAEPLLIYPHTY			
	GBM9R	DLKAFSAEPLLIYP			
		DLKAFSAEPLLIYPT			
		DLKAFSAEPLLIYPHT			
		DLKAFSAEPLLIYPHTY			
	GBM10R	DLKAFSAEPLLIYP			
		DLKAFSAEPLLIYPT			
		DLKAFSAEPLLIYPHT			
		DLKAFSAEPLLIYPHTY			
	GBM16P	DLKAFSAEPLLIYPT			
	DLKAFSAEPLLIYPHT				
	DLKAFSAEPLLIYPHTY				
	LKAFSAEPLLIYPHTY				
GBM20R	DLKAFSAEPLLIYPT				
ZH645	DLKAFSAEPLLIYPT				
ZH678	DLKAFSAEPLLIYPT				
ZH681	DLKAFSAEPLLIYPT				
ZH757	DLKAFSAEPLLIYPT				
	DLKAFSAEPLLIYPHT				
ZH761	DLKAFSAEPLLIYPHTY				
Nucleolar protein 16 (NOP16)	<u>29% P / 4% R</u>			Q9Y3C1 ■ 10	
	GBM5P	PKAKGKTRRQKF			
	GBM6P	PKAKGKTRRQKF			
	GBM13P	PKAKGKTRRQKF			
	GBM16R	PKAKGKTRRQKF			

Appendix: Supplement of CHAPTER 2

	GBM18P	PKAKGKTRRQKF		
	ZH613	PKAKGKTRRQKF		
	ZH617	PKAKGKTRRQKF		
	ZH631	PKAKGKTRRQKF		
	ZH645	PKAKGKTRRQKF		
	ZH678	PKAKGKTRRQKF		
	ZH681	PKAKGKTRRQKF		
	ZH802	PKAKGKTRRQKF		
N-acetyltransferase ESCO1 (ESCO1)	<u>18% P / 17% R</u>		Q5FWF5	12
	GBM11R	KVLEVKSDSKEDENLVINEVINSPK		
	GBM12R	KVLEVKSDSKEDENLVINEVINSPK		
	GBM14P	KVLEVKSDSKEDENLVINEVINSPK		
	GBM15R	KVLEVKSDSKEDENLVINEVINSPK		
	GBM18P	KVLEVKSDSKEDENLVINEVINSPK		
	GBM18R	KVLEVKSDSKEDENLVINEVINSPK		
	GBM19P	KVLEVKSDSKEDENLVINEVINSPK		
	GBM22P	KVLEVKSDSKEDENLVINEVINSPK		
	ZH617	KVLEVKSDSKEDENLVINEVINSPK		
	ZH645	KVLEVKSDSKEDENLVINEVINSPK		
	ZH791	KVLEVKSDSKEDENLVINEVINSPK		
Gamma-butyrobetaine dioxygenase (BBOX1)	<u>16% P / 21% R</u>		O75936	10
	GBM5P	KLGKRMGFLYLTFYGHWTWQVQDK		
	GBM9P	KAEALDGAHLMQIL		
	GBM9R	KAEALDGAHLMQIL		
	GBM10R	HKIIELDDKGQVVR		
		KAEALDGAHLMQIL		
		KHKIIELDDKGQVVR		
	GBM11P	KAEALDGAHLMQIL		
	GBM11R	KAEALDGAHLMQIL		
	GBM13P	HKIIELDDKGQVVR		
		KAEALDGAHLMQIL		
		KHKIIELDDKGQVVR		
		SKHKIIELDDKGQVVR		
	GBM13R	SKHKIIELDDKGQVVR		
	GBM14R	KAEALDGAHLMQIL		
	GBM16P	HKIIELDDKGQVVR		
		KAEALDGAHLMQIL		
		KHKIIELDDKGQVVR		
		SKHKIIELDDKGQVVR		
	GBM18P	HKIIELDDKGQVVR		
		KHKIIELDDKGQVVR		
Malignant fibrous histiocytoma-amplified sequence 1 (MFHAS1)	<u>13% P / 21% R</u>		Q9Y4C4	4
	GBM2P	KLNLSHNQLPALPAQLGALAHL		
	GBM7P	KLNLSHNQLPALPAQLGALAHL		
	GBM7R	KLNLSHNQLPALPAQLGALAHL		
	GBM11R	KLNLSHNQLPALPAQLGALAHL		
	GBM13P	KLNLSHNQLPALPAQLGALAHL		
	GBM20P	KLNLSHNQLPALPAQLGALAHL		
	GBM20R	KLNLSHNQLPALPAQLGALAHL		
	GBM21R	KLNLSHNQLPALPAQLGALAHL		
	ZH753	KLNLSHNQLPALPAQLGALAHL		
	ZH761	KLNLSHNQLPALPAQLGALAHL		
Polypeptide N-acetylgalactosaminyl-transferase 15 (GALNT15)	<u>13% P / 17% R</u>		Q8N3T1	2
	GBM4R	GGSYRLIKQPRRQD		
	GBM6P	GGSYRLIKQPRRQD		
		GGSYRLIKQPRRQDK		
		RGGSYRLIKQPRRQD		
		RGGSYRLIKQPRRQDK		
	GBM10R	GGSYRLIKQPRRQD		
		RGGSYRLIKQPRRQD		
	GBM16P	GGSYRLIKQPRRQD		
	GBM16R	GGSYRLIKQPRRQD		
	GBM17R	GGSYRLIKQPRRQDK		
		GGSYRLIKQPRRQDKE		
	GBM18P	LPEVRHPLCLQQHPQ		
		RNRVRIAETWLGSEFK		
	ZH616	GGSYRLIKQPRRQD		
		GGSYRLIKQPRRQDK		
		GGSYRLIKQPRRQD		
Kynurenine-oxoglutarate transaminase 1 (CCBL1)	<u>16% P / 13% R</u>		Q16773	11
	GBM4R	FPPPDFAVEAFQHAVSG		
	GBM5P	FPPPDFAVEAFQHAVSG		
	GBM6P	FPPPDFAVEAFQHAVSG		
	GBM7P	RDHMIRSLQSVGLKPIIP		
	GBM12R	GLVAIPVSIYFYSVPHQKHFDHYIRF		
	GBM18P	LDPMELAGKFTSRTKALVLNTPNNP		
	GBM18R	EQLLFRQPSSYFVQ		
	ZH645	FPPPDFAVEAFQHAVSG		
	ZH654	FPPPDFAVEAFQHAVSG		

Appendix: Supplement of CHAPTER 2

Ras-specific guanine nucleotide-releasing factor RalGPS1 (RALGPS1)	<u>13% P / 13% R</u> GBM11R GBM17R GBM19P ZH654 ZH750 ZH753 ZH802 ZH829	PTPPVPRHRKSHS PTPPVPRHRKSHS KRTREYIRSLKMVP PTPPVPRHRKSH PTPPVPRHRKSHS PTPPVPRHRKSH PTPPVPRHRKSHS PTPPVPRHRKSH PTPPVPRHRKSHS PTPPVPRHRKSH PTPPVPRHRKSHS PTPPVPRHRKSHS	Q5JS13 ■	1
Tripartite motif-containing protein 58 (TRIM58)	<u>16% P / 8% R</u> GBM12R GBM13P GBM16P GBM22P ZH645 ZH757 ZH761 ZH784	KKTVIWKEKQVEMQRQFRLEFEKHR KKTVIWKEKQVEMQRQFRLEFEKHR KKTVIWKEKQVEMQRQFRLEFEKHR KKTVIWKEKQVEMQRQFRLEFEKHR KKTVIWKEKQVEMQRQFRLEFEKHR KKTVIWKEKQVEMQRQFRLEFEKHR KKTVIWKEKQVEMQRQFRLEFEKHR KKTVIWKEKQVEMQRQFRLEFEKHR	Q8NG06 ■	3
Anaphase-promoting complex subunit CDC26 (CDC26)	<u>5% P / 25% R</u> GBM8P GBM8R GBM12P GBM14R GBM15R GBM17R GBM19R GBM21R	AIGLSSDPKSRE AIGLSSDPKSRE AIGLSSDPKSRE AIGLSSDPKSRE AIGLSSDPKSRE AIGLSSDPKSRE AIGLSSDPKSRE AIGLSSDPKSRE	Q8NHZ8 ■	1
NKG2D ligand 2 (ULBP2) / retinoic acid early transcript 1G protein (RAET1G)	<u>8%/11% P</u> <u>17%/13% R</u> GBM4P GBM4R GBM7R GBM8R GBM10R GBM13P ZH791 ZH829	KAQNPVLRVVDILTEQLL (RAET1G/RAET1L) LILCCLLIILPCFILP (ULBP2/RAET1L) KLNVTTAWKAQNPVLRVVDILT (ULBP2/RAET1G) KLNVTTAWKAQNPVLRVVDILT (ULBP2/RAET1G) KLNVTTAWKAQNPVLRVVDILT (ULBP2/RAET1G) KLNVTTAWKAQNPVLRVVDILT (ULBP2/RAET1G) KLNVTTAWKAQNPVLRVVDILT (ULBP2/RAET1G) KLNVTTAWKAQNPVLRVVDILT (ULBP2/RAET1G)	Q9BZM5 ■ Q6H3X3 ■	2 3
Hepatocyte nuclear factor 6 (ONECUT1)	<u>13% P / 13% R</u> GBM9R GBM11P GBM11R GBM13P GBM14P GBM16R GBM21P ZH802	KRKEQEHGKDRGNTPKKP KRKEQEHGKDRGNTPKKP KRKEQEHGKDRGNTPKKP KRKEQEHGKDRGNTPKKP KRKEQEHGKDRGNTPKKP KRKEQEHGKDRGNTPKKP KRKEQEHGKDRGNTPKKP KRKEQEHGKDRGNTPKKP	Q9UBC0 ■	2
Sushi repeat-containing protein SRPX2 (SRPX2)	<u>11% P / 21% R</u> GBM2P GBM9R GBM14P GBM14R GBM18R GBM20P GBM20R GBM21P GBM21R	IDRDRYMEPVTPEE APDPSNRYKMQISMLQQST GEHVIRYAYDR GEHVIRYAYDRAYN GEHVIRYAYDR GEHVIRYAYDRAY GEHVIRYAYDRAYN IDRDRYMEPVTPEE APDPSNRYKMQISMLQQST APDPSNRYKMQISMLQQST EGEHVIRYAYDRAY GEHVIRYAYDR GEHVIRYAYDRAY GEHVIRYAYDRAYN GEHVIRYAYDRAYN GPEPGSHFPEGEHVIRYAYDRAYN	Q60687 ■	7
Complement C1q-like protein 3 (C1QL3)	<u>8% P / 21% R</u> GBM7P GBM7R GBM12R GBM14R GBM21P	EPGDEVYIKLDGGKAHGG EPGDEVYIKLDGGKAHGGN EPGDEVYIKLDGGKAHGGN EPGDEVYIKLDGGKAHGGN TVPKIAFYAGLKRQHEG VPKIAFYAGLKRQHEG TVPKIAFYAGLKRQHEG VPKIAFYAGLKRQH	Q5VWW1 ■	1

Appendix: Supplement of CHAPTER 2

	GBM21R	TVPKIAFYAGLKRQH TVPKIAFYAGLKRQHEG VPKIAFYAGLKRQH VPKIAFYAGLKRQHE VPKIAFYAGLKRQHEG		
	ZH616 ZH753	KGEPGRQGLPGPPGAP EPGDEVYIKLDGGKAHG EPGDEVYIKLDGGKAHGGN		
Zinc finger protein GLIS1 (GLIS1)	<u>5% P / 21% R</u> GBM4 GBM9R GBM10R GBM11R GBM16P GBM16R ZH616	LPSKPSYPPFQSPPPPPLP LPSKPSYPPFQSPPPPPL LPSKPSYPPFQSPPPPPLP LPSKPSYPPFQSPPPPPLP LPSKPSYPPFQSPPPPPLP LPSKPSYPPFQSPPPPPLP LPSKPSYPPFQSPPPPPLP	Q8NBF1	6
Roundabout homolog 2 (ROBO2)	<u>13% P / 13% R</u> GBM10R	KKDKVRIDDKEER KKDKVRIDDKEERISIR GRYDIKDDYTLRIKK KKDKVRIDDKEERISIR KDKVRIDDKEERISIR KKDKVRIDDKEERIS KKDKVRIDDKEERISIR WKKDKVRIDDKEERISIR KDKVRIDDKEERIS KKDKVRIDDKEER KKDKVRIDDKEERIS KKDKVRIDDKEERISIR WKKDKVRIDDKEERIS WKKDKVRIDDKEERISIR KKDKVRIDDKEERISIR KKDKVRIDDKEERISIR LTDRPPPIILQGPANQTL RNEVVITENNNSIT	Q9HCK4	3
Striatin-4 (STRN4)	<u>13% P / 8% R</u> GBM11P GBM14R GBM18P GBM18R ZH613 ZH654 ZH802	SGSHDCSLRLWSLDNK KGQENLKT DDRGIRFLDNRTGKPV DDRGIRFLDNRTGKPV NSPLVWKEGRQLLR KGQENLKT DDRGIRFLDNRTGKPV	Q9NRL3	4
Beta-crystallin S (CRYGS)	<u>13% P / 4% R</u> GBM16P GBM18P GBM20R ZH645 ZH681 ZH802	RGRQYLLDKKEYRKPID GRQYLLDKKEYRKPID KITFYEDKNFQGR GRQYLLDKKEYRKPID RGRQYLLDKKEYRKPID GRQYLLDKKEYRKPID GRQYLLDKKEYRKPID KGFDFSGQMYETTED	P22914	1
Aftiphilin (AFTPH)	<u>8% P / 13% R</u> GBM9P GBM10R GBM17R GBM18P GBM18R ZH750	LYELTTSKLEISTSSL LYELTTSKLEISTSSL LYELTTSKLEISTSSL LYELTTSKLEISTSSL LYELTTSKLEISTSSL LYELTTSKLEISTSSL	Q6ULP2	1
Latent-transforming growth factor beta-binding protein (LTBP3)	<u>13% P / 8% R</u> GBM5P GBM13P GBM13R GBM14P GBM14R ZH654 ZH681	ESNSFWDTSPLLLKGPP ESNSFWDTSPLLLKGPP SNSFWDTSPLLLKGPP ESNSFWDTSPLLLKGPP SNSFWDTSPLLLKGPP VQVHRIESSNAESAAPS ASVQVHRIESSNAESAAPS QVHRIESSNAESAAPS SVQVHRIESSNAESAAPS VQVHRIESSNAESAAPS ESNSFWDTSPLLLKGPP SNSFWDTSPLLLKGPP ESNSFWDTSPLLLKGPP SNSFWDTSPLLLKGPP	Q9NS15	3
DNA repair protein RAD51 homolog 1 (RAD51)	<u>8% P / 8% R</u> GBM4P GBM17P GBM18R GBM20P	KLVPMGFTTATEFHQRRSEII KLVPMGFTTATEFHQRRSEII NDVKKLEEAGFHTV KLVPMGFTTATEFHQRRSEII	Q06609	2

Appendix: Supplement of CHAPTER 2

Protein Dos (DOS)	GBM22R	KTQICHTLAVTCQLPI	Q8N350 ■ 1
	<u>8% P / 8% R</u>		
	GBM6P	KVKKWKLEPSQRAAS	
		KVKKWKLEPSQRAASL	
	GBM7P	KVKKWKLEPSQRAAS	
		KVKKWKLEPSQRAASL	
	GBM10R	RRDYSIDEKTDALFHEFLRHDP	
GBM12P	KVKKWKLEPSQRAAS		
	KVKKWKLEPSQRAASL		
GBM20R	KVKKWKLEPSQRAAS		
	KVKKWKLEPSQRAASL		
	VKKWKLEPSQRAAS		
Copper-transporting ATPase 2 (ATP7B)	<u>8% P / 8% R</u>		P35670 ■ 4
	GBM9P	LMAGKAEIKYDPEVIQP	
	GBM10R	KSIEDRISNLKGIIS	
	GBM13P	KSIEDRISNLKGIIS	
	GBM18R	GEDNLIIEEEQVPME	
	ZH617	KGGKPLEMAHKIKTVMFDKTGTITH	
Putative mitochondrial ribosome-binding factor A (RBFA)	<u>8% P / 8% R</u>		Q8N0V3 ■ 11
	GBM2P	KNWLKFFASKTKK	
	GBM3R	KNWLKFFASKTKK	
	GBM5P	KNWLKFFASKTKK	
	GBM6P	KNWLKFFASKTKK	
	GBM7R	KNWLKFFASKTKK	
		KNWLKFFASKTKK	

Supplementary Table 3. Glioblastoma-associated HLA class I ligands presented on at least six primary and four recurrent tumors of a minimum of eight different patients. Peptides already reported to derive from glioblastoma-associated antigens were excluded from this listing. In turn, some of those antigens not designated as glioblastoma-associated due to a CNS-associated expression profile are listed herein with glioblastoma-associated peptides. The number of positive tumors other than glioblastoma was based on n=824 HLA class I peptidome datasets. HLA restrictions not passing manual assessment as quality control are indicated in *italics*. These combinations of sequence and HLA restriction were excluded from downstream analyses such as calculation of peptides matching per patient worldwide. All peptides were restricted to at least one HLA allotype covered by the CNS-related subset (brain, cerebellum, and spinal cord) of the benign database. Frequencies of positive tumors are given separately for n=38 primary (P) and n=24 recurrent (R) glioblastomas.

Peptide sequence	HLA restriction	Frequency of positive tumors	Antigen (UniProt accession)	Protein frequency on glioblastomas	Peptide-positive non-GBM tumors	Protein frequency on benign samples (n=418)
ALAAELNQL	A*02:01 A*02:05	<u>55% P</u>	<u>42% R</u>	Glial fibrillary acidic protein (GFAP; P14136)	100% P	6
		GBM2P	GBM20P		88% R	12%
	GBM2R	GBM20R				
	GBM3P	GBM21				
	GBM6P	ZH613				
	GBM6R	ZH616				
	GBM7P	ZH617				
	GBM7R	ZH645				
	GBM10P	ZH678				
	GBM10R	ZH681				
	GBM11P	ZH720				
	GBM11R	ZH750				
	GBM12R	ZH757				
	GBM13R	ZH761				
	GBM14P	ZH784				
GBM14R	ZH829					
GBM15P						
FLHDISDVQL	A*02:01 A*02:05	<u>47% P</u>	<u>42% R</u>	Ceramide synthase 1 (CERS1; P27544)	68% P	3
		GBM2P	GBM19P		71% R	2%
	GBM2R	GBM20R				
	GBM3P	GBM21P				
	GBM6P	ZH613				
	GBM6R	ZH616				
	GBM7P	ZH617				
	GBM7R	ZH645				
	GBM10R	ZH678				
	GBM11P	ZH681				
	GBM11R	ZH720				
	GBM13P	ZH753				
	GBM13R	ZH757				
	GBM14P	ZH761				
	GBM14R	ZH784				

Appendix: Supplement of CHAPTER 2

YVSSGEMMV	A*02:01 A*02:05 C*02:02 C*04:01 C*05:01 C*15:02 C*16:01	<u>47% P</u> GBM3P GBM6P GBM6R GBM7P GBM7R GBM10R GBM11P GBM12R GBM13P GBM13R GBM14P GBM14R GBM15P	<u>42% R</u> GBM21P GBM23R ZH613 ZH616 ZH617 ZH645 ZH678 ZH681 ZH753 ZH757 ZH761 ZH802 ZH829	Glial fibrillary acidic protein (GFAP; P14136)	100% P 88% R	2 12%	16%
GLLDGVFNV	A*02:01 B*13:02	<u>45%</u> GBM2P GBM2R GBM3P GBM5P GBM7P GBM7R GBM10R GBM11R GBM12R GBM13P GBM13R GBM14P GBM14R GBM19P	<u>46%</u> GBM19R GBM21P GBM21R ZH617 ZH645 ZH678 ZH681 ZH720 ZH750 ZH753 ZH757 ZH761 ZH784 ZH829	Carnosine synthase 1 (CARNS1; A5YM72)	63% P 71% R	13 2%	0%
YQDLLNVKL	A*02:01 A*02:05 B*13:02 C*02:02 C*04:01 C*05:01 C*08:02 C*15:02	<u>47% P</u> GBM3P GBM7P GBM7R GBM9P GBM9R GBM11P GBM11R GBM12R GBM13P GBM14P GBM14R GBM15P GBM19P GBM19R	<u>38% R</u> GBM20P GBM20R ZH613 ZH616 ZH617 ZH678 ZH681 ZH720 ZH753 ZH757 ZH761 ZH784 ZH802	Glial fibrillary acidic protein (GFAP; P14136)	100% P 88% R	7 12%	16%
SLWAGVVVL	A*02:01	<u>42% P</u> GBM2P GBM2R GBM3P GBM7P GBM7R GBM10R GBM12P GBM12R GBM13P GBM13R GBM14P GBM14R GBM19P	<u>42% R</u> GBM19R GBM20P GBM21P GBM21R ZH617 ZH645 ZH681 ZH750 ZH753 ZH757 ZH761 ZH784 ZH829	Chitinase-3-like protein 2 (CHI3L2; Q15782)	63% P 67% R	2 2%	1%
ALVSNLYVI	A*02:01	<u>42% P</u> GBM2P GBM3P GBM7P GBM11P GBM13P GBM13R GBM14R GBM15P GBM20P GBM20R	<u>17% R</u> GBM21P ZH617 ZH645 ZH678 ZH681 ZH720 ZH753 ZH757 ZH761 ZH829	Protein transport protein Sec61 subunit alpha isoform 1/2 (SEC61A1/2; P61619 / Q9H9S3)	97% / 97% P 100% / 100% R	31 60% / 51%	63% / 61%
ALIEVGEGVNL	A*02:01	<u>37% P</u> GBM2P GBM2R GBM7P GBM10R GBM11P GBM13P GBM13R GBM14R GBM19P	<u>29% R</u> GBM21P ZH617 ZH645 ZH681 ZH720 ZH753 ZH757 ZH761 ZH784	PNMA-like protein 1 (PNMAL1; Q86V59)	45% P 42% R	8 2%	0%

Appendix: Supplement of CHAPTER 2

		GBM20P GBM20R	ZH829				
ILDHNTMQV	A*02:01 C*05:01	<u>32% P</u> GBM3P GBM7P GBM7R GBM10R GBM11R GBM12R GBM13P GBM13R GBM9R GBM21P	<u>33% R</u> ZH617 ZH645 ZH678 ZH681 ZH720 ZH753 ZH757 ZH761 ZH784 ZH829	Pleckstrin homology domain-containing family H member 1 (PLEKHH1; Q9ULM0)	63% P 79% R	0 4%	2%
ALAQYLITA	A*02:01	<u>34% P</u> GBM2R GBM3P GBM7P GBM7R GBM10R GBM11P GBM11R GBM12R GBM13P GBM13R	<u>29% R</u> GBM20P ZH617 ZH645 ZH678 ZH681 ZH720 ZH753 ZH757 ZH761 ZH829	Poly(rC)-binding protein 4 (PCBP4; P57723)	61% P 59% R	5 4%	11%
GLLDQIQAL	A*02:01	<u>32% P</u> GBM3P GBM7P GBM7R GBM10R GBM12R GBM13R GBM14P GBM14R GBM20R GBM21P	<u>29% R</u> ZH617 ZH678 ZH681 ZH720 ZH750 ZH753 ZH757 ZH761 ZH829	Neuroigin-2/3 / X-/Y-linked neuroigin-4 (NLGN2/3/4X/4Y; Q8NFZ4 / Q9NZ94 / Q8N0W4 / Q8NFZ3)	34% / 61% / 50% / 50% P 29% / 54% / 42% / 42% R	7 2% / 3% / 2% / 2%	1% / 4% / 2% / 2%
VLDSHIHAY	A*01:01 A*03:01 B*15:01 C*01:02 C*04:01 C*07:01	<u>37% P</u> GBM3P GBM4P GBM4R GBM5P GBM5R GBM6P GBM9P GBM9R GBM10R GBM13P GBM13R GBM16P	<u>38% R</u> GBM16R GBM17P GBM17R GBM18P GBM22R GBM23P GBM23R ZH617 ZH645 ZH654 ZH761	Receptor-type tyrosine- protein phosphatase zeta (PTPRZ1; P23471)	97% P 83% R	6 6%	5%
KLTEENTTL	A*02:01 A*02:05 B*13:02	<u>37% P</u> GBM3P GBM7P GBM11P GBM12R GBM13P GBM14P GBM14R GBM15P GBM20P	<u>17% R</u> GBM20R GBM21P ZH616 ZH617 ZH678 ZH681 ZH753 ZH757 ZH761	Retrotransposon- derived protein PEG10 (PEG10; Q86TG7)	66% P 46% R	18 10%	6%
YYTVRNFTL	A*23:01 A*24:02 C*06:02 C*07:02 C*07:04	<u>34% P</u> GBM2P GBM4P GBM4R GBM8P GBM10R GBM11P GBM11R GBM15P GBM16P GBM16R GBM18R	<u>33% R</u> GBM19P GBM19R GBM22P GBM22R GBM23P ZH616 ZH681 ZH757 ZH784 ZH791	Receptor-type tyrosine- protein phosphatase zeta (PTPRZ1; P23471)	97% P 83% R	0 6%	5%
GLVEKVVQAA	A*02:01 A*02:05	<u>34% P</u> GBM2R GBM3P GBM6P GBM7P GBM7R GBM10R GBM11P GBM11R	<u>29% R</u> GBM13R GBM15P GBM20P GBM20R GBM21P ZH613 ZH617 ZH645	Apolipoprotein E (APOE; P02649)	76% P 67% R	25 16%	12%

Appendix: Supplement of CHAPTER 2

AIIDGVESV	A*02:01 A*02:05	GBM12R GBM13P <u>34% P</u> GBM7P GBM10R GBM11P GBM12P GBM12R GBM13P GBM14P GBM14R GBM15P	ZH678 ZH681 21% R GBM20R GBM21P ZH617 ZH645 ZH678 ZH681 ZH753 ZH757 ZH761	Receptor-type tyrosine- protein phosphatase zeta (PTPRZ1; P23471)	97% P 83% R	0 6%	5%
SLPELVHAV	A*02:01 A*02:05	<u>32% P</u> GBM3P GBM6P GBM7P GBM7R GBM10R GBM11P GBM11R GBM12R GBM13P GBM13R	<u>29% R</u> GBM14R GBM21P ZH613 ZH617 ZH678 ZH681 ZH753 ZH757 ZH761	Sestrin-3 (SESN3; P58005)	42% P 42% R	19 12%	4%
LLWGNAILF	A*02:01	<u>34% P</u> GBM2P GBM2R GBM3P GBM7P GBM7R GBM12R GBM13R GBM14P GBM19P	<u>17% R</u> GBM21P ZH616 ZH617 ZH678 ZH681 ZH750 ZH761 ZH829	Kinesin-like protein KIF1A (KIF1A; Q12756)	87% P 79% R	9 14%	15%
AIIGGMFTV	A*02:01 A*02:05	<u>32% P</u> GBM6P GBM10R GBM11P GBM11R GBM12R GBM13P GBM13R GBM14P GBM14R GBM20P	<u>29% R</u> GBM20R GBM21P ZH613 ZH617 ZH681 ZH720 ZH753 ZH757 ZH761	Endoplasmic reticulum- Golgi intermediate compartment protein 3 (ERGIC3; Q9Y282)	71% P 63% R	22 39%	26%
KIGPVGAVV	A*02:01 A*02:05 C*01:02 C*15:02	<u>18% P</u> GBM6R GBM7R GBM10R GBM11R GBM12R GBM13R GBM19R GBM21P	<u>33% R</u> ZH613 ZH678 ZH681 ZH720 ZH753 ZH757 ZH829	Myelin-associated glycoprotein (MAG; P20916)	50% P 63% R	0 0%	1%
ALQTIQLFL	A*02:01 B*13:02	<u>32% P</u> GBM2P GBM2R GBM3P GBM3R GBM7P GBM7R GBM13P GBM13R GBM14P GBM14R	<u>29% R</u> GBM15P GBM21P ZH617 ZH645 ZH681 ZH720 ZH753 ZH761 ZH784	Dystonin (DST; Q03001)	97% P 92% R	9 41%	55%
QLNEQVHSL	A*02:01 A*02:05	<u>32% P</u> GBM3P GBM10R GBM11P GBM13P GBM13R GBM14P GBM14R GBM20P GBM20R	<u>21% R</u> GBM21P ZH617 ZH678 ZH681 ZH753 ZH757 ZH761 ZH829	Microtubule-associated protein RP/EB family member 2 (MAPRE2; Q15555)	39% P 21% R	7 6%	9%
SLGLFLAQV	A*02:01	<u>29% P</u> GBM3P GBM3R GBM7P	<u>25% R</u> GBM20R GBM21P ZH617	Scavenger receptor class A member 3 (SCARA3; Q6AZY7)	53% P 38% R	10 4%	5%

Appendix: Supplement of CHAPTER 2

		GBM7R	ZH645				
		GBM12R	ZH678				
		GBM13R	ZH750				
		GBM14R	ZH757				
		GBM15P	ZH761				
		GBM20P					
ALLDGTVFEI	A*02:01	29% P GBM3P GBM3R GBM7P GBM10R GBM11P GBM13P GBM13R GBM14R GBM19P	25% R GBM20P GBM20R GBM21P ZH645 ZH681 ZH720 ZH757 ZH784	Protein DGCR6 / DGCR6L (DGCR6/6L; Q9BY27 / Q14129	34% / 34% P 33% / 33% R	24 7% / 6%	3% / 2%
ALSPNNHEV	A*02:01	29% P GBM3P GBM7P GBM7R GBM12R GBM13P GBM14R GBM20P GBM20R	21% R GBM21P ZH617 ZH678 ZH681 ZH753 ZH757 ZH761 ZH829	Actin-related protein 2/3 complex subunit 1A (ARPC1A; Q92747)	29% P 21% R	9 7%	10%
KIPPVTPSI	A*02:01 A*02:05 C*01:02 C*02:02 C*03:03 C*12:03 C*15:02	29% P GBM3P GBM5P GBM10R GBM11P GBM12R GBM13P GBM13R GBM14P	21% R GBM14R GBM21P ZH617 ZH645 ZH678 ZH681 ZH753 ZH757	Arrestin domain- containing protein 4 (ARRDC4; Q8NCT1)	63% P / 50% R	12	12%
LLLDVTISI	A*02:01	26% P GBM3P GBM7P GBM10R GBM13P GBM13R GBM14R GBM20P GBM20R	25% R GBM21P ZH681 ZH720 ZH753 ZH757 ZH761 ZH784 ZH829	Microtubule-associated protein 1A (MAP1A; P78559)	76% P 67% R	2	6%
GLLPSPLAV	A*02:01 B*13:02	26% P GBM3P GBM5P GBM5R GBM7P GBM10R GBM12R GBM13P GBM13R	25% R GBM14R GBM21P ZH617 ZH645 ZH678 ZH753 ZH761 ZH829	Zinc finger protein 385A (ZNF385A; Q96PM9)	71% P 67% R	25	15%
TLQEQLKA	A*02:01 A*02:05	26% P GBM3P GBM7P GBM10R GBM11P GBM12R GBM13R GBM14P GBM14R	25% R GBM15P GBM20P GBM20R GBM21P ZH616 ZH617 ZH681 ZH753	Pinin (PNN; Q9H307)	63% P 42% R	21	21%
TLYEQEIEV	A*02:01	24% P GBM2P GBM2R GBM3P GBM7P GBM7R GBM10R GBM11P GBM11R GBM12R	38% R GBM13P GBM13R GBM14R GBM20R ZH617 ZH678 ZH681 ZH753 ZH757	Procollagen galactosyltransferase 2 (COLGALT2; Q8IYK4)	39% P 54% R	3	1%
GTLEIPVAQK	A*03:01 A*11:01	29% P GBM4P GBM4R GBM6P GBM6R GBM7P GBM7R GBM10R	25% R GBM16P GBM17R GBM18P GBM22P GBM23P ZH631 ZH678	Neuronal cell adhesion molecule (NRCAM; Q92823)	47% P 29% R	0	1%

Appendix: Supplement of CHAPTER 2

		GBM12P GBM12R	ZH791				
RVSLPSYPR	A*03:01 A*11:01 A*31:01	<u>29% P</u> GBM4P GBM6P GBM7P GBM7R GBM10R GBM16P GBM16R GBM17R	<u>21% R</u> GBM18P GBM22P GBM23P GBM23R ZH631 ZH654 ZH678 ZH802	Neurocan core protein (NCAN; O14594)	34% P 21% R	2	1%
ILNVDGLIGV	A*02:01	<u>29% P</u> GBM7P GBM10R GBM11P GBM13P GBM13R GBM14R GBM19P GBM20P	<u>17% R</u> GBM20R GBM21P ZH645 ZH681 ZH720 ZH757 ZH829	ATP-citrate synthase (ACLY; P53396)	89% P 63% R	11	30%
ILKDGIIHNV	A*02:01 A*02:05	<u>29% P</u> GBM3P GBM11P GBM13P GBM13R GBM14R GBM20P GBM20R GBM21P	<u>17% R</u> ZH616 ZH617 ZH645 ZH678 ZH681 ZH753 ZH761	Prolow-density lipoprotein receptor- related protein 1 (LRP1; Q07954)	74% P 71% R	14	38%
KLQEANAQL	A*02:01	<u>26% P</u> GBM3P GBM7P GBM7R GBM10R GBM11P GBM12R GBM14P GBM14R	<u>25% R</u> GBM20P GBM20R GBM21P ZH617 ZH678 ZH681 ZH753 ZH757	Lethal(2) giant larvae protein homolog 1 (LLGL1; Q15334)	47% P 54% R	10	6%
QLNEKVAQL	A*02:01 B*08:01	<u>26% P</u> GBM9P GBM12R GBM13P GBM13R GBM14R GBM16P GBM20P GBM20R	<u>21% R</u> GBM21P ZH617 ZH678 ZH681 ZH753 ZH761 ZH829	Lanosterol 14-alpha demethylase (CYP51A1; Q16850)	82% P 58% R	32	31%
NIIPRFVQV	A*02:01 A*02:05 B*08:01 C*16:01	<u>26% P</u> GBM7P GBM11P GBM13R GBM14R GBM19P GBM20P GBM20R	<u>17% R</u> GBM21P ZH617 ZH678 ZH681 ZH753 ZH757 ZH761	SLIT-ROBO Rho GTPase-activating protein 2 / 2C (SRGAP2 / 2C; O75044 / PODJJ0)	66% / 66% P 54% / 54% R	14 14% / 11%	15% / 14%
SLNGTIFTV	A*02:01	<u>26% P</u> GBM3P GBM7P GBM12R GBM13P GBM13R GBM14R GBM20P	<u>17% R</u> GBM21P ZH617 ZH678 ZH681 ZH753 ZH757 ZH761	Bromodomain and PHD finger-containing protein 3 (BRPF3; Q9ULD4)	29% P 21% R	11 3%	1%
VIFDLPTTV	A*02:01 A*02:05 C*12:03 C*16:01	<u>26% P</u> GBM3P GBM7P GBM10R GBM11P GBM13P GBM13R GBM14R	<u>17% R</u> GBM21P ZH617 ZH645 ZH678 ZH753 ZH757 ZH761	Uncharacterized protein KIAA0556 (KIAA0556; O60303)	39% P 29% R	17 8%	5%
ALDGKIYEL	A*02:01	<u>26% P</u> GBM3P GBM7P GBM10R GBM11P GBM13P GBM13R GBM14R	<u>17% R</u> GBM20R GBM21P ZH617 ZH681 ZH720 ZH757 ZH761	Rho GTPase-activating protein 5 (ARHGAP5; Q13017)	42% P 42% R	11 11%	13%

Appendix: Supplement of CHAPTER 2

GLVAGGIIGA	A*02:01	<u>26% P</u> GBM3P GBM7P GBM10R GBM12R GBM13P GBM13R GBM14R	<u>17% R</u> GBM20P GBM21P ZH617 ZH678 ZH681 ZH757 ZH761	Translocase of inner mitochondrial membrane domain-containing protein 1 (TIMMDC; Q9NPL8)	39% P 21% R	38 15%	10%
AVATFLQSV	A*02:01 A*02:05 C*15:02	<u>24% P</u> GBM6P GBM6R GBM10R GBM11P GBM11R GBM13R GBM14R GBM20P	<u>29% R</u> GBM20R GBM21P ZH613 ZH617 ZH678 ZH681 ZH753 ZH757	Ubiquitin-like modifier-activating enzyme 1 (UBA1; P22314)	87% P 83% R	8 48%	54%
YLWTDVYSA	A*02:01	<u>24% P</u> GBM2R GBM3P GBM7P GBM7R GBM10R GBM12R GBM13P GBM13R	<u>29% R</u> GBM19P GBM19R ZH617 ZH678 ZH681 ZH753 ZH757 ZH829	Protein-arginine deiminase type-2 (PADI2; P22314)	87% P 83% R	2 13%	6%
SLMGTVFLL	A*02:01	<u>24% P</u> GBM3P GBM7P GBM10R GBM11P GBM11R GBM12R GBM13R GBM14P	<u>25% R</u> GBM14R ZH645 ZH681 ZH720 ZH750 ZH753 ZH757	Sphingomyelin synthase-related protein 1 (SAMD8; Q96LT4)	55% P 50% R	21 8%	7%
GLIEISNA	A*02:01 A*02:05	<u>24% P</u> GBM3P GBM6P GBM6R GBM7P GBM10R GBM11P GBM12R	<u>21% R</u> GBM13R GBM14R ZH613 ZH645 ZH678 ZH681 ZH757	U5 small nuclear ribonucleoprotein 200 kDa helicase (SNRNP200; O75643)	100% P 88% R	14 72%	74%
NLLYPVPLV	A*02:01	<u>21% P</u> GBM3P GBM7P GBM7R GBM10R GBM12R GBM13R GBM21P	<u>25% R</u> ZH645 ZH678 ZH681 ZH750 ZH753 ZH757 ZH784	Kinesin-like protein KIF1A (KIF1A; Q12756)	87% P 79% R	2 14%	15%
TLSTVIATV	A*02:01 A*02:05	<u>21% P</u> GBM3P GBM6P GBM7P GBM10R GBM12R GBM13R GBM14R	<u>21% R</u> GBM21P ZH617 ZH681 ZH720 ZH753 ZH761	Atrophin-1 (ATN1; P54259)	68% P 71% R	10 12%	10%
SLLEQAIAL	A*02:01	<u>18% P</u> GBM2R GBM3P GBM7P GBM7R GBM10R GBM12R GBM13R	<u>29% R</u> ZH678 ZH681 ZH753 ZH757 ZH761 ZH784 ZH829	Suppression of tumorigenicity 18 protein (ST18; O60284)	21% P 29% R	0 0%	0%
APSGTRVVQV	B*07:02	<u>29% P</u> GBM2P GBM4P GBM4R GBM7P GBM7R GBM8P GBM10R GBM11P GBM11R	<u>25% R</u> GBM16P GBM16R GBM18P GBM18R ZH616 ZH681 ZH757 ZH791	Protocadherin gamma-C3 (PCDHGC3; Q9UN70)	66% P 63% R	2 8%	11%

Appendix: Supplement of CHAPTER 2

ALADLQEAV	A*02:01 A*02:05 B*13:02	<u>29% P</u> GBM3P GBM7P GBM7R GBM10R GBM11P GBM11R GBM13P GBM13R	<u>21% R</u> GBM14P GBM14R GBM21P ZH616 ZH617 ZH645 ZH681 ZH757	Protein TANC1 (TANC1; Q9C0D5)	63% P 54% R	12 7%	10%
KLAPPPKKA	A*02:01	<u>29% P</u> GBM3P GBM7P GBM7R GBM14P GBM14R GBM20P GBM20R GBM21P	<u>17% R</u> ZH616 ZH617 ZH645 ZH678 ZH681 ZH753 ZH829	Astrocytic phosphoprotein PEA-15 (PEA15; Q15121)	76% P 58% R	22 28%	36%
SPYSKTLVL	B*07:02 B*14:02 B*35:03	<u>26% P</u> GBM4P GBM4R GBM7P GBM10R GBM11P GBM11R GBM14R GBM16P GBM16R	<u>25% R</u> GBM18P GBM18R GBM22P GBM22R ZH616 ZH681 ZH757 ZH791	E3 ubiquitin-protein ligase TRIM9 (TRIM9; Q9C026)	53% P 42% R	1 0%	0%
SPSGLRDSTV	B*07:02	<u>26% P</u> GBM2P GBM2R GBM4P GBM4R GBM7P GBM8P GBM10R GBM16P	<u>21% R</u> GBM16R GBM18P ZH616 ZH681 ZH757 ZH784 ZH791	ATP-sensitive inward rectifier potassium channel 10 (KCNJ10; P78508)	92% P 79% R	0 7%	12%
GVIESVVTI	A*02:01 A*02:05 B*13:02 C*02:02	<u>26% P</u> GBM3P GBM6P GBM6R GBM7P GBM11P GBM11R GBM12R GBM13P	<u>17% R</u> GBM13R GBM14R ZH613 ZH617 ZH681 ZH757 ZH761	Microtubule-associated protein 2 (MAP2; P11137)	66% P 50% R	1 4%	7%
GLLGGLPRL	A*02:01	<u>26% P</u> GBM7P GBM7R GBM12R GBM13P GBM13R GBM21P ZH678	<u>29% R</u> ZH681 ZH720 ZH750 ZH753 ZH757 ZH761 ZH829	Homeobox protein Nkx-6.2 (NKX6-2; Q9C056)	32% P 33% R	0 0%	1%
GLAPSIRTK	A*03:01 A*11:01	<u>24% P</u> GBM4P GBM4R GBM6P GBM6R GBM8P GBM10R GBM16P GBM16R GBM17R	<u>33% R</u> GBM18P GBM18R GBM22R GBM23P GBM23R ZH678 ZH761 ZH791	Tenascin (TNC; P24821)	87% P 83% R	11 14%	13%
RLFDEPQLA	A*02:01 B*13:02	<u>24% P</u> GBM3P GBM5P GBM5R GBM7P GBM10R GBM13R GBM14P	<u>21% R</u> GBM14R GBM21P ZH617 ZH681 ZH753 ZH757 ZH761	BTB/POZ domain- containing protein 1/2 (BTBD1/2; Q9H0C5 / Q9BX70)	74% / 74% P 58% / 67% R	8 34% / 38%	33% / 36%
SILDDVAMV	A*02:01	<u>24% P</u> GBM10R GBM12R GBM13P GBM13R GBM14P GBM20P	<u>17% R</u> ZH617 ZH678 ZH720 ZH753 ZH757 ZH761	RNA-binding protein 25 (RBM25; P49756)	50% P 33% R	31 17%	10%

Appendix: Supplement of CHAPTER 2

IPKAKPLTL	B*07:02 B*08:01	GBM21P					
		<u>21% P</u>	<u>33% R</u>	Stearoyl-CoA	68% P	4	4%
		GBM4P	GBM16P	desaturase 5 (SCD5;	58% R	6%	
		GBM4R	GBM16R	Q86SK9)			
		GBM7P	GBM18R				
		GBM9P	ZH617				
		GBM9R	ZH681				
		GBM10R	ZH753				
		GBM13P	ZH757				
		GBM13R	ZH784				
GLDPQGDRSFL	A*02:01 B*07:02 C*05:01	<u>21% P</u>	<u>25% R</u>	Protein LCHN (LCHN;	29% P	24	2%
		GBM7P	GBM21P	A4D1U4)	29% R	5%	
		GBM7R	ZH617				
		GBM10R	ZH678				
		GBM13R	ZH681				
		GBM14R	ZH753				
		GBM20P	ZH757				
		GBM20R	ZH761				
GVIDFSMYL	A*02:01 C*02:02 C*15:02 C*16:01	<u>21% P</u>	<u>21% R</u>	RUN and FYVE	42% / 34%	6	2% / 0%
		GBM7P	ZH720	domain-containing	29% / 38% R	4% / 3%	
		GBM10R	ZH750	protein 2/3 (RUFY2/3;			
		GBM12R	ZH753	Q8WXA3 / Q7L099)			
		GBM13P	ZH757				
		GBM13R	ZH761				
		ZH617	ZH784				
ZH681							
KMDENQFVAV	A*02:01	<u>18% P</u>	<u>25% R</u>	Dihydropyrimidinase-	71% / 79% /	11	30% / 41%
		GBM2P	ZH617	related protein 1/2/3	68% P	19% / 25% / 29%	/ 33%
		GBM10R	ZH681	(CRMP1 / DPYSL2/3;	67% / 79% /		
		GBM11P	ZH720	Q14194 / Q16555 /	67% R		
		GBM13R	ZH753	Q14195			
		GBM14R	ZH757				
		GBM20P	ZH784				
		GBM20R					
NLYEGQITV	A*02:01	<u>18% P</u>	<u>25% R</u>	ATP-binding cassette	37% P	3	4%
		GBM10R	ZH645	sub-family A member 3	29% R	5%	
		GBM11P	ZH678	(ABCA3; Q99758)			
		GBM11R	ZH681				
		GBM12R	ZH753				
		GBM13R	ZH757				
		GBM14R	ZH761				
ALTPVVVTL	A*02:01	<u>18% P</u>	<u>21% R</u>	Cyclin-dependent	50% P	28	8%
		GBM3P	GBM21P	kinase 4 (CDK4;	54% R	13%	
		GBM7P	ZH681	P11802)			
		GBM10R	ZH720				
		GBM12R	ZH753				
		GBM13R	ZH757				
		GBM14R	ZH761				
VLYEDSLSSQV	A*02:01	<u>29% P</u>	<u>21% R</u>	Integral membrane	55% P	10	18%
		GBM2P	GBM13P	protein 2C (ITM2C;	46% R	16%	
		GBM3P	GBM13R	Q9NQX7)			
		GBM7P	GBM20P				
		GBM7R	GBM20R				
		GBM10P	ZH617				
		GBM10R	ZH678				
		GBM11P	ZH720				
		GBM11R	ZH757				
IAFPGDILM	B*35:02 C*01:02 C*02:02 C*03:03 C*03:04 C*05:01 C*08:02 C*12:03 C*15:06	<u>26% P</u>	<u>25% R</u>	Excitatory amino acid	66% P	0	4%
		GBM3P	GBM21P	transporter 2 (SLC1A2;	58% R	3%	
		GBM6P	GBM22P	P43004)			
		GBM6R	GBM22R				
		GBM7P	GBM23P				
		GBM7R	GBM23R				
		GBM12R	ZH613				
		GBM14P	ZH631				
		GBM14R	ZH654				
KPKPTPDYL	B*07:02	<u>24% P</u>	<u>29% R</u>	Protein quaking (QKI;	92% P	8	58%
		GBM2R	GBM16P	Q96PU8)	88% R	52%	
		GBM4P	GBM16R				
		GBM4R	GBM18P				
		GBM7P	GBM18R				
		GBM7R	ZH616				
		GBM10R	ZH681				
		GBM11P	ZH757				
		GBM11R	ZH791				

Appendix: Supplement of CHAPTER 2

SPSEARQDVDL	B*07:02	<u>24% P</u> GBM2R GBM4P GBM4R GBM7P GBM7R GBM10R GBM11P GBM16P	<u>25% R</u> GBM16R GBM18P GBM18R ZH616 ZH681 ZH757 ZH791	Microtubule-associated protein 1B (MAP1B; P46821)	100% P 88% R	9 24%	29%
SLSSGPLTQK	A*03:01 A*11:01	<u>21% P</u> GBM2R GBM4P GBM4R GBM6P GBM6R GBM10R GBM16P GBM16R	<u>29% R</u> GBM17R GBM18P GBM23P GBM23R ZH631 ZH761 ZH791	Brain and acute leukemia cytoplasmic protein (BAALC; Q8WXS3)	45% P 54% R	2 2%	3%
SLDSTLHAV	A*02:01	<u>21% P</u> GBM3P GBM10R GBM11P GBM13P GBM13R GBM14R GBM20P	<u>21% R</u> GBM20R ZH616 ZH617 ZH645 ZH681 ZH753	Leucine-rich repeat and coiled-coil domain-containing protein 1 (LRRCC1; Q9C099)	39% P 21% R	11 4%	3%
ATYYGAFIK	A*03:01 A*11:01	<u>21% P</u> GBM4P GBM4R GBM7P GBM10R GBM16P GBM16R GBM17R	<u>21% R</u> GBM18R GBM23P ZH631 ZH678 ZH761 ZH791	Mitogen-activated protein kinase kinase kinase 4 / misshapen-like kinase 1 / TRAF2 and NCK-interacting protein kinase (MAP4K4 / MINK1 / TNIK; Q95819 / Q8N4C8 / Q9UKE5)	61% / 63% / 66% P 58% / 54% / 58% R	2 20% / 22% / 19%	22% / 23% / 23%
FLQGTIIAL	A*02:01	<u>21% P</u> GBM2P GBM2R GBM3P GBM7P GBM10R GBM12R	<u>17% R</u> ZH678 ZH681 ZH753 ZH757 ZH761 ZH829	Myelin regulatory factor (MYRF; Q9Y2G1)	47% P 63% R	1 1%	1%
KMLDEAVFQV	A*02:01	<u>18% P</u> GBM3P GBM7P GBM10R GBM11P GBM13R GBM14R	<u>17% R</u> ZH645 ZH681 ZH720 ZH757 ZH784	Neuron navigator 1 (NAV1; Q8NEY1)	53% P 38% R	12 10%	11%
VPRGFPSDTQL	B*07:02	<u>18% P</u> GBM2P GBM2R GBM4P GBM4R GBM7P GBM7R GBM10R GBM11R	<u>33% R</u> GBM16P GBM16R GBM18R ZH681 ZH757 ZH784 ZH791	Chondroadherin-like protein (CHADL; Q6NUI6)	24% P 46% R	0 2%	0%
SVMSILPKI	A*02:01 C*15:02	<u>18% P</u> GBM3P GBM7P GBM7R GBM13R GBM14R ZH645	<u>21% R</u> ZH678 ZH681 ZH720 ZH753 ZH757 ZH784	Serine incorporator 1 (SERINC1; Q9NRX5)	39% P 59% R	29 7%	10%
HLDFISIMTY	A*01:01	<u>24% P</u> GBM3P GBM5P GBM5R GBM9P GBM9R GBM13P GBM13R GBM16P	<u>25% R</u> GBM16R GBM17P GBM17R ZH617 ZH645 ZH654 ZH784	Chitinase-3-like protein 1 (CHI3L1; P36222)	68% P 63% R	8 4%	3%
SPFLQQQAL	B*07:02	<u>26% P</u> GBM2P GBM2R	<u>25% R</u> GBM11P GBM11R	Adenomatous polyposis coli protein 2 (APC2; O95996)	58% P 54% R	0 2%	1%

Appendix: Supplement of CHAPTER 2

		GBM4P GBM4R GBM7P GBM7R GBM10P GBM10R	GBM16P GBM16R GBM18P ZH616 ZH681 ZH791					
FLDYGALSLY	A*01:01	24% P GBM3P GBM5P GBM5R GBM9P GBM9R GBM13P GBM13R GBM16P	25% R GBM16R GBM17P GBM17R ZH617 ZH645 ZH654 ZH784	Progesterone and adiponectin receptor family member 6 (PAQR6; Q6TCH4)	32% P 29% R	1 1%	0%	
GTEKLIETY	A*01:01	24% P GBM3P GBM5P GBM5R GBM9P GBM9R GBM13P GBM13R GBM16P	25% R GBM16R GBM17P GBM17R ZH617 ZH645 ZH654 ZH784	Myelin proteolipid protein (PLP1; P60201)	71% P 71% R	1 1%	10%	
KPHSTPATL	B*07:02	24% P GBM2P GBM2R GBM4P GBM4R GBM7P GBM7R GBM8P GBM10R	25% R GBM16P GBM16R GBM18P GBM18R ZH616 ZH681 ZH791	Transcription factor RFX4 (RFX4; Q33E94)	55% P 46% R	0 0%	0%	
QLDHLSLYY	A*01:01	24% P GBM3P GBM5P GBM5R GBM9P GBM9R GBM13P GBM13R GBM16P	25% R GBM16R GBM17P GBM17R ZH617 ZH645 ZH654 ZH784	Electroneutral sodium bicarbonate exchanger 1 (SLC4A8; Q2Y0W8)	26% P 29% R	6 5%	3%	
FPDNQRPLL	B*07:02 B*35:02 C*04:01	24% P GBM4P GBM4R GBM7P GBM8P GBM10R GBM11P GBM16P	21% R GBM16R GBM18P GBM18R GBM23P GBM23R ZH681 ZH757	ETS translocation variant 1 (ETV1; P50549)	47% P 33% R	7 5%	3%	
MTDPSKNLGY	A*01:01	21% P GBM3P GBM5P GBM5R GBM9P GBM13P GBM13R GBM16P	21% R GBM16R GBM17R ZH617 ZH645 ZH654 ZH784	Protein FAM5B (FAM5B; Q9C0B6)	24% P 25% R	1 1%	1%	
TMMSRPPVL	A*02:01 B*08:01 B*14:02 C*01:02 C*07:02 C*12:03	24% P GBM6P GBM10P GBM10R GBM11P GBM11R GBM14P GBM14R	17% R ZH616 ZH617 ZH678 ZH720 ZH753 ZH757	Protein wntless homolog OS=Homo sapiens (WLS; Q5T9L3)	76% P 58% R	9 12%	15%	
VSDPKATMY	A*01:01	21% P GBM3P GBM5P GBM5R GBM9P GBM9R GBM13P GBM13R	25% R GBM16P GBM16R GBM17R ZH617 ZH645 ZH654 ZH784	Gamma-aminobutyric acid receptor subunit beta-1 (GABRB1; P18505)	42% P 42% R	1 2%	4%	
SYIGLGHYI	C*07:02	21% P GBM2P GBM2R GBM4P GBM4R	25% R GBM16P GBM16R GBM18P GBM18R	Chloride transport protein 6 (CLCN6; P51797)	26% P 33% R	14 3%	1%	

Appendix: Supplement of CHAPTER 2

VVDPSNLYY	A*01:01	GBM8P	ZH681	Cyclic nucleotide-gated cation channel alpha-3 (CNGA3; Q16281)	24% P 25% R	4 1%	1%
		GBM10R	ZH757				
		GBM11P	ZH784				
		<u>21% P</u>	<u>25% R</u>				
		GBM3P	GBM16P				
		GBM5P	GBM16R				
		GBM5R	GBM17R				
		GBM9P	ZH617				
		GBM9R	ZH645				
		GBM13P	ZH654				
SSDKVTVNY	A*01:01	GBM13R	ZH784	Protein-arginine deiminase type-2 (PADI2; Q9Y2J8)	87% P 83% R	22 13%	6%
		<u>21% P</u>	<u>21% R</u>				
		GBM3P	GBM16R				
		GBM5P	GBM17R				
		GBM5R	ZH617				
		GBM9P	ZH645				
		GBM9R	ZH654				
		GBM13P	ZH784				
		GBM16P					
YPHSGGSEL	B*07:02 B*35:01 B*35:02 B*35:03	<u>18% P</u>	<u>29% R</u>	T-box brain protein 1 (TBR1; Q16650)	18% P 33% R	0 2%	3%
		GBM2P	GBM16R				
		GBM2R	GBM18R				
		GBM4P	GBM21P				
		GBM7P	GBM22P				
		GBM12R	GBM22R				
		GBM14P	GBM23P				
		GBM14R	GBM23R				
SPVPATPIL	B*07:02 B*35:01 B*35:03	<u>18% P</u>	<u>25% R</u>	E3 ubiquitin-protein ligase TRIM9 (TRIM9; Q9C026)	53% P 42% R	0 0%	0%
		GBM4P	GBM16R				
		GBM4R	GBM18P				
		GBM6P	GBM18R				
		GBM7P	GBM21P				
		GBM10R	GBM22R				
		GBM14R	GBM23R				
		GBM16P					
ELDVVREIY	A*01:01 B*15:01	<u>18% P</u>	<u>25% R</u>	Formin-like protein 2 (FMNL2; Q96PY5)	58% P 71% R	18 17%	14%
		GBM3P	GBM16R				
		GBM5P	GBM17R				
		GBM5R	ZH617				
		GBM9P	ZH645				
		GBM9R	ZH654				
		GBM13R	ZH784				
		GBM16P					
FMVDKAIYL	A*02:01	<u>16% P</u>	<u>21% R</u>	Ecto-NOX disulfide-thiol exchanger 1 (ENOX1; Q8TC92)	26% P 21% R	18	0%
		GBM10R	ZH681				
		GBM11P	ZH720				
		GBM11R	ZH753				
		GBM13R	ZH757				
		ZH645	ZH784				
		ZH678					
LLQDRLVSV	A*02:01	<u>18% P</u>	<u>21% R</u>	Pleckstrin homology domain-containing family A member 4 (PLEKHA4; Q9H4M7)	18% P 21% R	7	1%
		GBM3P	GBM20P				
		GBM10R	GBM20R				
		GBM11P	GBM21P				
		GBM11R	ZH617				
		GBM13P	ZH681				
		GBM14R	ZH753				
ALYGKTEVV	A*02:01	<u>18% P</u>	<u>21% R</u>	Caskin-2 (CASKIN2; Q8WXE0)	32% P 46% R	8	16%
		GBM3P	ZH617				
		GBM10R	ZH645				
		GBM13P	ZH681				
		GBM13R	ZH753				
		GBM20R	ZH757				
		GBM21P					
LLYDQPLQV	A*02:01 B*13:02	<u>18% P</u>	<u>17% R</u>	Protein LAP2 (ERBB2IP; Q96RT1)	76% P 75% R	10 36%	35%
		GBM10R	ZH645				
		GBM11P	ZH678				
		GBM13R	ZH681				
		GBM20P	ZH753				
		GBM20R	ZH757				
		GBM21P					
LLYEHQNNL	A*02:01	<u>18% P</u>	<u>17% R</u>	Growth arrest-specific protein 8 (GAS8; Q95995)	21% P 17% R	14 4%	3%
		GBM10R	ZH617				
		GBM13P	ZH678				
		GBM13R	ZH681				
		GBM14R	ZH753				
		GBM20P	ZH757				
		GBM21P					

Appendix: Supplement of CHAPTER 2

LMYPYIYHV	A*02:01	<u>18% P</u> GBM10R GBM11P GBM13P GBM13R GBM19P GBM20R	<u>17% R</u> GBM21P ZH617 ZH681 ZH753 ZH757	Constitutive coactivator of PPAR-gamma-like protein 2 (FAM120C; Q9NX05)	50% P 50% R	3 8%	8%
YLDPRITVA	A*02:01	<u>18% P</u> GBM3P GBM7R GBM10R GBM20P GBM20R GBM21P	<u>17% R</u> ZH616 ZH617 ZH678 ZH681 ZH753	DNA topoisomerase 1 (TOP1; P11387)	53% P 50% R	12 32%	19%
FLDEKSGSFV	A*02:01 C*04:01 C*05:01	<u>18% P</u> GBM2P GBM10R GBM11P GBM14R GBM20P GBM20R	<u>17% R</u> ZH616 ZH617 ZH681 ZH753 ZH757	F-box only protein 32 (FBXO32; Q969P5)	63% P 63% R	12 16%	12%
YITEGQIYV	A*02:01 A*02:05	<u>18% P</u> GBM2R GBM7P GBM10R GBM11P GBM11R GBM20P	<u>17% R</u> ZH617 ZH645 ZH681 ZH753 ZH757	V-type proton ATPase subunit B, brain isoform (ATP6V1B2; P21281)	71% P 71% R	17 35%	29%
YLEDFYTRM	A*02:01 A*02:05 C*01:02 C*02:02 C*05:01 C*08:02	<u>18% P</u> GBM3R GBM11P GBM13R GBM14R GBM19P GBM20P	<u>17% R</u> GBM20R GBM21P ZH617 ZH681 ZH757	Peroxisomal sarcosine oxidase (PIPOX; Q9P0Z9)	29% P 17% R	2 1%	3%
LLYPVPLVH	A*03:01	<u>16% P</u> GBM2R GBM4P GBM4R GBM6P GBM6R GBM8P GBM10R	<u>33% R</u> GBM16P GBM16R GBM17R GBM18P GBM18R GBM22R GBM23P	Kinesin-like protein KIF1A (KIF1A; Q12756)	87% P 79% R	11 14%	15%
LPASPSVSL	B*07:02 B*35:01 B*35:02 B*35:03	<u>16% P</u> GBM4P GBM7P GBM10R GBM12R GBM14R GBM16P GBM16R	<u>29% R</u> GBM18R GBM21P GBM22P GBM22R GBM23P GBM23R	Ectoderm-neural cortex protein 1 (ENC1; O14682)	89% P 75% R	15 23%	15%
VLLEGELIDV	A*02:01	<u>16% P</u> GBM2R GBM10R GBM11P GBM13P GBM13R GBM20R	<u>21% R</u> ZH645 ZH720 ZH753 ZH757 ZH829	UPF0552 protein C15orf38 (C15orf38; Q7Z6K5)	21% P 25% R	4 2%	2%
ALDASILNV	A*02:01 B*13:02	<u>16% P</u> GBM3P GBM5P GBM10R GBM12R GBM13R	<u>17% R</u> GBM14R GBM21P ZH645 ZH678 ZH757	Regulator of G-protein signaling 12 (RGS12; O14924)	26% P 17% R	11 8%	5%
GLLPLLREA	A*02:01	<u>16% P</u> GBM2R GBM3P GBM12R GBM14R GBM15P	<u>17% R</u> GBM20R GBM21P ZH617 ZH645 ZH678	Stabilin-1 (STAB1; Q9NY15)	82% P 63% R	34 34%	31%
VPWQGTMTL	B*07:02 B*35:01 B*35:03 B*39:10 B*56:01	<u>16% P</u> GBM4P GBM6P GBM7P GBM10R GBM14R	<u>17% R</u> GBM16P GBM18R GBM22P ZH720 ZH784	Cystatin-C (CST3; P01034)	29% P 38% R	10 5%	7%

Appendix: Supplement of CHAPTER 2

AVASVIIYR	A*03:01 A*11:01 A*31:01 A*68:01	<u>21% P</u> GBM4P GBM4R GBM6P GBM6R GBM8P GBM10R GBM12P	<u>25% R</u> GBM12R GBM16P GBM16R GBM18P GBM18R ZH631 ZH802	Cadherin EGF LAG seven-pass G-type receptor 2 (CELSR2; Q9HCU4)	50% P 63% R	2 10%	11%
ISDHGTVTY	A*01:01	<u>21% P</u> GBM3P GBM5P GBM5R GBM9P GBM9R GBM13P GBM13R	<u>21% R</u> GBM16P GBM16R GBM17R ZH617 ZH645 ZH654	Lysosome-associated membrane glyco- protein 2 (LAMP2; P13473)	39% P 46% R	27 16%	12%
VSESHGQLSY	A*01:01	<u>21% P</u> GBM3P GBM5P GBM5R GBM9P GBM9R GBM13P GBM13R	<u>21% R</u> GBM16P GBM16R GBM17R ZH617 ZH645 ZH654	OTU domain-containing protein 4 (OTUD4; Q01804)	26% P 21% R	35 6%	3%
AVFPEGALTK	A*03:01 A*11:01	<u>21% P</u> GBM4P GBM4R GBM7P GBM7R GBM10R GBM16P GBM16R	<u>21% R</u> GBM18P GBM18R GBM23P ZH631 ZH678 ZH791	Ankyrin-2 OS=Homo sapiens (ANK2; Q01484)	87% P 75% R	12 19%	33%
STEERTFQY	A*01:01	<u>21% P</u> GBM3P GBM5P GBM5R GBM9P GBM9R GBM13P GBM13R	<u>21% R</u> GBM16P GBM16R GBM17R ZH617 ZH645 ZH654	Peroxisomal carnitine O-octanoyltransferase (CROT; Q9UKG9)	37% P 29% R	13 7%	3%
LDSHIHAY	A*01:01	<u>21% P</u> GBM3P GBM5P GBM9P GBM9R GBM13P GBM13R	<u>17% R</u> GBM16P GBM16R GBM17R ZH617 ZH645 ZH654	Receptor-type tyrosine- protein phosphatase zeta (PTPRZ1; P23471)	97% P 83% R	6 6%	5%
SVPYFVTAL	A*02:05 C*01:02 C*12:03	<u>21% P</u> GBM6P GBM6R GBM7P GBM7R GBM11P GBM11R	<u>17% R</u> GBM12R ZH613 ZH645 ZH757 ZH761 ZH829	Transmembrane 6 superfamily member 1 (TM6SF1; Q9BZW5)	55% P 58% R	3 18%	23%
APSGLR SQVQF	B*07:02	<u>18% P</u> GBM2R GBM4P GBM4R GBM7P GBM7R GBM10R GBM11P	<u>29% R</u> GBM11R GBM16P GBM16R GBM18P GBM18R ZH681 ZH757	GRAM domain- containing protein 3 (GRAMD3; Q96HH9)	47% P 54% R	9 11%	13%
HTDMADIEQY	A*01:01	<u>16% P</u> GBM3P GBM5P GBM5R GBM9P GBM9R GBM13R	<u>25% R</u> GBM16P GBM16R GBM17R ZH617 ZH645 ZH784	N-acetylaspartate synthetase (NAT8L; Q8N9F0)	53% P 50% R	6 5%	5%
LLDPAQRTLY	A*01:01	<u>18% P</u> GBM3P GBM5P GBM5R GBM9P GBM9R GBM13P GBM13R	<u>25% R</u> GBM16P GBM16R GBM17R ZH617 ZH654 ZH784	Zinc finger protein 557/558 (ZNF557/558; Q8N988 / Q96NG5)	21% / 26% P 33% / 38% R	33 6% / 6%	2% / 1%

Appendix: Supplement of CHAPTER 2

SPIERNEQL	B*07:02 B*08:01 B*35:02 B*35:03	<u>18% P</u> GBM4P GBM4R GBM10R GBM14P GBM14R GBM16P GBM18P	<u>25% R</u> GBM18R GBM21P GBM22R GBM23P GBM23R ZH681	Zinc finger protein 226 (ZNF226; Q9NYT6)	29% P 33% R	7 3%	2%
ISEELVQKY	A*01:01	<u>18% P</u> GBM3P GBM5P GBM5R GBM9P GBM9R GBM13R	<u>21% R</u> GBM16P GBM16R GBM17R ZH617 ZH645 ZH654	Reticulon-4 (RTN4; Q9NQC3)	79% P 75% R	34 32%	38%
KVQAGNSSL	B*07:02 C*01:02 C*02:02 C*16:01	<u>18% P</u> GBM2R GBM4P GBM4R GBM7P GBM7R GBM10R	<u>21% R</u> GBM16P GBM16R GBM18P ZH616 ZH681 ZH761	Phosphoserine aminotransferase (PSAT1; Q9Y617)	50% P 54% R	5 8%	9%
AVYDTNPAK	A*03:01 A*11:01	<u>18% P</u> GBM4P GBM4R GBM7P GBM16P GBM16R GBM17R	<u>17% R</u> GBM18P GBM23R ZH631 ZH761 ZH791	Glycolipid transfer protein (GLTP; Q9NZD2)	39% P 46% R	0 9%	8%
KIIDEDGLLNL	A*02:01 A*02:05	<u>18% P</u> GBM6P GBM6R GBM11P GBM11R GBM20R ZH613	<u>17% R</u> ZH617 ZH681 ZH720 ZH753 ZH757	Replication factor C subunit 1 (RFC1; P35251)	63% P 63% R	2 30%	17%
SRAPSTYTY	C*07:01 C*07:02	<u>18% P</u> GBM4P GBM4R GBM8P GBM10R GBM11P GBM16P	<u>17% R</u> GBM16R GBM18R ZH616 ZH681 ZH757	Radial spoke head protein 3 homolog (RSPH3; Q86UC2)	26% P 21% R	4 6%	4%
VLFDELLM	A*02:01	<u>18% P</u> GBM10R GBM13P GBM13R GBM20P GBM20R ZH616	<u>17% R</u> ZH617 ZH681 ZH753 ZH757 ZH761	Non-syndromic hearing impairment protein 5 (DFNA5; O60443)	55% P 38% R	7 4%	7%
VVAEELENV	A*02:01 A*02:05	<u>18% P</u> GBM6P GBM6R GBM10R GBM11P GBM11R GBM14R	<u>17% R</u> GBM21P ZH613 ZH617 ZH681 ZH761	F-box only protein 22 (FBXO22; Q8NEZ5)	24% P 21% R	8 12%	6%
TLLLWPINK	A*03:01 A*11:01	<u>18% P</u> GBM4P GBM4R GBM6R GBM7P GBM16P GBM16R	<u>17% R</u> GBM17P GBM18R ZH631 ZH678 ZH761	1-acyl-sn-glycerol-3- phosphate acyltransferase delta (AGPAT4; Q9NRZ5)	34% P 33% R	3 4%	3%
ESDLYSLAHSY	A*01:01	<u>16% P</u> GBM3P GBM5P GBM5R GBM9R GBM13R GBM16P	<u>21% R</u> GBM16R ZH617 ZH645 ZH654 ZH784	Nuclear protein 1 (NUPR1; O60356)	18% P 21% R	32 5%	1%
GTDYINASY	A*01:01	<u>16% P</u> GBM3P GBM5P GBM5R GBM9R GBM13R GBM16P	<u>21% R</u> GBM16R GBM17R ZH617 ZH645 ZH654	Receptor-type tyrosine- protein phosphatase gamma/zeta (PTPRG / PTPRZ; P23470 / P23471)	61% / 97% P 46% / 83% R	0 7% / 6%	12% / 5%

Appendix: Supplement of CHAPTER 2

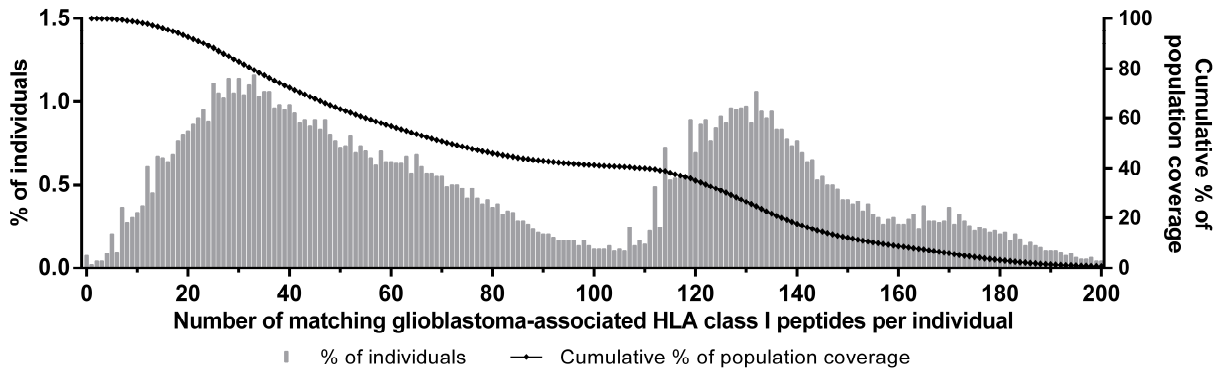
KTIEDTLMTV	A*02:01 A*02:05 C*16:01	<u>16% P</u> GBM6P GBM6R GBM10R GBM11P GBM11R GBM13R	<u>21% R</u> GBM20R ZH613 ZH617 ZH720 ZH757	Arfaptin-1 (ARFIP1; P53367)	47% P 38% R	15 14%	7%
RTDTALTNTY	A*01:01	<u>16% P</u> GBM3P GBM5P GBM5R GBM9R GBM13R GBM16P	<u>21% R</u> GBM16R GBM17R ZH617 ZH645 ZH654	Paired box protein Pax-6 (PAX6; P26367)	24% P 21% R	2 1%	0%
IPDRSGPEL	B*07:02 B*35:02 B*35:03	<u>16% P</u> GBM4R GBM7P GBM10R GBM16P GBM16R GBM18R	<u>21% R</u> GBM21P GBM23P GBM23R ZH616 ZH681	Progressive ankylosis protein homolog (ANKH; Q9HCJ1)	76% P 79% R	13 16%	12%
GLIDEQIL	A*02:01	<u>16% P</u> GBM7P GBM10R GBM13P GBM13R GBM14R	<u>17% R</u> ZH645 ZH678 ZH681 ZH753 ZH757	Dystonin (DST; Q03001)	97% P 92% R	8 41%	55%
KILDTSVAYV	A*02:01	<u>16% P</u> GBM10R GBM11P GBM13R GBM20P GBM20R	<u>17% R</u> GBM21P ZH617 ZH720 ZH753 ZH757	Kinesin-like protein KIF1B (KIF1B; O60333)	95% P 79% R	0 27%	26%
TAISRIYTV	A*02:01 A*02:05 B*08:01 B*51:01 C*12:03	<u>21% P</u> GBM6P GBM6R GBM9P GBM11P GBM11R GBM13P	<u>17% R</u> GBM16P GBM16R GBM18P GBM18R ZH613 ZH654	Carboxypeptidase E (CPE; P16870)	87% P 71% R	0 10%	14%
VTAQVVGTERY	A*01:01	<u>18% P</u> GBM5P GBM5R GBM9P GBM9R GBM13P GBM13R	<u>21% R</u> GBM16P GBM16R GBM17R ZH617 ZH645 ZH654	Phospholipase D2 (PLD2; O149399)	32% P 29% R	23 9%	8%
FPAGPPSHSL	B*07:02 B*35:02 B*35:03	<u>18% P</u> GBM4P GBM10R GBM16P GBM16R GBM18P GBM18R	<u>21% R</u> GBM21P GBM22P GBM22R GBM23P GBM23R ZH681	Peptidyl-prolyl cis-trans isomerase FKBP10 (FKBP10; Q96AY3)	42% P 25% R	11 9%	5%
RLKEGANINK	A*03:01	<u>18% P</u> GBM4P GBM4R GBM6P GBM6R GBM16P GBM16R	<u>21% R</u> GBM17R GBM18P GBM23P GBM23R ZH761 ZH791	Kinesin-like protein KIF1A/B/C (KIF1A/B/C; Q12756 / O60333 / O43896)	87% / 95% / 37% P 79% / 79% / 29% R	1 14% / 27% / 11%	15% / 26% / 9%
AVDPGLLGY	A*01:01 B*15:01	<u>18% P</u> GBM3P GBM5P GBM5R GBM9P GBM13P GBM13R	<u>17% R</u> GBM16P GBM16R GBM17R ZH617 ZH645	Atrophin-1 (ATN1; P54259)	68% P 71% R	17 12%	10%
FSSSHEGFSY	A*01:01 B*57:01 C*02:02	<u>18% P</u> GBM3P GBM5P GBM5R GBM9P GBM13P GBM13R	<u>17% R</u> GBM16P GBM16R GBM17R ZH617 ZH654	ETS translocation variant 5 (ETV5; P41161)	63% P 54% R	7 11%	8%

Appendix: Supplement of CHAPTER 2

GQDGSVVQF	B*15:01 C*04:01 C*05:01	<u>18% P</u> GBM2P GBM2R GBM5P GBM5R GBM12R GBM15P	<u>17% R</u> GBM20P GBM20R ZH616 ZH617 ZH802	Small ubiquitin-related modifier 2/3/4 (SUMO2/3/4; P61956 / P55854 / Q6EEV6)	26% / 34% / 18% P 29% / 38% / 17% R	27 24% / 21% / 7%	13% / 12% / 2%
LSSGPLTQK	A*03:01 A*11:01	<u>18% P</u> GBM4P GBM4R GBM6P GBM7P GBM7R GBM16P	<u>17% R</u> GBM16R GBM17R ZH631 ZH678 ZH791	Brain and acute leukemia cytoplasmic protein (BAALC; Q8WXS3)	45% P 54% R	2 2%	3%
VTDESIPSY	A*01:01	<u>18% P</u> GBM3P GBM5P GBM9P GBM9R GBM13P GBM13R	<u>17% R</u> GBM16P GBM16R GBM17R ZH617 ZH654	A-kinase anchor protein 9 OS=Homo sapiens GN=AKAP9; Q99996)	61% P 50% R	11 34%	32%
YRPLTVLTF	C*07:02	<u>16% P</u> GBM2P GBM4P GBM4R GBM10R GBM11P GBM11R	<u>25% R</u> GBM16P GBM16R GBM18P GBM18R ZH757 ZH784	Transmembrane and TPR repeat-containing protein 3/4 (TMTC3/4; Q6ZXV5 / Q5T4D3)	53% / 39% P 63% / 46% R	15 18% / 7%	18% / 7%
FLDPAQRDLY	A*01:01	<u>16% P</u> GBM5P GBM5R GBM9P GBM9R GBM13R GBM16P	<u>21% R</u> GBM16R GBM17R ZH617 ZH645 ZH654	Zinc finger protein 14 homolog (ZFP14; Q9HCL3)	18% P 25% R	13 4%	3%
TPASAGHVW	B*07:02 B*35:01	<u>16% P</u> GBM4P GBM4R GBM6P GBM7P GBM10R GBM12R	<u>21% R</u> GBM16R GBM18P GBM18R ZH681	Transcription factor SOX-9 (SOX9; P48436)	82% P 79% R	11 15%	7%
SVDSNLLSDY	A*01:01	<u>16% P</u> GBM3P GBM5P GBM5R GBM9P GBM9R GBM13R	<u>21% R</u> GBM16P GBM16R GBM17R ZH617 ZH645	Oxidative stress-induced growth inhibitor 2 (OSGIN2; Q9Y236)	26% P 33% R	39 13%	7%
YADGESFLGY	A*01:01 C*02:02	<u>16% P</u> GBM3P GBM5P GBM5R GBM9P GBM9R GBM16P	<u>21% R</u> GBM16R GBM17R ZH617 ZH645 ZH784	Proteasome subunit beta type-4 (PSMB4; P28070)	58% P 42% R	19 28%	20%
AVAPQVPAL	A*02:01 A*02:05 C*01:02 C*12:03 C*15:02	<u>16% P</u> GBM6P GBM6R GBM7P GBM10R GBM11P	<u>17% R</u> GBM11R ZH613 ZH681 ZH753 ZH757	Protein FAM118B (FAM118B; Q9BPY3)	18% P 21% R	2 2%	0%
MTEVLPNQRY	A*01:01	<u>16% P</u> GBM3P GBM5P GBM9P GBM9R GBM13R	<u>17% R</u> GBM16P GBM16R GBM17R ZH617 ZH645	SEC14-like protein 2 (SEC14L2; O76054)	32% P 25% R	2 1%	1%
NRYINIVAY	B*27:05 C*07:01 C*07:02	<u>16% P</u> GBM4P GBM4R GBM10R GBM11P GBM16P	<u>17% R</u> GBM16R GBM18R ZH616 ZH681 ZH757	Receptor-type tyrosine-protein phosphatase zeta (PTPRZ1; P23471)	97% P 83% R	0 6%	5%
FVDPYPVNKY	A*01:01 C*02:02	<u>16% P</u> GBM3P GBM5P GBM5R	<u>17% R</u> GBM16R GBM17R ZH617	Kelch-like protein 15 (KLHL15; Q96M94)	24% P 29% R	18 12%	15%

Appendix: Supplement of CHAPTER 2

Antigen (UniProt accession)	Protein frequency on glioblastomas	Peptide sequence	Frequency of positive tumors	Protein frequency on non-GBM tumors	Protein frequency on benign samples (n=364)
RPLVGPLAL	B*07:02	GBM9P	ZH645	Potassium/sodium hyperpolarization-activated cyclic nucleotide-gated channel 2 (HCN2; Q9UL51)	16% P 21% R
		GBM9R	ZH654		
		16% P	17% R		
		GBM2P	GBM16P		
		GBM4P	GBM16R		
RVFSTSPAK	A*03:01	GBM4R	GBM18R	Calcium and integrin-binding protein 1 (CIB1; Q99828)	76% P 71% R
		GBM6P	GBM23P		
		GBM16P	GBM23R		
		GBM16R	ZH761		
		GBM17R	ZH791		
TADGKTYYY	A*01:01 C*02:02	16% P	17% R	Transcription elongation regulator 1 (TCERG1; O14776)	29% P 38% R
		GBM3P	GBM16P		
		GBM5P	GBM16R		
		GBM5R	GBM17R		
		GBM9R	ZH617		
TVMQLRNEL	B*07:02 C*01:02 C*02:02	16% P	17% R	Neuron navigator 2 (NAV2; Q8IVL1)	63% P 38% R
		GBM4P	GBM16R		
		GBM4R	GBM18R		
		GBM7P	ZH616		
		GBM10R	ZH681		
		GBM16P	ZH757		



Supplementary Figure 3. Population coverage of glioblastoma-associated HLA-A, -B, and -C ligands. Using the population coverage tool provided by the IEDB Analysis Resource, the world population coverage of the 357 glioblastoma-associated peptides was calculated. The percentage of individuals with a specific number of matching peptides (max. of 235) is indicated by bar charts (associated with the left y-axis). The line diagram (associated with the right y-axis) shows the cumulative percentage of population coverage. The candidate target peptides cover 99.93% of the world population (first diamond on line diagram counted from the left) meaning that only 0.07% of all individuals are negative for all HLA-A, -B, and -C allotypes for which glioblastoma-associated peptides were defined. On average, 84 peptides are expected to match per patient worldwide.

Supplementary Table 4. Glioblastoma-exclusive HLA class II-presented peptides derived from glioblastoma-associated HLA presentation hotspots. Peptides already reported to derive from glioblastoma-associated antigens were excluded from this listing. In turn, some of those antigens not designated as glioblastoma-associated due to a CNS-associated expression profile are listed herein with glioblastoma-associated peptides. The number of positive tumors other than glioblastoma was based on n=585 HLA class II peptidome datasets. Frequencies of positive tumors are given separately for n=38 primary (P) and n=24 recurrent (R) glioblastomas.

Antigen (UniProt accession)	Protein frequency on glioblastomas	Peptide sequence	Frequency of positive tumors	Protein frequency on non-GBM tumors	Protein frequency on benign samples (n=364)
Fatty acid-binding protein, brain (FABP7; O15540)	26% P	DKVVIRTLSTFKN	3% P / 0% R	ZH616	1%
	29% R	GDKVVIRTLSTFKN	3% P / 0% R	ZH616	0
		GDKVVIRTLSTFKNTE	3% P / 0% R	ZH616	0

Appendix: Supplement of CHAPTER 2

		KPTVIISQEGDKVVI	3% P / 5% R	GBM20P	1	
			GBM20R			
		KPTVIISQEGDKVVIR	24% P / 25% R	GBM5P	7	
			GBM8P	GBM9R		
			GBM12P	GBM13P		
			GBM13R	GBM14R		
			GBM15P	GBM18P		
			GBM18R	GBM20P		
			GBM20R	GBM22P		
			GBM22R	ZH645		
		KPTVIISQEGDKVVIRT	8% P / 4% R	GBM12P	0	
			GBM13P	GBM20P		
			GBM20R			
		VIRTLSTFKNTEISF	0% P / 4% R	GBM10R	0	
Antithrombin-III (SERPINC1; P01008)	89% P 83% R				50%	48%
		ASMMYQEGKFRYRR	5% P / 4% R	GBM11P	0	
			GBM17R	ZH681		
		SASMMYQEGKFRYR	0% P / 4% R	GBM14R	0	
		SASMMYQEGKFRYRR	18% P / 17% R	GBM4R	5	
			GBM6P	GBM7P		
			GBM11P	GBM11R		
			GBM14P	GBM14R		
			GBM21R	ZH616		
			ZH757	ZH791		
		SASMMYQEGKFRYRRV	3% P / 0% R	GBM6P	0	
Fibronectin (FN1; P02751)	95% P 88% R				54%	65%
		GQQMIFEEHGFRRTPP	8% P / 8% R	GBM6P	5	
			GBM14P	GBM14R		
			GBM21P	GBM21R		
		QMIFEEHGFRRTPPT	5% P / 0% R	GBM11P	0	
			GBM14P			
		QQMIFEEHGFRRTPP	16% P / 21% R	GBM9R	11	
			GBM10R	GBM14P		
			GBM14R	GBM16P		
			GBM16R	GBM21P		
			GBM21R	ZH757		
			ZH791	ZH829		
		VGQQMIFEEHGFRRTPP	3% P / 0% R	GBM6P	0	
		VGQQMIFEEHGFRRTPPT	3% P / 0% R	GBM16P	3	
Superoxide dismutase [Mn], mitochondrial (SOD2; P04179)	68% P 54% R				19%	23%
		EHAYYLQYKNVRPD	3% P / 0% R	ZH645	0	
		EHAYYLQYKNVRPDY	3% P / 0% R	ZH645	0	
		GTTGLIPLLIDVWEH	13% P / 13% R	GBM6P	9	
			GBM7P	GBM12P		
			GBM12R	GBM14P		
			GBM14R	GBM19P		
			ZH753			
		GTTGLIPLLIDVWEHA	11% P / 8% R	GBM6P	6	
			GBM12P	GBM14P		
			GBM14R	GBM19P		
			ZH742			
		TGLIPLLIDVWEH	0% P / 8% R	GBM14R	3	
			ZH753			
		TTGLIPLLIDVWE	3% P / 4% R	GBM19P	0	
			ZH753			
		TTGLIPLLIDVWEH	19% P / 21% R	GBM2P	15	
			GBM2R	GBM6P		
			GBM6R	GBM7P		
			GBM12P	GBM12R		
			GBM14P	GBM14R		
			GBM15P	GBM19P		
			ZH753			
		TTGLIPLLIDVWEHA	13% P / 8% R	GBM6P	4	
			GBM7P	GBM12P		
			GBM14P	GBM14R		
			GBM19P	ZH753		
		WEHAYYLQYKNVRP	3% P / 0% R	ZH645	0	
		WEHAYYLQYKNVRPD	5% P / 0% R	ZH645	2	
			ZH681			
		WEHAYYLQYKNVRPDY	3% P / 0% R	ZH645	2	
Collagen alpha- 2(V) chain (COL5A2; P05997)	34% P 29% R				12%	3%
		ARLPIIDLAPVDVGGTD	11% P / 4% R	GBM5P	21	
			GBM13P	GBM18P		
			GBM18R	ZH645		
		GNVGKTVFEYRTQNVAR	0% P / 4% R	GBM14R	5	
		RLPIIDLAPVDVGG	0% P / 4% R	GBM18R	7	
		RLPIIDLAPVDVGGTD	13% P / 4% R	GBM5P	26	
			GBM12P	GBM13P		
			GBM18P	GBM18R		
			ZH645			

Appendix: Supplement of CHAPTER 2

	VARLPIIDLAPVDVGGTD	0% P / 4% R	GBM18R	16	
	VGKTVFEYRTQNVAR	8% P / 13% R	GBM11P	14	
		GBM14P	GBM14R		
		GBM16R	GBM21P		
		GBM21R			
Secretogranin-2				7%	5%
(SCG2; P13521)				0	
	DDVSKVIAYLKRL	3% P / 4% R	GBM3P	0	
		GBM23R			
	DDVSKVIAYLKRLVNA	3% P / 4% R	GBM3P	1	
		GBM22R			
	DDVSKVIAYLKRLVNAA	3% P / 0% R	GBM3P	1	
	DDVSKVIAYLKRLVNAAG	3% P / 4% R	GBM3P	5	
		GBM22R			
	DDVSKVIAYLKRLVNAAGS	3% P / 0% R	GBM3P	0	
	DDVSKVIAYLKRLVNAAGSG	3% P / 4% R	GBM3P	2	
		GBM22R			
	DVSKVIAYLKRL	3% P / 0% R	GBM3P	0	
	DVSKVIAYLKRLVNA	3% P / 4% R	GBM3P	0	
		GBM22R			
	DVSKVIAYLKRLVNAA	3% P / 4% R	GBM3P	5	
		GBM22R			
	DVSKVIAYLKRLVNAAG	11% P / 13% R	GBM3P	6	
		GBM3R	GBM22P		
		GBM22R	GBM23P		
		GBM23R	ZH810		
	DVSKVIAYLKRLVNAAGSG	3% P / 4% R	GBM3P	0	
		GBM22R			
	KVIAYLKRLVNA	0% P / 4% R	GBM3R	0	
	KVIAYLKRLVNAA	3% P / 4% R	GBM3P	0	
		GBM3R			
	KVIAYLKRLVNAAG	3% P / 4% R	GBM3P	0	
		GBM3R			
	LSDDVSKVIAYLKRLVNAAAG	0% P / 4% R	GBM22R	0	
	LSDDVSKVIAYLKRLVNAAGSG	3% P / 4% R	GBM3P	1	
		GBM22R			
	SDDVSKVIAYLKRLVNAAAG	3% P / 4% R	GBM3P	2	
		GBM22R			
	SDDVSKVIAYLKRLVNAAGSG	3% P / 4% R	GBM3P	1	
		GBM22R			
	SKVIAYLKRLVNA	3% P / 4% R	GBM3P	0	
		GBM3R			
	SKVIAYLKRLVNAA	3% P / 8% R	GBM3P	1	
		GBM3R	GBM22R		
	SKVIAYLKRLVNAAG	3% P / 8% R	GBM3P	0	
		GBM22R	GBM23R		
	VSKVIAYLKRLVNA	5% P / 13% R	GBM3P	3	
		GBM3R	GBM22P		
		GBM22R	GBM23R		
	VSKVIAYLKRLVNAA	21% P / 21% R	GBM3P	11	
		GBM3R	GBM5P		
		GBM5R	GBM19P		
		GBM22P	GBM22R		
		GBM23R	ZH678		
		ZH750	ZH784		
		ZH791	ZH810		
	VSKVIAYLKRLVNAAG	21% P / 21% R	GBM3P	11	
		GBM3R	GBM5P		
		GBM5R	GBM22P		
		GBM22R	GBM23P		
		GBM23R	ZH678		
		ZH750	ZH784		
		ZH791	ZH810		
	VSKVIAYLKRLVNAAGSG	0% P / 4% R	GBM23R	0	
	FPNPYNQEKVLPRLP	3% P / 4% R	GBM10R	0	
		GBM11P			
	FPNPYNQEKVLPRLPY	21% P / 21% R	GBM4R	4	
		GBM6P	GBM7P	0	
		GBM9P	GBM9R		
		GBM10R	GBM11P		
		GBM11R	GBM16P		
		GBM16R	ZH616		
		ZH757	ZH791		
	FPNPYNQEKVLPRLPYG	21% P / 25% R	GBM4R	4	
		GBM6P	GBM7P		
		GBM9P	GBM9R		
		GBM10R	GBM11P		
		GBM11R	GBM16P		
		GBM16R	GBM17R		
		ZH616	ZH757		
		ZH791			

Appendix: Supplement of CHAPTER 2

		FPNPYNQEKVLPRLPYGA	11% P / 13% R	GBM4R	0	
			GBM6P	GBM7P		
			GBM11P	GBM11R		
			GBM16P	GBM16R		
		FPNPYNQEKVLPRLPYGAG	3% P / 8% R	GBM11P	1	
			GBM11R	GBM17R		
		NPYNQEKVLPRLPYGAG	3% P / 4% R	GBM11P	0	
			GBM11R			
		TSYFPNPYNQEKVLPRLPYG	3% P / 0% R	GBM6P	0	
		YFPNPYNQEKVLPRLPYG	8% P / 4% R	GBM6P	0	
			GBM7P	GBM16P		
			GBM16R			
		YFPNPYNQEKVLPRLPYGA	3% P / 0% R	GBM7P	0	
Neural cell adhesion molecule 1 (NCAM1; P13591)	61% P 63% R				5%	6%
		DVRFIVLSNNYLQ	8% P / 0% R	GBM6P	0	
			GBM7P	GBM12P		
		DVRFIVLSNNYLQIR	8% P / 4% R	GBM6P	1	
			GBM7P	GBM19P		
			ZH753			
		FIVLSNNYLQIRG	3% P / 0% R	ZH802	0	
		KDVRFIVLSNNYLQ	3% P / 4% R	GBM14R	1	
			ZH761			
		KDVRFIVLSNNYLQIR	5% P / 4% R	GBM7R	0	
			GBM19P	ZH761		
		KDVRFIVLSNNYLQIRG	3% P / 0% R	GBM7P	0	
		LSNNYLQIRGIKKTDE	13% P / 17% R	GBM4R	2	
			GBM6P	GBM7P		
			GBM7R	GBM10R		
			GBM16P	GBM16R		
			ZH616	ZH757		
		LSNNYLQIRGIKKTDEG	5% P / 4% R	GBM4R	0	
			GBM16P	ZH616		
		NNYLQIRGIKKTDE	11% P / 8% R	GBM4R	0	
			GBM6P	GBM7P		
			GBM10R	GBM16P		
			ZH616			
		NYLQIRGIKKTDE	3% P / 0% R	ZH616	0	
		SNNYLQIRGIKK	5% P / 8% R	GBM4R	0	
			GBM7P	GBM10R		
			ZH616			
		SNNYLQIRGIKKT	11% P / 4% R	GBM4R	1	
			GBM6P	GBM7P		
			GBM16P	ZH616		
		SNNYLQIRGIKKT	8% P / 4% R	GBM7P	0	
			GBM10R	GBM16P		
			ZH616			
		SNNYLQIRGIKKTDE	13% P / 21% R	GBM4R	0	
			GBM6P	GBM7P		
			GBM9R	GBM10R		
			GBM11P	GBM11R		
			GBM16P	GBM16R		
			ZH757			
		SNNYLQIRGIKKTDEG	8% P / 8% R	GBM4R	0	
			GBM7P	GBM10R		
			GBM16P	ZH616		
		SNNYLQIRGIKKTDEGT	3% P / 0% R	ZH616	0	
		VRFIVLSNNYLQIR	3% P / 0% R	ZH802	0	
Receptor-type tyrosine-protein phosphatase zeta (PTPRZ1; P23471)	8% P 4% R				2%	4%
		IDEDLTQVNVNKKLFQGW	3% P / 0% R	GBM19P	0	
		KQSPINIDEDLTQVN	0% P / 4% R	GBM10R	0	
		KQSPINIDEDLTQVNVN	5% P / 8% R	GBM10R	1	
			GBM16P	GBM20P		
			GBM20R			
		NSPKQSPINIDEDLTQVNVN	3% P / 0% R	GBM16P	0	
		NSPKQSPINIDEDLTQVNVN	5% P / 0% R	GBM13P	0	
			GBM16P			
		QSPINIDEDLTQVN	21% P / 17% R	GBM9P	2	
			GBM9R	GBM10R		
			GBM13P	GBM15P		
			GBM16P	GBM16R		
			GBM18P	GBM20R		
			ZH617	ZH654		
			ZH802			
		QSPINIDEDLTQVNV	5% P / 4% R	GBM20R	0	
			ZH654	ZH802		

Appendix: Supplement of CHAPTER 2

		QSPINIDEDLTQVNVN	18% P / 25% R	GBM9P GBM9R GBM13P GBM16P GBM18P GBM20R ZH654	GBM10R GBM13R GBM16R GBM18R ZH617 ZH802	2	
		QSPINIDEDLTQVNVNL	3% P / 4% R	GBM16P	GBM10R	0	
		SPINIDEDLTQVN	3% P / 4% R	ZH802	GBM10R	0	
		SPINIDEDLTQVNV	3% P / 0% R		ZH802	0	
		SPINIDEDLTQVNVN	16% P / 13% R	GBM13P GBM16R GBM20R ZH654	GBM10R GBM16P GBM18P ZH617 ZH802	0	
		SPINIDEDLTQVNVNL	5% P / 8% R	GBM16R ZH802	GBM10R GBM18P	0	
		SPKQSPINIDEDLTQVN	16% P / 17% R	GBM9R GBM16P GBM18R ZH617 ZH802	GBM9P GBM10R GBM18P GBM20R ZH654	1	
		SPKQSPINIDEDLTQVNV	0% P / 4% R		GBM20R	1	
		SPKQSPINIDEDLTQVNVN	18% P / 17% R	GBM9P GBM13P GBM16R GBM20P ZH617	GBM8P GBM10R GBM16P GBM18R GBM20R ZH802	1	
		SPKQSPINIDEDLTQVNVNL	5% P / 13% R	GBM13P GBM16R GBM20R	GBM10R GBM16P GBM20R	1	
		SPKQSPINIDEDLTQVNVNLK	0% P / 4% R		GBM10R	0	
Tenascin (TNC; P24821)	76% P 67% R	ARVATYLPAPEGLKFKS	3% P / 0% R		GBM16P	0	
		IPVSARVATYLPAPEGLKFKS	3% P / 0% R		GBM16P	0	
		RVATYLPAPEGLKFKS	8% P / 0% R	GBM16P	GBM6P ZH616	0	
		VATYLPAPEGLKFK	8% P / 17% R	GBM6P GBM10R GBM16R	GBM4R GBM9R GBM16P ZH616	1	
		VATYLPAPEGLKFKS	16% P / 13% R	GBM6P GBM10R GBM16P ZH616	GBM4R GBM7P GBM11P GBM16R ZH757	2	
		EPGQEYNVLLTAEKGRH	11% P / 8% R	GBM21R GBM22R ZH761	GBM21P GBM22P ZH654	0	
		EPGQEYNVLLTAEKGRHKS	11% P / 8% R	GBM21R GBM22R ZH761	GBM21P GBM22P ZH654	1	
		NVLLTAEKGRHKS	5% P / 8% R	GBM6P GBM16P	GBM4R GBM10R	0	
		QEYNVLLTAEKGRHK	5% P / 4% R		GBM21P ZH654	0	
		YNVLLTAEKGRHKS	3% P / 0% R		GBM3P	0	
Chitinase-3-like protein 1 (CHI3L1; P36222)	89% P 96% R	AEFIKEAQP GK	3% P / 13% R	GBM10R GBM16R	GBM4R GBM16P	0	8%
		AEFIKEAQP GKQ	8% P / 8% R	GBM6P GBM16P	GBM4R GBM10R ZH616	0	
		AGKVTIDSSYDIA	0% P / 4% R		GBM10R	0	
		AGKVTIDSSYDIAK	0% P / 4% R		GBM10R	0	
		AQPGKKQLLSAALSAGKV	3% P / 0% R		ZH654	0	
		DKQHFTTLIKEMK	3% P / 0% R		ZH791	0	
		DKQHFTTLIKEMKA	3% P / 4% R		GBM11P GBM17R	0	

Appendix: Supplement of CHAPTER 2

DKQHFTTLIKEMKAE	13% P / 8% R	GBM11P	1
	GBM11R	GBM17P	
	GBM17R	ZH645	
	ZH681	ZH802	
DKQHFTTLIKEMKAEF	3% P / 0% R	GBM11P	0
DKQHFTTLIKEMKAEFIKEAQPG	11% P / 4% R	GBM3P	1
	GBM5P	GBM11P	
	GBM22P	GBM22R	
	ZH791		
EAQPGKKQLLSAALSAGK	3% P / 0% R	ZH654	0
EAQPGKKQLLSAALSAGKV	3% P / 0% R	ZH654	0
EMKAEFIKEAQPGKKQ	3% P / 4% R	GBM10R	0
	GBM16P		
FTTLIKEMKAEFIKE	0% P / 4% R	GBM14R	0
FTTLIKEMKAEFIKEA	0% P / 4% R	GBM14R	0
FTTLIKEMKAEFIKEAQPG	5% P / 8% R	GBM2R	1
	GBM12P	GBM14R	
	GBM19P		
GKKQLLSAALSAGKV	3% P / 0% R	ZH654	0
IKEAQPGKKQLLSAALSA	3% P / 0% R	ZH654	0
IKEAQPGKKQLLSAALSAGKV	5% P / 4% R	GBM20P	0
	GBM20R	ZH654	
IKEMKAEFIKEA	0% P / 4% R	GBM14R	0
IKEMKAEFIKEAQPG	5% P / 4% R	GBM12P	1
	GBM14R	ZH654	
KAEFIKEAQPGKK	0% P / 8% R	GBM4R	0
	GBM10R		
KAEFIKEAQPGKKQ	11% P / 13% R	GBM4R	0
	GBM6P	GBM10R	
	GBM11P	GBM16P	
	GBM16R	ZH616	
KEAQPGKKQLLSAALSAGK	3% P / 0% R	GBM12P	0
LIKEMKAEFIKE	0% P / 4% R	GBM14R	0
LIKEMKAEFIKEA	0% P / 4% R	GBM14R	0
LIKEMKAEFIKEAQPG	3% P / 4% R	GBM12P	1
	GBM14R		
MKAEFIKEAQPGKK	5% P / 4% R	GBM6P	0
	GBM9P	GBM10R	
MKAEFIKEAQPGKKQ	8% P / 8% R	GBM4R	0
	GBM6P	GBM9P	
	GBM10R	GBM16P	
QPGKKQLLSAALSAGK	3% P / 4% R	GBM20R	0
	ZH654		
QPGKKQLLSAALSAGKV	11% P / 8% R	GBM5P	0
	GBM20P	GBM20R	
	GBM23R	ZH645	
	ZH654		
SAGKVTIDSSYDIAK	0% P / 4% R	GBM10R	0
TLIKEMKAEFIK	5% P / 4% R	GBM14R	0
	GBM21P	ZH616	
TLIKEMKAEFIKE	8% P / 4% R	GBM12P	1
	GBM14R	GBM21P	
	ZH616		
TLIKEMKAEFIKEA	8% P / 8% R	GBM2R	1
	GBM12P	GBM14P	
	GBM14R	ZH616	
TLIKEMKAEFIKEAQPG	16% P / 25% R	GBM2R	3
	GBM6P	GBM7P	
	GBM12P	GBM12R	
	GBM14P	GBM14R	
	GBM15P	GBM15R	
	GBM21P	GBM21R	
	ZH753		
TTLIKEMKAEFIK	0% P / 4% R	GBM14R	0
TTLIKEMKAEFIKE	5% P / 4% R	GBM12P	0
	GBM14P	GBM14R	
TTLIKEMKAEFIKEA	5% P / 13% R	GBM2R	0
	GBM12P	GBM14R	
	GBM15P	ZH753	
TTLIKEMKAEFIKEAQPG	3% P / 17% R	GBM2R	1
	GBM12P	GBM12R	
	GBM14R	ZH753	
YPGRRDQHFHTTLIKEMKAE	3% P / 0% R	GBM11P	0
ATVHRILGQQVPYATKG	3% P / 0% R	ZH654	1
DDQESVSKSVQYLKDRQLAG	0% P / 4% R	GBM14R	0
DQESVSKSVQYLKDRQLAG	0% P / 4% R	GBM14R	0
ESVSKSVQYLKDRQ	3% P / 4% R	GBM18P	1
	GBM18R		
ESVSKSVQYLKDRQLAG	0% P / 4% R	GBM14R	0
GATVHRILGQQVPYATKG	5% P / 4% R	GBM20P	0
	GBM20R	ZH654	

Appendix: Supplement of CHAPTER 2

		GNQWVGYYDDQESVKS	0% P / 4% R	GBM20R	0	
		KSKVQYLKDRQLA	3% P / 0% R	ZH654	0	
		KSKVQYLKDRQLAG	0% P / 4% R	GBM10R	0	
		SVKSKVQYLKDRQLAG	0% P / 4% R	GBM14R	0	
		TVHRILGQQVPYA	3% P / 0% R	ZH654	0	
		TVHRILGQQVPYAT	3% P / 0% R	ZH654	0	
		TVHRILGQQVPYATK	8% P / 4% R	GBM18P	1	
			GBM20P	GBM20R		
			ZH654			
		TVHRILGQQVPYATKG	11% P / 13% R	GBM9P	2	
			GBM9R	GBM18P		
			GBM18R	GBM20P		
			GBM20R	ZH654		
		TVHRILGQQVPYATKGN	3% P / 0% R	ZH654	0	
		TVHRILGQQVPYATKGNQ	3% P / 0% R	ZH654	0	
		VHRILGQQVPYA	3% P / 0% R	ZH654	0	
		VHRILGQQVPYAT	3% P / 0% R	ZH654	0	
		VHRILGQQVPYATK	8% P / 0% R	GBM18P	0	
			ZH654	ZH802		
		VHRILGQQVPYATKG	11% P / 4% R	GBM18P	1	
			GBM20P	GBM20R		
			ZH654	ZH802		
		VKSKVQYLKDRQLA	3% P / 0% R	ZH654	0	
		VKSKVQYLKDRQLAG	16% P / 21% R	GBM4R	3	
			GBM6P	GBM9P		
			GBM9R	GBM10R		
			GBM11P	GBM14P		
			GBM14R	GBM16P		
			GBM16R	ZH791		
		VKSKVQYLKDRQLAGA	0% P / 4% R	GBM10R	0	
		WVGYYDDQESVKS	5% P / 4% R	GBM9P	0	
			GBM20P	GBM20R		
		WVGYYDDQESVKS	5% P / 8% R	GBM9P	1	
			GBM9R	GBM20P		
			GBM20R			
		WVGYYDDQESVKS	3% P / 0% R	GBM20P	0	
		YDDQESVKS	0% P / 4% R	GBM14R	0	
Transforming growth factor beta-2 (TGFB2; P61812)	37% P 38% R				4%	3%
		AEFRVFRLQNP	8% P / 0% R	GBM18P	2	
			ZH654	ZH802		
		AEFRVFRLQNP	3% P / 0% R	ZH654	0	
		AEFRVFRLQNP	16% P / 8% R	GBM6P	4	
			GBM10R	GBM16P		
			GBM18P	GBM18R		
			ZH616	ZH654		
			ZH802			
		AEFRVFRLQNP	5% P / 0% R	ZH654	0	
			ZH802			
		EFRVFRLQNP	5% P / 0% R	ZH654	0	
			ZH802			
		EFRVFRLQNP	3% P / 0% R	ZH654	0	
		EFRVFRLQNP	21% P / 13% R	GBM4R	3	
			GBM6P	GBM7P		
			GBM9P	GBM10R		
			GBM11P	GBM16P		
			GBM16R	ZH616		
			ZH654	ZH802		
		FRVFRLQNP	0% P / 4% R	GBM10R	0	
		FRVFRLQNP	16% P / 13% R	GBM4R	1	
			GBM6P	GBM7P		
			GBM10R	GBM11P		
			GBM16P	GBM16R		
			ZH616	ZH654		
Vasorin (VASN; Q6EMK4)	39% P 38% R				10%	7%
		DNELRALPPLRLPR	8% P / 4% R	GBM4R	7	
			GBM6P	GBM12P		
			GBM16P			
		GKNRIRHIQPGAFD	3% P / 0% R	ZH616	0	
		GKNRIRHIQPGAFDT	3% P / 0% R	ZH616	0	
		IQPGAFDTLDRLELK	3% P / 0% R	GBM3P	2	
		KLQDNELRALPPLRLPR	11% P / 0% R	GBM6P	5	
			GBM12P	GBM16P		
			ZH616			
		KLQDNELRALPPLRLPRL	5% P / 0% R	GBM6P	1	
			GBM16P			
		LQDNELRALPPLRLPR	8% P / 4% R	GBM4R	7	
			GBM6P	GBM12P		
			GBM16P			
		LQDNELRALPPLRLPRL	5% P / 0% R	GBM6P	2	
			GBM16P			

Appendix: Supplement of CHAPTER 2

		QDNELRALPPLRLPR	3% P / 8% R	GBM6P	13	
			GBM10R	ZH753		
		QDNELRALPPLRLPRL	3% P / 4% R	GBM6P	7	
			GBM10R			
		QPGAFDTLDRLLELK	5% P / 4% R	GBM3P	2	
			GBM22P	GBM22R		
Receptor expression- enhancing protein 4 (REEP4; Q9H6H4)	24% P 25% R	SLSRHEKEIDAYIVQAKERSYETV	24% P / 21% R	GBM7R	1%	1%
			GBM10R	GBM12R	0	
			GBM13P	GBM13R		
			GBM18P	GBM19R		
			GBM23P	ZH678		
			ZH681	ZH750		
			ZH761	ZH791		
			ZH802			
Adseverin (SCIN; Q9Y6U3)	32% P 42% R	AGLQVWRIEKLELVPVPQ	3% P / 4% R	GBM16R	4%	2%
			ZH757		0	
		GDFYVGDAYLVLHTA	3% P / 8% R	GBM4R	0	
			GBM20R	ZH791		
		GLQVWRIEKLELVPVPQ	13% P / 17% R	GBM6P	1	
			GBM9P	GBM9R		
			GBM10R	GBM16P		
			GBM16R	GBM20R		
			GBM21P	ZH757		
		LQVWRIEKLELVPVP	0% P / 4% R	GBM9R	0	
		LQVWRIEKLELVPVPQ	13% P / 17% R	GBM6P	5	
			GBM9P	GBM9R		
			GBM10R	GBM16P		
			GBM16R	GBM20R		
			ZH757	ZH791		
		VPVQSAHGDFYVGDAYLVLHTA	0% P / 4% R	GBM20R	0	
		DKPLIYKNGTSK	8% P / 21% R	GBM4R	1	
			GBM9P	GBM9R		
			GBM10R	GBM11P		
			GBM11R	GBM16P		
			GBM16R			
		DKPLIYKNGTSKK	16% P / 25% R	GBM4R	3	
			GBM6P	GBM7R		
			GBM9P	GBM9R		
			GBM10R	GBM11P		
			GBM11R	GBM16P		
			GBM16R	ZH757		
			ZH791			
		DKPLIYKNGTSKKG	16% P / 21% R	GBM4R	2	
			GBM6P	GBM9P		
			GBM9R	GBM10R		
			GBM11P	GBM11R		
			GBM16P	GBM16R		
			ZH757	ZH791		
		DKPLIYKNGTSKKGQAPAPP	5% P / 4% R	GBM6P	0	
			GBM10R	GBM16P		
		FKDKPLIYKNGTSKKG	3% P / 0% R	GBM6P	0	
		KDKPLIYKNGTSK	3% P / 0% R	GBM6P	0	
		KDKPLIYKNGTSKK	16% P / 21% R	GBM4R	1	
			GBM6P	GBM9P		
			GBM9R	GBM10R		
			GBM11P	GBM11R		
			GBM16P	GBM16R		
			ZH757	ZH791		
		KDKPLIYKNGTSKKG	5% P / 4% R	GBM6P	0	
			GBM10R	GBM11P		
		KEPVHLLSLFKDKPLIYKNGTSK	0% P / 4% R	GBM23R	0	
Scavenger receptor cysteine-rich type 1 protein M130 (CD163; Q86VB7)	37% P 33% R	AAELISVSKFLPIS	8% P / 4% R	GBM9P	14%	12%
			GBM9R	GBM16P	11	
			ZH616			
		AAELISVSKFLPISG	11% P / 4% R	GBM9P	5	
			GBM9R	ZH616		
			ZH757	ZH791		
		AELISVSKFLPIS	5% P / 4% R	GBM9P	10	
			GBM9R	ZH791		
		AELISVSKFLPISG	18% P / 13% R	GBM4R	10	
			GBM9P	GBM9R		
			GBM12R	GBM15P		
			GBM16P	ZH616		
			ZH681	ZH757		
			ZH791			
		ELISVSKFLPIS	5% P / 4% R	GBM9P	1	
			GBM9R	ZH791		

Appendix: Supplement of CHAPTER 2

		ELISVSKFLPISG	5% P / 4% R	GBM9R	2	
			GBM15P	ZH791		
		ENSHESADFSAAELISVSKFLPIS	0% P / 4% R	GBM12R	2	
		HESADFSAAELISVSKFLPIS	3% P / 0% R	GBM16P	0	
		SAAELISVSKFLPIS	3% P / 4% R	GBM12R	4	
			GBM15P			
		SENSHESADFSAAELISVSKFLPIS	3% P / 4% R	GBM9R	0	
			GBM16P			
		SHESADFSAAELISVSKFLPIS	8% P / 13% R	GBM3P	24	
			GBM5R	GBM9P		
			GBM9R	GBM12R		
			GBM16P			
		SHESADFSAAELISVSKFLPISG	3% P / 4% R	GBM9R	4	
			GBM16P			
Brevican core protein (BCAN; Q96GW7)	63% P 38% R	AEDLNGELFLGD	8% P / 4% R	GBM5P	1%	1%
			GBM10R	ZH757	0	
			ZH802			
		AEDLNGELFLGDPP	32% P / 25% R	GBM4R	1	
			GBM5P	GBM5R		
			GBM6P	GBM7P		
			GBM10R	GBM16P		
			GBM16R	GBM17R		
			GBM23P	GBM23R		
			ZH616	ZH631		
			ZH645	ZH654		
			ZH678	ZH681		
			ZH802			
		AEDLNGELFLGDPPE	39% P / 25% R	GBM4R	1	
			GBM5P	GBM5R		
			GBM6P	GBM7P		
			GBM10R	GBM16P		
			GBM16R	GBM17R		
			GBM18P	GBM19P		
			GBM23P	GBM23R		
			ZH616	ZH631		
			ZH645	ZH654		
			ZH681	ZH757		
			ZH802	ZH810		
		DLNGELFLGDPP	3% P / 4% R	GBM5P	0	
			GBM10R			
		DLNGELFLGDPPE	13% P / 8% R	GBM5P	0	
			GBM6P	GBM10R		
			GBM18P	GBM23P		
			GBM23R	ZH802		
		EDLNGELFLGDPP	21% P / 17% R	GBM5P	0	
			GBM6P	GBM10R		
			GBM16R	GBM17R		
			GBM23P	GBM23R		
			ZH631	ZH645		
			ZH681	ZH757		
			ZH802			
		EDLNGELFLGDPPE	11% P / 17% R	GBM6P	0	
			GBM10R	GBM16R		
			GBM17R	GBM23P		
			GBM23R	ZH757		
			ZH802			
		LNGELFLGDPP	3% P / 0% R	ZH802	0	
		LNGELFLGDPPE	3% P / 0% R	ZH802	0	
		YAEDLNGELFLGD	3% P / 0% R	GBM5P	0	
		YAEDLNGELFLGDPP	29% P / 21% R	GBM4R	1	
			GBM5P	GBM5R		
			GBM6P	GBM7P		
			GBM10R	GBM17R		
			GBM23P	GBM23R		
			ZH631	ZH645		
			ZH654	ZH681		
			ZH757	ZH802		
			ZH810			
		YAEDLNGELFLGDPPE	37% P / 25% R	GBM4R	0	
			GBM5P	GBM5R		
			GBM6P	GBM7P		
			GBM10R	GBM16P		
			GBM16R	GBM17R		
			GBM19P	GBM23P		
			GBM23R	ZH631		
			ZH645	ZH654		
			ZH678	ZH681		
			ZH757	ZH802		
			ZH810			

Appendix: Supplement of CHAPTER 2

Prolow-density lipoprotein receptor-related protein 1 (LRP1; Q07954)	95% P 96% R	YAEDLNGELFLGDPPEK	3% P / 0% R ZH757	GBM23P	0	51% 51%			
		DFHLSQSALYW	3% P / 8% R GBM22P	GBM12R GBM22R	0				
		HKGDYSVLVPGLRN	3% P / 4% R GBM10R	GBM6P	0				
		HKGDYSVLVPGLRNT	5% P / 8% R GBM6P ZH616	GBM4R GBM10R	1				
		HKGDYSVLVPGLRNTIA	0% P / 4% R	GBM10R	0				
		IALDFHLSQSAL	0% P / 4% R	GBM22R	0				
		IALDFHLSQSALY	3% P / 0% R	GBM22P	0				
		IALDFHLSQSALYW	5% P / 8% R GBM12R GBM22R	GBM12P GBM22P	0				
		IALDFHLSQSALYWT	5% P / 4% R	GBM12P	0				
		IALDFHLSQSALYWTD	3% P / 4% R GBM22R	GBM22R GBM22P	0				
		KGDYSVLVPGLRN	0% P / 8% R GBM10R	GBM4R	0				
		KGDYSVLVPGLRNT	3% P / 8% R GBM6P	GBM4R GBM10R	0				
		LDFHLSQSALYW	3% P / 4% R GBM22R	GBM22P	1				
		LDFHLSQSALYWT	3% P / 0% R	GBM22P	0				
		LRNTIALDFHLSQS	3% P / 0% R	GBM16P	0				
		LVPGLRNTIALDFHL	5% P / 8% R GBM5R GBM23R	GBM5P GBM13P	2				
		VPLRNTIALDFHL	3% P / 0% R	GBM13P	0				
		Contactin-1 (CNTN1; Q12860)	45% P 46% R	KPIPTIRWLKNGYAYH	16% P / 21% R GBM6P GBM10R GBM14R GBM18R ZH753		GBM4R GBM7P GBM14P GBM18P ZH654 ZH802	2	4%
				KPIPTIRWLKNGYAYHK	21% P / 29% R GBM6P GBM7R GBM14R GBM18R GBM23P ZH753 ZH761		GBM4R GBM7P GBM10R GBM18P GBM21R ZH654 ZH757 ZH802	1	
				KPIPTIRWLKNGYAYHKG	11% P / 13% R GBM6P GBM10R GBM18P		GBM4R GBM7P GBM14R ZH761	2	
KPIPTIRWLKNGYAYHKGE	3% P / 4% R GBM18P			GBM4R	0				
AYIIEVIPDTPAE	5% P / 4% R ZH654			GBM18R ZH802	3				
AYIIEVIPDTPAEA	8% P / 4% R GBM18R ZH802			GBM18P ZH654	4				
AYIIEVIPDTPAEAG	8% P / 4% R GBM18R ZH802			GBM18P ZH654	4				
DVIISINGQSVVS	16% P / 4% R GBM7P GBM14R GBM19P			GBM6P GBM14P GBM15P ZH761	11				
DVIISINGQSVVSA	8% P / 4% R GBM14P GBM19P			GBM6P GBM14R	3				
DVIISINGQSVVSAN	13% P / 8% R GBM7P GBM14P GBM19P			GBM6P GBM12P GBM14R ZH753	3				
Serine protease HTRA1 (HTRA1; Q92743)	71% P 71% R	DVIKRESTLNMVV	0% P / 4% R	GBM18R	1	17%			
		DVIKRESTLNMVVR	8% P / 4% R GBM18R ZH802	GBM18P ZH654	5				
		DVIKRESTLNMVVR	0% P / 4% R	GBM18R	1				
		DVIKRESTLNMVVR	0% P / 4% R	GBM13R	0				

Appendix: Supplement of CHAPTER 2

		DVSDVIKRESTLNMVVR	8% P / 8% R	GBM18P	11	
			GBM18R	GBM20R		
			ZH654	ZH802		
		DVSDVIKRESTLNMVRR	5% P / 4% R	GBM18P	5	
			GBM18R	ZH802		
		ENDVIISINGQSVVS	16% P / 4% R	GBM2P	20	
			GBM6P	GBM7P		
			GBM14P	GBM14R		
			GBM15P	GBM19P		
		ENDVIISINGQSVVSA	11% P / 8% R	GBM6P	5	
			GBM7P	GBM12P		
			GBM14P	GBM14R		
			ZH753			
		ENDVIISINGQSVVSAN	8% P / 13% R	GBM6P	4	
			GBM7P	GBM12R		
			GBM14R	GBM19P		
			ZH753			
		ENDVIISINGQSVVSAND	3% P / 0% R	GBM6P	1	
		GAYIIEVIPDTPAE	0% P / 4% R	GBM18R	1	
		GAYIIEVIPDTPAEA	3% P / 4% R	GBM18R	4	
			ZH654			
		GAYIIEVIPDTPAEAG	5% P / 4% R	GBM18P	4	
			GBM18R	ZH654		
		GLKENDVIISINGQSVVSA	3% P / 0% R	GBM6P	0	
		IEVIPDTPAEAGGL	0% P / 4% R	GBM10R	0	
		IIEVIPDTPAEA	3% P / 0% R	ZH654	3	
		IIEVIPDTPAEAG	0% P / 4% R	GBM18R	1	
		IIEVIPDTPAEAGGL	3% P / 4% R	GBM16P	3	
			GBM16R			
		IKRESTLNMVRRRGNE	0% P / 4% R	GBM18R	0	
		KENDVIISINGQSVVS	3% P / 8% R	GBM14R	3	
			GBM18R	ZH802		
		KENDVIISINGQSVVSA	5% P / 4% R	GBM6P	0	
			GBM14R	GBM19P		
		SDVIKRESTLNM	5% P / 4% R	GBM18R	3	
			ZH654	ZH802		
		SDVIKRESTLNMVV	8% P / 4% R	GBM18P	3	
			GBM18R	ZH654		
			ZH802			
		SDVIKRESTLNMVVR	8% P / 4% R	GBM18P	4	
			GBM18R	ZH654		
			ZH802			
		SDVIKRESTLNMVRR	0% P / 4% R	GBM13R	0	
		VIISINGQSVV	3% P / 4% R	GBM18R	2	
			ZH802			
		VIISINGQSVVS	5% P / 0% R	ZH761	3	
			ZH802			
		VIISINGQSVVSA	0% P / 4% R	ZH753	0	
		VIKRESTLNMVV	0% P / 4% R	GBM18R	1	
		VIKRESTLNMVVR	3% P / 0% R	ZH802	1	
		VIPDTPAEAG	3% P / 0% R	ZH802	0	
		VSDVIKRESTLNM	0% P / 4% R	GBM18R	1	
		VSDVIKRESTLNMVV	8% P / 8% R	GBM18P	5	
			GBM18R	GBM20P		
			GBM20R	ZH654		
		VSDVIKRESTLNMVVR	11% P / 13% R	GBM9R	16	
			GBM18P	GBM18R		
			GBM20P	GBM20R		
			ZH654	ZH802		
		VSDVIKRESTLNMVRR	8% P / 0% R	GBM18P	1	
			ZH654	ZH802		
		YIIEVIPDTPAEA	8% P / 4% R	GBM18P	3	
			GBM18R	ZH654		
			ZH802			
		YIIEVIPDTPAEAG	8% P / 4% R	GBM18P	1	
			GBM18R	ZH654		
			ZH802			
Neuronal cell	79% P				5%	
adhesion	75% R	EKKILTFQGSKTHG	0% P / 4% R	GBM10R	0	
molecule		EKKILTFQGSKTHGMLPG	3% P / 0% R	GBM12P	0	
(NRCAM;		HIEKKILTFQGSKTHG	3% P / 0% R	ZH616	0	
Q92823)		IEKKILTFQGSKTH	16% P / 13% R	GBM4R	0	
			GBM6P	GBM9P		
			GBM10R	GBM16P		
			GBM16R	ZH616		
			ZH757	ZH791		

Appendix: Supplement of CHAPTER 2

	IEKKILTFQGSKTHG	18% P / 17% R	GBM4R	1	
		GBM6P	GBM7P		
		GBM9P	GBM10R		
		GBM14R	GBM16P		
		GBM16R	ZH616		
		ZH757	ZH791		
	IEKKILTFQGSKTHGM	8% P / 8% R	GBM4R	0	
		GBM6P	GBM10R		
		ZH616	ZH791		
	IEKKILTFQGSKTHGMLPG	0% P / 8% R	GBM4R	0	
		GBM10R			
	ILTFQGSKTHGMLPG	3% P / 4% R	GBM12P	0	
		GBM22R			
	KILTFQGSKTHGMLP	3% P / 0% R	GBM12P	0	
	KILTFQGSKTHGMLPG	11% P / 8% R	GBM12P	0	
		GBM12R	GBM22P		
		GBM22R	ZH645		
		ZH681			
	KKILTFQGSKTHG	3% P / 8% R	GBM10R	0	
		GBM14R	GBM16P		
	KKILTFQGSKTHGMLPG	3% P / 0% R	GBM12P	0	
Sodium-coupled	18% P			2%	7%
neutral amino	17% R			0	
acid transporter 3		EGLLPVITPMAGNQRVEDPA	3% P / 4% R	GBM14R	
(SLC38A3;			GBM21P		
Q99624)		GLLPVITPMAGNQRVEDPA	13% P / 8% R	GBM6P	1
			GBM14P	GBM14R	
			GBM16P	GBM21P	
			GBM21R	ZH616	
	LLPVITPMAGNQRVE	3% P / 4% R	GBM6P	0	
		GBM14R			
	LLPVITPMAGNQRVED	0% P / 4% R	GBM14R	0	
	LLPVITPMAGNQRVEDP	3% P / 4% R	GBM6P	0	
		GBM14R			
	LLPVITPMAGNQRVEDPA	13% P / 13% R	GBM4R	2	
		GBM6P	GBM14P		
		GBM14R	GBM16P		
		GBM21P	GBM21R		
		ZH616			
	LPVITPMAGNQR	0% P / 4% R	GBM14R	0	
	LPVITPMAGNQRVE	8% P / 8% R	GBM14P	1	
		GBM14R	GBM21P		
		GBM21R	ZH616		
	LPVITPMAGNQRVED	0% P / 4% R	GBM14R	0	
	LPVITPMAGNQRVEDP	5% P / 13% R	GBM10R	2	
		GBM14R	GBM21P		
		GBM21R	ZH616		
	LPVITPMAGNQRVEDPA	16% P / 17% R	GBM4R	3	
		GBM6P	GBM10R		
		GBM11P	GBM14P		
		GBM14R	GBM16P		
		GBM21P	GBM21R		
		ZH616			
	PVITPMAGNQRVE	0% P / 4% R	GBM14R	0	
	PVITPMAGNQRVED	0% P / 4% R	GBM14R	0	
	PVITPMAGNQRVEDP	0% P / 4% R	GBM14R	0	
	PVITPMAGNQRVEDPA	5% P / 13% R	GBM6P	0	
		GBM10R	GBM14P		
		GBM14R	GBM21R		
	SEGLLPVITPMAGNQRVEDPA	3% P / 4% R	GBM6P	0	
		GBM14R			

Supplementary Table 5. Established TAAs and CTAs identified as glioblastoma-exclusive antigens on both primary and recurrent tumors or represented by glioblastoma-exclusive peptides on ≥ 2 primary as well as ≥ 2 recurrent neoplasms of a minimum of four different patients. HLA restrictions not passing manual assessment as quality control are indicated in *italic*. The number of positive tumors other than glioblastoma was based on n=824 HLA class I and n=585 HLA class II peptidome datasets. The frequency of positive benign HLA peptidomes was calculated from n=418 (HLA class I) or n=364 (HLA class II) benign human specimens. Glioblastoma exclusivity of HLA class II-restricted peptides was evaluated for the exact sequence match. Frequencies of positive tumors are given separately for n=38 primary (P) and n=24 recurrent (R) glioblastomas.

Peptide sequence	HLA restriction	Frequency of positive tumors	Protein frequency on glioblastomas	Protein frequency on non-GBM tumors	Protein frequency on benign samples
Glioblastoma-exclusive HLA class I-presented antigens derived from established TAAs and CTAs					
Oligodendrocyte transcription factor (OLIG2; Q13516)			34% P / 33% R	1%	0%
Supplementary Table 2					
EMKRLVSEI	<i>B*08:01</i>	0% P / 4% R	ZH753	0	
SIRPPHGLLK	A*03:01	3% P / 0% R	ZH761	0	
SLPGSGLPSV	A*02:01	3% P / 0% R	ZH757	0	
Transmembrane protein 255A (TMEM255A; Q5JRV8)			34% P / 17% R	1%	0%
Supplementary Table 2					
Paired box protein Pax-6 (PAX6; P26367)			24% P / 21% R	1%	0%
Supplementary Table 3					
FTQEIQEAL	A*02:05; C*12:03	3% P / 0% R	GBM6P	1	
RYYETGSIRPR	A*31:01	8% P / 0% R	ZH613 ZH654	3	
SALPPMPSF	C*12:03	3% P / 0% R	GBM6P	1	
Immunoglobulin superfamily member 11 (IGSF11; Q5DX21)			18% P / 17% R	0%	0%
Supplementary Table 2					
Protein AF1q (MLLT11; Q13015)			16% P / 21% R	2%	0%
APIASIHFS	B*07:02; B*35:01	8% P / 21% R	GBM4P GBM6P GBM12R GBM16R	7	
			GBM4R GBM6R GBM16P GBM18R		
ATYKVKDSSVGK	A*03:01; A*11:01	5% P / 0% R	ZH631 ZH761	0	
NPEGDGLLEY	B*35:01	3% P / 0% R	GBM6P	1	
QEKNPEGDGL	B*44:02	3% P / 0% R	GBM15P	0	
CD276 antigen (CD276; Q5ZPR3)			5% P / 4% R	4%	0%
AQLNLIWQL	A*02:01; B*13:02	5% P / 4% R	GBM5P GBM20P	6	
			GBM13R		
Interleukin-13 receptor subunit alpha-2 (IL13RA2; Q14627)			5% P / 4% R	0%	0%
LLDTNYNLFY	A*01:01	3% P / 0% R	GBM3P	0	
PLPPVYLTF	<i>A*23:01</i>	0% P / 4% R	GBM23R	0	
Glioblastoma-exclusive HLA class I ligands derived from established TAAs and CTAs					
Ankyrin repeat domain-containing protein 40 (ANKRD40; Q6A112)			55% P / 42% R	10%	6%
ELDRQELTY	A*01:01	18% P / 13% R	GBM3P GBM9P GBM13P GBM16P ZH617	12	
			GBM5P GBM9R GBM13R GBM16R ZH645		
Adenomatous polyposis coli protein (APC; P25054)			68% P / 58% R	15%	19%
LPSSSSSRGSL	B*07:02	16% P / 21% R	GBM4P GBM7P GBM10R GBM16R GBM18R ZH681	24	
			GBM4R GBM7R GBM16P GBM18P ZH616		
ELDTPINY	A*01:01	13% P / 17% R	GBM5P GBM9P GBM16P GBM17R ZH654	3	
			GBM9R GBM13R GBM16R ZH645		
KVMEEVSAI	A*02:01; C*02:02; C*15:02	11% P / 8% R	GBM3P GBM14R ZH678	4	
			GBM7R ZH617 ZH618		

Appendix: Supplement of CHAPTER 2

Brevican core protein (BCAN; Q96GW7)				58% P / 21% R	1%	1%
YEVDTVLRY	B*18:01; B*44:03	8% P / 8% R	GBM3P GBM17R ZH720	GBM3R ZH678	0	
Carbonic anhydrase 9 (CA9; Q16790)				18% P / 8% R	3%	2%
SPRAAEPVQL	B*07:02	13% P / 8% R	GBM16P GBM18P ZH616 ZH757	GBM16R GBM18R ZH681	11	
Cyclin-dependent kinase 4 (CDK4; P11802)				50% P / 54% R	13%	8%
Supplementary Table 3						
Ceramide synthase 1 (CERS1; P27544)				68% P / 71% R	2%	2%
Supplementary Table 3						
VLTGQVHEL	A*02:01	16% P / 13% R	GBM10R GBM14R ZH678 ZH753 ZH761	GBM11P ZH616 ZH681 ZH757	0	
Contactin-2 (CNTN2; Q02246)				37% P / 58% R	0%	2%
IVRNGGTSM	B*07:02	11% P / 17% R	GBM4P GBM7P GBM16P ZH681	GBM4R GBM7R GBM16R	0	
TEADIGSNLRW	B*44:02; B*44:03	11% P / 8% R	GBM17P GBM19R ZH761	GBM17R ZH678 ZH802	0	
Cysteine and glycine-rich protein 2 (CSRP2; Q16527)				26% P / 21% R	2%	3%
LTEKEGEIY	A*01:01	16% P / 17% R	GBM3P GBM9P GBM13P GBM16P GBM17R	GBM5P GBM9R GBM13R GBM16R ZH654	1	
Catenin beta-1 (CTNNB1; P35222)				92% P / 96% R	75%	72%
ATVGLIRNL	A*02:01; A*02:05; B*13:02; B*57:01; C*03:03; C*06:02; C*07:01; C*12:03; C*15:06	21% P / 13% R	GBM5P GBM6P GBM11P GBM17R ZH654 ZH791	GBM5R GBM6R GBM13P GBM23P ZH681	18	
Dedicator of cytokinesis protein 7 (DOCK7; Q96N67)				95% P / 79% R	29%	27%
AMASIINRL	A*02:01; A*02:05	13% P / 8% R	GBM6P GBM11P ZH613 ZH757	GBM6R GBM11R ZH617	3	
ELKSSISAL	B*08:01	11% P / 13% R	GBM13P GBM16P GBM18P ZH753	GBM13R GBM16R ZH617	3	
Dihydropyrimidinase-related protein 4 (DPYSL4; O14531)				47% P / 38% R	6%	12%
GLYDGPVHEV	A*02:01	13% P / 8% R	GBM7P GBM12P ZH616 ZH753	GBM7R GBM21P ZH681	0	
Epidermal growth factor receptor (EGFR; P00533)				58% P / 58% R	11%	6%
KITDFGLAK	A*03:01; A*11:01	11% P / 8% R	GBM6P GBM16R ZH631	GBM16P GBM17R ZH678	1	
SPSTSRTPLL	B*07:02	5% P / 17% R	GBM4R GBM16P ZH616	GBM10R GBM16R ZH784	0	
KLFGTSGQK	A*03:01	5% P / 13% R	GBM6P GBM16R GBM22R	GBM16P GBM17R	2	
QMDVNPEGKY	A*01:01	5% P / 8% R	GBM5P GBM17R	GBM16R ZH654	0	
Eukaryotic translation initiation factor 4E (EIF4E; P06730)				11% P / 21% R	8%	4%
RLISKFDTV	A*02:01	5% P / 8% R	GBM3P GBM13R	GBM11P ZH753	2	

Appendix: Supplement of CHAPTER 2

Elongation of very long chain fatty acids protein 2 (ELOVL2; Q9NXB9)			39% P / 25% R	2%	1%
YLPTFFLTV	A*02:01; A*02:05	26% P / 13% R	GBM3P GBM7P GBM11P GBM13R GBM20R ZH720 ZH829	GBM6P GBM7R GBM13P GBM19P GBM21P ZH757	1
Fatty acid-binding protein, brain (FABP7; O15540)			21% P / 13% R	1%	0%
EYMKALGVGF	A*23:01; A*24:02	11% P / 8% R	GBM15P GBM22P GBM23P	GBM19P GBM22R GBM23R	1
Constitutive coactivator of PPAR-gamma-like protein 2 (FAM120C; Q9NX05)			50% P / 50% R	8%	8%
Supplementary Table 3					
HAFSEDPML	B*35:02; B*35:03; C*03:04; C*12:03	8% P / 13% R	GBM14R GBM22P GBM23P	GBM21P GBM22R GBM23R	2
Neuronal membrane glycoprotein M6-b (GPM6G; Q13491)			84% P / 79% R	5%	14%
ATTYNYAVLK	A*11:01	11% P / 8% R	GBM7P GBM18P ZH631	GBM7R GBM18R ZH678	0
Glutamate receptor ionotropic, kainate 3 (GRIK3; Q13003)			39% P / 25% R	2%	6%
LLYDAVHIV	A*02:01	11% P / 13% R	GBM10R GBM13R ZH617 ZH757	GBM11P GBM14R ZH681	2
HEAT repeat-containing protein 1 (HEATR1; Q9H583)			58% P / 42% R	28%	24%
KMVEDLISV	A*02:01	5% P / 8% R	GBM3P GBM14R	GBM10R ZH617	11
Hepatocyte cell adhesion molecule (HEPACAM; Q14CZ8)			50% P / 33% R	0%	1%
VPISRPQVL	B*07:02	11% P / 13% R	GBM4P GBM7P GBM10R ZH681	GBM4R GBM7R GBM16P	0
Integrin alpha-7 (ITGA7; Q13683)			79% P / 63% R	10%	16%
LLYPMQVEL	A*02:01; C*01:02	24% P / 13% R	GBM10R GBM13P GBM20P GBM21P ZH645 ZH681	GBM11P GBM13R GBM20R ZH617 ZH678 ZH757	4
ATP-sensitive inward rectifier potassium channel 10 (KCNJ10; P78508)			92% P / 79% R	7%	12%
Supplementary Table 3					
RLNQVNVTF	A*32:01; B*15:01	8% P / 13% R	GBM2P GBM5P GBM12R	GBM2R GBM5R ZH631	0
Melanoma-associated antigen F1 (MAGEF1; Q9HAY2)			39% P / 33% R	12%	22%
ALAAKALAR	A*03:01	5% P / 13% R	GBM4P GBM8P GBM23R	GBM4R GBM17R	3
Membrane-associated guanylate kinase, WW and PDZ domain-containing protein 2 (MAGI2; Q86UL8)			24% P / 21% R	1%	2%
AVAPGPWKV	A*02:01; C*15:02	11% P / 13% R	GBM13R ZH617 ZH681 ZH757	GBM14R ZH678 ZH753	2
C-1-tetrahydrofolate synthase, cytoplasmic (MTHFD1; P11586)			47% P / 21% R	25%	30%
TTESEVMKY	A*01:01	18% P / 8% R	GBM3P GBM9P GBM16P ZH617 ZH654	GBM5P GBM13R GBM16R ZH645	17
Max-interacting protein 1 (MXI1; P50539)			11% P / 21% R	3%	3%
FPSMPSPRL	B*07:02; B*35:03; B*56:01	8% P / 21% R	GBM7P GBM10R GBM16P GBM18P	GBM7R GBM14R GBM16R GBM18R	11
Neuroigin-4, X-linked (NLGN4X; Q8N0W4)			50% P / 42% R	2%	1%
NLDTLMTYV	A*02:01; C*05:01; C*08:02	21% P / 8% R			1

Appendix: Supplement of CHAPTER 2

Neuronal cell adhesion molecule (NRCAM; Q92823)			47% P / 29% R		1%	1%
Supplementary Table 3						
SEPDNLVITW	B*44:02; B*44:03	16% P / 8% R	GBM17P GBM20P ZH617 ZH678	GBM17R GBM20R ZH631 ZH761	0	
Poly(A) polymerase alpha (PAPOLA; P51003)			53% P / 50% R		25%	24%
KIPTPIGVV	A*02:01	8% P / 8% R	GBM14R ZH678 ZH753	GBM21P ZH681	3	
Protocadherin gamma-C5 (PCDHGC5; Q9Y5F6)			68% P / 67% R		5%	7%
VSSDGLTKY	A*01:01; B*57:01	16% P / 13% R	GBM5P GBM9P GBM13P ZH617 ZH654	GBM5R GBM9R GBM17R ZH645	1	
Pecanex-like protein (PCNXL3; Q9H6A9)			29% P / 12% R		12%	10%
GVLENIFGV	A*02:01; C*16:01	24% P / 13% R	GBM3P GBM12R GBM14P GBM20P ZH617 ZH681	GBM7P GBM13R GBM14R GBM21P ZH678 ZH720	23	
E3 ubiquitin-protein ligase Praja-2 (PJA2; O43164)			87% P / 79% R		43%	40%
GSSPEQVVRPK	A*11:01	8% P / 8% R	GBM12R GBM18R ZH678	GBM18P ZH631	5	
Pleckstrin homology domain-containing family A member 4 (PLEKHA4; Q9H4M7)			18% P / 21% R		2%	1%
Supplementary Table 3						
Receptor-type tyrosine-protein phosphatase zeta (PTPRZ1; P23471)			97% P / 83% R		6%	5%
Supplementary Table 3						
EEFETLKEF	B*18:01; B*44:02; B*44:03	32% P / 8% R	GBM3P GBM17P GBM20P GBM21P ZH617 ZH678 ZH761	GBM8P GBM19R GBM20R ZH616 ZH631 ZH720 ZH802	3	
KVFAGIPTV	A*02:01; A*02:05; A*32:01; B*13:02; C*15:02	29% P / 13% R	GBM5P GBM10R GBM13P GBM14R ZH617 ZH678 ZH757	GBM7P GBM11P GBM13R GBM21P ZH631 ZH681 ZH761	2	
SENPETITY	B*18:01; B*44:02; B*44:03	26% P / 8% R	GBM3P GBM17R GBM21P ZH617 ZH678 ZH761	GBM8P GBM20R ZH616 ZH631 ZH750	1	
FLLPDTDGLTAL	A*02:01	26% P / 8% R	GBM3P GBM10R GBM21P ZH645 ZH753 ZH761	GBM7P GBM19P ZH617 ZH678 ZH757 ZH829	1	
VVYDTMIEK	A*03:01; A*11:01	18% P / 13% R	GBM7 GBM12P GBM16R ZH631 ZH761	GBM10R GBM16P GBM17R ZH678 ZH791	0	
FPTEVTPHAF	B*07:02; B*35:03	16% P / 21% R	GBM4P GBM14R GBM21P GBM22R	GBM10R GBM16P GBM22P	2	
SVDVYQVAK	A*11:01	13% P / 13% R	GBM7P GBM12R GBM18R ZH678	GBM7R GBM18P ZH631 ZH791	2	
FLYKVILSL	A*02:01; B*13:02; C*03:03	13% P / 8% R	GBM5P GBM13R ZH617 ZH829	GBM13P GBM14R ZH750	1	

Appendix: Supplement of CHAPTER 2

ALTTLMHQL	A*02:01; A*02:05	11% P / 17% R	GBM6P GBM11P GBM14R ZH613	GBM6R GBM11R GBM20R ZH757	0
FPSKATSEL	B*07:02; B*35:03	11% P / 13% R	GBM4P GBM14R GBM21P GBM22R	GBM10R GBM16P GBM22P	0
SPISKTFEL	B*07:02; B*08:01; B*35:01; B*35:03	8% P / 13% R	GBM6P GBM16P GBM22P	GBM10R GBM16R GBM22R	0
Cell differentiation protein RCD1 homolog (RQCD1; Q92600)					55% P / 46% R 17% 13%
LLDDTGLAY	A*01:01; B*15:01	8% P / 8% R	GBM5P GBM13R GBM17R	GBM9P GBM16P	5
Structural maintenance of chromosomes protein 4 (SMC4; Q9NTJ3)					71% P / 46% R 38% 24%
AVNPKEIASK	A*03:01	11% P / 17% R	GBM4P GBM6P GBM16R GBM23R	GBM4R GBM16P GBM17R ZH761	31
Alpha-2,8-sialyltransferase 8E (ST8SIA5; O15466)					11% P / 17% R 1% 1%
NTDVSIRVKY	A*01:01	5% P / 8% R	GBM13R ZH617	GBM17R ZH654	
Transforming growth factor beta-2 (TGFB2; P61812)					18% P / 21% R 3% 1%
RPYFRIVRF	B*07:02; B*08:01	11% P / 13% R	GBM4R GBM9P GBM16R GBM18R	GBM7P GBM16P GBM18P	10
Tenascin (TNC; P24821)					87% P / 83% R 14% 13%
Supplementary Table 3					
GVLKKVIRH	A*03:01; A*11:01	13% P / 25% R	GBM4P GBM6P GBM16P GBM17R GBM18R ZH631	GBM4R GBM6R GBM16R GBM18P GBM23R	10
ATEYEIELY	A*01:01	13% P / 17% R	GBM3P GBM5P GBM9R GBM16P ZH645	GBM3R GBM9P GBM13R GBM16R	7
SPRDLTATEV	B*07:02	5% P / 13% R	GBM4R GBM16P GBM18P	GBM10R GBM16R	0
NRLLETVEY	C*07:01; C*07:02	5% P / 8% R	GBM4P GBM16P	GBM10R GBM18R	0
Vacuolar protein sorting-associated protein 13B (VPS13B; Q7Z7G8)					74% P / 67% R 30% 25%
SLLQKQIML	A*02:01	11% P / 8% R	GBM10R GBM21P ZH753	GBM11P ZH681 ZH757	7
Glioblastoma-exclusive HLA class II-presented antigens derived from established TAAs and CTAs					
Fatty acid-binding protein, brain (FABP7; O15540)					26% P / 29% R 1% 0%
Supplementary Table 4					
Cyclin-dependent kinase 4 (CDK4; P11802)					8% P / 8% R 1% 0%
DPHSGHFVALKSVRVPN		5% P / 4% R	GBM7P GBM14R	GBM14P	6
DPHSGHFVALKSVRVPNG		8% P / 8% R	GBM7P GBM12P GBM14R	GBM7R GBM14P	3
DPHSGHFVALKSVRVPNGG		3% P / 4% R	GBM7P	GBM7R	4
DPHSGHFVALKSVRVPNGGG		3% P / 0% R	GBM7P		0
SGHFVALKSVRVPNGG		3% P / 0% R	GBM7P		0
DNA repair protein RAD51 homolog 1 (RAD51; Q06609)					8% P / 8% R 0% 0%
Supplementary Table 2					
Ceramide synthase 1 (CERS1; P27544)					5% P / 8% R 0% 0%
DLREYDTAEQSLKPS		5% P / 4% R	GBM6P ZH753	GBM12P	0
DLREYDTAEQSLKPSK		5% P / 0% R	GBM6P	GBM12P	0
GGSYHRLHALAADLG		3% P / 0% R	GBM6P		0
KVLYATSHCSLRTVPDI		0% P / 4% R	GBM2R		0
LREYDTAEQSLKPS		3% P / 0% R	GBM6P		0
LREYDTAEQSLKPSK		3% P / 0% R	GBM6P		0

Appendix: Supplement of CHAPTER 2

Lipase member I (LIPI; Q6XZB0)		3% P / 8% R		0%	0%
FISFPCRSYKDYKT	0% P / 4% R	GBM5R		0	
KSIFSGIQFIKCNHQRAVHLFM	0% P / 4% R	GBM21R		0	
PDKTMMDGFSFKLLNQLGMIEEP	3% P / 0% R	GBM13P		0	
Eukaryotic translation initiation factor 4E (EIF4E; P06730)		3% P / 4% R		1%	0%
IEPMWEDEKKNRGGR	0% P / 4% R	GBM10R		1	
QEVANPEHYIKHPLQNRWALWFFKN	3% P / 0% R	GBM16P		0	
Protein AF1q (MLLT11; Q13015)		3% P / 4% R		1%	0%
FWRAPIASIHSEFEL	0% P / 4% R	GBM22R		1	
MRDPVSSQYSSFLF	3% P / 0% R	ZH802		2	
WRAPIASIHSEFEL	0% P / 4% R	GBM22R		4	
WRAPIASIHSEFDLL	0% P / 4% R	GBM22R		3	
Kinetochore protein Nuf2 (NUF2; Q9BZD4)		3% P / 4% R		1%	0%
KTKIVDSPEKLNKYK	3% P / 4% R	GBM13R	GBM16P	0	
Transcription factor ETV6 (ETV6; P41212)		3% P / 4% R		1%	0%
MPSPIMHPLILNP	0% P / 4% R	GBM5R		0	
PGQRLLFRFMKTPDEI	3% P / 0% R	GBM16P		0	
Melanoma-associated antigen 1 (MAGEA1; P43355)		3% P / 4% R		1%	0%
APEEEIWEELSVMEVYDGREHSAY	3% P / 4% R	GBM10R	GBM16P	1	
Transcriptional repressor CTCFL (CTCF; Q8NI51)		3% P / 4% R		1%	0%
NQLLAERTKEQLF	3% P / 4% R	GBM18R	ZH654	1	
Glioblastoma-exclusive HLA class II-restricted peptides derived from established TAAs and CTAs					
A-kinase anchor protein 3 (AKAP3; O75969)		5% P / 17% R		1%	1%
EPKVPEQPVKEDRKLKERPLASSPP	5% P / 13% R	GBM9R	GBM10R GBM16P GBM16R ZH757	0	
Brevican core protein (BCAN; Q96GW7)		63% P / 38% R		1%	1%
Supplementary Table 4					
DAGWLSDQTVRYPIQ	5% P / 13% R	GBM10R	GBM13R GBM16P GBM16R ZH617	2	
EAYRFRVALPAYPA	32% P / 13% R	GBM4R	GBM5P GBM5R GBM6P GBM7P GBM10R GBM11P GBM16P GBM22P ZH613 ZH616 ZH678 ZH681 ZH757 ZH802	0	
RPRLRYEVDTVLRYR	8% P / 13% R	GBM10R	GBM13R GBM16P GBM16R GBM18P ZH617	0	
SPGWLADGSRYPPI	11% P / 13% R	GBM10R	GBM13P GBM13R GBM16P GBM16R GBM18P ZH617	0	
SPGWLADGSRYPPIV	8% P / 13% R	GBM10R	GBM13R GBM16P GBM16R GBM18P ZH617	1	
SPGWLADGSRYPPIVT	8% P / 13% R	GBM10R	GBM13R GBM16P GBM16R GBM18P ZH617	0	
SPGWLADGSRYPPIVTPS	11% P / 13% R	GBM10R	GBM13P GBM13R GBM16P GBM16R GBM18P ZH617	0	
SPRVKWTFLSRGREA	13% P / 8% R	GBM5P	GBM11P GBM17R GBM22P GBM22R ZH678 ZH750 ZH757	0	
VNEAYRFRVALPAYPA	37% P / 13% R	GBM3P	GBM4R GBM5R GBM5P GBM6P GBM7P GBM10R GBM11P GBM16P GBM22P ZH613 ZH616 ZH645 ZH678 ZH681 ZH757 ZH802	0	

Appendix: Supplement of CHAPTER 2

Clusterin (CLU; P10909)		87% P / 96% R		53%	59%
DNELQEMSNQGSK	11% P / 13% R	GBM9P GBM18P GBM20R ZH802	GBM9R GBM18R ZH654	24	
DNELQEMSNQGSKY	13% P / 13% R	GBM9P GBM18P GBM20P ZH654 ZH802	GBM9R GBM18R GBM20R ZH802	23	
DQTVSDNELQEMSNQGSK	8% P / 13% R	GBM9R GBM18R ZH654 ZH802	GBM18P GBM20R ZH802	8	
DQTVSDNELQEMSNQGSKY	11% P / 13% R	GBM9P GBM18P GBM20R ZH802	GBM9R GBM18R ZH654	14	
DQTVSDNELQEMSNQGSKYVN	8% P / 13% R	GBM9R GBM18R ZH654 ZH802	GBM18P GBM20R ZH802	16	
DQTVSDNELQEMSNQGSKYVNK	11% P / 8% R	GBM9P GBM18R ZH654 ZH802	GBM18P GBM20R ZH802	11	
DQTVSDNELQEMSNQGSKYVNKE	11% P / 13% R	GBM9P GBM18P GBM20R ZH802	GBM9R GBM18R ZH654	6	
DSDPITVTPVEVSRKNPK	5% P / 17% R	GBM5R GBM20R ZH645	GBM13R GBM23R ZH654	9	
ERLTRKYNELLKSYQ	11% P / 8% R	GBM21P GBM22P ZH654	GBM21R GBM22R ZH761	1	
GVTEVVVKLFDSDPIT	5% P / 13% R	GBM4R GBM14R GBM16R	GBM11P GBM16P	6	
NELQEMSNQGSK	8% P / 8% R	GBM18P GBM20R ZH802	GBM18R ZH654	14	
NELQEMSNQGSKY	11% P / 8% R	GBM9P GBM18R ZH654 ZH802	GBM18P GBM20R ZH802	14	
SDNELQEMSNQGSK	16% P / 13% R	GBM9P GBM15P GBM18R GBM20R ZH802	GBM9R GBM18P GBM20P ZH654	35	
SDNELQEMSNQGSKYY	8% P / 13% R	GBM9R GBM18R ZH654 ZH802	GBM18P GBM20R ZH802	16	
SDNELQEMSNQGSKYVNK	11% P / 8% R	GBM9P GBM18R ZH654	GBM18P GBM20R	12	
TVSDNELQEMSNQGSK	11% P / 8% R	GBM9P GBM18R ZH654 ZH802	GBM18P GBM20R ZH802	13	
TVSDNELQEMSNQGSKY	13% P / 13% R	GBM9P GBM18P GBM20P ZH654 ZH802	GBM9R GBM18R GBM20R ZH802	17	
TVSDNELQEMSNQGSKYVNK	8% P / 8% R	GBM18P GBM20R ZH802	GBM18R ZH654	10	
VPSGVTEVVVKLFDSDPIT	8% P / 25% R	GBM4R GBM11R GBM14R GBM16R ZH753	GBM11P GBM13P GBM16P GBM23R	17	
VSDNELQEMSNQGSK	11% P / 13% R	GBM9P GBM18P GBM20R ZH802	GBM9R GBM18R ZH654	12	

Appendix: Supplement of CHAPTER 2

VSDNELQEMSNQGSKYVN	8% P / 8% R	GBM18P GBM20R ZH802	GBM18R ZH654	9	
VSDNELQEMSNQGSKYVNK	8% P / 8% R	GBM18P GBM20R ZH802	GBM18R ZH654	9	
VSDNELQEMSNQGSKYVNKE	8% P / 8% R	GBM9R GBM20R ZH802	GBM18P ZH654	4	
VTEVVVKLFDSDPIT	8% P / 17% R	GBM4R GBM14P GBM16R GBM23R	GBM11P GBM14R GBM23P	5	
Epidermal growth factor receptor (EGFR; P00533)				42% P / 33% R	9%
LQRYSSDPTGALTEDS	5% P / 13% R	GBM10R GBM16P GBM18P	GBM13R GBM16R	2	12%
LRILKETEFKKIKV	8% P / 8% R	GBM6P GBM16P ZH631	GBM14R GBM16R	0	
Ephrin type-B receptor 2 (EPHB2; P29323)				16% P / 21% R	3%
TPGMKIYIDPFTYE	13% P / 17% R	GBM4R GBM7P GBM10R GBM16P ZH791	GBM6P GBM7R GBM11P GBM16R	8	4%
TPGMKIYIDPFTYEDP	5% P / 17% R	GBM4R GBM7R GBM11P	GBM7P GBM10R GBM16R	5	
Glypican-1 (GPC1; P35052)				26% P / 25% R	4%
IMQLKIMTNRLRSA	16% P / 8% R	GBM4R GBM7P GBM14R GBM21P	GBM6P GBM14P GBM16P ZH616	1	2%
Hepatocyte cell adhesion molecule (HEPACAM; Q14CZ8)				47% P / 54% R	0%
EPGPPGYSVSPAVPGRSPG	8% P / 17% R	GBM2R GBM7P GBM12R ZH753	GBM6P GBM12P GBM20R	0	1%
Legumain (LGMN; Q99538)				71% P / 75% R	29%
DVTPQNFLAVLRGDAEA	16% P / 13% R	GBM3P GBM22P ZH678 ZH784 ZH810	GBM5R GBM22R ZH750 ZH791	8	46%
EDVTPQNFLAVLRGDAEAVKG	11% P / 8% R	GBM3P GBM22P ZH678	GBM5R GBM22R ZH750	7	
GEDVTPQNFLAVLRGDAEAVK	13% P / 13% R	GBM3R GBM5R GBM22R ZH750	GBM5P GBM22P ZH678 ZH791	6	
GEDVTPQNFLAVLRGDAEAVKG	16% P / 8% R	GBM3P GBM22P ZH678 ZH791	GBM5R GBM22R ZH750 ZH810	7	
HLPDNINVYATTAANPRE	5% P / 13% R	GBM14P GBM16P GBM21R	GBM14R GBM18R	24	
HLPDNINVYATTAANPRES	5% P / 8% R	GBM16P GBM21R	GBM18R ZH654	11	
INVYATTAANPRES	11% P / 13% R	GBM4R GBM10R GBM16R	GBM9P GBM16P ZH616	4	
KDLNETIHYMYKHKMYRKMVFYI	8% P / 17% R	GBM2R GBM10R GBM16P ZH631	GBM4R GBM14R ZH616	0	
NHLPDNINVYATTAANPRE	8% P / 8% R	GBM14P GBM18R	GBM16P GBM21R	5	
TGEDVTPQNFLAVLRGDAEAVKG	5% P / 8% R	GBM5R ZH678	GBM22R ZH791	4	

Appendix: Supplement of CHAPTER 2

VTPQNFLAVLRGDAEA	16% P / 13% R	GBM3P GBM22P ZH678 ZH784 ZH810	GBM5R GBM22R ZH750 ZH791	8	
Neuronal cell adhesion molecule (NRCAM; Q92823)				79% P / 75% R	5% 6%
Supplementary Table 4					
ALGAIHHTISVRVKAA	13% P / 13% R	GBM5P GBM13R GBM23R ZH654	GBM13P GBM17R ZH645 ZH681	2	
AQLKLSPIVYNYSFR	8% P / 8% R	GBM4R GBM11P ZH616	GBM10R GBM16P	0	
EDGSFIGQYSGKKEKEPA	5% P / 8% R	GBM4R GBM10R	GBM6P ZH616	0	
GAIHHTISVRVKAAP	8% P / 8% R	GBM13P GBM17R ZH681	GBM13R ZH645	2	
GAIHHTISVRVKAAPY	13% P / 17% R	GBM5P GBM13P GBM17R ZH645 ZH681	GBM5R GBM13R GBM23R ZH654	1	
NGVPIEIPDDPSR	8% P / 8% R	GBM18P GBM20R ZH802	GBM18R ZH654	1	
NGVPIEIPDDPSRK	13% P / 8% R	GBM18P GBM20P ZH645 ZH802	GBM18R GBM20R ZH654	4	
SPLPTIEWFKGAKGSA	11% P / 13% R	GBM9P GBM11P GBM16P GBM21R	GBM10R GBM14R GBM21P	4	
VPIEIPDDPSR	8% P / 8% R	GBM18P GBM20R ZH802	GBM18R ZH654	3	
Palladin (PALLD; Q8WX93)				24% P / 25% R	6% 14%
SPSPPPPPPPVFSPTAAFPVPDV	8% P / 8% R	GBM13P GBM22P ZH654	GBM13R GBM23R	9	
Protocadherin gamma-C5 (PCDHGC5; Q9Y5F6)				34% P / 25% R	2% 4%
KPSENHYSLLTSQPLDR	11% P / 8% R	GBM2P GBM7P GBM12R	GBM6P GBM12P ZH753	0	
KPSENHYSLLTSQPLDRE	11% P / 8% R	GBM2P GBM7P GBM12R	GBM6P GBM12P ZH753	0	
Prostaglandin F2 receptor negative regulator (PTGFRN; Q9P2B2)				53% P / 33% R	15% 16%
GSDAYRLSVSRALSA	8% P / 8% R	GBM12P GBM13R ZH654	GBM13P GBM22R	8	
Receptor-type tyrosine-protein phosphatase zeta (PTPRZ1; P23471)				79% P / 58% R	2% 4%
Supplementary Table 4					
DSHIHAYVNALLIPG	8% P / 13% R	GBM4R GBM11P GBM16P	GBM10R GBM11R ZH791	0	
DSHIHAYVNALLIPGP	16% P / 21% R	GBM4R GBM9R GBM11P GBM16P ZH616 ZH791	GBM6P GBM10R GBM11R GBM16R ZH757	0	
IGTKYNEAKTNRSPTR	11% P / 8% R	GBM8P GBM15P GBM20P	GBM9P GBM15R GBM20R	1	
LDSHIHAYVNALLIPG	21% P / 21% R	GBM4R GBM7P GBM9R GBM11P GBM16P ZH616 ZH791	GBM6P GBM9P GBM10R GBM11R GBM16R ZH757	0	

Appendix: Supplement of CHAPTER 2

LDSHIHAYVNALLIPGP	21% P / 21% R	GBM4R GBM7P GBM9R GBM11P GBM16P ZH616 ZH791	GBM6P GBM9P GBM10R GBM11R GBM16R ZH757	0		
LDSHIHAYVNALLIPGPA	24% P / 21% R	GBM4R GBM7P GBM9R GBM10R GBM11P GBM16P ZH616 ZH757 ZH791	GBM6P GBM9P GBM10P GBM11P GBM16P ZH616 ZH791	0		
THYNRIGTKYNEAKT	13% P / 8% R	GBM8P GBM21R GBM22R ZH761	GBM21P GBM22P ZH654	0		
THYNRIGTKYNEAKTN	13% P / 8% R	GBM8P GBM21R GBM22R ZH761	GBM21P GBM22P ZH654	0		
Plasminogen activator inhibitor 1 (SERPINE1; P05121)				61% P / 63% R	14%	9%
APEEIIMDRPFLFVVRHNP	8% P / 25% R	GBM3R GBM11P GBM14R GBM15R GBM16R	GBM4R GBM11R GBM15P GBM16P	3		
EIIMDRPFLFVVR	8% P / 13% R	GBM13P GBM16R ZH617	GBM16P GBM18R ZH753	9		
EIIMDRPFLFVVRHNPT	5% P / 8% R	GBM3R GBM11P	GBM4R GBM16P	1		
TQQQIQAAAMGFKIDDK	11% P / 25% R	GBM6P GBM12R GBM14P GBM15R GBM22R	GBM12P GBM13R GBM14R GBM22P ZH753	7		
TQQQIQAAAMGFKIDDKG	8% P / 21% R	GBM12P GBM14R GBM20P GBM22R	GBM12R GBM15R GBM22P ZH753	7		
Sperm-associated antigen 1 (SPAG1; Q07617)				16% P / 25% R	1%	1%
EIENSEDEEGKSGRKHED	8% P / 13% R	GBM4R GBM10R GBM16R	GBM6P GBM16P ZH616	3		
ERRKIEIQEVNEGKEEPPG	5% P / 8% R	GBM13R GBM23R	GBM18P ZH645	3		
Transforming growth factor beta-2 (TFB2; P61812)				37% P / 38% R	4%	3%
Supplementary Table 4						
STRDLLQEKASRRAA	8% P / 13% R	GBM6P GBM14P GBM21R	GBM10R GBM14R ZH616	0		
Tenascin (TNC; P24821)				76% P / 67% R	15%	18%
Supplementary Table 4						
DITGLREATEYEIEL	11% P / 8% R	GBM12P GBM18R GBM22P	GBM18P GBM19P GBM22R	1		
EPLEITLLAPERTRD	11% P / 8% R	GBM6P GBM12P GBM14R	GBM7P GBM14P GBM15R	4		
GGWIVFLRRKNGREN	8% P / 13% R	GBM3P GBM5P GBM22R	GBM3R GBM22P GBM23R	3		
GVIQGYRTPVLS	8% P / 8% R	GBM10R GBM14R	GBM14P GBM16P	0		
GVIRGYRTPVL	18% P / 25% R	GBM4R GBM7P GBM9R GBM11P GBM16P GBM21R ZH791	GBM6P GBM9P GBM10R GBM14R GBM16R ZH616	4		

Appendix: Supplement of CHAPTER 2

GVIRGYRTPVLS	21% P / 25% R	GBM4R GBM9P GM10R GBM14R GBM16R GBM21R ZH757	GBM7P GBM9R GBM11P GBM16P GBM21P ZH616 ZH791	3	
GVIRGYRTPVLSA	16% P / 17% R	GBM4R GBM7P GBM9R GBM14R ZH616	GBM6P GBM9P GBM10R GBM16P ZH757	0	
GVIRGYRTPVLSAE	24% P / 21% R	GBM4R GBM7P GBM9R GBM11P GBM14R GBM16R ZH616	GBM6P GBM9P GBM10R GBM14P GBM16P GBM21P ZH791	1	
GVIRGYRTPVLSAEA	11% P / 8% R	GBM4R GBM7P GBM16P	GBM6P GBM10R ZH616	1	
GVIRGYRTPVLSAEASTAKEPE	11% P / 17% R	GBM4R GBM7P GBM14R GBM16R	GBM6P GBM10R GBM16P ZH616	1	
ITGLREATEYEIEL	11% P / 8% R	GBM12P GBM18R GBM22P	GBM18P GBM19P GBM22R	0	
IYGVIIQGYRTPVLSAE	5% P / 8% R	GBM4R GBM16P	GBM10R ZH616	0	
IYGVIRGYRTPVL	8% P / 8% R	GBM4R GBM10R	GBM6P GBM16P	2	
IYGVIRGYRTPVLS	13% P / 21% R	GBM4R GBM7P GBM9R GBM11P GBM16P	GBM6P GBM9P GBM10R GBM14R GBM16R	3	
IYGVIRGYRTPVLSA	11% P / 8% R	GBM4R GBM7P GBM16P	GBM6P GBM14R ZH616	0	
IYGVIRGYRTPVLSAE	13% P / 8% R	GBM4R GBM7P GBM11P ZH616	GBM6P GBM10R GBM16P	1	
IYGVIRGYRTPVLSAEA	5% P / 8% R	GBM4R GBM16P	GBM10R ZH616	1	
SIYGVIIQGYRTPVLSAE	5% P / 8% R	GBM4R GBM16P	GBM10R ZH616	0	
TVDSYVISYTGEKVPE	13% P / 8% R	GBM4R GBM7P GBM11P ZH616	GBM6P GBM10R GBM16P	1	
VDSYVISYTGEKVPE	11% P / 13% R	GBM4R GBM9R GBM11P ZH616	GBM9P GBM10R GBM16P	4	
VDSYVISYTGEKVPEIT	18% P / 17% R	GBM4R GBM7P GBM9R GBM11P GBM16R ZH791	GBM6P GBM9P GBM10R GBM16P ZH616	3	
Testis-specific gene 10 protein (TSGA10; Q9BZW7)				8% P / 8% R	1%
KLELITAEAEGNRLKEK	8% P / 8% R	GBM5P GBM7P GBM10R	GBM6P GBM9R	1	

Supplementary Table 6. Primary and recurrence-exclusive antigens presented on HLA class I and II molecules. HLA class I restrictions not passing manual assessment as quality control are indicated in *italic*, whereas HLA class II-presented proteins neither identified with peptides exceeding a length of twelve AA nor with different sequences across patients were not considered for this listing. FTSJ3, TDRD12, and AMER1 were detected with only one HLA class II peptide sequence across all patients. Frequencies of positive tumors are given for n=38 primary (P) and n=24 recurrent (R) glioblastomas.

Antigen	Frequency of positive tumors	Peptide sequence	HLA restriction	UniProt accession		
Primary glioblastoma-associated HLA class I-presented antigens						
PDZ domain-containing protein 2 (PDZD2)	<u>29% P</u>			Q15018		
	GBM5P	LLDDETLNQY	A*01:01			
	GBM13P	GLFHKQVTV	A*02:01			
	GBM15P	NYSRNFSSF	A*24:02			
	GBM22P	NYSRNFSSF	A*24:02			
	ZH613	HTQPSPVSR	A*31:01			
	ZH631	ASQEYHIVK	A*11:01			
	ZH645	SEAPAANAV	B*49:01			
	ZH654	HTQPSPVSR	A*31:01			
	ZH678	ASQEYHIVK	A*11:01			
		SSLQTAIRK	A*11:01			
	ZH761	AEQEMSRSF	B*44:02			
		GLFHKQVTV	A*02:01			
		HLTENLPKA	A*02:01			
	HTQPSPVSR	A*31:01				
Roundabout homolog 1 (ROBO1) 1 peptide multi-maps to ROBO2 (Q9HCK4)	<u>26% P</u>			Q9Y6N7		
	GBM3P	NSDSNLTTY	A*01:01			
	GBM4P	NPRDPSSSSSM	B*07:02			
	GBM7P	IPFLVPGIRY	B*56:01			
		KPRDQVVAL	B*07:02			
		NPRDPSSSSSM	B*07:02			
	GBM16P	NSDSNLTTY	A*01:01			
	GBM18P	NPRDPSSSSSM	B*07:02			
	ZH613	SSSSIEVHW	B*58:01			
	ZH645	AEGRPTPTI	B*49:01			
		NSDSNLTTY	A*01:01			
	ZH681	NPRDPSSSSSM	B*07:02			
	ZH802	RQREQANVGR	A*31:01			
	ZH829	IPFLVPGIRY	B*55:01			
Sodium- and chloride-dependent glycine transporter 1 (SLC6A9) 1 peptide multi-maps to SLC6A14/A7 (Q9UN76 / Q99884)	<u>24% P</u>			P48067		
	GBM3P	VAYPEALTL	C*02:02			
	GBM5P	VAYPEALTL	C*03:03			
	GBM6P	EFVLTSVGY	<i>B*35:01</i>			
		VAYPEALTL	C*12:03			
		VAYPEALTL	C*12:03			
	GBM7P	GAFDGMYY	C*02:02			
	GBM12P	EFVLTSVGY	<i>B*35:01</i>			
	GBM13P	VAYPEALTL	<i>B*13:02</i>			
	GBM19P	AFVAYPEALTL	A*24:02			
	GBM20P	AFVAYPEALTL	C*16:01			
	ZH654	KSSGKVVYF	B*57:01			
	Protein FAM65C (FAM65C)	<u>24% P</u>				Q96MK2
		GBM6P	GKYPGQLEI		B*15:03	
GBM8P		DIADFFTTR	A*68:01			
GBM9P		DIADFFTTR	A*33:05			
GBM10P		RPLPPPSSL	B*07:02			
GBM21P		PLQEVLELL	A*02:01			
ZH617		SLFGGSQGL	A*02:01			
ZH720		PLQEVLELL	A*02:01			
ZH757		RPLPPPSSL	B*07:02			
ZH791		RPLPPPSSL	B*07:02			
Centrosomal protein of 192 kDa (CEP192)		<u>24% P</u>			Q8TEP8	
		GBM3P	DELLVTEVY	B*18:02		
			SAAPFAQRY	C*02:02		
		GBM5P	VLDLFGDLTY	A*01:01; B*15:01		
	GBM6P	DVLDLFGDLTY	B*35:01			
	GBM9P	VLDLFGDLTY	A*01:01			
	GBM11P	TQVELLTRL	<i>A*02:05</i>			
	GBM15P	SAAPFAQRY	C*02:02			
	GBM23P	HYINMPVQF	A*23:01			
	ZH654	VRNPRITSL	C*06:02			
	ZH802	VRNPRITSL	B*14:02			
	Actin-related protein 8 (ACTR8)	<u>21% P</u>				Q9H981
		GBM4P	VIWSHAIQK	A*03:01		
		GBM5P	IQSNFIIVI	B*13:02		

Appendix: Supplement of CHAPTER 2

	GBM7P	APMALFYPATF	B*07:02	
		LPASIPHVIA	B*07:02; B*56:01	
	GBM16P	VIWSHAIQK	A*03:01	
	ZH613	LPASIPHVI	B*51:01	
	ZH631	LPASIPHVI	B*51:01	
	ZH654	KSASKPIGF	B*57:01	
		LPASIPHVI	B*51:01	
	ZH678	KQQGQPLYK	A*11:01	
		LPASIPHVI	B*51:01	
Oligophrenin-1 (OPHN1)	<u>21% P</u>			
	GBM3P	DEINIAESF	B*18:01	O60890
	GBM6P	FQDFFIGDTL	C*04:01	
		LGISWVKYY	C*12:03	
	GBM15P	NYSSAVQKF	A*24:02	
	GBM22P	NYSSAVQKF	A*24:02	
	ZH613	FQDFFIGDTL	A*02:05	
	ZH678	RTVGSNIQVQK	A*11:01	
	ZH720	DEINIAESF	B*18:01	
	ZH750	NYSSAVQKF	A*24:02	
Mitotic checkpoint serine/threonine-protein kinase BUB1 beta (BUB1B)	<u>21% P</u>			O60566
	GBM3P	EEYEARENF	B*18:01	
	GBM5P	SQKIPGRTL	B*13:02; B*15:01	
	GBM6P	GIADLAHLL	A*02:05	
		RAFYEIRF	B*15:03; C*12:03	
	GBM20P	YLHNQIGV	A*02:01	
	GBM21P	RAFYEIRF	C*12:03	
	ZH613	GIADLAHLL	A*02:05	
	ZH617	YLHNQIGV	A*02:01	
	ZH645	AELTVIKV	B*49:01	
Lymphocyte antigen 6 complex locus protein G6f (LY6G6F)	<u>21% P</u>			Q5SQ64
	GBM2P	RVYDVLVLK	A*03:01	
	GBM18P	RVYDVLVLK	A*03:01	
	GBM20P	AVLGQHHNY	A*29:02	
	GBM23P	RVYDVLVLK	A*03:01	
	ZH616	AVLGQHHNY	A*29:02	
	ZH631	RVYDVLVLK	A*11:01	
	ZH678	RVYDVLVLK	A*11:01	
	ZH757	SPAAGSFRTL	B*07:02	
Nuclease-sensitive element-binding protein 1 (YBX1)	<u>21% P</u>			P67809
	GBM3P	RRFPPYYMR (YBX1)	B*27:05	
		VRNGYGFNR (YBX1/2/3)	B*27:05	
	GBM6P	SKYAADRNYH (YBX1)	B*15:03	
	GBM9P	NVRNGYGFNR (YBX1/2/3)	A*33:05	
	ZH613	GTVKWFNVR (YBX1/2/3)	A*31:01	
	ZH645	GEKGAEAAV (YBX1/3)	B*49:01	
		GETVEFDVV (YBX1/2/3)	B*49:01	
	ZH654	ATKVLGTVKW (YBX1/3)	B*57:01	
		GTVKWFNVR (YBX1/2/3)	A*31:01	
		RNHYYRYP (YBX1)	A*31:01	
		RYRRNFNYRRR (YBX1)	A*31:01	
	ZH757	RYRRNFNYRRR (YBX1)	B*27:05	
	ZH802	GTVKWFNVR (YBX1/2/3)	A*31:01	
		NVRNGYGFNR (YBX1/2/3)	A*33:01	
		RNHYYRYP (YBX1)	A*31:01	
		RYRRNFNYRRR (YBX1)	A*31:01	
Tumor necrosis factor receptor superfamily member 21 (TNFRSF21)	<u>18% P</u>			O75509
	GBM3P	SEREVAAF	B*18:01	
	GBM6P	RVIEEIPQA	A*02:05	
	GBM22P	VYSHLPDLL	A*24:02	
	ZH613	RVIEEIPQA	A*02:05	
	ZH617	GLMEDTTQL	A*02:01	
	ZH681	RVIEEIPQA	A*02:01	
	ZH761	TSPSSSTAL	C*01:02	
Left-right determination factor 1/2 (LEFTY1/2)	<u>18% P</u>			O00292
	GBM3P	SLIDSRLVSV	A*02:01	
	GBM7P	SLIDSRLVSV	A*02:01	O75610
	GBM21P	SLIDSRLVSV	A*02:01	
	ZH617	SLIDSRLVSV	A*02:01	
	ZH645	SLIDSRLVSV	A*02:01	
	ZH681	SLIDSRLVSV	A*02:01	
	ZH757	SLIDSRLVSV	A*02:01	
PHD finger protein 1 (PHF1)	<u>18% P</u>			O43189
	GBM3P	WVDVAHLVLY	A*01:01	
	GBM5P	WVDVAHLVLY	A*01:01	
	GBM6P	VQFEDDSQFL	C*04:01	
	GBM9P	WVDVAHLVLY	A*01:01	
	GBM16	WVDVAHLVLY	A*01:01	
	ZH613	VQFEDDSQFL	A*02:05	
	ZH654	WVDVAHLVLY	A*01:01	

Appendix: Supplement of CHAPTER 2

tRNA (guanine-N(7)-methyltransferase subunit WDR4 (WDR4))	18% P			P57081
	GBM6P	TFDENVTSYL	C*04:01	
	GBM7P	ATFDNVTSYLK	A*11:01	
	GBM17P	SSGDGTLRLW	B*57:01	
	GBM18P	ATFDNVTSYLK	A*11:01	
	ZH631	ATFDNVTSYLK	A*11:01	
	ZH678	ATFDNVTSYLK	A*11:01	
5'-AMP-activated protein kinase subunit gamma-2 (PRKAG2)	18% P			Q9UGJ0
	GBM3P	SLFDVAVYSL	A*02:01	
	ZH613	DIYSKFDVI	B*51:01	
	ZH616	SESGVYMRP	B*44:02	
	ZH645	AEVHRLVVV	B*49:01	
	ZH654	DIYSKFDVI	B*51:01	
	ZH750	SLFDVAVYSL	A*02:01	
2 peptides multi-map to PRKAG1 (P54619)	ZH757	SLFDVAVYSL	A*02:01	
	18% P			Q96LW7
	GBM8P	DTPFLTGHGR	A*68:01	
	GBM23P	IILQLNRYR	A*03:01	
	ZH645	QEFYRALYI	B*49:01	
	ZH654	RYYPQILTNK	A*31:01	
	ZH678	RLVQDTPFL	A*02:01	
Bcl10-interacting CARD protein (C9orf89)	ZH757	RLVQDTPFL	A*02:01	
	ZH802	RYYPQILTNK	A*31:01	
	18% P			Q4KMP7
	GBM5P	AQAPVAAVL	B*13:02	
	GBM7P	GTAPLVAPPR	A*11:01	
	ZH631	RTLTPWASVL	A*32:01; C*03:03	
	ZH645	QEDFLVHEV	B*49:01	
TBC1 domain family member 10B (TBC1D10B)	ZH654	RTLTPWASVL	C*15:06	
	ZH678	GTAPLVAPPR	A*11:01	
	ZH750	RTLTPWASVL	B*15:17; C*07:01	
	18% P			Q9NWL6
	GBM3P	EECTMPTTF	B*18:01	
	GBM7P	KTMPPTFNR	A*11:01	
	GBM18P	KTMPPTFNR	A*03:01; A*11:01	
Asparagine synthetase domain-containing protein 1 (ASNSD1)	GBM23P	LPIWEKANLTL	B*35:02	
	ZH645	GEIFSGIKV	B*49:01	
	ZH654	KTMPPTFNR	A*31:01	
	ZH678	KTMPPTFNR	A*11:01	
	18% P			P40197
	GBM2P	AMIKIGQLF	B*15:01	
	GBM14P	LPTNLTHIL	B*35:03	
Platelet glycoprotein V (GP5)	GBM15P	SEAPVHPAL	B*44:02; B*44:03	
	GBM22P	SEAPVHPAL	B*40:01	
	ZH678	ALLDKMVLL	A*02:01	
		LPTNLTHI	B*51:01	
		SEAPVHPAL	B*44:03	
		TEVLLGHNSW	B*44:03	
	ZH802	DRLPNLSSL	B*14:02	
		LRYLGVTL	B*14:02	
		RTLPAAAFRR	A*31:01	
	ZH829	SEAPVHPAL	B*44:05	

Recurrence-associated HLA class I-presented antigens

Hormone-sensitive lipase (LIPE)	17% R			Q05469
	GBM10R	PLYSSPIVK	A*03:01	
	GBM16R	PLYSSPIVK	A*03:01	
	GBM17R	PLYSSPIVK	A*03:01	
T-cell receptor beta-1/2 chain C region (TRBC1/2)	ZH753	RLSGVFAGV	A*02:01	
	17% R			P01850
	GBM4R	ILYEILLGK	A*03:01	
	GBM12R	ATILYEILLGK	A*11:01	A0A5B9
	GBM16R	ILYEILLGK	A*03:01	
GBM18R	ATILYEILLGK	A*11:01		
		ILYEILLGK	A*03:01	

Primary glioblastoma-associated HLA class II-presented antigens

Receptor-type tyrosine-protein phosphatase gamma (PTPRG)	29% P			P23470
	GBM5P	FVCLILLIADVLYWRGCKNI		
	GBM11P	SSNQLHSYVNSILIPG		
	GBM13P	SSPRVVPNESIPIIPD		
	GBM21P	KSVEYLRNNFRPQQ		
	ZH613	SSPRVVPNESIPIIP		
		SSPRVVPNESIPIIPD		
	ZH645	SPRVVPNESIPIIP		
	SSPRVVPNESIPIIP			
	SSPRVVPNESIPIIPD			

Appendix: Supplement of CHAPTER 2

	ZH678	SSPRVVPNESIPIPIP	
	ZH681	SPRVVPNESIPIPIP	
		SPRVVPNESIPIPIPD	
		SSPRVVPNESIPIPIP	
		SSPRVVPNESIPIPIPD	
	ZH750	SPRVVPNESIPIPIP	
		SSPRVVPNESIPIPIP	
		SSPRVVPNESIPIPIPD	
	ZH791	SSNLHSHYVNSILIPG	
	ZH802	SPRVVPNESIPIPIP	
		SSPRVVPNESIPIPIP	
Zinc finger protein 302 (ZNF302)	<u>18% P</u>		Q9NR11
	GBM10P	QRIHSMKKKYECNKCLKVFSSFSFL	
	GBM11P	QRIHSMKKKYECNKCLKVFSSFSFL	
	GBM14P	QRIHSMKKKYECNKCLKVFSSFSFL	
	GBM16P	QRIHSMKKKYECNKCLKVFSSFSFL	
	ZH631	QRIHSMKKKYECNKCLKVFSSFSFL	
	ZH678	QRIHSMKKKYECNKCLKVFSSFSFL	
	ZH761	QRIHSMKKKYECNKCLKVFSSFSFL	
Pre-rRNA processing protein FTSJ3 (FTSJ3)	<u>18% P</u>		Q8IY81
	GBM18P	GKKGKVGKSRDKFY	
	GBM23P	GKKGKVGKSRDKFY	
	ZH613	GKKGKVGKSRDKFY	
	ZH631	GKKGKVGKSRDKFY	
	ZH645	GKKGKVGKSRDKFY	
	ZH681	GKKGKVGKSRDKFY	
	ZH761	GKKGKVGKSRDKFY	
Patatin-like phospholipase domain-containing protein 7 (PNPLA7)	<u>18% P</u>		Q6ZV29
	GBM13P	PTPQYRFRKRDKVMFYGRKIMRKVT	
	GBM19P	VFYGEEERLKKPPRLQESCDSD	
	GBM20P	SFTDLAEIVSRIEPAK	
	ZH750	PTPQYRFRKRDKVMFYGRKIMRKVT	
	ZH757	PTPQYRFRKRDKVMFYGRKIMRKVT	
		SFTDLAEIVSRIEPAK	
	ZH761	SFTDLAEIVSRIEPAK	
	ZH802	PTPQYRFRKRDKVMFYGRKIMRKVT	
Maltase-glucoamylase, intestinal (MGAM)	<u>18% P</u>		O43451
1 peptide multi-maps to Putative inactive maltase-glucoamylase-like protein LOC93432 (Q2M2H8)	GBM6P	VVQEYLELIGRPALPS	
	GBM12P	KFAGFPALINRMKADG	
	GBM16P	DTPEELCRRWMLGAFYPFSRNHN	
	GBM18P	TLMHKAHTEGVTVVRPLLH	
	GBM19P	IDSQFLGPAFLVSPV	
	ZH681	TIGGILDFYVFLGNTPEQ	
	ZH810	RKKLKKFTTLEIVLSVLLLVLFIS	

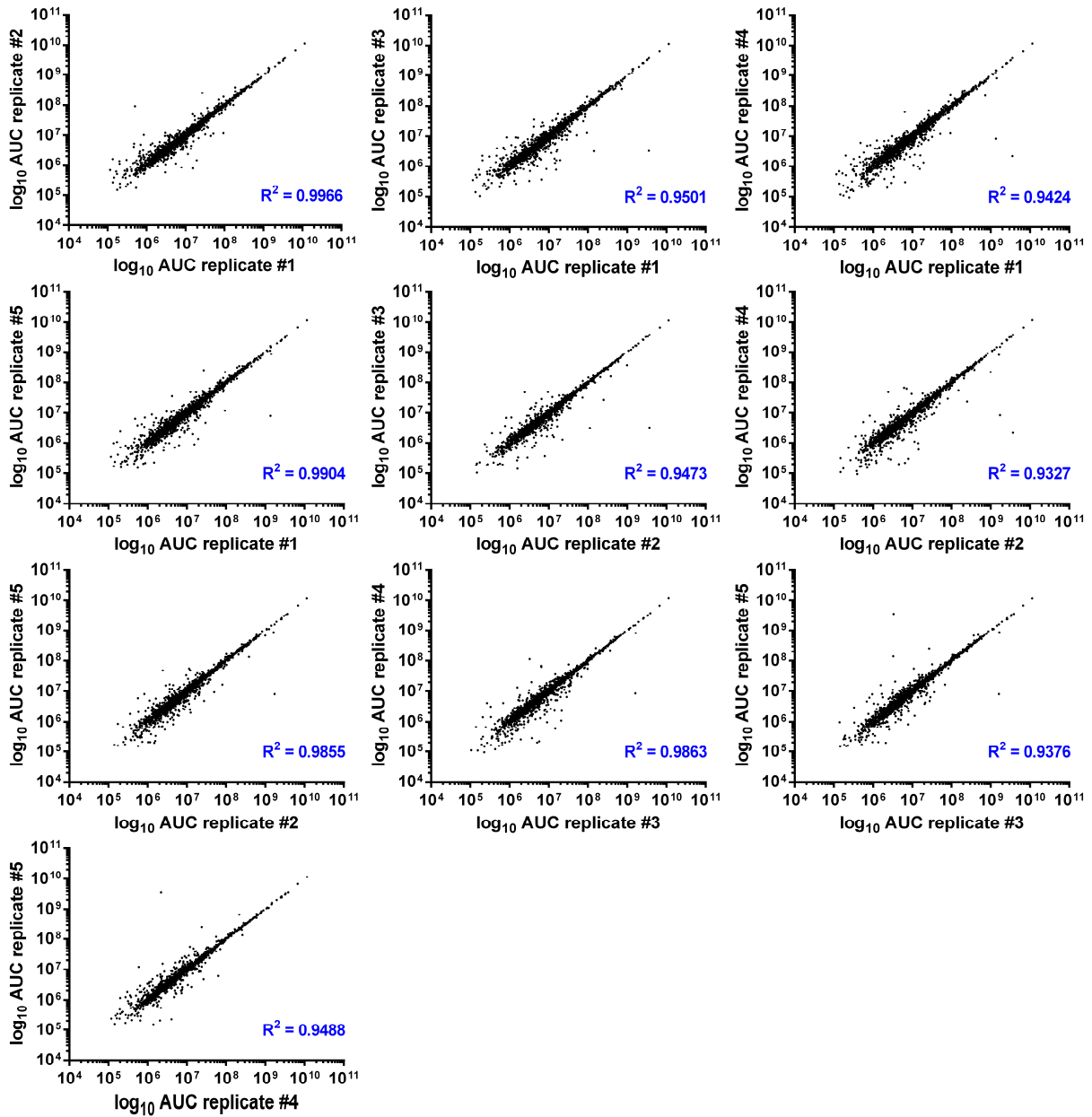
Recurrence-associated HLA class II-presented antigens

Thy-1 membrane glycoprotein (THY1)	<u>29% R</u>		Q7Z4Q2
	GBM2R	EIVLKYLRSRFP	
	GBM3R	EIVLKYLRSRFP	
	GBM9R	EIVLKYLRSRFP	
	GBM11R	EIVLKYLRSRFP	
	GBM14R	EIVLKYLRSRFP	
	GBM16R	VSILGITGSVLAKEDG	
	GBM20R	WNLKDIIPCKSQAEII	
HEAT repeat-containing protein 3 (HEATR3)	<u>25% R</u>		P04216
	GBM5R	FSLTRETKKHVLF	
		LTRETKKHVLF	
	GBM11R	LTRETKKHVLF	
	GBM12R	LTRETKKHVLF	
	GBM14R	YNMKVLYLSAFTSKDE	
	GBM16R	LTRETKKHVLF	
	GBM21R	LTRETKKHVLF	
Arf-GAP with SH3 domain, ANK repeat and PH domain-containing protein 3 (ASAP3)	<u>17% R</u>		Q8TDY4
	GBM9R	KAAQSLFPFIEKLAASVHA	
	GBM10R	PEQFSVAEFL	
	GBM18R	KAAQSLFPFIEKLAASVHA	
	GBM22R	KAAQSLFPFIEKLAASVHA	
		PEQFSVAEFL	
Tudor domain-containing protein 12 (TDRD12)	<u>17% R</u>		Q587J7
	GBM7R	KNIPVKSNIIRVVESFM	
	GBM10R	KNIPVKSNIIRVVESFM	
	GBM12R	KNIPVKSNIIRVVESFM	
	GBM17R	KNIPVKSNIIRVVESFM	
Serine/threonine-protein kinase LMTK2 (LMTK2)	<u>17% R</u>		Q8IWU2
	GBM2R	GLVSALSSDSTSQDSLLEDSL	
	GBM5R	GLVSALSSDSTSQDSLLEDSL	
	GBM9R	GLVSALSSDSTSQDSLLEDSL	
	GBM22R	KSEDLPSHQKIFDLMEINGVQADF	

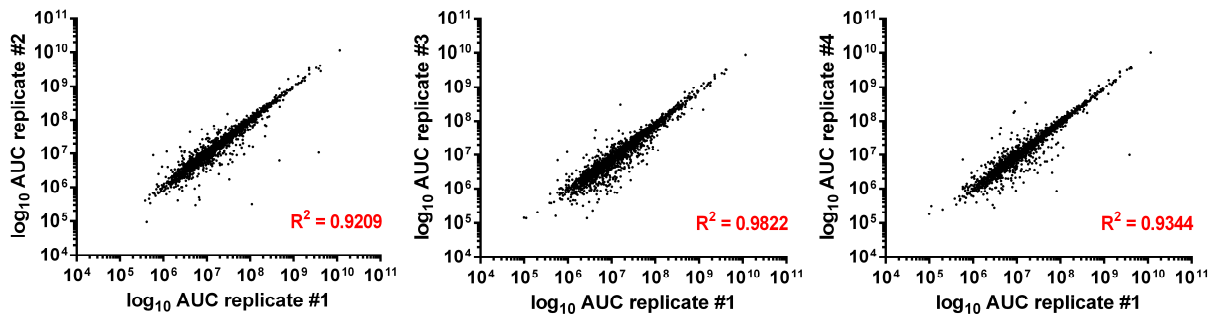
Appendix: Supplement of CHAPTER 2

Seipin (BSCL2)	<u>17% R</u> GBM5R GBM13R GBM14R GBM23R	ENSYVPTTGAIIIEIH ENSYVPTTGAIIIEHS SKRIQLYGAYLRIH ENSYVPTTGAIIIEIH ENSYVPTTGAIIIEHS	Q96G97
APC membrane recruitment protein 1 (AMER1)	<u>17% R</u> GBM12R GBM14R GBM20R GBM21R	QQEDSDEEDEEEEEEGEWSRDSPLSL QQEDSDEEDEEEEEEGEWSRDSPLSL QQEDSDEEDEEEEEEGEWSRDSPLSL QQEDSDEEDEEEEEEGEWSRDSPLSL	Q5JTC6
1-phosphatidylinositol 4,5-bisphosphate phosphodiesterase delta-4 (PLCD4)	<u>17% R</u> GBM10R GBM14R GBM15R ZH753	EEAQIWMRGLQLLVDLVTSMDH EEAQIWMRGLQLLVDLVTSMDH EEAQIWMRGLQLLVDLVTSMD EEAQIWMRGLQLLVDLVTSMDH	Q9BRC7
Cholecystokinin (CCK)	<u>17% R</u> GBM11R GBM14R GBM17R GBM21R	PAGSGLQRAEEAP GALLARYIQQARKA PAGSGLQRAEEAP GALLARYIQQARK GALLARYIQQARKA GALLARYIQQARKAPS	P06307
Treslin (TICRR)	<u>17% R</u> GBM3R GBM12R GBM14R GBM18R	DSEVPAAYQTPKKS KIPSGRTVDKLEDRGRTLRSKPK KSIAEVSQNLRQIEIPK KDTVQEVTKVRRNLFNQELLSP	Q7Z2Z1
Hematopoietic lineage cell-specific protein (HCLS1)	<u>17% R</u> GBM4R GBM8R GBM10R ZH753	KAKFESMAEEKRKRE AVALGISAVAV KAKFESMAEEKRKR KAKFESMAEEKRKRE KAKFESMAEEKRKREE VNDISEKEQRWGAKTIEGSGRTEHI	P14317
Proline-rich acidic protein 1 (PRAP1)	<u>17% R</u> GBM4R GBM16R GBM18R GBM23R	DQGEERPRLLWVMPNHQVLLGPE EERPRLLWVMPNHQVLLGPE ERPRLWVMPNHQVLL ERPRLWVMPNHQVLL ERPRLWVMPNHQVLLG ERPRLWVMPNHQVLLGPE ERPRLWVMPNHQVLL AWGARVVEPPEKDDQL WGARVVEPPEKDD WGARVVEPPEKDDQ WGARVVEPPEKDDQL WGARVVEPPEKDDQLV WGARVVEPPEKDDQLV	Q96NZ9
Proteolipid protein 2 (PLP2)	<u>17% R</u> GBM3R GBM5R GBM14R GBM21R	PVRQPRHTAAPTDPADGPV PVRQPRHTAAPTDPADGPV VTFPVRQPRHTAAPTDPADGPV PVRQPRHTAAPTDPADGP PVRQPRHTAAPTDPADGPV PVRQPRHTAAPTDPADGPV	Q04941
Complement factor D (CFD)	<u>17% R</u> GBM4R GBM5R GBM18R GBM20R	GGVLVAEQWVLSAA GGVLVAEQWVLSAA GGVLVAEQWVLSAAH KPGIYTRVASYAAWI KPGIYTRVASYAAW KPGIYTRVASYAAWI KPGIYTRVASYAAWID RPLPWQRVDRDVAPG VRPLPWQRVDRDVAPG VRPLPWQRVDRDVAPG GGVLVAEQWVLSAAH VRPLPWQRVDRDVAPG	P00746

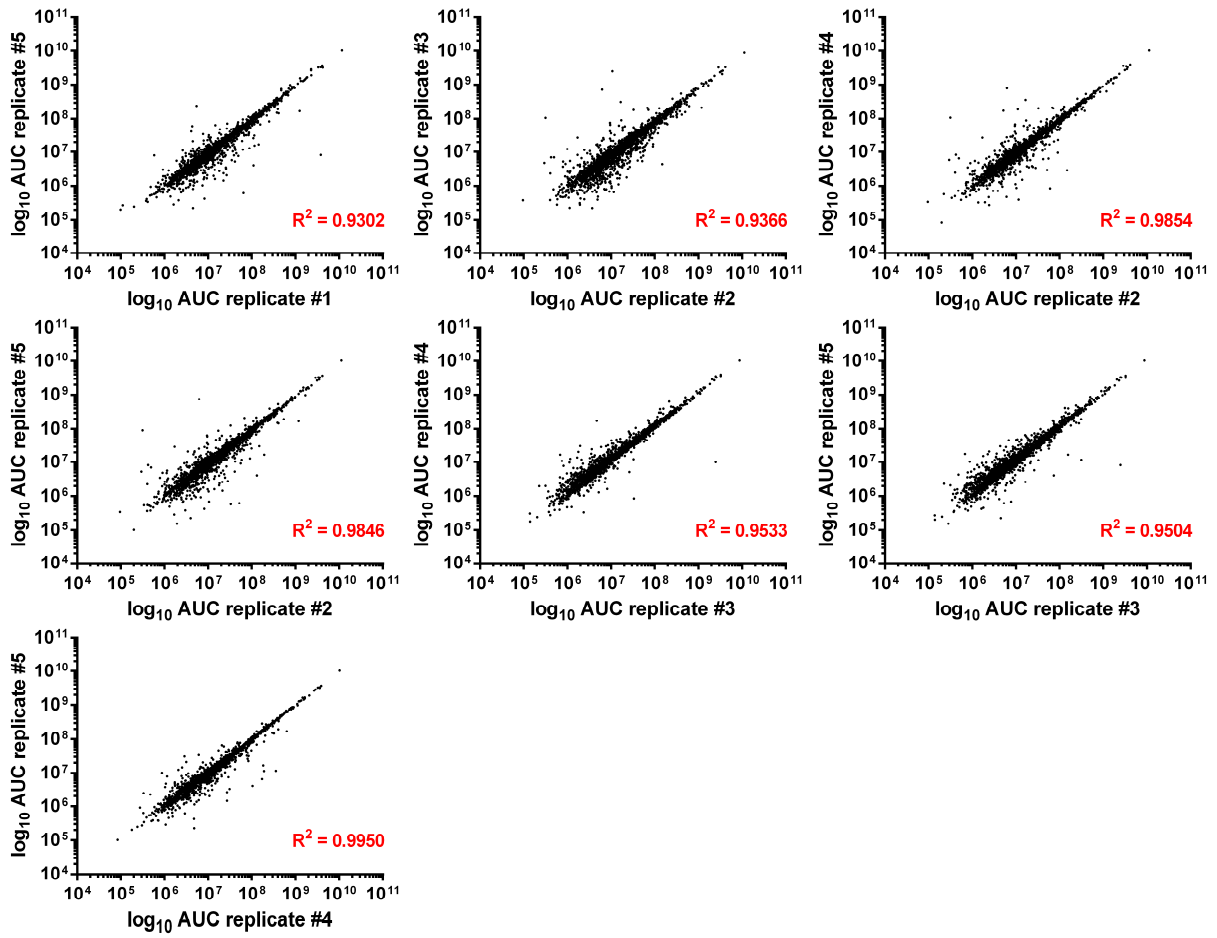
A



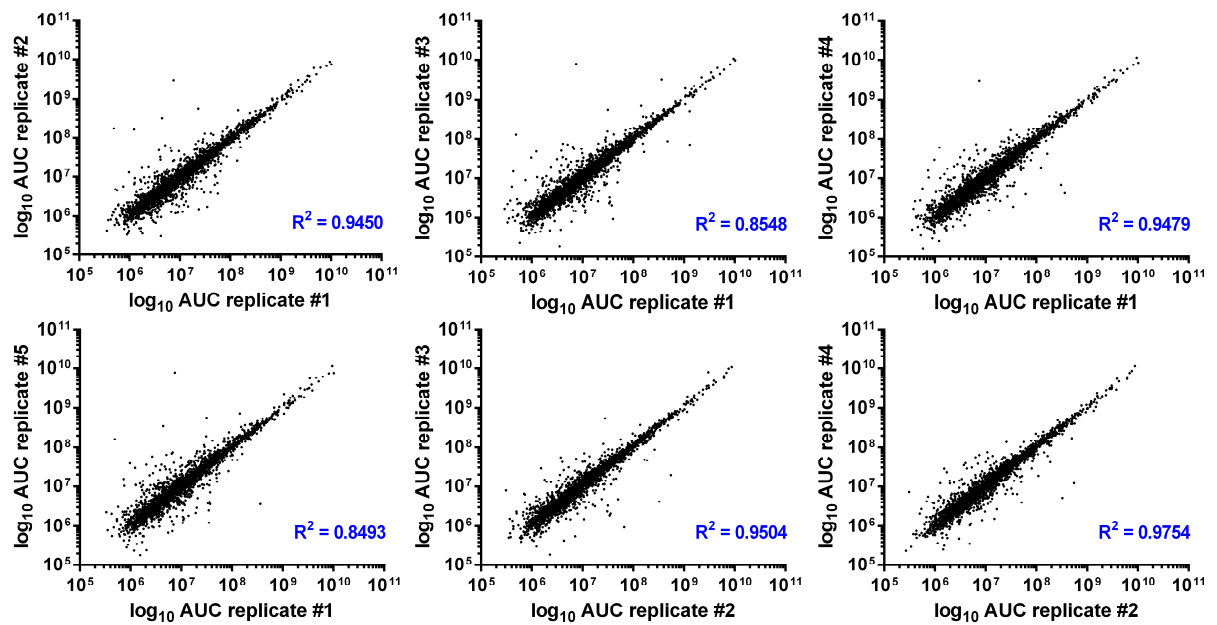
B



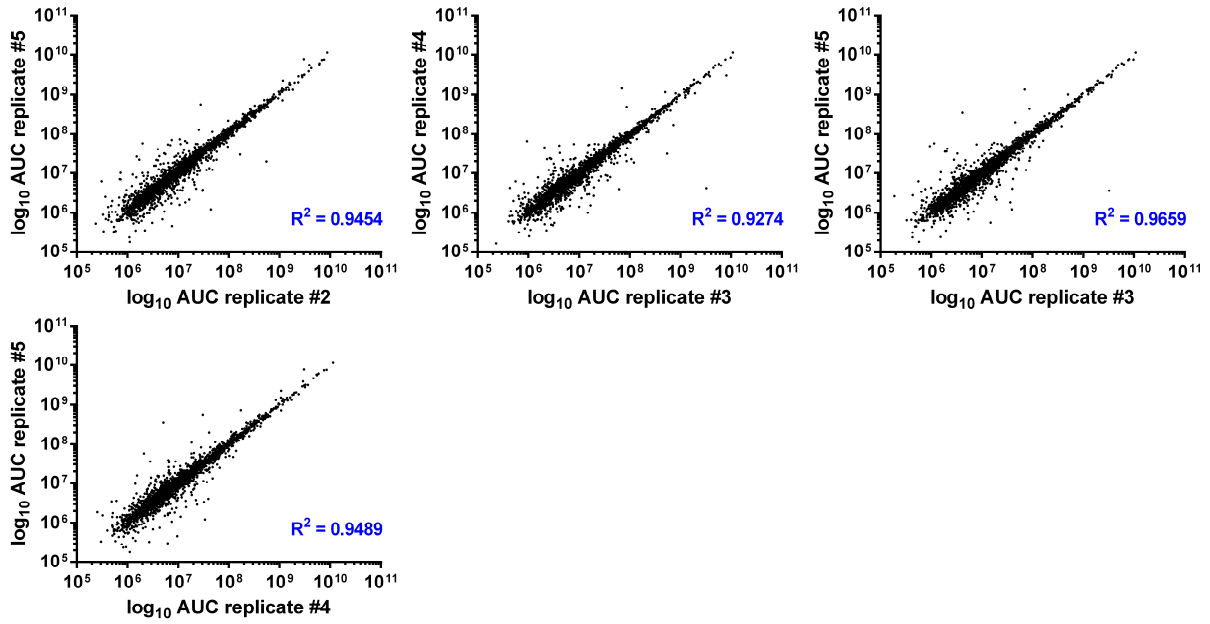
Appendix: Supplement of CHAPTER 2



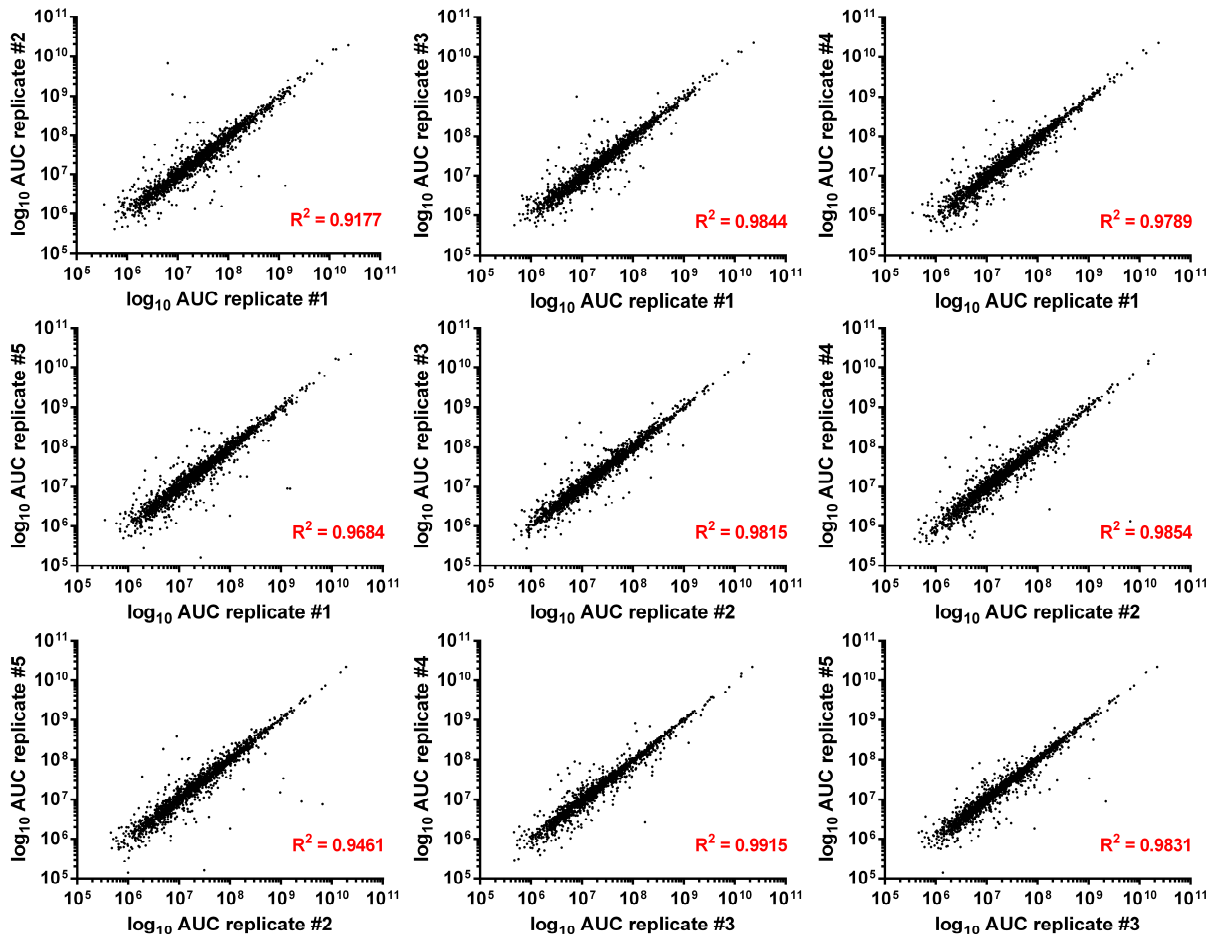
C

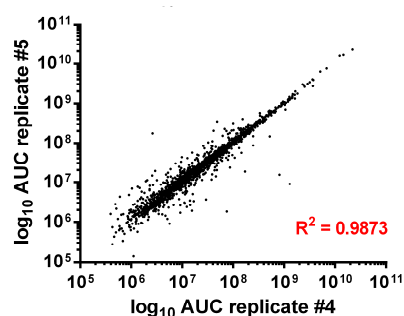


Appendix: Supplement of CHAPTER 2



D





Supplementary Figure 4. Reproducibility of precursor ion intensities across technical replicates exemplarily shown for GBM16. Scatter plots depicting raw MS¹ intensities prior to normalization in pairwise comparisons of technical replicates acquired from (A) HLA class I ligands eluted from primary glioblastoma, (B) HLA class I ligands identified at disease recurrence, (C) HLA class II-presented peptides eluted from primary glioblastoma, and (D) HLA class II-presented peptides identified at disease recurrence. Correlation coefficients were calculated by linear regression and amounted to > 0.92 except for HLA class II peptide intensity comparisons between replicate #1 and #5 as well as between replicate #1 and #3 acquired from primary glioblastoma.

Supplementary Table 7. Peptide sequences and level of modulation for antigens exclusively represented by up- or down-modulated HLA class I- and II-presented peptides on recurrent versus primary glioblastoma. Oxidized (m) and reduced (M) methionine were not treated equally in LFQ-MS and are listed separately. Multi-mapping peptides were censored when the second annotated protein diverged in assignment to groups of modulation according to comparative profiling. HLA restrictions not passing manual assessment as quality control are indicated in italic (HLA class I ligands not matching the motif of any of the patient's HLA allotypes; HLA class II-presented proteins neither identified with peptides exceeding a length of twelve AA nor with different sequences across samples). Abbreviation not introduced in the text above: fold change recurrence/primary (fc R/P).

UniProt accession	Antigen	Patients with significant modulation	Peptide sequence	HLA restriction	Fc (R/P)	Corrected p-value
Antigens exclusively represented by HLA class I ligands up-modulated at recurrence						
P02745	Complement C1q subcomponent subunit A (C1QA)	18% GBM4 GBM5	QPRPAFSAI GQVRRSLGF	B*07:02 <i>B*51:02</i>	173.79 30.26	0.00009 0.00044
P19878	Neutrophil cytosol factor 2 (NCF2)	18% GBM5 GBM20	SQVEALFSY VLYNIAFmY	<i>B*51:01</i> A*29:02	17.08 7.96	0.00432 0.00001
P26572	Alpha-1,3-mannosyl-glycoprotein 2-beta-N-acetylglucosaminyltransferase (MGAT1)	18% GBM5 GBM6	FRFPAVVV DASRPELLY	C*06:02 B*35:01; C*12:03	13.81 40.85	0.00021 0.00052
Q6P4A8	Phospholipase B-like 1 (PLBD1)	18% GBM5 GBM9	VTDTASMKY VTDTASmKY	A*01:01 A*01:01	54.44 5.01	0.00141 0.00406
Q7Z4Q2	HEAT repeat-containing protein 3 (HEATR3)	18% GBM5	IQIKLLSAL	B*13:02; <i>B*51:01</i>	10.06	0.00931
Q86Y82	Syntaxin-12 (STX12)	18% GBM14 GBM12 GBM14	VLDNVKMNL KLQENLQQL KLQENLQQL	<i>C*08:02</i> A*02:01 A*02:01	6.27 7.09 4.28	0.00002 0.00014 0.00117
Q8N7J2	APC membrane recruitment protein (AMER2)	18% GBM6	KKNPGVVAY SKKNPGVVAY VPGPGKPAL	<i>B*15:03</i> <i>B*15:03</i> B*07:02	19.38 57.84 48.50	0.00010 0.00016 0.00002
Q8WTW4	Nitrogen permease regulator 2-like protein (NPRL2)	18% GBM12 GBM20	HPTLGPKITY EEQSHPARLY	B*35:01 B*44:02	10.09 4.63	0.00003 0.00839
Q96PV0	Ras/Rap GTPase-activating protein SynGAP (SYNGAP1)	18% GBM11 GBM14	mLDEDEIHPL YPDEQTSRTL	A*02:01 B*35:03; <i>C*08:02</i>	16.18 4.56	0.00001 0.00025

Appendix: Supplement of CHAPTER 2

Antigens exclusively represented by HLA class I ligands down-modulated at recurrence							
Q53EL9	Seizure protein 6 homolog (SEZ6)	27%					
		GBM5	QSDPGTSLVGY	A*01:01	0.004	0.00002	
		GBM9	QSDPGTSLVGY	A*01:01	0.07	0.00017	
		GBM16	QSDPGTSLVGY	A*01:01	0.001	0.000003	
Q9Y2R0	Cytochrome c oxidase assembly protein 3 homolog, mitochondrial (COA3)	18%					
		GBM4	AQWQKVLPR	A*03:01	0.02	0.00697	
		GBM12	RQAELAQQWQK	A*11:01	0.18	0.00792	
Q9NPD8	Ubiquitin-conjugating enzyme E2 T (UBE2T)	18%					
		GBM7	ASQLVGIEK	A*11:01	0.06	0.00007	
		GBM14	EPNPDDPLm	B*35:03	0.15	0.00005	
Q9H095	IQ domain-containing protein G (IQCG)	18%					
		GBM5	TTDQLSILNY	A*01:01	0.18	0.00604	
		GBM11	SQNEYIANL	A*02:01;	0.10	0.00016	
				A*02:05			
Q9BVV7	Mitochondrial import inner membrane translocase subunit Tim21 (TIMM21)	18%					
		GBM5	RSHPEVIGV	B*13:02	0.13	0.00046	
		GBM12	RQHVRFTEY	B*15:01	0.02	0.00020	
Q96SC8	Doublesex- and mab-3-related transcription factor A2 (DMRTA2)	18%					
		GBM5	GIIPRPAY	B*15:01	0.02	0.00707	
		GBM12	GIIPRPAY	B*15:01	0.02	0.00171	
Q8NI35	InaD-like protein (INADL)	18%					
		GBM5	AQGLVQLEI	B*13:02	0.05	0.00009	
		GBM16	SPAGKTNAL	B*07:02	0.19	0.00596	
Q86YD5	Low-density lipoprotein receptor class A domain-containing protein 3 (LDLRAD3)	18%					
		GBM5	LLDQRPAWY	A*01:01;	0.04	0.00031	
				B*15:01			
		GBM16	ASEVGSPPSY	A*01:01	0.01	0.00006	
			LLDQRPAWY	A*01:01	0.07	0.00020	
Q86VE9	Serine incorporator 5 (SERINC5)	18%					
		GBM4	AISPWVQNR	A*03:01	0.01	0.00315	
		GBM20	ALSSKPAEV	A*02:01	0.06	0.000001	
Q6P499	NIPA-like protein 3 (NIPAL3)	18%					
		GBM5	AVSEASFYSY	B*15:01	0.08	0.00016	
		GBM7	APLSLIVPLSA	B*07:02;	0.08	0.00327	
				B*56:01			
Q5VYS8	Terminal uridylyltransferase 7 (ZCCHC6)	18%					
		GBM5	GQVSLILDV	B*13:02	0.06	0.00383	
		GBM20	LESFIRQDF	B*44:02	0.11	0.00020	
Q16538	Probable G-protein coupled receptor 162 (GPR162)	18%					
		GBM7	TPREPGSFL	B*07:02	0.02	0.00023	
		GBM16	TPREPGSFL	B*07:02	0.02	0.00034	
P62244	40S ribosomal protein S15a (RPS15A)	18%					
		GBM4	VRmNVLADAL	C*07:02	0.07	0.00055	
		GBM20	VLADALKSI	A*02:01	0.03	0.00002	
P28562	Dual specificity protein phosphatase 1 (DUSP1)	18%					
		GBM12	RAAQVFFLK	A*11:01	0.03	0.00137	
		GBM20	KLDEAFEFV	A*02:01	0.05	0.00004	
P23743	Diacylglycerol kinase alpha (DGKA)	18%					
		GBM9	DNVPRHLSL	B*08:01	0.01	0.00017	
		GBM16	NPRQVFNLL	B*07:02	0.14	0.00098	
P18031	Tyrosine-protein phosphatase non-receptor type 1 (PTPN1)	18%					
		GBM9	DIKSYTTR	A*33:05	0.06	0.00008	
				YRFLFNSNT	B*14:02	0.04	0.00075
		GBM14	DIKSYTTR	A*02:01	0.07	0.00075	
P14780	Matrix metalloproteinase-9 (MMP9)	18%					
		GBM9	DAFARAFAL	B*14:02	0.04	0.00034	
		GBM14	DAFARAFAL	B*14:02	0.02	0.00000	
P02788	Lactotransferrin (LTF)	18%					
		GBM12	LLFKDSAIGF	B*15:01	0.06	0.00043	
		GBM20	TLDGGFIYEA	A*02:01	0.02	0.00003	
O75832	26S proteasome non-ATPase regulatory subunit 10 (PSMD10)	18%					
		GBM16	LAYSGKLEEL	C*12:03	0.01	0.00005	
		GBM11	LAYSGKLEEL	A*02:01	0.05	0.00040	
O15230	Laminin subunit alpha-5 (LAMA5) 1 peptide multi-maps to LAMA3 (Q16787)	18%					
		GBM5	SYSPLREF	C*06:02	0.06	0.00019	
			SSYGGTLRY	A*01:01;	0.07	0.00014	
		GBM16	SPRPDLWVL	B*15:01			
				B*07:02	0.06	0.00004	
Q9UQR1	Zinc finger protein 14 (ZNF148)	18%					
		GBM5	QTISPLSTY	B*15:01	0.03	0.00006	
		GBM6	ALNVPISVK	A*03:01	0.07	0.00033	
Antigens exclusively represented by HLA class II-restricted peptides up-modulated at recurrence							
O60293	Zinc finger C3H1 domain-containing protein (ZFC3H1)	17%					
		GBM11	ENCVEETFEDLLLK	Class II	27.90	0.00549	
		GBM21	ENCVEETFEDLLLK	Class II	6.96	0.00046	

Appendix: Supplement of CHAPTER 2

P07148	Fatty acid-binding protein, liver (FABP1)	17% GBM2	TITAGSKVIQNEF IVQNGKHFKF IQKGDIKGVSE IQKGDIKGVSE	Class II Class II Class II Class II	18.38 14.19 4.76 10.18	0.00236 0.00175 0.00959 0.00002
P07492	Gastrin-releasing peptide (GRP)	17% GBM7 GBM11 GBM14	RGRAVPLPAG RGRAVPLPAG	Class II Class II	8.33 17.06	0.00013 0.0000004
Q5T5U3	Rho GTPase-activating protein 21 (ARHGAP21)	17% GBM7 GBM20	WSGFTEQDDRRGICERPRQEIHK SIPFIDEPTSPSIDH	Class II Class II	314.25 15.28	0.00762 0.00017
Q7Z2Z2	Elongation factor Tu GTP-binding domain-containing protein 1 (EFTUD1)	17% GBM7 GBM21	EAYSHLKNILEQINALTGT EAYSHLKNILEQINALTGT	Class II Class II	46.53 32.65	0.00000003 0.000003
Q8NDZ6	Transmembrane protein 161B (TMEM161B)	17% GBM12 GBM16	KNIFTPLFRGLLSFLTWWIAA KNIFTPLFRGLLSFLTWWIAA	Class II Class II	688.01 292.53	0.00043 0.00071
Q99767	Amyloid beta A4 precursor protein-binding family A member 2 (APBA2)	17% GBM7 GBM14	KNIRMMQAQEAVSRVKRmQKA NPSKNIRMMQAQEAVSR	Class II Class II	44.65 10.02	0.00002 0.00248
Q9ULX3	RNA-binding protein NOB1 (NOB1)	17% GBM7 GBM11	KNIYTIREVVTEIRDKATR KNIYTIREVVTEIRDKATR	Class II Class II	193.58 265.85	0.00009 0.00010
Antigens exclusively represented by HLA class II-restricted peptides down-modulated at recurrence						
O00469	Procollagen-lysine,2-oxoglutarate 5-dioxygenase 2 (PLOD2)	17% GBM5 GBM12	DASTFTINIALNNVG SPRKGWSFmHPGRLTH	Class II Class II	0.10 0.02	0.00422 0.00116
O95810	Serum deprivation-response protein (SDPR)	17% GBM12 GBM14	RLENNHAQLRRNHFKVLIF RLENNHAQLRRNHFKVLIF	Class II Class II	0.005 0.003	0.00159 0.000004
P51153	Ras-related protein Rab-13 (RAB13)	17% GBM2 GBM16	EHGIRFFETSAKSS ISTIGIDFKIRTV	Class II Class II	0.08 0.21	0.00170 0.00067
Q5T447	E3 ubiquitin-protein ligase HECTD3 (HECTD3)	17% GBM11 GBM16	LPARIYIPDKLGYE LPARIYIPDKLGYE	Class II Class II	0.05 0.06	0.00152 0.00098
Q86UP2	Kinectin (KTN1)	17% GBM7 GBM16	LKAQIQFHSQIAAQT KAQIQFHSQIAAQT LKAQIQFHSQIAAQT	Class II Class II Class II	0.11 0.17 0.01	0.00037 0.00001 0.00009
Q86VH5	Leucine-rich repeat transmembrane neuronal protein 3 (LRRTM3)	17% GBM11 GBM13	SGNEIEAFSGPSVFQ SGNEIEAFSGPSVFQ	Class II Class II	0.04 0.06	0.00045 0.00010
Q8N0V3	Putative ribosome-binding factor A, mitochondrial (RBFA)	17% GBM2 GBM5	KNWLKFFASKTKK KNWLKFFASKTKK	Class II Class II	0.05 0.07	0.00372 0.00100
Q8NEZ3	WD repeat-containing protein 19 (WDR19)	17% GBM11 GBM16	QSVIRIYLDHLNPE QDLYLASSCPAALEMRRD	Class II Class II	0.09 0.05	0.00098 0.00024
Q96QR8	Transcriptional activator protein Pur-beta (PURB)	17% GBM12 GBM16	VKPSYRNAITVPFK GTSITVDSKRFFFD GTSITVDSKRFFFDVG ELPEGTSITVDSKRFFFDVG	Class II Class II Class II Class II	0.005 0.01 0.07 0.12	0.00230 0.00007 0.00387 0.00375
Q9BRB3	Phosphatidylinositol N-acetylglucosaminyltransferase subunit Q (PIGQ)	17% GBM7 GBM12	ANTVASVLLDV ATTASTGGLAAVF	Class II Class II	0.09 0.04	0.00003 0.00097
Q9H492	Microtubule-associated proteins 1A/1B light chain 3A (MAP1LC3A)	17% GBM3 GBM5	SELVKIIRRRRLQLNPT SELVKIIRRRRLQLNPT	Class II Class II	0.24 0.05	0.00215 0.00493
Q9UPV9	Trafficking kinesin-binding protein 1 (TRAK1)	17% GBM12 GBM14	KAPVTLTSGILMGAKLSK KAPVTLTSGILMGAKLSK	Class II Class II	0.03 0.15	0.00193 0.000004

Supplementary Table 8. Functional annotation clustering of source proteins exclusively presented at recurrent or primary disease and/or represented by up- or down-modulated HLA class I- or II-restricted peptides on recurrent *versus* autologous primary glioblastoma. Clustering for biological processes was performed on the basis of Gene Ontology (GO) terms using DAVID Bioinformatic Resources 6.8 ('Homo sapiens' as background, medium classification stringency, GO BP_ALL). As recommended by Huang *et al.* (Ref. 419 CHAPTER 1), only clusters with an enrichment score ≥ 1.0 were reported.

Biological process Gene Ontology IDs	Enrichment score
Primary-exclusive antigens and proteins exclusively represented by HLA class I ligands down-modulated at recurrence	
amino acid transport	3.11
GO:0003333 GO:1905039 GO:1903825 GO:0006865 GO:1902475 GO:0015804 GO:0015807	
GO:0015849 GO:0015711 GO:0046942 GO:0006820	
metal ion transport	2.32
GO:0055085 GO:0006812 GO:0098655 GO:0006811 GO:0034220 GO:0030001 GO:0015672	
GO:0098662 GO:0006813 GO:0098660 GO:0034765 GO:0043269 GO:0071804 GO:0071805	
GO:0034762 GO:0006816 GO:0070838 GO:0072511 GO:0010959 GO:1904062	
intraspecies interaction	1.76
GO:0051705 GO:0051703 GO:0035176	
coenzyme biosynthesis	1.59
GO:0051188 GO:0009108 GO:0006732 GO:0051186	
protein folding	1.59
GO:0018208 GO:0000413 GO:0006457	
synaptic transmission	1.56
GO:0099536 GO:0099537 GO:0098916 GO:0007268 GO:0050804 GO:0007267	
tRNA modification	1.49
GO:0030488 GO:0006400 GO:0009451 GO:0006399 GO:0008033 GO:0001510 GO:0034470	
adaptive thermogenesis	1.44
GO:0002024 GO:1990845 GO:0002021	
response to alkaloid	1.33
GO:0007274 GO:0007271 GO:0035094 GO:0035095 GO:0043279	
respiratory chain complex IV assembly	1.31
GO:0008535 GO:0017004 GO:0033617 GO:0097034	
insemination	1.29
GO:0007320 GO:0007620 GO:0007618	
action potential transmission	1.21
GO:0019228 GO:0001508 GO:0035637 GO:0042391 GO:0019226	
quinone biosynthesis	1.20
GO:0006744 GO:1901663 GO:0006743 GO:0042181 GO:1901661 GO:0042180	
protein complex disassembly	1.14
GO:0032543 GO:0070125 GO:0070126 GO:0006415 GO:0006414 GO:0043624 GO:0043241	
GO:0032984 GO:0022411	
mRNA catabolism	1.10
GO:0043928 GO:0000291 GO:0000288	
azole transport	1.06
GO:0006867 GO:1902024 GO:0089709 GO:0006868 GO:0045117	
postsynaptic transmission	1.01
GO:0060078 GO:0060079 GO:0099565 GO:2000463 GO:0098815	
Recurrence-exclusive antigens and proteins exclusively represented by HLA class I ligands up-modulated at recurrence	
negative regulation of fatty acid metabolism	3.98
GO:1904223 GO:1904224 GO:2001030 GO:0052697 GO:2001029 GO:0045922 GO:0009410	
GO:0052696 GO:0071466 GO:0052695 GO:0051552 GO:0006805 GO:0010677 GO:0006063	
GO:0019585 GO:0042573 GO:0019217 GO:0009812 GO:0045912 GO:0009813 GO:0045833	
GO:0034754 GO:0010565 GO:0042440 GO:0010675 GO:0042180 GO:0019216 GO:0006109	
GO:0044262	
humoral immune response	3.16
GO:0006958 GO:0002455 GO:0006956 GO:0016064 GO:0072376 GO:0002250 GO:0019724	
GO:0002449 GO:0002460 GO:0038096 GO:0002433 GO:0002431 GO:0038094 GO:0006959	
GO:0002443 GO:0006909 GO:0002757 GO:0038095 GO:0006898 GO:0050778 GO:0002764	
GO:0002253 GO:0050776 GO:0002429 GO:0002376 GO:0006955 GO:0002684 GO:0002768	
GO:0002682 GO:0006897 GO:0038093 GO:0002252 GO:0016192 GO:0048584	
lipid metabolism	2.03
GO:0006631 GO:0019752 GO:0043436 GO:0006082 GO:0032787 GO:0044255 GO:0044281	
GO:0006629	
isoprenoid metabolism	3.05
GO:0045922 GO:0042573 GO:0001523 GO:0006721 GO:0016101 GO:0006720 GO:0034754	
GO:0042445 GO:0010817	
drug metabolism	2.69
GO:0017144 GO:0009698 GO:0009804 GO:0019748	
citrulline biosynthesis	1.98
GO:0019240 GO:1901607 GO:0000052	
drug catabolism	1.73
GO:0017144 GO:0042738 GO:0042737	
intermediate filament organization	1.60
GO:0045104 GO:0045103 GO:0045109	

Appendix: Supplement of CHAPTER 2

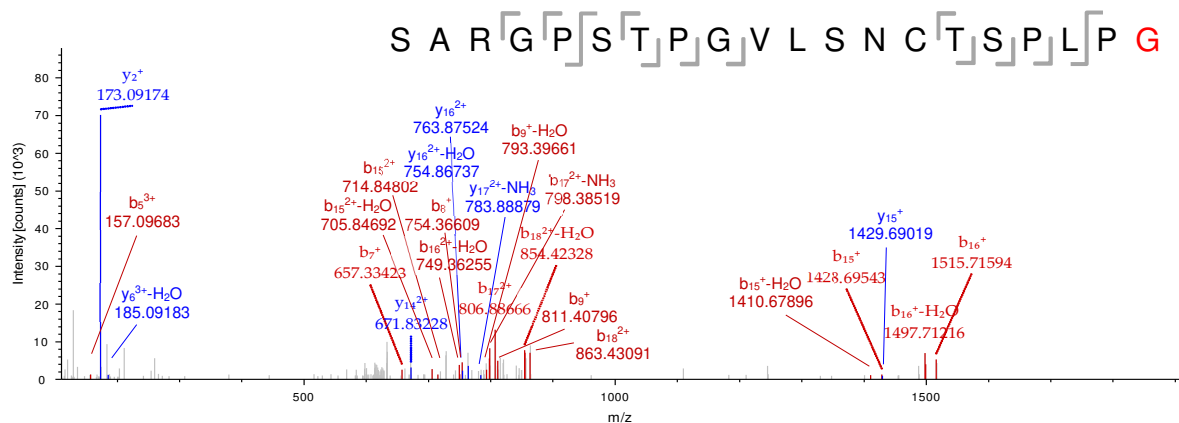
glutamate biosynthesis					1.54	
GO:0009064	GO:1901605	GO:0009084	GO:1901607	GO:0006541	GO:0009065	GO:0006537
GO:0006520	GO:0043648	GO:0008652	GO:1901606	GO:0043650	GO:0006536	
amino acid catabolism					1.47	
GO:0016054	GO:1901606	GO:0009063				
negative regulation of molecular function					1.36	
GO:0043086	GO:0010563	GO:0045936	GO:0044092	GO:0032269	GO:0051248	GO:0051338
cellular process					1.35	
GO:0044699	GO:0044763	GO:0009987				
ion transport					1.22	
GO:0006814	GO:0006813	GO:0071804	GO:0071805	GO:0035725	GO:0030001	GO:0055085
GO:0006811	GO:0042391	GO:0098662	GO:0006812	GO:0098655	GO:0098660	GO:0015672
GO:0070588	GO:0034220	GO:0043269	GO:0034762	GO:0034765	GO:0006816	GO:0072511
GO:0070838						
fatty acid oxidation					1.21	
GO:0016054	GO:0046395	GO:0016042	GO:0044282	GO:0072329	GO:0009062	GO:0044242
GO:0006635	GO:0019395	GO:0034440	GO:0030258			
unsaturated fatty acid metabolism					1.15	
GO:0019369	GO:0019373	GO:0001676	GO:0006690	GO:0033559		
heme metabolism					1.10	
GO:0042440	GO:0006787	GO:0033015	GO:0042167	GO:0046149	GO:0051187	GO:0006778
GO:0033013	GO:0042168					
glutamate secretion					1.03	
GO:0014047	GO:0006835	GO:0006820	GO:0015711	GO:0046942	GO:0051966	
Primary-exclusive antigens and proteins exclusively represented by HLA class II peptides down-modulated at recurrence						
organelle organization					2.51	
GO:0071840	GO:0006996	GO:0016043				
microtubule cytoskeleton organization					2.27	
GO:0007017	GO:0000226	GO:0007010				
histone H4 acetylation					2.15	
GO:0043984	GO:0043981	GO:0043982	GO:0043967			
chromatin organization					2.07	
GO:0016569	GO:0016570	GO:0018205	GO:0051276	GO:0006325		
cell projection assembly					2.00	
GO:0070925	GO:0030031	GO:0044782	GO:0042384	GO:0060271	GO:0010927	
embryonic morphogenesis					1.97	
GO:0043009	GO:0009792	GO:0001701	GO:0009790	GO:0048568	GO:0048598	
histone modification					1.87	
GO:0016570	GO:0018205	GO:0018394	GO:0018393	GO:0016573	GO:0006475	GO:0006473
GO:0043543	GO:0043967					
cell differentiation					1.80	
GO:0044767	GO:0032502	GO:0048856	GO:0007275	GO:0044707	GO:0048731	GO:0007399
GO:0048513	GO:0048869	GO:0048468	GO:0032501	GO:0030154		
regulation of TOR signaling					1.79	
GO:0032006	GO:0031929	GO:0032008	GO:0032007			
neural precursor cell proliferation					1.76	
GO:0072089	GO:2000648	GO:0061351	GO:1902692	GO:0007405	GO:0002052	GO:0072091
GO:2000177	GO:2000179					
DNA-templated transcription					1.74	
GO:0010468	GO:0051171	GO:0034645	GO:0010467	GO:0009059	GO:0090304	GO:0044260
GO:0006807	GO:0060255	GO:0034641	GO:0031323	GO:0016070	GO:0044249	GO:2000112
GO:1901576	GO:0019222	GO:0008152	GO:0044237	GO:0010556	GO:0071704	GO:0043170
GO:0031326	GO:1901360	GO:0009058	GO:0046483	GO:0044271	GO:0080090	GO:0006351
GO:0006139	GO:0009889	GO:0006725	GO:0051252	GO:0019219	GO:0044238	GO:0006366
GO:0006355	GO:0097659	GO:1903506	GO:2001141	GO:1901362	GO:0018130	GO:0019438
GO:0006357	GO:0032774	GO:0034654				
positive regulation of cellular component biogenesis					1.69	
GO:0033043	GO:0010638	GO:0044087	GO:0044089	GO:0051128	GO:0051130	
neuronal stem cell division					1.68	
GO:0048103	GO:0017145	GO:0021846	GO:0036445	GO:0055057	GO:0021873	GO:0048103
positive regulation of stress-activated MAPK cascade					1.63	
GO:0043506	GO:0032872	GO:0070302	GO:0046328	GO:0032874	GO:0070304	GO:0051403
GO:0007254	GO:0031098	GO:0043507	GO:0046330	GO:0080135	GO:0043405	GO:0043406
GO:0043410	GO:0007257					
regulation of cytoskeleton organization					1.57	
GO:0051493	GO:0051493	GO:0051493	GO:0051493			
ribonucleoprotein complex assembly					1.54	
GO:0000245	GO:0022618	GO:0071826	GO:0022613			
phosphatidylcholine biosynthesis					1.50	
GO:0046470	GO:0006656	GO:0097164				
positive regulation of NF-kappaB transcription factor activity					1.49	
GO:0051091	GO:0051090	GO:0051092				
protein localization to microtubule cytoskeleton					1.41	
GO:0072698	GO:0044380	GO:0035372	GO:0071539			
blastocyst development					1.40	
GO:0001832	GO:0001833	GO:0001824				
stress fiber assembly					1.32	
GO:0051492	GO:0030038	GO:0043149	GO:0032231	GO:0051493	GO:0051496	GO:0061572
GO:0051017	GO:0032233	GO:0032970	GO:0031032	GO:0032956	GO:0051495	GO:0030029
GO:0030036	GO:0007015					

Appendix: Supplement of CHAPTER 2

hematopoietic stem cell proliferation						1.24
GO:0071425	GO:1902033	GO:1902035				
negative regulation of proteasomal protein catabolism						1.21
GO:1903051	GO:1903363	GO:1901799	GO:0031330	GO:0032435	GO:0042177	GO:0032434
GO:0009895						
nonmotile primary cilium assembly						1.20
GO:0045724	GO:0035058	GO:1902855	GO:1902857			
sensory organ development						1.19
GO:0007423	GO:0090596	GO:0043583	GO:0048839	GO:0001654	GO:0042471	GO:0042472
GO:0048562						
negative regulation of cyclin-dependent protein kinase activity						1.17
GO:0045736	GO:1904030	GO:0008054	GO:1904029	GO:0000079	GO:0071901	
neural tube formation						1.17
GO:0021915	GO:0014020	GO:0001841	GO:0001843	GO:0060606	GO:0060562	GO:0035148
GO:0035239	GO:0001838	GO:0072175	GO:0016331			
regulation of translation						1.16
GO:0010608	GO:0006417	GO:0034248	GO:0006412	GO:0043043	GO:0043604	GO:0006518
GO:0043603	GO:1901564	GO:1901566				
positive regulation of megakaryocyte differentiation						1.14
GO:0045654	GO:0045652	GO:0030219	GO:0045639			
mRNA splicing						1.13
GO:0008380	GO:0008380	GO:0008380	GO:0008380	GO:0008380	GO:0008380	
rRNA modification						1.12
GO:0000154	GO:0031167	GO:0001510	GO:0070475			
histone deacetylation						1.10
GO:0016575	GO:0006476	GO:0035601	GO:0070932	GO:0098732		
positive regulation of MAPK cascade						1.09
GO:0043412	GO:0044260	GO:0032874	GO:0070304	GO:0006468	GO:0006464	GO:0036211
GO:0032268	GO:0044267	GO:0046330	GO:0016310	GO:0031399	GO:1902531	GO:0006793
GO:0051246	GO:0019220	GO:0042325	GO:0051174	GO:0006796	GO:0023014	GO:0000165
GO:0043408	GO:0001932	GO:0009967	GO:0010647	GO:0023056	GO:0051338	GO:0043549
GO:0071900	GO:0045859	GO:0019538	GO:0043405	GO:0043406	GO:0043410	GO:0032270
GO:0051347	GO:0033674	GO:1902533	GO:0051247	GO:0031401	GO:0042327	GO:0045860
GO:0032147	GO:0001934	GO:0071902	GO:0045937	GO:0010562	GO:0000187	
positive regulation of RNA biosynthesis						1.09
GO:0031323	GO:0019222	GO:0051173	GO:0080090	GO:0006366	GO:0031328	GO:0009891
GO:0010628	GO:0010557	GO:0031325	GO:0045935	GO:0051254	GO:0009893	GO:0006357
GO:1902680	GO:1903508	GO:0045893	GO:0010604	GO:0048518	GO:0048522	GO:0045944
regulation of mRNA splicing <i>via</i> spliceosome						1.08
GO:0043484	GO:1903311	GO:0048024	GO:0050684	GO:0000381		
smoothed signaling pathway						1.06
GO:0045880	GO:0021904	GO:0007224	GO:0008589	GO:0060831	GO:0021532	GO:0009953
positive regulation of GTPase activity						1.06
GO:0044093	GO:0043547	GO:0051345	GO:0043087	GO:0043085	GO:0051336	GO:0050790
GO:0065009						
protein ubiquitination						1.06
GO:0070647	GO:0032446	GO:0016567				
leptin-mediated signaling pathway						1.05
GO:0044321	GO:0044320	GO:0033210				
negative regulation of cell cycle transition due to DNA damage						1.02
GO:0000075	GO:0007049	GO:0000278	GO:1903047	GO:1901987	GO:0010564	GO:0031570
GO:0000077	GO:0022402	GO:0045786	GO:1901988	GO:0010389	GO:0045930	GO:0044770
GO:0007093	GO:1901991	GO:0051726	GO:0044839	GO:0000086	GO:0044772	GO:0007346
GO:1901990	GO:0072331	GO:0010948	GO:0044773	GO:0042770	GO:0044774	GO:0072395
GO:0030330	GO:0072401	GO:0072422	GO:2000134	GO:0044783	GO:0006977	GO:1902807
GO:1902403	GO:1902400	GO:1902402	GO:0072413	GO:0072431	GO:1902806	GO:0044843
GO:0031571	GO:0044819	GO:0007050	GO:0071158	GO:0000082	GO:2000045	GO:0071156
regulation of cell cycle process						1.01
GO:0010564	GO:0090068	GO:0045787				
G2/M DNA damage checkpoint						1.01
GO:1902749	GO:0010389	GO:0031572	GO:1902750	GO:0010972	GO:0007095	GO:0044818
mitotic sister chromatid cohesion						1.01
GO:0007064	GO:0007063	GO:0045876	GO:0034088	GO:0034086	GO:0034091	GO:0034182
GO:0034184	GO:0034093	GO:0051984	GO:0051785	GO:0045840		
Recurrence-exclusive antigens and proteins exclusively represented by HLA class II peptides up-modulated at recurrence						
positive regulation of hydrolase activity						2.25
GO:0043085	GO:0044093	GO:0051345	GO:0050790	GO:0065009	GO:0051336	GO:0043547
GO:0043087						
gene expression						1.97
GO:0034641	GO:1903506	GO:0006139	GO:0006355	GO:2001141	GO:0090304	GO:0044238
GO:0051252	GO:0046483	GO:0019219	GO:0006725	GO:1901360	GO:0071704	GO:0008152
GO:2000112	GO:0010556	GO:0006351	GO:0097659	GO:0044237	GO:0051171	GO:0010468
GO:0006357	GO:0006807	GO:0016070	GO:0043170	GO:0034654	GO:0060255	GO:0032774
GO:0010467	GO:0006366	GO:0044271	GO:0009889	GO:0031326	GO:1901362	GO:0018130
GO:0044260	GO:0019438	GO:0080090	GO:0019222	GO:0009058	GO:1901576	GO:0031323
GO:0009059	GO:0034645	GO:0044249	GO:0009892	GO:0010605	GO:0031324	GO:0048523
GO:0048519						

Appendix: Supplement of CHAPTER 2

mitotic cell cycle						1.73
GO:0022402	GO:0044772	GO:0044770	GO:1903047	GO:0000075	GO:1901990	GO:0007049
GO:0000278	GO:1901987	GO:0010564	GO:0007067	GO:0000280	GO:0048285	GO:0000070
GO:0000819	GO:0090068	GO:0051726	GO:0010948	GO:0045787	GO:0098813	GO:0007346
GO:0007059	GO:0045786	GO:1901991	GO:1901988	GO:0007093	GO:0045930	GO:0051301
GO:0007062						
response to xenobiotic stimulus						1.54
GO:0006805	GO:0071466	GO:0009410				
regulation of metaphase/anaphase transition						1.43
GO:0030071	GO:1902099	GO:0010965	GO:0051784	GO:0051983	GO:0044784	GO:0045839
GO:0051306	GO:0000070	GO:0000819	GO:0007091	GO:0033047	GO:0051304	GO:0031577
GO:0007094	GO:0045841	GO:0071174	GO:2000816	GO:0071173	GO:1902100	GO:0033048
GO:0051783	GO:0033045	GO:0033046	GO:0051985	GO:0007088	GO:1901991	GO:1901988
GO:0007093	GO:0033044	GO:0010639	GO:2001251			
positive regulation of G1/S phase transition						1.42
GO:1901992	GO:0090068	GO:1901989	GO:1900087	GO:0007089	GO:1902808	GO:0045931
chromatin organization						1.36
GO:0016570	GO:0016569	GO:0051276	GO:0006325	GO:0018205		
cerebellum morphogenesis						1.32
GO:0022037	GO:0030902	GO:0021549	GO:0021695	GO:0021696	GO:0021575	GO:0021587
GO:0021533	GO:0021697	GO:0021692	GO:0021702	GO:0021694	GO:0021680	
DNA repair						1.30
GO:0006974	GO:0006259	GO:0006281				
polyketide metabolism						1.21
GO:0071395	GO:0009753	GO:1901661	GO:0044598	GO:0044597	GO:0030638	GO:0030647
GO:0042448	GO:0016137	GO:0019748	GO:0008207	GO:0001523		
triglyceride metabolism						1.17
GO:0006639	GO:0006638	GO:0006641	GO:0046486			
negative regulation of DNA-templated transcription						1.13
GO:0006357	GO:0006366	GO:0000122	GO:0045934	GO:0051253	GO:1902679	GO:0051172
GO:1903507	GO:0009892	GO:0031327	GO:0045892	GO:0010558	GO:0010605	GO:0009890
GO:0031324	GO:0010629	GO:2000113				
proton-transporting ATP synthase complex assembly						1.12
GO:0043461	GO:0070272	GO:0070071				
activation of phospholipase activity						1.05
GO:0007202	GO:0060193	GO:1900274	GO:0060191	GO:0010518	GO:0010863	GO:0010517
negative regulation of muscle cell differentiation						1.04
GO:0051153	GO:0051154	GO:0051148	GO:0051147	GO:0010832	GO:0010830	
behavioral defense response						1.03
GO:0042596	GO:0033555	GO:0001662	GO:0002209			
positive regulation of pri-miRNA transcription						1.01
GO:1902895	GO:1902893	GO:0061614				



Supplementary Figure 5. Fragment spectrum of candidate neo-antigenic HLA class II-restricted peptide derived from mutant ATG9B (ENST00000377974 / ENSG00000181652 c.2294A>G; UPI00015E055A p.756E>G) detected in patient ZH750. The mutated amino acid is marked in red within the sequence, whereas b and y ions are indicated as red and blue peaks in the fragment spectrum, respectively. SARGPSTPGVLSNCTSP L P G was identified with 2.8% FDR (q value = 0.028) and on rank 1 by MHCquant, but annotated on rank 2 by SEQUEST and was therefore excluded from further validation steps.

Supplementary Table 9. Effect of the p.343P>T mutation in patient ZH681 on the phosphorylation state of PDGFR α . Using the PhosphoMotif Finder of the Human Protein Reference Database, the presence of phosphorylation motifs in PDGFR α was assessed for the WT sequence, the p.343P>T mutant version of patient ZH681, and the p.343P>S variant listed in the COSMIC database for two glioblastoma patients. Neo-phosphorylated tyrosine, threonine, and serine residues were subsequently investigated for being part of a neo-phospho binding motif for proteins. Listed phosphorylation motifs and binding sites refer to mutated position 343 plus the first site before and after the mutation.

Position in PDGFR α	Sequence in PDGFR α Mutated AA in red	Corresponding motif Phosphorylated AA in blue	Features of motif
Tyrosine phosphorylation motifs			
WT PDGFRα			
288-289	AE	pY [A/G/S/T/E/D]	Src kinase substrate motif
372-375	EIRY	[E/D]XX pY	ALK kinase substrate motif
ZH681 PDGFRα p.343P>T: 1 neo-phosphorylation motif			
288-289	AE	pY [A/G/S/T/E/D]	Src kinase substrate motif
342-343	YT	pY [A/G/S/T/E/D]	Src kinase substrate motif
372-375	EIRY	[E/D]XX pY	ALK kinase substrate motif
COSMIC PDGFRα p.343P>S: 1 neo-phosphorylation motif			
288-289	AE	pY [A/G/S/T/E/D]	Src kinase substrate motif
342-343	YS	pY [A/G/S/T/E/D]	Src kinase substrate motif
372-375	EIRY	[E/D]XX pY	ALK kinase substrate motif
Serine / threonine phosphorylation motifs			
WT PDGFRα			
322-325	SQLE	[pS/pT]XX[E/D]	Casein kinase II substrate motif
346-348	RIS	RX pS	PKA kinase substrate motif
ZH681 PDGFRα p.343P>T: 8 neo-phosphorylation motifs			
322-325	SQLE	[pS/pT]XX[E/D]	Casein kinase II substrate motif
339-347	VRAY T PPRI	[M/V/L/I/F][R/K/H]XX[pS/pT]XXX[M/V/L/I/F]	AMP-activated protein kinase substrate motif
340-343	RAY T	RXX[pS/pT]	Calmodulin-dependent protein kinase II substrate motif
340-343	RAY T	[R/K]XX[pS/pT]	PKC kinase substrate motif
340-346	RAY T PPR	RXX[pS/pT]XXR	CLK1 kinase substrate motif
342-344	YTP	X[pS/pT]P	GSK-3, ERK1, ERK2, CDK5 substrate motif
343-346	T PPR	[pS/pT]PX[R/K]	CDK1, 2, 4, 6 kinase substrate motif
343-346	T PPR	[pS/pT]PX[R/K]	Growth associated histone H1 kinase substrate motif
343-346	T PPR	[pS/pT]PX[R/K]	Cdc2 kinase substrate motif
346-348	RIS	RX pS	PKA kinase substrate motif
COSMIC PDGFRα p.343P>S: 13 neo-phosphorylation motifs, 1 neo-phosphatase motif			
322-325	SQLE	[pS/pT]XX[E/D]	Casein kinase II substrate motif
339-347	VRAYS P PPRI	[M/L/V/I/F][R/K/H]XXSXXX[M/L/V/I/F]	HMGCoA reductase kinase substrate motif
339-347	VRAYS P PPRI	[M/L/V/I/F][R/K/H]XX[pS/pT]XXX[M/L/V/I/F]	AMP-activated protein kinase substrate motif
340-343	RAY S	RXX pS	Calmodulin-dependent protein kinase II substrate motif
340-343	RAY S	RXX pS	PKA kinase substrate motif
340-343	RAY S	RXX[pS/pT]	Calmodulin-dependent protein kinase II substrate motif
340-343	RAY S	[R/K]XX[pS/pT]	PKC kinase substrate motif
340-346	RAY S PPR	RXX[pS/pT]XXR	CLK1 kinase substrate motif
341-344	AY S P	XX pS P	GSK-3, ERK1, ERK2, CDK5 substrate motif
342-344	Y S P	X[pS/pT]P	GSK-3, ERK1, ERK2, CDK5 substrate motif
343-344	S P	pS P	ERK1, ERK2 kinase substrate motif
343-346	S PPR	[pS/pT]PX[R/K]	CDK1, 2, 4, 6 kinase substrate motif
343-346	S PPR	[pS/pT]PX[R/K]	Growth associated histone H1 kinase substrate motif
343-346	S PPR	[pS/pT]PX[R/K]	Cdc2 kinase substrate motif
343-347	S PPRI	pS PX[R/K]X	CDK kinase substrate motif
346-348	RIS	RX pS	PKA kinase substrate motif

Appendix: Supplement of CHAPTER 2

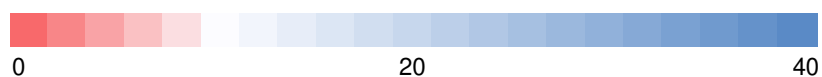
Phospho-tyrosine binding motifs			
WT PDGFRα: p.342Y not phosphorylated			
136-139	YLVI	pY[M/I/L/V]X[M/I/L/V]	GRB2, 3BP2, Csk, Fes, Syk C-terminal SH2 domain binding motif
555-557	YEI	pY[E/M/V][N/V/I]	3BP2 SH2 domain binding motif
ZH681 PDGFRα p.343P>T: 2 neo-phospho-tyrosine binding motifs			
136-139	YLVI	pY[M/I/L/V]X[M/I/L/V]	GRB2, 3BP2, Csk, Fes, Syk C-terminal SH2 domain binding motif
342-345	YTPP	pYXXP	Crk SH2 domain binding motif
342-345	YTPP	pYXXP	RasGAP C-terminal SH2 domain binding motif
555-557	YEI	pY[E/M/V][N/V/I]	3BP2 SH2 domain binding motif
COSMIC PDGFRα p.343P>S: 2 neo-phospho-tyrosine binding motifs			
136-139	YLVI	pY[M/I/L/V]X[M/I/L/V]	GRB2, 3BP2, Csk, Fes, Syk C-terminal SH2 domain binding motif
342-345	YSPP	pYXXP	Crk SH2 domain binding motif
342-345	YSPP	pYXXP	RasGAP C-terminal SH2 domain binding motif
555-557	YEI	pY[E/M/V][N/V/I]	3BP2 SH2 domain binding motif
Phospho-serine / -threonine binding motifs			
WT PDGFRα			
157-158	TP	[pS/pT]P	WW domain binding motif
374-377	RYRS	RXXpS	14-3-3 domain binding motif
ZH681 PDGFRα p.343P>T: 1 neo-phospho-threonine binding motif			
157-158	TP	[pS/pT]P	WW domain binding motif
343-344	T	[pS/pT]P	WW domain binding motif
374-377	RYRS	RXXpS	14-3-3 domain binding motif
COSMIC PDGFRα p.343P>S: 2 neo-phospho-serine binding motifs			
157-158	TP	[pS/pT]P	WW domain binding motif
340-343	RAYS	RXXpS	14-3-3 domain binding motif
343-344	SP	[pS/pT]P	WW domain binding motif
374-377	RYRS	RXXpS	14-3-3 domain binding motif

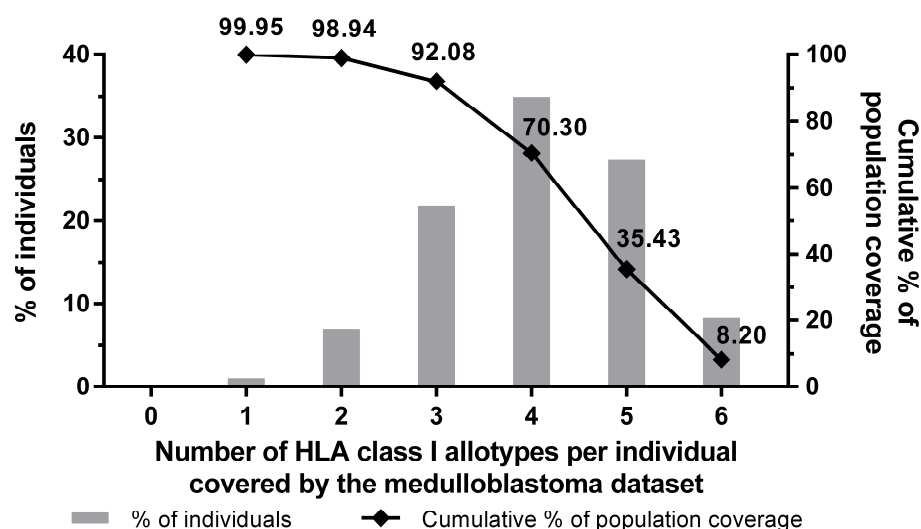
Supplement of CHAPTER 3

Supplementary Table 10. HLA class I allotype and allele frequencies in the medulloblastoma collective comprising n=28 patients. The top three ranking HLA-A, -B, and -C allotypes within the study cohort are marked in bold.

HLA allotype	Positive patients	Allele frequency	HLA allotype	Positive patients	Allele frequency
A*01:01	14%	7%	B*37:01	4%	2%
A*02:01	39%	21%	B*38:01	4%	2%
A*02:02	4%	2%	B*40:02	7%	4%
A*02:05	4%	2%	B*41:01	4%	2%
A*02:11	4%	2%	B*41:02	4%	2%
A*03:01	32%	16%	B*44:02	25%	13%
A*11:01	21%	11%	B*44:03	11%	5%
A*24:02	14%	7%	B*44:05	4%	2%
A*25:01	7%	4%	B*49:01	4%	2%
A*26:01	11%	5%	B*50:01	7%	4%
A*29:02	7%	4%	B*51:01	14%	9%
A*30:01	4%	2%	B*52:01	7%	4%
A*31:01	7%	4%	B*57:01	11%	5%
A*32:01	7%	4%	B*58:01	4%	2%
A*68:01	14%	7%	C*01:02	11%	5%
A*68:02	4%	2%	C*02:02	18%	9%
A*80:01	4%	2%	C*03:03	4%	2%
B*07:02	11%	5%	C*04:01	21%	13%
B*08:01	7%	4%	C*05:01	14%	9%
B*13:02	11%	5%	C*06:02	32%	16%
B*15:01	4%	2%	C*07:01	21%	11%
B*15:08	4%	2%	C*07:02	11%	5%
B*15:18	4%	2%	C*07:04	14%	7%
B*18:01	11%	5%	C*12:02	7%	4%
B*27:02	4%	2%	C*12:03	7%	4%
B*27:05	11%	5%	C*14:02	7%	4%
B*35:01	11%	5%	C*15:02	11%	5%
B*35:02	4%	2%	C*16:01	7%	4%
B*35:03	7%	4%	C*16:04	4%	2%
B*35:08	4%	2%	C*17:01	4%	2%

frequency of positive medulloblastoma patients [%]





Supplementary Figure 6. HLA class I allotype population coverage. Using the population coverage tool provided by the IEDB Analysis Resource, the world population coverage of the 60 distinct HLA-A, -B, and -C allotypes was calculated. The percentage of individuals positive for a specific number of HLA class I allotypes (max. of 6) is indicated by bar charts (associated with the left y-axis). The line diagram (associated with the right y-axis) shows the cumulative percentage of population coverage. The HLA class I allotypes of the medulloblastoma cohort cover 99.95% of the world population (first diamond on line diagram counted from the left) meaning that only 0.05% of all individuals are negative for all HLA-A, -B, and -C allotypes included in the present study (first bar counted from the left). 92.08% of all individuals are positive for at least three HLA class I allotypes (third diamond on line diagram counted from the left).

Supplementary Table 11. Medulloblastoma-associated HLA class I- and II-presented antigens identified on at least three tumors. GTEx profiles were assessed from all available datasets excepting EBV-transformed lymphocytes and cultured fibroblasts. Medulloblastoma-exclusive antigens with a brain-specific expression profile > 10 TPM were not reported (HLA class I: n=13; HLA class II: n=6) as candidate targets. Color codes were defined as follows: ■ < 10 TPM in any tissue, ◆ > 10 TPM in testes and < 10 TPM in other tissues (CTA-like expression profile), ■ 10-20 TPM in any tissue, ■ 20-30 TPM in any tissue, ■ > 30 TPM in any tissue. The number of positive tumors other than medulloblastoma was based on n=874 HLA class I and n=626 HLA class II peptidome datasets. HLA restrictions not passing manual assessment as quality control are indicated in *italics*. These peptides were excluded from downstream analyses such as calculation of peptides matching per patient worldwide. HLA class II-presented proteins neither identified with peptides exceeding a length of twelve AA nor with different sequences across patients were not considered for this listing of candidate target antigens. SYCP3 was detected with only one HLA class II peptide sequence across all patients. To indicate the distribution of antigens across subgroups and age classes, the following abbreviations were used: WNT-activated (W), SHH-activated (S), non-WNT/non-SHH (including those subclassified in Group 3 or Group 4; N), childhood medulloblastoma (≤ 15 years; C), adult medulloblastoma (≥ 25 years; A).

Antigen	Frequency of positive patients	Peptide sequence	HLA restriction	UniProt accession GTEx profile	Positive non-MB tumors
Medulloblastoma-associated HLA class I antigens					
Serine protease inhibitor Kazal-type 8 (SPINK8)	29% / NSW / C			P0C7L1 ■	5
	HH-06	ILFEGLNITK	A*11:01		
	SA2	ILFEGLNITK	A*11:01		
	SA5	ILFEGLNITK	A*11:01		
	Wü-N998/13	ILFEGLNITK	A*03:01		
	ZH513	ILFEGLNITK	A*03:01		
	ZH713	ILFEGLNITK	A*03:01		
	ZH732	ILFEGLNITK	A*03:01		
	ZH872	ILFEGLNITK	A*03:01		

Appendix: Supplement of CHAPTER 3

Protein Wnt-5a (WNT5A)	<u>25% / NSW / AC</u> HH-01 Wü-N391/17 ZH703 ZH718 ZH741 ZH868 ZH937	AMSSKFFLV AMSSKFFLV AMSSKFFLV AMSSKFFLV AMSSKFFLV AMSSKFFLV AMSSKFFLV	A*02:01 A*02:01 A*02:01 A*02:01 A*02:01 A*02:01 A*02:01	P41221 ■	51
Protein shisa-9 (SHISA9)	<u>18% / N / C</u> HH-02 HH-06 SA2 ZH513 ZH732	KVNDDFYTK KVNDDFYTK KVNDDFYTK KVNDDFYTK KMPHPPLAY	A*11:01 A*11:01 A*11:01 A*03:01; A*11:01 A*80:01	B4DS77 ■	11
Insulinoma-associated protein 2 (INSM2)	<u>14% / NS / AC</u> HH-06 SA2 ZH872 ZH913	STFFSSPGLTR STFFSSPGLTR ESFPGGAAAV STFFSSPGLTR	A*11:01 A*11:01 A*68:02 A*68:01	Q96T92 ■	1
Transcription factor HES-4 (HES4) 1 peptide multi-maps to non-MB-exclusive HES1 (Q14469) and HES5 (Q5TA89)	<u>14% / NS / C</u> HH-06 ZH703 ZH872 ZH890	LEKADILEM RINESLAQLK RINESLAQLK SSKPVMEKR	B*41:02 A*03:01 A*03:01 A*31:01	Q9HCC6 ■	19
Solute carrier family 22 member 1 (SLC22A1) peptides multi-map to non-MNG-exclusive SLC22A2 (O15244)	<u>14% / N / C</u> Wü-N526/17 ZH703 ZH513 ZH732	RLIQGLVSK RLIQGLVSK RLIQGLVSK RLIQGLVSK	A*03:01 A*03:01 A*03:01 A*03:01	O15245 ■	7
Insulin-like growth factor-binding protein-like 1 (IGFBPL1)	<u>14% / NS / C</u> HH-02 ZH513 ZH859 ZH872	FPAPDDRM STVTVLDLSK FPAPDDRM RAVPTPVITW	B*35:01 A*11:01 B*35:02 B*57:01	Q8WX77 ■	24
Mitochondrial coenzyme Q-binding protein COQ10 homolog A (COQ10A)	<u>14% / N / C</u> HH-06 SA5 Wü-N526/17 ZH713	ATMFFDEVVK EVVSNVQEY EVVSNVQEY EVVSNVQEY	A*11:01 A*26:01 A*26:01 A*26:01	Q96MF6 ■	16
NADH dehydrogenase [ubiquinone] 1 alpha subcomplex subunit 4-like 2 (NDUFA4L2)	<u>14% / NSW / AC</u> Wü-N391/17 Wü-N998/13 ZH890 ZH913	DQYKFLAV DQYKFLAV GASLGARFY AGASLGARFY AGASLGARFYR ASLGARFYR GASLGARFY	B*52:01 B*51:01 A*29:02 A*01:01 A*31:01 A*31:01 A*29:02	Q9NRX3 ■	77
Neuronal migration protein doublecortin (DCX) 1 peptide multi-maps to non-MB-exclusive doublecortin-like kinase 1/2 (DCLK1/2; O15075/Q8N568)	<u>11% / NS / C</u> SA2 ZH703 ZH859	GTSSSQLSTPK SLDDSDSLGDSM LLADLTRSL TAHSFEQVL	A*11:01 A*01:01 A*02:02; B*13:02 B*35:02	O43602 ■	13
Oligodendrocyte transcription factor 3 (OLIG3) 1 peptide multi-maps to MB-exclusive OLIG2 (Q13516) with brain-associated expression	<u>11% / NS / AC</u> HH-06 Wü-N526/17 ZH913	EVMPYAHGPSVR RLSAESKDLLK EVMPYAHGPSVR	A*68:01 A*03:01 A*68:01	Q7RTU3 ■	20
BTB/POZ domain-containing protein 17 (BTBD17)	<u>11% / NSW / AC</u> HH-06 Wü-N998/13 ZH913	AVFDKFIRY AVFDKFIRY AVFDKFIRY	A*11:01 A*03:01; A*29:02 A*29:02	A6NE02 ■	8
Embryonal Fyn-associated substrate (EFS)	<u>11% / NSW / AC</u> Wü-N998/13 ZH732 ZH913	STGDLQLLY STGDLQLLY AESPQELSF STGDLQLLY	A*03:01; A*29:02 A*80:01; C*02:02 B*44:02; B*44:03 A*29:02	O43281 ■	21
Vacuolar ATPase assembly integral membrane protein VMA21 (VMA21)	<u>11% / SW / C</u> Wü-N998/13 ZH868 ZH872	MSNRDSYFY STLKTLLFF STLKTLLFF	A*29:02 B*57:01 B*57:01	Q3ZAQ7 ■	18

Appendix: Supplement of CHAPTER 3

SERTA domain-containing protein 4 (SERTAD4)	<u>11% / SW / AC</u> Wü-N998/13	FYDYFETGY	A*29:02; C*14:02 A*03:01 A*29:02	Q9NUC0 ■	18
	ZH872	GISNPITTSK			
	ZH913	FYDYFETGY			
Medulloblastoma-associated HLA class II antigens					
Insulin-like growth factor-binding protein-like 1 (IGFBPL1)	<u>36% / NS / AC</u> HH-03	AVPTPVITWRKVTKSPE VPTPVITWRKVTKSPE VPTPVITWRKVTKSPEG ATAWILINPLRKED ATAWILINPLRKEDE GPSDHEATAWILINPLRKEDE GPSDHEATAWILINPLRKEDEG		Q8WX77 ■	7
	SA2	AVPTPVITWRKVTKSPEGTQ PTPVITWRKVTKSPEG TPVITWRKVTKSPEG TPVITWRKVTKSPEGTQ VPTPVITWRKVTKSPE VPTPVITWRKVTKSPEG VPTPVITWRKVTKSPEGT VPTPVITWRKVTKSPEGTQ VRAVPTPVITWRKVTKSPEGTQA			
	SA3	AVPTPVITWRKVTKSPE AVPTPVITWRKVTKSPEG VPTPVITWRKVTKSPE VPTPVITWRKVTKSPEG VPTPVITWRKVTKSPE AVPTPVITWRKVTKSPE AVPTPVITWRKVTKSPEG PTPVITWRKVTKSPE RAVPTPVITWRKVTKSPEG TPVITWRKVTKSPE VPTPVITWRKVTK VPTPVITWRKVTKSP VPTPVITWRKVTKSPE VPTPVITWRKVTKSPEG			
	ZH513	LLLPLLPPLSP DLSKYRSFHFPAPDD DLSKYRSFHFPAPDDR DLSKYRSFHFPAPDDRM KYSRFHFPAPDD LSKYRSFHFPAPDD LSKYRSFHFPAPDDR LSKYRSFHFPAPDDRM SHSTVLDLDSKYRSFHFPAPDDRM SKYRSFHFPAPDD SKYRSFHFPAPDDR SKYRSFHFPAPDDRM STVTVLDLDSKYRSFHFPAPDDRM VLDLDSKYRSFHFPAPDD VLDLDSKYRSFHFPAPDDRM VTVLDLDSKYRSFHFPAPDDRM			
	ZH713	ATAWILINPLRKED GPSDHEATAWILINPLRKEDE GPSDHEATAWILINPLRKEDEG			
	ZH718				
	ZH732	LPGDHVNIAVQVRGGPS			
E3 SUMO-protein ligase CBX4 (CBX4)	<u>21% / NSW / AC</u> HH-02	GIGGKMKIVKNKNKNGRIVMSKY		Q00257 ■	10
	SA5	RERQEQLMGYRKRGP			
	Wü-N998/13	GIGGKMKIVKNKNKNGRIVMSKY			
	ZH513	IVKNKNKNGRIVMSKY			
	ZH718	GIGGKMKIVKNKNKNGRIVMSKY			
	ZH913	GIGGKMKIVKNKNKNGRIVMSKY			
N-acetyltransferase ESCO1 (ESCO1)	<u>21% / NSW / AC</u> HH-02	KVLEVKSDESKEDENLVINEVINSK		Q5FWF5 ■	17
	HH-05	WVFSMMRRKIASRMIECLRSNFIY			
	ZH713	KVLEVKSDESKEDENLVINEVINSK			
	ZH718	KVLEVKSDESKEDENLVINEVINSK			
	ZH859	KVLEVKSDESKEDENLVINEVINSK			
	ZH937	KVLEVKSDESKEDENLVINEVINSK			
Synaptonemal complex protein 3 (SYCP3)	<u>18% / NS / C</u> HH-02	KASLKTSNQKIEHVWKTQQDQRQKL		Q8IZU3 ◆	2
	Wü-N526/17	KASLKTSNQKIEHVWKTQQDQRQKL			
	ZH713	KASLKTSNQKIEHVWKTQQDQRQKL			
	ZH732	KASLKTSNQKIEHVWKTQQDQRQKL			
	ZH859	KASLKTSNQKIEHVWKTQQDQRQKL			

Appendix: Supplement of CHAPTER 3

Thyroid transcription factor 1-associated protein 26 (CCDC59)	<u>18% / SW / AC</u> HH-01 SA2 Wü-N998/13 ZH868 ZH913	RKLKIQQSYKKLL RKLKIQQSYKKLL RKLKIQQSYKKLL RRKLKIQQSYKKLL VREGQGFARRRKLKIQQSYKKLL RRKLKIQQSYKKLL RRKLKIQQSYKKLL	Q9P031 ■	3
Protein LLP homolog (LLPH)	<u>14% / NSW / C</u> HH-04 HH-05 SA1 ZH868	AKSLRSKWKRKMRAEKRRK AKSLRSKWKRKMRAEKRRK KNAPKEASRLKSILK KNAPKEASRLKSILK	Q9BRT6 ■	5
Platelet-activating factor acetylhydrolase (PLA2G7)	<u>11% / NS / C</u> ZH680 ZH718 ZH919	KASLAFLLQKHLGLHK KASLAFLLQKHLGLHK NKASLAFLLQKHLGLHK KASLAFLLQKHLGLHK	Q13093 ■	30
Protocadherin-20 (PCDH20)	<u>11% / NS / AC</u> ZH703 ZH913 ZH919	KGEKHPREDENLEVIPLKGGKIDLH KPMDYELQQFYEVAVVAVNSE IIVIFRPPEIVPR	Q8N6Y1 ■	5
Something about silencing protein 10 (UTP3)	<u>11% / NW / C</u> HH-02 SA1 Wü-N998/13	RRKKIDRNPRVKHREKFRRAKIRRR SGELSGIRAGVKKSIKLL SGELSGIRAGVKKSIKLL	Q9NQZ2 ■	5
CGG triplet repeat-binding protein 1 (CGGBP1)	<u>11% / NS / AC</u> SA2 ZH680 ZH913	ADHPAVRAFLSRHVKN DHPAVRAFLSRHVKN DHPAVRAFLSRHVKN	Q9UFW8 ■	4

Supplementary Table 12. Medulloblastoma-associated HLA class I ligands presented on at least five tumors. Peptides already reported to derive from medulloblastoma-associated antigens were excluded from this listing. In turn, some of those antigens not designated as medulloblastoma-associated due to a CNS-associated expression profile are listed herein with medulloblastoma-associated peptides. The number of positive tumors other than medulloblastoma was based on n=874 HLA class I peptidome datasets. HLA restrictions not passing manual assessment as quality control are indicated in *italic*. These combinations of sequence and HLA restriction were excluded from downstream analyses such as calculation of peptides matching per patient worldwide. Peptides with an HLA restriction not covered by the CNS-related subset (brain, cerebellum, and spinal cord) of the benign database were excluded as well, since it is possible that these are false positive tumor-exclusive peptides arising owing to insufficient depth of the benign dataset (marked in grey). To indicate the distribution of antigens across subgroups and age classes, the following abbreviations were used: WNT-activated (W), SHH-activated (S), non-WNT/non-SHH (including those subclassified in Group 3 or Group 4; N), childhood medulloblastoma (≤ 15 years; C), adult medulloblastoma (≥ 25 years; A).

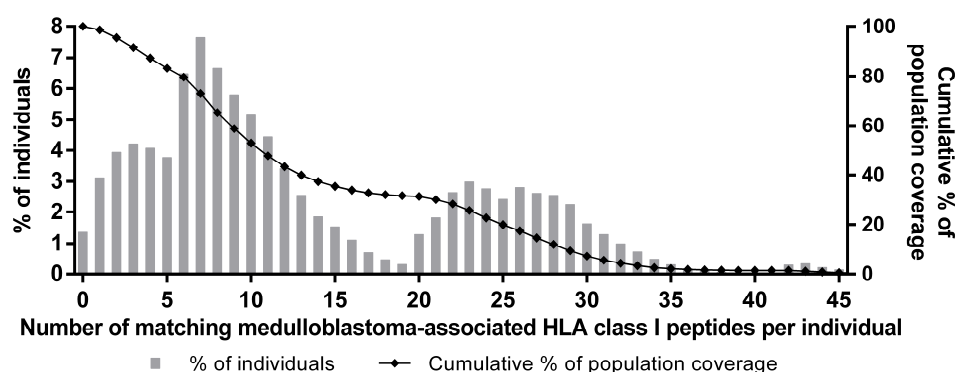
Peptide sequence	HLA restriction	Frequency of positive patients	Antigen (UniProt accession)	Protein frequency on medulloblastomas	Peptide-positive non-MB tumors	Protein frequency on benign samples (n=418)
ASYQEALARL	A*24:02 C*02:02 <i>C*04:01</i> C*16:01 C*17:01	29% HH-04 HH-06 Wü-N526/17 ZH513	<u>NSW / C</u> HH-05 SA5 Wü-N998/13 ZH859	Glial fibrillary acidic protein (GFAP; P14136)	100% 17%	16%
GDRYDGMVGF	B*37:01 B*41:02 B*44:02 B*44:03 C*06:02 <i>C*07:01</i> <i>C*07:02</i>	25% HH-02 HH-05 SA2 Wü-N998/13	<u>NW / C</u> HH-04 HH-06 SA4	Heterogeneous nuclear ribonucleoprotein K (HNRNPK; P61978)	75% 68%	64%
SAASLLLNR	A*03:01 A*11:01 A*68:01	25% HH-03 SA2 ZH513 ZH913	<u>NSW / AC</u> HH-05 SA5 ZH872	Sorting nexin-14 (SNX14; Q9Y5W7)	39% 16%	16%
ALLDGRVQL	A*02:01	25% HH-01 SA3 ZH741 ZH937	<u>NSW / AC</u> SA1 ZH718 ZH868	Aggrin (AGRN; O00468)	46% 19%	11%

Appendix: Supplement of CHAPTER 3

GSLNVTLEH	A*03:01 A*11:01 A*80:01	<u>25%</u> HH-02 SA2 Wü-N998/13 ZH732	<u>NW / C</u> HH-06 SA5 ZH513	DNA (cytosine-5)- methyltransferase 3A (DNMT3A; Q9Y6K1)	46%	8 11%	6%
LLYPVPLVH	A*03:01	<u>25%</u> Wü-N526/17 ZH513 ZH732 ZH872	<u>NSW / C</u> Wü-N998/13 ZH703 ZH859	Kinesin-like protein KIF1A (KIF1A; Q12756)	57%	19 18%	15%
SVYSTPVFSQK	A*03:01 A*11:01	<u>25%</u> HH-06 Wü-N998/13 ZH713 ZH872	<u>NSW / C</u> SA2 ZH703 ZH732	Gamma-aminobutyric acid receptor subunit gamma-2 (GABRG2; P18507)	25%	1 1%	0.5%
AAAGGAFPR	A*11:01 A*68:01	<u>21%</u> HH-02 HH-06 SA2	<u>N / C</u> HH-03 SA1 ZH513	Sortilin (SORT1; Q99523)	29%	6 6%	5%
ATFYSSPGLTR	A*03:01 A*11:01 A*68:01	<u>21%</u> HH-02 SA2 ZH872	<u>NS / AC</u> HH-06 ZH513 ZH913	Insulinoma-associated protein 1 (INSM1; Q01101)	21%	3 1%	0.2%
GLAEEVQRL	A*02:01 A*02:02 A*02:05 B*13:02	<u>21%</u> HH-02 Wü-N391/17 ZH718	<u>NS / C</u> HH-03 ZH703 ZH868	Alpha-internexin (INA; Q16352)	64%	6 27%	29%
KSYTHPSSLRK	A*03:01	<u>21%</u> Wü-N526/17 ZH703 ZH859	<u>NS / C</u> ZH513 ZH732 ZH872	Zinc finger protein ZIC 1/2/3/5 (ZIC1/2/3/5; Q15915 / Q95409 / O60481 / Q96T25)	61% / 39% / 25% / 25%	7 4% / 5% / 2% / 6%	1% / 1% / 0% / 1%
MIMFPLFGK	A*03:01 A*11:01	<u>21%</u> HH-02 Wü-N998/13 ZH713	<u>N / C</u> SA2 ZH513 ZH732	Interphotoreceptor matrix proteoglycan 2 (IMP G2; Q9BZV3)	25%	0 1%	1%
AEIYVNSSFY	B*18:01 B*44:02 B*44:03	<u>18%</u> Wü-N526/17 ZH741 ZH913	<u>NSW / AC</u> ZH718 ZH872	ATP-binding cassette sub-family G member 2 (ABCG2; Q9UNQ0)	71%	3 8%	8%
FLDEPTTGL	A*02:01 C*05:01	<u>18%</u> HH-01 ZH718 ZH937	<u>S / AC</u> SA3 ZH868	ATP-binding cassette sub-family G member 2 (ABCG2; Q9UNQ0)	71%	0 8%	8%
AIFDDSYLGY	A*11:01 A*25:01 A*26:01	<u>18%</u> SA5 ZH680 ZH718	<u>NS / C</u> Wü-N526/17 ZH713	Integrin alpha-V (ITGAV; P06756)	89%	21 48%	41%
AILEQILSH	A*03:01 A*11:01	<u>18%</u> HH-06 ZH513 ZH872	<u>NS / C</u> SA2 ZH732	RUN domain-containing protein 3A/3B (RUNDC3A/3B; Q59EK9 / Q96NL0)	18% / 18%	1 0% / 0%	0% / 1%
ATYGLNVER	A*11:01 A*68:01	<u>18%</u> HH-02 SA2 ZH513	<u>N / C</u> HH-06 SA5	Arf-GAP with GTPase, ANK repeat and PH domain-containing protein 1/3 (AGAP1/3; Q9UPQ3 / Q96P47)	50% / 54%	6 9% / 11%	9% / 9%
GLYAGDPVSK	A*03:01	<u>18%</u> Wü-N526/17 ZH703 ZH872	<u>NSW / C</u> Wü-N998/13 ZH732	RNA pseudouridylate synthase domain- containing protein 1 (RPUSD1; Q9UJJ7)	21%	14 3%	4%
NIYEVVNPk	A*03:01 A*11:01 A*68:01	<u>18%</u> HH-02 SA5 ZH732	<u>N / C</u> HH-06 ZH513	Copine-5 (CPNE5; Q9HCH3)	46%	1 16%	16%
NLDPGAALYLY	A*01:01 A*29:02 A*80:01	<u>18%</u> SA2 ZH732 ZH913	<u>NSW / AC</u> Wü-N998/13 ZH868	BarH-like 1 homeobox protein (BARHL1; Q9BZE3)	18%	2 1%	0.5%
QEADATLRL	B*40:02 B*44:02 B*44:03 B*44:05	<u>18%</u> Wü-N526/17 ZH732 ZH913	<u>NSW / AC</u> Wü-N998/13 ZH741	Glial fibrillary acidic protein (GFAP; P14136)	100%	8 17%	16%
RTYDPEGFK	A*03:01	<u>18%</u> Wü-N998/13 ZH732 ZH872	<u>NSW / C</u> ZH703 ZH859	Diphosphoinositol polyphosphate phosphohydrolase 3- alpha/beta (NUD10/11; Q8NFP7 / Q96G61)	36% / 36%	2 4% / 4%	4% / 4%

Appendix: Supplement of CHAPTER 3

SVDVYQVAK	A*11:01	18% HH-02 SA2 ZH513	<u>N / C</u> HH-06 SA5	Receptor-type tyrosine- protein phosphatase zeta (PRPRZ1; P23471)	57%	7 11%	5%
VSLGTPIMK	A*11:01	18% HH-02 SA2 ZH513	<u>N / C</u> HH-06 SA5	Protein ECT2 (ECT2; Q9H8V3)	43%	8 19%	8%
YEAPVSYTF	B*18:01 B*40:02 B*44:02 B*44:03	18% SA3 ZH718 ZH913	<u>NSW / AC</u> ZH703 ZH741	Cingulin-like protein 1 (CGNL1; Q0VF96)	21%	6 12%	13%
YQDLLNVKL	B*13:02 B*38:01 B*52:01 C*02:02 C*05:01	18% Wü-N391/17 ZH718 ZH937	<u>NSW / AC</u> ZH713 ZH741	Glial fibrillary acidic protein (GFAP; P14136)	100%	25 17%	16%
AVADFLFNV	A*02:01 A*68:02	18% Wü-N391/17 ZH741 ZH872	<u>SW / C</u> ZH718 ZH868	Chemokine-like receptor 1 (CMKKLR1; Q99788)	25%	10 6%	1%
DVIGTLSGF	A*25:01 A*26:01	18% SA5 ZH680 ZH718	<u>NS / C</u> Wü-N526/17 ZH713	Magnesium transporter NIPA2 (NIPA2; Q8N8Q9)	39%	27 11%	14%
EAIKIFNSL	A*25:01 B*08:01 B*35:01 B*35:02 B*35:03	18% HH-02 ZH680 ZH890	<u>NS / C</u> ZH513 ZH859	Unconventional myosin- X (MYO10; Q9HD67)	64%	11 25%	17%
ETFPGVTALF	A*25:01 A*26:01 A*68:02 B*57:01	18% SA5 ZH680 ZH872	<u>NS / C</u> Wü-N526/17 ZH718	Major histocompatibility complex class I-related gene protein (MR1; Q95460)	25%	29 11%	5%
EVIFSLETY	A*25:01 A*26:01	18% SA5 ZH680 ZH718	<u>NS / C</u> Wü-N526/17 ZH713	Asparagine synthetase [glutamine-hydrolyzing] (ASNS; P08243)	36%	17 17%	17%
GSVSININR	A*11:01 A*68:01	18% HH-03 SA1 ZH913	<u>NS / AC</u> HH-06 SA2	A-kinase anchor protein 9 AKAP9; Q99996)	64%	5 35%	32%
QVIEEIEEM	A*02:05 A*26:01 B*35:01	18% HH-02 Wü-N526/17 ZH859	<u>NS / C</u> SA5 ZH713	Fasciculation and elongation protein zeta- 1/2 (FEZ1/2; Q99689 / Q9UHY8)	29% / 39%	15 6% / 9%	7% / 9%
SGSFVVVQK	A*11:01 A*68:01	18% HH-03 SA2 ZH913	<u>NS / AC</u> HH-06 ZH513	Heterochromatin protein 1-binding protein 3 (HP1BP3; Q5SSJ5)	36%	16 35%	24%
SIYDDSYLGY	A*25:01 A*26:01	18% SA5 ZH680 ZH718	<u>NS / C</u> Wü-N526/17 ZH713	Integrin alpha-5 (ITGA5; P08648)	21%	19 10%	6%
STFSGFLVY	A*03:01 A*11:01 A*29:02 B*57:01 C*02:02	18% SA5 ZH513 ZH913	<u>NSW / AC</u> Wü-N998/13 ZH872	Complement C1q tumor necrosis factor-related protein 5 (C1QTFB5; Q9BXJ0)	21%	26 4%	1%
SVLATVQQV	A*02:01 A*02:11	18% HH-01 Wü-N391/17 ZH868	<u>SW / C</u> SA3 ZH741	Laminin subunit gamma-3 (LAMC3; Q9Y6N6)	43%	13 4%	4%
TVIIHIPQY	A*25:01 A*26:01	18% SA5 ZH680 ZH718	<u>NS / C</u> Wü-N526/17 ZH713	Integrin alpha-2 (ITGA2; P17301)	25%	23 7%	6%



Supplementary Figure 7. Population coverage of medulloblastoma-associated HLA-A, -B, and -C ligands. Using the population coverage tool provided by the IEDB Analysis Resource, the world population coverage of the 66 medulloblastoma-associated peptides was calculated. The percentage of individuals with a specific number of matching peptides (max. of 53) is indicated by bar charts (associated with the left y-axis). The line diagram (associated with the right y-axis) shows the cumulative percentage of population coverage. The candidate target peptides cover 98.64% of the world population (first diamond on line diagram counted from the left) meaning that only 1.36% of all individuals are negative for all HLA-A, -B, and -C allotypes for which medulloblastoma-associated peptides were defined. On average, 14 peptides are expected to match per patient worldwide.

Supplementary Table 13. Medulloblastoma-exclusive HLA class II-presented peptides derived from medulloblastoma-associated HLA presentation hotspots. Peptides already reported to derive from medulloblastoma-associated antigens were excluded from this listing. The number of positive tumors other than medulloblastoma was based on n=626 HLA class II peptidome datasets. To indicate the distribution of antigens across subgroups and age classes, the following abbreviations were used: WNT-activated (W), SHH-activated (S), non-WNT/non-SHH (including those subclassified in Group 3 or Group 4; N), childhood medulloblastoma (≤ 15 years; C), adult medulloblastoma (≥ 25 years; A).

Antigen (UniProt accession)	Protein frequency on medulloblastomas	Peptide sequence	Frequency of positive patients	Protein frequency on non-MB tumors	Protein frequency on benign samples (n=364)
Zinc finger C3H1 domain-containing protein (ZFC3H1; O60293)	25%	ENCVEETFEDLLLK	NSW / C HH-06 SA2 ZH703	3% 8	2%
			NS / AC ZH872 SA1 ZH703	9% 3 1 8	6%
Neural cell adhesion molecule 1 (NCAM1; P13591)	32%	KDVRFIVLSNNYLQIR KDVRFIVLSNNYLQIRG LSNNYLQIRGIKKTDE	NS / AC ZH872 SA1 SA2 ZH913	9% 3 1 8	6%
			SA2 ZH703	2 4	
			SA1 ZH703 ZH913	4 18% 4	
			SA2 ZH913	2 4	
Coxsackievirus and adenovirus receptor (CXADR; P78310)	18%	AIPVMIPAQSKDGSIV IPAQSKDGSIV	N / C SA2 ZH732	6% 0	3%
			SA1	0	
Follistatin-related protein 4 (FSTL4; Q6MZW2)	32%	PPVIRVYPESQAQEPGV THVLQVNVPPVIRVYPESQAQEPG VPPVIRVYPESQAQ VPPVIRVYPESQAQEPG	NSW / C ZH680 ZH718 ZH872 ZH680 ZH703 ZH872	2% 0 0 1 3	5%
			NSW / AC SA3 SA1 SA1 SA1 SA2	18% 0 0 0 0	
			NSW / AC SA3 SA1 SA1 SA1 SA2	18% 0 0 0 0	
			NSW / AC SA3 SA1 SA1 SA1 SA2	18% 0 0 0 0	
			NSW / AC SA3 SA1 SA1 SA1 SA2	18% 0 0 0 0	
Programmed cell death 6-interacting protein (PDCD6IP; Q8WUM4)	54%	AKQKQKFGEEIARLQH ARLQHAELIKTV FGEEIARLQHAELIKTV HAELIKTV	NSW / AC SA3 SA1 SA1 SA1 SA2	18% 0 0 0 0	17%
			NSW / AC SA3 SA1 SA1 SA1 SA2	18% 0 0 0 0	
			NSW / AC SA3 SA1 SA1 SA1 SA2	18% 0 0 0 0	
			NSW / AC SA3 SA1 SA1 SA1 SA2	18% 0 0 0 0	
			NSW / AC SA3 SA1 SA1 SA1 SA2	18% 0 0 0 0	
			NSW / AC SA3 SA1 SA1 SA1 SA2	18% 0 0 0 0	

Appendix: Supplement of CHAPTER 3

		KFGEEIARLQHAA	4%	SA1	0		
		KFGEEIARLQHAEL	7%	SA1	0		
			SA3				
		KFGEEIARLQHAELIK	4%	SA1	0		
		KFGEEIARLQHAELIKTV	43%	HH-03	0		
			HH-04	HH-05			
			SA1	SA2			
			SA3	SA4			
			Wü-N391/17	Wü-N526/17			
			ZH913	ZH919			
			ZH937				
		KQKKKFGEEIARLQH	4%	SA3	1		
		QKKKFGEEIARLQH	4%	SA3	2		
				<u>NW</u> / <u>C</u>	0.5%	2%	
Cadherin-related family member 1 (CDHR1; Q96JP9)	46%	ANDEAPRFIQEPYVAL	4%	ZH680	0		
		ANDEAPRFIQEPYVALVPEDIPA	7%	ZH680	0		
				ZH741			
		ANDEAPRFIQEPYVALVPEDIPAG	4%	ZH680	0		
		ANDEAPRFIQEPYVALVPEDIPAGS	4%	ZH680	0		
		APRFIQEPYVAL	4%	ZH680	0		
		APRFIQEPYVALVPE	14%	ZH680	0		
				ZH713	ZH732		
				ZH741			
		DANDEAPRFIQEPYVAL	4%	ZH680	0		
		DANDEAPRFIQEPYVALVPE	4%	ZH680	0		
		DANDEAPRFIQEPYVALVPED	4%	ZH680	0		
		DANDEAPRFIQEPYVALVPEDIPA	7%	ZH680	0		
				ZH713			
		DANDEAPRFIQEPYVALVPEDIPAG	4%	ZH680	0		
		DEAPRFIQEPYVAL	11%	ZH680	0		
				ZH713	ZH732		
		DEAPRFIQEPYVALVP	7%	ZH680	0		
				ZH713			
		DEAPRFIQEPYVALVPE	18%	ZH513	0		
				ZH680	ZH713		
				ZH732	ZH741		
		DEAPRFIQEPYVALVPED	4%	ZH680	0		
		DEAPRFIQEPYVALVPEDIP	4%	ZH680	0		
		DEAPRFIQEPYVALVPEDIPA	14%	ZH680	0		
				ZH713	ZH732		
		ZH741					
DEAPRFIQEPYVALVPEDIPAG	4%	ZH680	0				
DEAPRFIQEPYVALVPEDIPAGS	4%	ZH680	0				
DEAPRFIQEPYVALVPEDIPAGSII	4%	ZH680	0				
EAPRFIQEPYVAL	14%	ZH680	0				
		ZH713	ZH732				
		ZH741					
EAPRFIQEPYVALVP	7%	ZH680	0				
		ZH713					
EAPRFIQEPYVALVPE	25%	Wü-N998/13	1				
		ZH513	ZH680				
		ZH713	ZH732				
		ZH741	ZH890				
EAPRFIQEPYVALVPED	4%	ZH680	0				
EAPRFIQEPYVALVPEDIPA	14%	ZH680	0				
		ZH713	ZH732				
		ZH741					
EAPRFIQEPYVALVPEDIPAG	4%	ZH680	0				
GTPVKIEAIDEDAEEP	4%	HH-02	0				
GTPVKIEAIDEDAEEP	18%	HH-02	0				
		HH-06	SA1				
		SA5	ZH713				
IQEPYVALVPEDIPA	4%	Wü-N998/13	0				
LGTPVKIEAIDEDAEEP	4%	HH-02	0				
NDEAPRFIQEPYVALVPEDIPA	4%	ZH680	0				
TPVKIEAIDEDAEEP	21%	HH-02	0				
		SA1	SA4				
		SA5	ZH713				
		ZH732					
			<u>NSW</u> / <u>AC</u>	0%	1%		
Insulinoma- associated protein 2 (INSM2; Q96T92)	25%	PRGFLVKRTKRTGGL	11%	SA3	0		
			ZH868	ZH913			
		PRGFLVKRTKRTGGLY	7%	HH-06	0		
			ZH913				
		PRGFLVKRTKRTGGLYRV	4%	ZH913	0		
		PRGFLVKRTKRTGGLYRVR	7%	Wü-N526/17	0		
		ZH913					
PRGFLVKRTKRTGGLYRVRL	21%	SA3	0				
		Wü-N526/17	Wü-N998/13				
		ZH513	ZH868				

Appendix: Supplement of CHAPTER 3

		ZH913					
Insulinoma-associated protein 1 (INSM1; Q01101)	32%	PRGFLVKRSKKSTPVSY		<u>NSW</u> / <u>AC</u>	0%	1%	
				32%	SA2	0	
				Wü-N391/17	Wü-N998/13		
				ZH513	ZH732		
				ZH741	ZH859		
Dihydropyrimidinase-related protein 1 (CRMP1; Q14194)	68%	AADDFFQGTRAALVGG AADDFFQGTRAALVGGT AADDFFQGTRAALVGGTT ADDDFFQGTRAALVGG ADDDFFQGTRAALVGGT DDFFQGTRAALVGGT DDFFQGTRAALVGGTT DDFFQGTRAALVGGT DFFQGTRAALVGGTT		<u>S</u> / <u>AC</u>	16%	14%	
			4%	SA3	0		
			11%	SA3	2		
			7%	SA4	ZH868		
			7%	SA3	1		
			4%	ZH868			
			4%	SA3	0		
			11%	SA3	5		
			14%	SA4	ZH868		
			14%	SA3	4		
			4%	ZH868	ZH872		
			4%	ZH937			
4%	SA3	0					
11%	SA3	2					
4%	ZH868	ZH872					
4%	SA3	0					
Nucleolar and coiled-body phosphoprotein 1 (NOLC1; Q14978)	57%	KFTKGKSFREKTK KFTKGKSFREKTKK KFTKGKSFREKTKKK		<u>SW</u> / <u>AC</u>	13%	2%	
			7%	Wü-N391/17	2		
			18%	HH-05	1		
			7%	Wü-N391/17	ZH741		
			7%	ZH868	ZH913		
Drebrin (DRBN1; Q16643)	50%	FMESAEQAVL MESAEQAVL MESAEQAVLA MFMESAEQAVLA		<u>NS</u> / <u>C</u>	11%	10%	
			4%	ZH513	0		
			18%	SA2	3		
			14%	ZH513	ZH703		
			14%	ZH718	ZH732		
			14%	SA2	2		
			4%	ZH513	ZH718		
4%	ZH872						
4%	SA2	1					

Supplementary Table 14. Established TAAs and CTAs identified as medulloblastoma-exclusive antigens or represented by medulloblastoma-exclusive peptides on ≥ 2 tumors. HLA restrictions not passing manual assessment as quality control are indicated in italic. The number of positive neoplasias other than medulloblastoma was based on n=874 HLA class I and n=626 HLA class II peptidome datasets. The frequency of positive benign HLA peptidomes was calculated from n=418 (HLA class I) or n=364 (HLA class II) benign human specimens. Medulloblastoma exclusivity of HLA class II-restricted peptides was evaluated for the exact sequence match with none of the peptides arising from a tumor-associated presentation hotspot.

Peptide sequence	HLA restriction	Frequency of positive patients	Protein frequency on medulloblastomas	Protein frequency on non-MB tumors	Protein frequency on benign samples
Medulloblastoma-exclusive HLA class I ligands derived from established TAAs and CTAs					
Regulator of G-protein signaling 5 (RGS5; O15539)					
KIKSPAKMAEK	A*03:01; A*30:01	14%	Wü-N998/13 ZH872 ZH937	31%	18%
KLLQNNYGL	A*02:01	11%	HH-01 ZH868	17	18
Catenin beta-1 (CTNNB1; P35222)					
ATVGLIRNL	<i>A*02:01; A*32:01; B*57:01; C*02:02; C*12:03</i>	14%	HH-02 ZH868	93%	76%
IENIQRVAA	B*41:01; B*50:01	7%	HH-02	Wü-N391/17	9
VNIMRTYTY	A*29:02	7%	Wü-N998/13 ZH913	6	
Retinoblastoma-associated protein (RB1; P06400)					
AETQATSAF	B*18:01; B*44:02; B*44:03; B*44:05	11%	ZH741 ZH913	46%	34%
GVLGGYIQK	A*11:01	7%	SA5	ZH513	10

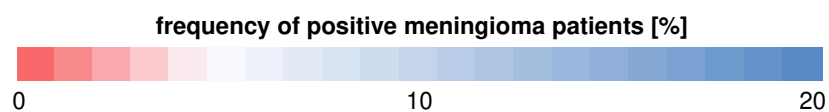
Appendix: Supplement of CHAPTER 3

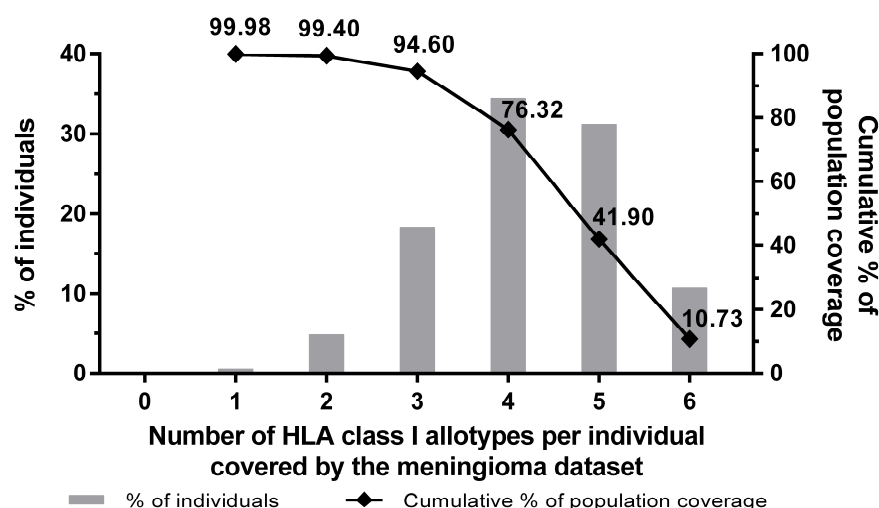
DNA repair protein RAD51 homolog 1 (RAD51; Q06609)				14%	13%	7%
ESFGPQPISR	A*68:01	11%	HH-03 ZH913	HH-06	11	
Arachidonate 12-lipoxygenase, 12S-type (ALOX12; P18054)					29%	6%
KRLDFEWTL	B*27:05	7%	ZH513	ZH680	2	9%
Axin-2 (AXIN2; Q9Y2T1)					14%	5%
ETVDSGYRSF	A*25:01	7%	ZH680	ZH718	16	3%
LTSDIYLEY	A*03:01; A*11:01; A*29:02	7%	ZH513	ZH913	15	
G2/mitotic-specific cyclin-B1 (CCNB1; P14635)					43%	15%
EEQAVRPKY	B*44:02; B*44:03	7%	Wü-N998/13	ZH868	13	13%
Cytochrome P450 1B1 (CYP1B1; Q16678)					50%	28%
DTVVFNQW	A*25:01	7%	ZH680	ZH718	9	41%
Glutamate carboxypeptidase 2 (FOLH1; Q04609)					14%	6%
DIVPPFSAF	A*25:01	7%	ZH680	ZH718	4	6%
UPF0378 protein KIAA0100 (KIAA0100; Q14667)					25%	20%
EVSTAKLTAFA	A*25:01	7%	ZH680	ZH718	11	17%
Leucine zipper putative tumor suppressor 1 (LZTS1; Q9Y250)					14%	3%
SPESASHQL	B*35:01; B*35:02; B*35:03	7%	ZH859	ZH890	8	0.5%
Outer dense fiber protein 2 (ODF2; Q5BJF6)					32%	3%
NVFGDGPYSTF	A*25:01	7%	ZH680	ZH718	8	13%
Platelet-derived growth factor receptor beta (PDGFRB; P09619)					61%	23%
YMDLVGFSY	A*29:02	7%	Wü-N998/13	ZH913	4	16%
Proteasome subunit beta type-9 (PSMB9; P28065)					43%	35%
AGVDHRVIL	C*07:04; C*16:01	7%	ZH872	ZH913	6	29%
Inactive rhomboid protein 2 (RHBDF2; Q6PJF5)					7%	5%
ISSTVQRQL	B*57:01	7%	SA3	ZH868	7	1%
Tyrosine-protein kinase receptor Tie-1 (TIE1; P35590)					32%	10%
SLFENFTYA	A*02:01	7%	HH-01	ZH868	1	16%
Medulloblastoma-exclusive HLA class II-presented antigens derived from established TAAs and CTAs						
DNA repair protein RAD51 homolog 1 (RAD51; Q06609)					7%	1%
KLVPMGFTTATEFHQRSEII		7%	HH-01	ZH680	4	0%
Glypican-2 (GPC2; Q8N158)					7%	0%
ARGYSLNLIPPALI		7%	ZH703	ZH718	0	0%
ERVFPPLLHPQYSFPPD		4%	ZH718		0	
GARGYSLNLIPPALI		4%	ZH703		0	
GARGYSLNLIPPALIS		7%	ZH703	ZH718	0	
GARGYSLNLIPPALISG		7%	ZH703	ZH718	0	
VLGARGYSLNLIPPALISGEHL		4%	ZH703		0	
Medulloblastoma-exclusive HLA class II-restricted peptides derived from established TAAs and CTAs						
Golgin subfamily A member 6-like protein 2 (GOLGA6L2; Q8N9W4)					75%	24%
EEMWQGEKKMWRQEKMREQEEMRE	14%		HH-06 ZH680	SA2 ZH872	2	43%
KMWEQEEKMREQEEMWRQEERLW	7%		Wü-N391/17	ZH680	2	
QKMRDQEERMWEQDERLREKEERM	7%		ZH718	ZH741	1	
Breast cancer type 1 susceptibility protein (BRCA1; P38398)					7%	1%
QPEVYKQSLPGSNCKHPEIKKQEY	7%		HH-01	ZH732	2	1%
Ephrin type-B receptor 2 (EPHB2; P29323)					11%	4%
HRPKFGQIVNTLDK	7%		SA5	ZH713	2	4%
Legumain (LGMN; Q99538)					50%	31%
HLPDNINVYATTAANPRE	7%		ZH868	ZH872	24	46%
HLPDNINVYATTAANPRESS	7%		ZH680	ZH868	22	
IPDEQIVVMYDDIAYSEDNPTPG	7%		HH-06	ZH868	2	
Mucin-1 (MUC1; P15941)					7%	6%
GVSFFFLSFHISNL	7%		SA4	ZH680	0	7%
Testis-expressed sequence 15 protein (TEX15; Q9BXT5)					7%	2%
KVEMQRSPLGSLLP	7%		ZH680	ZH732	1	1%

Supplement of CHAPTER 4

Supplementary Table 15. HLA class I allotype and allele frequencies in the study cohort comprising n=33 meningioma patients. The HLA-A, -B, and -C allotypes with the top three highest frequencies within the collective are marked in bold.

HLA allotype	Positive patients	Allele frequency	HLA allotype	Positive patients	Allele frequency
A*01:01	11%	12%	B*39:31	2%	2%
A*02:01	20%	23%	B*40:01	2%	2%
A*03:01	12%	12%	B*40:02	3%	3%
A*11:01	3%	3%	B*41:01	2%	2%
A*23:01	3%	3%	B*44:02	2%	2%
A*24:02	11%	12%	B*44:03	8%	9%
A*26:01	2%	2%	B*49:01	2%	2%
A*29:02	8%	8%	B*50:01	2%	2%
A*30:01	2%	2%	B*51:01	9%	9%
A*30:02	5%	5%	B*51:02	2%	2%
A*31:01	3%	3%	B*51:08	2%	2%
A*32:01	5%	5%	B*55:01	3%	3%
A*33:01	2%	2%	B*57:01	5%	5%
A*34:01	2%	2%	C*01:02	5%	5%
A*66:01	2%	2%	C*02:02	8%	8%
A*68:01	8%	8%	C*03:03	6%	6%
B*07:02	9%	11%	C*03:04	3%	3%
B*08:01	6%	6%	C*04:01	14%	17%
B*13:02	5%	5%	C*05:01	2%	2%
B*14:02	2%	2%	C*06:02	11%	11%
B*15:01	5%	5%	C*07:01	12%	14%
B*15:35	2%	2%	C*07:02	9%	11%
B*18:01	11%	11%	C*08:02	2%	2%
B*27:05	3%	3%	C*12:03	9%	9%
B*35:01	9%	11%	C*14:02	2%	2%
B*35:03	2%	2%	C*15:02	3%	5%
B*37:01	2%	2%	C*16:01	6%	6%
B*38:01	2%	2%	C*16:02	2%	2%
B*39:01	2%	2%	C*17:01	2%	2%





Supplementary Figure 8. HLA class I allotype population coverage. Using the population coverage tool provided by the IEDB Analysis Resource, the world population coverage of the 58 distinct HLA-A, -B, and -C allotypes was calculated. The percentage of individuals positive for a specific number of HLA class I allotypes (max. of 6) is indicated by bar charts (associated with the left y-axis). The line diagram (associated with the right y-axis) shows the cumulative percentage of population coverage. The HLA class I allotypes of the meningioma cohort cover 99.98% of the world population (first diamond on line diagram counted from the left) meaning that only 0.02% of all individuals are negative for all HLA-A, -B, and -C allotypes included in the present study (first bar counted from the left). 94.60% of all individuals are positive for at least three HLA class I allotypes (third diamond on line diagram counted from the left).

Supplementary Table 16. Meningioma-associated HLA class I- and II-presented antigens identified on at least three tumors. GTEx profiles were assessed from all available datasets excepting EBV-transformed lymphocytes and cultured fibroblasts. Color codes were defined as follows: ■ < 10 TPM in any tissue, ◆ > 10 TPM in testes and < 10 TPM in other tissues (CTA-like expression profile), ■ 10-20 TPM in any tissue, ■ 20-30 TPM in any tissue, ■ > 30 TPM in any tissue. The number of positive non-meningeal tumors was based on n=841 HLA class I and n=593 HLA class II peptidome datasets. HLA restrictions not passing manual assessment as quality control are indicated in *italic*. These peptides were excluded from downstream analyses such as calculation of peptides matching per patient worldwide. HLA class II-presented proteins neither identified with peptides exceeding a length of twelve AA nor with different sequences across patients were not considered for this listing of candidate target antigens. Eight of the listed HLA class II-presented antigens (DRGX, KIR2DS4, SGK3, PCED1B, STAT5B, ESCO1, ANGEL2, RFWD3) were detected with only one peptide in each case.

Antigen	Frequency of positive patients	Peptide sequence	HLA restriction	UniProt accession GTEx profile	Positive non-meningeal tumors
Meningioma-associated HLA class I antigens					
Nicotinamide mononucleotide adenylyltransferase 2 (NMNA2)	<u>30% / WHO I-III</u> MNG1 MNG3 MNG6 MNG499 MNG501 MNG636 MNG642 MNG661 MNG734 MNG814	EEIELRILL ENANLGTVMR ENANLGTVMR NANLGTVMR ENANLGTVMR IVSPVHDSY EEIELRILL SVLEHHRDLMK IVSPVHDSY SIVSSTKSR ENANLGTVMR	B*18:01 A*68:01 A*68:01 A*68:01 A*68:01 B*15:01 B*44:03 A*11:01 A*30:02 A*66:01 A*68:01	Q9BZQ4 ■	8

Appendix: Supplement of CHAPTER 4

Protein Wnt-5a (WNT5A)	<u>18% / WHO I+II</u>			P41221 ■	43
	MNG6	AMSSKFFLV	A*02:01		
	MNG628	AMSSKFFLV	A*02:01		
		NPVQMSEVY	B*35:01		
	MNG637	AMSSKFFLV	A*02:01		
	MNG638	AMSSKFFLV	A*02:01		
	MNG641	AMSSKFFLV	A*02:01		
	MNG702	AMSSKFFLV	A*02:01		
T-box transcription factor TBX15/18 (TBX15/18)	<u>18% / WHO I-III</u>			Q96SF7 ■	15
	MNG7	GLDPHQYY (TBX15/18)	A*01:01;	Q95935 ■	9
			A*30:02		
2 peptides multi-map to non- MNG-exclusive TBX20 (Q9UMR3) or to MNG- exclusive TBX22 (Q9Y458)	MNG635	SQMSVHMV (TBX15)	B*13:02		
	MNG636	FHDIGTEMI (TBX15/22)	B*38:01		
		THQGSYNTF (TBX18)	B*38:01		
		DIVPVDNKRYR (TBX15/18/20)	A*33:01		
		THQGSYNTF (TBX18)	B*38:01		
	MNG646	GLDPHQYY (TBX15/18)	A*01:01		
	MNG682	KTFNFPETVF (TBX15)	B*15:01		
	MNG734	GLDPHQYYI (TBX15/18)	A*02:01		
		YQNQQITRL (TBX15/18)	C*02:02		
Protein odd-skipped-related 1 (OSR1)	<u>15% / WHO I+II</u>			Q8TAX0 ■	6
	MNG7	APVPIHPSL	B*07:02		
	MNG501	FPWFPHVI	B*51:01		
	MNG628	SLVDARFQL	A*02:01		
	MNG641	SLVDARFQL	A*02:01;		
			C*17:01		
	MNG814	APVPIHPSL	B*07:02		
Protein SSX5/9 (SSX5/9) peptides multi-map to MNG- exclusive obsolete UniProt IDs of SSX10 (A6NEJ1) and SSX11 (A6NNU9); not in GTE _x	<u>12% / WHO I+II</u>			O60225 ■	13
	MNG1	SEKIIYVY	B*18:01	Q7RTT3 ■	12
	MNG623	SEKIIYVY	B*18:01		
	MNG673	SEKILYVY	B*44:03		
	MNG679	SEKIIYVY	B*44:03		
Frizzled-7 (FZD7) 3 peptides multi-map to non- MNG-exclusive FZD1 (Q9UP38) or FZD2 (Q14332)	<u>12% / WHO I+II</u>			O75084 ■	7
	MNG635	HQFYPLVKV (FZD1/2/7)	B*13:02		
	MNG661	TYLVDMRRF (FZD1/7)	A*24:02		
	MNG673	FSDDGYRTV (FZD7)	C*03:04;		
			C*16:01		
	MNG814	VPAVKTITI (FZD2/7)	B*07:02		
E3 ubiquitin-protein ligase ZNRF2 (ZNRF2)	<u>12% / WHO I+II</u>			Q8NHG8 ■	8
	MNG1	DEMDLHLVM	B*18:01		
	MNG6	DEMDLHLVM	B*18:01		
	MNG628	DEMDLHLVM	B*18:01		
	MNG638	DEMDLHLVM	B*18:01		
Tctex1 domain-containing protein 2 (TC1D2)	<u>12% / WHO I</u>			Q8WW35 ■	5
	MNG7	KLKEMGFDRY	A*30:02		
	MNG632	KLKEMGFDRY	A*30:02		
	MNG661	KLKEMGFDRY	A*30:02		
	MNG702	LSENIKDKL	C*06:02		
Insulin-like growth factor- binding protein 6 (IGFBP6)	<u>12% / WHO I+II</u>			P24592 ■	2
	MNG1	DEAPLRAL	B*18:01		
	MNG628	DEAPLRAL	B*18:01		
		TPHRLLPPL	B*35:01		
	MNG661	DEAPLRAL	B*18:01		
	MNG666	TPHRLLPPL	B*07:02		
Uncharacterized protein C8orf34 (C8orf34)	<u>12% / WHO I+II</u>			Q49A92 ■	3
	MNG499	YPAEPQAKV	B*51:01;		
			B*51:02		
	MNG635	YPAEPQAKV	B*55:02		
	MNG642	YPAEPQAKV	B*51:01		
	MNG833	YPAEPQAKV	B*51:01		
Globoside alpha-1,3-N- acetylgalactosaminyltrans- ferase 1 (GBGT1)	<u>12% / WHO I+II</u>			Q8N5D6 ■	26
	MNG6	ESAEEFFMR	A*68:01		
	MNG635	AVFGGQVAR	A*31:01		
	MNG814	ESAEEFFMR	A*68:01		
		RPTQLLTL	B*07:02		
	MNG833	KYTHFIQSF	A*24:02		
Xyloside xylosyltransferase 1 (XXLT1)	<u>12% / WHO I-III</u>			Q8NB16 ■	13
	MNG3	ETFSSATKR	A*68:01		
	MNG642	ETFSSATKR	A*34:01		
	MNG734	ETFSSATKRL	A*66:01		
	MNG833	YYSDSIFFL	A*24:02		
Solute carrier family 25 member 44 (SLC25A44)	<u>12% / WHO I-III</u>			Q96H78 ■	10
	MNG7	ILQADGLRGFY	A*01:01		
	MNG641	SLVAQSITV	A*02:01		
	MNG702	SLVAQSITV	A*02:01		
	MNG734	SLVAQSITV	A*02:01		

Appendix: Supplement of CHAPTER 4

Forkhead box protein (FOX) E3, D4-like 1/2/3/5/6 peptides multi-map to FOXB2 (Q5VYV0) and to non-MNG-exclusive FOXD1 (Q16676), FOXD2 (O60548), FOXD3 (Q9UJU5), FOXD4 (Q12950), FOXB1 (Q99853), FOXC1 (Q12948), FOXC2 (Q99958), FOXE1 (O00358), FOXG1 (P55316), FOXI1 (Q12951), FOXI2 (Q6ZQN5), FOXI3 (A8MTJ6), FOXJ1 (Q92949), FOXK1 (P85037), FOXK2 (Q01167), FOXL1 (Q12952), FOXL2 (P58012), FOXS1 (O43638)	<u>12% / WHO I+II</u> MNG6 MNG7 MNG646 MNG814	DMFDNGSFLR QNSLRHNL QNSLRHNL DMFDNGSFLR	A*68:01 B*08:01 B*08:01 A*68:01	Q13461 ■ Q9NU39 ■ Q6VB85 ■ Q6VB84 ■ Q5VV16 ■ Q3SYB3 ■	6 6 5 4 5 4
Sterol O-acyltransferase 2 (SOAT2) 2 peptides multi-map to non-MNG-exclusive SOAT1 (P35610)	<u>9% / WHO I+II</u> MNG501 MNG624 MNG833	YPMVLILFL NAFAEMLRF NAFAEMLRF	B*51:01 B*35:01 B*35:01	O75908 ■	7
Cadherin-3 (CDH3)	<u>9% / WHO I+II</u> MNG641 MNG666 MNG814	LPRGPLASLL LPRGPLASLL LPRGPLASLL	B*07:02 B*07:02 B*07:02	P22223 ■	17
Folate receptor gamma (FOLR3) peptides multi-map to non-MNG-exclusive FOLR2	<u>9% / WHO I+II</u> MNG635 MNG646 MNG661	SYFPTPAAL FESYFPTPAA SYFPTPAAL	C*06:02 B*40:02 A*24:02	P41439 ■	9
Transmembrane protein 87A (TMEM87A)	<u>9% / WHO II+III</u> MNG642 MNG635 MNG734	DAPYIFIV HPSPLSFFSA AAWLQVLPV	B*51:01 B*55:01 C*12:03	Q8NBN3 ■	41
Transmembrane protein 255B (TMEM255B)	<u>9% / WHO I+II</u> MNG632 MNG819 MNG833	NPAQQILAY YYPGIILGF YYPGIILGF	B*35:01 A*23:01 A*24:02	Q8WV15 ■	16
Ninjurin-2 (NINJ2)	<u>9% / WHO I+III</u> MNG7 MNG632 MNG734	EQGPSSHYY EQGPSSHYY NEVEKQWRL	A*30:02 A*30:02 B*40:02	Q9NZG7 ■	13
Rho-related GTP-binding protein RhoD (RHOD)	<u>9% / WHO I-III</u> MNG3 MNG642 MNG734	EVALSSRGR EVALSSRGR EVALSSRGR	A*68:01 A*34:01 A*66:01	O00212 ■	7
Beta-1,4-galactosyltransferase 4 (B4GALT4)	<u>9% / WHO I</u> MNG673 MNG679 MNG682	FNLTFHLSY FNLTFHLSY FNLTFHLSY	A*29:02 A*29:02 A*29:02	O60513 ■	6
cAMP-responsive element-binding protein-like 2 (CREBL2)	<u>9% / WHO I-III</u> MNG6 MNG638 MNG734	IPSEIKALL LRYQYLEEL LRYQYLEEL	B*35:03 C*07:01 B*39:31	O60519 ■	19
Mitochondrial tRNA-specific 2-thiouridylylase 1 (MTU1)	<u>9% / WHO I</u> MNG3 MNG673 MNG679	EVFEQKHVKK NFEHLLQY NFEHLLQY	A*68:01 A*29:02 A*29:02	O75648 ■	10
NKG2-C type II integral membrane protein (NKG2C) / NKG2-E type II integral membrane protein (NKG2E)	<u>9% / WHO I+II</u> MNG499 MNG501 MNG642	VTINGLAFK LPSSWIGVF VTINGLAFK	A*11:01 B*51:01 A*11:01	P26717 ■ Q07444 ■	1 1
Protein AF-9 (AF-9)	<u>9% / WHO I+II</u> MNG6 MNG628 MNG661	SEALFKSF SEALFKSF SEALFKSF	B*18:01 B*18:01 B*18:01	P42568 ■	3
1-phosphatidylinositol 4,5-bisphosphate phosphodiesterase delta-4 (PLCD4)	<u>9% / WHO I-III</u> MNG1 MNG673 MNG734	EELPLEQGF ALSSLVIYL ILFKDVVATV	B*18:01 A*02:01 A*02:01	Q9BRC7 ■	2
Paraneoplastic antigen Ma2 (PNMA2)	<u>9% / WHO I+II</u> MNG1 MNG3 MNG673	AYVLRLETL SEVQGGGGVW AEIQEVLQETL SEVQGGGGVW	A*24:02 B*44:03 B*40:01 B*44:03	Q9UL42 ■	32

Appendix: Supplement of CHAPTER 4

Meningioma-associated HLA class II antigens			
Inactive serine protease 35 (PRSS35)	<u>30% / WHO I-II</u>		Q8N3Z0 ■ 3
	MNG6	SRFSILDKRFLTNFPFS	
	MNG7	LTPSLSELEDY	
	MNG501	LTPSLSELEDYL	
	MNG634	LTPSLSELEDYL	
		LTPSLSELEDYLSYE	
		SRFSILDKRFLTNFPFS	
		SRFSILDKRFLTNFPFS	
	MNG638	KVPRIVSERTFHLTSP	
		KVPRIVSERTFHLTSPA	
		LTPSLSELED	
		LTPSLSELEDY	
		LTPSLSELEDYL	
		LTPSLSELEDYLSY	
		LTPSLSELEDYLSYE	
MNG641	GTDSRFSILDKRFLTNFPFS		
	SRFSILDKRFLTNFPFS		
	SRFSILDKRFLTNFPFST		
MNG673	DSRFSILDKRFLTNFPFS		
	DSRFSILDKRFLTNFPFST		
	GTDSRFSILDKRFLTNFPF		
	GTDSRFSILDKRFLTNFPFS		
	GTDSRFSILDKRFLTNFPFST		
	SRFSILDKRFLTNFPF		
	SRFSILDKRFLTNFPFS		
	SRFSILDKRFLTNFPFST		
MNG702	SRFSILDKRFLTNFPFS		
MNG814	RFSILDKRFLTNFPFS		
	SRFSILDKRFLTNFPFS		
MNG833	DSRFSILDKRFLTNFPFS		
	GTDSRFSILDKRFLTNFPFS		
	RFSILDKRFLTNFPFS		
	SRFSILDKRFLTNFPF		
	SRFSILDKRFLTNFPFS		
	SRFSILDKRFLTNFPFST		
Lactosylceramide 4-alpha-galactosyltransferase (A4GALT)	<u>27% / WHO I-III</u>		Q9NPC4 ■ 0
	MNG7	KPPDLLLRLLRGAP	
	MNG623	TQSRVYVNGAFLAFERR	
	MNG661	QSRVYVNGAFLAFER	
	MNG666	QSRVYVNGAFLAFER	
		TQSRVYVNGAFLAFER	
		TQSRVYVNGAFLAFERR	
	MNG673	GTQSRVYVNGAFLAFERRH	
		TQSRVYVNGAFLAFER	
	MNG682	TQSRVYVNGAFLAFER	
	MNG734	QSRVYVNGAFLAFERR	
	MNG819	TQSRVYVNGAFLAFER	
	MNG833	QSRVYVNGAFLAFER	
		QSRVYVNGAFLAFERR	
		TQSRVYVNGAFLAFER	
	TQSRVYVNGAFLAFERR		
	TQSRVYVNGAFLAFERRH		
Fibrillin-2 (FBN2)	<u>21% / WHO I-III</u>		P35556 ■ 7
	MNG1	DDSVFRIHQRNGLSY	
		DDSVFRIHQRNGLSYL	
		GNDDSVFRIHQRNGLSYLH	
		IQPLNNHIRYVISQG	
		NDDSVFRIHQRNGLSY	
	MNG3	DDSVFRIHQRNGLSY	
	MNG612	LRPAIQPLNNHIRYV	
	MNG641	LRPAIQPLNNHIRYV	
	MNG700	KKDSRQKRSI	
	MNG702	DSVFRIHQRNGLSY	
		GNDDSVFRIHQRNGLSY	
		GNDDSVFRIHQRNGLSYLH	
		IQPLNNHIRYVISQG	
		NDDSVFRIHQRNGLSY	
MNG734	LRPAIQPLNNHIRYV		
	RPAIQPLNNHIRYV		
Sushi, nidogen and EGF-like domain-containing protein 1 (SNED1)	<u>21% / WHO I-III</u>		Q8TER0 ■ 1
	MNG7	QTVLITDGKLSFTIFN	
	MNG638	DRFTFRALLPGKRY	
	MNG642	DRFTFRALLPGKRYT	
		EPAHLYIITSPRDG	
		EPAHLYIITSPRDGAD	
	MNG666	TKSRYVPNGKLASYT	
MNG679	TRLFSETKAFPVWE		

Appendix: Supplement of CHAPTER 4

MAGUK p55 subfamily member 6 (MPP6)	MNG702 MNG734 <u>18% / WHO I-III</u> MNG1 MNG2 MNG6 MNG623 MNG641 MNG734	TKSRYVPNGKLASYT ASTISVQWALHRIR INNQLLPVDAIRILG INNQLLPVDAIRILG INNQLLPVDAIRILGIH DRHEIQIYEEVAKMPP INNQLLPVDAIRILG DRHEIQIYEEVAKMPP DRHEIQIYEEVAKMPPF DRHEIQIYEEVAKMPPFQ FDRHEIQIYEEVAKMPP FDRHEIQIYEEVAKMPPFQ DRHEIQIYEEVAKMPP DRHEIQIYEEVAKMPPF	Q9NZW5 ■ 5
Dorsal root ganglia homeobox protein (DRGX)	<u>15% / WHO I+II</u> MNG3 MNG501 MNG666 MNG702 MNG833	LAMKINL TEARVQVWF LAMKINL TEARVQVWF LAMKINL TEARVQVWF LAMKINL TEARVQVWF LAMKINL TEARVQVWF	A6NNA5 ■ 6
Melanoma-associated antigen 10 (MAGEA10) 1 peptide multi-maps to non-MNG-exclusive MAGEA9 (P43362)	<u>15% / WHO I+II</u> MNG499 MNG624 MNG641 MNG682 MNG700	KLLTQDWVQENYLEYRQVPGSDP KLLTQDWVQENYLEYRQVPGSDP KLLTQDWVQENYLEYRQVPGSDP ESLPRSEIDEKVTDLVQFLLFKYQM KLLTQDWVQENYLEYRQVPGSDP	P43363 ■ 3
Nuclear factor of activated T-cells, cytoplasmic 2 (NFATC2)	<u>15% / WHO I+II</u> MNG1 MNG6 MNG7 MNG624 MNG702	DQTYLDDVNEIIR LDQTYLDDVNEIIR KDKSQPNMLFVEIPEYR DQTYLDDVNEIIR DQTYLDDVNEIIR LDQTYLDDVNEIIR DQTYLDDVNEIIR KPHAFYQVHRITGKT LDQTYLDDVNEIIR	Q13469 ■ 20
Uncharacterized protein KIAA1586 (KIAA1586)	<u>15% / WHO I+II</u> MNG5 MNG501 MNG637 MNG642 MNG702	EVDLNDFREFVNNNIK ELETEIIKIGRVMGPRW ELETEIIKIGRVMGPRW ELETEIIKIGRVMGPRW ELETEIIKIGRVMGPRW	Q9HC16 ■ 5
ZAR1-like protein (ZAR1L)	<u>12% / WHO I+II</u> MNG501 MNG638 MNG702 MNG833	MGPPTFLARPGLLVPANAP SPRLCKPNTKEVGVQVSPRVDAKAV MGPPTFLARPGLLVPANAP MGPPTFLARPGLLVPANAP	A6NP61 ■ 1
G protein-regulated inducer of neurite outgrowth 2 (GPRIN2)	<u>12% / WHO I+II</u> MNG638 MNG679 MNG682 MNG702	IQKHLEMQFEQLQRAPASEDS IQKHLEMQFEQLQRAPASEDSL IQKHLEMQFEQLQRAPASEDSL IQKHLEMQFEQLQRAPASEDSL	O60269 ■ 2
Bone morphogenetic protein 5 (BMP5) 1 peptide multi-maps to non-MNG-exclusive BMP6 (P18075)	<u>12% / WHO I+II</u> MNG638 MNG642 MNG679 MNG702	SNVILKKYRNMVVR AAEFRIYKDRSNN AAEFRIYKDRSNNR AAEFRIYKDRSNNR TAAEFRIYKDRSNN TAAEFRIYKDRSNNR RDADLFLLDTRK YTNRDADLFLLDTRK AFFKATEVHFR SSNVILKKYRNMVVR	P22003 ■ 0
Transcription factor SOX-6 (SOX6)	<u>12% / WHO I+II</u> MNG4 MNG499 MNG642 MNG679	ASMQVSPGAKMPS KTDGGSLAGNEMINGEDEMEMYDDY EMEMYDDYEDDP ITQLISLREQLLAHDEQKKLAAS	P35712 ■ 5
Zinc finger E-box-binding homeobox 2 (ZEB2)	<u>12% / WHO I+II</u> MNG7 MNG623 MNG624 MNG635	SVNGRMRNNIKTGSSP EEYFAKRKLEERDGHAVSIEEYLQ EEYFAKRKLEERDGHAVSIEEYLQ EEYFAKRKLEERDGHAVSIEEYLQ	O60315 ■ 1
Mucin-4 (MUC4)	<u>12% / WHO I+II</u> MNG499 MNG501	GRRDLRFQPVSIGR GRRDLRFQPVSIGRWG DNGQIIFPESDYQIFSYPNPLPT	Q99102 ■ 12

Appendix: Supplement of CHAPTER 4

	MNG628 MNG638	SNILHASASLPP APIPILPERGVSLFPY APIPILPERGVSLFPYG		
Kinesin light chain 2 (KLC2) peptides multi-map to non-MNG-exclusive KLC1 (Q07866)	<u>12% / WHO I+III</u> MNG6 MNG612 MNG636 MNG734	HNLVIQYASQGRYE LHNLVIQYASQGRYE LHNLVIQYASQGRYE LHNLVIQYASQGRYE	Q9H0B6 ■	6
Calcium-binding protein 39-like (CAB39L)	<u>12% / WHO I+II</u> MNG638 MNG641 MNG666 MNG702	GKKDVTQIFNNILRRQ DRHNFAIMTKYISKPE DRHNFAIMTKYISKPE DRHNFAIMTKYISKPE	Q9H9S4 ■	2
Calpain-14 (CAPN14)	<u>9% / WHO I</u> MNG7 MNG499 MNG673	MLRVENMEDVFNQ IMLSDDVCQLMLIRYGGPR LPPEFFQRNTPLSQPDRFLKEKE	A8MX76 ■	1
Methylenetetrahydrofolate reductase (MTHFR)	<u>9% / WHO I+II</u> MNG499 MNG638 MNG814	IKDVIEPIKDNDAAIR KGENITNAPELQPNVAVT IKDVIEPIKDNDAAIR	P42898 ■	9
Killer cell immunoglobulin-like receptor 2DS4 (KIR2DS4)	<u>9% / WHO I</u> MNG7 MNG623 MNG624	MSLMVIIMACVGFLLQGAW MSLMVIIMACVGFLLQGAW MSLMVIIMACVGFLLQGAW	P43632 ■	1
Probable allantoicase (ALLC)	<u>9% / WHO I+II</u> MNG6 MNG642 MNG673	PSSICLLRPREKPM DFFAPAENLIKSDSPCF IPERGTRTGAATPEEFEAIAELKS	Q8N6M5 ■	1
Tubulin polyglutamylase TTL6 (TTL6)	<u>9% / WHO I+II</u> MNG632 MNG702 MNG833	QMKKKVEMQGE QMKKKVEMQGE SEEKGDSSKEDPKETVALAFV	Q8N841 ◆	2
Serine/threonine-protein kinase Sgk3 (SGK3)	<u>9% / WHO I+II</u> MNG682 MNG702 MNG833	TFCGTPEYLAPEVIRKQPYDNT TFCGTPEYLAPEVIRKQPYDNT TFCGTPEYLAPEVIRKQPYDNT	Q96BR1 ■	4
PC-esterase domain-containing protein 1B (PCED1B)	<u>9% / WHO I-III</u> MNG634 MNG641 MNG734	NFMVGPQLPMPFFPTPRYQ NFMVGPQLPMPFFPTPRYQ NFMVGPQLPMPFFPTPRYQ	Q96HM7 ■	4
Mitochondrial import inner membrane translocase subunit TIM44 (TIMM44)	<u>9% / WHO I</u> MNG4 MNG6 MNG682	KRTEFAGDKFKEEKVFE KWYQQWKDFKENVVFNRFEMKMK KWYQQWKDFKENVVFNRFEMKMK	O43615 ■	1
Ubiquitin conjugation factor E4 B (UBE4B)	<u>9% / WHO I+II</u> MNG641 MNG666 MNG702	KDLIGQILMEVLMSTQTRDEN VDMFHILTKQVQKPF VDMFHILTKQVQKPF	O95155 ■	5
Protein SGT1 (ECD)	<u>9% / WHO I</u> MNG5 MNG6 MNG632	DSDDLDEDFECLDSDDDLDF LRDPIDLRACRVFKTFLPETRIMTS EKIQASLHRAHCFL	O95905 ■	4
T-lymphocyte activation antigen CD86 (CD86)	<u>9% / WHO I</u> MNG7 MNG623 MNG624	DKTRLLSSPFSIELEDQPPPP TDKTRLLSSPFSIELEDQPPPP DKTRLLSSPFSIELEDQPPPP DKTRLLSSPFSIELEDQPPPP	P42081 ■	22
Signal transducer and activator of transcription 5B (STAT5B)	<u>9% / WHO I+II</u> MNG3 MNG702 MNG833	DGVMEVLKHKHLKPH DGVMEVLKHKHLKPH DGVMEVLKHKHLKPH	P51692 ■	13
Nucleoporin GLE1 (GLE1)	<u>9% / WHO I+II</u> MNG628 MNG634 MNG814	ISGIIRASSESSYPTAE KEEGQIRLRALYALQEEML KQAEQERLRKEEGQI	Q53GS7 ■	3
N-acetyltransferase ESCO1 (ESCO1)	<u>9% / WHO I+II</u> MNG499 MNG635 MNG641	KVLEVKSDSKEDENLVINEVINSPK KVLEVKSDSKEDENLVINEVINSPK KVLEVKSDSKEDENLVINEVINSPK	Q5FWF5 ■	14
Protein angel homolog 2 (ANGEL2)	<u>9% / WHO I-III</u> MNG634 MNG734 MNG833	DHYGAEIRPSLESLEY DHYGAEIRPSLESLEY DHYGAEIRPSLESLEY	Q5VTE6 ■	0

Appendix: Supplement of CHAPTER 4

Meteorin-like protein (METRNL)	<u>9% / WHO I+II</u> MNG666	GFQYELVRRHRASD TGFQYELVRRHRASD	Q641Q3 ■	3
	MNG702	GFQYELVRRHRASD TGFQYELVRRHRASDLH		
	MNG833	GFQYELVRRHRASD		
E3 ubiquitin-protein ligase RFD3 (RFD3)	<u>9% / WHO I</u> MNG3	TNFISGLQRLHGMLEFL	Q6PCD5 ■	2
	MNG666	TNFISGLQRLHGMLEFL		
	MNG702	TNFISGLQRLHGMLEFL		
Highly divergent homeobox (HDX)	<u>9% / WHO I+II</u> MNG634	QRSYKPEHTGPAHNLNLC	Q7Z353 ■	2
	MNG635	FIENELEIQKQKYFKLQ		
	MNG666	SEMTVPQKPSVCHRPKIEP		
Signal-regulatory protein delta (SIRPD)	<u>9% / WHO I+II</u> MNG1	PLPSLLLYLLELA	Q9H106 ◆	3
	MNG3	PLPSLLLYLLELAG		
	MNG673	PLPSLLLYLLELA		
Uncharacterized protein C1orf112 (C1orf112)	<u>9% / WHO I+II</u> MNG3	FVSSLGKLF	Q9NSG2 ◆	1
	MNG6	FVSSLGKLF		
	MNG642	KAVFYSEFQCSGELSLP		

Supplementary Table 17. Meningioma-associated HLA class I ligands presented on at least five tumors. Peptides already reported to derive from meningioma-associated antigens were excluded from this listing. The number of positive non-meningeal tumors was based on n=841 HLA class I peptidome datasets. HLA restrictions not passing manual assessment as quality control are indicated in italic. These combinations of sequence and HLA restriction were excluded from downstream analyses such as calculation of peptides matching per patient worldwide.

Peptide sequence	HLA restriction	Frequency of positive patients	Antigen (UniProt accession)	Protein frequency on meningiomas	Peptide-positive non-meningeal tumors	Protein frequency on non-meningeal tumors	Protein frequency on dura (n=9) / benign samples (n=418)
TLQSTLLLL	A*02:01 C*17:01	<u>30%</u>	<u>WHO I-III</u>	Mimecan (OGN; P20774)	61%	1 2%	11% 5%
		MNG501	MNG612				
		MNG628	MNG638				
		MNG641	MNG666				
		MNG673	MNG700				
MNG702	MNG734						
QTFPNVREM	B*57:01 C*03:04 C*06:02 C*12:03	<u>30%</u>	<u>WHO I-III</u>	Forkhead box protein C2 (FOXC2; Q99958)	85%	0 7%	67% 8%
		MNG2	MNG3				
		MNG5	MNG628				
		MNG634	MNG635				
		MNG636	MNG661				
MNG666	MNG734						
IPISNILMV	B*07:02 B*51:01 B*51:02 B*55:01	<u>24%</u>	<u>WHO I-III</u>	Interferon-induced protein 44-like (IF144L; Q53G44)	30%	37 12%	11% 3%
		MNG499	MNG501				
		MNG612	MNG635				
		MNG642	MNG702				
MNG814	MNG833						
LLLPPVVSFA	A*02:01	<u>21%</u>	<u>WHO I-III</u>	Cathepsin K (CTSK; P43235)	21%	29 7%	0% 4%
		MNG612	MNG628				
		MNG641	MNG666				
		MNG673	MNG702				
MNG734							
SLPELVHAV	A*02:01	<u>21%</u>	<u>WHO I-III</u>	Sestrin-3 (SESN3; P58005)	11%	23 11%	33% 4%
		MNG6	MNG628				
		MNG641	MNG666				
		MNG673	MNG702				
MNG734							
YSLEKVFGI	A*02:01 C*02:02 C*06:02 C*07:01 C*12:03 C*17:01	<u>21%</u>	<u>WHO I-III</u>	Melanoma-associated antigen D2 (MAGED2; Q9UNF1)	94%	24 52%	56% 48%
		MNG2	MNG5				
		MNG612	MNG638				
		MNG641	MNG666				
		MNG734					
EYVGTGVASTR	A*34:01 A*66:02 A*68:01	<u>21%</u>	<u>WHO I-III</u>	Serine palmitoyl-transferase 3 (SPTLC3; Q9NUV7)	76%	2 20%	33% 17%
		MNG3	MNG6				
		MNG499	MNG632				
		MNG642	MNG734				
		MNG814					

Appendix: Supplement of CHAPTER 4

KAIDYIRFL	C*03:04 C*12:03 C*16:01	<u>21%</u> MNG1 MNG628 MNG666 MNG734	<u>WHO I-III</u> MNG4 MNG636 MNG673	Sterol regulatory element-binding protein 1 (SREBF1; P36956)	55%	12 23%	11% 13%
KLNNLFLY	A*03:01 A*29:02 A*30:02 B*15:01	<u>21%</u> MNG1 MNG641 MNG673 MNG814	<u>WHO I+II</u> MNG632 MNG646 MNG682	Mimecan (OGN; P20774)	61%	2 2%	11% 5%
SSFPTVVIY	C*02:02 C*12:03	<u>21%</u> MNG628 MNG637 MNG666 MNG734	<u>WHO I-III</u> MNG636 MNG661 MNG702	GPN-loop GTPase 1 (GPN1; Q9HCN4)	49%	32 25%	22% 15%
YPSGIHLEL	B*07:02 B*35:01	<u>21%</u> MNG2 MNG632 MNG642 MNG814	<u>WHO I+II</u> MNG7 MNG634 MNG666	Sulfate transporter (SLC26A2; P50443)	70%	2 4%	33% 3%
LPYNTSLVEM	B*07:02 B*35:01	<u>18%</u> MNG7 MNG632 MNG641 MNG814	<u>WHO I+II</u> MNG628 MNG634 MNG814	Tropomodulin-1 (TMOD1; P28289)	67%	2 8%	22% 11%
NYAGALMYF	A*24:02	<u>18%</u> MNG1 MNG635 MNG661	<u>WHO I+II</u> MNG628 MNG638 MNG833	Sodium leak channel non-selective protein (NALCN; Q8IZF0)	24%	2 2%	0% 1%
SELLVVKM	B*18:01 B*40:02	<u>18%</u> MNG1 MNG628 MNG646	<u>WHO I+II</u> MNG6 MNG638 MNG661	Obscurin-like protein 1 (OBSL1; O75147)	45%	5 17%	33% 15%
VYGLYTSFF	A*24:02	<u>18%</u> MNG5 MNG635 MNG661	<u>WHO I+II</u> MNG628 MNG638 MNG833	Sulfate transporter (SLC26A2; P50443)	70%	3 4%	33% 3%
DGYIEVIGF	B*35:01 B*51:01	<u>18%</u> MNG624 MNG632 MNG682	<u>WHO I+II</u> MNG628 MNG634 MNG833	Diacylglycerol kinase iota / zeta (DGKI / DGKZ; O75912 / Q13574)	18% / 39%	34 6% / 19%	0% / 0% 3% / 16%
DVIDGPISQR	A*66:01 A*68:01	<u>18%</u> MNG3 MNG499 MNG734	<u>WHO I-III</u> MNG6 MNG632 MNG814	Signal-induced proliferation-associated 1-like protein 1 (SIPA1L1; O43166)	49%	7 20%	33% 18%
EVQDRVMLTGR	A*33:01 A*68:01	<u>18%</u> MNG3 MNG499 MNG634	<u>WHO I</u> MNG6 MNG632 MNG636	Protein yippee-like 5 (YPEL5; P62699)	70%	28 47%	56% 41%
SMVEDITGLRL	A*02:01	<u>18%</u> MNG501 MNG638 MNG666	<u>WHO I-III</u> MNG612 MNG641 MNG673	Desmoplakin (DSP; P15924)	97%	26 34%	56% 32%
SVFAGVVG V	A*02:01	<u>18%</u> MNG6 MNG641 MNG673	<u>WHO I-III</u> MNG612 MNG666 MNG702	Guanylate cyclase soluble subunit alpha-3 (GUCY1A3; Q02108)	64%	42 17%	56% 16%
VPYSRALIM	B*35:03 B*51:01 B*51:02	<u>18%</u> MNG6 MNG612 MNG702	<u>WHO I-III</u> MNG499 MNG642 MNG833	Lysoplasmalogenase-like protein TMEM86A (TMEM86A; Q8N2M4)	24%	27 5%	11% 2%
YENLLKASF	B*18:01 B*15:35	<u>18%</u> MNG1 MNG628 MNG642	<u>WHO I+II</u> MNG6 MNG638 MNG661	Desmoplakin (DSP; P15924)	97%	12 34%	56% 32%
AANGVFHV V	C*12:03	<u>15%</u> MNG628 MNG661 MNG734	<u>WHO I-III</u> MNG636 MNG666	Stabilin-1 (STAB1; Q9NY15)	79%	19 34%	56% 31%
AEPPELA AF	B*18:01 B*40:02 B*44:03	<u>15%</u> MNG1 MNG636 MNG646	<u>WHO I+II</u> MNG6 MNG638	Uncharacterized protein KIAA1755 (KIAA1755; Q5JYT7)	45%	0 2%	0% 2%

Appendix: Supplement of CHAPTER 4

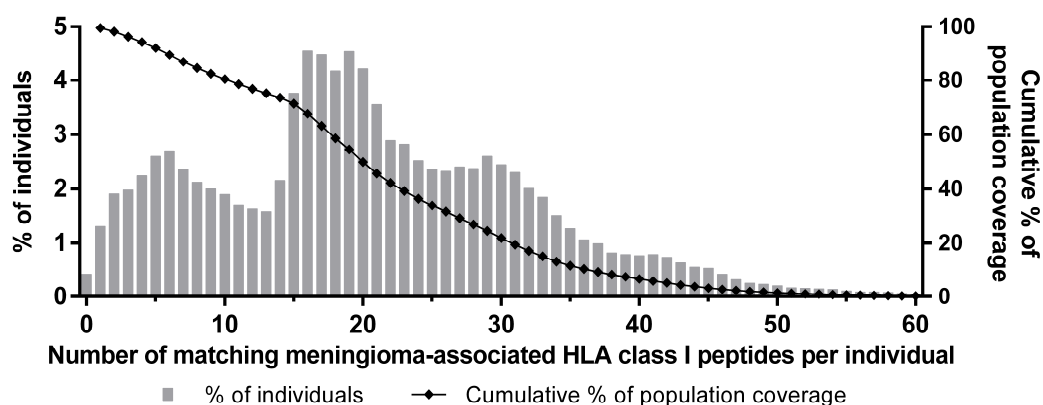
DEDRFMMQF	B*18:01	15% MNG1 MNG628 MNG661	<u>WHO I+II</u> MNG6 MNG638	Formin-like protein 2 (FMNL2; Q96PY5)	48%	3 18%	11% 14%
DEKFHIAY	B*18:01	15% MNG1 MNG623 MNG661	<u>WHO I+II</u> MNG6 MNG628	Sestrin-1 (SESN1; Q9Y6P5)	67%	6 28%	56% 34%
DMFATPQYR	A*33:01 A*68:01	15% MNG3 MNG499 MNG814	<u>WHO I</u> MNG6 MNG636	Adiponectin receptor protein 2 (ADIPOR2; Q86V24)	24%	18 8%	0% 3%
DVFQHSQSR	A*33:01 A*34:01 A*66:01 A*68:01	15% MNG3 MNG636 MNG734	<u>WHO I-III</u> MNG632 MNG642	Constitutive coactivator of PPAR-gamma-like protein 1 (FAM120A; Q9NZB2)	85%	3 42%	33% 36%
DYTIGFGKF	A*24:02	15% MNG1 MNG628 MNG833	<u>WHO I+II</u> MNG5 MNG661	Integrin beta-4 (ITGB4; P16144)	76%	7 21%	22% 27%
EIVGNLPSAMR	A*68:01	15% MNG3 MNG499 MNG814	<u>WHO I+II</u> MNG6 MNG632	Kelch-like protein 23 (KLHL23; Q8NBE8)	21%	3 3%	0% 2%
ETASVLVNYR	A*66:01 A*68:01	15% MNG3 MNG632 MNG814	<u>WHO I-III</u> MNG6 MNG734	Intersectin-2 (ITSN2; Q9NZM3)	24%	6 19%	11% 13%
EVASEIQPFLR	A*68:01	15% MNG3 MNG499 MNG814	<u>WHO I+II</u> MNG6 MNG632	Desmoplakin (DSP; P15924)	97%	1 34%	56% 23%
FEGNVFMY	B*18:01	15% MNG1 MNG628 MNG661	<u>WHO I+II</u> MNG6 MNG638	Cell cycle control protein 50A (TMEM30A; Q9NV96)	64%	7 30%	44% 18%
GLFQKLENI	A*02:01	15% MNG501 MNG666 MNG700	<u>WHO I+II</u> MNG641 MNG673	Desmoplakin (DSP; P15924)	97%	1 34%	56% 32%
HSIGAVGPTGR	A*68:01	15% MNG3 MNG499 MNG814	<u>WHO I+II</u> MNG6 MNG632	Serine palmitoyl-transferase 3 (SPTLC3; Q9NUV7)	76%	0 20%	33% 17%
IYNGKVTSI	A*24:02	15% MNG1 MNG635 MNG833	<u>WHO I+II</u> MNG628 MNG661	ATP-dependent RNA helicase DHX8 (DHX8; Q14562)	58%	6 23%	11% 18%
LAFPGEMLL	C*03:03 C*12:03	15% MNG628 MNG661 MNG734	<u>WHO I-III</u> MNG636 MNG666	Neutral amino acid transporter A (SLC1A4; P43007)	18%	23 9%	0% 3%
LPIGIALMF	B*51:01	15% MNG499 MNG632 MNG833	<u>WHO I+II</u> MNG501 MNG682	Multidrug and toxin extrusion protein 1 (SLC47A1; Q96FL8)	70%	1 5%	33% 5%
LPIIANMI	B*51:01	15% MNG499 MNG612 MNG833	<u>WHO I-III</u> MNG501 MNG642	Armadiillo repeat-containing X-linked protein 2 (ARMCX2; Q7L311)	45%	11 12%	33% 11%
MEYFPTTRF	B*18:01	15% MNG1 MNG623 MNG638	<u>WHO I+II</u> MNG6 MNG628	Phospholipase D4 (PLD4; Q96BZ4)	39%	1 5%	33% 4%
PYFDKPLFI	A*24:02	15% MNG628 MNG638 MNG833	<u>WHO I+II</u> MNG635 MNG661	Sodium leak channel non-selective protein (HSBP1; Q8IZF0)	24%	1 2%	0% 1%
QTMSDQIIGR	A*68:01	15% MNG3 MNG499 MNG814	<u>WHO I+II</u> MNG6 MNG632	Heat shock factor-binding protein 1 (O75506)	15%	8 3%	0% 3%

Appendix: Supplement of CHAPTER 4

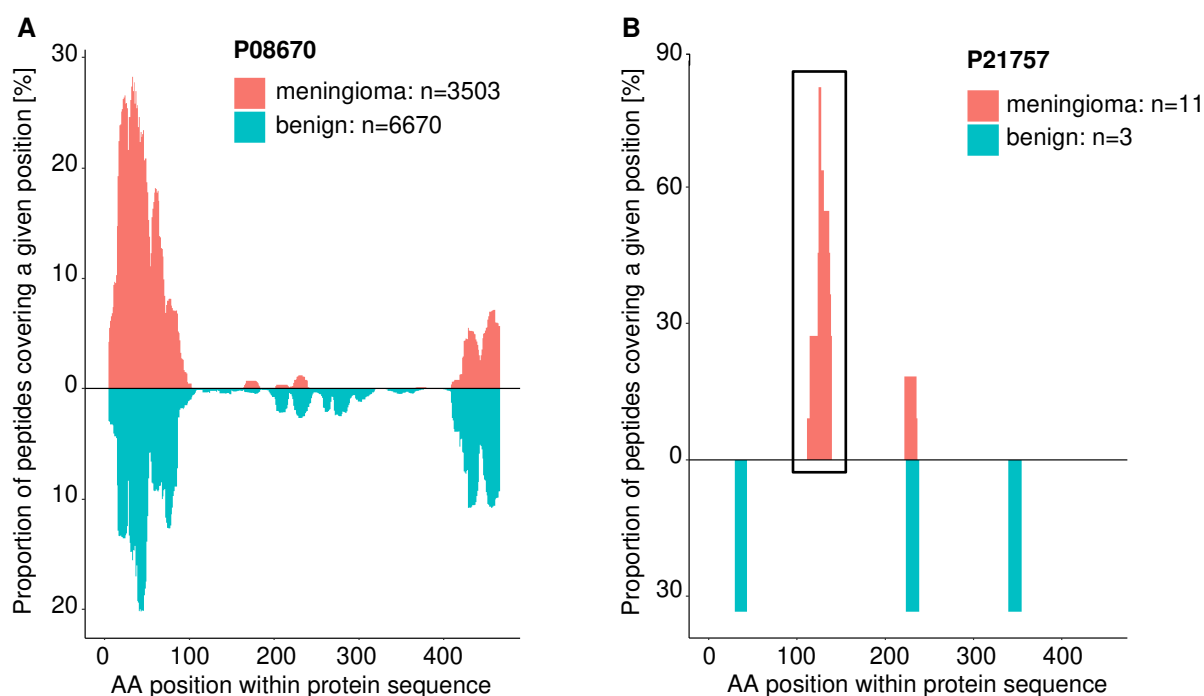
STITPTSTR	A*66:01 A*68:01	15% MNG3 MNG499 MNG734	<u>WHO I+III</u> MNG6 MNG632	Prolow-density lipoprotein receptor-related protein 1 (LRP1; Q07954)	88%	7 32%	67% 38%
TPHDFIEHF	B*35:01	15% MNG624 MNG632 MNG833	<u>WHO I+II</u> MNG628 MNG682	G1/S-specific cyclin-D1 (CCND1; P24385)	79%	13 36%	67% 39%
VALPVYLLI	B*51:01	15% MNG499 MNG612 MNG833	<u>WHO I-III</u> MNG501 MNG702	Phosphatidylinositol N-acetylglucosaminyltransferase subunit P (PIGP; P57054)	30%	27 9%	11% 2%
VAVGFPMMI	C*12:03	15% MNG628 MNG661 MNG734	<u>WHO I-III</u> MNG636 MNG666	Putative sodium-coupled neutral amino acid transporter 10 (SLC38A10; Q9HBR0)	48%	19 24%	33% 19%
VEVQLPELY	B*18:01 B*44:03	15% MNG1 MNG636 MNG661	<u>WHO I+II</u> MNG6 MNG638	Voltage-gated potassium channel subunit beta-1 (KCNAB1; Q14722)	21%	9 5%	11% 4%
YGYSNPKIL	C*03:04 C*12:03	15% MNG3 MNG636 MNG734	<u>WHO I-III</u> MNG628 MNG661	Transcription factor AP-1 (JUN; P05412)	33%	27 24%	11% 26%
YNFEYSVVF	B*38:01 C*12:03	15% MNG628 MNG637 MNG734	<u>WHO I-III</u> MNG636 MNG666	Renin receptor (REN1; O75787)	70%	16 42%	33% 41%
YRNAKVELV	B*51:01 B*51:08	15% MNG4 MNG501 MNG702	<u>WHO I+II</u> MNG499 MNG702	PDZ and LIM domain protein 4 (PDLIM4; P50479)	28%	17 8%	0% 4%
YYASAFSMM	A*24:02	15% MNG628 MNG638 MNG833	<u>WHO I+II</u> MNG635 MNG661	Dolichyl-diphosphooligosaccharide-protein glycosyltransferase 48 kDa subunit (DDOST; P39656)	58%	0 39%	44% 41%
YYKSTSSAF	A*24:02	15% MNG1 MNG635 MNG833	<u>WHO II</u> MNG628 MNG638	Galactose-3-O-sulfotransferase 4 (GAL3ST4; Q96RP7)	30%	9 6%	11% 1%
DAFDGHAAR	A*33:01 A*34:01 A*66:01 A*68:01	15% MNG3 MNG636 MNG734	<u>WHO I-III</u> MNG632 MNG642	CDP-diacylglycerol-inositol 3-phosphatidyltransferase (CDIPT; O14735)	28%	6 9%	0% 6%
DSERFFIRY	A*01:01	15% MNG4 MNG7 MNG646	<u>WHO I</u> MNG5 MNG624	Tubulin-specific chaperone cofactor E-like protein (TBCEL; Q5QJ74)	18%	30 7%	11% 9%
EAENTLQSFR	A*68:01	15% MNG3 MNG499 MNG814	<u>WHO I+II</u> MNG6 MNG632	Vimentin (VIM; P08670)	100%	1 88%	100% 96%
EAIQLEVKY	A*26:01 A*29:02 B*35:01	15% MNG624 MNG679 MNG833	<u>WHO I+II</u> MNG634 MNG682	Vacuolar protein sorting-associated protein 13D (VPS13D; Q5THJ4)	61%	1 30%	33% 35%
EVFAGSGTSGQR	A*66:01 A*68:01	15% MNG3 MNG632 MNG814	<u>WHO I-III</u> MNG6 MNG734	Procollagen C-endopeptidase enhancer 1 (PCOLCE; Q15113)	21%	1 1%	0% 1%
EVPSFTMGR	A*34:01 A*66:01 A*68:01	15% MNG3 MNG642 MNG814	<u>WHO I+II</u> MNG6 MNG734	PRKR-interacting protein 1 (PRKRIP1; Q9H875)	15%	5 1%	0% 0.5%
FFNIPQIQY	A*29:02	15% MNG1 MNG673 MNG682	<u>WHO I+II</u> MNG623 MNG679	28S ribosomal protein S25, mitochondrial (MRPS25; P82663)	15%	12 4%	0% 5%

Appendix: Supplement of CHAPTER 4

FLMEMGFRM	A*02:01	15% MNG6 MNG628 MNG673	<u>WHO I-III</u> MNG612 MNG638	Mediator of RNA polymerase II transcription subunit 18 (MED18; Q9BUE0)	24%	13 7%	11% 4%
FVFGENMVER	A*68:01	15% MNG3 MNG499 MNG814	<u>WHO I+II</u> MNG6 MNG632	Ran-binding protein 3-like (RANBP3L; Q86VV4)	24%	1 1%	0 1%
GAFGLPITV	C*02:02 C*12:03	15% MNG636 MNG666 MNG734	<u>WHO I+III</u> MNG661 MNG702	Glutathione S-transferase kappa 1 (GSTK1; Q9Y2Q3)	24%	10 27%	11%
GLLPLLREA	A*02:01	15% MNG641 MNG673 MNG734	<u>WHO I-III</u> MNG666 MNG702	Stabilin-1 (STAB1; Q9NY15)	79%	34 34%	56%
HTNDTIGSVR	A*66:01 A*68:01	15% MNG3 MNG632 MNG814	<u>WHO I-III</u> MNG6 MNG734	Probable ubiquitin carboxyl-terminal hydrolase FAF-X / FAF-Y (USP9X/Y; Q93008 / O00507)	82% / 64%	18 53% / 41%	67% / 44% 57% / 41%
NLMGKTSER	A*34:01 A*66:01 A*68:01	15% MNG3 MNG632 MNG734	<u>WHO I-III</u> MNG6 NBG642	Transcription factor 12 (TCF12; Q99081)	61%	3 43%	33% 29%
RVYDIPPKF	A*30:02 A*32:01 B*15:35 C*12:03	15% MNG7 MNG634 MNG661	<u>WHO I+II</u> MNG632 MNG642	Cytochrome b-245 heavy chain (CYBB; P04839)	88%	4 34%	56% 32%
SLSLENVLYY	A*29:02 B*15:01	15% MNG1 MNG673 MNG682	<u>WHO I+II</u> MNG623 MNG679	Sortilin-related receptor (SORL1; Q92673)	45%	14 23%	11% 17%
SPNNFLSYY	B*35:01	15% MNG628 MNG634 MNG833	<u>WHO I+II</u> MNG632 MNG682	G1/S-specific cyclin-D1 (CCND1; P24385)	79%	8 36%	67% 39%
SVDSNLLSDY	A*01:01	15% MNG3 MNG624 MNG702	<u>WHO I</u> MNG7 MNG646	Oxidative stress-induced growth inhibitor 2 (OSGIN2; Q9Y236)	42%	41 12%	33% 7%
SVIEGVRSR	A*66:01 A*68:01	15% MNG3 MNG632 MNG814	<u>WHO I-III</u> MNG6 MNG734	BTB/POZ domain-containing protein 9 (BTBD9; Q96Q07)	27%	13 12%	0% 6%
SYFPTVPGVYI	A*24:02	15% MNG1 MNG635 MNG833	<u>WHO I+II</u> MNG5 MNG638	Filamin-B (FLNB; O75369)	94%	7 46%	67% 60%
TEEPLKQSF	B*18:01	15% MNG1 MNG628 MNG661	<u>WHO I+II</u> MNG6 MNG638	GRAM domain-containing protein 3 (GRAMD3; Q96HH9)	42%	9 12%	11% 13%
VELLMHNDY	B*18:01	15% MNG1 MNG628 MNG661	<u>WHO I+II</u> MNG6 MNG638	Importin subunit alpha-5/6/7 (KPNA1/5/6; P52294 / O15131 / O60684)	73% / 58% / 64%	12 52% / 45% / 46%	78% / 67% / 78% 53% / 45% / 46%
VGVDFAKLV	C*12:03	15% MNG628 MNG661 MNG734	<u>WHO I-III</u> MNG636 MNG666	Ras-related protein Rab-7L1 (RAB7L1; O14966)	27%	12 4%	11% / 2%



Supplementary Figure 9. Population coverage of meningioma-associated HLA-A, -B, and -C ligands. Using the population coverage tool provided by the IEDB Analysis Resource, the world population coverage of the 141 meningioma-associated peptides was calculated. The percentage of individuals with a specific number of matching peptides (max. of 74) is indicated by bar charts (associated with the left y-axis). The line diagram (associated with the right y-axis) shows the cumulative percentage of population coverage. The candidate target peptides cover 99.57% of the world population (first diamond on line diagram counted from the left) meaning that only 0.43% of all individuals are negative for all HLA-A, -B, and -C allotypes for which meningioma-associated peptides were defined. On average, 21 peptides are expected to match per patient worldwide.



Supplementary Figure 10. Hotspot analysis of antigens represented by meningioma-exclusive HLA class II-restricted peptides. Peptides were aligned to source protein sequences, whereby identifications on meningioma (n=33) or autologous tumor-free dura (n=9) / benign tissues (n=364) are shown in red or green, respectively. The proportion of all peptides covering a given position is indicated on the y-axis (separately for malignant and benign hits). **(A) Vimentin (VIM; P08670).** Comparative profiling identified a total of 29 meningioma-exclusive peptides derived from vimentin. However, identical peptide sequences differing only in 1 AA in length were identified on benign tissues, which cannot be reflected by comparative profiling. HLA class II molecules are renowned for promiscuous binding of peptides due to decreased length preferences and degenerate peptide motifs and TCRs of CD4⁺ T cells rather recognize the core sequence of HLA class II-presented peptides than distinguishing between length variants. This refutes all meningioma-exclusive peptides originating from vimentin to be candidate targets for cancer immunotherapy, as they derived from regions presented on both benign and

malignant tissues. **(B) Macrophage scavenger receptor types I and II (MSR1; P21757)**. Despite one part of the protein sequence was covered by both malignant and benign peptide identifications, eight distinct sequences derived from a meningioma-associated presentation hotspot were identified between position 112 and 139 (indicated by box).

Supplementary Table 18. Meningioma-exclusive HLA class II-presented peptides derived from meningioma-associated HLA presentation hotspots. Peptides already reported to derive from meningioma-associated antigens were excluded from this listing. The number of positive non-meningeal tumors was based on n=593 HLA class II peptidome datasets.

Antigen (UniProt accession)	Protein frequency on meningiomas	Peptide sequence	Frequency of positive patients	Protein frequency on non-meningeal tumors	Protein frequency on dura (n=9) / benign samples (n=364)
Unconventional myosin-Ic (MY11C; O00159)	49%	ENQLKYLTRLLSVE	WHO 12%	I+II MNG6 1	11% 0% / 17%
			MNG623 MNG666	MNG702	
			6% MNG6 5	MNG623	
			6% MNG6 0	MNG623	
			3% MNG623 0	MNG623 MNG635	
12% MNG6 5	MNG623 MNG666				
E3 ubiquitin-protein ligase MARCH6 (MARCH6; O60337)	15%	DQTPLFYWQDWALGVLH	WHO 15%	I+II MNG637 0	0% / 2%
			MNG642 MNG666	MNG673 MNG833	
			6% MNG637 0	MNG833	
Slit homolog 2 protein (SLIT2; O94813)	52%	DHIAVELYRGRVRAS	WHO 12%	I-III MNG6 0	22% / 7%
			MNG634 MNG641	MNG734	
			6% MNG6 0	MNG641	
			6% MNG6 0	MNG641	
			3% MNG636 0	MNG641	
			3% MNG6 1	MNG636 0	
EGF-containing fibulin-like extracellular matrix protein 2 (EFEMP2; O95967)	45%	DVFQIQATSVYPG	WHO 9%	I-III MNG6 0	33% / 6%
			MNG638 MNG734	MNG636 0	
			3% MNG636 0	MNG814 1	
			3% MNG814 1	MNG636 1	
			6% MNG636 1	MNG638	
			24% MNG3 12	MNG6 MNG624	
			MNG636 MNG638	MNG641 MNG682	
Coagulation factor XIII A chain (F13A1; P00488)	79%	LSANITFYTGVPKAEF	WHO 9%	I+III MNG6 1	44% / 32%
			MNG634 MNG636	MNG636 0	
			6% MNG636 0	MNG734	
			6% MNG612 0	MNG734	
Antithrombin-III (SERPINC1; P01008)	85%	SDQIHFFFAKLN	WHO 15%	I-III MNG6 1	89% / 48%
			MNG612 MNG636	MNG641 MNG734	
			6% MNG641 MNG734		
Insulin-like growth factor II (IGF2; P01344)	70%	PAHGGAPPEM	WHO 3%	I+II MNG637 0	44% / 18%
			3% MNG637 1	MNG637 0	
			6% MNG637 0	MNG702	
			6% MNG637 0		

Appendix: Supplement of CHAPTER 4

		PAHGGAPPEMASN	33%	MNG3	8	
				MNG624	MNG637	
				MNG638	MNG641	
				MNG666	MNG673	
				MNG679	MNG702	
				MNG833		
Fibronectin (FN1; 94% P02751)				<u>WHO</u>	<u>I-III</u>	54%
		LTPGVEYVYTIQVLRDGGQERDAPI	3%	MNG632	0	100% / 65%
		TPGVEYVYTIQVLRDG	6%	MNG638	6	
				MNG679		
		TPGVEYVYTIQVLRDGQE	9%	MNG1	1	
				MNG638	MNG679	
		TPGVEYVYTIQVLRDGGQER	3%	MNG638	1	
		TPGVEYVYTIQVLRDGGQERDAPI	3%	MNG632	0	
		YVYTIQVLRDGGQERDAPI	3%	MNG642	2	
		VYTIQVLRDGGQERDAPI	3%	MNG642	3	
		VGQQMIFEEHGFRRTTPPT	6%	MNG635	1	
				MNG638		
		GQQMIFEEHGFRRTTPP	12%	MNG612	2	
				MNG635	MNG638	
				MNG641		
		GQQMIFEEHGFRRTTPPT	6%	MNG635	1	
				MNG638		
		QQMIFEEHGFRRTTPP	12%	MNG6	9	
				MNG612	MNG635	
				MNG734		
		IFEEHGFRRTTPP	3%	MNG734	0	
Collagen alpha-2(V) chain (COL5A2; P05997)	36%			<u>WHO</u>	<u>I-III</u>	11%
		GNVGKTVFEYRTQNVAR	6%	MNG636	3	11% / 3%
				MNG638		
		VGKTVFEYRTQNVAR	12%	MNG612	10	
				MNG636	MNG638	
				MNG734		
		VARLPIIDLAPVDVGGTD	9%	MNG499	13	
				MNG642	MNG700	
		ARLPIIDLAPVDVGGTD	9%	MNG1	21	
				MNG499	MNG642	
		RLPIIDLAPVDVGGTD	6%	MNG499	28	
				MNG642		
		LPIIDLAPVDVGGT	3%	MNG499	25	
		LPIIDLAPVDVGGTD	9%	MNG1	35	
				MNG499	MNG642	
Secretogranin-2 (SCG2; P13521)	30%			<u>WHO</u>	<u>I-III</u>	9%
		LSDDVSKVIAYLKRLVNAAGSG	3%	MNG4	1	0% / 5%
		SDDVSKVIAYLKRLVNAAG	3%	MNG4	2	
		SDDVSKVIAYLKRLVNAAGSG	3%	MNG4	1	
		DDVSKVIAYLKRLVNAAG	3%	MNG4	1	
		DDVSKVIAYLKRLVNAAG	9%	MNG4	3	
				MNG6	MNG702	
		DDVSKVIAYLKRLVNAAGSG	6%	MNG4	1	
				MNG702		
		DVSKVIAYLKRLVNAAG	6%	MNG4	4	
				MNG6		
		DVSKVIAYLKRLVNAAG	9%	MNG4	8	
				MNG6	MNG702	
		VSKVIAYLKRL	3%	MNG6	0	
		VSKVIAYLKRLVNA	6%	MNG4	4	
				MNG6		
		VSKVIAYLKRLVNAAG	15%	MNG4	16	
				MNG6	MNG635	
				MNG641	MNG702	
		VSKVIAYLKRLVNAAG	15%	MNG4	16	
				MNG6	MNG635	
				MNG641	MNG702	
		SKVIAYLKRLVNAAG	3%	MNG6	2	
		SGYPKTPGRAGTEALPDG	3%	MNG682	0	
		YPKTPGRAGTEALPDG	9%	MNG6	6	
				MNG682	MNG734	
		TPGRAGTEALPDG	9%	MNG6	12	
				MNG682	MNG734	
Prolyl 4-hydroxylase subunit alpha-1 (P4HA1; P13674)	24%			<u>WHO</u>	<u>I+II</u>	7%
		DKVSVLDYLSYA	6%	MNG501	5	0% / 3%
				MNG638		
		DKVSVLDYLSYAVYQ	9%	MNG3	7	
				MNG7	MNG638	
		DKVSVLDYLSYAVYQQ	9%	MNG501	9	
				MNG635	MNG638	
		DKVSVLDYLSYAVYQQG	3%	MNG3	11	

Appendix: Supplement of CHAPTER 4

Inter-alpha-trypsin inhibitor heavy chain H2 (ITI2; P19823)	73%	FEIPINGLSE	WHO	I-II	35%	33% / 32%
			6%	MNG638	3	
			MNG702			
			18%	MNG6	1	
FEIPINGLSEF			MNG501	MNG638		
			MNG702	MNG814		
			MNG833			
			6%			
FEIPINGLSEFVD			MNG501	MNG702	0	
Macrophage scavenger receptor types I and II (MSR1; P21757)	15%	EVFMEHMSNMEKRIQH MEHMSNMEKRIQH MEHMSNMEKRIQHILD RIQHILDMEANLMDTE	WHO	I-III	3%	0% / 1%
			3%	MNG642	3	
			3%	MNG635	2	
			3%	MNG6	0	
			6%	MNG638	1	
			MNG734			
			3%	MNG734	0	
			3%	MNG734	0	
			3%	MNG638	0	
			3%	MNG638	1	
Cellular retinoic acid-binding protein 1 (CRABP1; P29762)	27%	INFKVGEGFEEETVD	WHO	I-II	2%	0% / 1%
			15%	MNG7	2	
			MNG623	MNG642		
			MNG661	MNG679		
INFKVGEGFEEETVDG			3%	MNG642	0	
			3%	MNG7	0	
Replication factor C subunit 4 (RFC4; P35249)	18%	KDRGVAASAGSSGENKKAKPVP	WHO	I-II	1%	11% / 1%
			18%	MNG7	3	
			MNG499	MNG628		
			MNG634	MNG638		
			MNG682			
Disintegrin and metalloproteinase domain-containing protein 17 (ADAM17; P78536)	24%	HVETLLTFSALKRH HVETLLTFSALKRHF HVETLLTFSALKRHF TSTHVETLLTFSALKRHF VETLLTFSALKRH VETLLTFSALKRHF VETLLTFSALKRHF	WHO	I-III	6%	0% / 3%
			3%	MNG734	1	
			3%	MNG641	0	
			15%	MNG6	3	
			MNG612	MNG634		
			MNG641	MNG734		
			3%	MNG641	0	
			6%	MNG641	0	
			MNG734			
			9%	MNG6	1	
			MNG641	MNG734		
			12%	MNG612		
MNG634	MNG641	3				
MNG734						
Probable cation-transporting ATPase 13A5 (ATP13A5; Q4VNC0)	18%	VDSCFKGTSVSNIIKP	WHO	I-III	0.3%	0% / 1%
			18%	MNG6	1	
			MNG612	MNG634		
			MNG641	MNG642		
Tetratricopeptide repeat protein 27 (TTC27; Q6P3X3)	18%	EIAIILGICTNFQKN	WHO	I-III	2%	0% / 2%
			15%	MNG624	1	
			MNG636	MNG638		
			MNG682	MNG734		
Chondroitin sulfate proteoglycan 4 (CSPG4; Q6UVK1)	24%	DFIYVDIFEGHLRA DFIYVDIFEGHLRAVV DFIYVDIFEGHLRAVVE FIYVDIFEGHLRA FIYVDIFEGHLRAV FIYVDIFEGHLRAVV FIYVDIFEGHLRAVVE IYVDIFEGHLRA IYVDIFEGHLRA IYVDIFEGHLRAVV IYVDIFEGHLRAVVE	WHO	I-III	8%	0% / 6%
			9%	MNG6	2	
			MNG634	MNG734		
			3%	MNG634	0	
			6%	MNG612	1	
			MNG734			
			15%	MNG6	5	
			MNG612	MNG636		
			MNG641	MNG734		
			3%	MNG734	1	
			6%	MNG612	2	
			MNG734			
			3%	MNG734	0	
			18%	MNG6	4	
MNG612	MNG634					
MNG636	MNG641					
MNG734						
6%	MNG634	2				
MNG734						
6%	MNG634	0				
MNG734						
Protocadherin Fat 4 (FAT4; Q6V0I7)	70%	GGNSQFTINPSTGQIIT GNSQFTINPSTGQII GNSQFTINPSTGQIIT	WHO	I-II	4%	11% / 20%
			3%	MNG702	0	
			3%	MNG702	0	
			9%	MNG3	0	
			MNG666	MNG702		

Appendix: Supplement of CHAPTER 4

		IGGNSQFTINPSTGQIIT	6%	MNG635	0		
				MNG673			
Interleukin-34 (IL34; Q6ZMJ4)	18%			<u>WHO</u>	<u>I+II</u>	0%	0% / 1%
		DKLQYRSRLQYMKHY	3%	MNG666	0		
		LRDKLQYRSRLQYMKHY	15%	MNG1	0		
				MNG3	MNG666	0	
				MNG673	MNG702		
		RDKLQYRSRLQYMKHY	6%	MNG666			
				MNG833			
Thrombospondin type-1 domain- containing protein 4 (THSD4; Q6ZMP0)	82%			<u>WHO</u>	<u>I+III</u>	9%	56% / 12%
		EMYKSNNYLALRSRSGRSIIN	3%	MNG682	0		
		KSNNYLALRSRSG	3%	MNG682	1		
		KSNNYLALRSRSGR	3%	MNG682	4		
		KSNNYLALRSRSGRS	9%	MNG624	5		
				MNG636	MNG682		
		KSNNYLALRSRSGRSI	15%	MNG6	6		
				MNG624	MNG682		
				MNG702	MNG734		
		KSNNYLALRSRSGRSIIN	3%	MNG682	0		
		KSNNYLALRSRSGRSIING	3%	MNG682	1		
		SNNYLALRSRSG	3%	MNG682	2		
		SNNYLALRSRSGR	3%	MNG682	2		
		SNNYLALRSRSGRS	3%	MNG682	1		
		SNNYLALRSRSGRSI	9%	MNG624	4		
				MNG682	MNG734		
		SNNYLALRSRSGRSIIN	6%	MNG3	1		
				MNG702			
		YKSNNYLALRSRSGRS	3%	MNG682	1		
		YKSNNYLALRSRSGRSI	3%	MNG682	0		
		YKSNNYLALRSRSGRSIIN	3%	MNG682	0		
Transmembrane protease serine 9 (TMPRSS9; Q7Z410)	21%			<u>WHO</u>	<u>I+II</u>	1%	0% / 1%
		SDYHRTLPTLEALLH	21%	MNG499	1		
				MNG635	MNG636		
				MNG637	MNG646		
				MNG666	MNG682		
Epidermal growth factor-like protein 6 (EGFL6; Q8IUX8)	27%			<u>WHO</u>	<u>I+II</u>	1%	0% / 1%
		GKGKGTGEIADVGVLLVSG	3%	MNG7	1		
		GKTGEIADVGVLLVSG	9%	MNG5	1		
				MNG7	MNG624		
		GKTGEIADVGVLLVSGL	6%	MNG7	3		
				MNG637			
		KSIIFEAERGKGTG	6%	MNG6	0		
				MNG638			
		KTGEIADVGVLLVS	3%	MNG7	0		
		KTGEIADVGVLLVSG	12%	MNG5	2		
				MNG7	MNG624		
				MNG646			
		KTGEIADVGVLLVSGL	12%	MNG5	4		
				MNG7	MNG624		
				MNG637			
		TKSIIFEAERGKGTG	3%	MNG6	0		
E3 ubiquitin- protein ligase UBR1 (UBR1; Q8IWW7)	21%			<u>WHO</u>	<u>I+II</u>	1%	0% / 1%
		TKDQDLIKQYNTLIEEMLQV	18%	MNG3	2		
				MNG6	MNG499		
				MNG641	MNG702		
				MNG682			
Phosphatidyl- inositol 3,4,5- trisphosphate- dependent Rac exchanger 1 protein (PREX1; Q8TCU6)	24%			<u>WHO</u>	<u>I+II</u>	3%	0% / 3%
		LRNDFKLVENILAKR	15%	MNG6	5		
				MNG634	MNG636		
				MNG637	MNG641		
		LRNDFKLVENILAKRL	3%	MNG637	2		
Protein KIAA1199 (KIAA1199; Q8WUJ3)	70%			<u>WHO</u>	<u>I-III</u>	10%	11% / 5%
		DPLKPREPAIIRHFIAYKNQD	3%	MNG638	0		
		DPLKPREPAIIRHFIAYKNQDH	3%	MNG638	0		
		DPLKPREPAIIRHFIAYKNQDHG	9%	MNG638	0		
				MNG641	MNG734		
		KPREPAIIRHFIAYKNQD	12%	MNG6	0		
				MNG636	MNG641		
				MNG734			
		KPREPAIIRHFIAYKNQDH	6%	MNG6	0		
				MNG734			
		KPREPAIIRHFIAYKNQDHG	3%	MNG734	0		
		EPAIIRHFIAYK	3%	MNG734	0		
		EPAIIRHFIAYKN	6%	MNG641	0		
				MNG734			
		EPAIIRHFIAYKNQ	6%	MNG641	0		
				MNG734			

Appendix: Supplement of CHAPTER 4

		EPAIRHFIAYKNQD	3%	MNG734	0	
		IIRHFIAYKNQDHG	3%	MNG642	0	
		IRHFIAYKNQDHG	3%	MNG642	0	
		IPDNSIVLMASKGRYV	36%	MNG1	0	
				MNG3	MNG6	
				MNG7	MNG634	
				MNG636	MNG638	
				MNG641	MNG642	
				MNG666	MNG702	
				MNG734		
		IPDNSIVLMASKGRYVS	45%	MNG1	1	
				MNG3	MNG6	
				MNG7	MNG612	
				MNG634	MNG635	
				MNG636	MNG638	
				MNG641	MNG642	
				MNG666	MNG702	
				MNG833	MNG833	
		IPDNSIVLMASKGRYVSR	27%	MNG1	0	
				MNG6	MNG634	
				MNG636	MNG638	
				MNG641	MNG666	
				MNG702	MNG734	
		PDNSIVLMASKGRYVS	3%	MNG702	0	
Cortactin-binding protein 2 (CTNBP2; Q8WZ74)	18%	QKKLEMEKLQLQALEQEHHK	18%	WHO I	1%	0% / 1%
				MNG499	1	
				MNG636	MNG679	
				MNG682	MNG700	
				MNG702		
SLIT and NTRK-like protein 6 (SLIRK6; Q9H5Y7)	18%	NDSRMSTKTTSSILKLP	18%	WHO I-III	2%	0% / 2%
				MNG6	8	
				MNG612	MNG634	
				MNG641	MNG642	
				MNG682		
Stabilin-1 (STAB1; Q9NY15)	85%	DELARIRAHRLVFR	9%	WHO I+II	32%	44% / 32%
				MNG1	3	
				MNG666	MNG702	
		DELARIRAHRLVFRYH	15%	MNG3	5	
				MNG666	MNG673	
				MNG702	MNG833	
		ELARIRAHRLVFRYH	15%	MNG1	2	
				MNG3	MNG666	
				MNG702	MNG833	
		GLVPQIEAATAYTIFVPT	3%	MNG638	1	
		IEAATAYTIFVPT	3%	MNG638	0	
		LARIRAHRLVFR	15%	MNG1	4	
				MNG3	MNG666	
				MNG702	MNG833	
		LARIRAHRLVFRYH	15%	MNG1	1	
				MNG3	MNG666	
				MNG702	MNG833	
		LVPQIEAATAYTIF	3%	MNG638	0	
		LVPQIEAATAYTIFVP	3%	MNG638	3	
		LVPQIEAATAYTIFVPT	12%	MNG623	6	
				MNG624	MNG638	
				MNG700		
		VPQIEAATAYTIF	3%	MNG638	0	
		VPQIEAATAYTIFV	3%	MNG638	2	
		VPQIEAATAYTIFVP	6%	MNG636	4	
				MNG638		
		VPQIEAATAYTIFVPT	9%	MNG623	4	
				MNG636	MNG638	
Carboxypeptidase A4 (CPA4; Q9UI42)	45%	IVSDYQRDPAITS	3%	WHO I+II	1%	22% / 0%
		SREWISQATAIWTARK	3%	MNG702	0	
		TARKIVSDYQRDPA	9%	MNG638	0	
				MNG661	1	
				MNG624	MNG642	
		TARKIVSDYQRDPAI	3%	MNG624	0	
		TARKIVSDYQRDPAIT	3%	MNG624	0	
		WTARKIVSDYQRDPA	3%	MNG642	0	
Carboxypeptidase Q (CPQ; Q9Y646)	48%	AGVPGASLLDDL	15%	WHO I+II	10%	22% / 7%
				MNG499	0	
				MNG632	MNG642	
				MNG666	MNG673	
Olfactomedin-like protein 2B (OLFM2B; Q68BL8)	55%	FSQEVIVLSKLNAAD	12%	WHO I+II	11%	11% / 1%
				MNG623	2	
				MNG635	MNG641	
				MNG661		
		FSQEVIVLSKLNAADL	9%	MNG623	6	

Appendix: Supplement of CHAPTER 4

			MNG635	MNG641		
		GAFYYNRAFTRNII	9%	MNG3	4	
			MNG501	MNG642		
		GAFYYNRAFTRNIIK	6%	MNG642	0	
			MNG700			
		GFSQEVIVLSKLNAAD	3%	MNG623	1	
		GFSQEVIVLSKLNAADL	6%	MNG623	3	
			MNG641			
		NGAFYYNRAFTRNII	6%	MNG638	0	
			MNG642			
		NGAFYYNRAFTRNIIK	6%	MNG638	0	
			MNG642			
		SQEVIVLSKLNAAD	9%	MNG635	3	
			MNG641	MNG661		
		SQEVIVLSKLNAADL	15%	MNG623	6	
			MNG635	MNG641		
			MNG661	MNG702		
		VIVLSKLNAAD	3%	MNG628	1	
		VIVLSKLNAADL	3%	MNG702	2	
		VYNGAFYYNRAFTRNIIK	3%	MNG642	0	
		YNGAFYYNRAFTRNII	12%	MNG3	1	
			MNG501	MNG638		
			MNG642			
		YNGAFYYNRAFTRNIIK	9%	MNG501	2	
			MNG638	MNG642		
		YYNRAFTRNII	6%	MNG638	0	
			MNG642			
Inter-alpha-	55%		<u>WHO</u>	<u>I+II</u>	8%	22% / 12%
trypsin inhibitor		GHKKQRTYLRTITILINKPE	6%	MNG623	0	
heavy chain H5			MNG679			
(ITIH5; Q86UX2)		KQRTYLRTITILINKPE	15%	MNG1	1	
			MNG2	MNG5		
			MNG623	MNG679		
Immunoglobulin	21%		<u>WHO</u>	<u>I+II</u>	1%	0% / 1%
superfamily		APKGPKIVMTPSRARVGD	15%	MNG1	1	
member 21			MNG3	MNG666		
(IGSF21;			MNG702	MNG833		
Q96ID5)						
CUB and sushi	18%		<u>WHO</u>	<u>I+II</u>	1%	0% / 1%
domain-contain-		KSPVCKSKGVREVN	15%	MNG7	1	
ing protein 1		TKTPVP	MNG499	MNG638		
(CSMD1;			MNG641	MNG666		
Q96PZ7)						
Hermansky-	21%		<u>WHO</u>	<u>I+II</u>	2%	11% / 1%
Pudlak		ERGLIFYINHSLYE	3%	MNG7	0	
syndrome 3		ERGLIFYINHSLYEN	9%	MNG3	4	
protein (HPS3;			MNG634	MNG638		
Q969F9)		KYERGLIFYINHSLY	12%	MNG3	3	
			MNG501	MNG702		
			MNG814			
Fibromodulin	94%		<u>WHO</u>	<u>I+II</u>	26%	56% / 18%
(FMOD; Q06828)		MPGGLPRSLRELHLDHNQI	9%	MNG499	10	
			MNG642	MNG700		
		MPGGLPRSLRELHLDHNQISR	9%	MNG499	21	
			MNG646	MNG700		
		MPGGLPRSLRELHLDHNQISRVPN	3%	MNG499	18	
		NLTRMPGGLPRSLRE	6%	MNG635	0	
			MNG646			
		NLTRMPGGLPRSLRELH	3%	MNG635	0	
		NNLTRMPGGLPRSLRE	6%	MNG635	0	
			MNG646			
		NNLTRMPGGLPRSLRELH	6%	MNG635	0	
			MNG646			
EGF-containing	61%		<u>WHO</u>	<u>I+II</u>	11%	33% / 16%
fibulin-like		GRNNFVIRRNADPQR	9%	MNG682	0	
extracellular			MNG702			
matrix protein 1		GRNNFVIRRNADPQRIP	3%	MNG833	0	
(EFEMP1;		GRNNFVIRRNADPQRIPS	9%	MNG702	1	
Q12805)			MNG666			
		GRNNFVIRRNADPQRIPSN	3%	MNG682	0	
		GRNNFVIRRNADPQRIPSNP	3%	MNG702	0	
		GRNNFVIRRNADPQRIPSNPS	3%	MNG702	0	
		NFVIRRNADPQR	9%	MNG628	1	
			MNG666	MNG702		
		NFVIRRNADPQRIPS	12%	MNG628	3	
			MNG682	MNG702		
			MNG833			
		NNFVIRRNADP	6%	MNG628	0	
			MNG702			

Appendix: Supplement of CHAPTER 4

		NNFVIRRNADPQR	6%	MNG682	0	
				MNG702		
		NNFVIRRNADPQRIPS	12%	MNG628	2	
				MNG682	MNG702	
				MNG833		
		NNFVIRRNADPQRIPSNPS	3%	MNG702	0	
		PQRIPSNPS	6%	MNG628	0	
				MNG702		
		TGRNNFVIRRNADPQR	3%	MNG666	0	
		TGRNNFVIRRNADPQRIPS	3%	MNG666	0	
		TGRNNFVIRRNADPQRIPSN	3%	MNG702	0	
		TGRNNFVIRRNADPQRIPSNPS	3%	MNG702	0	
		TGRNNFVIRRNADPQRIPSNPSH	3%	MNG702	0	
		VIRRNADPQR	3%	MNG628	0	
		VIRRNADPQRIPS	6%	MNG628	1	
				MNG702		
Collagen alpha-3(IX) chain (COL9A3; Q14050)	24%			<u>WHO</u>	<u>I-III</u>	2%
		EQIAQLAAHLRKPL	6%	MNG636	1	0% / 2%
				MNG734		
		EQIAQLAAHLRKPLAPG	3%	MNG734	0	
		GGMISEQIAQLAAHLRKPLAPG	6%	MNG641	0	
				MNG734		
		IAQLAAHLRKPLAPG	6%	MNG501	1	
				MNG702		
		ISEQIAQLAAHLRKPL	9%	MNG612	2	
				MNG636	MNG734	
		ISEQIAQLAAHLRKPL	18%	MNG6	6	
				MNG612	MNG636	
				MNG638	MNG641	
				MNG734		
		ISEQIAQLAAHLRKPLA	6%	MNG641	3	
				MNG734		
		ISEQIAQLAAHLRKPLAP	15%	MNG6	6	
				MNG612	MNG636	
				MNG641	MNG734	
		ISEQIAQLAAHLRKPLAPG	21%	MNG6	6	
				MNG501	MNG612	
				MNG636	MNG638	
				MNG641	MNG734	
		QIAQLAAHLRKPL	3%	MNG734	1	
		QIAQLAAHLRKPL	3%	MNG734	1	
		SEQIAQLAAHLRKPL	6%	MNG636	2	
				MNG734		
		SEQIAQLAAHLRKPL	15%	MNG6	4	
				MNG612	MNG636	
				MNG641	MNG734	
		SEQIAQLAAHLRKPLA	3%	MNG734	1	
		SEQIAQLAAHLRKPLAP	3%	MNG734	1	
Nidogen-2 (NID2; Q14112)	73%			<u>WHO</u>	<u>I-III</u>	14%
		DTSPAVLGLAARYVRAGFPR	3%	MNG1	0	11% / 13%
		EDTSPAVLGLAARYVRAGFPR	12%	MNG1	0	
				MNG666	MNG673	
				MNG833		
		LPSGELNTFQAVLASDG	15%	MNG3	2	
				MNG6	MNG638	
				MNG641	MNG734	
		LPSGELNTFQAVLASDGSYSAL	3%	MNG6	0	
		SPAVLGLAARYVRAG	6%	MNG3	1	
				MNG638		
		SPAVLGLAARYVRAGFP	9%	MNG1	0	
				MNG3	MNG833	
		SPAVLGLAARYVRAGFPR	9%	MNG1	0	
				MNG702	MNG833	
		TSPAVLGLAARYVRAG	3%	MNG638	1	
Importin subunit beta-1 (KPNB1; Q14974)	18%			<u>WHO</u>	<u>I+II</u>	11%
		KTTLVIMERLQQ	3%	MNG6	1	0% / 8%
		KTTLVIMERLQQVL	3%	MNG623	3	
		KTTLVIMERLQQVLQ	15%	MNG6	16	
				MNG623	MNG641	
				MNG666	MNG702	
Splicing factor 1 (SF1; Q15637)	15%			<u>WHO</u>	<u>I+II</u>	6%
		GVAGMPPFGMPPAPPPPPQN	12%	MNG6	13	0% / 2%
				MNG628	MNG638	
				MNG702		
		MGMGVAGMPPFGMPPAPPPPPQN	6%	MNG666	20	
				MNG702		
Proteoglycan 4 (PRG4; Q92954)	42%			<u>WHO</u>	<u>I+II</u>	3%
		GGLTGQIVAALSTAKYKNWPE	3%	MNG6	0	0% / 5%
		GLTGQIVAALSTAKYKN	6%	MNG3	0	
				MNG638		

GLTGQIVAALSTAKYKNWPE	6%	MNG6	1
		MNG666	
GQIVAALSTAKYKN	3%	MNG3	0
TGQIVAALSTAKYK	3%	MNG642	0
TGQIVAALSTAKYKN	9%	MNG3	0
		MNG638	MNG642

Supplementary Table 19. Established TAAs and CTAs identified as meningioma-exclusive antigens or represented by meningioma-exclusive peptides on ≥ 2 tumors. HLA restrictions not passing manual assessment as quality control are indicated in italic. The number of positive non-meningeal tumors was based on n=841 HLA class I and n=593 HLA class II peptidome datasets. The frequency of positive benign HLA peptidomes was calculated from n=9 tumor-free duras and n=418 (HLA class I) or n=364 (HLA class II) benign human specimens. Meningioma exclusivity of HLA class II-restricted peptides was evaluated for the exact sequence match with none of the peptides arising from a tumor-associated presentation hotspot.

Peptide sequence	HLA restriction	Frequency of positive patients	Protein frequency on meningiomas	Protein frequency on non-meningeal tumors	Protein frequency on dura / benign samples
Meningioma-exclusive HLA class I-presented antigens derived from established TAAs and CTAs					
Protein SSX5/SSX9 (SSX5/9; O60225 / Q7RTT3)					
Supplementary Table 16					
Probable ATP-dependent RNA helicase DDX43/54 (DDX43/53; Q9NXZ2 / Q86TM3)					
YLMPGFIHL	A*02:01; C*17:01	6%	MNG628 MNG641	0	0% / 0% 0.5% / 0.5%
Meningioma-exclusive HLA class I ligands derived from established TAAs and CTAs					
Neurofibromin (NF1; P21359)					
LPYLFHVV	B*51:01	12%	MNG499 MNG612 MNG642 MNG833	13	56% / 22%
NYPDEFKTL	A*24:02	12%	MNG1 MNG628 MNG635 MNG661	8	
AETVLADRF	B*44:03	6%	MNG1 MNG636	2	
DEFDQRILY	B*18:01	6%	MNG1 MNG661	5	
AVIAFRSSY	A*30:02	6%	MNG7 MNG632	3	
DYAELIVKF	A*24:02	6%	MNG628 MNG833	5	
Catenin beta-1 (CTNNB1; P35222)					
ATVGLIRNL	A*32:01; <i>B*13:02</i> <i>C*02:02</i>	9%	MNG634 MNG635 MNG702	22	100% / 72%
KTNVKFLAI	C*15:02	6%	MNG499 MNG501	7	
TYTYEKLLW	A*23:01; A*24:02	6%	MNG638 MNG679	9	
Platelet-derived growth factor receptor beta (PDGFRB; P09619)					
YMDLVGFSY	A*29:02	9%	MNG623 MNG673 MNG682	1	33% / 16%
MPYHIRSI	B*51:01	9%	MNG499 MNG833	7	
Regulator of G-protein signaling 5 (RGS5; O15539)					
KAKQIYEEF	<i>B*15:35</i> ; B*57:01	9%	MNG3 MNG642 MNG673	11	11% / 18%
KIKSPAKMAEK	A*03:01	6%	MNG636 MNG814	15	
Mothers against decapentaplegic homolog 3 (SMAD3; P84022)					
HASQPSMTV	B*51:01; C*15:02	9%	MNG499 MNG702 MNG833	11	
Werner syndrome ATP-dependent helicase (WRN; Q14191)					
ILQDLQPFL	A*02:01	9%	MNG612 MNG638 MNG673	5	11% / 4%
Cytochrome P450 1B1 (CYP1B1; Q16678)					
NRNFSNFIL	B*39:01; B*39:31	6%	MNG666 MNG734	0	89% / 41%
RVMIFSVGK	A*03:01	6%	MNG636 MNG666	3	
SMMRNFFTR	A*31:01	6%	MNG623 MNG635	2	
Zinc phosphodiesterase ELAC protein 2 (ELAC2; Q9BQ52)					
EISSPAVER	A*68:01	6%	MNG3 MNG632	1	22% / 22%
Retinoblastoma-associated protein (RB1; P06400)					
DEVKNVYF	B*18:01	6%	MNG6 MNG661	13	33% / 39%
TEINSALVL	B*40:01; B*40:02	6%	MNG3 MNG646	5	
Cytochrome c oxidase subunit 1 (MT-CO1; P00395)					
LPVLAAGITM	B*07:02; B*35:01	6%	MNG628 MNG666	3	11% / 18%

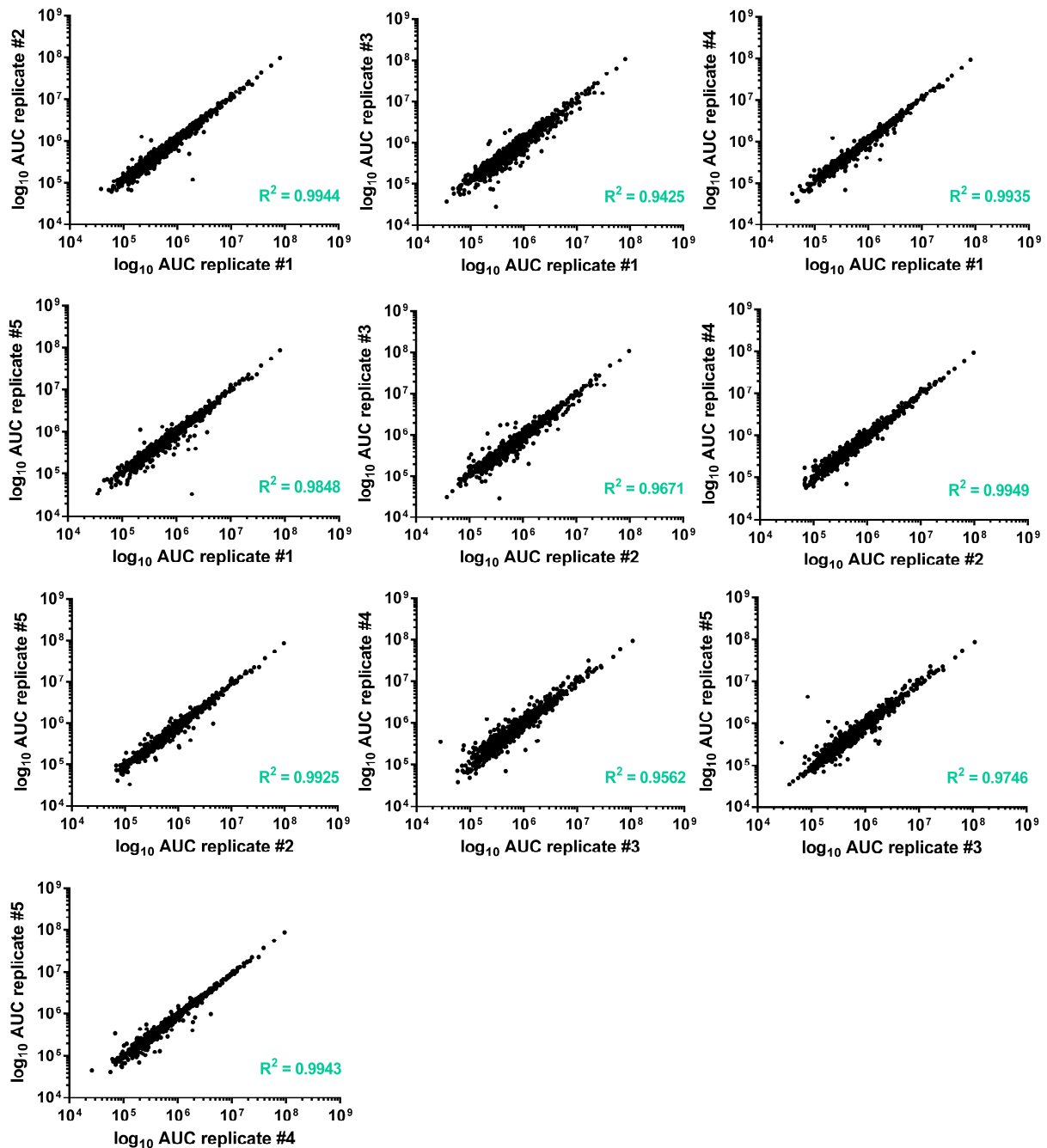
Appendix: Supplement of CHAPTER 4

DNA polymerase epsilon catalytic subunit A (POLE; Q07864)		33%		19%		11% / 25%
FYVDTVRAF	A*24:02	6%	MNG661	MNG833		18
EPSSLTYVTR	A*68:01	6%	MNG3	MNG814		2
Short transient receptor potential channel 1 (TRPC1; P48995)		33%		5%		0% / 4%
NEIRDLLGF	B*18:01	6%	MNG1	MNG628		1
DNA mismatch repair protein Msh2 (MSH2; P43246)		30%		34%		11% / 32%
SAAEVGFVR	A*68:01	6%	MNG3	MNG814		3
Epidermal growth factor receptor (EGFR; P00533)		24%		13%		0% / 6%
YQDPHSTAV	C*02:02; B*39:31	6%	MNG702	MNG734		28
Adenomatous polyposis coli protein (APCP; P25054)		24%		18%		0% / 19%
GELDTPINY	B*18:01; B*44:03	6%	MNG1	MNG636		1
LPSSSSSRGSL	B*07:02	6%	MNG7	MNG814		30
Mismatch repair endonuclease PMS2 (PMS2; P54278)		18%		7%		11% / 7%
DALHNLFYI	B*51:01	6%	MNG501	MNG833		4
Mothers against decapentaplegic homolog 4 (SMAD4; Q13485)		18%		11%		0% / 5%
KGFPVHIYA	C*12:03	6%	MNG636	MNG661		6
HRQGGSEETF	B*38:01 B*39:31	6%	MNG636	MNG734		6
POTE ankyrin domain family member A (POTEA; Q6S8J7)		30%		3%		11% / 5%
EVPRADLIVM	B*35:01	6%	MNG628	MNG833		2
Meningioma-exclusive HLA class II-presented antigens derived from established TAAs and CTAs						
Melanoma-associated antigen 10 (MAGEA10; P43363)						
Supplementary Table 16						
A/G-specific adenine DNA glycosylase (MUTYH; Q9UIF7)		6%		1%		0% / 0%
WRRRAEDEMDDLDRRAYAVWVSEVM		6%	MNG1	MNG679		2
Calcium-binding tyrosine phosphorylation-regulated protein (CABYR; O75952)		6%		0.5%		0% / 0%
DVLMVDVATSMPPVVIKEVPS		3%	MNG666			0
PVTEGVVYIEQLPEQIV		3%	MNG636			2
Meningioma-exclusive HLA class II-restricted peptides derived from established TAAs and CTAs						
Platelet-derived growth factor receptor-like protein (PDGFRL; Q15198)		48%		5%		33% / 2%
APKTQSIMMQVLDKGRFQKPA		15%	MNG499 MNG673 MNG700	MNG623 MNG679		5
TQSIMMQVLDKGRFQKPA		15%	MNG499 MNG637 MNG700	MNG623 MNG679		5
TQSIMMQVLDKGRFQKP		15%	MNG499 MNG637 MNG679	MNG623 MNG642		5
IQDTWRLIHRGLGHTT		9%	MNG666 MNG833	MNG702		3
QDTWRLIHRGLGHT		6%	MNG666	MNG833		2
Alpha-1,6-mannosylglycoprotein 6-beta-N-acetylglucosaminyl-transferase A (MGAT5; Q09328)		30%		15%		0% / 7%
DNILQRIGKLESKVDN		12%	MNG6 MNG642	MNG623 MNG666		15
LDLSKRYIKALAEENR		9%	MNG642 MNG679	MNG673		13
Cadherin-1 (CDH1; P12830)		64%		22%		56% / 32%
GTDGVITVKRPLRFHNPQ		9%	MNG1 MNG702	MNG673		3
TGRQRTAYFSLDTRF		6%	MNG7	MNG623		2
Serine/threonine-protein kinase ATR (ATR9; Q13535)		15%		4%		11% / 5%
GLPLSIEGHVHYLIQEATDE		9%	MNG501 MNG702	MNG700		0
Neurofibromin (NF1; P21359)		12%		3%		0% / 4%
GNPIFYVARRFK		9%	MNG6 MNG734	MNG641		0
Legumain (LGMN; Q99538)		49%		31%		22% / 46%
VPKDYTGEDVTPQNFLAVLR		6%	MNG1	MNG833		21
Matrix-remodeling-associated protein 5 (MXRA5; Q9NR99)		24%		16%		11% / 5%
DPWPRILWRLPSK		6%	MNG666	MNG702		10
GDPWPRILWRLPSK		6%	MNG666	MNG702		12
DPWPRILWRLPSKR		6%	MNG666	MNG702		12
C-1-tetrahydrofolate synthase, cytoplasmic (MTHFD1; P11586)		6%		15%		0% / 18%
GVSGALTVLMKDAIKPNLMQ		6%	MNG624	MNG682		2

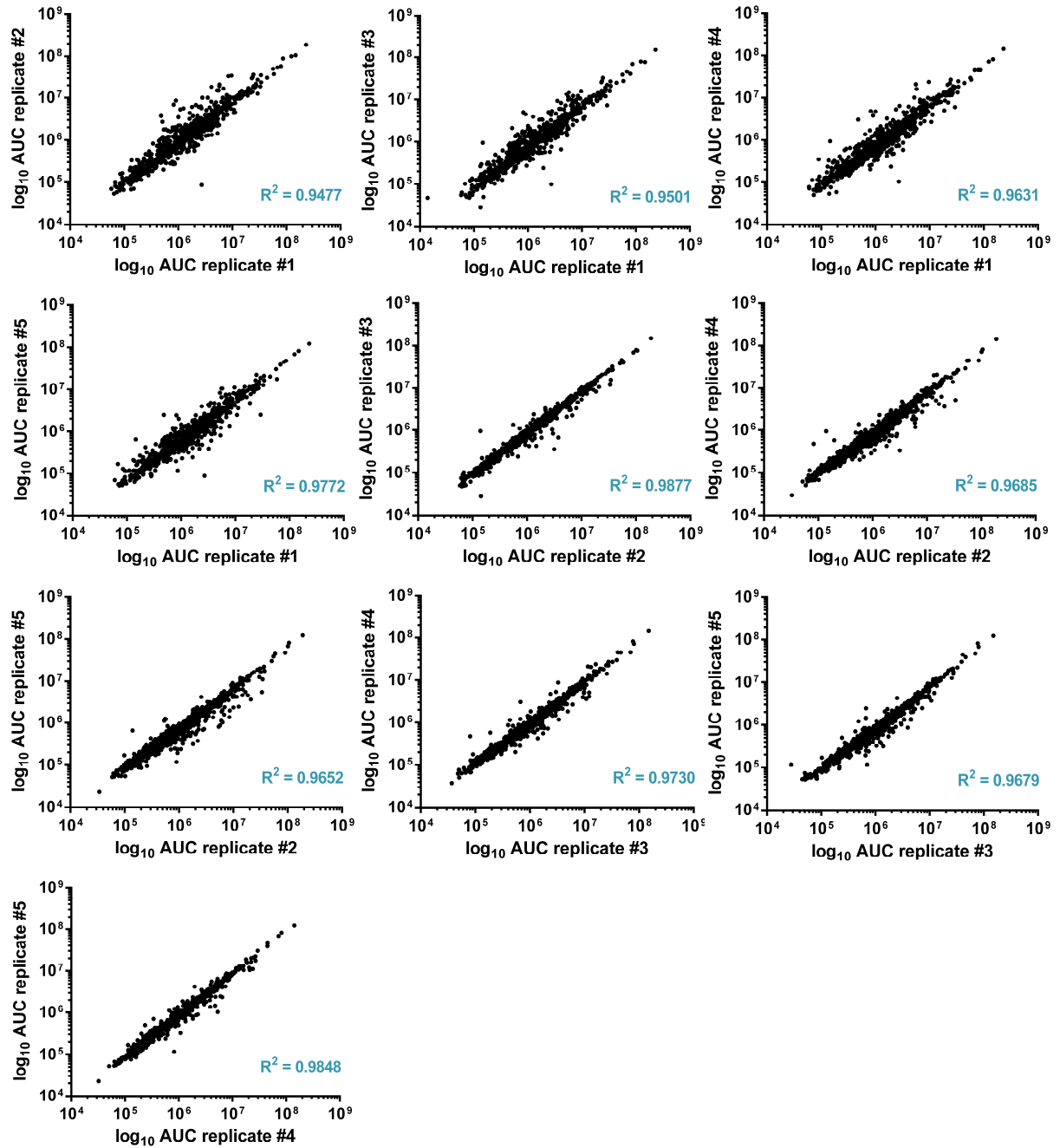
Appendix: Supplement of CHAPTER 4

Macrophage scavenger receptor types I and II (MSR1; P21757)	15%	3%	0% / 1%
RIQHILDMEANLMDTE	6%	MNG638 MNG734	1
Zinc phosphodiesterase ELAC protein 2 (ELAC2; Q9BQ52)	12%	1%	0% / 1%
LSGMILTLLKETGLPKCVLSGPP	6%	MNG7 MNG499	0
IIFLGTGSAIPMKIRNVSATLVNI	6%	MNG638 MNG702	0
Poly(A) polymerase alpha (PAPOLA; P51003)	9%	2%	0% / 1%
LSVDLTYDIQSFTD	6%	MNG1 MNG3	6
Ephrin type-B receptor 2 (EPHB2; P29323)	9%	3%	0% / 4%
TPGMKIYIDPFTYED	6%	MNG3 MNG638	1
Tyrosine-protein kinase receptor Tie-1 (TIE1; P35590)	9%	2%	0% / 15%
QTDVIWKSNGSYFYT	6%	MNG499 MNG814	0
A/G-specific adenine DNA glycosylase (MUTYH; Q9UIF7)	6%	1%	0% / 0.5%
WRRRAEDEMMLDRRAYAVVWSEVM	6%	MNG1 MNG679	0
ALK tyrosine kinase receptor (ALK; Q9UM73)	6%	1%	0% / 1%
PHNEAAREILLMPTPG	6%	MNG7 MNG638	0

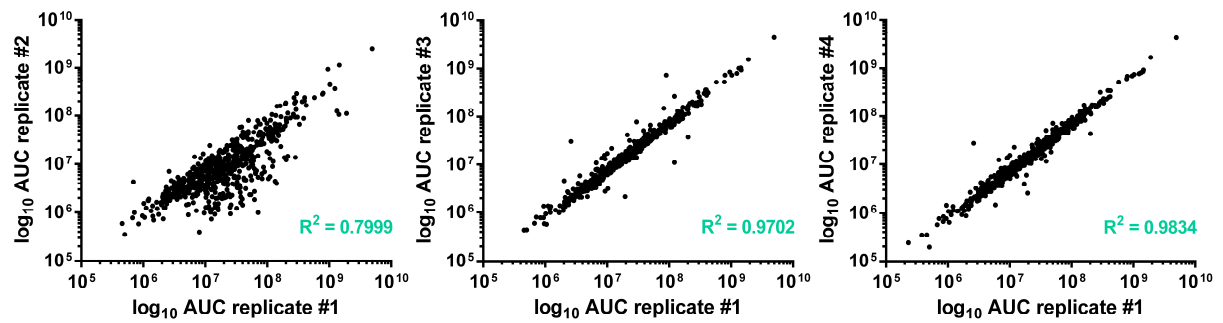
A



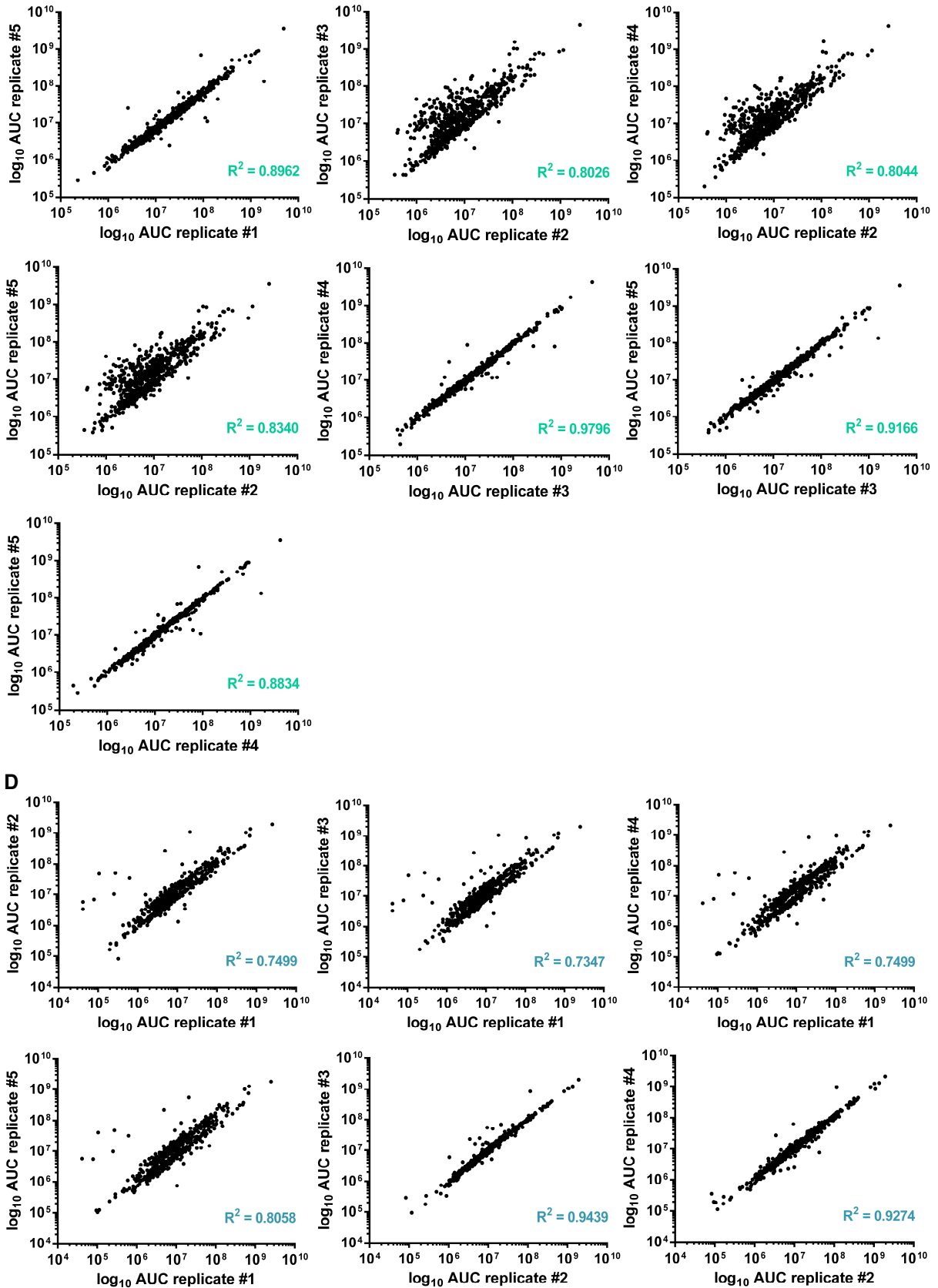
B

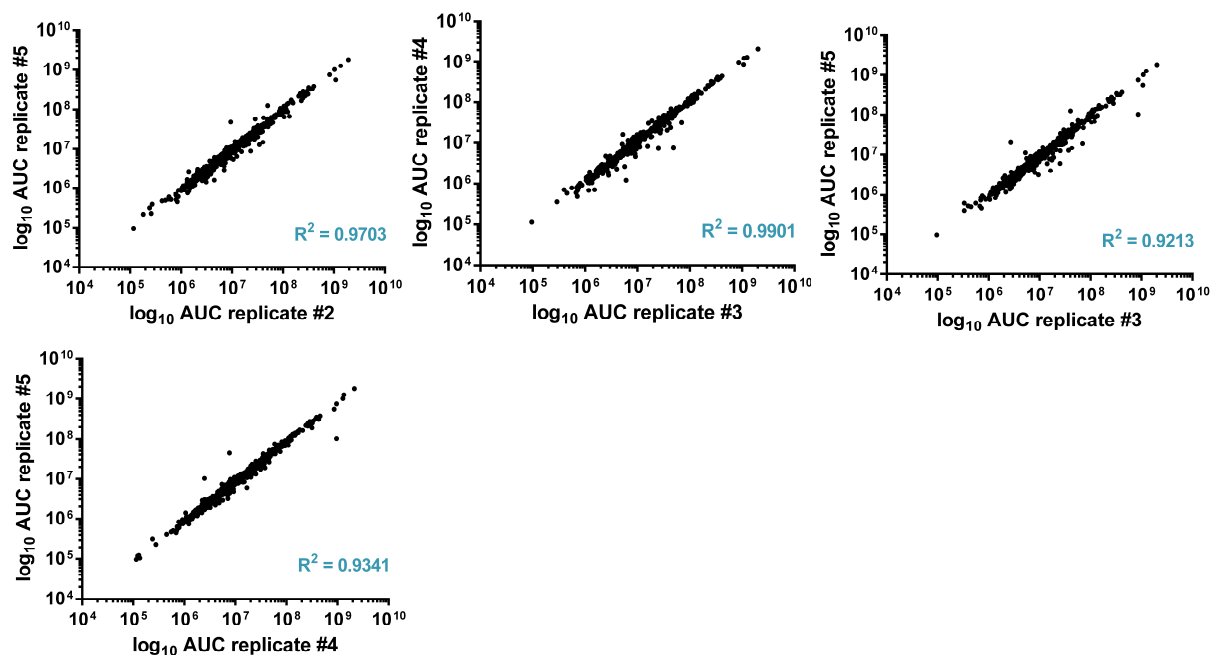


C



Appendix: Supplement of CHAPTER 4





Supplementary Figure 11. Reproducibility of precursor ion intensities across technical replicates exemplarily shown for MNG679. Scatter plots depicting raw MS¹ intensities prior to normalization in pairwise comparisons of technical replicates acquired from (A) HLA class I ligands eluted from tumor-free dura, (B) HLA class I ligands identified in meningioma, (C) HLA class II-presented peptides eluted from tumor-free dura, and (D) HLA class II-presented peptides identified in meningioma. Correlation coefficients were calculated by linear regression and amounted to > 0.85 except for HLA class II peptide intensity comparisons including replicate #2 acquired from dura and replicate #1 acquired from meningioma. HLA class II peptide intensities were in general slightly less reproducible as compared with HLA class I ligand intensities.

Supplementary Table 20. Peptide sequences and level of modulation for antigens exclusively represented by up- or down-modulated HLA class I- and II-presented peptides. Oxidized (m) and reduced (M) methionine were not treated equally in LFQ-MS and are listed separately. Multi-mapping peptides were censored when the second annotated protein diverged in assignment to groups of modulation according to comparative profiling. HLA restrictions not passing manual assessment as quality control are indicated in italic (HLA class I ligands not matching the motif of any of the patient's HLA allotypes; HLA class II-presented proteins neither identified with peptides exceeding a length of twelve AA nor with different sequences across patients). Abbreviation not introduced in the text above: fold change meningioma/dura (fc M/D).

UniProt accession	Antigen	Patients with significant modulation	Peptide sequence	HLA restriction	Fc (M/D)	Corrected p-value
Antigens exclusively represented by HLA class I ligands up-modulated on meningioma						
P05387	60S acidic ribosomal protein P2 (RLA2)	60% MNG679	MRYVASYLL	<i>C*04:01</i>	67.32	0.00093
			mRYVASYLL	<i>C*04:01</i>	20.86	0.00011
		MNG702	MRYVASYLL	<i>C*06:02</i>	22.02	0.00161
			mRYVASYLL	<i>C*06:02</i>	60.94	0.00014
			MRYVASYL	<i>C*06:02</i>	68.11	0.00005
			mRYVASYL	<i>C*06:02</i>	7.47	0.00014
MNG833	mRYVASYLL	<i>C*04:01</i>	18.48	0.00089		
P0DJ07	Protein PET100 homolog, mitochondrial (PT100)	40% MNG819	IYLTFPVAmF	A*23:01	5.82	0.00333
		MNG833	IYLTFPVAmF	A*24:02	10.58	0.00208
P28039	Acyloxyacyl hydrolase (AOAH)	40% MNG679	KFTNFNLFY	A*29:02	23.01	0.00002
		MNG702	SVIEQLAQV	A*02:01	18.33	0.00112
Q14126	Desmoglein-2 (DSG2)	40% MNG679	RFLDDLGLKF	<i>C*04:01</i>	44.61	0.00002
		MNG819	Manual HLA annotation: RFLDDLGLKF	A*23:01		
				A*23:01	28.79	0.00176

Appendix: Supplement of CHAPTER 4

Q15796	Mothers against decapentaplegic homolog 2 (SMAD2) 1 peptide multi-maps to SMAD1/3/5/9 (Q15797 / P84022 / Q99717 / O15198)	40% MNG702 MNG679	LTELPLDDY FVKGWGAEY	A*01:01 A*29:02	10.83 6.52	0.00052 0.00049
Q2TAY7	WD40 repeat-containing protein SMU1 (SMU1)	40% MNG679 MNG833	DVIRLIMQY DVIRLImQY DVIRLImQY	A*29:02 A*29:02 B*35:01	856.09 209.76 5.15	0.00025 0.00256 0.00037
Q68CP4	Heparan-alpha-glucosaminide N-acetyltransferase (HGNAT)	40% MNG679 MNG819	NYFPFQWKL NYFPFQWKL	A*23:01 A*23:01	25.65 12.97	0.00473 0.00090
Q6KC79	Nipped-B-like protein (NIPBL)	40% MNG679 MNG814	DVIERVIQY EVVAVDPSILAR	A*29:01 A*68:01	93.70 4.53	0.00012 0.00840
Q6PI26	Protein SHQ1 homolog (SHQ1)	40% MNG679 MNG833	EAIEQILKY NVHDIImVSF	A*29:02 B*35:01	28.28 6.39	0.00002 0.00072
Q6PKG0	La-related protein 1 (LARP1)	40% MNG679 MNG819	YGLEKFWAF YGLEKFWAF	A*23:01 A*23:01	45.79 11.98	0.00012 0.00169
Q96T76	MMS19 nucleotide excision repair protein homolog (MMS19)	40% MNG679 MNG702	EVVHLILFY VDTLVTKF	A*29:02 B*37:01	125.12 21.09	0.00043 0.000009
Q9BS91	Probable UDP-sugar transporter protein SLC35A5 (S35A5)	40% MNG679 MNG833	KWSIPAFLY IFIQNSKLYF	A*29:01 A*24:02	17.63 10.08	0.000005 0.00070
Q9H799	Ciliogenesis and planar polarity effector 1 (CPLN1)	40% MNG679 MNG819	KFLDLFLSY EYIKFLDLF	A*29:01 A*23:01	6.92 15.21	0.00727 0.00279

Antigens exclusively represented by HLA class I ligands down-modulated on meningioma

Q9Y520	Proline-rich and coiled-coil-containing protein 2C (PRC2C)	60% MNG679 MNG819 MNG833	FYmDTSHLF FYmDTSHLF FYmDTSHLF	A*23:01 A*23:01 A*24:02	0.0491 0.0957 0.1108	0.0000002 0.00013 0.00030
Q9UL54	Serine/threonine-protein kinase TAO2 (TAOK2) 1 peptide multi-maps to TAOK3 (Q9H2K8)	40% MNG679 MNG702	SEVVAIKKm QTELGQNQLEY	B*44:03 A*01:01	0.1283 0.0457	0.00119 0.00005
Q9BXC9	Bardet-Biedl syndrome 2 protein (BBS2)	40% MNG679 MNG819	AEQDLIREL IRSNNINTL	B*44:03 C*06:02	0.0303 0.0793	0.00047 0.00205
Q9BRK3	Matrix-remodeling-associated protein 8 (MXRA8)	40% MNG702 MNG814	RSEDIQLDY ALPSRILLWK	A*01:01 A*03:01	0.0470 0.0240	0.00002 0.000002
Q99733	Nucleosome assembly protein 1-like 4 (NP1L4) peptides multi-map to NP1L1 (P55209)	40% MNG679 MNG833	EEVHDLERKY QPmSFVLEF	B*44:03 B*35:03	0.0603 0.1462	0.00027 0.00007
Q8NG06	Tripartite motif-containing protein 58 (TRI58)	40% MNG702 MNG819	GLLEGVRGV GLLEGVRGV	A*02:01 A*02:01	0.0168 0.0444	0.000006 0.00034
Q8IUQ4	E3 ubiquitin-protein ligase SIAH1 (SIAH1)	40% MNG679 MNG814	VFDTSIAQL ATALPTGTSK	C*04:01 A*03:01	0.0425 0.2459	0.00030 0.00541
Q6N022	Teneurin-4 (TEN4)	40% MNG679 MNG819	AYSDGHFLF AYSDGHFLF	A*23:01 A*23:01	0.0951 0.0517	0.00045 0.00163
Q53FT3	Protein Hikeshi	40% MNG679 MNG819	KmLDNFYFN KmLDNFYFN	A*23:01 A*23:01	0.0579 0.2422	0.00001 0.00099
Q15746	Myosin light chain kinase, smooth muscle (MYLK)	40% MNG702 MNG814	DAFEEKANI SPQQVDFRSVL	B*51:01 B*07:02	0.0115 0.1016	0.00001 0.00024
Q15005	Signal peptidase complex subunit 2 (SPCS2)	40% MNG679 MNG819	AEFTKSIKAF REAEFTKZIA	B*44:03 B*50:01	0.0469 0.0947	0.00114 0.00709
Q01459	Di-N-acetylchitinase (DIAC)	40% MNG679 MNG819	REIEGSQVTF SQITTVATF	B*44:03 B*15:01	0.0492 0.1910	0.000003 0.00014
P57740	Nuclear pore complex protein Nup107 (NU107)	40% MNG679 MNG819	AEDLNFNRY AYLEAHETF	B*44:03 A*23:01	0.0275 0.1817	0.000001 0.00013
P43243	Matrin-3	40% MNG679 MNG702	FFGETSHNY RTEEGPTLSY	A*29:02 A*01:01	0.2240 0.0696	0.00004 0.0000003

Appendix: Supplement of CHAPTER 4

P29966	Myristoylated alanine-rich C-kinase substrate (MARCS)	40% MNG679 MNG819	AESGAKEEL AERPGEAAVA	B*44:03 B*50:01	0.0649 0.0866	0.00006 0.00604
P24821	Tenascin (TN-C)	40% MNG679 MNG819	TYLPAPEGLKF TYLPAPEGLKF	A*23:01 A*23:01	0.0468	0.00029 0.00017
P12755	Ski oncogene (SKI)	40% MNG814 MNG819	KPSSWLRTL QELEFLRVA	B*07:02 B*50:01	0.0073 0.0619	0.00008 0.00006
O15066	Kinesin-like protein KIF3B (KIF3B)	40% MNG679 MNG819	VYVKDLSSF VYVKDLSSF	A*23:01 A*23:01	0.0474 0.1181	0.00005 0.00039

Antigens exclusively represented by HLA class II-restricted peptides up-modulated on meningioma

Q6PCB0	von Willebrand factor A domain-containing protein 1 (VQA1)	33% MNG700 MNG819	ADSGYYVLELVPSAQPG DSGYYVLELVPSAQPG SGYYVLELVPSAQPG ADSGYYVLELVPSAQPG DSGYYVLELVPSAQPG SGYYVLELVPSAQPG	Class II Class II Class II Class II Class II Class II	23.73 49.63 18.03 21.16 10.57 4.18	0.00107 0.00150 0.00140 0.00066 0.00112 0.00053
O14949	Cytochrome b-c1 complex subunit 8 (QCR8)	33% MNG700 MNG702	FRVVPQFVVF FRVVPQFVVF	Class II Class II	5.25 22.51	0.00119 0.00019

Antigens exclusively represented by HLA class II-restricted peptides down-modulated on meningioma

Q9UBX1	Cathepsin F (CATF)	33% MNG700 MNG819	LPSNAYSAIKNLGGLE LPSNAYSAIKNLGGLE	Class II Class II	0.1075 0.0996	0.00486 0.00112
Q9GZZ6	Neuronal acetylcholine receptor subunit alpha-10 (ACH10)	33% MNG700 MNG819	YTSALRPVADTDQTLNV YTSALRPVADTDQTLNV	Class II Class II	0.0148 0.0014	0.00733 0.00073
Q96NH3	Protein broad-minded (BROMI)	33% MNG700 MNG819	TLCEKLTVLSLSDPDPVF TLCEKLTVLSLSDPDPVF	Class II Class II	0.0075 0.0014	0.00722 0.00073
P46459	N-ethylmaleimide-sensitive vesicle-fusing ATPase (NSF)	33% MNG700 MNG819	AAEFIQQFNNQAFS AAEFIQQFNNQAFS	Class II Class II	0.0573 0.0379	0.00639 0.00006

Supplementary Table 21. Functional annotation clustering of source proteins exclusively represented by up- or down-modulated HLA class I- or II-presented peptides on meningioma versus autologous tumor-free dura. Clustering for biological processes was performed on the basis of Gene Ontology (GO) terms using DAVID Bioinformatic Resources 6.8 ('Homo sapiens' as background, medium classification stringency, GO BP_ALL). As recommended by Huang *et al.* (Ref. 419 CHAPTER 1), only clusters with an enrichment score ≥ 1.0 were reported.

Biological process Gene Ontology IDs	Enrichment score
Antigens exclusively represented by HLA class I ligands up-modulated on meningioma	
organelle organization GO:0071840 GO:0016043 GO:0006996	3.50
ribosome biogenesis GO:0034470 GO:0034660 GO:0006364 GO:0016072 GO:0006396 GO:0022613 GO:0042254	2.04
cellular protein localization GO:0051641 GO:0008104 GO:0034613 GO:0033036 GO:0070727 GO:1902580 GO:0033365 GO:0046907 GO:1902582 GO:0015031 GO:0006605 GO:0045184 GO:0051649 GO:0006886 GO:0051179 GO:0072594 GO:0071702 GO:0051234 GO:0006810 GO:1902578 GO:0044765	2.03
DNA-templated transcription GO:0032784 GO:0034243 GO:0006354 GO:0032786 GO:0006368	1.84
histone modification GO:0016570 GO:0051276 GO:0016569 GO:0006325 GO:0018205	1.69
protein complex biogenesis GO:0043933 GO:0044085 GO:0022607 GO:0065003 GO:0006461 GO:0070271 GO:0071822 GO:0034622 GO:0043623	1.61
intracellular protein transport GO:1903829 GO:0090316 GO:0015031 GO:0051222 GO:0032388 GO:0006605 GO:1904951 GO:0032880 GO:0006886 GO:1903827 GO:0051223 GO:0070201 GO:0033157 GO:1903533 GO:0032386 GO:0032386 GO:0032386 GO:0032386 GO:0032386 GO:0032386 GO:0032386	1.57
cellular component organization GO:0051130 GO:0033043 GO:0051128	1.37
membrane protein localization GO:1902580 GO:0061024 GO:0044802 GO:0072657 GO:0007009 GO:0010256 GO:0072659 GO:1990778	1.32
protein oligomerization GO:0070206 GO:0070207 GO:0051259 GO:0051260	1.19
positive regulation of GTPase activity GO:0044093 GO:0043547 GO:0043085 GO:0065009 GO:0051345 GO:0043087 GO:0050790 GO:0051336 GO:0051338 GO:0007264	1.15

Appendix: Supplement of CHAPTER 4

DNA damage response						1.15
GO:2001020	GO:0006282	GO:0006281	GO:0006974	GO:0006259	GO:2001022	GO:2000779
GO:0045739	GO:0051052	GO:0006302	GO:0051054			
positive regulation of cell cycle						1.11
GO:0051983	GO:0090068	GO:0045787				
response to endogenous cyclic compound						1.10
GO:0009719	GO:0071363	GO:0070848	GO:0071407	GO:0010033	GO:0070887	GO:0071495
GO:0071310	GO:0042221					
amino acid biosynthesis						1.10
GO:0071265	GO:0009086	GO:0006555	GO:0009067	GO:0000096	GO:0046394	GO:0008652
GO:1901607	GO:0016053	GO:0009066	GO:0006790	GO:0006520	GO:1901605	
nuclear protein import						1.08
GO:0006913	GO:0051169	GO:1902582	GO:1900182	GO:0051170	GO:1903533	GO:0034504
GO:0046824	GO:0044744	GO:0006606	GO:1902593	GO:0042991	GO:0042307	GO:0042993
GO:1904591	GO:0017038	GO:1900180	GO:0046822	GO:0042990	GO:0042306	GO:1904589
chromosome segregation						1.07
GO:0051983	GO:0007059	GO:0007062	GO:0000819	GO:0033045	GO:0051304	GO:0098813
GO:0033044	GO:0007091	GO:0010965	GO:0044784	GO:0051306	GO:0051784	GO:0033047
GO:0000070	GO:0007094	GO:0034502	GO:0071173	GO:0022402	GO:2001251	GO:2000816
GO:0051985	GO:0031577	GO:0000280	GO:1903047	GO:0010948	GO:0045786	GO:0045839
GO:0030071	GO:1902099	GO:1901990	GO:0010639	GO:0007346	GO:0007067	GO:0048285
GO:1901991	GO:0007049	GO:0051301	GO:1901987	GO:0051783	GO:1901988	GO:0010564
GO:0000075	GO:0007126	GO:1903046	GO:0051726	GO:0044772	GO:0007088	GO:0044770
GO:0051129	GO:0007093	GO:0051321	GO:0000086	GO:1902589	GO:0044839	GO:0051129
regulation of organelle organization						1.05
GO:0033043	GO:0010638	GO:0051493				
ribonucleoprotein complex assembly						1.05
GO:0022613	GO:0001731	GO:0022618	GO:0071826			
amide biosynthesis						1.02
GO:0006412	GO:0043043	GO:0043604	GO:1901564	GO:1901566	GO:0006518	GO:0006417
GO:0010608	GO:0043603	GO:0034248				
Antigens exclusively represented by HLA class I ligands down-modulated on meningioma						
antigen processing and presentation						3.98
GO:0002478	GO:0019884	GO:0048002	GO:0019882	GO:0019886	GO:0002495	GO:0002504
GO:0002479	GO:0042590	GO:0002474				
intracellular signal transduction						2.90
GO:0035556	GO:0023051	GO:0010646	GO:0048583	GO:0007165	GO:0044700	GO:0023052
GO:0007154	GO:0051716	GO:0050794	GO:0009966	GO:0050789	GO:0050896	GO:0065009
GO:0065007	GO:1902531					
negative regulation of signal transduction						2.89
GO:0023051	GO:0010646	GO:0010648	GO:0023057	GO:0009966	GO:0009968	GO:0048585
membrane protein localization						2.87
GO:1902580	GO:1990778	GO:0090150	GO:0072657	GO:0072659	GO:0090002	GO:0010256
GO:0034613	GO:0070727	GO:0007009	GO:0061024	GO:0044802		
viral process						2.60
GO:0044403	GO:0044419	GO:0016032	GO:0044764	GO:0044033	GO:0019080	GO:0019083
GO:0019058	GO:0051704					
protein complex biogenesis						2.56
GO:0006996	GO:0065003	GO:0043933	GO:0071840	GO:0044085	GO:0016043	GO:0034622
GO:0070271	GO:0022607	GO:0006461	GO:0071822			
cellular protein localization						2.27
GO:1902580	GO:0051641	GO:0008104	GO:0045184	GO:0034613	GO:0033036	GO:0070727
GO:1902582	GO:0051234	GO:0051179	GO:0051649	GO:0015031	GO:1902578	GO:0072594
GO:0006810	GO:0046907	GO:0033365	GO:0006605	GO:0044765	GO:0006886	GO:0071702
apoptosis						2.25
GO:0051402	GO:0043523	GO:0070997	GO:1901214	GO:0043524	GO:1901215	GO:0006915
GO:0042981	GO:0010941	GO:0043067	GO:0043069	GO:0008219	GO:0012501	GO:0043066
GO:0060548	GO:0010942	GO:0043065	GO:0043068			
inhibition of kinase activity						2.23
GO:0031400	GO:0043549	GO:0010563	GO:0051338	GO:0032269	GO:0051248	GO:0051348
GO:0033673	GO:0045859	GO:0042325	GO:0031324	GO:0006469	GO:0001933	GO:0042326
GO:0001932	GO:0043086	GO:0044092	GO:0045936			
cellular response to peptide hormone						2.19
GO:0010033	GO:0071310	GO:0009725	GO:1901700	GO:0010243	GO:0071417	GO:0071495
GO:0032870	GO:1901698	GO:0070887	GO:0009719	GO:0043434	GO:1901653	GO:1901652
GO:0071375	GO:1901699	GO:1901701	GO:0007166	GO:0042221	GO:0032868	GO:0032869
EGFR signaling						1.98
GO:0007173	GO:0038127	GO:0007169				
cell development						1.92
GO:0044767	GO:0032502	GO:0048731	GO:0048856	GO:0044707	GO:0007275	GO:0048869
GO:0030154	GO:0048513	GO:0032501	GO:0007399			
ribonucleoprotein complex assembly						1.73
GO:0022613	GO:0022618	GO:0071826				
platelet activation						1.63
GO:0007596	GO:0042060	GO:0050817	GO:0007599	GO:0009611	GO:0030168	GO:0050878
nucleosome organization						1.61
GO:0071103	GO:0006323	GO:0034728	GO:0006334	GO:0006333	GO:0031497	GO:0071824
GO:0065004						

Appendix: Supplement of CHAPTER 4

regulation of MAPK cascade						1.50
GO:0051246	GO:0032268	GO:0031399	GO:0044267	GO:0006464	GO:0036211	GO:0043549
GO:0006468	GO:0019538	GO:0016310	GO:0043412	GO:0051338	GO:0045860	GO:0033674
GO:0045859	GO:0050790	GO:0051347	GO:0065009	GO:0032147	GO:0043406	GO:0042325
GO:0001932	GO:0019220	GO:0051174	GO:0060255	GO:0043085	GO:1902531	GO:0006796
GO:0006793	GO:0031401	GO:0044093	GO:0001934	GO:0042327	GO:0045937	GO:0010562
GO:0019222	GO:0071902	GO:0071900	GO:0023014	GO:0000165	GO:0032270	GO:0043170
GO:0051247	GO:0070372	GO:0043405	GO:0043410	GO:0043408	GO:0044260	GO:0080090
GO:0000187	GO:0009893	GO:0010604	GO:0048584	GO:0010647	GO:0031323	GO:0023056
GO:0051336	GO:0070371					
T-cell activation						1.46
GO:0050852	GO:0007155	GO:0022610	GO:0031295	GO:0031294	GO:0050851	GO:0030155
GO:0098609	GO:0002429	GO:0002768	GO:0050865	GO:0002376	GO:0001775	GO:0022407
GO:0002764	GO:0002757	GO:0050863	GO:1903037	GO:0002253	GO:0045321	GO:0002694
GO:0050870	GO:0038095	GO:0070486	GO:0045785	GO:0007159	GO:1903039	GO:0006952
GO:0046649	GO:0045087	GO:0002682	GO:0002252	GO:0071593	GO:0070489	GO:0042110
GO:0002223	GO:0051249	GO:0002220	GO:0050778	GO:0022409	GO:0050867	GO:0098602
GO:0031349	GO:0050776	GO:0006955	GO:0031347	GO:0002684	GO:0016337	GO:0002696
GO:0002758	GO:0038093	GO:0051251	GO:0002218	GO:0045089	GO:0045088	GO:0002221
GO:0002683						
membrane fusion						1.41
GO:0022406	GO:0006904	GO:0048278	GO:0061025	GO:0048284	GO:0022406	GO:0006904
microtubule-associated transport						1.37
GO:0030705	GO:0072386	GO:0072383	GO:0072384	GO:0007018	GO:0010970	GO:0047496
GO:0099518	GO:0051656	GO:0051640	GO:0007017	GO:0051648	GO:0051650	
stress-activated MAPK cascade						1.32
GO:0080135	GO:0032872	GO:0070302	GO:0046328	GO:0023014	GO:0000165	GO:0031098
GO:0051403	GO:0046330	GO:0043408	GO:0043410	GO:0032874	GO:0070304	GO:0043507
GO:0007254	GO:0043506					
respiratory system development						1.30
GO:0060541	GO:0030324	GO:0030323	GO:0060425	GO:0035295		
regulation of cell proliferation						1.29
GO:0008283	GO:0008285	GO:0042127	GO:0008284			
cell physiology						1.28
GO:0065007	GO:0009987	GO:0044763	GO:0044699			
response to vitamin						1.26
GO:0071305	GO:0031670	GO:0031669	GO:0071295	GO:0031668	GO:0033280	GO:0071496
GO:0031667	GO:0009991	GO:0033273	GO:0007584	GO:0042594		
negative regulation of TGF- β / bone morphogenetic protein signaling						1.22
GO:0071560	GO:0071559	GO:0090101	GO:0007179	GO:1903845	GO:0030512	GO:0007167
GO:0090288	GO:1903844	GO:0017015	GO:0007178	GO:0070848	GO:0071363	GO:0060021
GO:0090092	GO:0030514	GO:0090287	GO:0030509	GO:0071773	GO:0071772	GO:0030510
neuron differentiation						1.21
GO:0048468	GO:0048666	GO:0022008	GO:0030154	GO:0030182	GO:0031175	GO:0048699
GO:0061564	GO:0048667	GO:0007399	GO:0000902	GO:0007409	GO:0000904	GO:0032989
GO:0048812	GO:0030030	GO:0048858	GO:0032990			
viral genome replication						1.21
GO:0019079	GO:0039703	GO:0039694				
cell-cell and cell-substrate adhesion						1.18
GO:0045216	GO:0034332	GO:0034330	GO:0051017	GO:0032231	GO:0061572	GO:0048010
GO:0001952	GO:0051492	GO:0007160	GO:0048041	GO:0007045	GO:0007044	GO:0034333
GO:2000114	GO:0001954	GO:0032878	GO:0031589	GO:1901888	GO:0034329	GO:0010810
GO:0090109	GO:0051893	GO:1903391	GO:0010811			
response to steroid hormone						1.17
GO:0009725	GO:0014070	GO:0071407	GO:0033993	GO:0030522	GO:0071396	GO:0048545
GO:0071383	GO:0043401	GO:0009755	GO:0030518			
nuclear protein import						1.09
GO:1902580	GO:0034613	GO:0070727	GO:1902582	GO:0051649	GO:0072594	GO:0046907
GO:0033365	GO:0006606	GO:0044744	GO:1902593	GO:0017038	GO:0034504	GO:0051170
GO:0006605	GO:0006913	GO:0051169	GO:0006886	GO:0042306	GO:1904589	GO:0046822
GO:0043433	GO:0042990	GO:0042991	GO:1900180	GO:1903827	GO:0032386	GO:1903533
GO:0033157	GO:1903829	GO:0090316	GO:0032388			
histone acetylation						1.04
GO:0051276	GO:0006325	GO:0016570	GO:0043970	GO:0018205	GO:0006475	GO:0016569
GO:2000615	GO:0016573	GO:0061647	GO:0018393	GO:0006473	GO:0018394	GO:0035065
GO:0035066	GO:0043543	GO:2000758	GO:2000756	GO:0043967	GO:1901983	GO:1901985
GO:0031056	GO:0031058	GO:1902275	GO:1905269	GO:0033044	GO:0043966	GO:2001252
establishment or maintenance of cell polarity						1.04
GO:0006939	GO:0007163	GO:0070830	GO:0043297	GO:0034329	GO:0030866	GO:0030865
GO:0007043						
cytokine-mediated signaling						1.04
GO:0045087	GO:0019221	GO:0071345	GO:0034097	GO:0002684		
actin organization						1.02
GO:0051017	GO:0030036	GO:0032231	GO:0061572	GO:1902589	GO:0051493	GO:0010638
GO:0051492	GO:0007010	GO:0032233	GO:0051130	GO:0044087	GO:0030029	GO:0032956
GO:0032970	GO:0031032	GO:0043254	GO:0051496	GO:0030038	GO:0043149	GO:0007015
GO:0051130	GO:0051130	GO:0051130	GO:0051130	GO:0051130	GO:0051130	
iron ion homeostasis						1.02
GO:0006880	GO:0097577	GO:0051651	GO:0006879	GO:0046916	GO:0051238	GO:0055072
GO:0055076	GO:0006826	GO:0000041				

Appendix: Supplement of CHAPTER 4

ribosome biogenesis						1.02
GO:0022613	GO:0042254	GO:0006364	GO:0016072	GO:0034660	GO:0006396	GO:0042274
negative regulation of RNA transcription						1.01
GO:0048519	GO:0048523	GO:0010605	GO:0051246	GO:0009892	GO:0032268	GO:0009058
GO:1901576	GO:0044267	GO:0043412	GO:0019538	GO:0031324	GO:0060255	GO:0019222
GO:0000122	GO:0043170	GO:0010629	GO:0080090	GO:0010468	GO:0009890	GO:0044260
GO:0045934	GO:0031323	GO:0006366	GO:0010558	GO:1902679	GO:0031327	GO:0010467
GO:1903507	GO:0051171	GO:0051172	GO:0051253	GO:2000113	GO:0090304	GO:0034654
GO:0045892	GO:0006139	GO:0008152	GO:0018130	GO:0034641	GO:0071704	GO:0019438
GO:0044238	GO:0016070	GO:0006357	GO:0019219	GO:0046483	GO:0006725	GO:1901362
GO:0044271	GO:0010556	GO:0032774	GO:1901360	GO:0051252	GO:0009889	GO:0006807
GO:0031326	GO:0097659	GO:2001141	GO:2000112	GO:0044237	GO:1903506	GO:0006355
GO:0009059	GO:0034645	GO:0044249	GO:0006351			
Antigens exclusively represented by HLA class II-restricted peptides up-modulated on meningioma						
cell-cell adhesion						3.94
GO:0007156	GO:0098742	GO:0098609	GO:0007155	GO:0022610	GO:0007399	
ribonucleoside metabolism						2.16
GO:0033275	GO:0030049	GO:0030048	GO:0006936	GO:0070252	GO:0003012	GO:0003009
GO:0006928	GO:0046034	GO:0050881	GO:0050879	GO:0009205	GO:0009199	GO:0009144
GO:0009167	GO:0009126	GO:0009161	GO:0009141	GO:0009123	GO:0003008	GO:0046128
GO:0042278	GO:0006941	GO:0009119	GO:0009116	GO:0030029	GO:1901657	GO:0007517
GO:0009150	GO:0009259	GO:0006163	GO:0019693	GO:0072521	GO:0061061	GO:0060537
GO:0009117	GO:0006753	GO:0055086	GO:0019637	GO:0014706	GO:1901135	GO:0006470
GO:0006796	GO:0006793	GO:0009888	GO:0044281	GO:0016311	GO:1901564	GO:0044710
actin organization						2.00
GO:0033275	GO:0030049	GO:0030048	GO:0070252	GO:0006941	GO:0030029	GO:0030239
GO:0031032	GO:0061061	GO:0055002	GO:0055001	GO:0010927	GO:0070925	GO:0030036
GO:0048646	GO:0051146	GO:1902589	GO:0032989	GO:0042692	GO:0007010	
Antigens exclusively represented by HLA class II-restricted peptides down-modulated on meningioma						
response to oxidative stress						1.74
GO:0098869	GO:1990748	GO:0098754	GO:0009636	GO:0055114	GO:0000302	GO:0006979
GO:1901700						
protein catabolism						1.14
GO:0044248	GO:0009056	GO:1901575	GO:0009057	GO:0044265	GO:0009894	GO:0042176
GO:0031329	GO:1903050	GO:1903362	GO:0030163	GO:0051603	GO:0044257	GO:0006508
GO:0043161	GO:0006511	GO:0019941	GO:0043632	GO:0010498	GO:0042787	GO:0030162
GO:0016567	GO:0032446	GO:0051246	GO:0032268	GO:0070647		

Supplement of CHAPTER 6

Supplementary Table 22. Peptide yields with PROCAL or heavy isotope-labeled RT peptides spiked into a complex matrix of HLA class I peptides eluted from JY cells. PROCAL peptides were spiked at 2.5 / 5 / 10 / 20 fmol/peptide/ μ l into JY17#3 and LC-MS/MS measurements were performed back-to-back on an Orbitrap Fusion Lumos. A selection of ten in-house produced heavy isotope-labeled RT peptides were diluted in JY17#3 (Orbitrap Fusion Lumos) or in JY17#4 (LTQ Orbitrap XL) to a concentration of 0.01 / 0.25 / 0.05 / 0.1 / 0.25 / 0.5 / 1 / 5 fmol/peptide/ μ l and LC-MS/MS data acquisition was performed in the order of ascending synthetic peptide concentration. Of note, neither PROCAL nor RT peptides had an apparent influence on the total number of unique peptide identifications at any of the evaluated concentrations. RT peptides were spiked at determined concentration into the newly produced LC-MS/MS standard JY19#1.

LC-MS/MS measurement	Concentration [fmol/ peptide/ μ l]	Unique peptides	Total PSMs	Total intensity
PROCAL peptides				
Orbitrap Fusion Lumos				
180628_LF_jpt_RTPeptides_12-5fmol-5ul_2-5fmol-ul_JY17#3_4-1diluted_thawed20180629_DDA#1_400-650mz_msms67	2.5	1057	3435	3.504E+10
180628_LF_jpt_RTPeptides_25fmol-5ul_5fmol-ul_JY17#3_4-1diluted_thawed20180629_DDA#1_400-650mz_msms66	5	1094	3936	6.012E+10
180628_LF_jpt_RTPeptides_50fmol-5ul_10fmol-ul_JY17#3_4-1diluted_thawed20180629_DDA#1_400-650mz_msms65	10	1080	3833	1.064E+11
180628_LF_jpt_RTPeptides_100fmol-5ul_20fmol-ul_JY17#3_4-1diluted_thawed20180629_DDA#1_400-650mz_msms64	20	1029	4404	2.333E+11
In-house heavy isotope-labeled RT peptides				
Orbitrap Fusion Lumos				
190605_LF_10_RTPeptides_in-house_0-fmol-ul_Aload_1-10_in_JY17#3_thawed20190604_DDA#1_400-650mz_Lumos_msms1	0	1254	2785	2.452E+10
190605_LF_10_RTPeptides_in-house_0-01fmol-ul_in_JY17#3_thawed20190604_DDA#1_400-650mz_Lumos_msms2	0.01	1201	2670	2.035E+10
190605_LF_10_RTPeptides_in-house_0-025fmol-ul_in_JY17#3_thawed20190604_DDA#1_400-650mz_Lumos_msms3	0.025	988	2197	1.718E+10
190605_LF_10_RTPeptides_in-house_0-05fmol-ul_in_JY17#3_thawed20190604_DDA#1_400-650mz_Lumos_msms4	0.05	1393	3014	2.621E+10
190605_LF_10_RTPeptides_in-house_0-1fmol-ul_in_JY17#3_thawed20190604_DDA#1_400-650mz_Lumos_msms5	0.1	1430	3106	2.807E+10
190605_LF_10_RTPeptides_in-house_0-25fmol-ul_in_JY17#3_thawed20190604_DDA#1_400-650mz_Lumos_msms6	0.25	1441	3269	2.817E+10
190605_LF_10_RTPeptides_in-house_0-5fmol-ul_in_JY17#3_thawed20190604_DDA#1_400-650mz_Lumos_msms7	0.5	1419	3182	3.003E+10
190605_LF_10_RTPeptides_in-house_1fmol-ul_in_JY17#3_thawed20190604_DDA#1_400-650mz_Lumos_msms8	1	1358	3201	3.150E+10
190913_AN_JY_Standard_19#1_RT_aufgetaut190913_DDA#1_400-650mz_msms7	0.05-1	2429	5453	5.347E+10
LTQ Orbitrap XL				
190604_LF_10_RTPeptides_in-house_0fmol-ul_Aload_1-10_inJY17#4_thawed20190604_Rep#1_400-650mz_XL_msms11	0	923	2525	9.267E+09
190604_LF_10_RTPeptides_in-house_0-025fmol-ul_inJY17#4_thawed20190604_Rep#1_400-650mz_XL_msms12	0.025	1004	2545	8.724E+09
190604_LF_10_RTPeptides_in-house_0-05fmol-ul_inJY17#4_thawed20190604_Rep#1_400-650mz_XL_msms13	0.05	915	2356	8.654E+09
190604_LF_10_RTPeptides_in-house_0-1fmol-ul_inJY17#4_thawed20190604_Rep#1_400-650mz_XL_msms14	0.1	947	2454	7.730E+09
190604_LF_10_RTPeptides_in-house_0-25fmol-ul_inJY17#4_thawed20190604_Rep#1_400-650mz_XL_msms15	0.25	974	2477	9.842E+09
190604_LF_10_RTPeptides_in-house_0-5fmol-ul_inJY17#4_thawed20190604_Rep#1_400-650mz_XL_msms16	0.5	976	2565	1.014E+10
190604_LF_10_RTPeptides_in-house_1fmol-ul_inJY17#4_thawed20190604_Rep#1_400-650mz_XL_msms17.msf	1	839	2227	7.066E+09
190604_LF_10_RTPeptides_in-house_5fmol-ul_inJY17#4_thawed20190604_Rep#1_400-650mz_XL_msms18.msf	5	912	2656	1.126E+10
191125_LM_Standard_JY19#1_W_10RTpeptides_20191112_Rep#4_400-650mz_XL_PerformanceCheck_msms25.msf	0.1-0.5	1350	3347	1.623E+10